NASA SP-80

IEEE-NASA SYMPOSIUM ON SHORT-TERM FREQUENCY STABILITY

GODDARD SPACE FLIGHT CENTER

GREENBELT, MARYLAND

NOVEMBER 23-24

1964

NASA SP-80

SHORT-TERM FREQUENCY STABILITY

Proceedings of the IEEE-NASA Symposium on the Definition and Measurement of Short-Term Frequency Stability held at the Goddard Space Flight Center, Greenbelt, Maryland, November 23–24, 1964

Prepared by Goddard Space Flight Center

Scientific and Technical Information Division 1965
NATIONAL AERONAUTICS AND SPACE ADMINISTRATION
Washington, D.C.

For sale by The Superintendent of Documents, U.S. Government Printing Office
Washington, D.C. 20402 Price $1.75

OFFICERS

Chairman	ANDREW R. CHI NASA/GSFC
Vice Chairman	JAMES H. ARMSTRONG IEEE/COMMITTEE-14
Secretary	THOMAS E. MCGUNIGAL
Public Affairs	CHARLES P. BOYLE NASA/GSFC

PROGRAM COMMITTEE

Chairman	A. R. CHI NASA/GSFC
Vice Chairman	J. H. ARMSTRONG IEEE/TC-14
Secretary	T. E. MCGUNIGAL NASA/GSFC

E. J. Baghdady	AD COM, INC.
A. S. Bagley	HEWLETT-PACKARD CO.
J. A. Barnes	NBS BOULDER LABS.
K. M. Brown	GENERAL DYNAMICS CORP.
M. H. C. Criswell	BUREAU OF SHIPS, U.S. NAVY
C. Friend	WPAFB, U.S. AIR FORCE
J. G. Gregory	NASA/MSFC
G. K. Guttwein	U.S.A.E.R.D.L.
D. J. Healey, III	WESTINGHOUSE ELECTRIC CO.
D. B. Leeson	HUGHES AIRCRAFT CO.
F. H. Reder	U.S.A.E.R.D.L.
W. K. Saunders	HARRY DIAMOND LABORATORY
H. P. Stratemeyer	GENERAL RADIO CO.
R. F. C. Vessot	VARIAN ASSOCIATES
F. O. Vonbun	NASA/GSFC

FOREWORD

This volume contains the papers and discussions presented at the Symposium on the Definition and Measurement of Short-Term Frequency Stability. The need for clarification in this field has been recognized for some time. To this end, the Symposium held at Goddard Space Flight Center on November 23 and 24, 1964, was sponsored jointly by NASA—GSFC and the Institute of Electrical and Electronic Engineers (Technical Committee, Standards 14—Piezoelectric and Ferroelectric Crystals).

The Proceedings are arranged into four Sessions, namely:

I. Users' Viewpoint and Requirements
II. Theory
III. Devices, and
IV. Measurement Techniques.

A panel discussion on the papers and related subject matter was conducted by the Session Chairman after each session. The panel was composed in each case of a group of experts in the field covered by the particular session.

It is interesting to note that this Symposium was the first devoted solely to the subject of *short-term* frequency stability. Because of the importance of this subject to missile and spacecraft tracking and guidance system designers as well as to manufacturers, the Symposium was enthusiastically supported and attended; therefore offered a unique opportunity for cross-fertilization of ideas. Of course, a good deal of work in this field had been done by many groups prior to the Symposium; but communication was severely hampered by the lack of commonly accepted terminology.

The results of the Symposium, from the standpoint of the quality of the papers, the wide representation of the participants, and the interest stimulated, were very rewarding. It is to be hoped that additional interest and work in short-term frequency stability will evolve in the fields of theory, frequency generating devices, and measurement techniques. Most of all, it is to be hoped that this Symposium has stimulated the interest of the users with whom we wish to open a channel of communication.

The original concept for the Symposium was generated within the Goddard Space Flight Center. Immediate and enthusiastic support for the idea was given by Dr. Harry J. Goett, Director of the Goddard Space Flight Center, and Messrs. Roger A. Sykes and James H. Armstrong of Bell Telephone Laboratory. Accordingly, joint Goddard/IEEE sponsorship was agreed upon between Goddard and Mr. Armstrong, Chairman of IEEE Committee—Standards 14. Following the decision to proceed with the Symposium, strong support and valuable guidance in the development of the Symposium was furnished to the officers by all members of the program committee.

The number of those who participated in the Symposium either as attendees, registrants, or in a more active capacity, amounted to 367. Twenty-four papers were selected for oral presentation. Numerous additional papers were submitted

which could not be presented because of the two-day time limitation. Eight inquiries were received from five foreign countries. Several representatives from abroad actually attended the Symposium.

The breadth of the organizations represented at the Symposium can be seen by reviewing the affiliations of the authors of the papers printed here. Twelve private companies presented papers and these may be further broadly classified in terms of their major products as aerospace, instrumentation, space communication, and research and development. In addition, papers were presented by representatives of three government agencies, two universities, and one foreign country. Incidentally, the demand for the Interim Proceedings greatly exceeded our expectations. Although 500 copies were printed, they were quickly distributed and many additional requests for copies had to be turned down until the printing of these final Proceedings

Readers of these Proceedings will be pleased to know that continuation of work leading toward the development of standards in this area has been insured by the organization within the IEEE of a subcommittee under Technical Committee Standards 14—Piezoelectric and Ferroelectric Crystals. The Technical Subcommittee, Standards 14.7—Frequency Stability will serve as a focal point for information in this field. The ultimate aim of the subcommittee will be an IEEE standard on the definition and measurement of both short-term and long-term frequency stability.

To this end, a special issue of the Proceedings of the IEEE devoted to the subject of frequency stability is scheduled for February 1966 to promote the further exchange of information. The members of Subcommittee 14.7 will serve as the editors of this special issue

It is the hope of the officers of this Symposium that the close cooperation of those working in this field will be extended in the same degree to the members of the Subcommittee as it was to us in the planning and execution of this Symposium. This will insure the development of useful and meaningful standards so much desired by us all.

It is a great pleasure to acknowledge the support and contributions of the officers, members of the Program Committee, chairmen of each session, panelists, authors, and the many others who helped behind the scenes and without whose cooperation these proceedings could not have been so complete.

A. R. CHI
Greenbelt, Maryland
May 1965

CONTENTS

IV: MEASUREMENT TECHNIQUES

APPENDIX A — ADDITIONAL PAPERS

APPENDIX B — LIST OF ATTENDEES

I. USERS' VIEWPOINT AND REQUIREMENTS

Call to Session	ANDREW R. CHI Chairman of Symposium, GSFC
Welcoming Remarks	HARRY J. GOETT Director, GSFC
Chairman	ROGER A. SYKES Bell Telephone Laboratories
Discussion Panel	ELIE J. BAGHDADY ADCOM, Inc. EDMUND J. HABIB GSFC DAVID B. LEESON Hughes Aircraft Company (now at Applied Technology, Inc.) GERALD M. HYDE Lincoln Laboratory, MIT

1. SHORT-TERM STABILITY FOR A DOPPLER RADAR: REQUIREMENTS, MEASUREMENTS, AND TECHNIQUES

D. B. LEESON AND G. F. JOHNSON

Hughes Aircraft Company
Culver City, California

Short-term frequency stability is an important parameter affecting resolution and range of a Doppler radar. This paper describes system and circuit requirements found in a typical airborne Doppler radar designed for operation in a severe vibration and acoustic environment. The characteristic of a Doppler radar which leads to short-term stability requirements is its use of a narrow-band receiver to detect a Doppler-shifted target return which is weaker than clutter.

The system short-term stability requirements are determined by the following two points:

1. Target return linewidth has a direct effect on sensitivity and velocity resolution; it determines the minimum useful Doppler filter bandwidth.
2. Transmitter and local oscillator noise sidebands appearing on clutter determine the maximum possible subclutter visibility.

Short-term stability for a Doppler radar is defined in terms of linewidth and spectrum. Oscillator and crystal requirements are derived from the system requirements. Measurements of linewidth and spectral purity under quiescent and environmental conditions are described, and vibration characteristics of quartz crystals are considered.

Modern airborne radar systems must provide ever-increasing detection ranges. In a typical long-range detection situation, the main lobe of the narrow-beam radar antenna illuminates both the target and the ground. Even by range-gating, an ordinary pulsed radar cannot discriminate between the target and ground clutter at the same range. Because of this, ground clutter is a severe limitation on a long-range airborne pulsed radar.

The radar return from a moving target is Doppler-shifted to a different frequency from that of the ground clutter. A Doppler radar overcomes the limitations of a pulsed radar by using this frequency difference to discriminate between target and clutter.

The resolution and range of a Doppler radar are dependent on linewidth and spectral purity, which are determined by short-term frequency stability. For this reason, short-term frequency stability is an important parameter in a Doppler system. The purpose of this paper is to outline the reasons for this dependence in a typical airborne Doppler radar and to touch on some specific requirements for short-term stability.

DOPPLER RADAR CHARACTERISTICS

A diagram of a typical long-range detection situation is shown in Figure 1–1. The return from the moving target is offset from the transmitter frequency f_0 because of Doppler shift.*
For a stationary radar, the ground clutter return and leakage appear at the transmitter frequency, as shown in Figure 1–2.

In an airborne radar the clutter spectrum becomes complex and consists of three major components:

1. *Altitude Return,* caused by direct reflection

*The doppler shift f_D is $2V/\lambda$, where V is the radial component of target velocity as seen by the radar and λ the transmitter wavelength.

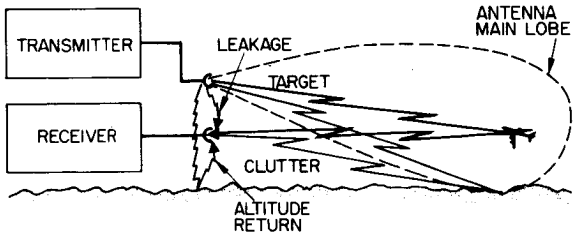

FIGURE 1–1.—Sources of clutter signals.

from the ground immediately below the aircraft. Since the aircraft velocity perpendicular to the ground is small, the altitude return is centered about the transmitter frequency.

2. *Main Lobe Clutter,* caused by the antenna main beam striking the ground. The main lobe clutter is Doppler-shifted because of the velocity of the aircraft relative to the ground.* Main lobe clutter is a particular problem in a long-range system because of the small angular separation between target and ground.

3. *Side Lobe Clutter,* caused by the side lobes of the antenna beam striking the ground. The side lobe clutter extends from the maximum positive to maximum negative Doppler frequency determined by the aircraft velocity.

A typical aircraft signal spectrum consisting of target, clutter, and leakage is shown in Figure 1–3. The spectrum at a missile receiver is different because of the relative velocity of the missile to the interceptor, but the same components are present.

The time-gating of the pulsed radar can be combined with the frequency discrimination of CW Doppler to reduce the effects of leakage. This leaves clutter as the principal interfering signal in a pulsed Doppler radar. Subclutter visibility is achieved by use of a narrow-band receiver at the target frequency. Even though the total clutter

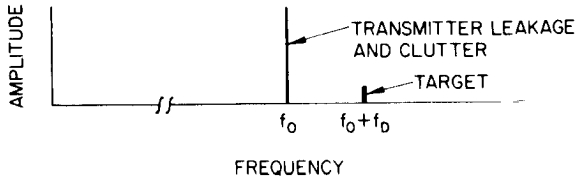

FIGURE 1–2.—Stationary clutter spectrum.

power far exceeds the total target return, the signal power density in the narrow receiver bandwidth can exceed the clutter and noise power density at the target Doppler frequency. The system requirements for short-term stability can be derived from the requirements for a narrow-band receiver and for subclutter visibility.

SYSTEM FREQUENCY STABILITY REQUIREMENTS

The system short-term stability requirements are determined by the following two points:

1. Target return linewidth has a direct effect on sensitivity and velocity resolution; it determines the minimum useful Doppler filter bandwidth.

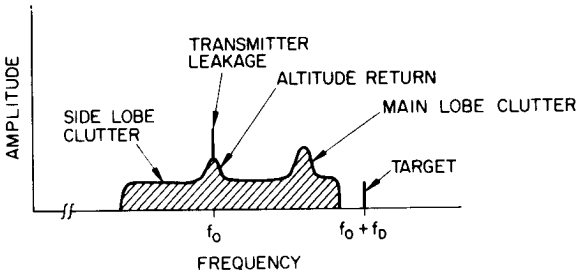

FIGURE 1–3.—Airborne clutter spectrum.

2. Transmitter and local oscillator noise sidebands appearing on clutter determine the maximum possible subclutter visibility.

Both of these statements refer to target and clutter as presented to the Doppler filter at IF. Correlation between the transmitter output and the receiver local oscillator can be obtained by synthesizing both from a common source. Use of correlation reduces frequency stability requirements, but the effect is only one of degree. The situation of an independent transmitter and receiver local oscillator will be considered here. In this case, the receiver local oscillator linewidth and noise sidebands are as important as those of the transmitter, because the local oscillator is mixed with the signal before filtering.

Consider first the linewidth requirement: In the situation of a filter excited by a narrow-band signal and broadband noise, narrowing the filter bandwidth increases its output signal-to-noise

ratio as long as the filter bandwidth exceeds the signal linewidth. Therefore, in the presence of broadband noise, receiver sensitivity—and hence range—improves as the receiver bandwidth is narrowed. This improvement continues until the receiver filter bandwidth matches the target linewidth. Target linewidth is dependent in part on transmitter and local oscillator linewidths. Thus, linewidth is a direct limit on sensitivity—a narrower linewidth makes possible an increase in radar range.

Further, in a Doppler radar the ability to discriminate between two targets of almost the same velocity is related to the Doppler filter bandwidth. Since velocity and frequency are proportional in a Doppler system, narrowing the Doppler filter provides increased velocity resolution. The limit on this improvement is again the target linewidth.

Thus, linewidth can be defined operationally as the narrowest filter bandwidth which will pass the major portion of the energy of the signal. Transmitter and local oscillator outputs of a Doppler radar are typically stable signals with incidental frequency modulation caused by noise. With the narrow signals required for a Doppler system, the major portion of the energy lies within the range of what is ordinarily called the peak-to-peak frequency deviation. Since the short-term frequency modulation is typically noiselike, extrapolation from an rms measurement is more rigorous.

Short term, as used here, refers to frequency variations which occur at a rate faster than the receiver can track. Typically, this rate corresponds to a modulating frequency smaller than the Doppler filter bandwidth and can be a few cycles per second or larger.

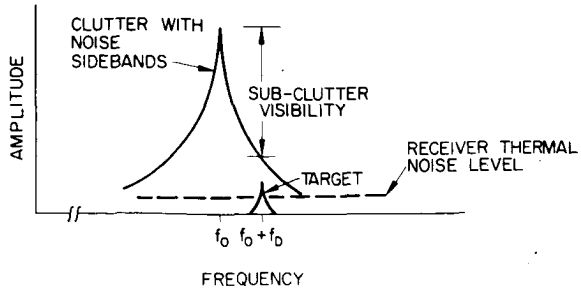

FIGURE 1–4.—Frequency relations for stationery radar with noise sidebands.

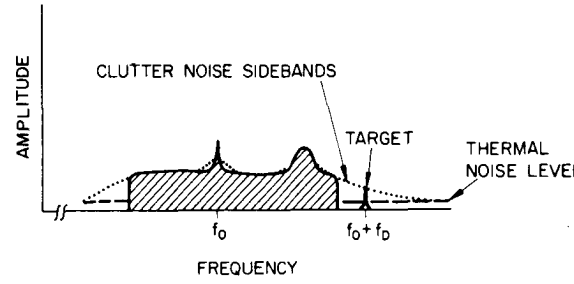

FIGURE 1–5.—Clutter spectrum with noise.

Other factors, such as target motion and target signal modulation due to antenna scanning, place a lower limit on the target linewidth which is independent of the transmitter and local oscillator linewidths. This lower limit with an X-band radar is in the range of 10 to 50 cps for typical airborne targets, and transmitter and receiver improvements below this level reach the point of diminishing returns.

The effect of noise sidebands on subclutter visibility can be seen even in the elementary case of a stationary radar. This example is used because of the simplicity of the clutter spectrum. Figure 1–4 shows the stationary radar spectrum of Figure 1–2 with noise sidebands added.

Subclutter visibility is limited by clutter noise sidebands at the Doppler frequency. Thus, the noise sidebands due to very short term frequency variations limit system sensitivity at Doppler frequencies for which clutter noise sidebands exceed the receiver thermal noise level.

Since narrow filtering of the target return cannot be accomplished ahead of the receiver mixer, the noise sidebands on the local oscillator have an effect similar to transmitter noise. The clutter and other large interfering signals are modulated by local oscillator noise, resulting in noise power at Doppler frequencies. Any requirements on the transmitter noise spectrum apply to the receiver local oscillator as well.

In actual systems the leakage and clutter spectra may be quite complex because of relative motion between transmitter, receiver, ground, and targets. However, the effects of FM noise sidebands are the same as in the simple example: Transmitter and local oscillator FM noise sidebands cause smearing of clutter energy to Doppler frequencies which would be clear if noise due to short-term frequency variations were not present.

The effect is shown in Figure 1–5, which is the clutter spectrum of Figure 1–3 with noise sidebands added.

Since the clutter spectrum with noise is the determining factor in subclutter visibility, short-term frequency stability requirements can be stated in terms of the transmitter and local oscillator power spectrum in the Doppler region. Typical noise spectral density requirements for an airborne Doppler radar are that FM noise sideband levels in 1 kc/sec bandwidth be more than 80 db below the main line power at modulation frequencies in the Doppler range.

Short-term stability in this connection refers to variations occurring at rates which result in energy in the frequency range of expected Doppler shifts. This range can extend from a few cps up to several hundred kc/sec.

OSCILLATOR REQUIREMENTS

The type of system under consideration here employs solid-state microwave sources for reasons of size, reliability, vibration insensitivity, and long-term frequency stability. The requirement for more than moderate frequency stability implies frequency multiplication from a lower frequency crystal oscillator. It has been found empirically that the oscillator is the major source of FM noise.

Oscillator instabilities are increased by the multiplication ratio; a factor of 100 is typical. Linewidth and modulation index increase directly with the multiplication ratio, and FM sideband power increases as the square of the ratio. A typical 10-gcps requirement of 100-cps linewidth and noise sidebands down 80 db in the Doppler region would require that a 100-Mc crystal oscillator have 1-cps linewidth and FM sidebands down 120 db. These stringent requirements also are placed on spurious outputs due to varactor multiplier instabilities. Modulation due to AM is ordinarily suppressed in multiplication, so the FM requirement predominates except in special systems such as a homodyne altimeter.

Short-term instabilities in the oscillator are related to the signal-to-noise ratio at the input of the oscillator amplifier. For modulation rates higher than the oscillator feedback loop bandwidth, an approximate calculation of signal-to-noise ratio can be made. If the signal level at the oscillator input is −10 dbm and the thermal noise level including a 4-db noise figure is −140 dbm/kc, the best expected signal-to-noise ratio is 130 db referred to 1 kc/sec bandwidth far from the center frequency. In practice, this limit is not achieved; and noise level increases rapidly as the carrier is approached. The role of drive level in determining signal-to-noise ratio is fairly clear; the highest drive level consistent with long-term stability requirements appears to give the best signal-to-noise ratio. The effect of noise enhancement by multiplication prompts the choice of a high oscillator frequency for a Doppler radar—this generally has been upheld in practice. Reduction of noise sidebands by narrow-band filtering is possible in a single-frequency application.

Since linewidth and low-lying sidebands are important to system operation, the effect of environment on these parameters is important. An airborne or missile-borne system must provide the required stability while experiencing high vibration and acoustic levels. Not merely the average frequency, but the detail spectrum and small frequency deviations at rates up to hundreds of kilocycles are important *during* environmental stress. A typical environment includes random vibration of 5 g's rms from 20 to 2000 cps and an overall sound pressure level of 130 db above 0.0002 dyne/cm^2 with energy up to 100 kc/sec.

QUARTZ CRYSTAL REQUIREMENTS

In a typical solid-state microwave source, the crystal is the element most sensitive to vibration. It has been found empirically that a standard wire-mount crystal will not provide the required linewidth and spectrum under a typical airborne vibration environment. The reason for this is the sensitivity of the resonator to vibration at the internal mount resonant frequencies.

Because of other system requirements, attempts to reduce vibration sensitivity must not degrade aging or temperature characteristics. This rules out presently available "ruggedized" or stiffly mounted crystals in the standard configuration. Aging or temperature performance of these devices is sacrificed to move the mount resonance above the critical vibration region of 20 to 2000 cps.

Attention has been turned to vibration iso-

TABLE 1–1

Crystal specifications

Crystal specification No. 1004	
1. Series resonant frequency	f_0=90 to 100 Mc/sec
2. Electrical capacity	C_0=3.5 pf±10%
3. Motional capacitance	$C_m=5\times10^{-4}$ pf±10%
4. Mode number	=5
5. Crystal cut	=AT
6. Series resistance	$R_s\leq80$ ohm
7. Frequency and series resistance of spurious responses.	−40 db R_s'/R_s within ±10 kc/sec, −20 db R_s'/R_s within ±50 kc/sec
8. Thermal time constant	$\tau_\theta\leq2$ min
9. Vibration sensitivity	$\Delta f/f_0\leq1.5\times10^{-8}$ peak deviation under stated vibration and shock environment
10. Thermal sensitivity	$\Delta f/f_0\leq\pm1\times10^{-6}$ for temperature range 79°±18°F
11. Aging	$\Delta f/f_0\leq\pm1\times10^{-6}$ per year after initial aging and with storage −65° to +165°F
12. Mount	Either 2- or 3-point ribbon mount with resonances of mount above 3 kc/sec
13. Case	TO–5 transistor case
14. Case seal	Cold-weld in vacuum, after complete cleaning and bake out. Seal will be leak tested.
15. Setting tolerances	$\pm5\times10^{-6}$ at 79°F

lation of standard crystal units. The improvement afforded by isolation is accompanied by an increase in the thermal time constant of the isolator-crystal system. This results in degraded altert times in systems requiring temperature stabilization before operating.

The use of a ribbon mount as developed by Bell Telephone Laboratories (BTL) appears to satisfy the requirement of a high-mount resonant frequency with no induced stress in the crystal blank. In theory, three short ideal ribbons will remove the 6 degrees of freedom of the blank without any redundancies. In practice, two-ribbon mounts also show promise. The BTL crystal employs three short ribbons which position the blank parallel to the base of a standard TO-5 can. The lowest resonant frequency of this assembly is well above 2000 cps.

Experience with this type of crystal at Hughes Aircraft Company shows a reduction of two orders of magnitude in vibration sensitivity compared with the standard wire mount. At the same time, aging characteristics are not degraded; and hard-mounting provides a satisfactory thermal time constant. Crystal specifications for a current system are shown in Table 1–1.

MEASUREMENTS AND TECHNIQUES

Short-term stability requirements for a Doppler radar have been defined in terms of linewidth and spectrum. These parameters are measured under both quiescent and vibration environments.

Typical measurement techniques and results are listed below:

1. The two-oscillator comparison method employs two similar microwave sources and a mixer to translate the combined microwave spectrum of both to a convenient frequency for measure-

X-BAND LINEWIDTH (2Δf)		
CRYSTAL TYPE	QUIESCENT	RANDOM VIBRATION, (5g's rms)
HC-18	50 cps	2400 cps
HC-18 WITH ISOLATOR	50 cps	300 cps
TO-5	50 cps	70 cps

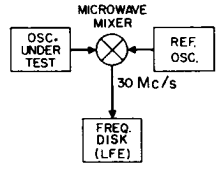

FIGURE 1–6.—Two-oscillator linewidth measurement.

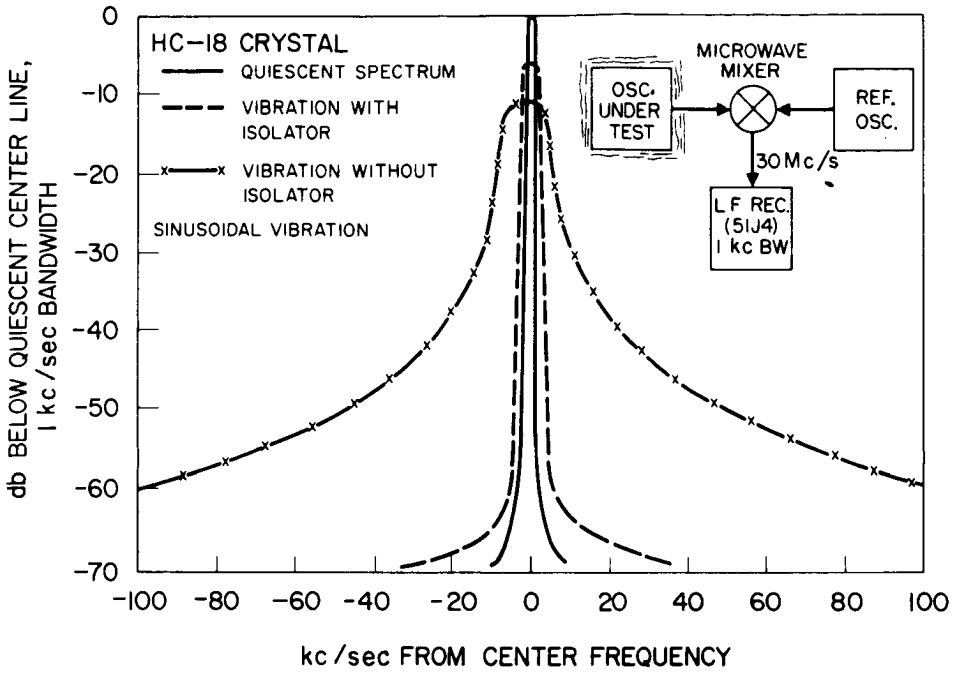

FIGURE 1–7.—Two-oscillator spectrum measurement.

ment. Vibration measurements are made by exposing one oscillator to vibration while isolating the other. Linewidth measurements have been made with a commercially available low frequency discriminator (Laboratory for Electronics Stalo Tester). A Collins 51J4 receiver or Hewlett-Packard HP-310A wave analyzer is used as a low-frequency narrow-band spectrum analyzer. Block diagrams and typical test results are shown in Figures 1–6 and 1–7.

2. A microwave frequency discriminator employing a transmission cavity is used for microwave spectrum measurements. This equipment gives the same spectrum information as the commercially available Allscott and Varian test sets without resorting to a critical carrier-nulling scheme. A particular advantage is that no reference oscillator is required in this system. The phase versus frequency characteristic of the microwave cavity is used to convert frequency variations to phase variaions. The phase detector compares cavity input and output phases to give a voltage proportional to frequency deviation. Typical data and a block diagram are shown in Figure 1–8.

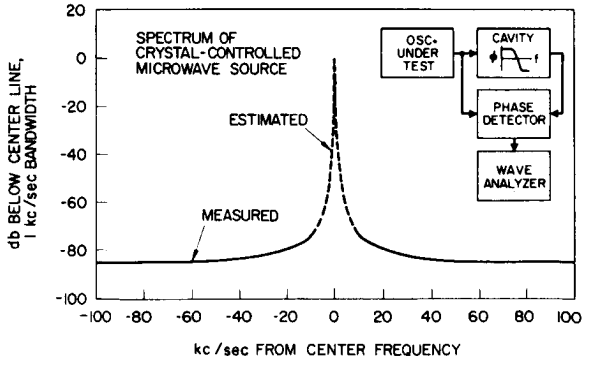

FIGURE 1–8.—Spectrum measurement with microwave bridge.

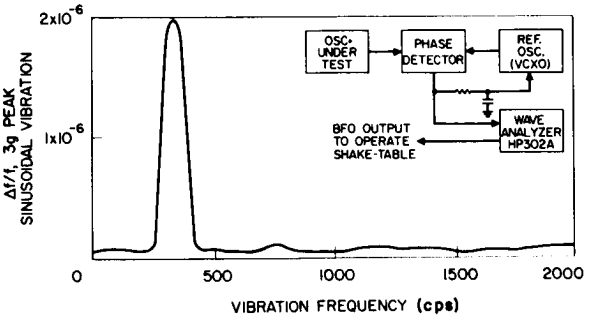

FIGURE 1–9.—Phase-locked discriminator measurement of crystal vibration sensitivity.

3. Measurements have been made at the oscillator frequency with a phase-locked discriminator. The test equipment consists of two similar oscillators phase-locked in a narrow-loop bandwidth. The phase detector output is a measure of phase deviations at rates higher than the loop bandwidth. This system has been used to obtain vibration information directly at the oscillator frequency without requiring the rest of the system. A block diagram and typical data appear in Figure 1–9.

Some techniques presently used to achieve short-term stability under environment have been derived from considerations reviewed in this paper. These are summarized here:

1. Use is made of the highest oscillator frequency and drive level consistent with other system requirements.

2. Foamed construction is used in all RF circuitry.

3. Crystal vibration isolators are necessary with present crystals; replacement with ribbon-mount TO–5 crystals is desirable.

CONCLUSION

Short-term frequency stability is a major problem in a Doppler radar. Because of their effect on range and resolution, linewidth and spectral purity are the parameters used to characterize short-term stability for a Doppler radar.

Measurements of linewidth and spectrum under quiescent and environmental conditions point to the need for increased understanding of oscillator short-term instabilities and for improved components such as the BTL TO-5 crystals.

Short-term frequency stability is one of the factors limiting the capabilities of present-day radars. This problem will become even more severe in the future as greater radar range and resolution are required.

ACKNOWLEDGMENT

The authors are pleased to acknowledge the contributions—direct and indirect—of G. O. D'Nelly, E. V. Phillips, and W. W. Maguire of Hughes Aircraft Company.

2. BASIC RELATION BETWEEN THE FREQUENCY STABILITY SPECIFICATION AND THE APPLICATION

J. D. HADAD

Raytheon Company
Bedford, Massachusetts

This paper classifies the requirements for short-term stability according to the application by examining applications ranging from velocity and acceleration measuring devices to coherent radars exposed to clutter.

FM noise is generated at substantially different levels in typical sources, and the effect of each is different as it affects performance and influences equipment design. FM noise is considered with respect to either the requirement or the accuracy of a measurement.

A stable reference signal is essential to the satisfactory operation of any coherent radar system. An unknown shift in phase of the signal from the reference oscillator during the interval between transmission of the radar signal and the reception of the return signal will produce an erroneous output and can lead to a degradation of the radar system performance. Any time-varying phase shifts in other parts of the system whose value during the same interval can be detected will produce a similar effect.

In designing a coherent system for a particular application, it is necessary to specify the stability that is required for satisfactory operation. This is often done for short-term stability by specifying the allowable modulation on the signal entering the predetection filters of the receiver. For frequency modulation (FM), this is specified in terms of allowable deviation ratio. Long-time stability is often specified by maximum permissible frequency drift rate, assuming this rate to be constant over the pertinent time interval. In this paper the short-time stability is of basic interest, while long-time stability is not significant as long as the drift can be controlled for proper operation of the radar. An attempt is made herein to present a review of the frequency stability requirements for coherent radars. The areas stressed are those which experience has shown to be the most important from a system design point of view.

The stability of a coherent system can be classified into four broad groups of application, which are:

1. Velocity measurement.
2. Acceleration measurement.
3. Fixed target and clutter suppression.
4. Airborne navigation.

VELOCITY MEASUREMENT

Applications such as radar guidance of ballistic missiles or precision trajectory measuring systems require three or more radars to measure with precision the velocity of a body, whereas applications such as airborne target tracking require the use of only a single radar. However, accuracies and frequency stabilities are usually imposed for each radar, thus making it possible to present a generalized coherent radar equipment specification.

Consider a hypothetical ICBM radar guidance system: The radar system for guidance uses a beacon in the rocket, a ground computer, and a radar command link to the vehicle. An achievable accuracy of 600 feet is desired for a 5500-nautical mile flight. Reference 1 shows that the velocity

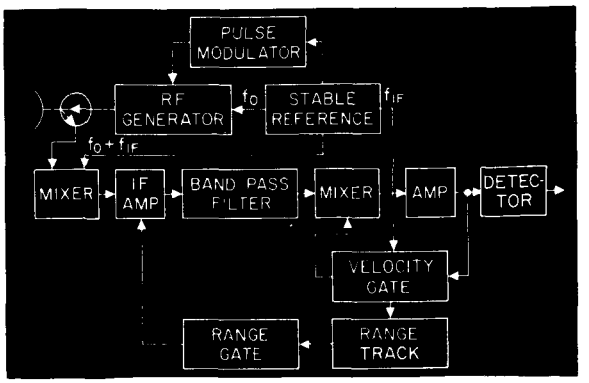

FIGURE 2-1.—Typical pulse Doppler radar.

must be known to within 0.1 ft/sec. Thus, a reasonable velocity specification for the radar equipment is 0.05 ft/sec. Assume that the rocket is traveling 30,000 ft/sec and accelerating 600 ft/sec^2, and that the measurement is performed at 600 nautical miles. The specification for the short-term stability for the transmitter and critical components in a pulse Doppler and a CW Doppler X-band radar is desired.

Similarities between a pulse Doppler (PD) radar and a CW Doppler radar are shown in Figures 2-1 and 2-2. The PD radar has a bandpass filter to extract the maximum amplitude spectrum line of a pulsed waveform. The requirement for the velocity gate is to measure velocity to an accuracy of 0.05 ft/sec, which is an equivalent Doppler frequency error of 1 cps at X-band. The bandwidth of the velocity gate is kept to a minimum consistent with the Doppler tracking changes. These changes are due to a rocket acceleration of 600 ft/sec^2, or 12 kc/sec^2. Thus, with a velocity gate tracking loop gain of 1000, the

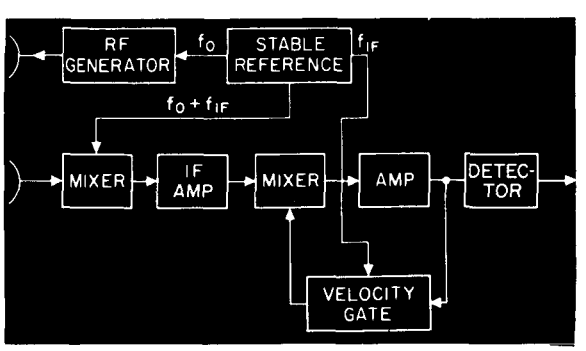

FIGURE 2-2.—Typical CW Doppler radar.

frequency tracking lag error is approximately 12 cps. This imposes a minimum predetection bandwidth B requirement on the velocity gate and the system of 24 cps. Reference 2 shows that the instantaneous 1-sigma frequency perturbation for a signal in noise in a band-limited third-order filter is obtained from Equation 1:

$$(\Delta f)_{rms} = (\pi/24)^{1/2}[B/(S/N)_v]. \quad (1)$$

The rms frequency perturbation over an observation time T, with BT independent samples, is determined by Equation 2:

$$\sigma_f \cong (\Delta f)_{rms}/(BT)^{1/2}$$

$$= [(\pi/24)(B/T)]^{1/2}(S/N)_v^{-1}. \quad (2)$$

Thus, for a 0.5-second observation time and a 68-percent probability that the observed frequency perturbation is less than 1 cps, a signal-to-noise ratio of 2.8—or 9 db—is required, thus resulting in an instantaneous frequency perturbation due to noise of 4.0 cps in a 24-cps band. The transmitter frequency stability should be 10 times better than this to prevent further velocity errors; therefore a frequency deviation of 0.40 cps in a 24-cps band will be required. Expressed in a standard 1-kc bandwidth, the maximum frequency deviation on the transmitter is 3 cps/kc.

The effects of direct leakage from the transmitter to the receiver can degrade system sensitivity, which in turn will increase the velocity error. The PD radar can range-gate out this leakage; however, a CW radar cannot and must therefore tolerate this leakage. Appendix A shows that the allowable frequency deviation of the transmitter can be expressed by Equation A13:

$$(\Delta f)_{rms} \leq (10^{-11}/\pi\tau)(NFB/P_G)^{1/2}. \quad (A13)$$

Consider a feedthrough power of 0.5 microwatt, which corresponds to 80-db isolation from a 50-watt transmitter. Also consider a double sideband receiver with a 10-db noise figure and a 0.15-μsec time delay in the leakage signal relative to reference. The transmitter frequency deviation must be less than 0.62 cps in a 24-cps band, or 4.0 cps/kc. Thus, the direct leakage or carrier feedthrough for the CW case has negligible effects on the accuracy of measurement.

ACCELERATION MEASUREMENT

Acceleration or deceleration can be determined by measuring the phase between the return signal and the master oscillator of the radar. The equations for making phase measurements at three equally spaced time intervals T_v are shown in Equation 3:

$$2\pi n_1+\phi_1-\phi_0=(4\pi/\lambda)v_0T_v+(2\pi/\lambda)aT_v^2,$$
$$2\pi n_2+\phi_2-\phi_0=(4\pi/\lambda)v_0T_v+(2\pi/\lambda)aT_v^2,$$
$$2\pi n_2+\phi_3-\phi_0=(4\pi/\lambda)v_0T_v+(2\pi/\lambda)aT_v^2. \quad (3)$$

Solving for acceleration and assuming the phase ambiguities are resolved, the error in measuring acceleration as a result of the phase measurement error is determined by Equation 4:

$$(\Delta a)_{rms}=(6^{1/2})\lambda(\Delta\phi)_{rms}/4\pi T_v^2. \quad (4)$$

In the radar, the phase error can be traced to three main causes: signal-to-noise limitations $(\Delta\phi_n)_{rms}$, radar phase modulation $(\Delta\phi_r)_{rms}$, and data handling errors $(\Delta\phi_d)_{rms}$. The equation relating the three errors is shown in Equation 5:

$$(\Delta\phi)_{rms}=[(\Delta\phi_n)_{rms}^2+(\Delta\phi_r)_{rms}^2+(\Delta\phi_d)_{rms}^2]^{1/2}. \quad (5)$$

The data handling error $(\Delta\phi_d)_{rms}$ is primarily a phase shift measurement error. For a digital phase shifter consisting of six phase shifting elements arranged in steps of $(2)^n$, a quantization level of 64 in a total phase shift range of 360 degrees is 5.62 degrees per step. The data handling rms error is determined by Equation 6:

$$(\Delta\phi_d)_{rms}=\epsilon/(12^{1/2})=5.62/(12^{1/2})=1.62 \text{ degrees}. \quad (6)$$

The signal-to-noise error $(\Delta\phi_n)_{rms}$ is determined from Equation 7 by integration of Equation 2. For this application the sampling time interval T_v is related to the noise bandwidth by $1/2B$.

$$(\Delta\phi_n)_{rms}=(\pi/24)^{1/2}(S/N)_v^{-1}. \quad (7)$$

A signal-to-noise ratio of 10 will introduce a phase error of 2.1 degrees rms.

The radar phase modulation $(\Delta\phi_r)_{rms}$ is determined by referring to Equations A7 and A17. The phase modulation error due to the frequency modulation of the transmitter is determined by Equation 8:

$$(\Delta\phi_r)_{rms}=2[(\Delta f)_{rms}/F_m]=2(P_{DS}/P_c)^{1/2}. \quad (8)$$

Thus, a measure of the double sideband power to the carrier power will give a direct indication of phase error. A 1-degree rms phase error will require a P_{DS}/P_c of -41.5 db. The frequency stability requirement of the transmitter at the lower end of the band, or 1 kc, is 8.25 cps in a $1/2T_v$ bandwidth.

Consider a hypothetical C-band coherent pulsed radar with the requirements of measuring deceleration from three pulses at a pulse repetition rate of 100 pps. Applying Equations 4 and 5, and assuming the previously stated phase errors, the resulting acceleration error is 22.4 ft/sec^2.

FIXED TARGET AND CLUTTER REJECTION

The first two sections of this paper considered applications with respect to receiver noise. This section will consider the requirements imposed on the frequency stability of the transmitter due to the presence of clutter and fixed target returns. The design objective is to maintain this clutter or fixed target-induced spectral noise in a desired band below receiver noise. Broadly, three conditions must be taken into account:

1. The clutter fluctuations have negligible energy at the target Doppler frequencies.
2. The clutter rejection filter and the target Doppler filter must reject the clutter frequencies.
3. Any fluctuations in the signal energy reflected from the clutter or from a fixed target, as a result of fluctuations in the transmitted signal, will appear as noise and must be kept at a minimum in the desired band.

The noise problem in a coherent Doppler system is best illustrated in terms of a hypothetical system. Consider the detection of a moving vessel at sea in the presence of 77-db clutter return above minimum detectable signal, which is 13 db above receiver noise. For clutter to have a negligible effect in the Doppler band, a 100-db reduction is needed. This actually results in clutter being 10 db below receiver noise.

Considering the *first* condition, the clutter frequency spectrum, Reference 3 shows that a Doppler return from sea clutter at X-band might

reasonably be assumed to be Gaussian, with a half-power point at 60 cycles. If the distribution is normal, the power density will be down 100 db (10^{-10}) at 5.8 times the half-power point, or at about 350 cycles. This would tend to indicate that the "tails" of the clutter spectrum at target Doppler frequencies would be entirely negligible.

With regard to the *second* condition, performance of clutter rejection filters, clutter rejection of 100 db using clutter notched filters and Doppler frequency filters is considered entirely feasible.

With regard to the third condition, the frequency modulation of the transmitted signal, a signal reflected from a fixed target appears as noise in the target Doppler band. This fluctuation will produce noise sidebands around the central line. Consider a 1- to 67-kc Doppler band for a CW radar, or the same band for a pulse radar limited to a pulse recurrence frequency of 67 kc. If the noise is uniformly distributed, then the noise in any 1-kc band will be 1/67 the total noise, or 18.3 db down. Thus, for a suppression of 100 db with respect to the power in the transmitted signal, the noise will be required to be 81.7 db below the carrier (clutter noise being negligible). Thus, from Equation 8, the deviation at the lower end of the band (1 kc) is 0.1 cps/kc. Note that this is at present a stringent requirement on the transmitter. This limitation applies to the master oscillator and to the power amplifier for either a CW or pulsed Doppler radar.

The limiting condition imposed on the frequency stability of the transmitter by a fixed target is an infinite plane perpendicular to the radar. Assume all the energy falling on the plane is reradiated isotropically. Radar Equation 9 is for this type of situation:

$$P_G = \bar{P}_t \lambda_0^2 G_0 / 8\pi^2 R^2, \qquad (9)$$

where G_0 is the gain of the smaller antenna. Combining Equations A13 and 9, and substituting the relation $\tau = 2R/c$, the frequency stability requirement for the transmitter is given by Equation 10:

$$(\Delta f)_{rms} \leq 10^{-11} f_0 (NFB/P_t G_0)^{1/2}. \qquad (10)$$

Substituting the parameters from the velocity measurement radars and assuming an antenna gain G_0 of 32 db, the allowable frequency deviation is 0.005 cps in a 24-cps band, or 0.03 cps/kc.

Note that this stringent requirement on the transmitter can be accomplished by an actively degenerated klystron.

AIRBORNE NAVIGATION

In the previous sections the coherent radar was required to operate in the presence of ground or sea clutter without system degradation. An equally important group of radar systems depends on ground and sea returns for intelligence. An application of this type of radar is a Doppler airborne navigation which is designed to measure an airborne vehicle's velocity with respect to the earth. An application would be the use of a Doppler radar for terminal phase guidance and attitude control of a lunar-landing vehicle.

Consider a coherent radar to control the touchdown velocity for a lunar landing. Assume an X-band Doppler navigator with three 7.5-degree antenna beams inclined at 45 degrees. A tracking time constant of 0.5 sec is desired for a velocity spectrum of 3000 to 25 ft/sec. From Equation B14 (Appendix B) the velocity error is 1.0 ft/sec for a touchdown velocity of 25 ft/sec:

$$\sigma_{V_R} = (1.08/\cos\gamma)\,(\lambda\beta V_R \sin\gamma/T)^{1/2}. \qquad \text{(B14)}$$

The effective bandwidth of 70 cps is obtained from Equation 11:

$$\sigma_{\omega_n} = \{(\pi/2T_g)[(24\pi^2\beta/\lambda)\,V_R \sin\gamma]\}^{1/2}. \qquad (11)$$

Thus, to have a negligible effect on the system performance, the transmitter frequency stability should be less than one-tenth of the Doppler error as determined from Equation 12, or 1.4 cps.

$$\Delta f \leq 0.1[2\sigma_{V_R} \cos\gamma/\lambda]. \qquad (12)$$

Based on the lower end of the Doppler spectrum of 350 cps, the requirement on the frequency stability of the transmitter is expressed as 11.7 cps in a 1-cps bandwidth centered at 350 cps. This requirement cannot be expressed by the standard 1-kc bandwidth expression.

In an airborne operation of a coherent system, the following additional limitations must be taken into account: (1) ripple resulting from size and weight limitations on the high power supply, (2) microphonics resulting from the moving platform, and (3) radome reflections resulting from the relative motion of the antenna and the reflecting surface of the radome. Appendix A treats these conditions by a composite frequency deviation determined from Equation A18.

TABLE 2–1

Summary of Measurement

Systems	Requirements	Maximum allowable deviations
Radar guidance of ballistic missiles	0.05 ft/sec accuracy	3 cps/kc.
Precision trajectory measurements	0.05 ft/sec accuracy	3 cps/kc.
Acceleration or deceleration of bodies	0.75 g accuracy	36 cps/kc.
Phase measurements	1° accuracy	36 cps/kc.
Targets in sea clutter	−100 db rejection	0.1 cps/kc.
Fixed targets	Infinite plane	0.03 cps/kc.
Direct leakage or feedthrough	0.5 μ watt feedthrough	4.0 cps/kc.
Lunar—landing vehicle	4% at 25 ft/sec	11.7 cps in a 1-cps band.

CONCLUSION

Table 2–1 summarizes the applications and the related frequency stability of the transmitter. The applications presented cover the majority of the cases for coherent systems. The method, analyses, and equations presented were varied intentionally so that a systems engineer can handle other related system applications for coherent systems.

REFERENCES

1. BUCKHEIM, R., "Space Hand Book," Random House.
2. BENDAT, J., "Principles and Applications of Random Noise Theory," J. Wiley and Sons.
3. KERR, "Propagation of Short Wave Radio Waves," Radiation Lab. Series.
4. HALL, W. M., "Noise in Pulse Doppler Systems," April 1964 (Raytheon Company).
5. LAWSON, J. L., and UHLENBECK, G., "Threshold Signals," Radiation Lab. Series.

GLOSSARY OF TERMS

a	acceleration of a target
Δ_a	acceleration error
B	effective receiver bandwidth
c	velocity of electromagnetic radiation
E_g	peak voltage from a target
E_r	peak reference voltage
E_t	peak transmitted voltage
e_g	instantaneous voltage from a target
e_o	output from phase detector
e_r	instantaneous reference voltage
e_t	instantaneous transmitted voltage
F_{d_n}	Doppler frequency
F_m	modulation frequency
ΔF_{d_n}	Doppler spectrum width
f_0	unmodulated transmitted frequency
Δf	peak frequency deviation
G_0	antenna gain of the smaller antenna
$G_{\omega_n}(0)$	power spectral density at $\omega=0$
m_r	effective receiver modulation index
m_t	transmitter modulation index
n_1, n_2, n_3	number of full wavelengths between target and measuring radar at time the three phase measurements are made
NF	receiver noise figure
$N(t)$	amplitude of narrow-band noise
P_c	carrier power
P_{DS}	double sideband power
P_G	transmitter power at receiver input terminal due to ground return
P_{nfm}	FM noise power at receiver input
$\bar{P}_t$	transmitter average power
R	range of target
T	absolute temperature (290°K)
T_g	frequency tracker equivalent time constant
T_v	time between the two phase measurements
V_P, V_Y, V_R	velocity components in pitch, yaw, and roll
v	velocity of moving target
$X(t), Y(t)$	independent Gaussian random functions
β	antenna beamwidth
γ	antenna beam inclined angle
ϵ	phase measurement error
θ	phase angle between two signals
λ	wavelength
τ_g	time delay of target signal

τ_r	time delay of reference signal	ϕ_1, ϕ_2, ϕ_3	three phase measurements taken less than 2
σ_{V_R}	fluctuations in components along the vehicle's roll axis	$\Delta\phi$	peak phase modulation error
σ_{ω_n}	rms output of frequency tracker	$\omega_n(t)$	output of frequency discriminator

APPENDIX A—COHERENT RADAR STABILITY REQUIREMENTS

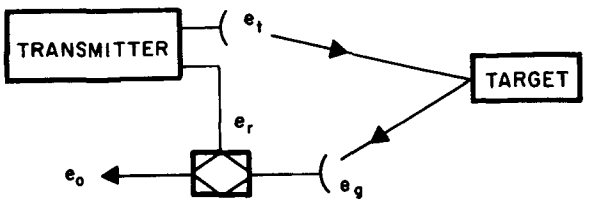

FIGURE 2-A1.

Consider a continuous wave (CW) radar that is frequency-modulated with a sine wave function. The voltage from the transmitter is given by

$$e_t = E_t \sin[2\pi f_0 t + (\Delta f/F_m) \sin 2\pi F_m t]. \quad \text{(A1)}$$

At the receiver two signals are processed. One is the reference voltage

$$e_r = E_r \sin[2\pi f_0(t-\tau_r) - (\Delta f/F_m) \sin 2\pi F_m(t-\tau_r)], \quad \text{(A2)}$$

and the other a returned signal from an object

$$e_g = E_g \sin[2\pi f_0(t-\tau_g(t)) + (\Delta f/F_m)(t-\tau_g(t))]. \quad \text{(A3)}$$

To insure linear application of a phase detector in a radar, the reference voltage is made much larger than the target return voltage. For convenience, we shall assume the phase detector to be of the balance type,

$$e_o = E_g \cos\theta. \quad \text{(A4)}$$

The phase angle θ between the two waves is

$$\theta = [2\pi f_0(t-\tau_r) + (\Delta f/F_m) \sin 2\pi F_m(t-\tau_r)] - \{2\pi f_0[t-\tau_g(t)] + (\Delta f/F_m) \sin 2\pi F_m[t-\tau_g(t)]\}. \quad \text{(A5)}$$

The output voltages from a linear detector is

$$e_o = E_g \cos\left[2\pi f_0[\tau_r - \tau_g(t)] + 2\pi\Delta f[\tau_r - \tau_g(t)] \frac{\sin\pi F_m[\tau_r-\tau_g(t)]}{\pi F_m[\tau_r-\tau_g(t)]} \times \cos 2\pi F_m \tfrac{1}{2}[t-\tau_r+\tau_g(t)]\right]. \quad \text{(A6)}$$

Equation A6 can be simplified by assuming the frequency deviation of the oscillators to be small. Thus, $2\pi\Delta f[\tau_r-\tau_g(t)] \ll 1$ and, by proper trigonometric manipulations,

$$e_o = E_g\Big[\underbrace{\cos 2\pi f_0[\tau_r-\tau_g(t)]}_{\text{DC TERM}} \underbrace{-2\pi\Delta f[\tau_r-\tau_g(t)]}_{\text{Amplitude Term}} \underbrace{\frac{\sin\pi F_m[\tau_r-\tau_g(t)]}{\pi F_m[\tau_r-\tau_g(t)]}}_{\text{Long-Range Term}} \underbrace{\sin 2\pi f_0[\tau_r-\tau_g(t)]}_{\text{Phase Term}} \underbrace{\cos 2\pi F_m\{t-\tfrac{1}{2}[\tau_r+\tau_g(t)]\}}_{\text{Modulation Rate Term}}\Big]. \quad \text{(A7)}$$

$$\underbrace{\qquad\qquad\qquad\qquad\qquad\qquad\qquad\qquad\qquad\qquad}_{\text{AC TERM}}$$

Considering only the ac term, the dc can be removed with a condenser. The equivalent power reference to the input terminal of the receiver is

$$P_{nfm} = P_G(2\pi\Delta f\tau)^2\left(\frac{\sin\pi F_m\tau}{\pi F_m\tau}\right)^2 (\sin 2\pi f_0\tau)^2, \quad \text{(A8)}$$

$$\tau = \tau_r - \tau_g(t). \quad \text{(A9)}$$

The maximum noise power will occur when τ is such that $\sin 2\pi f_0\tau = 1$. At these points,

$$P_{nfm} = P_G(2\pi\Delta f\tau)^2 (\sin\pi F_m\tau/\pi F_m\tau)^2. \quad \text{(A10)}$$

In order to maintain this noise power below the receiver noise power;

$$P_{nfm}(max) = P_G(2\pi\Delta f\tau)^2 \times (\sin\pi F_m\tau/\pi F_m\tau)^2 \leq NFKTB\,\tfrac{1}{10}. \quad \text{(A11)}$$

Thus, the allowable oscillator frequency deviation becomes

$$(\Delta f)_{rms} \leq (10^{-11}/\pi\tau)\,(NFB/P_G)^{1/2} \times (\pi F_m \tau/\sin\pi F_m \tau). \quad \text{(A12)}$$

For short time delays compared with a modulation cycle, $\tau \ll 1/F_m$, Equation A2 reduces to an expression for short ranges to

$$(\Delta f)_{rms} \leq (10^{-11}/\pi\tau)\,(NFB/P_G)^{1/2}. \quad \text{(A13)}$$

An examination of Equation A13 reveals that a coherent radar only becomes sensitive to angular modulation of the carrier by the mechanisms of time-delay correlation. This fact is useful in reducing the effects of carrier feedthrough and local oscillator stability on system sensitivity.

It is convenient to consider the stability requirements also in terms of sideband-to-carrier power levels. For a small modulation index m, the ratio of the double sideband power to the carrier power is

$$P_{DS}/P_c = 2(m_r/2)^2. \quad \text{(A14)}$$

The process of coherent detection of a time-delayed signal alters the angular modulation index as shown by Equation A6.

$$m_r = 2m_t \sin\pi F_m \tau, \quad \text{(A15)}$$

where

$$m_t = \Delta f/F_m. \quad \text{(A16)}$$

For long time delays, the two indices are on the average equal. This being the worst case,

$$P_{DS}/P_c = (\Delta f_{rms}/F_m)^2 \quad \text{(A17)}$$

or

$$\Delta f_{rms} = F_m (P_{DS}/P_c)^{1/2}. \quad \text{(A17a)}$$

The frequency spectrum of an oscillator is not limited to only one modulating frequency but can have a number of unwanted coherent FM modulations (HVPS ripple, microphonic, etc.). The composite deviation in a given bandwidth is the rms of the individual deviation-rate products.

$$\Delta f_{rms} = \sqrt{2}\pi\tau[(\Delta f_1 F_{m_1})^2 + (\Delta f_2 F_{m_2})^2 \cdots (\Delta f_n F_{m_n})^2]. \quad \text{(A18)}$$

The unwanted noncoherent FM modulation (noise) is usually expressed by an rms noise power in any bandwidth of interest, usually 1 kc/sec, in a noise spectrum removed from the carrier by 1 kc/sec or more. For example, suppose the FM noise power in a 1 kc/sec bandwidth centered at 10 kc/sec from the carrier is 80 db below the carrier power:

$$\Delta f_{rms} = F_m (P_{DS}/P_c)^{1/2} = 10^4 (10^{-8})^{1/2} = 1.0 \text{ cps}.$$

Thus, the 1.0-cps rms FM noise is the same as the power in the first-order sidebands which would be generated by intentionally modulating the carrier at a frequency F_m of 10 kc/sec to a rms deviation of 1.0 cps.

APPENDIX B—DOPPLER NAVIGATION

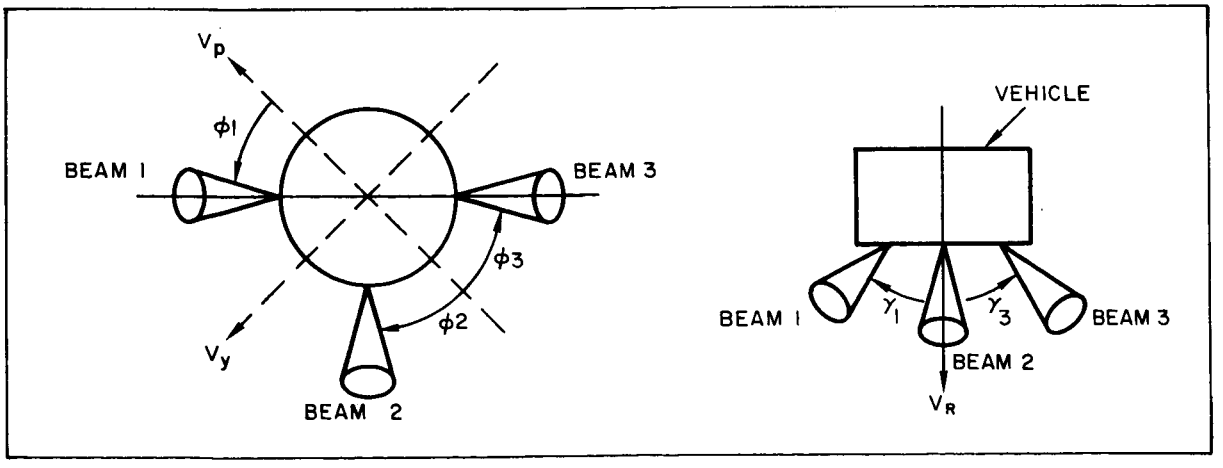

FIGURE 2-B1.—A basic Doppler configuration.

A basic Doppler configuration is shown in Figure 2-B1. The analysis, based on a 3-beam "T" configuration, is valid for essentially all types of Doppler navigators. To simplify the analysis,

assume the pitch and yaw velocities are zero:

$$V_P = V_Y = 0; \tag{B1}$$

also,

$$\gamma_1 = \gamma_2 = \gamma_3 = \gamma. \tag{B2}$$

The Doppler frequencies of the signals received are given by:

$$F_{d_n} = (2V_R/\gamma)\ \cos\gamma. \tag{B3}$$

Because of the finite width of each beam, the Doppler frequencies will be spread over a spectrum whose width is a function of the width of the beam β. This Doppler spectrum width received by each receiver is:

$$\Delta F_{d_n} = (2\beta/\lambda)\, V_R \sin\gamma. \tag{B4}$$

To determine velocity from a Doppler radar, it is necessary to determine the center frequency of the radar return signal by means of a frequency tracker. For the purposes of simplifying the analysis, it is assumed that the radar return signal can be represented by narrow-banded noise whose amplitude $N(t)$ is given by

$$N(t) = X(t)\ \cos\omega_c t + Y(t)\ \sin\omega_c t, \tag{B5}$$

where ω_c represents the carrier frequency. The quantities $X(t)$ and $Y(t)$ are independent Gaussian random functions. A more useful form of Equation B5 is:

$$N(t) = R(t)\ \cos[\omega_c t - \tan^{-1}(Y/X)], \tag{B6}$$

where $R = (X^2 + Y^2)^{1/2}$. It will be assumed that B6 is amplitude-limited and then passed through an FM discriminator. The output of the discriminator is given by

$$\begin{aligned}\omega_n(t) &= (d/dt)\ [\tan^{-1}(Y/X)] \\ &= (Y\dot{X} - X\dot{Y})/(X^2 + Y^2),\end{aligned} \tag{B7}$$

where $\omega_n(t)$ represents the instantaneous Doppler frequency shift relative to the carrier ω_c. The power spectral density for a narrow-band rectangular-shaped spectrum of width B, corresponding to an ω of zero, is obtained from Reference 5 to be:

$$G_{\omega_n}(0) = 12B. \tag{B8}$$

Assume that the frequency tracker can be represented dynamically by a first-order filter having the transfer function $(1 + j\omega T_g)^{-1}$. Under realistic conditions, the bandwidth of the frequency tracker will be much narrower than the bandwidth of the instantaneous Doppler frequency shift ω_n. Accordingly, it is reasonable to determine the rms output of the frequency tracker from the zero-frequency value of $G_{\omega_n}(\omega)$ by the following relation:

$$\sigma_{\omega_n}^2 = \int_0^\infty G_{\omega_n}(0)[d\omega/(T_g^2\omega^2 + 1)], \tag{B9}$$

$$\sigma_{\omega_n} = [(\pi/2T_g) G_{\omega_n}(0)]^{1/2}. \tag{B10}$$

To obtain the component of velocity along the vehicle's roll axis V_R, it is necessary to add the signals from beams (1) and (3). Thus, from Equation B3

$$V_R = (\lambda/4\ \cos\gamma)\,(F_{d_1} + F_{d_3}). \tag{B11}$$

The fluctuation in the components of velocity along the vehicle's roll axis is therefore

$$\begin{aligned}\sigma_{V_R} &= (\lambda/4\ \cos\gamma)\,(1/2\pi) \\ &\quad \times \{(\pi/2T_g)[G_{\omega_{n_1}}(0) + G_{\omega_{n_3}}(0)]\}^{1/2}.\end{aligned} \tag{B12}$$

Relation $G_{\omega_n}(0)$ to the physical parameters of the radar can be obtained by combining Equations B8 and B4 as follows:

$$G_{\omega_n}(0) = (12)\,(2\pi)\,(\tfrac{1}{2}\pi)\,(2\beta/\lambda)\ |\ V_R \sin\gamma\ |, \tag{B13}$$

where β represents the width of the individual radar beam. The factor (2π) is used to convert $G_{\omega_n}(0)$ from cycles/sec to radians/sec. The $\frac{1}{2}\pi$ is to approximate a conversion from an assumed rectangular-shaped input spectrum to a more realistic Gaussian shape spectrum. Thus,

$$\sigma_{V_R} = (1.08/\cos\gamma)\,(\lambda\beta V_R \sin\gamma/T_g)^{1/2}. \tag{B14}$$

3. MASTER OSCILLATOR REQUIREMENTS FOR COHERENT RADAR SETS

L. P. GOETZ AND W. A. SKILLMAN

Defense Center
Westinghouse Electric Corporation
Baltimore, Maryland

Stability requirements for pulse Doppler MTI radars which operate in a severe clutter environment are derived on the basis of required performance. Performance factors considered are spurious generation, signal loss, ranging, and lobing noise. Requirements are shown to be different for common modulation, where the range time delay modifies phase relations, and for independent modulation, where no delay is involved. A stability requirement given in parts per million is seen to be inadequate; rather, a more complex "deviation spectrum" is required. A typical state-of-the-art radar is postulated, and its requirements are calculated.

This paper discusses the master oscillator requirements for coherent radar sets. Coherent radars are most widely used where the Doppler information is to be extracted from a return radar signal. One application of Doppler radar (commonly called *moving target indicator*, or MTI) is to separate the moving target from the ground, sea, and cloud clutter which may appear at the same range as the target but produces a different Doppler shift on the return radar signal. A second application (called *synthetic aperture radar*) is the use of the Doppler history of ground targets as seen from a moving platform to sharpen synthetically the radar display in azimuth. In addition, the "chirp" technique can be used to obtain large average transmitter power with a peak-power-limited device and at the same time maintain an effective short pulse for range resolution. Chirp techniques can be used in combination with Doppler techniques.

Doppler radars require extremely high short-term stability; in some applications, the incidental modulation sidebands on the carrier must be limited to values of the order of 100 decibels below the carrier level. On the other hand, the long-term frequency stability may be quite poor when compared with other applications, such as broadcast stations which must maintain their assigned frequency within 20 cps, and reference clocks, where the long-term "average" is important.

In this paper the master oscillator stability requirements will be discussed for MTI Doppler radars. Examination of these requirements will show that a single number (such as a specification of parts per million) is not adequate to specify clearly the requirements for Doppler radars.

TYPES OF DOPPLER RADAR

The Doppler phenomenon, the change in frequency of a traveling wave introduced when there is a relative velocity difference between the transmitter and the point of observation (see Reference 1) is used in many types of radar. This paper discusses the use of the Doppler effect to separate targets from large unwanted signals, such as ground clutter, using the difference in frequency associated with the velocity between the unwanted and wanted signals for separation by means of frequency filtering.

There are many mechanizations which can be used in Doppler radar. In this paper, they are divided into two types:

1. Radars which detect the Doppler shift unambiguously.
2. Low prf (pulse recurrence frequency) radars

which receive ambiguous Doppler information.

Examples of the first type are CW (continuous wave) and high prf PD (pulse Doppler) radars. The stability requirements of the two are identical, ignoring the leak through problem. The low prf radar category can be further divided into three types:

1. MTI (moving target indicator) and AMTI (airborne MTI).
2. Coherent Doppler radars.
3. Noncoherent Doppler radars.

To detect Doppler shift, the phase and/or frequency of the transmitted signal must be retained for reference during the receive time. In MTI and coherent types of radar this may be done by locked local oscillator techniques. MTI radars use a delay line equal to the interpulse (prf) period. Alternate pulses are subtracted; and the residual pulse, introduced by the phase change of moving targets, is the signal detected by the radar. Stationary targets introduce no change in phase and hence give no output. Coherent radars use filter(s) to separate out the Doppler shift introduced by moving targets. Noncoherent radars, instead of remembering the transmitted phase, use the stationary clutter at the same range as the target for the reference signal. Moving targets introduce a phase shift different from this fixed reference; and it is this change in phase, equivalent to a change in frequency, which is detected. Essentially, all low prf radars have the same frequency stability requirements; and these requirements are satisfactorily covered in the literature (see References 1 and 2).

In this paper airborne PD radar stability requirements will be discussed. Further, the examples given are for typical operational radars and are included to show the order of magnitude of the frequency stability requirements. It will be obvious from the development that no single number, such as the fractional frequency stability (parts per million), can be used; rather, the allowable deviation or first-order sideband levels must be specified as a function of modulating frequency.

DOPPLER CLUTTER IN AIRBORNE RADAR

In Doppler radars, clutter considerations determine some of the frequency stability requirements, as will be shown later. The types of Doppler clutter are briefly described below (see References 1, 2, 3, and 4).

When a Doppler radar set is flown in an airplane, clutter can come from three sources as illustrated in Figure 3–1.

Main beam clutter comes from weather effects, and from the ground and sea if the main beam dips below the horizon; it is generally a very strong signal because of the high main beam gain of the antenna. *Side lobe clutter* comes from the antenna side lobes striking the ground at various angles, giving Doppler shifts both above and below the transmitted frequency; this produces a range of Doppler frequencies with a spread equal to twice the Doppler velocity of the aircraft. At any particular instant, one of the side lobes will be looking straight down at the earth and will return a signal with zero Doppler shift. This is analogous to the altitude line in ordinary pulse radar.

The general characteristic of the main beam and side lobe clutter is that it is a random signal, as in most cases the ground can be considered as consisting of many random scatters. The references given above discuss the characteristics of all types of clutter in more detail.

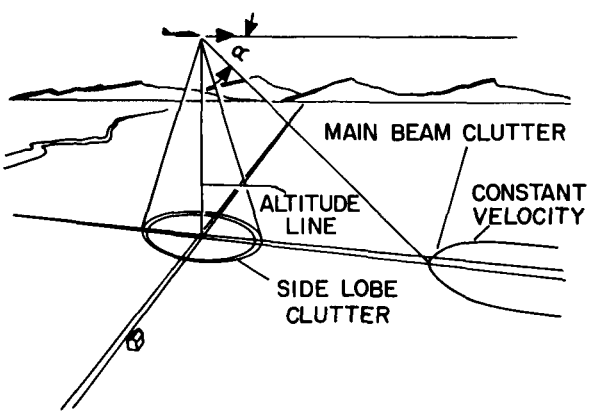

FIGURE 3–1.—Clutter in airborne Doppler radar.

STABILITY REQUIREMENTS FOR PULSE DOPPLER RADAR

A basic requirement of a Doppler radar system is the generation of a stable RF source for use in the transmitter. Also, since a practical receiver requires an IF greater than zero frequency, the generation of an additional stable radio frequency is required to heterodyne the transmitted frequency to the desired IF.

The frequency stability can be described in terms of allowable modulation on the signal entering the predetection filters of the receiver. For frequency modulation (FM), this is specified in terms of allowable deviation ratio. Short-time stabilities are of basic concern, since long-term stability is not significant as long as the drift does not increase the mutual interference, reduce the power output, or result in an incorrect indication of target velocity.

The permissible spectrum broadening in the receiver is determined by: (1) allowable spurious signals (false targets), (2) loss of sensitivity in the presence of interference (clutter), (3) loss of small signal sensitivity in the interference free region, and (4) interference with range or angle tracking due to spurious signals entering the tracking loops.

Consider a carrier ω_c modulated by one AM signal ω_b and one FM signal ω_m. The resultant spectrum is given by Equation 1:

$$\begin{aligned} S(\omega) = {} & J_0(\delta)\ \cos\omega_c t + \sum_{n=1}^{\infty} J_n(\delta) \\ & \times[\cos(\omega_c + n\omega_m)t + (-1)^n \cos(\omega_c - n\omega_m)t] \\ & + \tfrac{1}{2} m J_0(\delta)\ [\cos(\omega_c+\omega_b)t + \cos(\omega_c-\omega_b)t \\ & + m \sin\omega_b t \sum_{n=1}^{\infty} J_n(\delta) \\ & \times[\cos(\omega_c + n\omega_m)t + (-1)^n \sin(\omega_c - n\omega_m)t]. \end{aligned} \quad (1)$$

It will be shown below that m must be small; therefore, the intermodulation terms can be neglected. It should be noted that there is a possibility that, in some applications, the large deviations at low frequencies permitted by the deviations below, may cause large enough values of m and $J_n(\delta)$ to give significant intermodulation terms. However, in most applications linear superposition is a valid assumption, and the requirements on AM and FM will be derived separately.

Generation of Spurious Signals

Spurious signals can appear in the receiver because of incidental modulation of the main beam and altitude line clutter signals, since these are usually the largest signals in the receiver. Since these spurious signals may be mistaken for targets, they must be maintained below the receiver noise level. Both of the clutter signals are removed from the receiver by rejection filters. Full sensitivity is not obtained for targets close to the clutter, but a certain guard band must be assumed. The width of this band is determined by the extent of main beam clutter spreading, rejection filter characteristics, and the positioning accuracy of the rejection filter. The spurious signal requirement is then that spurious signals from the clutter be R db down from the clutter amplitude for sideband frequencies separated more than Δf_{min} from the clutter. Usually, the clutter is sufficiently narrow so that it can be assumed to be a single frequency, easing the calculation considerably. As an example, if the clutter is 80 db above noise, a sideband requirement of 86 db on AM and FM independently will assure that, in the worst case of in-phase signals, the spurious will be no more than equal to the noise level. Additional safety factors may be required, depending on system usage—assuming a 4-db safety factor, $R = -90$ db.

In amplitude modulation, a pair of sidebands are generated, each of amplitude $\frac{1}{2}m$, as shown in Equation 1. The maximum incidental AM modulation index m_{max} is then

$$m_{max} = 2R^{1/2}; \quad (2)$$

for $R = -90$ db, $m_{max} = 6.3 \times 10^{-5}$.

Similarly, for FM the maximum allowable deviation as a function of frequency can be found from Equation 1 by calculations of the Bessel coefficients. For frequencies below Δf_{min}, the higher order sidebands set the requirement; that is, at $\Delta f_{min}/2$, the second order sideband must be below R, etc. Figure 3–2 shows the permissible deviation as a function of modulating frequency for $R = -90$ db. The dashed curve in this figure

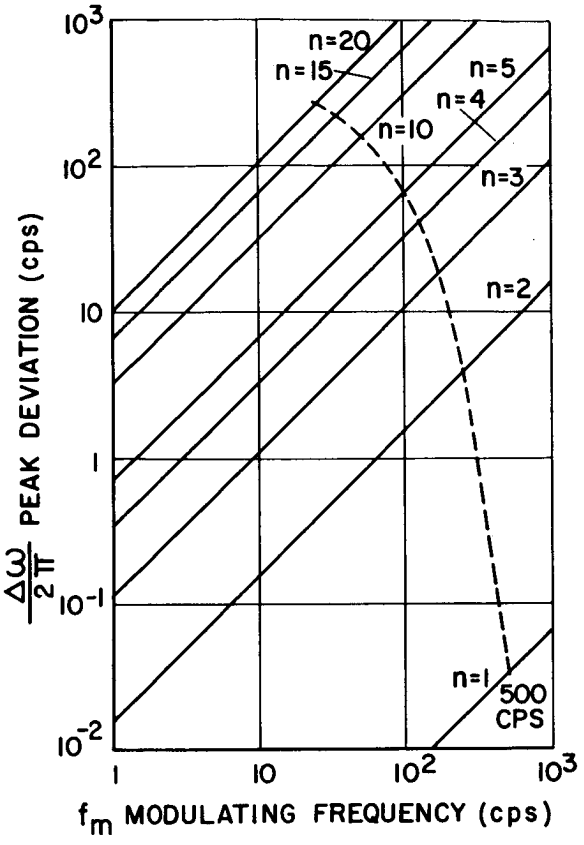

FIGURE 3-2.—Maximum deviation allowed to maintain a particular FM sideband 90 db below the carrier.

indicates the maximum peak deviation for a particular modulating frequency such that all sidebands removed 500 cps or more from the carrier will be at least 90 db below the carrier.

Loss of Signal Energy at the Output of the Predetection Filter

Loss of signal energy occurs in the predetection filter when the signal is frequency-modulated; this results from the fact that the sum of the powers in all of the sidebands plus the carrier must be equal to the unmodulated carrier power. When sidebands of the FM signal fall outside of the receiver detection filter passband, the signal power is reduced. AM will not result in signal loss, since the carrier level is unaffected by AM.

For the frequency modulation components, three cases must be considered:

1. Small δ and a modulation frequency greater than one-half the predetection filter bandwidth.
2. Large δ and a modulation frequency that approaches zero.
3. A δ that produces significant higher order modulation components $J_2(\delta)$, $J_3(\delta)$, etc.

For the first case, a typical criterion is that the reduction in $J_0(\delta)$ be 0.1 db. This is equivalent to $J_0(\delta)=0.9886$ or $\delta=0.213$.

The second case may be evaluated by assuming that the receiver bandpass filter has a two-pole Butterworth response. This network has a transfer function of the form (where the carrier is much greater than β):

$$P_o/P_i=[1+(2\Delta/\beta)^4]^{-1}. \quad (3)$$

For a large δ as ω_m approaches zero, the power frequency spectrum $H(\omega)$ can be represented as (see Reference 5)

$$H(\omega)=(\pi\Delta\omega)^{-1}[1-(\Delta/\Delta\omega)^2]^{-1/2}, \quad \Delta\leq\Delta\omega. \quad (4)$$

Solving for the total power output,

$$\frac{P_o}{P_i}=\frac{2}{\pi\Delta\omega}\int_0^{\Delta\omega}\frac{d\Delta}{[1+(2\Delta/\beta)^4][1-(\Delta/\Delta\omega)^2]^{1/2}}. \quad (5)$$

Evaluation of this integral gives $\Delta\omega=\beta/4$ for a 0.1-db loss in signal strength. For example, if filters of 350-cycle bandwidth are used, the peak deviation is restricted to 88 cps.

The third case can be handled by considering the power in each of the discrete sidebands rather than by using a continuum. The number of sidebands N that must be included within a rectangular filter to have no more than 0.1-db

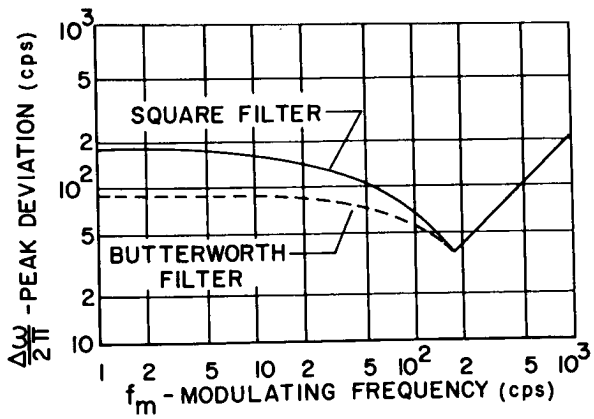

FIGURE 3-3.—Stability requirements for signal loss.

power loss is found from the equation,

$$P_o/P_i = 0.9773 = J_0^2(\delta) + \sum_{n=1}^{N} 2J_n^2(\delta). \quad (6)$$

The modulating frequency is related to the filter width by the relation,

$$f_m = \beta/2(N+1), \quad (7)$$

where the assumption is made that the sidebands corresponding to the $N+1$ term are just outside the band edge. The upper solid curve in Figure 3–3 shows the resulting deviation requirement at low frequencies. The curve is asymptotic at low frequencies to one-half the filter bandwidth, 350/2 cps in this case. This curve must be modified when practical filters are considered. For example, if the Butterworth filter discussed above is used, the maximum deviation permitted at low frequencies is 88 cps. The dotted curve has been sketched in approximately parallel to the solid curve and has been made to intercept the solid curve at one-half the filter bandwidth, 175 cps. This is a transition to the first case where the first-order sideband is specified in terms of carrier loss.

FM Ranging Modulation Requirements

In a CW or high prf pulse Doppler radar, range may be measured by FM techniques. Basically, these techniques involve introduction of a modulation in the frequency domain on the transmitted signal, recovery of the modulation from the range delayed received signal, and measurement of the time delay by suitable demodulation. Two basic types of FM used are:

1. *Linear FM*—a constant rate of change of frequency is put on both transmitted and local oscillator signals. An apparent Doppler shift which is proportional to range appears.
2. *Sinusoidal FM*—a small deviation sinusoidal modulation is applied to both transmitter and local oscillator. The phase shift of the IF signal, compared with the original modulation, is directly proportional to range. Requirements for both techniques are discussed below.

Linear FM Requirements

The linear FM requirements can be considered as three separate requirements: *range accuracy requirements, signal loss requirements,* and *spurious signal requirements.*

Range Accuracy Requirements—The transmitter and local oscillator are linearly swept at a rate df/dt. The time delay τ_r of the target return is then measured by the apparent Doppler shift Δf_r:

$$\tau_r = \Delta f_r (df/dt)^{-1}; \quad (8)$$

or, the range of the target is

$$r = c(\Delta f_r/2)\,(df/dt). \quad (9)$$

Differentiating and solving for the fractional error due to an error in the slope of the linear FM waveform,

$$dr/r = -\frac{d(df/dt)}{df/dt}; \quad (10)$$

or, a given percentage error in slope causes the same percentage error in range measurement. If a filter bank is used to detect the apparent Doppler shift, then the absolute error in frequency need be no better than about one-fourth of a filter width. If a target at maximum range is shifted by N filters, the maximum error in slope is then

$$\frac{d(df/dt)}{df/dt} = (4N)^{-1}. \quad (11)$$

Signal Loss Requirements—As shown above in the section on Loss of Signal Energy, for 0.1-db allowable loss the maximum deviation is one-fourth of the predetection filter bandwidth. This requirement also holds for linear FM except that the deviation is measured with reference to the average slope.

Spurious Signal Requirements—Again, the deviation requirements are as derived in the section on Generation of Spurious Signals, except that the deviation is measured with reference to the average slope.

Sinusoidal FM Requirements

It can be shown that the range r, in nautical miles, measured by the sinusoidal FM technique is found by the equation,

$$r = (c/\omega_m)\,\sin^{-1}(\Delta\omega'/2\Delta\omega)$$
$$= (c/\omega_m)\,\sin^{-1}(\delta'/2\delta). \quad (12)$$

Range Accuracy Requirements—The accuracy of the modulating frequency is determined by

the required ranging accuracy. Since, as seen from the above equation, the percentage error in modulating frequency is equal to the percentage error in measured range, the allowed error in frequency is some fraction of the required overall accuracy. For example, if 2-percent accuracy is required, then 0.2-percent accuracy of the frequency will render this error negligible. Similarly, the accuracy of the transmitted deviation is the same as for the frequency, provided $\Delta\omega'$ is small; this is usually the case in order to obtain an essentially linear relation between range and phase. If larger phase shifts are used, a compensating network can be employed to linearize the equation, in which case the same accuracy requirement holds.

Signal Loss Requirements—This requirement is the same as derived in the section on Loss of Signal Energy.

Spurious Signal Requirements—Outside the ranging frequency region, the requirements are the same as derived in the section on Generation of Spurious Signals. Near the ranging frequency, spurious modulation sidebands must be sufficiently far below the desired ranging signal that the accuracy will be essentially unaffected.

Consider the use of sinusoidal FM ranging with a modulating (ranging) frequency of 85 cps and a peak transmitted deviation of 1000 cps. Assuming that range must be measured at ranges beyond 0.5 nautical mile, the minimum received deviation ratio is

$$\delta_{min}' \cong (\Delta\omega'/\Delta\omega)\,\delta = \tau_r \Delta\omega,$$

$$\cong 2\pi \times 6.2 \times 10^{-6} \times 1000,$$

$$\cong 0.0386.$$

For negligible effect, assume a 10-db signal-to-spurious-noise ratio is required. The received spurious deviation ratio (at 85 cps) must then be less than

$$\delta' = \delta_{min}'/(10^{1/2}) = 1.21 \times 10^{-2}.$$

The peak allowed received spurious deviation at 85 cps is

$$\Delta\omega'/2\pi = \delta'\omega_m/2\pi = 1.21 \times 10^{-2} \times 85,$$

$$= 1.03 \text{ cps}.$$

This value is the independent modulation requirement which holds for the remainder of the transmit-receive system exclusive of the master oscillator. The common, or master oscillator requirement, is that the spurious transmitted sideband be 10 db below the intentional modulation sideband; so that the allowable deviation at 85 cps is 1000 cps/$10^{1/2}$ = 316 cps.

Lobing Noise Requirement

In a conical scan tracking radar, incidental modulation (AM) sidebands that fall in the vicinity of the lobing frequency can affect the tracking accuracy. FM sidebands will not affect the tracking, since the amplitude detector used is insensitive to FM. Considerations of the tracking loop bandwidth and permissible angular error permit the specification of the percentage modulation permitted at or near the lobing frequency. Typically, 1-percent modulation is permitted at the lobing frequency. The requirement on the master oscillator may be relaxed from this value, depending on the degree of saturation of the transmitter amplifiers.

Requirement on Transmitted Frequency Stability

Let the transmitted carrier be frequency-modulated by $\Delta\omega \sin\omega_m t$; then the transmitted frequency ω_r is

$$\omega_r = \omega_c + \Delta\omega \sin\omega_m t. \tag{13}$$

Now assume a point source target moving at a constant radial velocity. The received signal ω_R, is shifted by the Doppler shift ω_D. The received signal is

$$\omega_R = \omega_c + \omega_D + \Delta\omega[(\omega_c+\omega_D)/\omega_c] \times \sin\omega_m[(\omega_c+\omega_D)/\omega_c](t-\tau_r)$$

$$\approx \omega_c + \omega_D + \Delta\omega \sin\omega_m(t-\tau_r). \tag{14}$$

When the transmitted signal is translated by a pure frequency ω_{IF}, the resultant is the local oscillator signal ω_{LO}:

$$\omega_{LO} = \omega_c - \omega_{IF} + \Delta\omega \sin\omega_m t. \tag{15}$$

When the received signal frequency ω_R is beat

against ω_{LO} in a mixer, the output is

$$\omega_R' = \omega_R - \omega_{LO},$$
$$= \omega_{IF} + \omega_D + \Delta\omega\,[\sin\omega_m(t-\tau_r) - \sin\omega_m t],$$
$$= \omega_{IF} + \omega_D - 2\Delta\omega \sin\tfrac{1}{2}(\omega_m\tau_r)\cos\omega_m(t-\tfrac{1}{2}\tau_r). \quad (16)$$

Comparison of Equations 16 and 13 shows that the magnitude of the ratio of the frequency deviation in the receiver to the transmitter frequency deviation is

$$\Delta\omega'/\Delta\omega = \left|\frac{2\Delta\omega\sin(\omega_m\tau_r/2)}{\Delta\omega}\right|$$
$$= 2\,|\sin(\omega_m\tau_r/2)\,|$$
$$= 2\,|\sin(\pi f_m\tau_r)\,|. \quad (17)$$

Examination of this equation shows that, for low modulating frequencies and short ranges, the deviation in the receiver may be considerably less than that of the transmitter; however, for large values of the product $f_m\tau_r$ the deviation in the receiver may exceed the deviation of the transmitter by a factor of 2. Figure 3–4 shows curves of $|\sin\pi f_m\tau_r|$ versus f_m for a radar with a maximum range of 130 nautical miles. Curves of $\tau_r < \tau_{r,max}$ fall to the right of the curve

$$\tau_r = \tau_{r,max},$$

so that the peaks of the sum of the curves completely fill the area under the envelope curve. The maximum deviation in the receiver can be represented by the envelope which can be described analytically as follows:

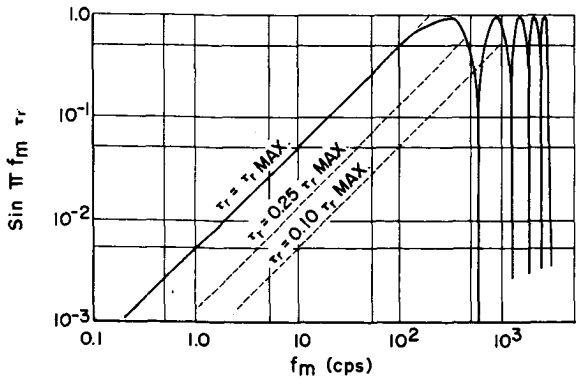

FIGURE 3–4.—Frequency deviation of received signal; maximum range, 130 nautical miles.

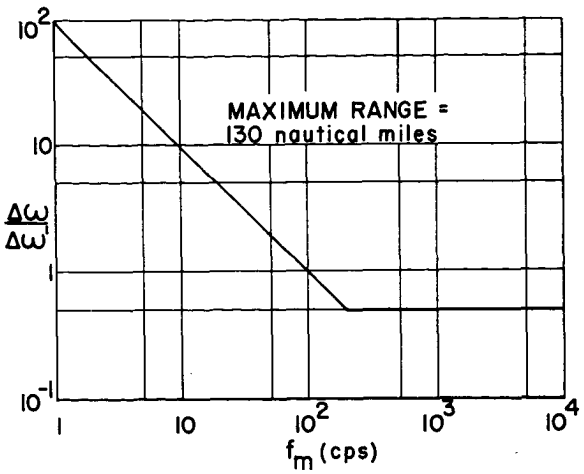

FIGURE 3–5.—Frequency deviation of transmitter vs. that of receiver.

$$|\sin\pi f_m\tau_r| \cong \pi f_m\tau_r, \qquad \pi f_m\tau_r \le 1,$$
$$\cong 1, \qquad \pi f_m\tau_r > 1. \quad (18)$$

In the log–log coordinates used, the envelope consists of a straight line with +1 slope intersecting the point

$$\pi f_m\tau_r = 1,$$

and a straight line with zero slope intersecting the same point. For the previous case of a radar with a maximum range of 130 nautical miles, the corner is at

$$\Delta\omega/\Delta\omega' = 0.5$$

and

$$f_m = 1/\pi \times 130 \times 12.3 \times 10^{-6} = 200.$$

This curve is plotted in Figure 3–5 and gives the ratio of frequency deviation permissible on the transmitter to that in the receiver.

The above discussion applies when the receiver-beating oscillator is phase-locked to the transmitter. However, when two stable oscillators are employed, the restrictions are that at all ranges the worst condition requires that the deviation allowed on either oscillator be only one-half the deviation allowed in the receiver IF signal.

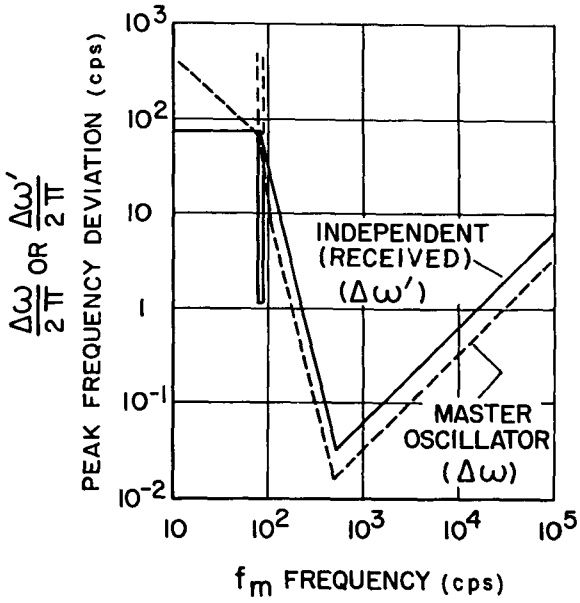

FIGURE 3–6.—Composite stability requirements.

COMBINED STABILITY REQUIREMENTS

The previous developments have indicated the factors which must be considered in computing the stability requirements for a PD radar. It is desirable to determine how these different requirements combine to form a stability spectrum. Consider a long-range PD radar representing the state of the art which must operate in a severe clutter environment (see Reference 3). The critical items for this radar are:

1. The clutter rejection is to be 90 db within 500 cps of the main beam clutter.

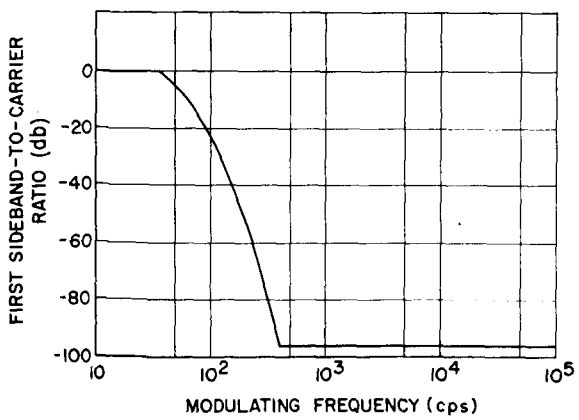

FIGURE 3–7.—Master oscillator stability requirements.

2. The carrier loss at low frequencies is to be restricted to 0.1 db.

3. The Doppler filters shall be two-pole Butterworth with a bandwidth of 350 cps.

4. The maximum range of the radar is to be 130 nautical miles.

5. Sinusoidal FM ranging is used with modulating frequency 85 cps, deviation of 1000 cps, and minimum range of 0.5 nautical miles.

The stability spectrum requirements of this PD radar are shown in Figure 3–6. Two curves are shown: one labeled "Independent," and the other "Master Oscillator." The independent curve represents the requirements of the signal in the receiver. The master oscillator requirement curve is obtained by multiplying the independent curve by the curve of Figure 3–5, except for the ranging frequency region which was derived in the section "Sinusoidal FM Requirements."

The requirements indicated in Figure 3–6 make it clear that no single number or simple statement can be used to specify the stability requirements of a PD radar.

Since it is generally easier to measure the sideband levels rather than the deviation, the master oscillator requirements can be expressed in terms of sideband levels. This is done by calculating the sidebands obtained using the allowable deviation curve of Figure 3–6. The result is shown in Figure 3–7.

REFERENCES

1. RIDENOUR, L. N., "Radar System Engineering," Vol. 1, MIT Rad. Lab. Series, New York: McGraw-Hill Book Co., Inc., 1947.
2. SKOLNIK, M. I., "Introduction to Radar Systems," New York: McGraw-Hill Book Co., Inc., 1962.
3. GOETZ, L. P., and ALBRIGHT, J. D., "Airborne Pulse-Doppler Radar," *IRE Transactions on Military Electronics* MIL-5 (2), April 1961.
4. MOONEY, D., and RALSTON, G., "Performance in Clutter of Airborne Pulse MTI, CW Doppler and Pulse Doppler Radar," in: *IRE International Convention Record*, Part 5, 1961.
5. GOLDMAN, S., "Frequency Analysis, Modulation and Noise," New York: McGraw-Hill Book Co., Inc., 1948.

SYMBOLS

c	velocity of light
df/dt	linear FM sweep rate
f_m	modulating frequency (cps)

Δf_{min} signal separation from clutter
Δf_r apparent Doppler shift
$H(\omega)$ power spectrum of low-frequency modulation and high-frequency deviation
$J_n(X)$ Bessel function of the first kind and nth order
m fractional amplitude modulation
m_{max} maximum AM modulation
n integer 0, 1, 2, etc,
P_i Doppler filter power input
P_o Doppler filter power output
R required sideband-to-carrier ratio
r range to target
$S(\omega)$ frequency spectrum (radians/sec)
t time
β filter bandwidth (cps)
Δ detuning from the center frequency of a filter (cps)
δ transmitted frequency deviation ratio, $\Delta\omega/\omega_m$
δ' received frequency deviation ratio, $\Delta\omega'/\omega_m$
τ_r radiation round-trip time
ω_b AM modulation frequency (radians/sec)
ω_c RF carrier frequency (radians/sec)
ω_D Doppler shift (radians/sec)
ω_{IF} translation (IF) frequency (radians/sec)
ω_{LO} local oscillator signal (radians/sec)
ω_m modulating radian frequency
ω_R received frequency, RF (radians/sec)
ω_R' received frequency, IF (radians/sec)
$\Delta\omega$ peak deviation of the transmitted carrier (radians/sec)
$\Delta\omega'$ peak deviation of the received frequency, (radians/sec)
ω_τ transmitted frequency (radians/sec)

4. COHERENT RADAR FM NOISE LIMITATIONS

D. M. RADUZINER AND N. R. GILLESPIE

Raytheon Company
Wayland, Massachusetts

The fundamental benefits of coherent radar are compromised by uncontrolled deviations in transmitted phase or frequency. An example illustrating the dependence of an adequate definition of short-term frequency stability on spectral content considerations is given, followed by a brief review of techniques employed to generate and measure short-term frequency stable sources for coherent radars. Illustrations are provided to compare the test data obtained from a klystron microwave exciter and an all solid-state microwave source which employs a piezoelectric crystal oscillator, transistor amplifiers, and varactor frequency multipliers. A practical problem is illustrated by experimental results obtained when the performance of the above microwave sources in a vibration environment are compared. Finally, a brief comparison of the operation of two coherent radar processors in the presence of unwanted FM discloses an interesting difference in clutter rejection degradation.

Two important parameters which aid in a performance description of a coherent radar are *clutter rejection* and *subclutter visibility*. This paper will relate these parameters to the performance of practical STAble Master OScillators, often referred to as *stamos*. Two basic means of generating stable reference signals will be compared by describing their noise properities in both quiescent and vibrating enviroments. This will be followed by a general discussion of the effects of radar transmitter FM noise and the resultant changes in clutter rejection and subclutter visibility performance obtained with two Doppler processing circuits.

The terms clutter rejection and subclutter visibility, as used in this paper, may be defined as follows (see Reference 1):

Clutter rejection is the measure of a system's ability to attenuate clutter below some specified level. It is usually defined as the maximum clutter amplitude which, after being attenuated, does not exceed this level. It is the ratio of the maximum clutter to receiver noise which can be rejected before crossing the specified threshold.

Subclutter visibility is a measure of a system's ability to detect weak moving targets in the presence of strong fixed clutter. It is specified as the maximum ratio of clutter to signal levels at which the signal is just discernible. In a pulse system, this ratio is measured for clutter and signal appearing in a single range gate while, in an unmodulated CW system, it must include the clutter return from all ranges.

Of course, signal detectability is always limited by nonclutter-related noise limits, and therefore a practical upper bound on subclutter visibility is determined by the clutter rejection ratio.

A coherent radar derives its advantage with respect to moving target and clutter resolution by effective use of stored or controlled measures of the transmitted energy phase and frequency characteristics. Consequently, transmission of uncontrolled or unstored modulations will deteriorate the clutter performance of the coherent system. The term "noise" may be used to identify all undesirable modulations.

Random or noncoherent noise will cause transmitter leakage or clutter returns to "jam" the receiver and reduce signal detectability. In other words, the subclutter visibility would be reduced. Simple CW systems encounter transmitter noise as a limiting factor in signal detectability, and consequently the distance at which a given target can be detected cannot be increased by simply increasing transmitter power.

On the other hand, coherent noise, which may

be characterized by the appearance of undesirable "lines" in the transmitter power spectrum, may cause transmitter leakage or clutter to be identified falsely as a moving target. Coherent noise therefore reduces the clutter rejection capabilities of the system.

Noise in the transmitted output may originate with the RF source or in any subsequent processing element. In general, noise sidebands about a desirable spectral line may be considered as the result of composite amplitude and angle (phase or frequency) modulations. These modulations or perturbations may be caused by both random and ordered processes. In a discussion of oscillator stability, the noise terms related to angle modulation are of particular interest. In fact, experience with coherent radars has shown that many clutter problems are due to unwanted FM of the transmitted energy.

A definition of oscillator short-term stability should discuss the spectral content of the oscillator output in terms of FM noise deviations, to simplify relating the results of actual coherent radar FM noise measurements to oscillator stability criteria which are useful in other areas of endeavor.

This paper will discuss FM microwave sources and noise measurement techniques briefly and will demonstrate their usefulness in some aspects of coherent radar design.

STABLE MICROWAVE SOURCES COMMONLY APPLIED TO COHERENT RADAR

A microwave signal for coherent radar applications must have microwave phase continuity from pulse-to-pulse or be a continuous single microwave tone for a CW application. One common generating technique uses a master oscillator and power amplifier transmitter chain. This section is limited to a discussion of radar master oscillators; however, the same power sources could be applied to any application requiring stable microwave signals such as the local oscillator in a phase-lock communication system.

Today there are a variety of sources without external stabilization circuitry which exhibit low spurious frequency modulation under quiescent laboratory conditions.

Table 4–1 relates measurements of typical spurious FM levels achievable in the laboratory with well-smoothed dc power supplies to the following four types of unstabilized sources: triode, reflex klystron, two-cavity klystron, and an all-solid-state stamo.

Because it is not as common in a power ampli-

TABLE 4.1—*Unstabilized Coherent Microwave Signal Source Characteristics**

Source types	Typical values of FM noise measured in a 1-kc band at $f_m = 10$ kc	
	Δf_{rms} (cps)	Both sidebands in db below carrier
1. Triodes TRAK 2970 with GE 7486 Triode (C-band), Reference 3	≈5	66
2. Reflex klystron such as the X–13	5 to 10	66 to 60
3. Non-gridded 2-cavity klystron SOX–239 at X-band, Reference 4	0.2 to 0.5	94 to 86
4. All solid-state source at X-band, Reference 2	≈2	74

*Note: The following definitions are used:

Sidebands in Terms of Δf and db Below Carrier—The relation between Δf_{rms} and the ratio between total sideband power P_{SB} and carrier power P_c for a very small index of modulation and single sinusoidal frequency modulation may be stated as follows:

$$P_{SB}/P_c \text{ (db)} = -20 \log_{10} (fm/\Delta f_{rms}).$$

Δf_{rms} in a 1-kc Band—This is the rms deviation of a single sinusoidal frequency modulation at the center of a 1-kc band that would equal the rms deviation of the total frequency modulation of the actual signal (perhaps random noise) contained in the whole 1-kc band.

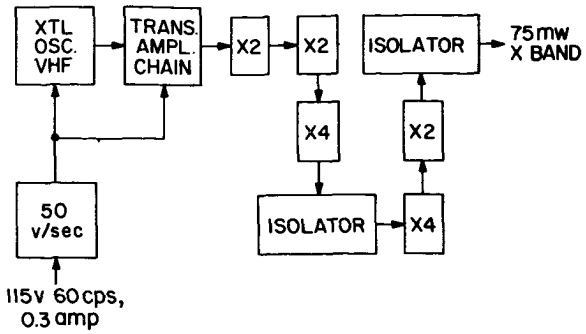

FIGURE 4–1.—All-solid-state microwave power source.

fier driver transmitter chain as the other three types listed, a typical solid-state stable master oscillator is briefly described here. It consists of a VHF crystal oscillator, a power transistor amplifier chain, and a series of varactor frequency multipliers as shown in Figure 4–1. Its frequency is deviable with 75 milliwatts output power, which is more than adequate to drive a multi-kilowatt, four-cavity power klystron amplifier. Its long-term frequency stability is better than one part in 10^6 per week, and it operates from a 50-volt dc power supply. A more detailed description may be found in Reference 2.

Lower FM noise klystron performance can be achieved when required by the coupling of a high-Q cavity to the stamo output. As much as 20-db improvement in FM noise is readily achievable with a passively stabilized reflex klystron at the expense of at least 10-db output power. Therefore, this *passive stabilization* technique can

TABLE 4–2.—*A Comparison of Frequency Modulation Noise Measuring Techniques at X-Band**

Techniques	Minimum f_m detectable for −60 db sidebands	Practical FM sensitivity measured in a 1-kc band at $f_m = 10$ kc		Practical AM rejection (db)
		Δf_{rms} (cps)	Both sidebands in db below carrier	
1. Spectrum analyzer	10 kc is common	≈10	≈60	None
2. Delay line analyzer (Figure 4–2)	100 kc	None (10 kc is not detectable)	None	None
3. Microwave discriminator, using direct video detection and video narrow-band analyzer (Figure 4–3).	Limited by video analyzer at <10 cps.	≈1	≈80	≈10
4. Discriminator using sidestepped L.O., a single IF channel, IF phase detection, and narrow-band analyzer (Figure 4–4).	<10 cps	≈0.1	≈100	≈10
5. Two-channel comparison using high-Q microwave bridge, L.O., two-channel IF mixing, IF phase comparison, and video narrow-band analyzer (Reference 5 and Figure 4–5).	<10 cps	≈0.01	≈120	≈30

*Definition of terms in Table 4–2:

f_m: frequency of modulation

Minimum f_m detectable: frequency of a −60 db sideband with minimum separation from the carrier that can be detected

Sidebands in terms of Δf and db below carrier: See Table 4–1

Δf_{rms} in a 1-kc band: See Table 4–1

Practical FM sensitivity and AM rejection: those values which can be achieved with reasonable care in tuning and adjustment; the thresholds of each equipment and the theoretical values are of course higher

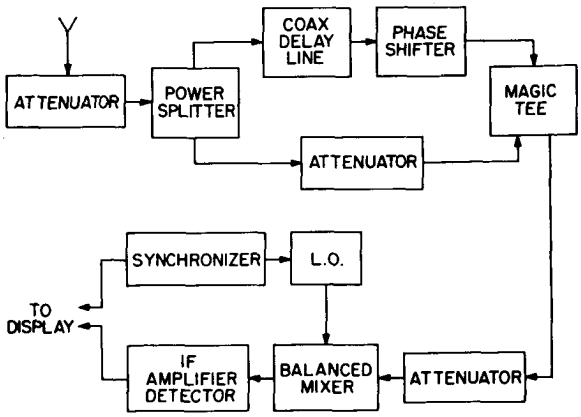

FIGURE 4–2.—Delay line analyzer.

be used only when the basic power source is much larger than required for the system application.

Any of the sources listed above can employ FM noise degeneration (or *active stabilization*) by the addition of a sensitive FM discriminator and a degeneration amplifier to complete a negative feedback loop. The FM noise degeneration circuitry is designed to have a gain and phase response consistent with the specific system requirements. With active degeneration, the lower noise limit is determined by the sensitivity of the discriminator. FM noise as low as 0.01 cps rms measured in a 1-kc band is available by this technique in quiescent laboratory conditions (Reference 2). An obvious disadvantage is the additional equipment complexity.

LOW-NOISE MEASURING TECHNIQUES

A brief outline of techniques used to measure the FM noise levels is presented in this section.

Table 4–2 lists three FM noise measuring techniques and compares sensitivity in 1-kc bands centered at 10 kc; also listed are two techniques for spectral displays. With the spectral displays, each sideband is presented separately, and the angular and amplitude components cannot be separated. These two display techniques are useful for FM measurements only when the known amount of AM is well below the FM. Figures 4–2, 4–3, 4–4, and 4–5 illustrate the basic configurations employed for the several techniques.

Calibration of the noise measuring equipment is particularly important because of the possibility of experimental error. The test equipment sensitivity is determined by inserting a microwave signal with a known deviation and then measuring the test equipment response.

One *common technique* for establishing a known deviation is to frequency-modulate the carrier with a single sinusoid at a known frequency and null the carrier or one of the sidebands by observing the output on a spectrum analyzer. From the known Bessel function relations, the peak deviation can be calculated. Care must be taken in this step that no other significant modulations are present and that the modulation is being applied linearly. The presence of harmonics of f_m will cause the carrier null to occur at a different modulation level.

Once null is established, the modulation is attenuated to a level that will not saturate the test equipment and that will insure a linear test equipment response. This level, however, must be at least 20 db above the spurious FM noise to assure that measurement error will be less than the inherent error in the test equipment. Test equipment sensitivity is now measured tuning the narrow-band analyzer to the deliberate f_m.

The spurious AM noise level must be measured to verify that it is 20 db below the spurious FM noise level. The AM noise may be permitted to be higher in direct proportion to the AM rejection provided by the test equipment.

In using a discriminator with direct video detection, caution must be exercised to distinguish between low-frequency source noise and 1/f

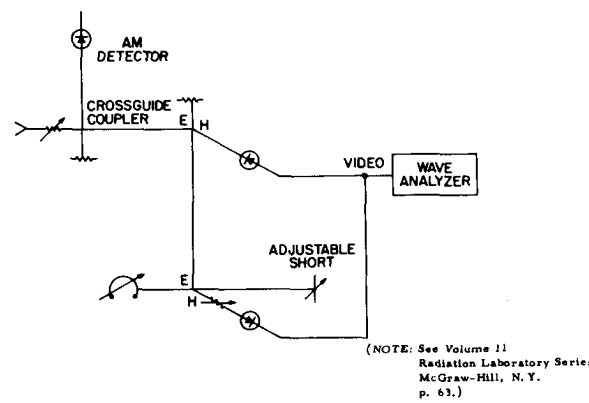

FIGURE 4–3.—Microwave discriminator using direct video detection and narrow-band analyzer.

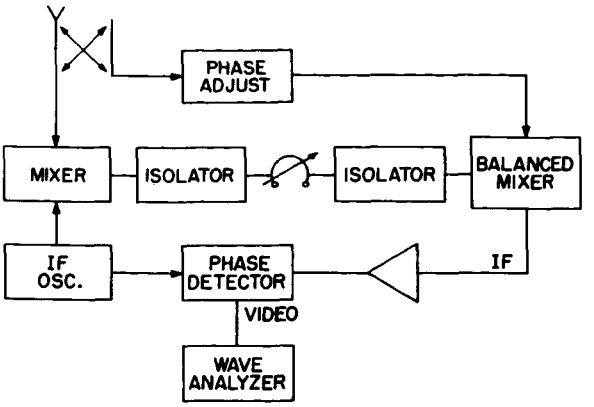

FIGURE 4–4.—Discriminator using side-stepped local oscillator (L.O.), single IF channel, IF phase detector, and wave analyzer.

crystal noise. Reference 6 discusses crystal noise at low frequencies.

A novel *dc offset method* of FM measurement calibration has become practical with the solid-state multiplier source. The method is practical because of the inherently high degree of stability of the source. Stability of one part in 10^8 is required over a 1-minute period. The dc offset method has been checked against the carrier null technique to within ± 0.5 db, which is well within the experimental error. The test setup is shown in Figure 4–6. The procedure is given below:

1. Using a dc bias, push the XTL OSC frequency from

$$f_o \text{ to } f_o + (\Delta f/\sqrt{2}X)$$

   using the VHF counter for frequency measurement.
2. Set the meter to full scale; then remove dc pushing bias.

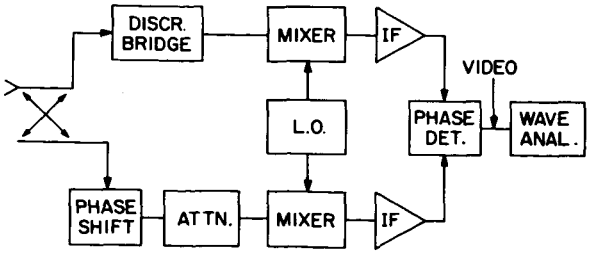

FIGURE 4–5.—Two-channel comparison using L.O., two-channel IF, IF phase detector, and wave analyzer (Reference 5).

3. Modulate with f_m to swing the meter to full scale.
4. The resultant Δf now equals the desired peak deviation.

The symbols are defined as:

f_o base oscillator frequency,
X multiplication factor of the varactor multipliers,
Δf desired peak deviation at output,
f_m desired modulating frequency.

Advantages to this method are that a microwave spectrum analyzer is not required and that f_m is not limited by the resolution of the microwave analyzer. However, the discriminator and

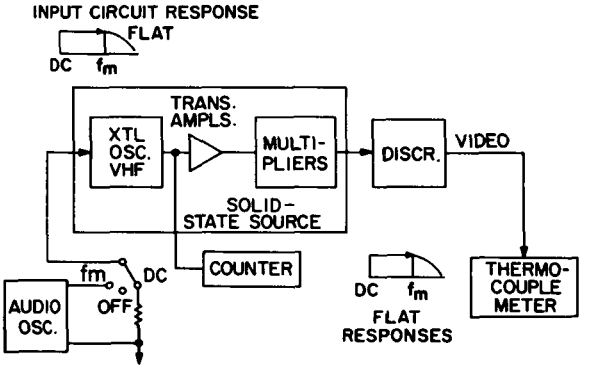

FIGURE 4–6.—Test setup for dc offset calibration of FM discriminator.

oscillator modulation circuit each must have a flat response from the calibrating frequency to dc. Two advantages for some solid-state sources with limited power output and limited linear pushing range are that a very low Δf can be used for a calibration level and that a lossy external modulator is not required.

MICROWAVE SOURCES UNDER VIBRATION

In radar systems required to function in a vibration environment, the stable microwave source must be chosen so that the noise generated under vibration is low enough to cause no degradation of system performance beyond the design objectives. However, it is the nature of most microwave sources to produce additional noise

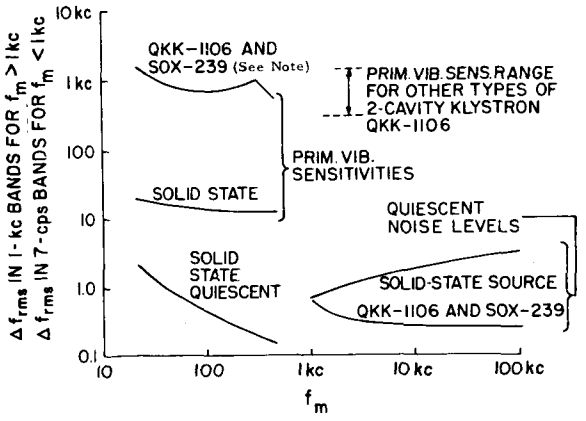

FIGURE 4–7.—Typical primary vibration sensitivity for 1-G peak acceleration. (NOTE: Actual bandwidth data are not given for this measure in Reference 4; however, similar measurements in a 7-cps BW give about the same results.)

sidebands when mechanically excited. Two obvious choices are:

1. Isolate the microwave source from mechanical excitation.
2. Reduce the sensitivity of the microwave source to mechanical excitation.

Mechanical isolation often is used, and active degeneration also is common. However, active degeneration is limited by the vibration sensitivity of the required discriminator. The ideal solution would be the development of a microwave source that has such low vibration sensitivity that it requires no special mechanical isolation or degeneration.

For purposes of discussion, *primary vibration sensitivity* may be defined as the effective value (rms) of deviation at the vibration frequency or its harmonics, which are produced by a 1-g acceleration of the speciment under test. Modulation of the source at any frequency other than the frequency of vibration and its harmonics is defined as *secondary sensitivity*.

Considerable development effort has been expended in recent years to achieve a low-noise unstabilized microwave source that also has low primary and secondary vibration sensitivity. Data were presented in Reference 4 for such a tube under vibration (a tunable non-gridded two-cavity klystron oscillator, SOX-239). The data are repeated in Figure 4–7 for reference purposes.

An all-solid-state microwave source similar to a unit being developed for a communication system, in cooperation with the Raytheon Communication and Data Processing Operation, was subjected to vibration. The resulting primary sensitivity data are plotted against f_m in Figure 4–7 as deviation in 7-cps or 1-kc bands for comparison with the SOX-239 data. The original solid-state-source quiescent data were taken in bandwidths smaller than 1 kc. However, because the resulting noise was observed to be of a random nature, a bandwidth conversion of the data to facilitate comparisons with the previously existing 1-kc SOX-239 quiescent noise data introduces errors that are less than the experimental error. Noise measuring equipment similar to that shown in Figure 4–3 was used for measuring the characteristics of the solid-state source.

For bandwidth conversion with random noise,

$$\Delta f_{n1} = \Delta f_{n2}(n_1/n_2)^{1/2},$$

where f_n is the deviation of the noise frequency modulation measured in a bandwidth n.

Test results indicate that the rise in FM noise due to primary vibration sensitivity of the solid-state stamo is about 30 db for a 1-g peak acceleration. The FM noise rise from a special klystron source (designed specifically for low-vibration sensitivity) assuming 1-cps rms quiescent noise, is about 60 db for the same excitation.

Reference 4 did not report quiescent noise below 1 kc; however, tests at Raytheon on two-cavity oscillators indicate noise close to the carrier ranges from about 0.5 to 1.5 cps rms as measured in 7-cps bands.

Secondary vibration sensitivity tests of the solid-state source have shown no increase in noise output at frequencies other than the primary vibration frequencies and its harmonics.

The advent of solid-state multiplying sources of RF energy, such as those developed by Raytheon, signifies a new vibration-resistant performance level for applications in mechanical or acoustical high noise environments.

RADAR PERFORMANCE VS. SPECTRAL CONTENT

As mentioned previously, specifications for the noise performance of a stamo or power amplifier are dependent on the spectral content of the RF

output. A common technique for identifying the FM components was used in Table 4–1; this technique consists of obtaining a measure of the equivalent FM deviation of the source in a specified bandwidth centered on a modulating frequency of interest. The usefulness of this measure with respect to exact radar performance predictions is in part dependent on the radar data processing circuit design.

Consider the two pulse Doppler radar data processors shown in Figures 4–8 and 4–9. The automatic target detector shown in these figures may be described either as a contiguous filter CFAR (Constant False Alarm Rate) detector or as a real-time spectrum analyzer with automatic threshold detectors associated with contiguous Doppler "bins." After range gating, if applicable, and clutter rejection filtering to reject slow-moving target returns with Doppler frequencies below those of interest, the Doppler audio is analyzed by the target detector. Ideally, clutter returns will not contain enough energy in the Doppler passbands to compete with either "front-end" noise or any possible moving target returns. On the other hand, a moving target will cause energy to appear in one or two contiguous filters in the Doppler passband and, after detection and comparison with a threshold, will "ring" a target alarm.

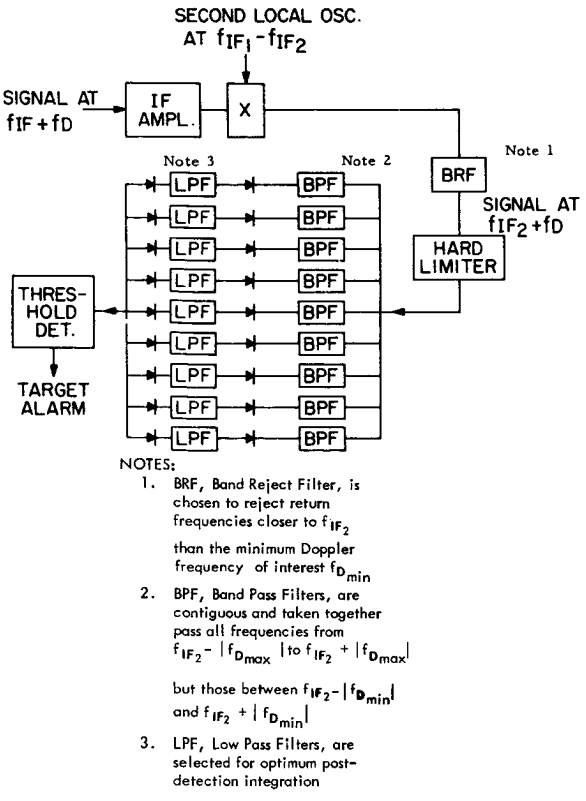

FIGURE 4–8.—Automatic target detector.

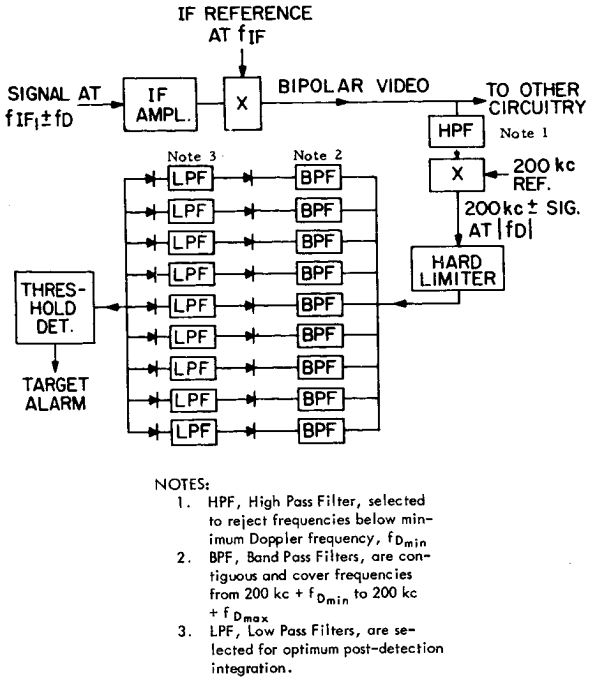

FIGURE 4–9.—Automatic target detector with folded Doppler processing.

The effect of transmitter output frequency modulation by a single "unwanted" sinusoid is completely different for the two data processors shown. For low-modulation indices, the waveform of the return from stationary clutter or of transmitter leakage into the receiver may be expressed as follows (Reference 7):

$$x(t) = \text{Real}\ \{\exp(j\omega_c t)[1-\tfrac{1}{2}\beta\exp(-j\omega_m t) + \tfrac{1}{2}\beta\exp(j\omega_m t)]\} \quad (1)$$

for $\beta \ll \pi/2$ (low-modulation index), where

ω_c transmitted carrier frequency,

ω_m frequency of modulation.

For the circuitry shown in Figure 4–8, the successive heterodyne operations may be interpreted as translations of ω_c down to a value of $2\pi f_{IF_1}$ and then to $2\pi f_{IF_2}$. Examination of the

above equation will show energy at the following frequencies:

$$f_{IF_2}, \qquad f_{IF_2}-f_m,$$

and

$$f_{IF_2}+f_m.$$

If

$$|f_{D_{min}}|<f_m<|f_{D_{max}}|,$$

then the automatic target detector will respond to the energy at both $f_{IF}+f_m$ and $f_{IF}-f_m$; and a false alarm will result. In accordance with the definitions discussed in the introduction, poor clutter rejection can result from the "unwanted" frequency modulation of the transmitted energy.

The circuitry shown in Figure 4–9 will behave in a different manner, as shown by the following argument. The synchronous detection of the IF amplifier output by the IF reference signal is tantamount to heterodyning to a second IF of zero frequency. However, the translation of the carrier term, ω_c in the previous equation, to zero results in the following waveform at the input to the high-pass filter (HPF).

$$y(t) = \underset{\text{Lim}\omega_c \to 0}{x(t)} = \text{Real}\,\{\exp(j[0t+\phi])$$
$$\times[1-\tfrac{1}{2}\beta\exp(-j\omega_m t)+\tfrac{1}{2}\beta\exp(j\omega_m t)]\}, \quad (2)$$

where ϕ is the phase angle between the signal at freq. f_{IF} and the reference oscillator at f_{IF}. When $\phi=0$,

$$\underset{\phi=0}{y(t)} = 1-\tfrac{1}{2}\beta\cos\omega_m t+\tfrac{1}{2}\beta\cos\omega_m t \quad (3)$$

and $y(t)=1$. Therefore, the spurious sidebands cancel and only a non-fluctuating (dc) term representing the carrier remains when ϕ is zero. When $\phi=\pi/2$,

$$y(t) = \text{Real}\,\{\exp(j\pi/2)[1-\tfrac{1}{2}\beta\exp(-j\omega_m t)$$
$$+\tfrac{1}{2}\beta\exp(j\omega_m t)]\},$$

$$\underset{\phi=\pi/2}{y(t)} = \beta\sin\omega_m t. \quad (4)$$

Therefore, the sidebands reinforce and no carrier term remains if the reference oscillator is in quadrature with the carrier ($\phi=\pi/2$). Therefore, the sidebands due to single sinusoidal frequency modulation may cancel in the processing circuitry for a folded Doppler processor. The following statements can be shown to be valid for *in-phase synchronous detection*:

1. Single sinusoid frequency modulation of *any deviation* will cancel in an ideal processing circuit of a folded Doppler or zero frequency second IF processor.
2. Complex frequency modulations with *very low modulation indices* will cancel in an ideal processing circuit of a folded Doppler or zero frequency second IF processor.

Of course, the cancellation will disappear with movement of the clutter target with respect to the radar.

In general, the probability density characteristic for the phase between a stationary clutter return and the synchronous detector reference oscillator signal is rectangular. However, the appearance of maximum clutter return on the displayed bipolar video always will be accompanied by maximum cancellation of transmitted FM sidebands.

An analysis of the effects of amplitude modulation on a folded Doppler data processor will show that the reverse situation applies and that maximum clutter video is accompanied by in-phase addition of the sidebands.

Coherent radar designs must reject moving clutter, and consequently the character of unintentional frequency modulations must be closely monitored during radar development and test.

When unwanted modulations are very complex or perhaps random, large numbers (perhaps all) of the contiguous filters in both of the previously discussed automatic target detectors will contain extra energy. The real target detection sensitivity of the circuitry therefore will be reduced and become a function of the clutter or transmitter feedthrough levels. Subclutter visibility, therefore, is directly related to the level of unwanted wideband modulations of the radar stamo or RF power amplifier.

The testing of coherent radar systems often is conducted at stationary facilities using the local environment as the test clutter for clutter rejection measurements. The return from the largest clutter appearing on a bipolar display is examined for alarm activity. An appreciation of the FM cancelling effects possible with a folded Doppler system may explain discrepancies in measured clutter rejection levels on a day-to-day or mo-

ment-to-moment basis. Wind at velocities much lower than the desired minimum target velocity may cause movement of the clutter reflectors (trees, waves, etc.) and reduce the degree of transmitted FM sideband cancellation obtained. If the unintentional modulation peaks in one of the alarm filters, false alarms on the clutter return will result.

The use of FM measuring techniques to determine coherent radar performance is valid and, under special circumstances, may be considered conservative in that the clutter rejection performance actually obtained may be better than that predicted on the basis of spectral energy content alone.

Upper tolerances on FM noise are determined by the clutter rejection and subclutter visibility performance desired and the sensitivity of the target detection circuitry. The following example may be considered as representative of one class of coherent radars:

System Requirements—

Clutter rejection = 100 db

(for $P(\text{alarm}) = 0.5$)

Subclutter visibility = 70 db

(for $P_D = 0.5$)

(and $P_{FA} = 10^{-6}$)

Considering an ideal version of the signal processor shown in Figure 4–8 (or Figure 4–9 with slowly moving clutter), an assumption is made that the filter characteristics are rectangular and that the hard limiter has infinite gain. This latter assumption will guarantee that the hard limiter output power will remain essentially constant even with severe clutter limiting and "front-end" noise suppression in the preceding IF circuitry.

To achieve a probability of detection of 0.5 and a false alarm probability of 10^{-6} with a nonfluctuating signal requires a signal-to-noise ratio *at the threshold detector* of about +11 db (see Reference 8). The signal-to-noise ratio *in the receiver (first IF amplifier) passband* which corresponds to this level may be in the order of −10 db.

Subclutter visibility of 70 db for this processor therefore requires that noncoherent sideband energy in the receiver passband be at least 60 db down from the carrier energy.

On the other hand, clutter rejection of 100 db requires that coherent sidebands (signals in a single CFAR filter) be greater than 110 db below the carrier energy.

In this example, ideal worse-case sorts of FM noise were postulated by considering the effect of band-limited "white" noise on subclutter visibility and the effect of narrow-band coherent noise on clutter rejection. Actual "non-white" random noise or multiple frequency coherent noise will cause intermediate results.

In the real world of nonideal circuitry, other problems such as internal data processor noise also must be considered and conquered.

CONCLUSIONS

The frequency stability of a radar master oscillator may be expressed in terms of equivalent frequency modulation deviations in specified bandwidths or as the db ratio between specific sidebands and the carrier. With the normally low unintentional modulation levels encountered, a sophisticated monitoring technique or the complete radar system is required to determine whether satisfactory radar clutter performance can be achieved. A simple dc offset technique for calibrating the frequency deviation measurement instrumentation used with a solid-state stamo multiplier chain has been discussed. The use of solid-state oscillator-multiplier chains as sources of RF energy has allowed a large reduction in unintentional noise created by a vibrating environment; and consequently a restriction on the maximum clutter rejection achievable from a moving, vibrating radar platform is relaxed.

ACKNOWLEDGMENT

The writers wish to express their thanks to Mr. J. B. Higley for his careful and helpful review of this paper.

REFERENCES

1. Gillespie, N. R., Higley, J. B., and Mackinnon, N., "The Evolution and Application of Coherent Radar Systems," *Trans. PGMIL*, Volume MIL–5, Number 2, April 1961.
2. Mager, H., Johnson, S. C., and Calder, D. A.,

"Noise Spectrum Properties of Low Noise Tube and Solid State Sources," *Symposium on Definition and Measurement of Short-Term Frequency Stability*, November 1964. [See Paper 16, *this Volume*].

3. JAMES SCOTT (Electronics Engineering) Ltd., Glasgow, E.Z., Scotland, "Technical Note on Improved High Power Noise Measuring Equipments Type 123," issued September 1962.
4. ASHLEY, F. R., MONTGOMERY, H. R., and POLKA, F. M., "Low Spurious Modulation Klystron Oscillators for Transmitter Applications," IEEE Winter General Meeting, January 31, 1963.
5. WHITWELL, A. L., and WILLIAMS, N., "A New Microwave Technique for Determining Noise Spectra at Frequencies Close to the Carrier," *Microwave Journal*, November 1959.
6. BOSCH, B. G., GAMBLING, W. A., and WILMSHURST, T. H., "Excess Noise in Microwave Mixer Crystals," *IRE Proceedings*, July 1961, pp. 1226–1227.
7. SCHWARTZ, M., "Information Transmission, Modulation and Noise," McGraw-Hill Book Company, Inc., 1959, p. 118.
8. HALL, W. M., "General Radar Equation," *Space/Aeronautics R&D Handbook*, 1962–1963.

5. SATELLITE RANGE AND TRACKING ACCURACY AS A FUNCTION OF OSCILLATOR STABILITY

J. J. CALDWELL, JR.

*TRW Systems**
Redondo Beach, California

Guidance, tracking, and communication requirements of earth satellites and space systems often demand high-stability oscillators. Some system types need high-order short-term, yet modest long-term, stability. In other systems emphasis must be placed on long-term stability with short-term stability playing a minor role. Under other circumstances stability over a wide range of observation periods must be considered. Systems of each type are briefly examined, and the effect of oscillator stability on system performance is discussed.

Oscillators are used in spacecraft for a variety of purposes, such as range and range-rate measurements for orbit determination, timing for telemetry systems, etc. Emphasis is on system simplicity, reliability, minimizing weight, and power consumption. Functions performed on the spacecraft are minimized at the expense of those which can be kept on the ground.

Cataloging of oscillators for spacecraft is difficult because the requirements are mission-dependent, a large variety of missions exists, and the development of the art is rapid. Oscillators for many (if not most) spacecraft uses are proved in the circuitry by operational tests and are not fully specified in purchase specifications.

Figure 5–1 shows the requirements for several systems. The system clock for OGO, POGO, EGO utilizes a 256-kc GT cut crystal operated in the environment of the spacecraft without the benefit of an oven. Stability of 10^{-5} is required over the expected $-14°$ to $+45°$C temperature range. Stability of 10^{-6} for 1 hour is required over a $\pm 1°$C range expected in the spacecraft during this period. Stability for periods shorter than 1 hour is unspecified.

The requirements for OMEGA (References 1 and 2), a Navy VLF navigation system, were placed on this figure for comparison purposes only. Recalibration is planned at 24-hour intervals.

The requirements labeled "Red Shift Experiment" in Figure 5–1 were purposely made lenient by the authors (Badessa, Kent, Howell, and Searle—Reference 3) to emphasize that measurements necessary to determine the altitude-dependence of the gravitational red shift could be made with oscillators available in 1959. The proposed experiment utilized measurements made

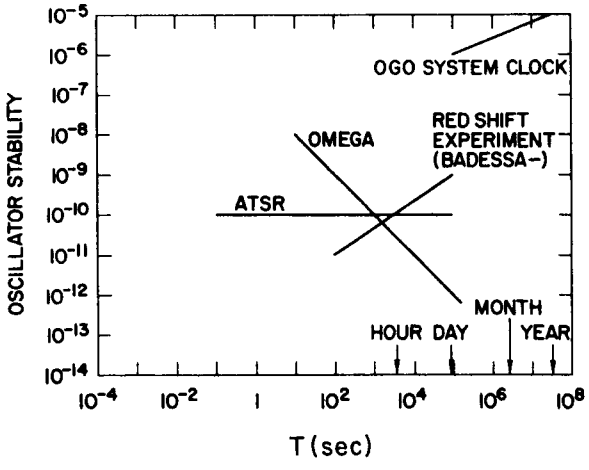

FIGURE 5–1.—Oscillator stability requirements for three satellite systems and a VLF navigation system.

* Formerly TRW Space Technology Laboratories, Inc.

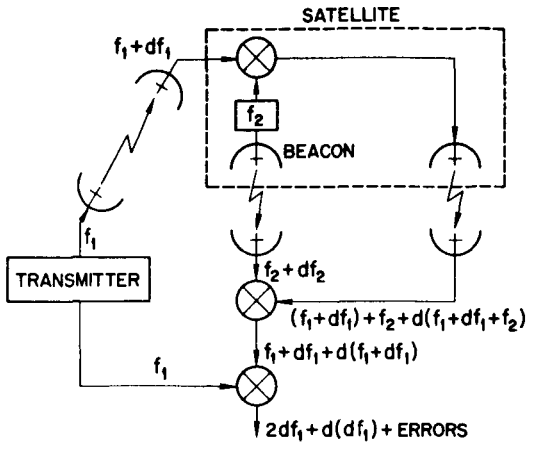

FIGURE 5-2.—The Syncom beacon Doppler measurement system.

on many satellite passes to minimize stability requirements of the oscillator in the satellite.

The line (Figure 5–1) marked ATSR represents the stability requirement of the master oscillator, located in ground equipment, for the Advanced Technical Satellite. The target accuracy for the range rate for this system is 0.01 meter/second. Requirements on the oscillator in the satellite are minimized by the use of a beacon system.

Figure 5–2 shows a block diagram of a beacon system as used in Syncom. The signal transmitted to the satellite is offset in frequency by a local oscillator in the satellite prior to retransmission. The oscillator output also is transmitted to the ground and is used in processing the received Doppler signal to remove long-term frequency shift and short-time fluctuations within loop capabilities. The advantage of transmitting the L.O. signal to the ground is that it allows the L.O. to be of poorer quality than would otherwise be necessary. For this technique to be effective, it is necessary that the phase-lock loops in the ground receivers be capable of following accurately the received signal fluctuations. Since the loop bandwidths are determined by other considerations, a limit must be imposed on the noise introduced by the L.O. and by other system oscillators.

The transmitter oscillator must meet the stability requirements imposed by range-rate accuracy requirements. Range measurements, made on side tones, place less severe requirements on transmitter oscillator stability.

An examination of the block diagram will show that both short- and long-term changes of the satellite local oscillation are completely cancelled out if the transit time for the beacon frequency and the offset frequency are equal and if the receiver loops track perfectly. However, each loop has a tracking error which is influenced by the satellite L.O. as well as by the phase-lock loop oscillators in each receiver.

Requirements on each of the oscillators can be estimated by an analysis of the entire system, assigning an error budget to each error source on the basis of achievability and available methods of calculating the individual errors. The satellite local oscillator, being in a hostile environment, might for instance be assigned a principal portion of the error budget.

PHASE-LOCK LOOP REQUIREMENTS

Oscillator noise introduces a tracking error into the second-order phase-lock loop of the receiver. Following the method of Develet (Reference 4), an estimate of the required equivalent coherence time of the several oscillators can be made. A stability requirement for the satellite local oscillator can now be determined under the assumption that it is the principal noise contributor.

Oscillator stability requirements for the phase-lock loop—assuming white-noise spectrum—are, according to Develet,

$$S=(2\epsilon/W_0)\,(\zeta W_n/\rho)^{1/2},$$

where

ϵ = allowable tracking error (radians),
W_0 = frequency (radians/sec),
W_n = noise bandwidth (radians/sec),
ρ = time for measurement of S (sec),
ζ = loop damping factor.

Phase-lock loops for earth satellites are typically 100 cps for the main receiver tracking loop and perhaps 1 cps for a tone filter loop. Allowable tracking errors, determined by many factors, range from 0.1 to 0.01 radian. Stability requirements for phase-lock loop oscillators are typically 2×10^{-8} to 1×10^{-11} for periods of 0.01 to 1 second.

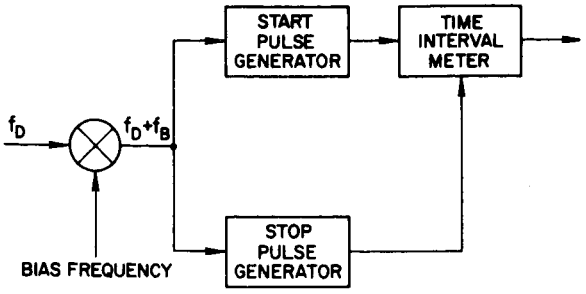

FIGURE 5–3.—The Doppler frequency measurement system.

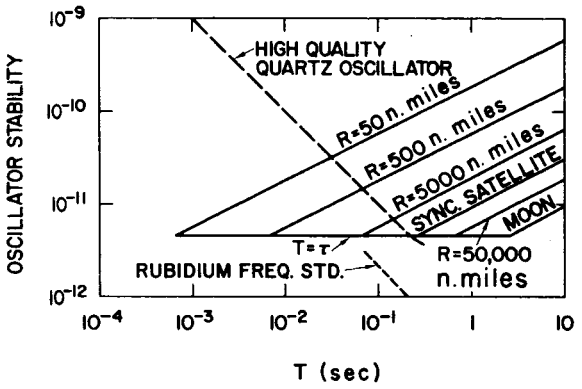

FIGURE 5–4.—Transmitter stability requirements assuming range-rate error of 0.001 meter/sec contributed by white-noise oscillator.

Third-overtone mode crystals are customarily used because of the requirement for a large pulling range. Performance of the crystal in the phase-lock loop is considerably better than Develet's expression would indicate.

TRANSMITTER OSCILLATOR STABILITIES

Consider the requirements which might be imposed on the transmitter oscillator of Figure 5–2. The transmitter is located on the ground, subject to a gentle environment; and it is reasonable to design so that its contribution to error is small compared with contributions from other sources. Develet (Reference 5) has shown that—for a system (Figure 5–2) where a frequency is generated, transmitted, coherently transponded, received, detected against the transmitted signal to yield the Doppler frequency, and the Doppler frequency measured by counting cycles (Figure 5–3) for a known time interval–the oscillator stability required is given by

$$S=(T/CR)^{1/2}\dot{r}_\epsilon=(2T/\tau)^{1/2}(\dot{r}_\epsilon/C),$$

$$0<(\tau/T)<1,$$

$$S=2(\dot{r}_\epsilon/C), \qquad 1\leq(\tau/T)<\infty,$$

where

S = oscillator stability for period T,
C = velocity of propagation,
τ = propagation time,
T = cycle counting period,
R = range,
$\dot{r}_\epsilon$ = range-rate error due to oscillator noise.

Assume that a system requirement is 0.01 meter/sec range-rate accuracy. Assign an error budget of 10 percent to the transmitter oscillator stability. The stability requirements for 0.001 meter/sec range-rate error are shown in Figure 5–4 as a function of counting period. The line marked $T=\tau$ represents the stability requirement for a counting period equal to the transit time. The counting period for most earth satellite range-rate measurements is 0.2 to 4 seconds—long enough to get good averaging, short enough to avoid errors from satellite acceleration. Note that, particularly for short ranges, limiting the range-rate error from this source to 0.001 m/sec places severe requirements on the transmitter oscillator stability.

REFERENCES

1. BROGDEN, J. W., COVEY, A. W., and WILLIAMS, M. F., "The Omega Navigation System," *Frequency*, March–April 1963.
2. Private Communication, C. J. Casselman, U.S. Naval Electronics Laboratory, San Diego, Calif.
3. BADESSA, R. S., KENT, R. L., NOWELL, J. C., and SEARLE, C. R., "A Doppler Cancellation Technique for Determining the Altitude Dependence of Gravitational Red Shift in an Earth Satellite," *Proc. IRE, 48*, p. 758.
4. DEVELET, JEAN A., Jr., "Fundamental Sensitivity Limitations for Second-Order Phase-Lock Loops," TRW Space Technology Laboratories, 8616–0002–NU–000. *Presented before International Scientific Union (URST), Spring Meeting*, May 4, 1961, Georgetown University, Washington, D.C.
5. DEVELET, JEAN A., Jr., "Fundamental Accuracy Limitations in a Two-Way Coherent Doppler Measurement System," *IRE Transactions on Space Electronics and Telemetry*, September 1961.

6. SHORT-TERM STABILITY REQUIREMENTS FOR DEEP SPACE TRACKING AND COMMUNICATIONS SYSTEMS*

R. L. SYDNOR

Jet Propulsion Laboratory
California Institute of Technology
Pasadena, California

The use of phase-locked receivers in unmanned deep space exploration requires a high degree of phase stability in the transmitter and receivers used in the Deep Space Network. Present requirements are based on available transmitter power, receiver noise temperature and range of planned targets, as well as required accuracy of measurements. The requirements are for the system phase noise, as measured in a double-sided noise bandwidth of 5 cps, to be less than 0.2 radian rms at S-band. The actual performance of an operational S-band system has been measured as less than 0.05 radian rms. Requirements and performance of a developmental X-band system are described.

Correlation techniques using a digital data handling system on line have been used for extreme range experiments. This system is used for planetary and lunar mapping experiments and is applicable to extreme range, low-bit-rate telemetry and communications. The requirements on this system are the same as for the phase-locked system with the additional requirement that the frequencies be continuously variable and controlled to an accuracy of 1×10^{-10} and a stability of 1×10^{-11} for a 4-second averaging period.

Several methods of measuring short-term stability are used, depending on the final requirements of the system and the use to which the system will be placed. These methods are discussed in detail, and representative data are presented.

Tracking of unmanned deep space probes and communications with these probes is performed by the NASA Deep Space Instrumentation Facility (DSIF), managed by the Jet Propulsion Laboratory. The DSIF is a precision tracking and data acquisition network which is designed to track, command, and receive data from deep space probes. It utilizes large antennas, low-noise phase-lock receiving systems, and high power transmitters at stations positioned approximately 120 degrees around the earth. Its policy is to continuously conduct research and development of new components and systems and to engineer them into the DSIF so as to maintain continuously a state-of-the-art capability.

*This paper presents results of one phase of research carried out at the Jet Propulsion Laboratory, California Institute of Technology, under Contract No. NAS 7-100, sponsored by the National Aeronautics and Space Administration.

DESCRIPTION OF DEEP SPACE COMMUNICATION SYSTEMS

Normal communication with a spacecraft is depicted in Figure 6-1. The ground transmitter-exciter is shown in Figure 6-2. The required submultiple of the transmitter frequency is synthesized from the station atomic frequency standard. This frequency is passed through a narrow-band phase-locked loop which serves to filter out any of the spurious signals remaining from the synthesis process and to produce a signal which has the short-term stability of the specially designed crystal oscillator and the long-term stability of the atomic standard. This output signal is multiplied to the required transmitter frequency and amplified to the full 10-kw output for transmission to the spacecraft. Communication to the spacecraft is achieved by means of phase modulation of the low-level signal before the final amplifier.

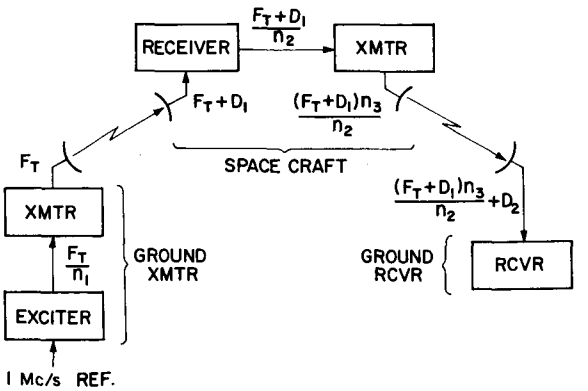

FIGURE 6–1.—Spacecraft communication system.

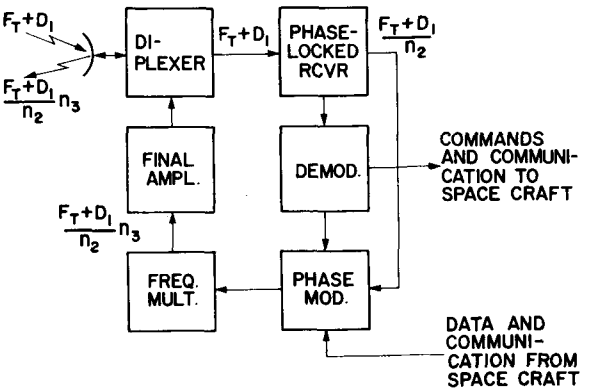

FIGURE 6–3.—Spacecraft receiver/transmitter.

This communication is in the form of commands for the spacecraft, or ranging codes.

The spacecraft transponder is shown in Figure 6–3. The phase-locked receiver produces several outputs: (1) a submultiple $(1/n_2)$ of the received signal for driving the spacecraft transmitter, (2) demodulated commands to the spacecraft, and (3) demodulated ranging codes.

The $1/n_2$ submultiple of the received signal is multiplied by n_3, amplified, and transmitted back to the ground. The ranging code is used to remodulate the transmitted signal as are the data signals from the spacecraft. The signal-to-noise ratio in the spacecraft receiver is high because of the high antenna gains both on the spacecraft and the ground and because of the high power output of the ground transmitter.

The ground receiver is shown in Figure 6–4. The receiver is a phase-locked loop and has demodulators for extracting the modulation on the received carrier. The recovered ranging modulation is compared with the modulation impressed on the signal transmitted from the ground, and the data modulation is decoded to complete the communication link with the spacecraft. Because of the power limitations in the spacecraft and the resulting low power output of the spacecraft transmitter, the bandwidth of the ground receiver is very narrow to maintain as high a signal-to-noise ratio in the receiver as is possible, commensurate with required tracking rates.

PHASE NOISE REQUIREMENTS FOR SEVERAL SYSTEMS

The short-term stability of the ground transmitter is made very high in the above system by means of a high-quality crystal oscillator. Since the signal-to-noise ratio in the spacecraft receiver

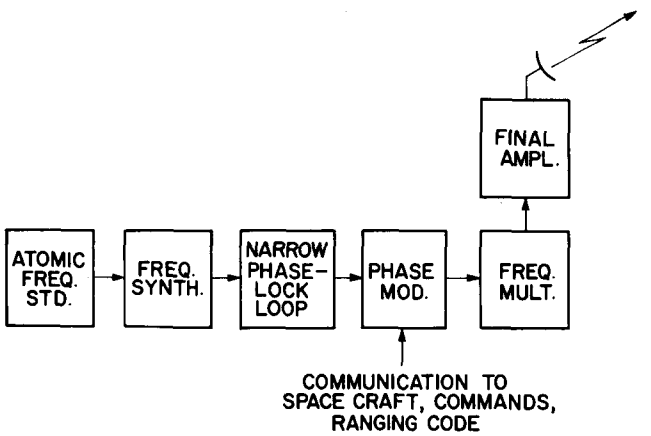

FIGURE 6–2.—Ground transmitter.

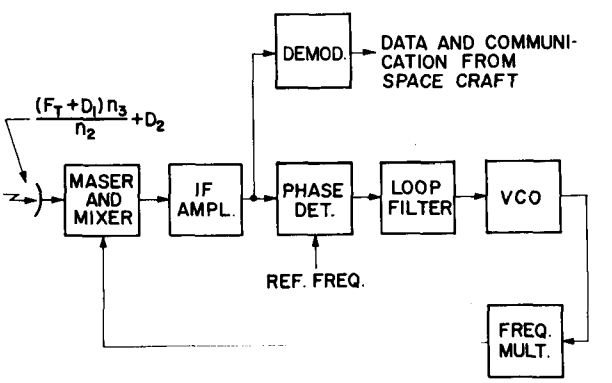

FIGURE 6–4.—Ground receiver.

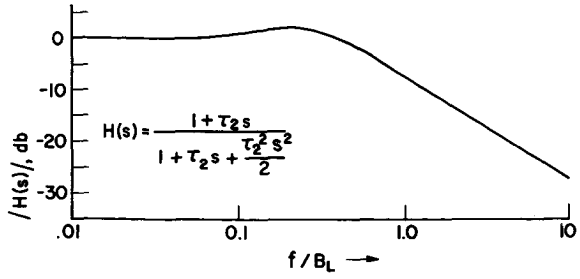

FIGURE 6–5.—Phase-locked loop frequency response.

is high and the bandwidth is large (compared with the ground receiver), the deterioration of the phase noise of the signal due to the spacecraft is negligible. The only effect the spacecraft has is to shift the frequency from input to output by the factor n_3/n_2. *The phase noise observed in the ground receiver is then due to the instability of the ground transmitter oscillator, the instability of the ground receiver oscillator, and any thermal noise introduced at the receiver input.* This statement is made under the assumption that none of the other parts of the system contributes significant amounts of phase noise. Extensive measurements over a period of many years with all the systems used to date indicate that this assumption is justified, since the total contribution due to these sources is no higher than 10 percent of that due to the oscillators.

The usual specification on phase noise is that it be low enough to degrade the system threshold a negligible amount. Threshold of the receiver is defined as the signal level at which the phase noise reaches 1 radian rms. The oscillator contribution is usually specified as some fraction of 1 radian rms at strong signal at a prescribed receiver bandwidth. The transfer function of the receiver

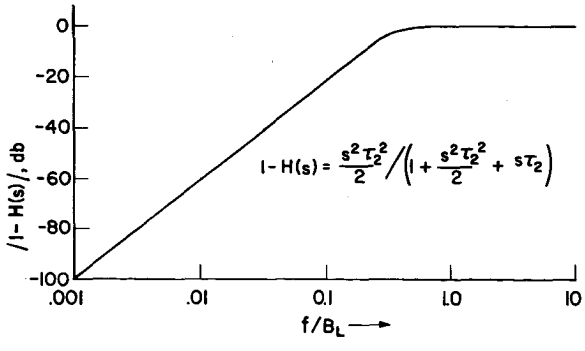

FIGURE 6–6.—Phase-locked loop frequency response.

at its design bandwidth is given by

$$H(s) = \frac{1 + s\tau_2}{1 + s\tau_2 + \frac{1}{2}(s^2\tau_2^2)}; \qquad (1)$$

this is plotted in Figure 6–5.

It is seen that the system is of second order with a damping factor of 0.7. The double-sided noise bandwidth of this system is given by

$$2B_L = \tfrac{3}{2}\,\tau_2^{-1}. \qquad (2)$$

The response of the loop is usually measured at the error point in the servo system. The transfer function measured at this point is given by

$$1 - H(s) = \frac{\frac{1}{2}(s^2\tau_2^2)}{1 + s\tau_2 + \frac{1}{2}(s^2\tau_2^2)};$$

this function is plotted in Figure 6–6.

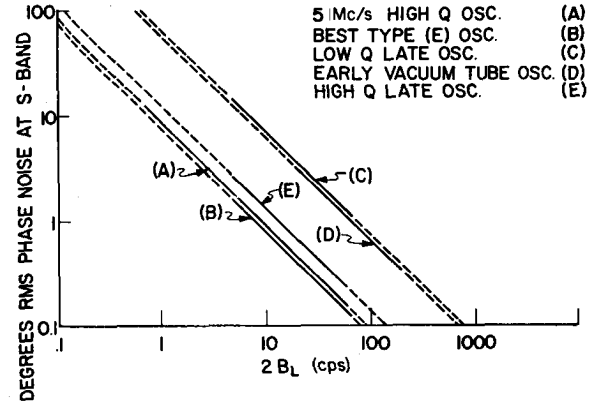

FIGURE 6–7.—Loop noise bandwidth.

Measured phase noise versus loop noise bandwidth for several different types of oscillators is shown in Figure 6–7. Several things may be noted from this figure: first, the characteristic $1/2B_L$ dependence of phase noise on bandwidth predictable from the thermal noise characteristics predominates (Reference 1); second, the gradual improvement with time may be noted from curve (D)—an early vacuum-tube oscillator circa 1958, and from curves (E) and (B)—a late model transistorized high-Q oscillator circa 1964.

PLANETARY RADAR SYSTEMS

An S-band system for use in planetary/lunar radar experiments was designed and built in 1962.

TABLE 6-1

Characteristic	Specification	Performance
Phase stability	<1 rad rms ($2B_L$=5 cps)	<0.05 rad rms
Frequency stability:		
10 hr	1×10^{-9}	$<5\times10^{-11}$
10 min	1×10^{-10}	$<5\times10^{-11}$
Tuning accuracy	1×10^{-9} continuously (4-sec gate time)	1.3×10^{-10}
Spectral purity	1×10^{-9} over tuning range	1.5×10^{-10}
Tuning range	±1.5 months of conjunction with Venus ($\pm1\times10^{-4}$)	±6 months ($\pm5\times10^{-4}$)

The specifications on this system and measured performance are presented in Table 6-1.

The phase stability of this system is the same as the value obtained from curve (E) in Figure 6-7 and is almost entirely due to the oscillators used in the receiver and transmitter. The 10-hour and 10-minute frequency stabilities are due to the station atomic frequency standard, a rubidium-vapor frequency standard. Tuning accuracy is measured as the error in the servo loop which slaves the output frequency of the local oscillator to a punched paper tape of Doppler frequency computed from the planet ephemeris. A diagram of the tuning servo on the latest system is shown in Figure 6-8. This particular arrangement is used to obtain the frequency stability and accuracy required without degrading the phase noise of the basic oscillators or the long-term stability of the frequency reference. The voltage-controlled oscillator (VCO) only covers enough of a frequency range to follow the Doppler variation for 1 day. This range is changed each day by changing the output frequency of the frequency synthesizer. The counter operates on a 4-second gate time for ±0.25 cps resolution ($\pm1\times10^{-10}$). The error is due to the ±1 count ambiguity of the counter, round-off errors in the Doppler tape, and instability of the 475 kc/sec VCO. Since the ±1 count ambiguity in the counter is $\pm1\times10^{-10}$ of the output frequency and the measured performance is 1.3×10^{-10} rms, it is obvious that the stability of the VCO represents only a small portion of the error. However, since 1×10^{-10} of the output frequency represents approximately 70×10^{-10} of the oscillator frequency, the oscillator requirements are not too severe and are easily met by a VCO with a $\pm2\times10^{-4}$ control range. The total tuning range of the local oscillator is the sum of the ranges of the VCO and the frequency synthesizer. The voltage-controlled oscillator covers $\pm3.2\times10^{-6}$ at the output, so that nearly the total range of $\pm5\times10^{-4}$ is covered by the frequency synthesizer.

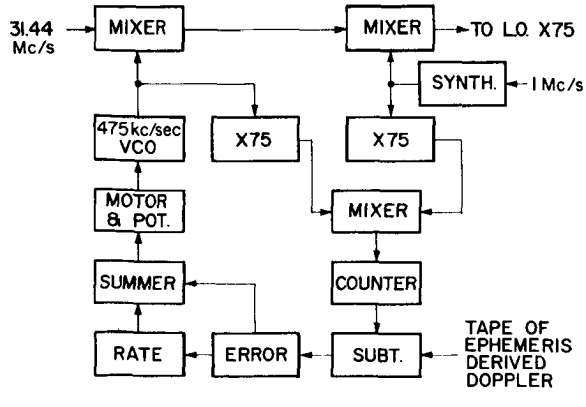

FIGURE 6-8.—Programmed local oscillator for planetary radar.

An X-band system similar to Figure 6-8 has been constructed. The only difference in the two systems is the frequency multipliers, which were changed to X240 to correspond to the multiplication factor of the local oscillator multiplier

TABLE 6-2

Characteristic	Specification	Performance
Phase stability	<0.2 rad rms ($2B_L$=5 cps)	0.15 rad rms
	<0.1 rad rms ($2B_L$=10 cps)	0.075 rad rms
Frequency stability:		
10 hr	5×10^{-10}	5×10^{-11}
11 min	5×10^{-11}	5×10^{-11}
Tuning accuracy	3×10^{-10} (4-sec gate time)	5×10^{-11}
Spectral purity	3×10^{-10}	1.3×10^{-10}
Tuning range	$\pm5\times10^{-4}$	$\pm5\times10^{-4}$

chain. The specifications and measured performance of this system are presented in Table 6-2.

Since the same type of oscillator is used in the receiver and in the transmitter as in the S-band system, the rms phase noise of the X-band system would be expected to be higher than the S-band system by the ratio of the frequencies, 3.5:1, as demonstrated by the above data. The improvement in tuning accuracy is due to the increase in the output frequency, since at X-band the ±1 count uncertainty of the counter represents only $\pm3\times10^{-11}$ instead of the $\pm1\times10^{-10}$ at S-band. The stability of the oscillator is estimated, from the above data and the characteristics of the round-off procedure in the Doppler tapes, as contributing approximately $\pm3\times10^{-11}$ to the stability of the system. At the oscillator itself this would be $\pm2\times10^{-9}$ for a 4-second gate. This stability does not approach that of a high-quality fixed-frequency standard, which can be as low as 1 part in 10^{11} or 10^{12} but is representative of the performance of a relatively high swing VCO operating with fundamental crystals at 500 kc/sec. The calculated stability of this oscillator due to thermal effects alone from (Reference 2) is $\Delta f/f=3\times10^{-13}$ for a 4-second gate time. The discrepancy between the actual and calculated values has been traced to several causes: (1) the stability of the voltage references used to generate the control voltage contributes nearly 1×10^{-9} of the measured stability; (2) the oven is a single-stage proportional-control device with relatively poor performance which contributes an estimated 5×10^{-10}, and (3) the noise and drift of several of the components have been found to be excessive and are being investigated. The oscillator itself is a Colpitts or Clapp type with ALC, as are all the oscillators described here.

SHORT-TERM STABILITY MEASUREMENTS

Several methods have been used to obtain data on the short-term stability of oscillators and standards. The usefulness of any one method depends mostly on the practical measuring difficulties of making the measurement and on the use to which the data are put. The different forms of the resulting data are useful for different purposes. While it is true that, if one set of data is

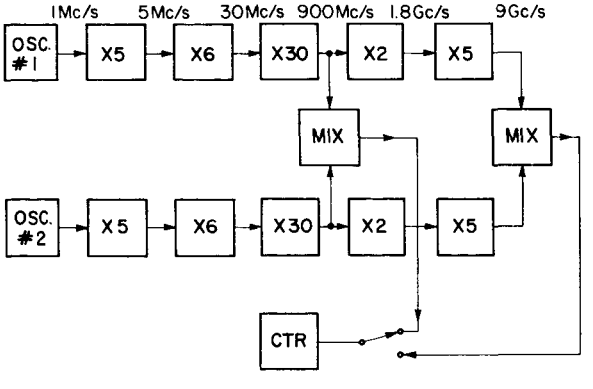

FIGURE 6-9.—Short-term measurements for histograms.

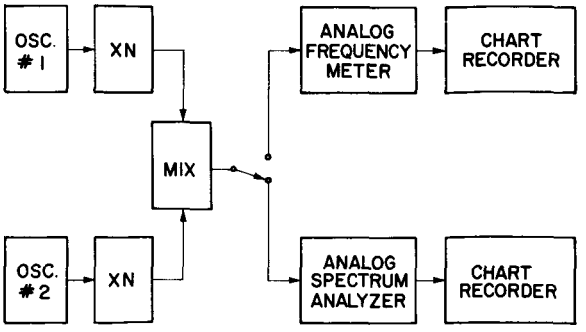

FIGURE 6-10.—Analog short-term stability measurements.

available, the other data may often be derived from it, a number of assumptions must be made to do this. To eliminate these assumptions, the data are taken in the required form directly.

Possibly the most straightforward measurement is the direct counting of the difference frequency between two standards with appropriate frequency multiplication to obtain the required accuracy. An implementation of this method, which has been used for evaluation of atomic standards, is shown in Figure 6–9. A histogram is made of the counts and the rms deviation—that is, standard deviation—from the mean calculated. Care must be made to insure that any long-term drifts are removed from the data so that they do not obscure the short-term data. A good indication as to the character of the short-term statistics may be obtained by this method by comparing a Gaussian error curve with the same standard deviation to the measured data and by calculating the second moments.

A second method, which is applicable to the evaluation of a planetary radar system, is to use

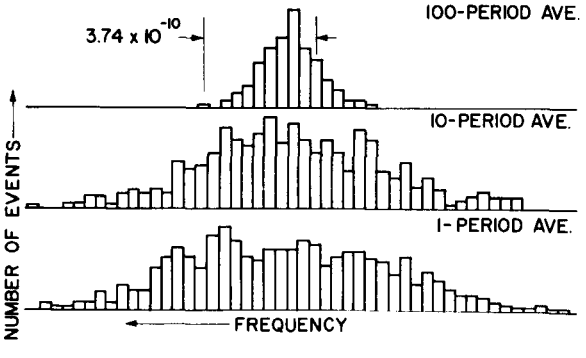

FIGURE 6-11.—Various histograms (5.4 sec, 540 msec, and 54 msec average) of cesium standards at 9 Gc/sec.

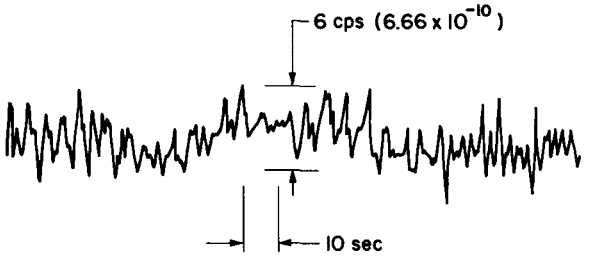

FIGURE 6-12.—Analog frequency recordings of cesium standards at 9 Gc/sec.

the actual radar system as described above with the Doppler tape programmed such as to produce a constant frequency. An on-line computer used during the experiment to obtain the spectrum of the return signal will now measure the spectrum of the overall system. The computer determines the spectrum by measuring the autocorrelation function and taking the sine transform to find the spectrum. The autocorrelation and computer

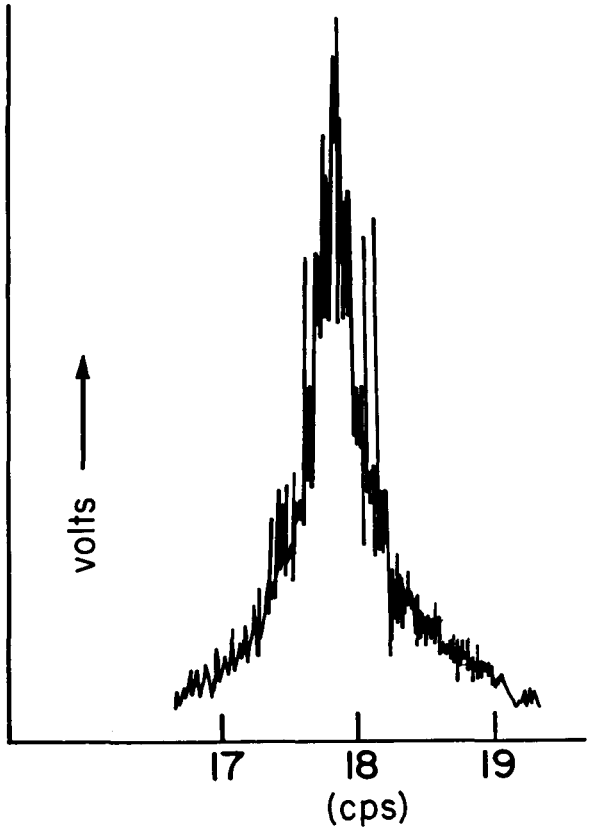

FIGURE 6-13.—Analog spectrum analysis, cesium standards at 900 Mc/sec; 2 atomichrons.

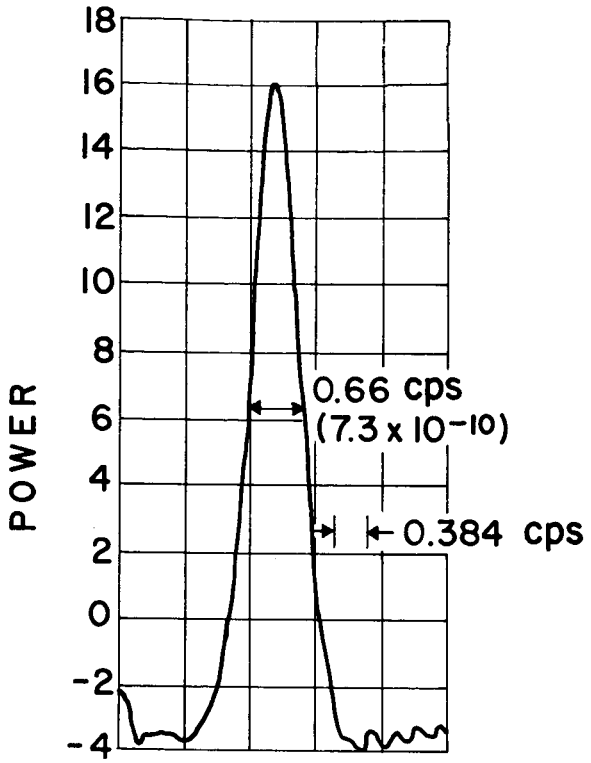

FIGURE 6–14.—Digital spectrum analysis, cesium standards at 900 Mc/sec; 2 atomichrons.

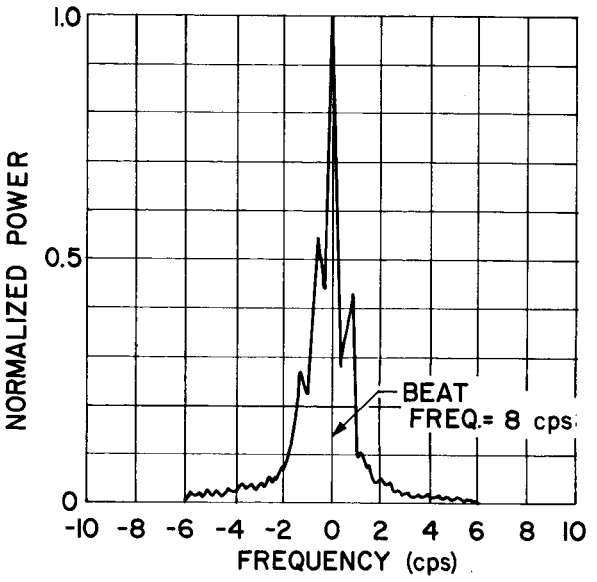

FIGURE 6–15.—Planetary radar system.

may be used independently of the rest of the system to measure spectra of oscillators and has been used for the evaluation of atomic standards.

A third method, which is useful for obtaining a measure of the behavior to be expected of a return Doppler signal from a spacecraft or from planetary

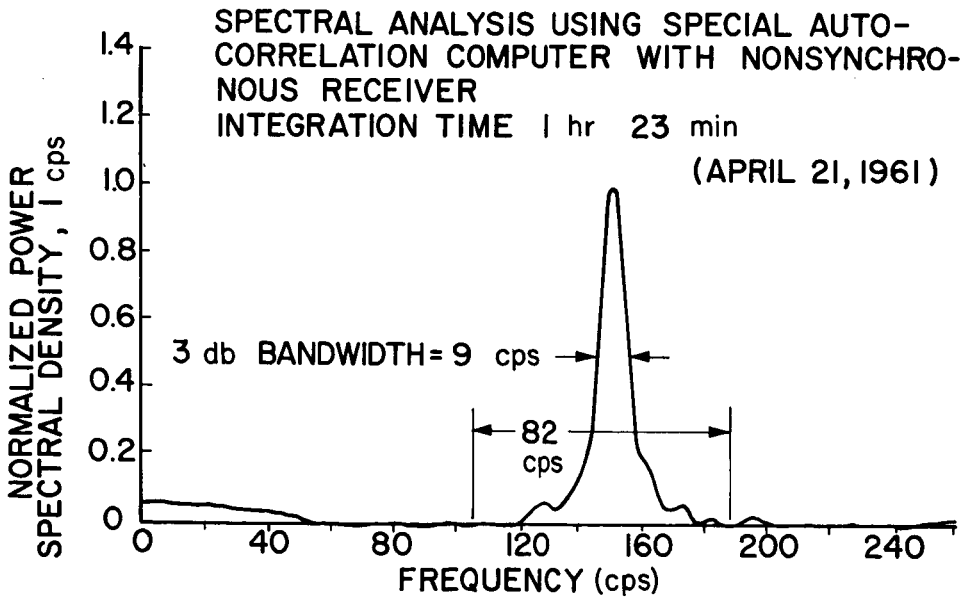

FIGURE 6–16.—Venus spectrum S-band radar.

TABLE 6-3

Measurement	Cesium standard	Commercial Rb standard	Lab. Rb standard	Radar receiver
50 msec av.	4.7×10^{-10}	5×10^{-11}	3×10^{-11}	—
500 msec av.	4.3×10^{-10}	2×10^{-11}	1.4×10^{-11}	—
5 sec av.	1.1×10^{-10}	0.5×10^{-11}	0.4×10^{-11}	—
8 min av.	1.1×10^{-10}	0.4×10^{-11}	0.5×10^{-11}	—
Spectrum width	3.7×10^{-10}	0.4×10^{-11}	0.5×10^{-11}	5×10^{-10} with Cs 5×10^{-11} with Rb

radar signals where the round-trip time is long enough that the data are essentially uncorrelated, is shown in Figure 6-10. A record is obtained of frequency vs. time in an analog form which is useful for estimating possible deviations due to the oscillator themselves, independent of spacecraft or planetary perturbations.

Representative data from these three methods are shown in Figures 6-11 through 6-16. A compilation of the data for a number of different types of standards and oscillators is shown in Table 6-3.

A fourth method of measuring short-term stability, which is useful in phase-lock systems, is the measurement of phase noise in a system as described above. While the data thus obtained are difficult to relate to the data obtained by other methods, a rough correlation may be obtained. For the evaluation of oscillators for use in such a system, this method is used exclusively because the data thus obtained are a direct measure of the quality of the oscillator for this particular puspose. Data for several oscillators obtained for this use were presented in the section on Phase Noise Requirements.

CONCLUSION

Short-term stability is a deciding factor in the design and implementation of spacecraft communications and planetary radar systems. With improved short-term stability in systems capable of continuous tuning, data rates may be lowered and/or communications distances increased with the same return power from the spacecraft or planetary echo.

As improved systems become available, experiments which depend on the improved performance are devised. Obtaining an accurate spectrum of the planet Venus requires narrow spectral width and high tuning accuracy as well as good medium- and short-term stability, since the return spectrum is only approximately 6-cps wide at S-band, the round-trip time is 6 minutes, and the integration time in the computer may be set at 6 minutes to several hours. With the improved performance available from the planetary oscillator system, mapping of planetary irregularities is being performed. Low-data-rate systems for long-lifetime, low-power unmanned solar system probes using the planetary radar receiver are possible.

REFERENCES

1. EDSON, W. A., "Noise in Oscillators," *Proceedings of the IRE*, Vol. 50, No. 7, pp. 1454–1456, July, 1962.
2. HAFNER, E., "Stability of Crystal Oscillators," *Proceedings of the 14th Annual Symposium of Frequency Control*, pp. 192–199, 1960.

PANEL DISCUSSION

SESSION I: USERS' VIEWPOINT AND REQUIREMENTS

Chairman	ROGER A. SYKES
Panel Members	ELIE J. BAGHDADY
	EDMUND J. HABIB
	DAVID B. LEESON
	GERALD M. HYDE
Authors	G. F. JOHNSON
	J. D. HADAD
	W. A. SKILLMAN
	N. R. GILLESPIE
	J. J. CALDWELL
	R. L. SYDNOR

Dr. Baghdady.—This field has needed quite a bit of organization for quite some time, and I hope that as a result of this conference we are going to have a good start in that direction.

The main problem that I see, which seems to dominate the whole issue and applies specifically in this session, is the fact that people have not yet very clearly distinguished between two important aspects of what we are really talking about; namely, (1) the RF spectrum of the signal we are looking at; and (2) the instantaneous frequency or phase fluctuations or instabilities of that signal. You might say that the first aspect is a question of spectral purity, and the second is more directly the question of frequency stability.

In any application, we have to make a decision as to whether we are really interested in spectral purity, or instantaneous frequency, or phase instabilities. To just confuse the issue and hop back and forth between these, as if they are completely interchangeable, is a very bad mistake.

Now, the spectral purity question, of course, includes the instantaneous frequency characteristics; but the trouble is that people have not been really inspecting spectral purity when they say they are. Although they say they *are* concerned with spectral purity, they turn around and only measure frequency deviation, and things like that, and really get into trouble.

Frequency deviation and spectral purity are not interchangeable. This is very easy to demonstrate. The only thing that you can learn from frequency fluctuations is a measure of asymmetries in the spectrum.

Thus, the spectral impurity could be very high, which would make the oscillation really look bad. And yet you may measure a very small deviation, which shows no significant frequency instability. So we have to be careful in our approach here.

Unfortunately, in all of these papers, with some minor exceptions, this confusion is evident. Also, it shows up in the method of measurement.

Now, I would like to direct some specific observations with regard to each paper in the remainder of my comments. There is an awful lot that can be said in this area, by the way, but I have to hustle along.

To start with, the above general comments are particularly applicable to the first paper, although they are also applicable to the other papers.

In the second paper, I see some relationships used which were derived on the basis of assumptions that ignored higher order derivatives. Specifically, in the measurement of velocity, I couldn't detect anything in the results that should emerge from effects of acceleration; or, in the case of the acceleration, the results do not include the effects of higher order derivatives of the range or the distance. In my mind there is a doubt about the value of the equations used unless, indeed, the effects of higher derivatives have been taken into account, estimated, and judged to be negligible.

Then, of course, there is the question of RF spectrum and frequency instability and deviation, and so forth.

In the third paper, you begin to see more consciousness of the fact that a lot of the spectrum could only be caused by an AM effect. If you are really concerned with spectral purity, yes, you want to look at the RF spectrum; but if you are concerned with frequency stability, such as in applications where you try to compare the phases at two different times or the frequencies at two different times, then you want to look at frequency and phase instability, and not at the RF power spectral density.

In one of the papers relating to the determination of requirements on stability for satellite applications, some work was quoted in which, if I am not mistaken (I had looked at it a while ago), the author made some very sweeping assumptions about the character of the spectral density of the instantaneous frequency fluctuations. Unfortunately, the choice of spectral density is selected by the quoted writer which happens to simplify the analysis. However, it is totally inapplicable to the satellite mission, so the numbers are in grave doubt in that paper, if they were based on that formula.

Finally, I would like to direct some remarks to

Dr. Sydnor. The question of what kind of rms criterion to use for the phase error is really one that should be tied down to what you might call system resolution capability, not just an arbitrary analytical convenience. In particular, one radian rms doesn't seem to have any friends anywhere, in real analysis. Everything seems to be against it. Perhaps if you choose something smaller, you are getting closer to what you might normally require, but a lot of things get messed up when you begin to talk about rms errors in phase-locked loops in the order of one radian or more. I saw 100° on the projected slide which is about two radians. So my point is that the criterion should really be related to the observable damages or effects that instability can cause, rather than just arbitrary analytical convenience.

There is a considerable amount of discussion that is warranted in the area of measurements, and I would like to reserve this to this afternoon's session when we will have more to say. In the meantime, I would like to give you a hint that there are a lot of questions on the value (the general purpose value, and in fact the value for any particular application short of a lot of specifications about the masking effects of the measuring instruments) of the period counting technique and some of the other measurement techniques that we have seen. I am dodging this question right now because this will be the subject of more discussion in the remainder of this program.

Dr. Leeson.—As a coauthor, I am in no position to criticize any of the other papers, so I will refrain from that for the moment. I think that one thing we can agree on is that particularly for someone who might not eat, drink, or sleep radar or space tracking some of these definitions seem pretty loose. I have noticed a number of listeners gnashing their teeth at a number of things.

I think one thing I might comment on is that it does seem that there are two separate requirements in airborne radar, and systems of that sort, which deal with Doppler frequencies of the order of kc's or hundreds of kc's, as against the requirements for space tracking, or satellite tracking in which the data concerns are of a different sort. So I think there is perhaps a dichotomy of requirement here, to which it would be well to pay some attention.

The radar requirements, I have noticed, are perhaps surprising to some who have worked on stability of oscillators as concerned with communications applications. I can only assure anybody who doubts these 80, 100, 120 db sort of figures, that these are not only real requirements but in many cases are representative of present systems.

The same thing is true of the very narrow line widths required or mentioned in terms of deep space tracking.

One thing that doesn't come out in the papers, I think because every author is anxious to cover up the sloppy areas of his field, is that there is a lot of work that is going on that is sort of below the surface, a lot of hidden data.

For example, in your comment, Dr. Baghdady, regarding AM and FM, in most of the situations in which AM is ignored, somebody at some time found out by measurement or theory or combination that in that particular sort of situation it was all right. But it doesn't show up in these papers, and I agree it is a good point.

The definition based on a power spectrum as required in the doppler radar case or the actual characteristics of the instantaneous frequency or time function is something which ought to be dwelled on longer in attempting to establish a general definition of short-term stability.

One thing I might point out is that in all of these measurements, there is the ever-present opportunity for some bandwidth to be hidden in the measurement. For example, in our paper we talked about line width, as measured on a particular instrument; this instrument has some lower and upper bounds on its bandwidth and I am afraid that didn't come out in the paper. This is also true in the phase jitter measurement of the type which JPL is talking about. There is some upper bandwidth or at least some integral convergence which has to be considered, if you are going to treat the relationship between the spectrum and some measurements such as phase deviation as a function of time in a rigorous fashion.

I think that you can get some feel from the first four papers that the radar requirements are pretty much the same sort of animal in spite of the considerably different philosophies of the companies responsible for presenting the papers. I think this session has brought out the sort of

variables which people working in the two fields are comfortable with.

I think perhaps there is plenty of room for introducing rigor, and this will be the purpose of the session this afternoon. But I think that all of the papers this morning did a good job in establishing what you might call scale factors for thinking about the types and magnitudes of stability which people in radar and space tracking are concerned with.

Mr. Habib.—I would just like to make an observation here. To me at least it has become clear that we are really talking about two distinct types of tracking systems: one which is a cooperative one and one which isn't a cooperative one. There are advantages, I feel, at least in the cooperative one, in that the return frequency can be arbitrarily displaced from the transmitted frequency, making the problem a little easier. I think this is even true in the Venus tracking case where the doppler of Venus with respect to Earth effectively translates the frequency and again makes the problem easier.

I do think the two types become similar when you get near zero doppler, though, and then you see common problems. I would like to pass that observation on because I think there are two distinct types of problems here.

Mr. Hyde.—My interests are primarily, of course, in the planetary radar systems, satellite tracking systems, and as such I have been quite unfamiliar until this morning with some of the problems in the wide-band pulse doppler radars. I think it is clear, as Mr. Habib has said, there are two distinctly different sets of requirements. The radar astronomy problem appears to be one of extreme short-term stability on first examination. Long-term stability, however, enters the problem as well, since the range accuracy is determined by the stability of the timing system: i.e., round-trip travel times of twenty (20) minutes are not uncommon today.

Certain radar astronomy experiments have been such that the filter bandwidths required were one-tenth (0.1) of a cycle per second. In fact, we have programmed, in a general-purpose digital computer, and utilized results from filters as narrow as one one-hundredth (0.01) of a cycle. Obviously, if such a filter is to be useful, one has to have both long- and short-term stability in his frequency and timing standards.

Although radar echoes returned from even the most slowly rotating planet, Venus, have a fairly broad spectrum in these terms, it is not true that one filter equal in bandwidth to the received spectra is optimum. Certain planetary mapping techniques allowing fine-grain study of the planetary surface are limited in resolution primarily by the frequency and timing stability of the experimenter's system. Since the echo received is extended in range by an amount equal to the radius of the planet, it is apparent that the energy returned at a discrete range must have been reflected from an area on the planetary sphere described by a circular belt or annulus. Further, since the planets do rotate about their polar axes, one half of the planet is apparently approaching while the other half is receding if the observer is in the plane of the rotational axis at a constant distance from the planet. Although these ideal conditions never prevail very long, it is not difficult to normalize the velocity, i.e., doppler, measurements to the on-axis doppler. By observing the normalized frequency of the energy returned from a particular range, apparently one can determine from where on the planet the signal was reflected—with one ambiguity. That is, there are always two areas or cells of such a map: one in the northern hemisphere and one in the southern hemisphere, which cannot be resolved easily. Albeit, such a radar map is still of extreme scientific interest, and obviously the cell size and therefore the granularity of such a map is largely determined by the frequency resolution of the radar astronomer's equipment.

Mr. Sykes.—You have heard the users' viewpoints and requirements, and the observations of our panelists. What we would like to do now is to open the discussion to everyone, including the authors themselves, if they wish.

Dr. Mullen, (Raytheon Research Division).—First, I would like to make a comment about the first paper, in which the authors assume that the transmitter and the receiver local oscillators were uncorrelated. In some cases there are advantages to be gained by making them correlated. Now there are some noise suppression effects that can be achieved this way that can't be if you have independent oscillators. Using this correlation creates

range dependent effects and target dependent effects and there is no doubt that it would have made the paper very much more complicated to have discussed them. But in some cases the use of this correlation can be worthwhile.

Well, secondly, I would like to defend the speakers from some of Dr. Baghdady's comments. It is perfectly possible to tie together spectral purity and frequency deviations if one has a model of the situation that is actually occurring. I think that most of these papers have been based, as Dr. Leeson said, on models of the radar situation in which there is really good reason to believe that there is a unique tie-in between the two quantities. From a users' point of view these specifications represent real statements which when satisfied will guarantee good performance of the system.

Furthermore, these noise problems are really quite delicate so that you can't see the second order effects and need only explain the first order effects. Therefore, when the theory predicts effects which match the needed system tests, we can't spend the taxpayers' money to research the next order of effects.

Dr. Baghdady.—But I have serious doubts about your methods of testing as a matter of fact. I can prove anything to you by those methods of testing. There are operational parameters in each of these measuring techniques that can be manipulated. Unfortunately, quite often, the user of the results of the test measurements is not provided with sufficient information about the tests, how much influence the method of testing has upon the quantities observed, or whether the method of testing is really applicable to the user's circumstances. So I have my doubts about the methods of testing, particularly the assumptions and interpretations often made of what the results signify.

I agree with you, when we have a clear model of what is going on, the tie-in can be established in a unique manner. But unfortunately, there is no visible indication in anything that we have heard today to show that people have really searched for such a thing. Merely to say, "look, here are my computed numbers and here is my test curve and look how close they are 'among friends', there is agreement," does not prove anything, even "among friends". Instantaneous frequency fluctuations spread the spectrum, instantaneous amplitude fluctuations spread the spectrum, imbalance in amplitude and phase in the spectral distribution can cause disturbances, and so on. It is not enough to merely attribute all of the blame to the one effect that we happen to be obsessed with.

There is a tendency or implication when you measure only the rms frequency deviation to draw an equivalent sine wave model for the RF disturbance. That is very bad. You are dealing with something that has a high peak factor and you turn around and choose a signal model with a low-peak factor. You measure one number using your biased eyes or sensors to judge what it is, and then you claim that this number is a sufficient characterization of the RF spectrum or of the statistical properties of the frequency perturbations. In the end you don't know what you have. So what can you do?

Dr. Mullen.—Well, it is certainly true that when you measure things there may be a lot of nasty surprises when you actually go out to measure what or how the radar is performing, or how well the oscillator is performing. Most of these papers, I believe, have been the results of measurements that do agree with the predictions that were made ahead of time, or possibly ex post facto. If one has theoretical models which are capable of explaining everything that is actually found, then I think that is really adequate for the moment.

You know, it is certainly true that good engineers can find and solve more problems than bad ones, and if the people are going to do bad experiments, then that certainly is going to present lots of problems. But if you have a theory that matches good experiments, then I think that is adequate enough for the moment.

Dr. Baghdady.—Yes, this is what I am wondering; do we have such things?

Dr. Leeson.—I wonder if I could speak on that as far as the spectral density measurement. I think there is pretty good agreement. Well, you saw agreement this morning among three competing, strongly competing corporations, regarding the measurement of spectral density as it applies to an airborne doppler radar. I think this is one area in which, by the way the doppler radar operates, you can see you are concerned with spectral density. I agree that it was sort of slipped in that the noise spectral density is largely due to frequency vari-

ations. However, this happens to be the case in the sort of physical system which ends up being used in a doppler radar. That is to say, there is almost always some limiting mechanism somewhere, frequency multipliers typically enhance the FM sidebands and tend to either limit or at least don't increase the AM sidebands.

Dr. Baghdady.—It also, unfortunately, changes some amplitude fluctuations to phase or frequency fluctuations.

Dr. Leeson.—This is true, and this is a point which requires considerable caution. The resultant measurements, though, of spectral density do seem to correlate very well with the sort of field sensitivities that you actually achieve when you take a radar which you measure on a test set. There are a number of commercially available test sets for this sort of thing. There is a sort of a mystique that has grown up around them which I guess the papers this morning have made an attempt to let us in on. It has been found that there is good agreement between spectral density measurements made on this sort of equipment and the kinds of results that you get with a radar system. Because this is due to the fact that the radar system actually is characteristically the same sort of measuring instrument.

Dr. Baghdady.—I would like to remind you that I tried to make a distinction. I wasn't saying that one of these, only that one or the other should be used. I was really trying to point out that there are applications in which this RF spectral density is really what you want to be concerned with. There are others. Whereas, in principle, the RF spectrum could characterize the frequency disturbances that you are looking for, what you measure about it actually—because of the method of measurement and so forth—winds up not being very applicable. In those situations you want to concentrate on the fluctuations themselves. So I am trying to distinguish between the two problems.

I am not saying that we all have one problem. We really have two general problems: one embodies all applications that are really ultimately concerned with spectral purity; another, embodies applications in which we are really concerned with jitter in phase and frequency. There are methods of testing and characterization that are adequately applicable in each case. I am not trying to cast doubt on either of these. I say both exist and both must be clearly distinguished.

Dr. Leeson.—I think all of the papers this morning did talk about two parameters. I think perhaps a convenient way to think about it in some cases would be to look directly at the signal. In other cases you are concerned with looking off to the side and trying to ignore it. Ordinarily, when you are trying to ignore it, you are not really concerned with the details of its frequency variation, but you are concerned with any energy which might be present in the region where you are looking. If you are trying to put it through a filter, treat it nicely, and get some information off it; then you are concerned with something entirely different. You are concerned with how much energy or information you can get through the filter. I have to agree that there is a tremendous difference between these two.

Dr. Baghdady.—You can't just hop from one to the other.

Dr. Leeson.—No, you can't. They are not inter-related, and this is something which people sooner or later find out when they try to relate measurements of one sort to another. You can't make a spectral density measurement and then from that make any reasonable sort of qualification as to what the statistics of the frequency or phase versus time are going to be.

It is true in what was pointed out in all of these papers this morning, the best way to find this sort of thing is to do what I think most of the practitioners of this art do now, that is, to make both measurements; and, at least in the back of their minds they have this division between the two sorts of characteristics fairly well sorted out.

Dr. Curry (Curry, McLaughlin & Len, Inc.).—I don't know whether to reserve this comment until this afternoon when I will hear Dr. Baghdady's talk or bring it up now, concerning the relationship between the time and frequency domain representation. Isn't it true that really what you are saying is that the spectra that we are using are just not properly measured?

Dr. Baghdady.—Not really. I would like to point out that the question I have raised is not really a question of time and frequency domain representations. It is a question of uniqueness of representation by a given abstraction. In other words, if you choose the RF power spectral density

and measure it and work with it, then this spectral density can represent a million and one signals that have completely different time behaviors. Some of them are extremely stable frequency-wise; and others, bad. In other words, the RF power spectral density by itself does not uniquely identify the signal and is not sufficient for characterization of the time behavior of the signal.

Dr. Curry.—I would agree, and I will be saying something on this this afternoon. I think that one problem that we run into right away is that we try to compare spectral data, power spectral data, which we take with instruments which really are taking cuts across the time-frequency domain. We really don't know what we have when we get through or at least we do not have what we can relate to one millisecond intervals. If we want something to relate to one millesecond intervals or, let's say, I am using that as an example, then we have to make certain that we do in fact or we have in fact measured a short-term spectra and we begin rapidly to get into problems there.

Dr. Baghdady.—Incidentally, there has been a sad lack of comment aimed at defining really in any given application, or in some general guiding way, what we mean by "short-term" for any situation. I would have liked to hear this. This being a requirements session, presumably somebody was going to announce "this kind of application requires this kind of thing." And I think a lot of people would like to see some clear quantitative definition, not in terms of deviation, like so much such and such a delta F doesn't say anything. I think what is meant by "short-term" ties with a lot of things that would require specification for each application.

Mr. Sykes.—It is probably a little early in the symposium to accomplish that. That is what we hope to be able to do.

Mr. Kruger (GSFC).—If you look at the doppler frequency value, what you generally do is integrate the frequency over a certain amount of time. That means you do not look at frequency, as such, you look at elapsed phase. And it therefore seems to me that phase deviation or phase jitter would be of more importance than frequency deviation or frequency jitter. However, all papers today have generally been concerned with frequency rather than with phase. I wonder if I could get some comments on that.

Dr. Baghdady.—There are two things that I would like to point out. Number one, the spectral density of the phase fluctuation and the spectral density of the frequency fluctuation are very simply related. So you can work with one or the other. Number two, it turns out that in systems this seems to be like a hierarchy, so I am going to give you a start of one and you can go down.

In systems where the effects of short-term stability disturb you because you are really trying to compare the phases of a continuing process at two different times, you find that because the effects are usually assumed to be random, people like to choose the rms or mean square measure of disturbance. You find that the rms disturbance that is caused by the instability comes out to be an integral in which one of the factors inside is the spectral density of the frequency fluctuations.

This happens to be the case, for example, in ranging, where you actually are comparing phases at two different times. In doppler measurements or velocity measurements where you are comparing frequencies at two different times, again it comes up. Actually, you can express the rms error due to instability in terms of the spectral density of the frequency fluctuations.

Because of the simplicity of the relationship between the spectral density of phase and frequency fluctuation, you can always wind up with the spectral density of one or the other, as you choose, inside of that integral. So if you pick one or the other, you are all right.

Mr. Kruger.—Well, I don't quite agree with that. I think an error analysis at some time makes a difference at what you look. At least, it is simple to look at phase—

Dr. Baghdady.—That is an instrumentation problem. On the other hand, there is a great deal to be said about watching frequencies, you see. I mean, it is an instrumentation problem, and some people are more skilled in one observation than another. It also depends on the shape of the spectral density of the phase fluctuations and the corresponding spectral density of the frequency fluctuations. The shape of one or the other may render it more amenable to measurement to within a specified error and confidence level with a given degree of instrumentation complexity.

Mr. Hyde.—I think it is clear that we need to look at both the frequency spectrum and the

phase in general. When we are doing extremely narrowband spectral analysis by Fourier integral, or other correlation techniques, we are correlating, essentially, a continuum of phase as has been pointed out. However, we don't know what is going on necessarily outside of this extremely narrow band filter, that has either been built in an analog machine or programmed in the computer, and it may be that we are almost unknowingly wasting a good deal of our transmitted power in sidebands which are only ten, twenty, or frequently sixth cycles away from our transmitted carrier. So some spectral analysis must be done in a wide frequency band as well as the extremely narrow band.

Mr. Mager (Raytheon Missiles System Division).—In response to Dr. Baghdady's request for a definition of short-term stability, I think the phrase "short-term stability" in a way begs the question. It almost by implication assumes a time domain definition. It seems to say, well, what do we mean, a millisecond, a tenth of a second, or what? And I think the first four papers made it clear that in many applications such an approach to the question is not too meaningful.

Another area that I wanted to comment on, with Dr. Baghdady, is the question of whether phase and frequency are really simply related; given different mechanisms for phase modulation and frequency modulation, which we don't always very clearly understand. I wonder if one can really derive a frequency deviation spectrum from a phase deviation spectrum.

Dr. Baghdady.—Yes. Divide by frequency.

Mr. Mager.—That implies that we know the frequency distribution.

Dr. Baghdady.—If you go from phase to frequency, multiply by frequency.

Mr. Mager.—Yes, this implies that we know $\Delta\phi = \Delta f/f_m$ where f_m is the modulation frequency, or some simple relation like this or an integral relation of this nature.

Dr. Baghdady.—I'm sorry, but I don't understand what you are saying.

Mr. Mager.—You say one can be derived from another by a simple multiplication.

Dr. Baghdady.—There is no condition at all—without any restriction—one is the derivative of the other in time; therefore, in frequency the spectrum gets divided or multiplied by ω, it is that simple.

Mr. Mager.—Well, given that one is the derivative of the other, we must know the function that we are taking the derivative of, and we don't always know it theoretically or analytically. This is what I am implying is the problem.

Dr. Baghdady.—I see what you mean.

Dr. Leeson.—Are you referring to the idea of the measurement of $\Delta\phi$, so many radians rms, and talking about that as opposed to a line width measurement? In other words, are you talking about measurements in which you haven't made a spectrum analysis or do I misunderstand?

Mr. Mager.—Well, as an example, if we were to use a frequency discriminator of some sort, some of the commercial equipment, to measure an rms frequency deviation in a given bandwidth, what I am saying is that an equivalent phase deviation is not readily or immediately derivable from this.

Dr. Baghdady.—That is true.

Dr. Leeson.—I have to agree with that entirely.

Dr. Baghdady.—That is true.

Mr. Mager.—That is my only point.

Dr. Baghdady.—I was talking spectral densities, and now you are right, any particular value, says rms value or peak value or something like this, measured on one, cannot be uniquely related to the other.

Mr. Mager.—All right.

Dr. Leeson.—This points up an interesting difference in the so-called airborne applications of the first four papers and the applications brought out in the last two, and that is primarily if the information which you are seeking is in the form of phase, then of course you are going to be concerned with random variations of phase over which you have no control.

On the other hand, if you are operating with a system which is in essence a frequency spectrum analyzer, then frequency becomes a more convenient variable to work with, only because of the fact that everything else in the offing is also in the same terms.

Mr. Sykes.—Now, we really haven't given the speakers a chance here, but as a result of this discussion, do any of the speakers have comments that they would like to make, clarification, or for that matter any questions?

Mr. Johnson.—I have a comment I would like

to make in answer to Dr. Baghdady's statement that nobody said what they mean by "short-term stability". I said in my paper "short-term stability" refers to the ability of the receiver to track the signal. If you receive a signal varying in frequency at a rate that a narrow band receiver can track, to me that is long-term stability. And if the rate of the frequency variation becomes such that the receiver no longer can track it, then it becomes short-term stability.

We are giving here what our user requirements are, how we measure it, and what we need to know. I think that is what the four papers this morning pointed out. The two papers following the radar papers showed a completely different requirement. This points out the necessity for each individual to determine from the system requirements what are his short-term stability requirements.

Dr. Baghdady.—I think it is possible to derive by some systematic arrangement;—we are going to offer one this afternoon—a definition in which parameters enter that identify gross features of the application. You assign values to these parameters to characterize different applications and you wind up with a number that says "five seconds" for the user, this is the user number now. Now, there is another number that the manufacturer must come up with. The manufacturer's number must be unrestricted by the users' numbers, unless he is catering to one very specific application. For general-purpose application, the manufacturer has to avoid any specific assumptions about the users' numbers. I would like to suggest that we come up with a guideline, a quantitative guideline.

Say here is our resolution, here is our application. It is characterized by this and that. And here is the way these things are tied together. Compute this number and you get five. Call it five seconds, depending upon the dimensions. This is this man's shortest interval of significance. You see, this is what we mean for him by short-term stability.

This is possible. We are going to recommend something in Session II.

Mr. Habib.—Could I ask a question of the JPL representative here. How do you handle the seven minutes delay to Venus and back on a stability basis?

Dr. Sydnor.—What do you mean by "stability basis"?

Mr. Habib.—Well, when you are doing planetary radar, and you have a seven-minute delay between the transmitted and the returned signal, or approximately that, what sort of stability problems do you run into there?

Dr. Sydnor.—We have to make a few assumptions in that case. We assume that the random variations of the transmitted signal are not correlated with the return variations. We have run a number of tests with a number of master oscillators, rubidium standards in this case, to see if they are independent over that length of time. We found that within our measuring technique limitations that they are. If they are not correlated, then we can measure the stability over this sort of time interval and find out what it is, so we can evaluate the quality of our data.

Mr. Van Duzer (Hewlett-Packard).—I have an observation to make here, that is, all of the users seem to be radar people. If we are going to use this discussion this morning as a basis for arriving at a definition of short-term stability, we ought to carefully consider that there are a lot of other applications in which people are interested in short-term frequency stability.

Mr. Sykes.—Well, I think that that will probably be apparent as we go along with some of the other sessions. I would hope that we wouldn't do this just for one group.

Mr. Gillespie.—We are never going to get complete statistics on the quality of oscillators. I don't think we will find them in a definition of short-term frequency stability, and we will end up talking about certain averages in rms phase deviation perhaps, or rms frequency deviation.

I showed one particular radar processor this morning that was sensitive in a peculiar way, perhaps, to frequency changes, frequency deviation. It also is sensitive to amplitude deviations. We haven't talked much about AM and I just choose not to talk about it. We certainly could have had a lot of problems if AM noise, either coherent or non-coherent, were present. If we are concerned with MTI (moving target indication) search radars for which specifications must be made in terms of oscillator rms phase deviation; or with tracking radars using something like the CFAR (constant false-alarm-rate) automatic-

target detection circuitry, then we would like to know more about deviations in averages of frequency. We will need all of the statistics. It is quite a job to come up with a standard.

Dr. Baghdady.—I think we will show in Session II an approach, actually some specific applications, and show how the thing always winds up. It turns out that it is possible, if you use as your measure of performance or measure of disturbance the mean square or the rms fluctuation error, you wind up with a result in which the instabilities are characterized by two things: Number one, the spectral density of the instantaneous frequency fluctuation and/or phase fluctuation; and number two, a measure of the peak factor of the fluctuations.

You might well say, is this all? Yes, this is all. It would be nice to determine, for example, the statistics of the instantaneous frequency fluctuation, so you would have a better idea about what value of peak factor to assign to the fluctuations that would suit your application. But in the absence of—it is a very costly process, the determination of this,—the probability density function of the fluctuations, we usually resort to some arm-waving tactic. For example we say if the fluctuations were characterized by gaussian statistics, then the peak factor is three or four. If it is something else you pick another number, you see? But ultimately you may want to know the probability distribution so that you can tell with what probability some value will be exceeded. In this way, you can pick that value that will be exceeded during a fraction of the time that is negligible in your application, or which would satisfy some criterion of negligibility, and use that value in estimating the peak factor. So it is possible to characterize the instabilities with a small number of gross parameters.

Mr. Grauling (Westinghouse Aerospace).—I think there is one point here that has been alluded to a little bit that hasn't really been brought out very clearly, and I know that this is something that Dr. Leeson mentioned. The question of spectral purity actually involves both AM and FM contributions, or if you want to call it AM and PM. I think that the thing that most of the users, at least in the radar papers, are interested in, is the total spectral content in the bandwidth of interest. Whether this arises from FM, or whether it arises from AM, it can be a problem in the system.

The reason these things usually wind up being stated in terms of short-term frequency stability is the fact that the AM contributions are small compared to the FM, and consequently if you can manage to measure the FM you have pretty well solved the problem.

Dr. Baghdady.—This is a debatable question.

Mr. Grauling.—Yes, this is. But from the users' standpoint we are concerned with the total noise or what have you in a given channel.

Dr. Baghdady.—I mean the relative weight of AM and FM is debatable. You mentioned that the AM contribution is usually negligible, and I don't know if it is. It depends on the mechanism. It depends on models. And if indeed you have established that it is negligible, neglect it, don't just assume it across the board.

Mr. Grauling.—Oh no, we can't assume that across the board. In fact, the sets have to be built to measure both AM and FM contributions. I think the reason, and this is the point that has not been brought out, is that it is the total contribution which is of significance to the user. It is a fact that the way the radar sets are highly mechanized, it is a single sideband receiving system, so consequently we are interested in the energy at a given point on one side of the carrier. The source of this in terms of AM or PM is unimportant, but it is the single sideband being passed through the receiver that does get picked up. The measuring sets, of course, must distinguish between the two.

Dr. Reder (Army Electronics Laboratory).—It seems to me we are going around in a circle on questions which actually should be asked and answered in this afternoon's session. On the other hand, you would have available now the representatives for the one question which is very pertinent to this session. I mention that there are many other applications of short-term stability, and I think the answer to this question is more pertinent in this session and it will be very important.

Mr. Sykes.—This is exactly right, and I had hoped to get more discussion specifically on this morning's papers.

I think there are a number of things from these papers that have been brought out. One that seems to be most important to me, while the title of this

Symposium is "Definition and Measurement of Short-Term Frequency Stability", it certainly has become obvious from the discussion and the papers that have been presented that it is just not that simple. Before you try to define "short-term frequency stability" you need to know what are the terms that need definition.

For example, the user says he wants to do such and such, and he wants this kind of an answer. It certainly seems apparent to me that we have to first obtain a language. What are the terms that are necessary to define in order to get the answers that the users really want? I think that if we establish only that this morning, we have gone a long way. It is expected that a subcommittee of one of the IEEE committees will be formed as a result of this symposium. I would hope that they would take on the job of establishing the terms that we need, arrive at some definitions for these terms so that we can, in the development of these systems, get a better language in which we can all get a common understanding.

II. THEORY

Call to Session	MERRICK E. SHAWE GSFC
Chairman	WILLIAM A. EDSON Electromagnetic Technology Corp.
Discussion Panel	MALCOLM W. P. STRANDBERG MIT
	MARCEL J. E. GOLAY Consultant, Perkin-Elmer Corp.
	JAMES A. MULLEN Raytheon Company
	ELIE J. BAGHDADY ADCOM, Inc.

7. SHORT-TERM FREQUENCY STABILITY: CHARACTERIZATION, THEORY, AND MEASUREMENT

E. J. BAGHDADY, R. N. LINCOLN, AND B. D. NELIN

ADCOM, Inc.
Cambridge, Massachusetts

An analysis of the manner in which oscillator short-term instabilities limit performance in a number of applications is presented. This analysis provides guidelines for theoretical formulations, the definition of *short-term stability*, and the development of measurement techniques for characterizing short-term instabilities. The factors that affect short-term stability are discussed, and basic models for theoretical analysis are formulated. The models are used in investigations of the characteristics of outputs of "stable" sources. Measurement techniques are proposed and compared with techniques employed by other investigators.

A treatment of the problems of characterizing, analyzing, and measuring short-term instabilities of ultrastable sinusoidal oscillation sources as well as of loop-controlled oscillations is presented.

The term *short-term stability* appears with increasing frequency in discussions of timing and synchronization systems, frequency synthesis techniques, and moving-target tracking systems of all types. But this term continues to mean different things to different individuals, even in the same applications. At the present time, and in almost all applications, there is:

1. No common understanding of what short-term stability means.
2. No common agreement on why it is needed.
3. No common understanding of how to characterize, model, analyze, and measure oscillation instabilities.
4. No widely accepted accounts of how the instabilities will affect performance in applications, and how the requirement for short-term stability should be specified.

Stable oscillators are used extensively as:

1. Original sources of timing and synchronization signals.
2. Original sources of carriers or subcarriers for target tracking applications, communication signals, and multiple-access utilization of aerospace vehicles as relay centers.
3. Local independent reference signals for timing, phase, or frequency measurement.
4. Local oscillation of controllable phase and frequency that tracks the instantaneous phase or frequency of an incoming signal, thereby providing a continuous estimate of its instantaneous phase or frequency.

In some of these operations, the emphasis is placed on the unavoidable fluctuations in phase or frequency caused by sources of instability and, in others, on the spectral structure or "spectral purity" of the oscillation. Thus, the characterization and measurement of oscillator instability may be pursued along the lines of:

1. Characterizing the fluctuations in the phase and frequency of the oscillator output.
2. Characterizing the structure of the spectrum of the oscillator output.

In general, one cannot concentrate on one and ignore the other of these two aspects of an oscillation completely, although either of them potentially can be made to provide a complete representation of the source output. Thus, exclusive

concentration on the structure of the spectrum or the mean-square spectral density obscures the fact that not all of the spectral components actually will cause phase and frequency fluctuations—fluctuations in the amplitude of the oscillation also spread out its spectrum and may be completely unrelated to the phase and frequency fluctuations. Similarly, exclusive concentration on the phase or frequency fluctuations obscures the fact that a considerable source of the observed instability actually may be spurious filterable components that will be reduced effectively in the ultimate system. In the final analysis, the type of characterization sought must be the one most clearly related to the intended application of the oscillation.

In the next section we explore the manner in which oscillator short-term instabilities limit system performance in a number of applications. This analysis shows that the mean-square spectral density of the instantaneous frequency fluctuations of the oscillation frequently provides the most direct basis for the characterization, measurement, and specification of the short-term frequency and phase instabilities. Although the probability density functions of the instantaneous phase and frequency fluctuations may be of interest, often only a practical estimate of the peak factor of the fluctuations is sufficient. Guidelines are provided for user estimation of the shortest interval of time over which instability errors will become noticeable in a specified application. A user quantitative interpretation of "short-term" is thereby made possible. Situations in which the mean-square spectral density of the oscillation itself provides an adequate abstraction are also discussed.

In the third section, on Models and Characteristics of Unstable Oscillations, a survey is made of mathematical models and associated characteristics of unstable oscillations. Two general approaches for modeling are presented, and several models in each category are discussed.

In the final section attention is directed to the problem of measuring the characteristics of frequency unstable oscillations. The general properties of satisfactory measurement systems, from which the basic structure of these systems is obtained, are developed. The gross performance of the class of recommended systems is contrasted with that of previous systems for the measurement of oscillator instability. Finally, the areas of unsolved problems in measurement are discussed.

EFFECT OF OSCILLATION INSTABILITY IN APPLICATIONS

The characterization, modeling, analysis, measurement, and specification of bounds on oscillation short-term, or rapid, instability ultimately must be made in the light of its effects on the performance of systems that rely on the oscillation. General guidelines now will be sought in terms of a number of specific applications.

Precision Range Measurement

An application of great current interest, and one whose methodology of treatment is representative of a number of other applications, is encountered in precision range (or radial distance to a vehicle) measurement systems. Such a system is illustrated in Figure 7–1. In this system, a tone of suitable frequency is transmitted to the vehicle to be tracked and is returned by it to the tracking station. Range from the tracking station to the vehicle is then determined from a measurement of the phase of the returned tone relative to the phase of the original transmitted tone, on the basis of a current segment of the continuing output of the source of the original tone. In the ensuing discussion we consider only the errors caused by the short-term instabilities of the source

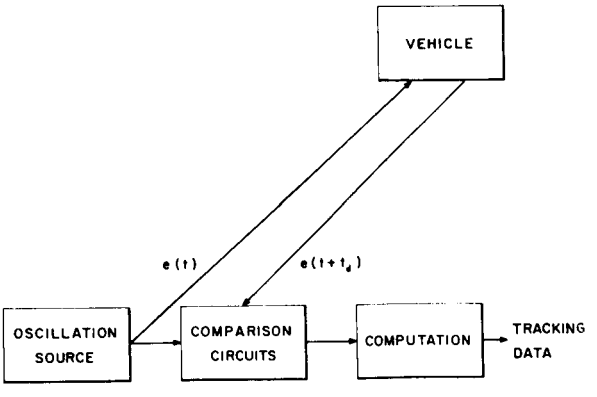

FIGURE 7–1.—Basic functions of a target-tracking system with sinusoidal ranging signal.

of the ranging tone that cause the current segment to differ from the original one (or a perfect replica of it), and ignore all other effects as extraneous to this discussion.

Thus, let t_d be the two-way signal propagation time between the tracking station and the vehicle. The radial distance to the vehicle is then

$$R = ct_d/2, \tag{1}$$

where c is the velocity of signal propagation in the intervening medium. If the original transmitted tone is expressed as

$$e_{trans}(t) = E(t) \cos \theta(t), \tag{2}$$

then—assuming ideal propagation conditions and no delay in turnaround at the vehicle—we have for the returned signal

$$e_{ret}(t) = E(t + t_d) \cos \theta(t + t_d). \tag{3}$$

The desired information is contained in

$$\begin{aligned}\Delta\theta(t, t_d) &= \theta(t+t_d) - \theta(t) \\ &= \int_t^{t+t_d} \dot{\theta}(\mu)\, d\mu \\ &= \dot{\theta}(t) \otimes p_{rect,t_d}(t+t_d/2),\end{aligned} \tag{4}$$

where $\dot{\theta}(t) = d\theta(t)/dt$, $\otimes$ denotes convolution, and $p_{rect,t_d}(t) =$ rectangular pulse of unit height extending from $t = -t_d/2$ to $t = t_d/2$.

Now, the instabilities in the oscillation frequency may be accounted for by writing

$$\theta(t) = 2\pi f_0 t + \phi(t) \tag{5}$$

so that

$$\dot{\theta}(t) = 2\pi f_0 + \dot{\phi}(t),$$

where $f_0 =$ the value of the instantaneous frequency of the tone at the start of the t_d round-trip time to be measured and $\phi(t) =$ instantaneous fluctuations in the phase of the oscillation about the phase $2\pi f_0 t$ of an absolutely stable source of frequency f_0. Substitution in Equation 4 yields

$$\Delta\theta(t, t_d) = 2\pi f_0 t_d + \dot{\phi}(t) \otimes p_{rect,t_d}(t+t_d/2). \tag{6}$$

This shows that the frequency instability of the ranging tone introduces an uncertainty in the measured value of t_d given by

$$\Delta t_d = (2\pi f_0)^{-1} \dot{\phi}(t) \otimes p_{rect,t_d}(t+t_d/2.) \tag{7}$$

In view of the random character of $\dot{\phi}(t)$, a convenient measure of the error it causes is usually the root-mean-square value (or standard, deviation). Thus, if σ_{t_d} denotes the rms value of αt_d,

$$\sigma_{t_d} = (2\pi f_0)^{-1} \{ E \langle [\dot{\phi}(t) \otimes p_{rect,t_d}(t+t_d/2)]^2 \rangle \}^{1/2}, \tag{8}$$

where $E\langle\ \rangle$ denotes "statistical average." Since the Fourier transform of the convolution of two functions equals the product of their Fourier transforms, we have

$$\sigma_{t_d}/t_d = (2\pi f_0)^{-1} \left[(2\pi)^{-1} \int_{-\infty}^{\infty} S_{\dot{\phi}}(\omega) \left(\frac{\sin \omega t_d/2}{\omega t_d/2} \right)^2 d\omega \right]^{1/2}, \tag{9}$$

where $S_{\dot{\phi}}(\omega)$ is the mean-square spectral density of $\dot{\phi}(t)$.

Equation 9 brings out the following important facts:

1. The fractional rms error caused by the frequency instability of the oscillator is determined by the *mean-square spectral density* $S_{\dot{\phi}}(\omega)$ of the *instantaneous frequency perturbations.*

2. The spectral density $S_{\dot{\phi}}(\omega)$ is weighted by a filtering effect,

$$\left(\frac{\sin \omega t_d/2}{\omega t_d/2} \right)^2, \tag{10}$$

plotted in Figure 7–2, which depends on the interval of time t_d—peculiar to the application—over which the oscillator instabilities may cumulate their influence on the measurement.

It is clear from Figure 7–2 that the weighting function favors only the part of the spectrum contained *within* $|\omega| \leq 2\pi/t_d$. As t_d increases, the edges of this interval shrink closer and closer to $\omega = 0$, indicating that the faster fluctuations in $\dot{\phi}(t)$ become less and less significant in determining the error in the measurement.

In practice, additional filtering is introduced to smooth out the effects of noise from various sources, the bandwidth being chosen to maximize the noise smoothing without intolerable conflict with requirements on the speed of response imposed by range resolution specifications and by the dynamics of the vehicle trajectory. The introduction of such a filter, characterized by $H_{lp}(j\omega)$, multiplies the integrand in Equation 9 by

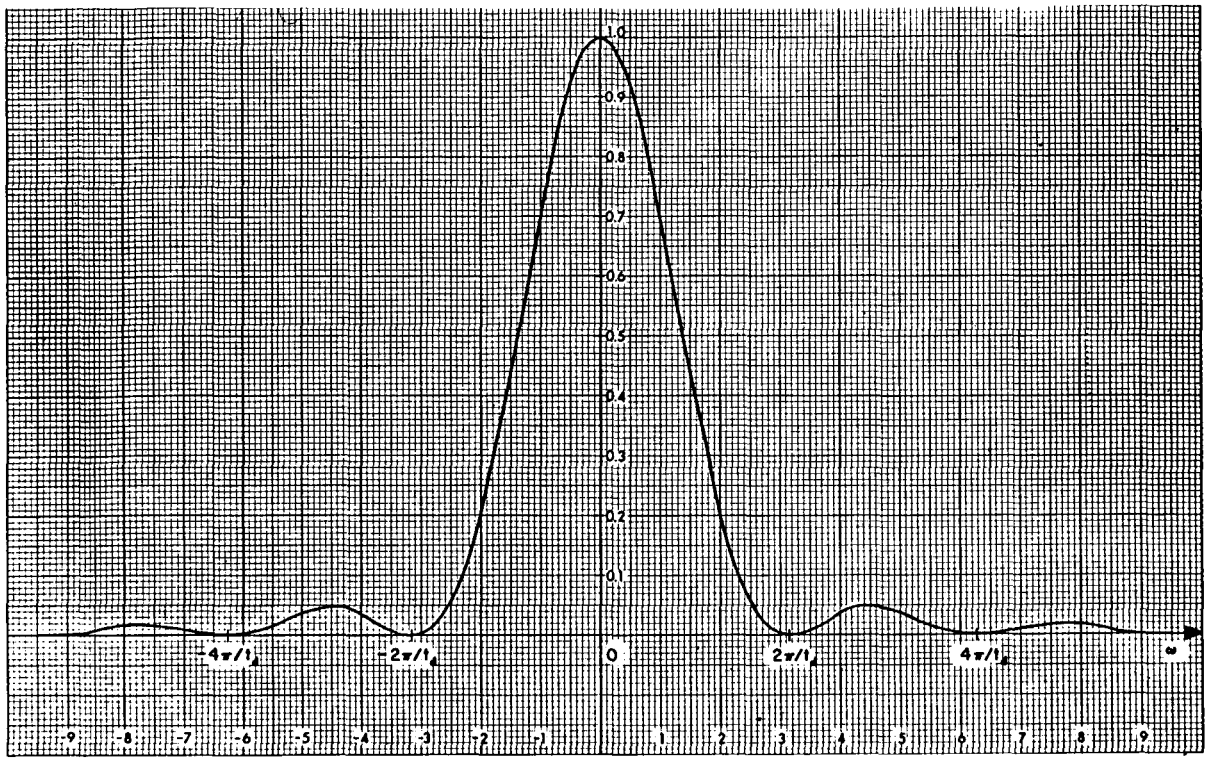

FIGURE 7–2.—Filtering effect of interval t_d over which the instabilities may cumulate their influence on the measurement.

$|H_{lp}(j\omega)|^2$. If the nominal passband of $H_{lp}(j\omega)$ is restricted to $|\omega| \leq 2\pi B_{lp}$, then for

$$B_{lp} \leq (1/t_d)/10$$

only the spectral components within $|\omega| \leq 2\pi B_{lp}$ will contribute instability errors. In the absence of this filter action, or when B_{lp} is of the order of 10 times $1/t_d$ or more, components with frequency up to B_{lp} cps may contribute [depending on $S_\phi(\omega)$] significantly to the instability error, although components within $|\omega| \leq 2\pi/t_d$ fall on the more favorable part of the curve in Figure 7–2.

Note that the range measurement application considered above is representative of all applications in which information is derived from a comparison of samples of the oscillation *phase* taken at different times. If the precision of the phase-shift measuring instrument is sufficient to resolve ρ_θ radians, then the effects of instability will be negligible provided that:

Phase uncertainty cumulated in t_d sec $\leq \rho_\theta/10$. (11)

The peak value of the error cumulated in t_d sec may be expressed as the product of the expected rms error σ_{t_d} and a peak factor, $(p.f.)_\phi$ associated with the fluctuation caused by oscillator instability. Thus, if the peak error is to satisfy Condition 11, we must have

$$[(p.f.)_\phi/2\pi f_0]t_d \times\left[\frac{1}{2\pi}\int_{-\infty}^{\infty} S_\phi(\omega)\left(\frac{\sin\omega t_d/2}{\omega t_d/2}\right)^2 |H_{lp}(j\omega)|^2\, d\omega\right]^{1/2} \leq \rho_\theta/10. \quad (12)$$

This shows that, as far as the rms error caused by instabilities of the oscillation source is concerned, each application is completely characterized by a smoothing filter $H_{lp}(j\omega)$, the nominal ranging tone frequency f_0, the value (or range of values) of the time separation t_d between the compared samples of tone phase, and the resolution of the phase measuring instrument ρ_θ. Of these only t_d is independent of equipment. Therefore, for a given setup, t_d may be considered to characterize the application. The oscillator instabilities are completely characterized by $S_\phi(\omega)$ and a nominal

peak factor for conversion from rms to peak phase fluctuation.

Close inspection of the left-hand member of (12) shows that the peak phase uncertainty caused by oscillator instability is an increasing function of the time separation t_d between the compared phase samples, all other factors (such as choice of B_{lp}) being the same. This is particularly evident when the smoothing filter bandwidth B_{lp} is much smaller than $1/t_d$; in which case the error will rise monotonically with increasing t_d. This observation combined with the fact that, of all the parameters in condition (12), only t_d is beyond the control of the designer suggests that in any specific application (specified equipment and oscillator) the equation

$$[(p.f)_\phi/2\pi f_0]t_d \times\left[\frac{1}{2\pi}\int_{-\infty}^{\infty} S_\phi(\omega)\left(\frac{\sin\omega t_d/2}{\omega t_d/2}\right)^2 |H_{lp}(j\omega)|^2\, d\omega\right]^{1/2} = \rho_\theta \quad (13)$$

may be solved for a value of t_d for which the expected peak error will equal the phase resolution capability ρ_θ. If this value of t_d is denoted $t_{d\rho}$, then from the viewpoint of the user the phase discrimination errors caused by oscillator instability become noticeable only for values of t_d that are comparable with, or in excess of, $t_{d\rho}$. In this way, the term *short-term* in a specified application may be interpreted to mean "over intervals of duration t_d that are comparable with $t_{d\rho}$."

A word of caution is necessary here. The preceding interpretation of *short-term* is strictly intended to provide a criterion for determining, in a specified application, whether or not measurements based on a comparison of two samples of the oscillation phase, separated in time by t_d sec, will be subject to noticeable errors attributable to instability of the oscillation source. We assumed knowledge of the application—specifically, f_0, $H_{lp}(j\omega)$ and ρ_θ—and the availability of properly measured data—specifically, $S_\phi(\omega)$ and $(p.f.)_\phi$—characterizing the instantaneous frequency perturbations of the oscillation. It should be clear that this interpretation is only a user guideline and definitely is not the criterion for the choice of "adequate" time interval in tests aimed at furnishing $S_\phi(\omega)$ and $(p.f.)_\phi$. The experimental determination of the instability characteristics of oscillators and the associated interpretation of *short-term* will be discussed later in this paper.

For specific illustrations, consider first the situation in which

$$S_\phi(\omega) = a^2 = \text{Constant for all } \omega. \quad (14)$$

Then, if

$$B_{lp} \gg 1/t_d, \quad (15)$$

the integral in (13) is closely approximated by $a^2 2\pi/t_d$. Solution for t_d yields

$$t_d = \left(\frac{2\pi f_0 \rho_\theta}{a(p.f.)_\phi}\right)^2 \triangleq t_{d\rho}. \quad (16)$$

On the other hand, if

$$B_{lp} \leq (1/t_d)/10, \quad (17)$$

then the integral in (13) becomes closely approximated by $4\pi a^2 B_{lp}$, and the corresponding $t_{d\rho}$ becomes

$$t_{d\rho} = \frac{2\pi f_0 \rho_\theta}{(p.f.)_\phi a(2B_{lp})^{1/2}}. \quad (18)$$

Consider next the situation in which

$$S_\phi(\omega) = b^2\omega^2, \qquad \text{for all } \omega. \quad (19)$$

Substitution in Equation 13 yields

$$\frac{(p.f.)_\phi b}{2\pi f_0}\left(\frac{1}{2\pi}\int_{-\infty}^{\infty} |H_{lp}(j\omega)|^2(1-\cos\omega t_d)\, d\omega\right)^{1/2} = \rho_\theta. \quad (20)$$

The quantity under the square-root sign equals

$$\tfrac{1}{2}\alpha[1-\exp(-\alpha t_d)] \text{ for } H_{lp}(j\omega) = \alpha/(\alpha+j\omega), \quad (21)$$

$$(4\pi\alpha)^{1/2}[1-\exp(-\alpha t_d^2)] \text{ for } |H_{lp}(j\omega)|^2 = \exp(-\omega^2/4\alpha), \quad (22)$$

$$2B_{lp}\left[1-\frac{\sin(2\pi B_{lp} t_d)}{(2\pi B_{lp} t_d)}\right] \text{ for } |H_{lp}(j\omega)| = 1, \quad |\omega| \leq 2\pi B_{lp}; \quad = 0, \quad |\omega| > 2\pi B_{lp}. \quad (23)$$

From Equations 21 and 22 we conclude that, when the smoothing filter is a simple RC or a Gaussian low-pass filter, the instability error associated with the spectral density specified by Equation 19 will always rise monotonically with t_d. With the rectangular filter, (23) shows that

the error rises monotonically with t_d for $0 \leq t_d \approx (4.5/2\pi B_{lp})$ but undulates thereafter with decreasing amplitude about the value

$$(p.f.)_{\phi} b(2B_{lp})^{1/2}/(2\pi f_0).$$

It is interesting to observe that, in each case, the rms instability error approaches a bounded value as $t_d \rightarrow \infty$. For each filter, an expression for t_{dp} may be obtained by substitution from Equations 21, 22, or 23 into Equation 13.

One final conclusion that may be drawn from inspection of the left-hand member of Equation 13 is that, in applications where comparisons are made of phase samples t_d apart in time, oscillator frequency instability phenomena that vary so slowly as to be almost constant within the interval t_d (*long-term* effects) always must be considered and that phenomena that vary rapidly within t_d (*short-term* effects) may not be of importance. This conclusion contradicts many statements made by other writers about the essential effect of oscillator instability in such applications.

Precision Range-Rate Measurement

The radial velocity, or range rate, of a moving target may be determined from a measurement of the Doppler frequency shift of a tone returned by the target, relative to the frequency of a current segment of the continuing output of the source of the original transmitted tone. Frequency comparisons are also employed in coherent Doppler and CW systems, in timing, and in synchronization operations. Just as the mean-square spectral density of $\dot{\phi}(t)$ of Equation 5 determines the mean-square instability error in measuring increments of $\theta(t)$, the mean-square spectral density of $\ddot{\phi}(t)$ may be expected to determine the mean-square error in the measurement of changes in $\dot{\theta}(t)$. That this is indeed the case is readily shown by starting with the fact that the desired information is now conveyed by

$$\begin{aligned}\Delta\dot{\theta}(t, t_d) &= \dot{\theta}(t+t_d) - \dot{\theta}(t) \\ &= \ddot{\theta}(t) \otimes p_{rect, t_d}(t+t_d/2). \end{aligned} \quad (24)$$

Thus, the error in the observed Doppler shift caused by frequency instability in the transmitted tone is given by

$$\Delta f_{Dop} = (4\pi)^{-1} \ddot{\phi}(t) \otimes p_{rect, t_d}(t+t_d/2), \quad (25)$$

with an rms value given by

$$\begin{aligned}\sigma_{f_d} &= \frac{t_d}{4\pi}\left[\frac{1}{2\pi}\int_{-\infty}^{\infty} \omega^2 S_{\dot{\phi}}(\omega)\left(\frac{\sin\omega t_d/2}{\omega t_d/2}\right)^2 |H_{lp}(j\omega)|^2 d\omega\right]^{1/2} \\ &= \frac{1}{2\pi}\left[\frac{1}{2\pi}\int_{-\infty}^{\infty} S_{\dot{\phi}}(\omega) |H_{lp}(j\omega)|^2 \sin^2(\omega t_d/2)\, d\omega\right]^{1/2}, \end{aligned} \quad (26)$$

in which we have introduced the effect of a post-detection low-pass filter aimed at reducing the effects of extraneous additive noise.

Again, we observe that:

1. The rms instability error in the Doppler shift measurement is determined by the mean-square spectral density $S_{\dot{\phi}}(\omega)$ of the *instantaneous frequency perturbations* of the unstable transmitted tone.

2. A filtering effect, $\sin^2(\omega t_d/2)$, weights the spectral density in a manner that favors alternate intervals of duration $2\pi/t_d$ rad/sec, one of which is defined by $|\omega| \leq \pi/t_d$.

The term *short-term* also may be given a user quantitative interpretation relative to Doppler measurements. Here we seek the value of t_d for which the effects of instability become noticeable in a measurement of Doppler shift. The equation to be solved for this value of t_d is

$$\text{Frequency shift cumulated in } t_d \text{ sec} = \rho_{\dot{\theta}}, \quad (27)$$

in which $\rho_{\dot{\theta}}$ defines the instrumental precision in masuring frequency changes. As before, we may assume a peak factor $(p.f.)_{\dot{\phi}}$ for the frequency fluctuations caused by instability, and write $(p.f.)_{\dot{\phi}}\sigma_{f_d}$ for the left-hand member of Equation 27.

Applications Affected by Oscillator RF Spectrum

As we have mentioned previously, there are applications in which the spectral composition of an oscillator signal is of primary importance. Doppler resolution radar is a good example; this system is used to resolve several targets moving with different radial velocities on the basis of the different Doppler shifts of the associated returned replicas of the illuminating signal. A bank of

filters is used to resolve the spectrum into "velocity regions," and the output of an individual filter will present only those targets whose radial velocities cause the returned signals to fall into the passband of the filter. The system works perfectly if the RF spectrum of the oscillator is a pure line. Amplitude, phase, and frequency instabilities of the illuminating signal broaden the "line width" and spectral occupancy of this signal, and thereby limit the ultimate velocity resolution of the system. It is quite clear that, to determine the effect of oscillator instability in such an application, we should work directly with the RF spectrum of the oscillator signal.

Spreading of the oscillator spectrum by unwanted amplitude and phase fluctuations also adds to the spectral density of background signals and noise that interfere with a desired return. This degrades the possibility of discriminating a desired target return from other unavoidable obstacle and sidelobe returns (or clutter) and from relatively strong additive background noise.

It should be clear that, in applications that are affected by the spectral splatter of the oscillation, the frequency or phase instabilities of the oscillation may or may not account for the significant sidebands and diffused linewidth of the oscillation. Only after it has been established in a clear manner that amplitude fluctuation effects on the spectrum are entirely negligible is it safe to attribute the oscillation spectral characteristics exclusively to the frequency or phase fluctuations.

Specification of Oscillator Instability Characteristics

For applications of the type discussed in the sections on precision range and range-rate measurements, the most direct determinant of the effects of oscillator instability is $S_{\dot\phi}(\omega)$. Since $\dot\phi(t) = d\phi/dt$,

$$S_{\dot\phi}(\omega) = \omega^2 S_\phi(\omega). \tag{28}$$

Hence either spectral density $S_{\dot\phi}(\omega)$ or $S_\phi(\omega)$ would suffice as a specification.

One particularly interesting form of presentation of $S_{\dot\phi}(\omega)$ is as a polynomial approximation, such as

$$S_{\dot\phi}(\omega) \approx \alpha_0 + \alpha_1\omega + \alpha_{-1}\omega^{-1} + \alpha_2\omega^2 + \alpha_{-2}\omega^{-2} + \cdots, \tag{29}$$

or as a piecewise representation using selected terms from this polynomial over specified frequency intervals. The values of the various coefficients plus the RF bandwidth of the oscillator signal (limited by filtering or amplifier bandwidths) could serve as characteristic parameters of $S_{\dot\phi}(\omega)$. This approach is suggested naturally by the theoretical models to be discussed in the next section. Integrals of $S_{\dot\phi}(\omega)$ that are suitable for specified applications may be sufficient in some cases.

Of the two related functions $S_{\dot\phi}(\omega)$ and $S_\phi(\omega)$, the one preferred as a general oscillator specification for a particular source is the one that is easier to measure economically and with low error. This question is often clearly resolvable on the basis of which of the two is expected to vary more slowly or uniformly with ω. For example, in unlocked oscillators, $\phi(t)$ is characterized by a random-walk behavior, and hence $S_\phi(\omega)$ will exhibit a nonintegrable singularity at the origin. In other cases, the principal effect of the instability on the oscillation is to result in a tantalizingly unending $1/\omega$ behavior of $S_{\dot\phi}(\omega)$ near $\omega = 0$.

For some applications, the properties of the RF spectrum of the oscillator signal must be specified; this is most directly and simply achieved by direct measurements on the RF spectrum itself. Unfortunately, current practice is heavily oriented toward indirect approaches involving the measurement of quantities of questionable significance—such as rms frequency deviation—based exclusively on the phase or frequency fluctuations. The difficulty with these indirect approaches arises from two fundamental considerations:

1. The possibility that the amplitude fluctuations cannot be neglected.
2. The fact that the RF spectrum *per se* is not uniquely determined by any one number (or even a few numbers) obtained by averaging some power of the phase or frequency fluctuations.

One might suppose that, inasmuch as the emphasis really is often on the RF spectral density *levels* rather than *shape*, it may be possible to determine upper bounds on the density level in terms of some average quantity derived from the

frequency fluctuations. This approach is quickly discouraged by the fact that the effect of components, in any part of the RF spectrum, on the frequency fluctuations depends not only on the spectral level of those components but also on their frequency separations from the undisturbed position of the oscillation frequency. Thus, if a given value of mean-square frequency deviation is to be used in bounding the level of RF spectral density, then it will be found that no one upper bound can be associated with it. In fact, concentrating the energy in one disturbing side component for bounding purposes would result in an upper bound that varies as $1/(\omega-\omega_o)^2$ around the long-time average oscillation frequency ω_o going to ∞ as $|\omega-\omega_o| \rightarrow 0$.

MODELS AND CHARACTERISTICS OF UNSTABLE OSCILLATIONS

Having discussed the manner in which oscillator instabilities introduce errors in applications and having identified the intrinsic characteristics of the instabilities that determine the errors, we now turn to the problem of the mathematical modeling of unstable oscillations and the characterization of instabilities caused by various mechanisms.

There are two approaches to the modeling of oscillations with frequency instabilities. These approaches may be called the *causal approach* and the *black-box approach*.

In the *causal* approach, a functional structure of the oscillation source is postulated, and various causes of instability are identified and combined with an assumed ideal oscillation signal. The model is thus centered on postulated occurrences *within* a box, and the consequences of these occurrences on the properties of the output signal are then pursued. This approach is essential for an understanding of the reasons for the instability, especially in the search for developing ultrastable sources.

In the *black-box* approach, the model is centered on the resultant disturbed oscillation at the output terminals of the box, the point where the oscillation is available to the user. Thus, a number of output signal models are postulated, their properties are explored, and the actual source output is identified piecewise (for different frequency regions) with one (or perhaps more) of these models.

Causal Approach

In the causal approach to the modeling of unstable oscillations, two types of disturbances that give rise to frequency instability are distinguished: namely, *additive noise* and *multiplicative noise*. In loop-controlled oscillators, the reference signal input also may contain a nonnegligible added noise component.

Additive noise models take account of noise added to the oscillator signal either in the oscillator loop or in the buffer amplifier following the oscillator, as illustrated in Figure 7–3. The spectrum of this type of noise occupies a frequency region that often extends widely around the oscillator frequency. The noise introduced into (or originating in) the oscillator loop will be called *internal additive noise*; the noise added in the amplifier following the oscillator will be called *external additive noise*.

In addition to the additive noise near the oscillator frequency, multiplicative low-frequency processes that effectively frequency-modulate the oscillator also are present. Examples of such processes are current and voltage fluctuations (flicker noise), mechanical vibrations, temperature variations, etc. The deviation ratio of the frequency modulation caused by these processes usually is large. Consequently, the shape of the resulting RF spectrum is essentially identical with the shape of the probability density function of the resultant baseband noise process.

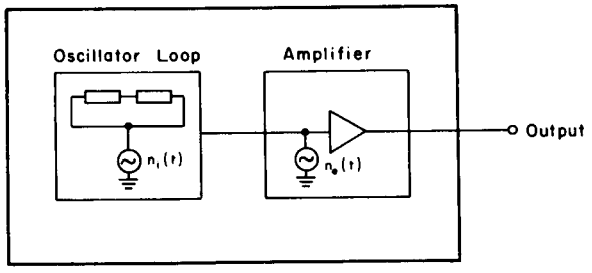

FIGURE 7–3.—An oscillator with a buffer amplifier, showing additive noise sources [$n_i(t)$, internal noise source; $n_e(t)$, external noise source].

Additive-Noise Model: External Noise

For this model, it is assumed that the oscillator delivers a perfectly stable signal, to which relatively white Gaussian noise is added. If the oscillator signal is expressed as

$$e_{osc}(t) = A\cos\omega_o t, \tag{30}$$

the additive noise may be expressed in the form

$$n_e(t) = n_c(t)\cos\omega_0 t + n_q(t)\sin\omega_0 t, \tag{31}$$

where $n_c(t)$ and $n_q(t)$ are white Gaussian processes. The sum of the oscillator signal and the additive noise is

$$e_{out}(t) = [A + n_c(t)]\cos\omega_o t + n_q(t)\sin\omega_o t. \tag{32}$$

Since we are dealing with very stable oscillators, it can be assumed that the rms value of the noise is much smaller than the rms value of the oscillator signal. Hence, only $n_q(t)\sin\omega_o t$ influences the phase of $e_{out}(t)$ significantly, and

$$e_{out}(t) \approx A[1 + n_c(t)/A]\cos\{\omega_o t + [n_q(t)/A]\}. \tag{33}$$

Thus, a relativeley weak externally added noise component results in envelope fluctuations $n_c(t)/A$ and phase fluctuations $\phi_e(t)$ given by

$$\phi_e(t) = n_q(t)/A. \tag{34}$$

If, over the frequency range of interest, the mean-square one-side spectral density of the added noise is N_0 volts²/cps, then the two-side spectral density of $n_q(t)$ will also be N_0 volts²/cps and the phase perturbations of $e_{out}(t)$ will have a spectral density N_0/A^2 rad²/cps. The added

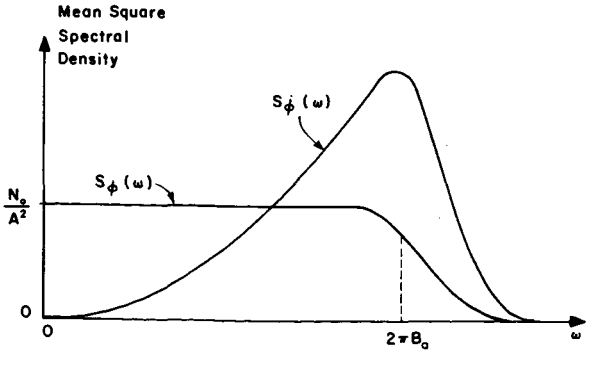

FIGURE 7–4.—Example of mean-square spectral density of phase fluctuations due to additive external noise.

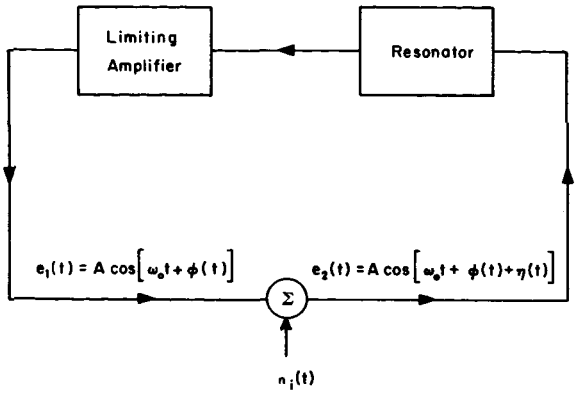

FIGURE 7–5.—Oscillator loop with internal additive noise.

noise will of course be modified by the RF filtering in the buffer amplifier. This filtering restricts the bandwidth of the phase perturbations so that their spectrum is confined to a frequency region extending up to one-half of the amplifier RF bandwidth. Thus, the mean-square spectral density $S_\phi(\omega)$ of the output signal phase fluctuations will be as illustrated in Figure 7–4, where B_a cps denotes one-half the amplifier bandwidth.

Since the instantaneous frequency fluctuations are given by the time derivative of the phase fluctuations, the mean-square spectral density $S_{\dot\phi}(\omega)$ of the frequency fluctuations is given by

$$S_{\dot\phi}(\omega) = \omega^2 S_\phi(\omega). \tag{35}$$

In the present case,

$$S_{\dot\phi}(\omega) = \omega^2 N_0/A^2, \qquad \text{for } |\omega| < 2\pi B_a. \tag{36}$$

If the RF amplifier frequency response beyond $\pm 2\pi B_a$ falls off faster than $1/\omega^2$, the mean-square spectral density of the frequency fluctuations will be as illustrated in Figure 7–4.

It is clear that this type of noise in unstable oscillator outputs can be characterized by the following two gross parameters:

1. The relative noise density N_0/A^2.
2. The buffer amplifier bandwidth $2B_a$.

Additive-Noise Model: Internal Noise

In this model the additive noise enters into the oscillator loop as shown in Figure 7–5. The noise $n_i(t)$ is assumed white in a frequency region around the oscillator frequency. The additive

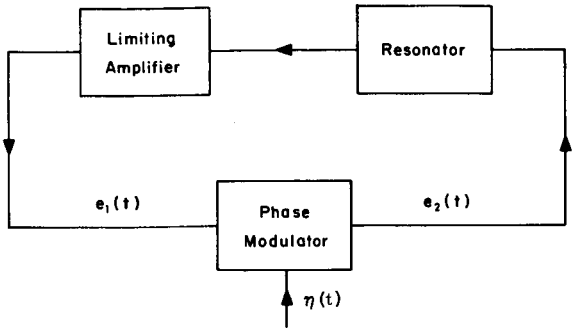

FIGURE 7–6.—Equivalent diagram of the oscillator in Figure 7–5.

noise $n_i(t)$ can be expressed in the form

$$n_i(t) = V_n(t)\cos[\omega_o t+\theta_n(t)], \qquad (37)$$

where $V_n(t)$ and $\theta_n(t)$ are low-pass processes. Then the sum of the output of the limiter and the noise is

$$\begin{aligned} e_2(t) &= e_1(t)+n_i(t) \\ &= \{A+V_n(t)\cos[\phi(t)-\theta_n(t)]\} \\ &\times \cos[\omega_o t+\phi(t)]+\{V_n(t)\sin[\phi(t)-\theta_n(t)]\} \\ &\times \sin[\omega_o t+\phi(t)]. \end{aligned} \qquad (38)$$

With $V_n(t) \ll A$ almost all of the time, the instantaneous phase of $e_2(t)$ is approximately $[\omega_o t+\phi(t)+\eta(t)]$, in which

$$\eta(t) \approx [V_n(t)/A]\sin[\phi(t)-\theta_n(t)]. \qquad (39)$$

Thus the effect of the additive noise is to introduce a fluctuating phase shift into the loop. Recognizing this, we can replace the adder in Figure 7–5 by an equivalent phase modulator as in Figure 7–6.

When the phase shift $\eta(t)$ is equal to zero, the oscillator will oscillate at the frequency for which the phase shift through the resonator is zero (i.e., at its resonance frequency). However, when $\eta(t) \neq 0$, the introduction of the phase shift will change the oscillator frequency so that the phase shift in the resonator is equal to $-\eta(t)$ and the total phase shift around the loop is zero. Thus the variations of $\eta(t)$ will cause fluctuations of the oscillator frequency. In fact, Figure 7–6 represents the block diagram of a familiar frequency-modulated oscillator. In this case, however, the control signal $V_n(t)\sin[\phi(t)-\theta_n(t)]$ is dependent on the phase $\phi(t)$ of the oscillator signal.

The frequency modulation sensitivity is determined by the phase slope (vs. frequency) of the resonator transfer function. Since the resulting frequency fluctuations will be small, only the part of the phase characteristic near the resonant frequency is of interest. In that region the phase characteristic can be assumed linear. For a resonator represented by a single tuned circuit with a half-power bandwidth of B_R cps, the phase shift $\phi(t)$ caused by a small frequency variation around the resonant frequency is approximately

$$\phi(t) \approx \dot{\phi}(t)/\pi B_R. \qquad (40)$$

Thus the phase condition for oscillations becomes

$$\eta(t)-(1/\pi B_R)\dot{\phi}(t)=0, \qquad (41)$$

whence

$$\dot{\phi}(t) = \pi B_R[V_n(t)/A]\sin[\phi(t)-\theta_n(t)]. \qquad (42)$$

This is a nonlinear differential equation with random input that seems very hard to solve. However, some observations about the mean-square spectral density of $\dot{\phi}(t)$ may be made. If, for example, $\phi(t)$ was absent from the right-hand side of Equation 42, then the mean-square spectral density of $\dot{\phi}(t)$ would be equal to the spectral density of $\pi B_R[V_n(t)/A]\sin\theta_n(t)$; that is, it would be white with a mean-square spectral density equal to $(\pi B_R/A)^2 N_0$. The presence of $\phi(t)$ in the right-hand side will spread out the spectrum with a downward slope away from

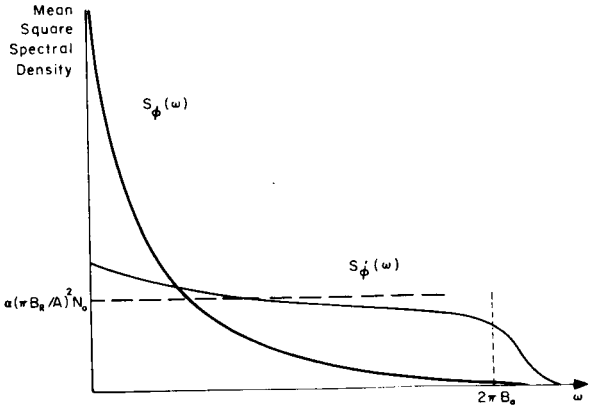

FIGURE 7–7.—Mean-square spectral densities of phase and frequency fluctuations due to internal noise source.

$\omega=0$. Aside from the tendency for peaking at $\omega=0$ [because of the spectral convolutions associated with the nonlinearities inherent in (42)], the general level of the spectral density of $\dot{\phi}(t)$ will be lower than $(\pi B_R/A)^2 N_0$. Since it seems reasonable to assume that this spectral density is approximately uniform over the frequency range of interest, we can express it as $\alpha(\pi B_R/A)^2 N_0$, where α is a positive constant smaller than unity.

As in the case of the external noise, it is clear that the amplifier following the oscillator will limit the spectrum of $\dot{\phi}(t)$ essentially to the frequencies up to B_a cps. The appearance of the mean-square spectral density of the phase and frequency fluctuations due to an internal noise source is shown in Figure 7–7. In the region where $S_{\dot{\phi}}(\omega)$ is uniform, the spectrum of the phase is given by

$$S_{\dot{\phi}}(\omega) = S_{\phi}(\omega)/\omega^2.$$

The above type of oscillator instability can then be characterized by the following parameters:

1. The mean-square spectral density

$$\alpha(\pi B_R/A)^2 N_0$$

of the oscillator frequency fluctuations.

2. The buffer amplifier bandwidth $2B_a$.

Multiplicative Noise Model

The frequency of an oscillator always is somewhat susceptible to variations in circuit parameters. An ultrastable oscillator is, of course, designed so that the sensitivity to the parameter variations is very small. Considerable effort also is directed to keeping the parameters as constant as possible. Examples of phenomena that can cause parameter variations in an oscillator are temperature variations, voltage supply variations, current variations, magnetic field variations, mechanical vibrations, etc. These low-frequency processes essentially frequency-modulate the oscillator. Some of them (as, for example, voltage supply variations due to hum or periodic vibrations) are periodic functions and will thus yield a discrete mean-square spectral density for the oscillator frequency or phase fluctuations. The other processes usually have continuous spectral densities that decrease monotonically with frequency.

The most common of the above processes are the low-frequency current fluctuations in the electronic tubes and transistors used in crystal oscillators. This type of fluctuation is called *flicker noise*. It has a spectral density of the form $S_{\dot{\phi}}(\omega)=\beta/\omega$, where β is a constant. Since the energy of the flicker noise must be finite, this spectral density must ultimately become flat as $\omega\rightarrow 0$. Thus, the spectrum of the frequency fluctuations resulting from flicker noise can be characterized by the gross parameter β.

Loop-Controlled (APC and AFC) Oscillators

There are two types of loop-controlled oscillators (Reference 1) that are of wide interest, namely, Automatic Phase-Controlled reference oscillators (APC) and Automatic Frequency-Controlled reference oscillators (AFC). The performance of these systems in the presence of a strong reference signal is well known: the instantaneous frequency noise caused by relatively white input additive Gaussian noise is also Gaussian with a mean-square spectral density that rises as the square of frequency and is ultimately bounded by the filtering effect of the driving filter in cascade with the low-pass equivalent closed-loop system function.

It is of interest here to consider the situation in which the input reference signal, if any, is weak compared with the noise present.

APC Oscillator—Consider the functional diagram of an APC loop shown in Figure 7–8. Let

$$e_{in}(t)=[E_s+n_{c,if}(t)]\cos[\omega_{if}t+\psi(t)] - n_{q,if}(t)\sin[\omega_{if}t+\psi(t)], \quad (43)$$

in which

E_s = constant amplitude of input reference signal,

$\psi(t)$ = instantaneous phase fluctuations of input reference signal,

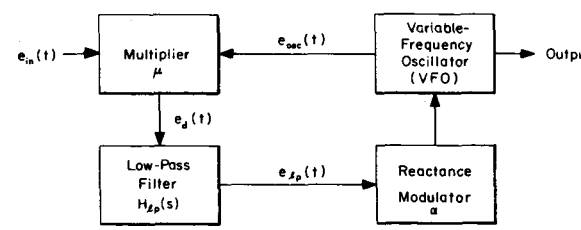

FIGURE 7–8.—APC oscillator.

and $n_{c,if}(t)$ and $n_{q,if}(t)$ are instantaneous amplitudes of cophasal and quadrature components of the input noise. Also, let the oscillation be represented by

$$e_{osc}(t) = E_{osc} \cos[\omega_{osc}t + \phi_{osc}(t)]. \quad (44)$$

Under the assumption of stable feedback operation, and in the absence of spurious byproducts in the output of the multiplier, we have, with $\omega_{if} = \omega_{osc}$,

$$(\mu\alpha)^{-1}\dot{\phi}_{osc}(t) = \{[1 + E_s^{-1}n_{c,if}(t)] \times \sin[\psi(t) - \phi_{osc}(t)] + E_s^{-1}n_{q,if}(t) \times \cos[\psi(t) - \phi_{osc}(t)]\} \otimes h_{lp}(t), \quad (45)$$

where $\otimes$ denotes convolution and $h_{lp}(t)$ is the impulse response of the low-pass filter. The existence of a feedback steady-state condition in which Equation 45 gives an adequate description of loop performance requires that

$$|\psi(t) - \phi_{osc}(t)| \leq \pi/2. \quad (46)$$

If a perfect bandpass limiter operates on the sum of signal and noise before it is applied to the APC loop, Equation 45 is replaced by

$$(\mu\alpha)^{-1}\dot{\phi}_{osc}(t) = h_{lp}(t) \otimes \sin[\psi(t) + \theta_{n,if}(t) - \phi_{osc}(t)], \quad (47)$$

where

$$\theta_{n,if}(t) = \tan^{-1}\frac{n_{q,if}(t)}{E_s + n_{c,if}(t)}. \quad (48)$$

It is generally convenient to set

$$\phi_{osc}(t) = \phi_{osc,s}(t) + \phi_{osc,n,d}(t), \quad (49)$$

in which $\phi_{osc,n,d}(t)$ combines all the distortion and noise products in the phase of the oscillation and $\phi_{osc,s}(t)$ represents a pure signal term given by $\psi(t) \otimes h_{eq}(t)$, $h_{eq}(t)$ being the impulse response of the low-pass linear equivalent strong-signal model of the closed-loop system.

When the input signal component is much weaker than the noise, Equation 45 can be reduced to

$$(\mu\alpha)^{-1}\dot{\phi}_{osc,n,d}(t) \approx h_{lp}(t) \otimes \{E_s^{-1}V_{n,if}(t) \times \sin[\theta_{n,if}(t) - \phi_{osc,n,d}(t)]\}, \quad (50)$$

where

$$\theta_{n,if}(t) \approx \tan^{-1}n_{q,if}(t)/n_{c,if}(t) \quad (51)$$

and

$$V_{n,if}(t) \approx [n^2_{c,if}(t) + n^2_{q,if}(t)]^{1/2}. \quad (52)$$

Formally, Equation 50 differs from Equation 42 for the effect of an internal noise source only by the low-pass filtering effect $h_{lp}(t)$.

The introduction of a perfect bandpass limiter to operate on the sum of signal and noise before the APC loop transforms Equation 50 to

$$(\mu\alpha)^{-1}\dot{\phi}_{osc,n,d}(t) \approx h_{lp}(t) \otimes \sin[\theta_{n,if}(t) - \phi_{osc,n,d}(t)]. \quad (53)$$

To understand the significance of Equations 50 and 53, we first note that in this discussion we are concerned primarily with the situations in which either

$\phi_{osc,n,d}(t)$ fluctuates much more slowly than

$$\theta_{n,if}(t), \quad (54)$$

or

$$|\phi_{osc,n,d}(t)| \ll |\theta_{n,if}(t)| \leq \pi/2. \quad (55)$$

These conditions correspond to an APC loop whose low-pass transmittance to the phase of the oscillation attenuates strongly all frequencies that are not much smaller than the bandwidth of the IF system preceding the loop.

Thus, under either of Conditions 54 and 55, Equations 50 and 53 can be approximated by

$$(\mu\alpha)^{-1}\dot{\phi}_{osc,n,d}(t) \approx h_{lp}(t) \otimes [E_s^{-1}x_{q,if}(t)] \quad (56)$$

and

$$(\mu\alpha)^{-1}\dot{\phi}_{osc,n,d}(t) \approx h_{lp}(t) \otimes \sin\theta_{n,if}(t). \quad (57)$$

Integration yields

$$\phi_{osc,n,d}(t) \approx (\mu\alpha/E_s)\int^t h_{lp}(u) \otimes x_{q,if}(u)\, du \quad (58)$$

in the absence of prelimiting, and

$$\phi_{osc,n,d}(t) \approx \mu\alpha\int^t h_{lp}(u) \otimes \sin\theta_{n,if}(u)\, du \quad (59)$$

when the input signal plus noise is prelimited. Equations 58 and 59 show that, irrespective of prelimiting or the lack of it, the APC loop treats

the noise presented to it in an essentially linear manner with an equivalent linear filter system function given by

$$H_{ol}(s) = \mu\alpha H_{lp}(s)/s \qquad (60)$$

as long as either of Conditions 54 and 55 is satisfied. Note that $H_{ol}(s)$ is the "open-loop" transfer function of the APC loop.

Some remarks about the physical significance of the above results are in order. First, note that $H_{lp}(s)/s$ has a pole at the origin as long as $H_{lp}(s)$ is not allowed to have a zero there. The effect of this pole is to cause $|H_{ol}(j\omega)|^2$ to weight a nonzero noise density around $\omega=0$ in a hyperbolic manner. Thus, even though $|H_{lp}(j\omega)/\omega|$ cuts off more rapidly than $|H_{lp}(j\omega)|$ at the higher frequencies, the behavior near $\omega=0$ does not allow the integral that yields the mean-squared value of the output noise to converge. The physical meaning of this is that, although the mean value of $\phi_{osc,n,d}(t)$ will be zero, the unboundedness of the mean square indicates unbounded excursions that require a reexamination of Condition 55. Physically, the oscillation beats continuously with the input noise. Heavy filtering of the higher frequency noise beats by $H_{lp}(s)/s$ causes $\phi_{osc,n,d}(t)$ to be rather slow compared with $\theta_{n,if}(t)$, thus allowing the noise modulation of the oscillator frequency to have an essentially Gaussian character and permitting the approximation of (50) by (56) and (53) by (57). The oscillator phase fluctuations wander out of step with the input noise fluctuations, causing the loop to treat the noise essentially in an open-loop manner. If the input signal component is much weaker than the noise, so that its contribution at the low-pass filter output is dominated by the noise, the loop will be unable to distinguish the signal from the equivalent of a weak noise component. No closed-loop control can therefore be established by the signal, and the oscillator frequency is modulated mainly by the Gaussian noise as filtered by the low-pass filter $h_{lp}(t)$. The effect of this modulation of the oscillator frequency is known to cause the oscillator phase to stray in random-walk-like manner. But, even though the mean-square error in identifying the oscillator phase will diverge (directly, for random walk) with the length of the observation interval (because of the cumulative action of the integration in Equations 58 and 59), the mean-square error in identifying the oscillator frequency will go to zero (inversely) with increasing length of the observation interval. Comparison of (59) and (58) also shows that prelimiting increases the noise level in the output.

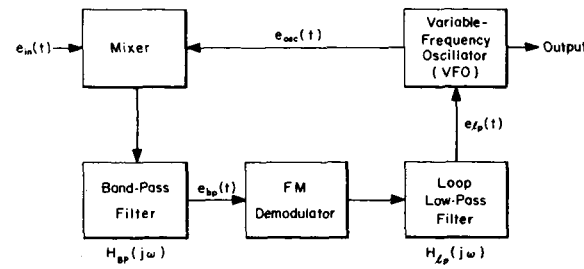

FIGURE 7–9.—AFC oscillator.

AFC Oscillator—The functional diagram of an oscillator with an automatic frequency control loop is shown in Figure 7–9. We assume that the closed-loop system can lock properly to the desired signal in the absence of noise, and let $e_{in}(t)$ and $e_{osc}(t)$ be described by Equations 43 and 44, respectively. The AFC loop is assumed to be driven with no prior amplitude limiting of signal plus noise. Under these conditions, we further assume that the mixer delivers in the nominal passband of the loop bandpass filter only the beat components

$$[E_s+n_{c,if}(t)]\cos[\omega_{bp}t+\psi(t)-\phi_{osc}(t)] - n_{q,if}(t)\sin[\omega_{bp}t+\psi(t)-\phi_{osc}(t)],$$

in which $\omega_{bp}\equiv\omega_{if}-\omega_{osc}=$ nominal center frequency of the bandpass filter within the loop. If an amplitude-insensitive linear FM demodulator and a linear feedback from the discriminator output to the instantaneous frequency of the VFO are assumed, we can show that

$$\phi_{osc}(t) = k_d\beta_{fb}\left[\tan^{-1}\frac{A_q(t)\otimes h_{LP}(t)}{A_c(t)\otimes h_{LP}(t)}\right]\otimes h_{lp}(t), \qquad (61)$$

where

$$A_c(t) \equiv [1+E_s^{-1}n_{c,if}(t)]\cos[\psi(t)-\phi_{osc}(t)] - E_s^{-1}n_{q,if}(t)\sin[\psi(t)-\phi_{osc}(t)],$$

$$A_q(t) \equiv [1+E_s^{-1}n_{c,if}(t)]\sin[\psi(t)-\phi_{osc}(t)] + E_s^{-1}n_{q,if}(t)\cos[\psi(t)-\phi_{osc}(t)],$$

and $h_{LP}(t)$ is the impulse response of the lowpass analog of the bandpass filter.

Now let the input reference signal be much weaker than the noise. Two cases are considered: In the first, we assume that

$$|\psi(t)-\phi_{osc}(t)| \ll 1.$$

We then have from Equation 61,

$$\phi_{osc}(t) \approx k_d\beta_{fb}h_{lp}(t) \otimes \tan^{-1}\frac{\{n_{q,if}(t)+n_{c,if}(t)[\psi(t)-\phi_{osc}(t)]\}\otimes h_{LP}(t)}{\{n_{c,if}(t)-n_{q,if}(t)[\psi(t)-\phi_{osc}(t)]\}\otimes h_{LP}(t)}. \quad (62)$$

If we introduce some additional assumptions, this expression can be simplified still further. For example, if the loop low-pass filter bandwidth is relatively "sharply" restricted to a value below one-half the bandpass filter bandwidth and if $k_d\beta_{fb}$ is not high enough to broaden the bandwidth of $\phi_{osc}(t)$ above one-half the bandpass filter bandwidth, then

$$\phi_{osc}(t) \approx k_d\beta_{fb}h_{lp}(t) \otimes \tan^{-1}\left\{\psi(t)-\phi_{osc}(t)+\frac{n_{q,if}(t)\otimes h_{LP}(t)}{n_{c,if}(t)\otimes h_{LP}(t)}\right\}$$

$$\approx k_d\beta_{fb}h_{lp}(t)\otimes[\psi(t)-\phi_{osc}(t)] + k_d\beta_{fb}h_{lp}(t)\otimes\phi_{n,LP}(t),$$

where

$$\phi_{n,LP}(t) = \tan^{-1}\frac{n_{q,if}(t)\otimes h_{LP}(t)}{n_{c,if}(t)\otimes h_{LP}(t)}.$$

Rearrangement of terms yields (with $u_0(t)=$ unit impulse)

$$[u_0(t)+k_d\beta_{fb}h_{lp}(t)]\otimes\phi_{osc}(t) \approx k_d\beta_{fb}h_{lp}(t)\otimes[\psi(t)+\phi_{n,LP}(t)],$$

whence

$$\phi_{osc}(t) = h_{eq'}(t)\otimes[\psi(t)+\phi_{n,LP}(t)], \quad (63)$$

where $h_{eq'}(t)$ is the impulse response of a linear filter with transmittance

$$H_{eq'}(s) = \frac{k_d\beta_{fb}H_{lp}(s)}{1+k_d\beta_{fb}H_{lp}(s)}. \quad (64)$$

This system function differs from the more complete closed-loop system function associated with strong-signal models of AFC systems and frequency-compressive feedback demodulators only in that the transmission effects of the loop bandpass filter on the frequency fluctuations of the input reference signal have been neglected (Reference 1).

If instead of requiring $|\psi(t)-\phi_{osc}(t)| \ll 1$, we express $\phi_{osc}(t)$ as a sum (see Equation 49) of a pure signal-modulation component $\phi_{osc,s}(t)$ and noise and distortion component $\phi_{osc,n,d}(t)$ and require only that

$$|\psi(t)-\phi_{osc,s}(t)|_{max} \ll 1,$$

then Equation 61 with the noise assumed much stronger than the signal leads to

$$\phi_{osc,s}(t) \approx \psi(t)\otimes h_{eq'}(t)$$

and

$$\phi_{osc,n,d}(t) \approx k_d\beta_{fb}h_{lp}(t) \otimes \tan^{-1}\frac{h_{LP}(t)\otimes \sin[\phi_{n,if}(t)-\phi_{osc,n,d}(t)]}{h_{LF}(t)\otimes \cos[\phi_{n,if}(t)-\phi_{osc,n,d}(t)]}, \quad (65)$$

where

$$\phi_{n,if}(t) \equiv \tan^{-1}[n_{q,if}(t)/n_{c,if}(t)].$$

In each case, the phase fluctuations of the weak input phase reference are transmitted, filtered by $h_{eq'}(t)$, to the controlled oscillator phase without compression by the noise. However, in practice the FM noise impulses and the dips of the noise envelope below the drive threshold of the FM demodulator within the loop will prevent this FM demodulator from operating in the "amplitude-insensitive linear" manner assumed in the analysis. Moreover, the various factors that contribute to improper AFC tracking of signal plus noise all will be in evidence below the AFC noise threshold. Consequently, the comparatively severe disruptive noise effects may well completely mask the frequency fluctuations contributed by the input reference signal.

Black-Box Approach

In the black-box approach to the modeling of unstable oscillations, the source output is represented in various frequency ranges by signal models whose properties fit the properties of the

source output over the specified portions of the spectrum. This approach is useful because it provides an alternate route to the characterization of source outputs with emphasis on the user needs. It also adds further insight into the mechanisms of instability in the signal structure, provides representations that are particularly suitable for analysis in subsequent parts of a system, bypasses the difficulties of dealing with nonlinear differential equations by assuming applicable signal representations or forms, and is naturally suited to the analysis of problems of spectral purity.

A common way to explain how an oscillation comes about in a properly designed loop without visible "provocation" is to rationalize that unavoidable random-current or voltage fluctuations in various parts of the loop provide an excitation in a feedback loop with sharp selectivity (determined principally by the phase shift of a high-Q resonator) about the frequency of in-phase feedback. The regeneration around the loop builds up the feeble provocation to a strong signal whose amplitude is limited ultimately by automatic nonlinear gain control action or by actual saturation. This, together with the fact that the regenerative loop selectivity is of nonzero (albeit small) width about the frequency of in-phase feedback, suggests that the resulting signal may actually consist of a band of Gaussian-like noise with or without a distinct sinewave at the center of the band. In the immediate vicinity of the oscillation frequency, the oscillation signal therefore may be modeled by a *band of amplitude-limited Gaussian noise.*

Other models for representing the signal over various frequency intervals are:

Sinewave plus Gaussian noise,
Constant-amplitude carrier frequency-modulated by narrow-band gaussian noise,
Sinewave plus one or more discrete-frequency components,
Combinations of the above.

Applicability of these various models depends on the origin of the signal. For example, if the signal is a processed form of an originally extremely stable source, then frequency-processing adds noise with a bandwidth extending over at least 10 times the original source width of band. Therefore, sinewave plus Gaussian noise would be a good model. If, however, the width of the source band is not too narrow relative to bandwidths of later processing circuits, then the appropriate model may be

1. A band of noise, if passive filters only are used for tone isolation;
2. A constant-amplitude signal frequency modulated by noise if a phase-locked loop is used for "tone isolation."

We now discuss some of the above models to bring out their characteristic properties.

Amplitude-Limited Narrow-Band Gaussian Noise

If the center frequency is denoted ω_o rad/sec, bandpass amplitude-limited narrow-band Gaussian noise may be expressed as

$$e_l(t) = A_l \cos[\omega_o t + \eta(t)], \tag{66}$$

where $\eta(t)$ is the instantaneous phase of a Gaussian noise process and hence has a uniform distribution over the range $|\eta| \leq \pi$. The mean-square spectral density $S_{\dot{\eta}}(\omega)$ of $\dot{\eta}(t)$ has been derived in a number of publications (References 2, 3, 4, and 5) for rectangular as well as for Gaussian shapes of the spectrum before limiting. Illustrative curves are sketched in Figures 7–10(a) and (b), $(\rho=0)$. It is interesting to observe the $1/\omega$ shape of $S_{\dot{\eta}}(\omega)$ over a narrow frequency range surrounding $\omega=0$ and extending principally over a few times the bandwidth of the prelimited process (defined by the resonator in the oscillator circuit).

The peak factor $(p.f.)_\eta$ of $\eta(t)$ is readily shown to be $\sqrt{3}$, whether η is considered to range over $|\eta| \leq \pi$ or over $0 \leq \eta \leq 2\pi$, modulo 2π.

The RF spectrum of this type of signal has also been studied (References 2 and 6) extensively, and is illustrated in Figure 7–11.

Sinewave Plus Gaussian Noise

The properties of the resultant of sinewave plus Gaussian noise are well known (References 3 and 7). Of principal interest here are the following facts: *First,* under conditions of very high ratio of the mean-square value of the sinewave to the mean-square value of the Gaussian noise, the statistics of the phase and frequency fluctuations of the resultant signal are practically Gaussian

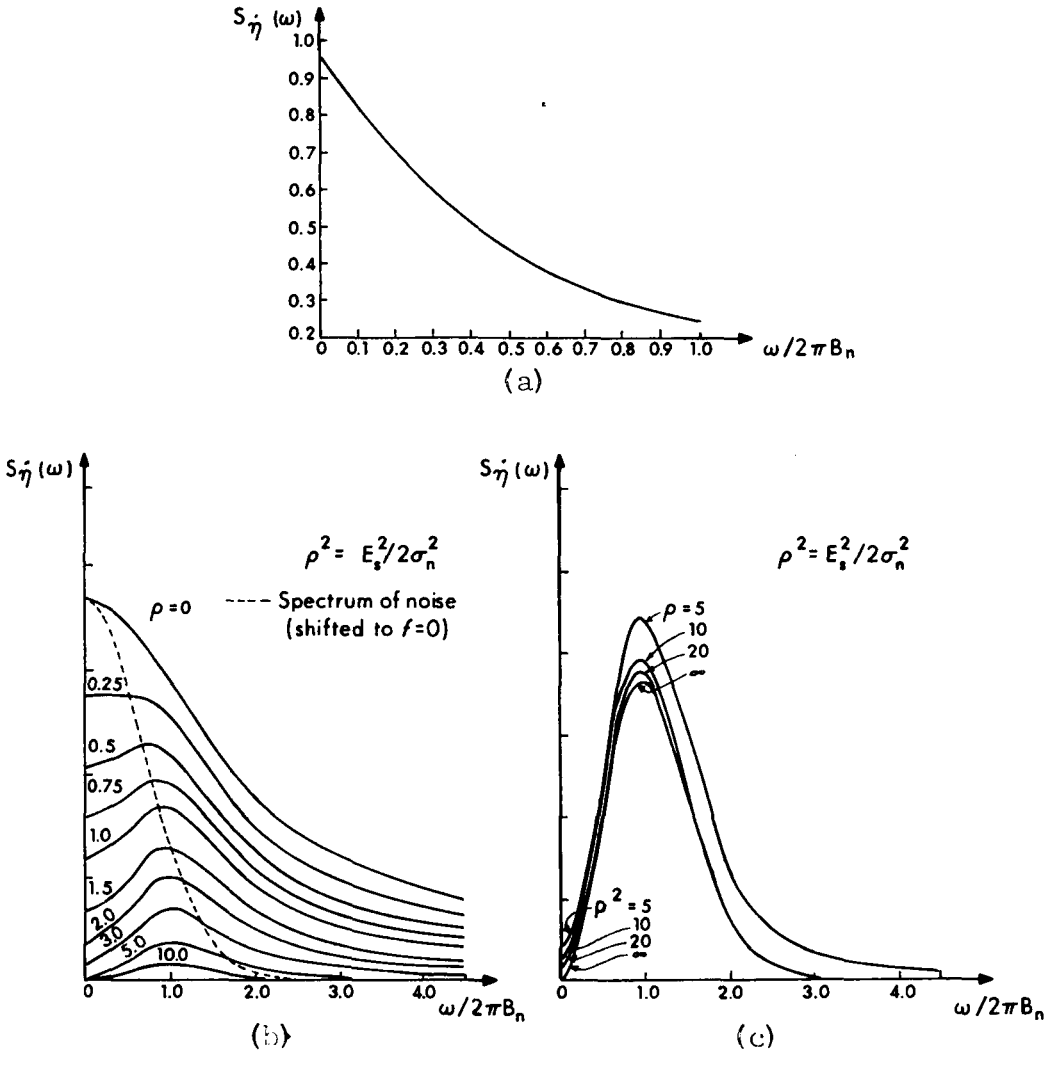

FIGURE 7–10.—(a) Mean-square spectral density of instantaneous frequency of narrow-band Gaussian noise with a rectangular input spectrum (adapted from Reference 2). (b) Mean-square spectral density of the frequency fluctuations $\dot\eta(t)$ of the resultant of sine wave plus Gaussian noise for different relative sine wave powers (adapted from Reference 5). (c) Same as (a) but for strong sine wave (note change in scale); B_n is equal to half the noise bandwidth before limiting (adapted from Reference 5).

and *second*, the mean-square spectral density of the phase fluctuations practically differs only by a constant multiplier from the sum of the positive-frequency half and the negative-frequency half of the spectral density of the input noise, after both halves have been shifted down to $\omega = 0$.

If the amplitude-limited resultant of the sine-wave plus the Gaussian component is expressed as in Equation 66 and $e_1(t)$ is used to represent the output of an oscillator, the "initial" phase ϕ of the sinewave must be assumed to be uniformly distributed over $-\pi \leq \phi \leq \pi$, since all values of ϕ are equally likely. Then the unconditional probability density function $p(\eta)$ of the total phase will also be uniform. However, the conditional probability density $P(\eta/\phi)$ of the total phase $\eta(t)$, given the phase ϕ of the sinewave, is shown in Figure 7–12 for different relative strengths of the sinewave.

The mean-square spectral density $S_{\dot\eta}(\omega)$ of $\dot\eta(t)$ is shown in Figures 7–10(b) and (c) for the case in which the noise spectral density before

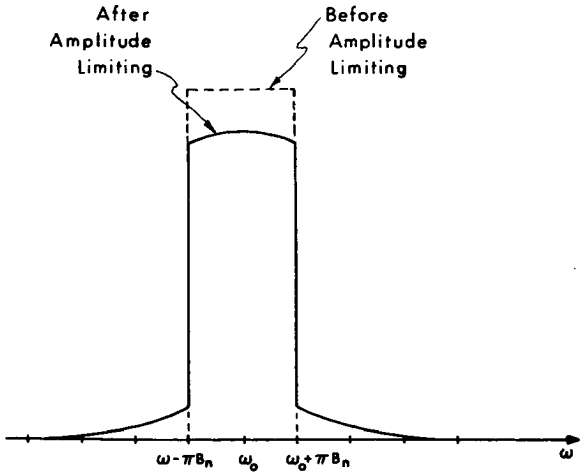

FIGURE 7–11.—Shape of RF spectral density of bandpass-limited Gaussian noise for rectangular prelimiting noise spectrum (adapted from Reference 6).

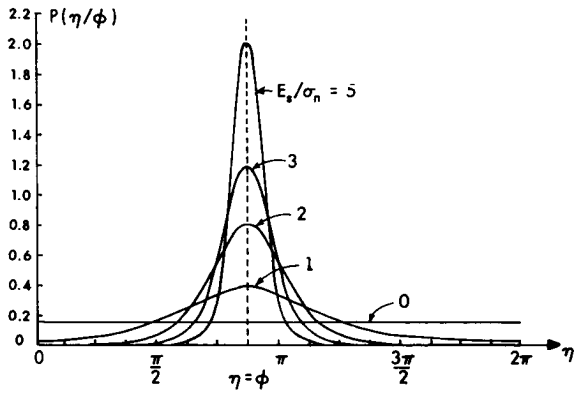

FIGURE 7–12.—Probability density function of the total phase η, conditioned on the phase ϕ of the sine wave, for various strengths of the sine wave (adapted from Reference 5).

limiting has a Gaussian shape. The shape of the input noise spectrum about the center frequency ω_0 is superimposed as a dashed curve on the low-frequency curves in Figure 7–10(b).

It is interesting to note from Figure 7–10(b) that, outside the frequency range defined for each solid curve by the intersection with the dashed curve, the solid curve under consideration shows a $1/\omega$ dropoff with ω, whereas inside of this range the solid curve either flattens out or actually bends down as $\omega \rightarrow 0$. The mean-square spectral density always will have a nonzero value

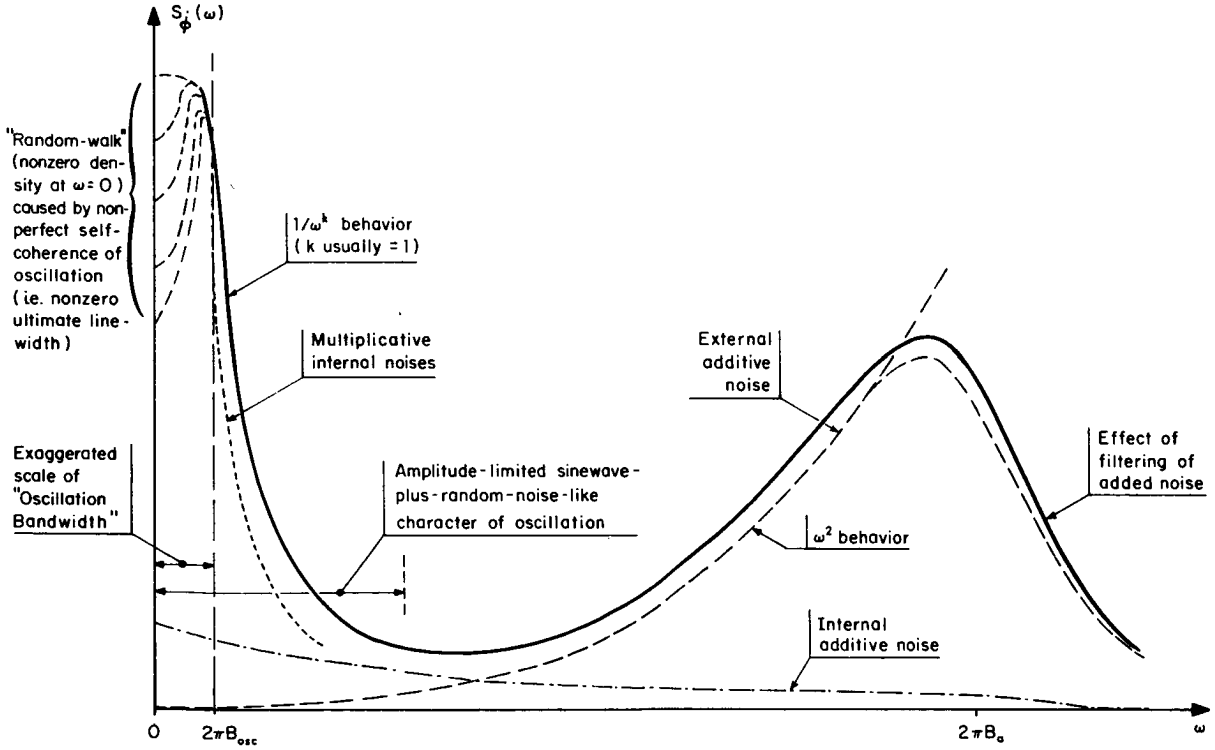

FIGURE 7–13.—Spectral density (solid curve) of instantaneous frequency fluctuations resulting from combination of various instability mechanisms (arbitrarily chosen relative levels for illustration only).

for $\omega=0$ because of the impulsive component present in the instantaneous frequency of the resultant. (Only in the case of an infinitely strong sinewave is the spectral density strictly zero for zero frequency.) In view of the extremely narrow postdetection processing bandwidths normally encountered in applications of ultrastable oscillations, no distinction between the impulsive component and the smooth component of the instantaneous frequency need be made.

For a nonzero spectral density for $\dot{\eta}(t)$ at $\omega=0$, the mean-square spectral density of $\eta(t)$ is infinite at $\omega=0$; this follows from the fact that the spectrum of the phase is obtained by dividing the frequency modulation spectrum by ω^2. The infinite spectral density for $\omega=0$ results in an infinite rms value of the phase in any frequency regions that includes $\omega=0$. These properties are characteristic of a so-called *random-walk* process.

Combined Effect of Various Mechanisms

The various mechanisms of oscillator frequency instability modeled in the preceding sections all may be expected to be present in varying degrees in practical oscillators. The net effect of the combined mechanisms on the spectral density of the resulting instantaneous frequency fluctuations is illustrated in Figure 7–13.

Of the various parts of the overall curve in Figure 7–13, the part contained within $0 \leq \omega \leq 2\pi B_{osc}$ merits further explanation. By definition, B_{osc} is a measure of the "width" of the oscillation band and is determined by the shape of the nominally "infinite-Q" selectivity curve for feedback around the oscillating loop. In an ultrastable oscillator, B_{osc} will be an extremely small fraction of a cps, perhaps corresponding to periods of hours, days, or longer. The scale of B_{osc} in Figure 7–13 is greatly exaggerated to illustrate a *guess* about what the heretofore unmeasured part of the spectral density $S_{\dot{\phi}}(\omega)$ might look like. The suggested extensions of the curve of $S_{\dot{\phi}}(\omega)$ toward $\omega=0$ are based on a model of the oscillation as a sinewave plus a band of Gaussian noise arising from the various irregularities of the electronic phenomena associated with the loop components and shaped spectrally by the selectivity of the feedback under conditions of sustained oscillation. Two significant consequences of such a physically motivated model are:

1. The ultimate "linewidth" of the oscillation, as gauged by B_{osc}, is nonzero. This causes $S_{\dot{\phi}}(\omega)$ to have a *nonzero* value at $\omega=0$, thus accounting for the inherent random-walk phenomenon in unlocked oscillators. $S_{\dot{\phi}}(0)=0$ (and hence the random-walk effect is absent) only if the oscillation is perfectly self-coherent; that is, its ultimate linewidth B_{osc} is zero.
2. The extremely slow fluctuations of the extremely narrow band of noise representing the ultimate oscillation signal are practically indistinguishable from the slow multiplicative noise phenomena (flicker noise, etc.). If one were to filter out the flicker and related noise effects within the loop by some high-pass filtering action, hyperbolic behavior of the spectral density of the frequency fluctuations immediately beyond $\omega=2\pi B_{osc}$ should persist.

MEASUREMENT OF OSCILLATOR INSTABILITIES

Any theoretical characterization of oscillator instabilities is of little practical value if some effective means cannot be devised to measure the pertinent parameters or properties brought out by the characterization. In this section, we examine the measurement problem for the purpose of developing satisfactory means for measuring the principal characteristics of unstable oscillations. The importance of the RF spectrum of the entire oscillator signal and of the mean-square spectral density of only the frequency fluctuations of the oscillator signal for different applications has been discussed in previous sections. Some general aspects of RF spectrum measurement are presented in this section. However, in view of the fact that frequency instability is the subject of paramount interest in this paper, major attention is directed to the measurement of the spectral densities $S_{\phi}(\omega)$ and $S_{\dot{\phi}}(\omega)$ of the instantaneous phase and frequency fluctuations. We shall identify the features that should be exhibited by techniques for measuring these spectral densities, and then outline the form and discuss the particular technique that is most suitable. We shall compare this technique with that most commonly

advocated and employed by others. Finally, we shall point out the general limitations of all approaches to the measurement problem that exist at the present time.

Representation of Oscillator Signal

In general, a perturbed oscillation signal may be expressed in the form

$$e(t) = A(t)\cos[2\pi\bar{f}t + \phi(t)], \qquad (67)$$

where $A(t)$ is the amplitude of the signal, $\bar{f}$ is the constant *long-time average* frequency, and $\phi(t)$ embodies the instantaneous phase fluctuations with zero *long-time* mean. It is important to observe the emphasis made here on *long-time averages*. In the second section of this paper, we treated a typical "one-shot" measurement in specified applications and emphasized that the error due to instability would, strictly speaking, result only from changes in the continuing oscillator signal that would cumulate during the time separation between the two compared samples of the oscillation. For that reason, we employed a representation of the oscillation phase in which $\phi(t) = 0$ at the time of the first sample; namely,

$$2\pi f_0 t + \phi(t),$$

where f_0= instantaneous frequency at the time of the first sample. The difference between the two representations is philosophically important, although it may turn out to be of no practical significance in a number of applications. Thus, if for the time being the $\phi(t)$ associated with f_0 is denoted $\phi_0(t)$ and that with $\bar{f}$ is denoted $\phi_-(t)$, then over a very long time interval (assuming the instability process to be at least wide-sense stationary)

$$\bar{f} - \bar{f}_0 = \overline{\dot{\phi}_0(t)}/2\pi, \qquad (68)$$

since $\overline{\dot{\phi}_-(t)} = 0$ and $\bar{\bar{f}} = \bar{f}$, where the overbar denotes "*long-time* average." This suggests that f_0 may not be convenient to work with for general-purpose measurement of the characteristics of oscillator frequency instability, because it is too tied down to the timing of the first sample in a specific one-shot application, and it may be expected to vary randomly from "one-shot" to "one-shot" in a sequence of application measurements. Consequently, for the purpose of general-purpose measurements of oscillator frequency instability characteristics, the representation

$$2\pi\bar{f} + \phi(t)$$

is preferable. The effect of the use of such general-purpose data in the computations of a specific application that entails a sequence of individual one-shot comparisons of time-spaced samples of oscillator phase or frequency is a problem in the well-developed field of statistical sampling, and therefore will not be considered here.

RF Spectrum Measurement

Direct spectral analysis is the most obvious way of measuring the RF spectrum of an oscillator signal. This technique has instrumentation problems that are treated extensively in the literature. In order to avoid these difficulties, it is frequently supposed that the RF spectrum can be determined in a straightforward manner from the spectrum of the instantaneous frequency fluctuations, $S_{\dot{\phi}}(\omega)$. The supporting argument is based on the assumption that the phase fluctuations caused by the frequency instabilities are sufficiently small so that only the first-order RF sidebands will be significant. We now shall show that the preceding assumption about the effects of the instabilities is untenable and hence that the RF spectrum is *not* related in the usually assumed manner to $S_{\dot{\phi}}(\omega)$.

Starting with the representation in Equation 67, we assume that the AM effects are negligible. Trigonometric expansion yields

$$e(t) = A[\cos\phi(t)\cos 2\pi\bar{f}t - \sin\phi(t)\sin 2\pi\bar{f}t]. \qquad (69)$$

If it can be assumed that

$$\overline{\phi^2(t)} \ll 1, \qquad (70)$$

then we can write

$$e(t) \approx A[\cos 2\pi\bar{f}t - \phi(t)\sin 2\pi\bar{f}t], \qquad (71)$$

which represents the so-called low-modulation-index approximation to $e(t)$. This shows that the spectrum of $e(t)$ would consist of a spectral line at $\omega = 2\pi\bar{f}$, plus the spectrum of $\phi(t)$ translated to this carrier frequency.

It is well known, however, that $\phi(t)$ always exhibits the characteristics of a random walk,

so that

$$\lim_{\omega \to 0} S_\phi(\omega) \to \infty \tag{72}$$

and the rms value of $\phi(t)$ is unbounded. Thus, Condition 70 never holds, and the phase fluctuations of the carrier cannot be assumed to be sufficiently small so that Approximation 71 is valid. Severe spectral spreading results from the highly nonlinear modulation characteristics indicated in Equation 69. Effects of AM that we have thus far neglected may also be present. Hence, a simple, unique relation between the spectrum of the frequency (or phase) fluctuations of an oscillator signal and the RF spectrum of the complete signal cannot be established.

Fundamental Properties of Satisfactory Measurement Systems for $S_\phi(\omega)$ and $S_{\dot\phi}(\omega)$

The first requirement for measuring $S_\phi(\omega)$ and $S_{\dot\phi}(\omega)$ is to extract $\phi(t)$ and $\dot\phi(t)$ for direct examination, free of the effects of $2\pi\bar{f}t$ and $A(t)$. Other desired characteristics of the measurement technique are sensitivity and accuracy, sensitivity being the more important because it bears on the observability of the fluctuations sought. Finally, provisions for monitoring the measurement errors are desirable.

We can evolve the basic structure of the measurement system by considering how to realize the above properties. By forming the product of two oscillator signals, we can obtain a signal $e_d(t)$ such that

$$e_d(t) = k \cos[2\pi(\bar{f}_1 - \bar{f}_2)t + \phi_1(t) - \phi_2(t)], \tag{73}$$

where the subscripts refer to the individual oscillators, at the sacrifice of including the instability of two oscillator signals in each measurement. Providing that the statistical independence of all oscillator signals is assured, two-at-a-time measurements on three members of a given class of oscillators are sufficient to determine the deviation spectra of each. In the limit as $\bar{f}_1 - \bar{f}_2$ approaches zero, the product operation becomes synchronous detection. If the inputs to the detector are in quadrature, Equation 73 becomes

$$e_d(t) = k \sin[\phi_1(t) - \phi_2(t)] \approx k\Delta\phi(t), \tag{74}$$

where

$$\Delta\phi(t) = \phi_1(t) - \phi_2(t), \tag{75}$$

providing $\Delta\phi(t)$ is sufficiently small. The resulting signal can be processed to yield the power spectrum of $\Delta\phi(t)$, $S_{\Delta\phi}(\omega)$ by several means. Differentiation of $e_d(t)$ results in a signal that can be processed for $S_{\Delta\dot\phi}(\omega)$. Because of the expected shapes of instability spectra for a highly stable oscillator, $S_{\Delta\dot\phi}(\omega)$ should be measured for spectral regions of relatively small ω, and $S_{\Delta\phi}(\omega)$ should be measured for relatively large ω.

The assurance of synchronous detection of quadrature signals establishes a self-error evaluation property for the system. If *one* signal is introduced at both inputs (except that one input is shifted 90 degrees in phase) to the detector, the power spectrum of the resulting output signal should be uniformly zero. A residual spectrum produced by the measurement circuitry will result, however, from the noise and distortion that are not completely crosscorrelated at the inputs to the detector. Evaluation of this residual spectrum establishes the measurement error as well as the effective measurement sensitivity of the system. Inasmuch as the introduction of one signal as an input to both signal channels of the system can be accomplished at any point before the detector, the residual spectrum contributed by predetection gain circuits such as amplifiers and multipliers, as well as frequency synthesizers that convert atomic resonance frequencies to standard outputs, can be measured in this way. Thus, we can provide additional gain, and perhaps sensitivity, by incorporating multiplication techniques before the detector.

Since both oscillator signals must be independent, the inputs to the product device are not guaranteed to be coherent or in quadrature. However, a system that ensures these necessary relations without affecting the independence of the signals has been conceived and analyzed by ADCOM, Inc.

The limitations of this type of system are the state of the art in circuitry required for its implementation and the general problem of spectral analysis of real-time data.

It is our opinion that this spectrum measuring technique does not suffer in comparison with any others. In some cases, it displays significant

advantages. We shall compare it with the period counting technique as an example of other methods for measuring the frequency instabilities of oscillators.

Period Counting Techniques

We shall consider the common technique of period measurement with a counter, although our arguments will pertain to the whole class of measurements that incorporate a moving-average calculation.

A standard period counting test setup is shown in Figure 7–14. Two independent oscillator signals, $e_1(t)$ and $e_2(t)$, are mixed to produce a beat signal $e_b(t)$ whose average frequency is much lower than that of the input signals. In this way, much of the average value contamination will be removed. $e_b(t)$ is introduced as a triggering signal to a gate in the counter. At one zero-crossing of $e_b(t)$, the gate opens to pass the high-frequency counter oscillator signal $e_c(t)$, which is "accumulated" or counted in the counter register. After an integral number of periods of $e_b(t)$, the gate is closed and the total count is read. As the period of $e_c(t)$ will be a simple decimal fraction of a second, say 0.1 microsecond, the counter will display the total number of 0.1 microseconds that equal the integral number of $e_b(t)$ periods. We define the length of time the gate is open as τ. Usually several consecutive measurements of length τ are made, and the resulting data are reduced to yield the average value and the mean-square deviation of the accumulated periods. The rms value of the deviation divided by the average of the period accumulated in a time τ is called $I(\tau)$, the frequency instability in a time τ of an oscillator signal. The assumption here is that the normalized rms deviation of frequency is essentially equal to the normalized rms deviation of period, which is valid for highly stable oscillator signals.

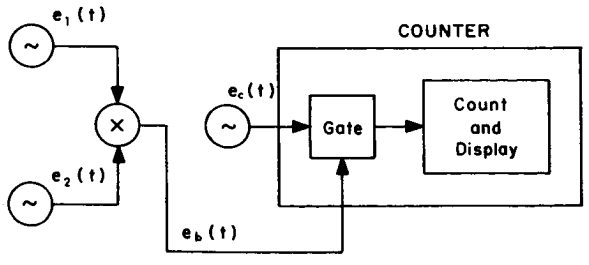

FIGURE 7–14.—A standard period counting test setup.

Existing literature describes the sensitivity of measurement of this technique in terms of the imperfections of counters (Reference 8). Here we are interested in comparing this technique with the spectral measurement we advocate.

In the first place, the two techniques measure different quantities, so we shall start by relating these quantities. Let us assume a perfect counter with such a high internal oscillator frequency that we can consider the period accumulation to be a continuous time process. In addition, let us assume that the display has so many digits that we can resolve the deviation in period by measuring one oscillator signal directly, instead of the beat between two oscillators. Let us represent the oscillator signal as in Equation 67. Then we may define the instantaneous frequency of the oscillator signal $f(t)$ as

$$f(t) = \bar{f} + \delta f(t), \tag{76}$$

where $\bar{f}$ is the average value and $\delta f(t)$ the deviation from it. We can define the instantaneous period of the signal as $T(t)$, such that

$$T(t) = \bar{T} + \delta T(t); \tag{77}$$

and, by definition,

$$T(t) = 1/f(t). \tag{78}$$

We can show that

$$N(\tau, t) = \int_t^{t+\tau} T(\mu)\, d\mu, \tag{79}$$

where $N(\tau, t)$ is the accumulation in the display for a given count of length τ. Following the same procedure as in the second section, we can show that as a consequence of Equation 79

$$I(\tau) = (2\pi\bar{f})^{-1}\left[\frac{1}{2\pi}\int_{-\infty}^{+\infty} S_\phi(\omega)\,\frac{\sin^2(\omega\tau/2)}{(\omega\tau/2)^2}\,d\omega\right]^{1/2} \tag{80}$$

Having established the relation between the two measured quantities, we are in a position to make three comparisons:

1. *$S_\phi(\omega)$ is a more fundamental parameter than $I(\tau)$.* Given $S_\phi(\omega)$, Equation 80 shows that $I(\tau)$

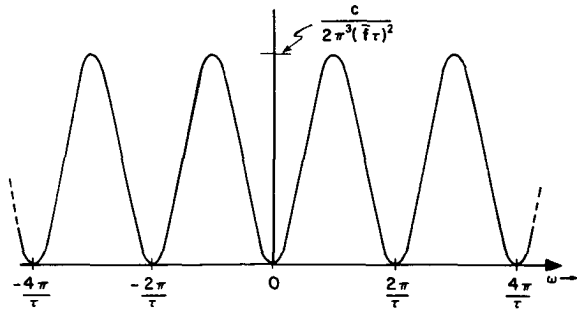

FIGURE 7–15.—The instability integral associated with a parabolic spectral density for the frequency fluctuations.

can easily be calculated from it. Reversing the process would indeed be difficult. Only after we have specified a form of the spectrum with a small number of parameters, such as

$$S_\phi(\omega) = (a/\omega) + b + c\omega^2, \qquad (81)$$

can we obtain spectral information from $I(\tau)$. Then, by solving Equation 80, we could obtain $I(\tau)$ in terms of complicated functions of a, b, c, and ω. The three chosen parameters could be evaluated through a high-order least-error curve fit to $I(\tau)$. Even so, this is not a direct calculation of $S_\phi(\omega)$ from $I(\tau)$, inasmuch as $S_\phi(\omega)$ has been forced to conform to a preconceived notion whose validity may be questioned. For evaluation of a variety of applications from one basic test, we must compute $S_\phi(\omega)$.

2. $I(\tau)$ *may well be ambiguous* in that there may be an additional degree of freedom inherent in $I(\tau)$ that is not a property of the oscillator.

To illustrate this second point, before listing point (3), let us consider the simple spectral density $S_\phi(\omega) = c\omega^2$. Then Equation 80 reduces to the square root of the area under the curve shown in Figure 7–15.

The area under the curve is infinite. But, in a real situation, there will be some filtering in a measurement system that will band-limit $S_\phi(\omega)$. Let us assume that this filtering is approximately rectangular with a rather wide bandwidth, such that

$$\omega_a \gg 2\pi/\tau,$$

where ω_a is the cutoff radian frequency of the filter. In this case, the curve shown in Figure 7–15 will go through many cycles as ω approaches ω_a. The area will then be approximately the average value of the curve multiplied by $2\omega_a$. Thus,

$$I(\tau) \approx (2\pi\bar{f}\tau)^{-1}(2c\omega_a/\pi)^{1/2}. \qquad (82)$$

This result shows a familiar $1/\tau$ shape, but the presence of ω_a makes Equation 82 unspecific about c. Thus, any description of $I(\tau)$ must contain the effective filtering characteristic as additional information in the data. In general, we cannot expect $I(\tau)$ to remain unchanged if the bandwidth of the measuring system is changed. Thus, a direct $I(\tau)$ measurement may not provide a specification of the oscillator alone and is generally unacceptable as a general-purpose specification of the oscillator frequency instability.

Others have shown that the moving average or "rectangular time window" that describes the period counting technique is an inefficient and relatively unstable operation for determining the power spectrum of a process (Reference 9).

3. *The period counting technique is not self-checking.* In the section on "The Fundamental Properties of Satisfactory Measurement Systems for $S_\phi(\omega)$ and $S_\varphi(\omega)$," we showed that the determination of the residual spectrum of the test equipment requires the introduction of two identical, completely crosscorrelated input signals to the equipment. It is obvious that this is useless in the case of a period measuring system such as illustrated in Figure 7–15, because the system requires presence of a beat frequency output from the the mixer. (A modified period-counting technique that avoids this difficulty has been described by Cutler, see Paper 8, these Proceedings).

In some applications, operations that are indistinguishable from the basic period counting operation are actually carried out. For these applications, period counting is definitely a useful testing method provided that it is designed as an accurate imitation of the eventual operations. More generally, period-counting tests may be designed to imitate a wide variety of *spot measurements* in specific applications. In this regard, period counting can be exploited as a useful simulation tool. But outside of these rather restricted circumstances, data on oscillator instability obtained by the period-counting technique are practically useless.

General Limitations of Spectral Measurements of Phase and Frequency Fluctuations

As stated previously, the general limitations of the measurement of oscillator frequency instability are those of extracting spectral information from real-time signals. Thus there are upper and lower limits on the magnitude of ω for which spectral information can be obtained. Since the analysis of oscillator frequency instability effects in coherent ranging and related systems involves integration of $S_\phi(\omega)$ around $\omega=0$, the lower limit is far more important. This limit is caused by the extreme averaging time required to resolve the spectra close to the origin, and the complicated nonstationary statistics of oscillator drift phenomena. Some authors have attempted to establish a lower limit on the magnitude of ω related to the total time that an oscillator can be operated without recalibration (References 10 and 11). The assumption is made that this lower limit bounds a region of the spectrum centered about the origin over which integration for analysis will not be needed, as the oscillator will not be operated for intervals longer than the time corresponding to this bound. This extension toward $\omega=0$ of resolution in the spectrum of frequency instability is worthy of further effort.

ACKNOWLEDGMENT

This paper is based on work performed for NASA Marshall Space Flight Center, Huntsville, Alabama, under Contract No. NAS8-11228. The authors are indebted to J. G. Gregory of Marshall Space Flight Center for his interest in, and many helpful discussions of, this work to Andrew R. Chi of Goddard Space Flight Center for his encouragement and invitation of this paper, and to A. F. Ghais of ADCOM, Inc. for helpful discussions and criticisms.

REFERENCES

1. Baghdady, E. J., "Theoretical Comparison of Exponent Demodulation by Phase-Lock and Frequency-Compressive Feedback Techniques," 1964 IEEE International Convention Record, Part 6, pp. 402–421.
2. Wang, M. C., in J. L. Lawson and G. E. Uhlenbeck, *Threshold Signals*, Vol. 18, Rad. Lab. Series, McGraw-Hill Book Company: New York, 1950.
3. Rice, S. O., "Statistical Properties of a Sinewave Plus Random Noise," *Bell Syst. Tech. Journ. 27*, 109 (1948).
4. Stumpers, F. L. H. M., "Theory of Frequency-Modulation Noise," *Proc. IRE 36*, 1081 (1948).
5. Middleton, D., *Statistical Communication Theory*, McGraw-Hill Book Company, New York; 1960.
6. Price, R., "A Note on the Envelope and Phase-Modulated Components of Narrow-Band Gaussian Noise," *IRE Trans. Inf. Th.*, pp. 9–13; September 1955.
7. North, D. O., "An Analysis of the Factors Which Setermine Signal/Noise Discrimination in Pulsed-Carrier Systems," RCA Laboratories, Princeton, N.J., Tech. Rept. No. PTR-6C; June 25, 1943. Republished in *Proc. IEEE*, pp. 1016–1027; July 1963.
8. Tanzman, H. D., "Short Term Stability Measurements," *IRE International Convention Record*, vol. 9, Part 9, pp. 191–206, 1961.
9. Blackman, R. B., and Tukey, J. W., *The Measurement of Power Spectra*, Dover Publications, Inc., New York, 1959.
10. Atkinson, W. R., et al., "Spectrum Analysis of Extremely Low Frequency Variations of Quartz Oscillators," *Proc. IEEE*, p. 379, February 1963.
11. Malakhov, A. N., "Spectra of Flickernoise," *Radiotekh. Elektron. 4*, 54 (1959).

8. SOME ASPECTS OF THE THEORY AND MEASUREMENT OF FREQUENCY FLUCTUATIONS IN FREQUENCY STANDARDS

L. S. CUTLER

Hewlett-Packard Company
Palo Alto, California

Precision quartz oscillators have three main sources of noise contributing to frequency fluctuations: thermal noise in the oscillator, additive noise contributed by auxiliary circuitry such as AGC, etc., and fluctuations in the quartz frequency itself as well as in the reactive elements associated with the crystal leading to an f^{-1} type of power spectral density in frequency fluctuations.

The influences of these sources of noise on frequency fluctuation versus averaging time measurements, using the multiple-period beat frequency measuring technique, will be discussed. The f^{-1} spectral density leads to results which depend on the length of time over which the measurements are made.

The characteristics of atomic standards using a servo-controlled quartz oscillator will be discussed. The choice of servo time constant influences the frequency fluctuations observed as a function of averaging time, and should be chosen for best performance with a given quartz oscillator and environmental condition.

The purpose of this paper is to present some of the theoretical and practical aspects of frequency fluctuations in frequency standards and their measurement. The main sources of noise in oscillators and their influences will be discussed. Several of the techniques for making fluctuation measurements will be analyzed.

The f^{-1} spectral density of frequency fluctuations in oscillators requires special attention. The fluctuations in an oscillator servo-controlled by atomic devices also will be described.

No attempt will be made to make the mathematics rigorous.

DEFINITIONS

The signal from an oscillator may be described by

$$f(t) = A(t)\ \cos[\omega_0 t + \Phi(t)], \qquad (1)$$

where $f(t)$ represents a voltage or current, $A(t)$ and $\Phi(t)$ are slowly varying real functions of time, and ω_0 is a constant. $A(t)$ is the variable amplitude of the signal and does not contribute to frequency fluctuations. The time origin and ω_0 are chosen so that $\Phi(t)$ has zero time average and $|\ \Phi(t)\ | \leq C < \infty$ for all time t where C is some positive constant. These conditions simplify the mathematics (but will have to be relaxed later). The instantaneous angular frequency is

$$\omega(t) = (d/dt)[\omega_0 t + \Phi(t)] = \omega_0 + \dot{\Phi}(t). \qquad (2)$$

In all that follows we will refer to angular frequency as *frequency*. The average frequency is

$$\langle \omega(t) \rangle = \lim_{T\to\infty} T^{-1} \int_{-T/2}^{T/2} \omega(t)\ dt$$

$$= \omega_0 + \lim_{T\to\infty} \frac{\Phi(T/2) - \Phi(-T/2)}{T}$$

$$= \omega_0. \qquad (3)$$

Therefore, $\Phi(t)$ is the instantaneous phase angle of the oscillator with respect to an ideal oscillator of frequency ω_0, and $\dot{\Phi}(t)$ is the instantaneous frequency departure from ω_0. Let $\dot{\Phi}(t) = \Omega(t)$.

The frequency departure averaged over time τ is

$$\langle \Omega_\tau(t) \rangle = \langle \dot{\Phi}_\tau(t) \rangle = \tau^{-1} \int_{t-\tau/2}^{t+\tau/2} \dot{\Phi}(t')\, dt'$$

$$= \tau^{-1}[\Phi(t+\tau/2) - \Phi(t-\tau/2)]. \quad (4)$$

$\langle \Omega \rangle$ signifies the average (time or statistical) of Ω, and $\langle \Omega_\tau(t) \rangle$ signifies the finite time average at time t:

$$\langle \Omega_\tau(t) \rangle = \tau^{-1} \int_{t-\tau/2}^{t+\tau/2} \Omega(t')\, dt'.$$

The phase averaged over time τ is

$$\langle \Phi_\tau(t) \rangle = \tau^{-1} \int_{t-\tau/2}^{t+\tau/2} \Phi(t')\, dt'. \quad (5)$$

The phase difference over time τ is

$$\Delta\Phi_\tau(t) = \Phi(t+\tau/2) - \Phi(t-\tau/2) = \langle \Omega_\tau(t)\tau \rangle. \quad (6)$$

$$R_\Phi(\tau) = \langle \Phi(t+\tau/2)\Phi(t-\tau/2) \rangle$$

$$= \lim T^{-1} \int_{-T/2}^{T/2} \Phi(t+\tau/2)\Phi(t-\tau/2)\, dt \quad (7)$$

is the autocorrelation function of the phase. Similarly, $R_\Omega(\tau)$ is the autocorrelation function of the frequency departure. Writing these both as functions of τ only implies that Φ and Ω are stationary in the wide sense (Reference 1).

$$S_\Phi(\omega) = \int_{-\infty}^{\infty} R_\Phi(\tau) \exp(-i\omega\tau)\, d\tau$$

$$= 2\int_0^{\infty} R_\Phi(\tau) \cos\omega\tau\, dr, \quad (8)$$

$$R_\Phi(\tau) = \frac{1}{2\pi} \int_{-\infty}^{\infty} S_\Phi(\omega) \exp(i\omega\tau)\, d\omega$$

$$= \pi^{-1} \int_0^{\infty} S_\Phi(\omega) \cos\omega\tau\, d\omega, \quad (9)$$

so that $S_\Phi(\omega)$ and $R_\Phi(\tau)$ are Fourier transforms of each other (Reference 2), where $S_\Phi(\omega)$ is the power spectral density of the phase (we use the two-sided power spectrum). In the same way $R_\Omega(\tau)$ and $S_\Omega(\omega)$ are Fourier transforms of each other, where $S_\Omega(\omega)$ is the power spectral density of the frequency departure.

A useful measure of fluctuation is the standard deviation σ.

$$\sigma(X) = [\langle (Y - \langle X \rangle)^2 \rangle]^{1/2} = (\langle X^2 \rangle - \langle X \rangle^2)^{1/2}. \quad (10)$$

The standard deviation of the various quantities defined earlier can be written in terms of the autocorrelation functions (References 3 and 4) (see Appendix A):

$$\sigma \langle \Phi_\tau(t) \rangle = \left(\frac{2}{\tau} \int_0^{\tau} R_\Phi(\tau')[1 - (\tau'/\tau)]\, d\tau' \right)^{1/2}$$

= Standard deviation of average phase, (11)

$$\sigma[\Delta\Phi_\tau(t)] = \{2[R_\Phi(0) - R_\Phi(\tau)]\}^{1/2}$$

= Standard deviation of phase difference, (12)

$$\sigma \langle \Omega_\tau(t) \rangle = \tau^{-1}\{2[R_\Phi(0) - R_\Phi(\tau)]\}^{1/2}$$

= Standard deviation of average frequency departure, (13)

$$\sigma[\langle \Omega_\tau(t) \rangle/\omega_0] = \frac{1}{\omega_0\tau}\{2[R_\Phi(0) - R_\Phi(\tau)]\}^{1/2}$$

= Standard deviation of average fractional frequency departure. (14)

The last two may equally well be written in terms of $R_\Omega(\tau)$:

$$\sigma \langle \Omega_\tau(t) \rangle = \left(\frac{2}{\tau} \int_0^{\tau} R_\Omega(\tau')[1 - (\tau'/\tau)]\, d\tau' \right)^{1/2}, \quad (15)$$

$$\sigma[\langle \Omega_\tau(t) \rangle/\omega_0] = \frac{1}{\omega_0} \left(\frac{2}{\tau} \int_0^{\tau} R_\Omega(\tau')[1 - (\tau'/\tau)]\, d\tau' \right)^{1/2}. \quad (16)$$

Also, we have:

$$\sigma[\Phi(t)] = [R_\Phi(0)]^{1/2} = \left(\pi^{-1} \int_0^{\infty} S_\Phi(\omega)\, d\omega \right)^{1/2}$$

= Standard deviation of phase, (17)

$$\sigma[\Omega(t)] = [R_\Omega(0)]^{1/2} = \left(\pi^{-1} \int_0^{\infty} S_\Omega(\omega)\, d\omega \right)^{1/2}$$

$$= \left(\pi^{-1} \int_0^{\infty} \omega^2 S_\Phi(\omega)\, d\omega \right)^{1/2}$$

= Standard deviation of frequency. (18)

The preceding formulas hold for wide-sense

stationary random processes or for time functions which have stationary means and autocorrelation functions which depend only on the time difference τ.

MEASUREMENT TECHNIQUES

There are several well-known techniques for making measurements of some of the standard deviations described above. Some of these will now be considered.

1. *Multiple-Period Measuring System*: The general system is shown in Figure 8–1. Two signal sources, slightly offset in average frequency, feed two identical channels through optional frequency multipliers to a phase detector. The difference frequency contains all the phase information and is used to trigger the Schmitt trigger at the zero crossings. The period (or multiple period) of the sharp leading edge of the Schmitt trigger is measured by the counter, displayed by the analog recorder, and each measurement printed out on a digital recorder.

The theory behind this technique is as follows: Oscillator number 1 has output

$$V_1(t) = A_1(t)\ \cos[\omega_1 t + \Phi_1(t)\,].$$

Similarly, oscillator number 2 has output

$$V_2(t) = A_2(t)\ \cos[\omega_2 t + \Phi_2(t)\,]. \qquad (19)$$

In the frequency multipliers the amplitude changes get removed by limiting processes (if they are carefully designed, there can be little conversion of the amplitude changes to phase changes). After multiplication, the signals are:

$$V_1'(t) \approx A_1 \cos[n\omega_1 t + n\Phi_1(t)\,],$$
$$V_2'(t) \approx A_2 \cos[n\omega_2 t + n\Phi_2(t)\,]. \qquad (20)$$

It is well known that both the instantaneous phase and the average frequency are multiplied by the factor n (provided the multiplier has sufficient bandwidth to encompass the full spectrum of the nth harmonic). The phase detector behaves as a multiplier. Its output is

$$V_0(t) \approx V_1'(t)\,V_2'(t) = \tfrac{1}{2}(A_1A_2)$$
$$\times(\cos\{n[\omega_1+\omega_2]t + n[\Phi_1(t)+\Phi_2(t)\,]\}$$
$$+\cos\{n(\omega_1-\omega_2)t + n[\Phi_1(t)-\Phi_2(t)\,]\}). \qquad (21)$$

The sum frequency is filtered out, leaving only the difference frequency term. If the two signal sources have exactly the same statistics for $\Phi_1(t)$ and $\Phi_2(t)$ but are uncorrelated, then all the fluctuation can be assumed to be in one channel $\sqrt{2}$ times as large as that channel alone, while the other channel can be assumed perfect. Let

$$\omega_1 - \omega_2 = \Delta\omega. \qquad (22)$$

Then the signal which feeds the Schmitt trigger is

$$V_0'(t) = \tfrac{1}{2}(A_1A_2)\ \cos[n\ \Delta\omega t + n\Phi(t)\,], \qquad (23)$$

where $\Phi(t) = \Phi_1(t) - \Phi_2(t)$. The Schmitt trigger gives a sharp pulse out each time the signal crosses zero going in, say, the negative direction. This occurs for t such that

$$n\ \Delta\omega t + n\Phi(t) = \tfrac{1}{2}\pi + 2\pi M,$$

where M is any integer. Suppose the counter is set to count N periods and the gate opens at t_0 such that

$$n\ \Delta\omega t_0 + n\Phi(t_0) = \tfrac{1}{2}\pi.$$

The gate will close at $t_0+\tau$ such that

$$n\ \Delta\omega(t_0+\tau) + n\Phi(t_0+\tau) = \tfrac{1}{2}\pi + 2\pi N.$$

Subtracting the first from the second, we get

$$n\ [\Delta\omega\tau + \Phi(t_0+\tau) - \Phi(t_0)\,] = 2\pi N. \qquad (24)$$

Let

$$\tau = (2\pi N/n\ \Delta\omega) - \Delta\tau \equiv \tau_0 - \Delta\tau,$$
$$\tau_0 = (2\pi N/n\ \Delta\omega). \qquad (25)$$

Then

$$\Phi(t_0+\tau) - \Phi(t_0) = \Delta\omega\ \Delta\tau. \qquad (26)$$

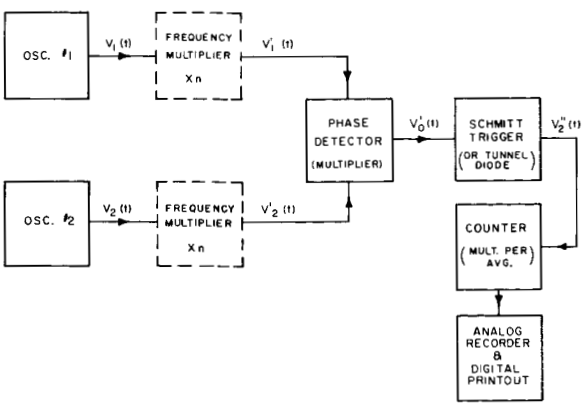

FIGURE 8–1.—Multiple-period measuring system.

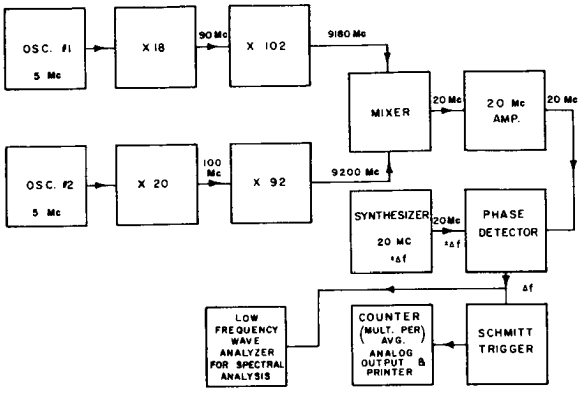

FIGURE 8–2.—Versatile multiple-period measuring system.

Since τ is not constant, the time difference $\Delta\tau$ between successive measurements is not constant; but, if $\Delta\omega\ \Delta\tau \ll 1$ and $\dot{\Phi}(t_0)\ \Delta\tau \ll 1$, then only very small error is caused by replacing $\Phi(t_0+\tau)$ by $\Phi(t_0+\tau_0)$. The process of averaging over many measurements helps here. The multiple-period technique thus measures essentially $\Phi(t+\tau_0) - \Phi(t) = \Delta\Phi_{\tau_0}(t)$. Therefore,

$$\Delta\Phi_{\tau_0}(t) \approx \Delta\omega\ \Delta\tau. \tag{27}$$

Almost any desired averaging time τ_0 can be obtained by varying N, n, or $\Delta\omega$. By making many measurements of τ in succession, the standard deviation may be estimated as

$$\sigma[\Delta\Phi_{\tau_0}(t)] \approx \Delta\omega\sigma(\Delta\tau)$$

$$\approx \Delta\omega[m^{-1}\sum_{i=1}^{m}\tau_i^2 - (m^{-1}\sum_{i=1}^{m}\tau_i)^2]^{1/2}, \tag{28}$$

where τ_i is the ith measurement and m is the total number of measurements, which should be large (of the order of 100) to give a good estimate. It is wise to remove the drift during the observation time by subtracting the best straight line based on a least-squares fit from the data. For $m=100$, this leads to

$$\sigma[\Delta\Phi_{\tau_0}(t)] = \Delta\omega\{[1/(99.99\times10^6)]$$

$$\times[999900\sum_{i=1}^{100}\tau_i^2 - 40602(\sum_{i=1}^{100}\tau_i)^2$$

$$-12(\sum_{i=1}^{100}\tau_i i)^2 + 1212(\sum_{i=1}^{100}\tau_i)(\sum_{i=1}^{100}\tau_i i)]\}^{1/2}. \tag{29}$$

The order of the data must be preserved for this formula. The other quantities of interest, such as Equations 13 and 14, may be estimated from Equation 29 in an obvious way. The subtraction of the best straight line corresponds to filtering out the low-frequency fluctuations, as will be discussed later.

Figure 8–2 shows a block diagram of a versatile system which allows the two oscillators to have zero offset. This feature allows the system noise to be evaluated by feeding both channels from one source. The offset is obtained by the frequency synthesizer, whose fluctuations do not degrade the measurement much since the oscillator fluctuations have been multiplied by 1840 times in the 20-Mc difference frequency before the comparison is made. Figure 8–3 shows some typical results obtained with this system.

From a practical standpoint the multiple-period system gives good results over a range of τ from about 10^{-4} sec to as long as is desired. The technique is particularly good for times greater than 10^{-2} sec.

2. *Phase Detector Techniques*: Figure 8–4 shows a typical phase detector or multiplier technique. If the two signals are identical in frequency and

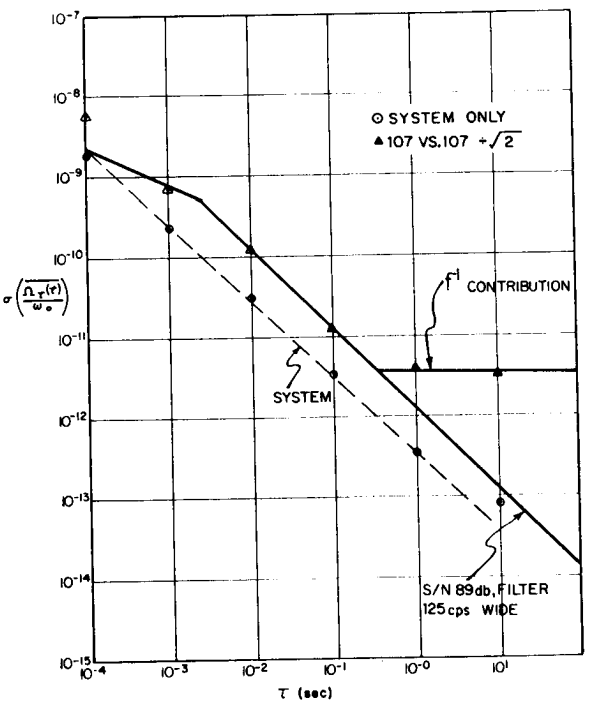

FIGURE 8–3.—Measurements with multiple-period system.

placed in quadrature, they may be represented as

$$V_1(t) = A_1(t)\cos[\omega_0 t + \Phi_1(t)],$$
$$V_2(t) = A_2(t)\sin[\omega_0 t + \Phi_2(t)]. \quad (30)$$

The product coming from the phase detector is

$$V_0(t) = V_1(t)V_2(t) = \tfrac{1}{2}[A_1(t)A_2(t)] \times \{\sin[2\omega_0 t + \Phi_2(t) + \Phi_1(t)] + \sin[\Phi_2(t) - \Phi_1(t)]\}. \quad (31)$$

As before, the sum frequency term is discarded. If $\Phi_2(t)$ and $\Phi_1(t)$ are small, then

$$V_0'(t) \approx \tfrac{1}{2}[A_1(t)A_2(t)][\Phi_2(t) - \Phi_1(t)]. \quad (32)$$

If the variations in A_1 and A_2 are small—as is usually the case—they may be neglected, and the phase detector output is essentially the difference between the instantaneous phases. Both signals may be heterodyned down to a convenient low frequency by means of two mixers and a common local oscillator. Because the approximation of small angles

$$\sin[\Phi_2(t) - \Phi_1(t)] \approx \Phi_2(t) - \Phi_1(t)$$

practically always fails for the very low frequency components of $\Phi_2(t) - \Phi_1(t)$, this technique is not good for very low frequency fluctuations. The phase detector output may be analyzed by a low-frequency narrow-band wave analyzer to estimate the spectral density of the phase $S_\Phi(\omega)$ directly. If the low-pass filter is omitted, then the rms voltmeter reading gives an estimate of $\sigma[\Phi_2(t) - \Phi_1(t)]$, provided the system has been calibrated in voltage versus phase difference. This may be accomplished by making one of the signals small

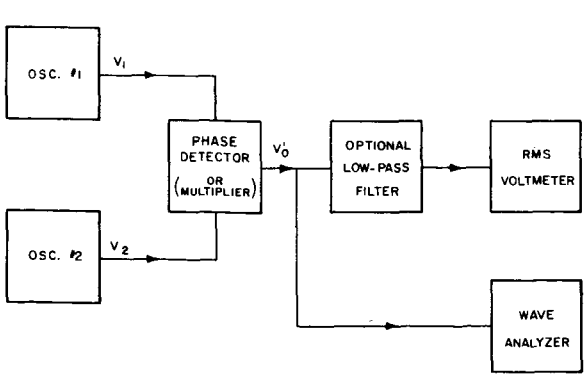

FIGURE 8–4.—Phase detector system.

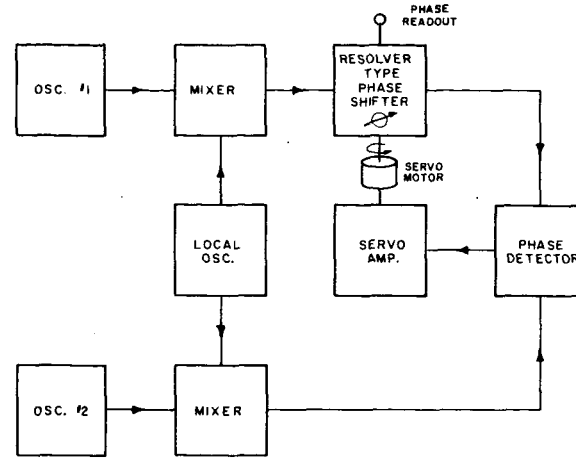

FIGURE 8–5.—Elapsed-phase method.

and offsetting it in frequency. Introduction of the low-pass filter produces two effects: First, the spectral density of the phase fluctuations is limited on the high-frequency end by the filter; second, the filter performs time averaging over a time roughly equal to the reciprocal of the band pass in radians per second. The system then gives an estimate of $\sigma\langle\Phi_r(t)\rangle$ for the phase fluctuations passed through the low-pass filter. Several systems of this general type have been described elsewhere (References 5 and 6).

The phase detector method thus gives estimates of $S_\Phi(\omega)$, $\sigma[\Phi(t)]$ for all but the low-frequency components of Φ and an estimate of $\sigma\langle\Phi_r(t)\rangle$ for the phase after modification by a low-pass filter. The technique works well for high-frequency components and, with the narrow bandwave analyzer, furnishes an excellent means of studying the power spectral density of the phase.

3. *Elapsed-Phase-Difference Method*: Figure 8–5 shows a simple elapsed- phase-difference method block diagram. The two signals are heterodyned down by means of a common local oscillator to a convenient low-frequency suitable for the resolver-type phase shifter. The servo system maintains the output phase from the phase shifter in fixed relation to the phase in the other channel Consequently, the phase shift introduced by the phase shifter is equal to the relative phase difference in the two channels. Since the relative phase is preserved in the heterodyning process it is equal to the relative phase of the two oscillators. A system of this type has been used by

J. Barnes at the NBS Laboratories in Boulder. The phase shift may be read electrically by an optical shaft encoder and thus fed directly to computation devices. If the phase is read at intervals of time τ, this technique gives an estimate of $\Delta\Phi_\tau(t)$. However, because of the slow speed of the servo and the low comparison frequencies involved, the high-frequency components of the spectrum are lost. The system thus works well for large τ ($\tau \approx 100$ sec or greater). If the signals being compared are at 5 Mc and the resolver can be read to 0.005 of one revolution, the resolution is 10^{-9} second, giving a sensitivity of 10^{-12} in $\sigma[\langle \Omega_\tau(t) \rangle/\omega_0]$ for a τ of 1000 sec.

NOISE IN OSCILLATORS

Practical oscillators appear to have three main sources of noise contributing to frequency fluctuations: (1) *thermal and shot noise in the oscillator* itself, which actually perturbs the oscillation; (2) *additive noise associated with the oscillator and accessory circuits*, such as AGC and amplifiers, which does not perturb the oscillation but is merely added to the signal; and (3) *fluctuations in the resonator frequency* either in the resonator itself or due to circuit parameter changes influencing the resonance frequency. The frequency fluctuations of an oscillator due to the last-mentioned source appear to have an f^{-1} power spectral density (Reference 7).

In oscillators used for precision frequency standards, great care is taken to couple very lightly into the oscillating circuit; and, because of the nonlinearity of the resonator, it is necessary to stabilize the oscillation at a very low power level (typically about 10^{-7} to 10^{-6} watt). As a consequence, the noise of the amplifiers following the oscillator is the predominant factor for fluctuations involving times of the order of 0.1 sec or less.

Assume the *additive noise* is band-limited by a narrow-band filter with transfer function,

$$F(\omega) \approx \frac{1}{1+i[(\omega-\omega_0)/\omega_1]}, \qquad (33)$$

where ω_1 is the half bandwidth of the filter. Such a transfer function is of course not realizable but is a good approximation for the narrow-band case. Assume also that the additive noise is white and that it has a power spectral density S_0. Then the power spectral density of the noise out of the filter will be

$$\frac{S_0}{1+[(\omega-\omega_0)/\omega_1]^2}.$$

The total noise power will be

$$P_n = \frac{1}{2\pi}\int_{-\infty}^{\infty} \frac{S_0}{1+[(\omega-\omega_0)/\omega_1]^2}\, d\omega = \tfrac{1}{2}(\omega_1 S_0). \qquad (34)$$

If the total signal power P_S is large in comparison with P_N so $P_N/P_S \ll 1$, then it is well known that half the noise power appears as amplitude modulation sidebands on the signal centered in the noise and the other half as phase modulation sidebands. The power spectral density of this effective phase modulation is then

$$S_\Phi(\omega) = \frac{1}{\omega_1}\frac{P_n}{P_S}\frac{\omega_1^2}{\omega^2+\omega_1^2}, \qquad (35)$$

and the autocorrelation function is

$$R_\Phi(\tau) = \frac{P_n}{P_S}\frac{\exp(-\omega_1 \mid \tau \mid)}{2}. \qquad (36)$$

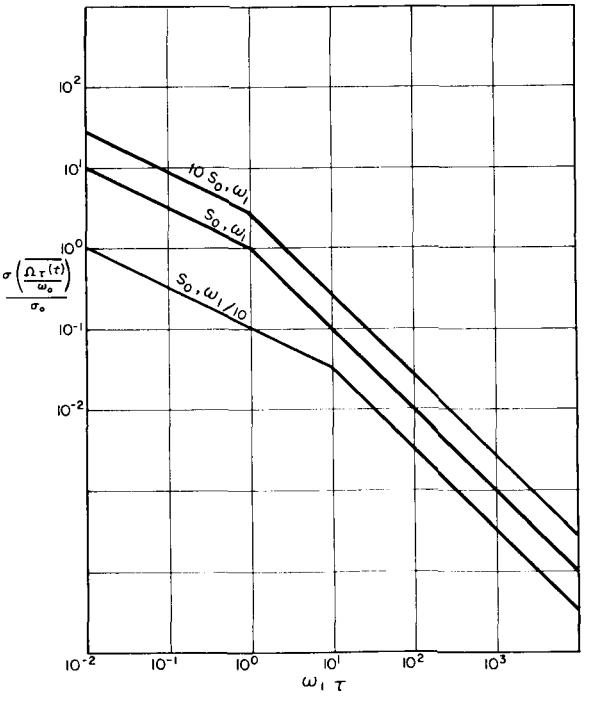

FIGURE 8–6.—normalized additive noise contributions to oscillator fluctuations.

From this, using Equation 14,

$$\sigma[\langle\Omega_\tau(t)\rangle/\omega_0]$$
Single filter

$$=(\omega_0\tau)^{-1}\{(P_n/P_S)[1-\exp(-\omega_1\tau)]\}^{1/2}. \quad (37)$$

A normalized plot of this function is shown in Figure 8–6. For $\omega_1\tau\gg1$,

$$\sigma\approx\frac{1}{\omega_0\tau}\left(\frac{P_n}{P_S}\right)^{1/2};$$

for $\omega_1\tau\ll1$,

$$\sigma\approx\frac{1}{\omega_0}\left(\frac{\omega_1}{\tau}\frac{P_n}{P_S}\right)^{1/2}.$$

For $\omega_1\tau\gg1$, σ is proportional to $\omega_1^{1/2}$ for constant noise spectral density and, for $\omega_1\tau\ll1$, it is proportional to ω_1. Consequently, using a narrow-band filter can greatly improve short-term stability. For cascaded filters each of half bandwidth ω_1, the result is

$$\sigma[\langle\Omega_\tau(t)\rangle/\omega_0]$$
Double filter

$$=(\omega_0\tau)^{-1}\{(P_n/P_S)[1-\exp(-\omega_1\tau)(\omega_1\tau+1)]\}^{1/2}. \quad (38)$$

In this case σ is constant for $\omega_1\tau\ll1$. For any shape of bandpass filter with white additive noise,

$$\sigma\approx(\omega_0\tau)^{-1}(P_n/P_S)^{1/2}$$

when τ is much greater than the reciprocal half bandwidth.

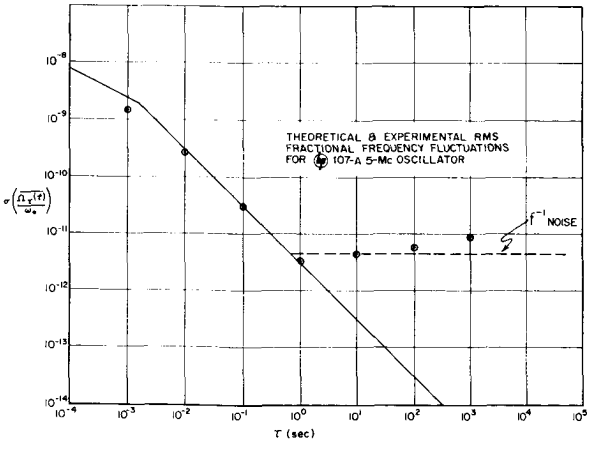

FIGURE 8–7.—Theoretical and experimental rms fractional frequency fluctuations in an oscillator.

As a practical example, consider a 5-Mc oscillator with a single filter of half bandwidth of 62.5 cps and $P_n/P_S=-87$ db. Then for $\tau=1$ sec,

$$\sigma[\langle\Omega_1(t)\rangle/\omega_0]=1.4\times10^{-12}.$$

For a comparison with experimental results, see Figures 8–3 and 8–7.

The perturbing effects of *thermal and shot noise* in oscillators are well known (Reference 8). The phase does a random walk because of the perturbations. It has been shown that this leads to

$$\sigma[\langle\Omega_\tau(t)\rangle/\omega_0]=(kT/2\tau PQ^2)^{1/2}, \quad (39)$$

where

k = Boltzmann constant,
T = effective noise temperature,
P = total power delivered to resonator and load,
Q = loaded Q of resonator.

As an example, consider a 5-Mc oscillator with $Q=2\times10^6$, $P=10^{-7}$ watt, and $T=10^3$ degrees K. For $\tau=1$ sec

$$\sigma[\langle\Omega_1(t)\rangle/\omega_0]=1.3\times10^{-13}.$$

From this example and the one above, it is apparent that the additive noise will dominate the perturbation-type noise for short averaging times in precision frequency standards. Here, the effects of the two sources of noise would become equal at about an averaging time of 100 sec, with at total fluctuation of about 2×10^{-14} if no other sources were effective. For times longer than 100 sec, the perturbation-type noise would dominate.

The *third main source of noise* is that which has an f^{-1} power spectral density of *frequency fluctuation*. In addition to this, oscillators drift in frequency (drift is usually accompanied by an f^{-1} power spectral density). Because of the drift in frequency, the phase is not a stationary process. Also, since an f^{-1} power spectral density for frequency fluctuations corresponds to $S_\Phi(\omega)$ proportional to $|\omega|^{-3}$,

$$\frac{1}{2\pi}\int_{-\infty}^{\infty}S_\Phi(\omega)[1-\exp(i\omega\tau)]\,d\omega$$

doesn't converge, since $1-\cos\omega\tau)$ only goes to zero as ω^2 for $\omega\to0$. This is not surprising. If the f^{-1} spectrum persisted down to zero frequency,

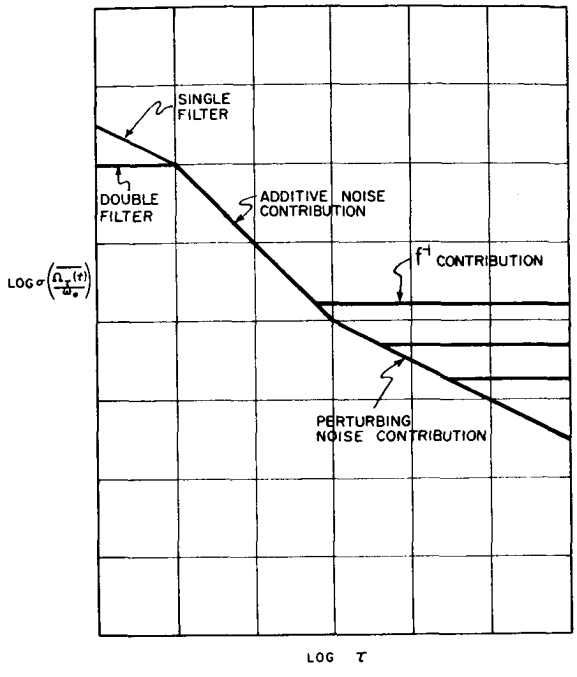

FIGURE 8–8.—Contributions to oscillator fluctuations.

we would see infinitely large fluctuations by observing over all time. In the actual situation, observations are made over a finite time T. If the frequency drift is removed during the time T by subtraction of the least-squares fit of a straight line, this corresponds to a high-pass filter acting on the low-frequency components of the phase. The output of this filter goes to zero as ω^2 for $\omega \to 0$, and the filter starts to cut off at $\omega \approx 2/T$ (see Appendix B); this gives finite results for $\sigma[\langle\Omega_\tau(t)\rangle/\omega_0]$ as shown in Appendix B. It is apparent from the functional form of the integral that, if the ratio of observing time to averaging time T/τ is constant (corresponding to a fixed number of samples), then $\sigma[\langle\Omega_\tau(t)/\omega_0]$ is constant. Since there is no theory giving the strength of the f^{-1} spectral density, no prediction can be made as to the constant value of σ. The dependence of σ^2 on T/τ is proportional to $1.04+\frac{1}{2}\log(T/2\tau)$.

Actual oscillators measured under the conditions of finite T and removal of drift exhibit the predicted behavior (see Figures 8–3 and 8–7). For T/τ of about 100, $\sigma[\langle\Omega_\tau(t)\rangle/\omega_0]$ flattens out at a value somewhat greater than 1×10^{-12}. Since this is larger than the fluctuations due to the perturbing type of noise at the τ for which additive noise becomes dominant, it is apparent that the effects of the perturbing type of noise are not seen at all in many frequency standards. Figure 8–8 shows the effects due to the three sources of fluctuations.

J. Barnes (Reference 9) of the NBS Laboratories of Boulder recently has shown that taking successive differences of the phase has interesting consequences. For example, taking second differences removes the linear frequency drift and also gives convergent results independent of observation time for an assumed f^{-1} power spectrum. As shown in Appendix A,

$$\sigma[\Delta^2_\tau\Phi(t)/\omega_0\tau]=(\omega_0\tau)^{-1}[6R_\Phi(0)-8R_\Phi(\tau)+2R_\Phi(2\tau)]^{1/2}, \quad (40)$$

where $\Delta^2_\tau\Phi(t)=\Phi(t+\tau)-2\Phi(t)+\Phi(t-\tau)$ is the second phase difference. Using this on an f^{-1} power spectral density of frequency fluctuation $S_\Phi(\omega)=K/|\omega|^3$ gives

$$\sigma=(8K\log 2)^{1/2}/\omega_0. \quad (41)$$

Since this is independent of observation time T, it appears to be a good measure for the f^{-1} characteristic of oscillators.

FLUCTUATIONS IN ATOMIC STANDARDS USING A SERVO CONTROLLED QUARTZ OSCILLATOR (REFERENCE 10)

Consider an oscillator compared against a reference such as an atomic beam device and controlled in frequency by a servo actuated by the error signal. Figure 8–9 shows a system block diagram. The power spectral density of the

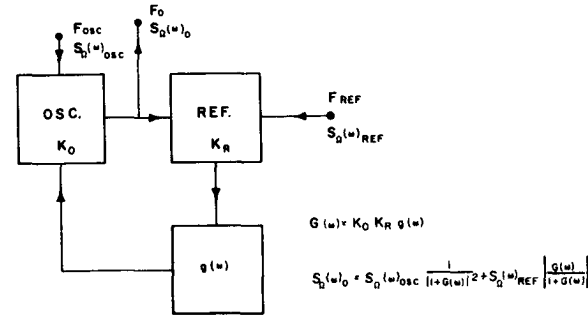

FIGURE 8–9.—The atomic standard.

fluctuations in the output frequency is

$$S_\Omega(\omega)_0 = S_\Omega(\omega)_{Osc} \frac{1}{|1+G(\omega)|^2} + S_\Omega(\omega)_{Ref} \left| \frac{G(\omega)}{1+G(\omega)} \right|^2, \quad (42)$$

where $S_\Omega(\omega)_{Osc}$ refers to the open-loop fluctuations in the oscillator, $S_\Omega(\omega)_{Ref}$ refers to the equivalent frequency fluctuations in the reference, and $G(\omega)$ is the total loop gain $K_0K_Rg(\omega)$. In deriving Equation 42 it is assumed that the system is linear and that the two noise sources are uncorrelated. The simplest useful form for $G(\omega)$, also a very practical one, is

$$G(\omega) = \omega_c/i\omega, \quad (43)$$

which is just gain and integration. This is a good approximation to what is done in many cases. Substituting, Equation 42 becomes

$$S_\Omega(\omega)_0 = S_\Omega(\omega)_{Osc}[\omega^2/(\omega^2+\omega_c^2)] + S_\Omega(\omega)_{Ref}[\omega_c^2/(\omega^2+\omega_c^2)], \quad (44)$$

so that the oscillator noise is high-pass filtered and the reference noise is low-pass filtered.

Consider first the fluctuations due to the oscillator only. If it is assumed to have characteristics similar to those previously discussed, namely additive noise filtered by a narrow-band filter of half width ω_l and an f^{-1} behavior, then—if $\omega_l \gg \omega_c$ (as is usually the case)— the additive noise contribution is virtually unchanged by the servo loop. The f^{-1} portion gives, in the closed-loop condition, (from Equations 42 and 14),

$$\sigma[\langle\Omega_\tau(t)\rangle/\omega_0] = (B/\omega_0\omega_c\tau)[1.16+2\log\omega_c\tau - \exp(-\omega_c\tau)\,Ei^*(\omega_c\tau) - \exp(\omega_c\tau)\,Ei(-\omega_c\tau)]^{1/2}, \quad (45)$$

where B is a constant depending on the strength of the f^{-1} noise. This behaves like

$$B/\omega_0[5/2-\gamma-\log(\omega_c\tau)]^{1/2}$$

(very slowly varying) for $\omega_c\tau \ll 1$ and like

$$(B/\omega_0\omega_c\tau)[2\log(\omega_c\tau)+2\gamma]^{1/2}$$

for $\omega_c\tau \gg 1$. $\gamma = 0.577$ is the Euler constant;

$$Ei(X) = \int_{-\infty}^{X} (e^t/t)\,dt, \qquad X<0,$$

is the exponential integral; and $Ei^*(X)$ is the principal value of the integral for $X>0$.

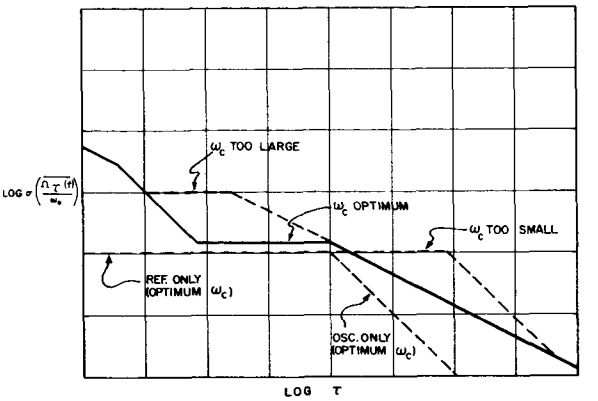

FIGURE 8–10.—Contributions to atomic standard fluctuations.

The contribution due to the reference noise, which is assumed to be white with power spectral density S_R, is (from Equations 42 and 14)

$$\sigma[\langle\Omega_\tau(t)\rangle/\omega_0] = \omega_0^{-1}\{(S_R/\omega_c\tau^2)[\omega_c\tau+\exp(-\omega_c\tau)-1]\}^{1/2}, \quad (46)$$

This approaches a constant value of $\omega_0^{-1}(S_R\omega_c/2)^{1/2}$ for $\omega_c\tau \ll 1$ and for $\omega_c\tau \gg 1$, $\sigma \approx \omega_0^{-1}(S_R/\tau)^{1/2}$. Figure 8–10 shows the behavior of the various contributions to the overall fluctuations. It is apparent that there is an optimum choice of loop ω_c for a given oscillator and beam tube.

It is of interest to calculate the power spectral density of the noise for the case of a cesium beam reference. For Ramsey excitation the response may be written for small departures from line center approximately as

$$I(t) = \tfrac{1}{2}I_m\{1+\cos\pi[\Delta\omega(t)/\omega_l]\}, \quad (47)$$

where I is the output current assumed to have maximum value I_m, $\Delta\omega$ is the departure from line center, and ω_l is the full line width. Let $\Delta\omega(t)/\omega_l = \epsilon+\alpha\cos\omega_m t$, to allow for the usual sinusoidal modulation. ω_m is the modulation frequency assumed small in comparison with ω_l so that the dynamic behavior is essentially the same as the static behavior. The result of synchronous detection of this signal is

$$I_0 = (I_m\omega_m/2\pi)\int_{-\pi/\omega_m}^{\pi/\omega_m} \tfrac{1}{2}[1+\cos\pi(\epsilon+\alpha\cos\omega_m t)] \times \cos\omega_m t\,dt = -I_m J_1(\pi\alpha)\tfrac{1}{2}(\sin\pi\epsilon) \approx \tfrac{1}{2}[-I_m J_1(\pi\alpha)]\epsilon\pi \quad (48)$$

for ϵ small. For a given offset ϵ this has the maximum absolute value of $0.91\ \epsilon I_m$ with $\pi\alpha \approx 1.8$, the first maximum of the Bessel function. This represents the signal output for a given fractional mistuning ϵ.

In a beam tube the noise is mainly due to shot noise, and so the power spectral density is proportional to $I(t)^{1/2}$ and is independent of ω. Since $I(t)$ is a function of time, the noise output is not a stationary function. If $i_n(t)$ is the instantaneous noise current under no modulation and $\epsilon = 0$, then

$$I_n(t) = i_n(t) \mid \cos[(\pi/2)\alpha \cos\omega_m t] \mid. \quad (49)$$

The autocorrelation function after synchronous detection is desired. Performing the statistical and the time averages gives

$$R_I(\tau) = \delta(\tau)(S_I/4)[1 + J_0(\pi\alpha) - J_2(\pi\alpha)], \quad (50)$$

where S_I is the spectral density of the noise current. From this and Equation 48 the spectral density S_R is

$$S_R = \frac{S_I[1 + J_0(\pi\alpha) - J_2(\pi\alpha)]\omega_l^2}{J_1^2(\pi\alpha) I_m^2 \pi^2}, \quad (51)$$

where S_I is the spectral density of the noise current, I_m is the peak signal current, $\alpha = (\Delta\omega)_{max}/\omega_l$ is the ratio of peak frequency swing due to the modulation to the full line width ω_l.

CONCLUSIONS

Some of the considerations of the theory and measurement of fluctuations in frequency standards have been presented. In some cases, many of the details have been lightly treated or omitted. It is hoped that the results will be useful in promoting understanding and in guiding designs.

ACKNOWLEDGMENT

The author would like to thank R. Vessot of Varian Associates and J. Barnes of NBS Boulder for interesting discussions, and Lee Bodily and Allen Foster of the Hewlett-Packard Company for making some of the measurements.

REFERENCES

1. Davenport and Root, "Random Signals and Noise," New York: McGraw-Hill, 1958. Section 4-5.
2. Davenport and Root (see Reference 1), Chapter 6.
3. Searle, C. L., and Brown, D. A., "Comparison of Performance Criteria of Frequency Standards," in: *Proc. 16th Annual Symposium on Frequency Control*, Atlantic City, April 1962, pp. 259–266.
4. Rarity, J., Saporta, L., and Weiss, G., "Study of Short Term Stability of Crystal Oscillators," Technical Report from New York University, Contract DA-36-039-SE-87450, DA Project No. 3A-99-15-02, 02-02.
5. Vessot, R., Private communication and also *These Proceedings*, paper 10.
6. Van Duzer, V., Private communication and also *These Proceedings*, paper 23.
7. Atkinson, W. R., Fey, L., and Newman, J., "Spectrum Analysis of Extremely Low Frequency Variations of Quartz Oscillators," *Proc. IEEE 51*, 379 (1963).
8. Edson, W. A., "Noise in Oscillators," *Proc. IRE 48*, 1454 (1960). See also Mullen, J. A., "Background Noise in Oscillators" and Golay, M., Monochromaticity and Noise in a Regenerative Electrical Oscillator." These articles follow Edson's article.
9. Barnes, J., Private communication and also *These Proceedings*, paper 11.
10. Bagnall, J. J., Jr., "The Effect of Noise on an Oscillator Controlled by a Primary Reference," in *NEREM 1959 Record*, pp. 84–86.

APPENDIX A

If $\Phi(t)$ is wide-sense stationary and has 0 mean,

$$\sigma^2[\Delta\Phi_\tau(t)] = \langle[\Phi(t+\tau/2) - \Phi(t-\tau/2)]^2\rangle = \langle\Phi(t+\tau/2)^2\rangle - \langle 2\Phi(t+\tau/2)\Phi(t-\tau/2)\rangle + \langle\Phi(t-\tau/2)^2\rangle$$
$$= 2[R_\Phi(0) - R_\Phi(\tau)], \quad (A1)$$

which gives Equation 12 in the text.

$$\sigma^2\langle\Phi_\tau(t)\rangle = \frac{1}{\tau^2}\int_{-\tau/2}^{\tau/2} dt' \int_{-\tau/2}^{\tau/2} dt'' \langle\Phi(t')\Phi(t'')\rangle = \frac{1}{\tau^2}\int_{-\tau/2}^{\tau/2} dt' \int_{-\tau/2}^{\tau/2} dt'' R_\Phi(t''-t'); \quad (A2)$$

let $(t''-t')=\tau'$. Using this substitution and interchanging the order of integration gives

$$\sigma^2\langle\Phi_\tau(t)\rangle=\frac{2}{\tau}\int_0^\tau R_\Phi(\tau')[1-(\tau'/\tau)]\,d\tau', \quad \text{(A3)}$$

which gives Equation 11.

The second phase difference, $\Delta^2\Phi_\tau(t)$, is $[\Phi(t+\tau)-\Phi(t)]-[\Phi(t)-\Phi(t-\tau)]$, or $\Phi(t+\tau)-2\Phi(t)+\Phi(t-\tau)$.

$$\sigma^2[\Delta^2\Phi_\tau(t)]=\langle[\Phi(t+\tau)-2\Phi(t)+\Phi(t-\tau)]^2\rangle$$
$$=6R_\Phi(0)-8R_\Phi(\tau)+2R_\Phi(2\tau), \quad \text{(A4)}$$

leading to Equation 40.

APPENDIX B

Assume that a signal $v(t)$ is observed for a time T and it is desired to remove the mean and the linear drift in a least-square departure sense. This requires that

$$\int_{-T/2}^{T/2}[v(t)-(a+bt)]^2\,dt=\text{Minimum}. \quad \text{(B1)}$$

For this to be satisfied,

$$a=\frac{1}{T}\int_{-T/2}^{T/2}v(t)\,dt,$$

$$b=\frac{12}{T^3}\int_{-T/2}^{T/2}v(t)t\,dt. \quad \text{(B2)}$$

Consider the Fourier transform of

$$v'(t)=v(t)-(a+bt), \qquad |t|<T/2$$
$$=0, \qquad |t|>T/2$$

$$V'(\omega)=\int_{-T/2}^{T/2}v'(t)\exp(-i\omega t)\,dt. \quad \text{(B3)}$$

Expanding the exponential which gives an approximation to $V'(\omega)$ for $\frac{1}{2}(\omega T)<1$ gives

$$V'(\omega)\approx\int_{-T/2}^{T/2}v'(t)[1-i\omega t-\tfrac{1}{2}(\omega^2t^2)+\cdots]dt$$

$$=\int_{-T/2}^{T/2}[v(t)-a-bt]$$
$$\times[1-i\omega t-\tfrac{1}{2}(\omega^2t^2)+\cdots]\,dt. \quad \text{(B4)}$$

If the integrals that can be done are carried out and the values of a and b substituted, it will be seen that $V'(\omega)$ has neither a constant term nor a term linear in ω. Also the transform of $a+bt$ goes to zero rapidly for $\omega\gg 2/T$. Effectively, $v(t)$ has been passed through a high-pass filter cutting off at about $\omega=2/T$. Another way to show this is to consider the minimization of

$$\frac{1}{2\pi}\int_{-\infty}^{\infty}|V'(\omega)|^2\,d\omega=\int_{-T/2}^{T/2}[v'(t)]^2\,dt, \quad \text{(B5)}$$

the equality holding because of Parseval's theorem. Adjusting the parameters a and b for minimum total energy is really removing the maximum amount of energy possible in the band of frequencies occupied by the transform of $a+bt$. Since this transform has a half width of the order of $2/T$, the whole process corresponds to the high-pass filter mentioned earlier. Subtracting a second-order and third-order term in t would about double the cutoff frequency.

Let us now calculate the fluctuation expected in a finite time of observation of an oscillator with f^{-1} power spectral density of frequency. Assume

$$S_\Omega(\omega)=K/|\omega|, \quad \text{(B6)}$$

so that

$$S_\Phi(\omega)=K/|\omega|^3.$$

If the oscillator were observed for an infinite time,

$$\sigma^2[\Delta\Phi_\tau(t)]=2[R_\Phi(0)-R_\Phi(\tau)]$$
$$=\frac{2K}{\pi}\int_0^\infty\frac{1-\cos\omega\tau}{\omega^3}\,d\omega,$$

which of course doesn't converge. If we cut off the integral at the lower limit $2/T$ corresponding to the filtering action of a finite time with drift removal,

$$\sigma^2=\frac{2K}{\pi}\int_{2/T}^\infty\frac{1-\cos\omega\tau}{\omega^3}\,d\omega$$

$$=\frac{2K\tau^2}{\omega}\int_{2\tau/T}^\infty\frac{1-\cos x}{x^3}\,dx.$$

For constant T/τ the integral is a constant and $\sigma^2 = C^2\tau^2$, C a constant.

$$\sigma[\langle\Omega_\tau(t)\rangle/\omega_0] = (\omega_0\tau)^{-1}\sigma[\Delta\Phi_\tau(t)] = \text{Constant}.$$

To get the dependence on T/τ, we can estimate the integration. (The integral can be done exactly in terms of the cosine integral.)

$$\sigma^2[\langle\Omega_\tau(t)\rangle/\omega_0] = \frac{2K}{\pi\omega_0^2}\int_{2\tau/T}^{\infty}\frac{1-\cos x}{x^3}\,dx$$

$$\approx \frac{2K}{\pi\omega_0^2}\{1.04+\tfrac{1}{2}\log(T/2\tau) + O[(2\tau/T)^2]\}.$$

So, for $T/2\tau \gg 1$, $\sigma^2[\langle\Omega_\tau(t)\rangle/\omega_0]$ is proportional to $\log(T/2\tau)$.

9. SPECIFICATION OF SHORT-TERM FREQUENCY STABILITY BY MAXIMUM LIKELIHOOD ESTIMATES

T. F. CURRY

Curry, McLaughlin and Len, Inc.
Syracuse, New York

This paper presents a fundamental basis for interpreting and processing measured short-term frequency stability data. This approach evolved from a need for quantitatively describing the short-term stability of microwave signal sources over microsecond-to-second time intervals in a reproducible fashion and from a desire to explain observed differences in the measured stabilities of such sources in terms of various hypotheses concerning the nature of the noise mechanisms which produce the measured phase or frequency fluctuations. The particular approach described here was suggested by a paper by Slepian (Reference 1).

PRELIMINARIES

We deal with the usual harmonic functions—or complex and composite representations thereof—functions, which can be expressed:

$$S(t) = Re\{|\psi(t)| \exp[j \operatorname{Arg}\psi(t)]\}$$
$$= |\psi(t)| \cos[\operatorname{Arg}\psi(t)]; \qquad (1)$$

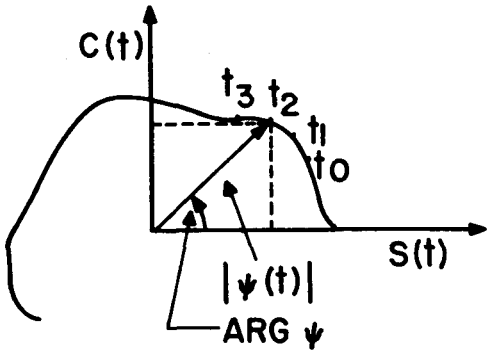

FIGURE 9–1.—The signal $S(t)$ as the real part of $\psi(t) = S(t) + jC(t)$. Instantaneous frequency is defined as the angular velocity of the phasor.

$|\psi(t)|$ can be considered the envelope of $S(t)$, and $\operatorname{Arg}\psi(t)$ the phase portion of $S(t)$. $\operatorname{Arg}\psi(t)$ will be referred to as the *phase function* associated with the signal $S(t)$, and the time derivative of $\operatorname{Arg}\psi(t)$ will be referred to as the *instantaneous frequency function* of the signal $S(t)$.

A technical description or specification of short-term frequency stability involves a description of the variations of the phase or frequency function over "short" intervals of time where, in practice, "short" means microseconds to seconds.

Representing Equation 1 as a phasor, as in Figure 9–1, we have the physical picture of the tangential component of the acceleration of the phasor as resulting from phase or frequency noise perturbations.

The instantaneous frequency, as conventionally defined, is the angular *velocity* of the phasor:

$$f_i = (1/2\pi)(d/dt) \operatorname{Arg}\psi(t), \qquad (2)$$

and the angular phasor acceleration is

$$a_i = (1/2\pi)(d^2/dt^2) \operatorname{Arg}\psi(t). \qquad (3)$$

To illustrate the preceding, for the real signal $S(t) = \cos[\omega t + \phi]$:

$$\psi(t) = \exp[j(\omega t + \phi)], \qquad \omega > 0,$$
$$f_i = \omega/2\pi,$$
$$a_i = (1/2\pi)\, d\omega/dt. \qquad (4)$$

Experimentally, we visualize Equation 2 as a

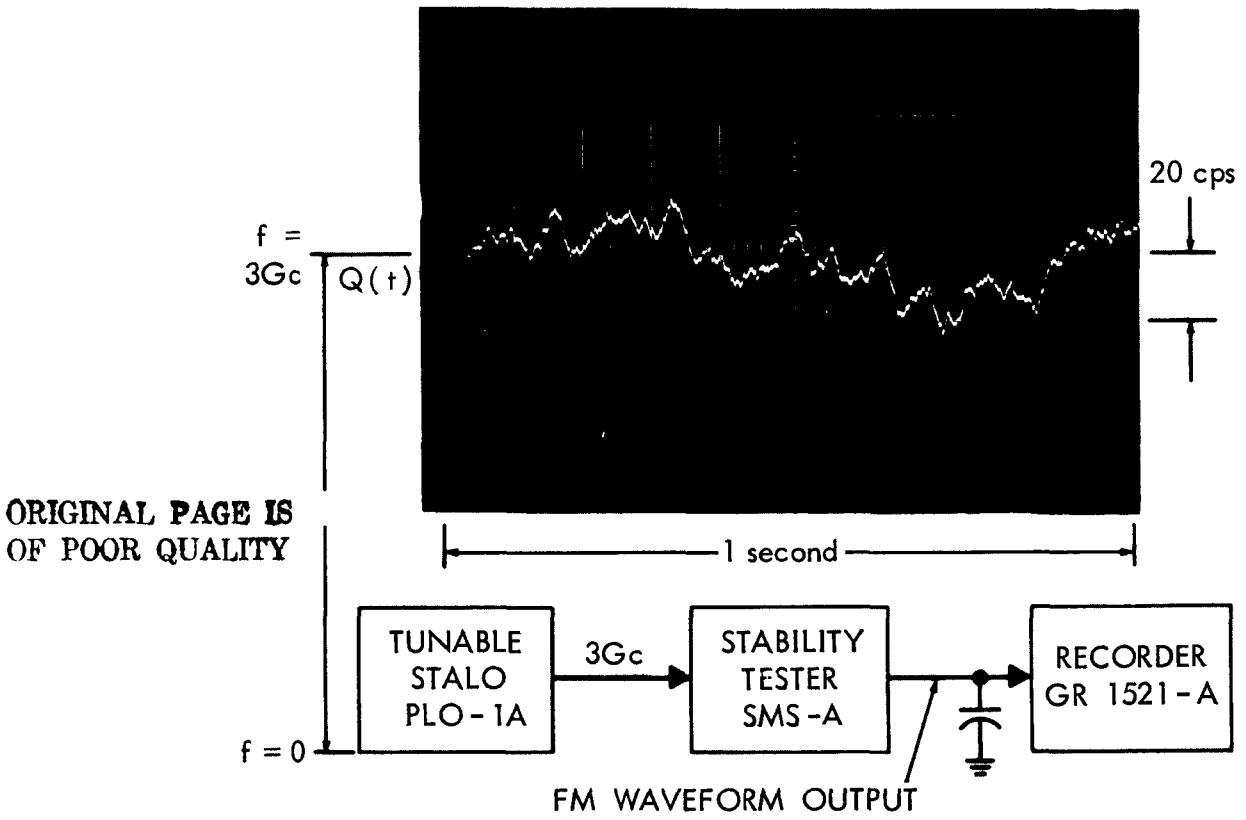

FIGURE 9–2.—A 1-sec epoch of frequency function obtained with the technique illustrated in Figure 9–3(a). ($1/RC$ at recorder input was set at 300 cps.)

function of time $Q(t)$, which is to be observed for a period of time T (Figure 9–2), to obtain a finite set of sample data values. In applications, we may be particularly interested in the magnitude of the function variations over shorter periods τ. We want to minimize the uncertainty of measurements and thereby obtain the highest possible reproducibility of results.

Two representative measurement techniques are shown in Figure 9–3. The process of mixing or translating the signal against an ideally stable reference, as illustrated in Figure 9–3, may in some cases "strip off" the periodic, or carrier, component; and $\text{Arg}\psi(t)$ may thereby be altered

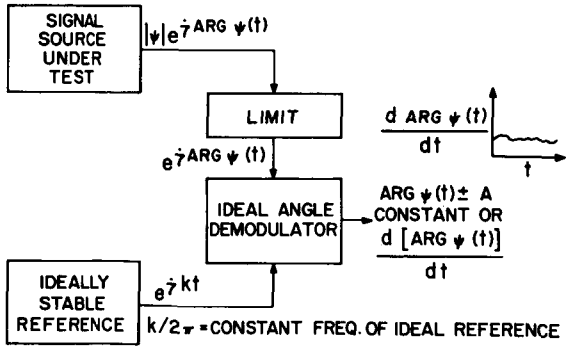

FIGURE 9–3a.—Ideal frequency translation and angle demodulation to give $\text{Arg}\psi(t)$ or its time derivative.

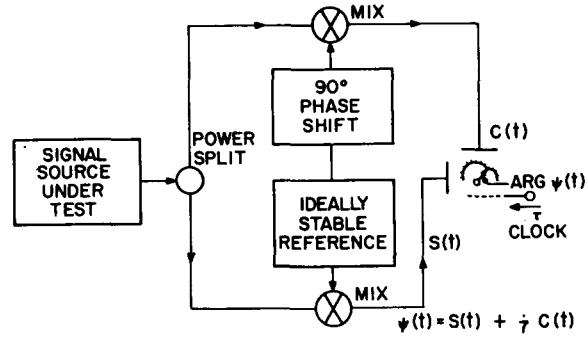

FIGURE 9–3(b).—Technique for measuring $\text{Arg}\psi(t)$.

by the linear term k, where k is the fixed ideally stable angular frequency of the reference. However, since we are concerned here only with the first derivative of $\text{Arg}\psi(t)$, such a frequency translation operation ideally has no effect, the k term being eliminated as a result of the differentiation.

The technique of Figure 3(b), giving direct $\psi(t)$ measurements over microsecond intervals, recently has been reported (Reference 2).

In general $Q(t)$ may exhibit both periodic and random variations. For a completely deterministic variation, there is no theoretical problem in specification. For example, in the case of a sinusoidal variation or waveforms which can be expressed as a Fourier series of sines and cosines, ideal sinusoids are postulated; and period measurements suffice to completely describe the function. Measurement experience indicates that the predominent noise mechanism for values of τ in the microsecond to 1-second range are of a random nature. Attention in this paper is therefore limited to $Q(t)$ functions which derive from wide-sense stationary random noise mechanisms.

The problem to be considered is as follows:

> *Given* sample measurements at intervals τ on $Q(t)$, say X_1, X_2, X_3, $\cdots$, X_n and an hypothesis concerning the general nature of the perturbing mechanisms, we require an estimate of a descriptive and useful statistic, possibly simply the rms value of $Q(t)$. That is, over a necessarily finite observation time T we obtain data to calculate the most probable value for the standard deviation of the fluctuation.

One method of choosing the most probable value is the method of *maximum likelihood estimation* (due to Fisher, Reference 3).

The signal data can, of course, be described in the form of estimates of the auto-covariance or power spectral functions. These must be *short-term* statistics* and not their classical forms, and are hence subject to the same statistical uncertainty as is the variance. As the period of observation increases, such short-term functions will of course approach their long-term averages, but these long-term averages are not what we seek. One important question is, in fact, concerned with the method and rate of approach of the short-term estimates to the long-term averages as τ increases.

Concerning the effects of additive "amplitude" noise, we intuitively would expect such noise to have negligible effect on instantaneous frequency as long as the carrier power is large compared with the noise—as is true, for example, in the case of low-noise FM analysis.

MAXIMUM LIKELIHOOD ESTIMATION

The principle of maximum likelihood estimation, as expressed in its simplest form, is as follows: Samples $X_1 \cdots X_n$ are taken of a random process $\{X_t\}$ which is known to be characterized by a class of probabilities $P(x, \alpha)$, where α is a parameter associated with the probability functions and is the number which is to be estimated using the measured samples. We then define a function

$$L = P(X_1, \alpha)\, P(X_2, \alpha) \cdots P(X_n, \alpha), \qquad (5)$$

which is, assuming statistical independence of the samples, the probability of obtaining the $X_1 \cdots X_n$ sample values. The most likely value of α is therefore given by maximizing L with respect to α (i.e., set $dL/d\alpha = 0$ and solve for α). Such an α value is termed the *Maximum Likelihood Estimator* (MLE) for α.

In application, one usually forms a functional of the original process $\{X_t\}$, $f[\{X_t\}]$ such that the desired quantity to be estimated can be considered a parameter of the probability distributions of $f[\{X_t\}]$, which can themselves (at least in principle) be derived from the probability distribution of the original random process. In general, the estimator is expressed directly as a function of the samples of the original process, $X_1 \cdots X_n$.

Maximum likelihood estimates have well-defined optimal properties (Reference 3) and have been used extensively in radar signal detection and parameter estimation problems.

We illustrate the procedure of finding the MLE for the mean and variance of a wide-sense stationary Gaussian random process with essentially flat (white) spectrum. The likelihood

*For various definitions of short-term autocorrelation and "instantaneous spectrum," see References 4 through 8.

function in this case is

$$L=\prod_{i=1}^{n}(\sqrt{2\pi}\sigma)^{-1}\exp[-(X_i-\mu)^2/2\sigma^2]$$
$$=(1/2\pi\sigma^2)^{n/2}\exp[-\sum(X_i-\mu)^2/2\sigma^2], \quad (6)$$

where

$\sigma^2=$ variance of process,

$\mu=$ mean of process,

$X_1, X_2, \cdots, X_n=n$ serial samples of a single function of the process ensemble.

In this case it is convenient to obtain the maxima of the *logarithm* of L rather than L, positions of maxima in terms of σ and μ being the same for any monotone function of L. Hence,

$$\ln L\equiv L'=-\tfrac{1}{2}n\ln(2\pi\sigma^2)-(1/2\sigma^2)\sum_{i=1}^{n}(X_i-\mu)^2 \quad (7)$$

and

$$\partial L'/\partial\mu=(1/\sigma^2)\sum_{i=1}^{n}(X_i-\mu), \quad (8)$$

$$\partial L'/\partial\sigma^2=\frac{-n/2}{\sigma^2}+\frac{1}{2\sigma^4}\sum(X_i-\mu)^2.$$

Setting these derivatives equal to zero and solving for μ and σ^2,

$$\hat{\mu}=n^{-1}\sum_{i=1}^{n}X_i=\bar{X}, \quad (9)$$

$$\hat{\sigma}^2=n^{-1}\sum_{i=1}^{n}(X_i-\bar{X})^2, \qquad \text{with } \hat{\mu} \text{ for } \mu, \quad (10)$$

where the carets indicate that these are the values of μ and σ^2 which maximize L and are hence the MLE for the parameters of the process. As it turns out, these are the estimators which intuition probably would lead us to calculate anyway.

CHOICE OF A FLUCTUATION STATISTIC

The first step in formulating a description of the short-term $Q(t)$ variations as a statistical estimation problem involves a choice of statistic, or function of $Q(t)$ sample values, which is to be estimated.

Maximum Excursion (cps)

Perhaps the simplest and most used fluctuation description of $Q(t)$ is the specification of the maximum difference of $Q(t)$ magnitudes over the time intervals of interest τ. We define a new function over a discrete ordered set of τ intervals:

$$Q_M(\tau)=Max_\tau\,|\,Q(t)-\bar{Q}\,|, \quad (11)$$

where $\bar{Q}$ is the estimate of the mean as obtained with Equation 9 for samples $q_1, q_2, \cdots, q_n$ taken at intervals $t_0=1/2W$, W being the bandlimits assumed for the $Q(t)$ process and $\tau\gg t_0$. $\bar{Q}$ also may be replaced with appropriate samples of a "moving average," as described in a following section.

The probability density for a maximum M of n samples of $Q(t)$ can be written as a product of probabilities for n independent Bernoulli trials over the interval τ:*

$$g(M)$$
$$=4n\left[\int_{-0}^{M}[(2\pi)^{1/2}\sigma]^{-1}\exp[-(q-\bar{Q})^2/2\sigma^2]\,dq\right]^{n-1}$$
$$\times\int_{M-\delta}^{M+\delta}[(2\pi)^{1/2}\sigma]^{-1}\exp[-(q-\bar{Q})^2/2\sigma^2]\,dq, \quad (12)$$

where

$\sigma^2=$ variance of $Q(t)$ process,

$\bar{Q}=$ estimate of mean process,

$\delta=(\sigma^2/n)^{1/2}, \quad n=\tau/t_0,$

and we have used the well-known fact that the variance of the sample mean is given by the assumed population variance σ^2, divided by the sample size n in specifying the probability element for M (second term of Equation 12).

If now we consider M as a parameter of the distribution given by Equation 12, we can form a likelihood function:

$$L=\prod_{i=1}^{k}g(M_i;q^i_1, q^i_2, \cdots, q^i_n), \qquad \text{for } k \text{ intervals } \tau. \quad (13)$$

Straightforward computation of the MLE from

* In applications where the probability of exceeding a specified value (threshold) must be very small, an alternate approach would apply the statistical theory of extreme values (see Gumbel, E. J., *NBS Applied Math Series* No. 33, 1954).

Equation 13 gets into difficulty rapidly, and we have yet to work through to a solution. Intuitively, one expects an estimator for M such that, for large n and k, the estimate will approach a value equal in magnitude to the point of inflection on the Gaussian curve accorded to the estimate $\hat{\sigma}^2$.

Mean-Square Fluctuation Power (cps²)

Consider now the mean-square difference of $Q(t)$ values τ seconds apart:

$$y(\tau)=\tau^{-1}\int_{-\tau/2}^{\tau/2}[Q(t)-Q(t+\tau)]^2\,dt \qquad (14)$$

$$=\tau^{-1}\int_{-\tau/2}^{\tau/2}Q^2(t)\,dt$$

$$-(2/\tau)\int_{-\tau/2}^{\tau/2}Q(t)Q(t+\tau)\,dt$$

$$+\tau^{-1}\int_{-\tau/2}^{\tau/2}Q^2(t+\tau)\,dt.$$

Assuming the process is stationary, the first and third terms may be combined to give

$$y(\tau)\approx Z(\tau)$$

$$=(2/\tau)\left[\int_{-\tau/2}^{\tau/2}Q^2(t)\,dt-\int_{-\tau/2}^{\tau/2}Q(t)Q(t+\tau)\,dt\right]. \qquad (15)$$

The first term of $Z(\tau)$ is recognized as corresponding to the "average power," in $(\text{cps})^2$, of $Q(t)$ and the second term as the short-term auto-covariance for $Q(t)$.*

Now, we have two cases to consider, depending on the correlation time of the $Q(t)$ process relative to the time intervals τ. [For processes with a rectangular spectrum (so-called *bandlimited-white*), we define correlation time t_0 as $1/2W$, where W is the spectrum width. For processes with spectrum $2\alpha/\alpha^2+\omega^2$ (so-called RC noise), correlation time is defined as $1/\alpha$.] If all τ values of interest are larger than $1/2W$, then we can direct attention solely to the statistic:

$$Z'(\tau)=(2/\tau)\int_{-\tau/2}^{\tau/2}Q^2(t)\,dt. \qquad (16)$$

If the τ intervals of interest are less than the correlation time for the process, the second term of Equation 15 is important; and, in this case, the short-term correlation function would certainly seem to be a sufficient statistic. We direct attention to Equation 16, allowing us to apply Slepian's results (Reference 1)—with appropriate interpretation—to the problem at hand.

Slepian derives the probability density function for (16), assuming $Q(t)$ is normally distributed with mean zero, and for three classes of spectra: RLC, RC, and band-limited white.

Before proceeding with Equation 16, we will summarize briefly the situation with respect to short-term power spectra and correlation (covariance) function estimation and suggest a "smoothing" operation on $Q(t)$.

Moving Average

One problem associated with the processing of short-term stability data concerns the fact that the observed process, $Q(t)$ in the present context, exhibits fluctuations due to both long- and short-term noise mechanisms. To separate the two data would seem to involve, from a practical standpoint, only a high-pass filter.* Generally, we may define a new function of $Q(t)$, the "moving average" function as follows:

$$Q'(t,\tau)=\tau^{-1}\int_{-\tau/2}^{\tau/2}Q(\xi+t)\,d\xi, \qquad (17)$$

$$Q'(t,\tau)\to Q(t) \quad \text{as} \quad \tau\to 0.$$

Use of this "smoothed" Q, Q', as the standardizing Q-average eliminates the long-term drift consideration in processing Equation 16 and might be accomplished in practice by well-known tracking filter techniques, with VCO closed loop bandwidth of approximately $1/2\tau$. $Q(t)$ smoothing and possible statistics [(11) and (16)] are illustrated in Figure 9–4.

In passing, it should be mentioned that a very useful approach, from a digital machine processing standpoint, to eliminating the long-term drift from experimental short-term data would be to apply simple linear regression analysis to the data. For normally distributed processes, maximum likelihood estimates for drift and short-term deviation are easily obtained.†

* Compare Equation 15 with Searle, et al., Equation 6, these Proceedings.

* For example, the CML stability measuring set, Model SMS–B uses a cutoff of 3 cps.

† Reference 3, Chapter 13.

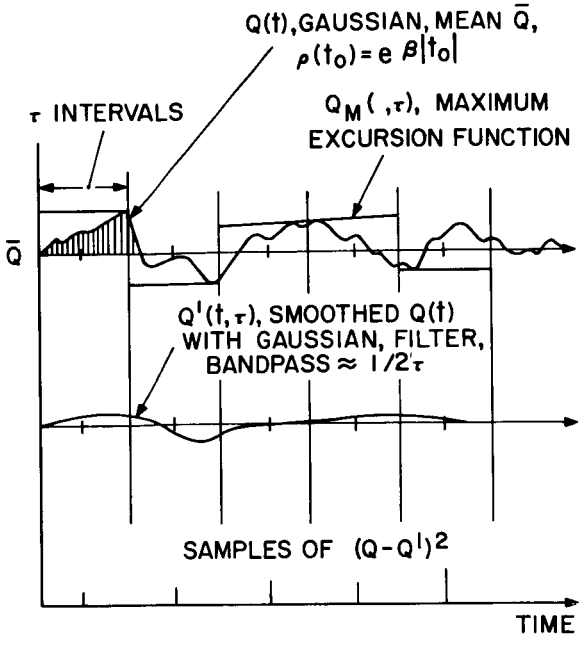

FIGURE 9–4.—Illustrating the possible fluctuation statistics and smoothing.

Spectral Density Estimates

Various methods for estimating the spectral density function for wide-sense stationary processes are described from a mathematical viewpoint by Grenander and Rosenblatt (Reference 9). Power spectral estimation from an engineering standpoint has been treated exhaustively by Blackman and Tukey (Reference 10†).

Despite some good arguments in favor of power spectra (Reference 10, Section B–3 for example), there appear to be limitations to the usefulness in the short-term stability estimation. For example, the shape of the scanning window enters the picture critically for the very narrow spectra we want to examine. If we multiply the frequency (with negligible added disturbance) high enough and scan slowly enough, window problems are eliminated. However, the slower we scan, the longer the averaging time. Measurements resulting from heterodyne scanning techniques are cuts across the time-frequency plane and, as such, are neither time-bird nor frequency-beast.

One possible approach to short-term power spectra measurement is shown schematically in Figure 9–5. Signal power is split into two banks of contiguous bandpass filters through ideal switches. The filters "impulse respond," the envelope of the response depending on the filter characteristic and amplitude depending on impulse energy. If we close the switches on the first bank of filters at $t=t_0$, and sample and hold the first maxima of the impulse response of each filter (which will occur sometime later than $t=t_0$) we obtain a set of numbers which will be called, for the purpose of this discussion, the *running spectrum* of the input at time $t=t_0$. We then close the switches on the second bank at $t_0=\tau$, τ being the desired interval for which a specification of short-term spectrum is desired. This second filter bank is necessary, since τ will—in general—always be much smaller than the filter "ringing" times for filter bandpass (frequency resolution) values of interest.

Suppose we observe a magnitude A at f_1 with the first filter bank. Then a description of the spectrum requires a specification of the probability of observing a magnitude B at f_1 with the second filter bank. This necessarily "probabilistic" description of the energy distribution over the

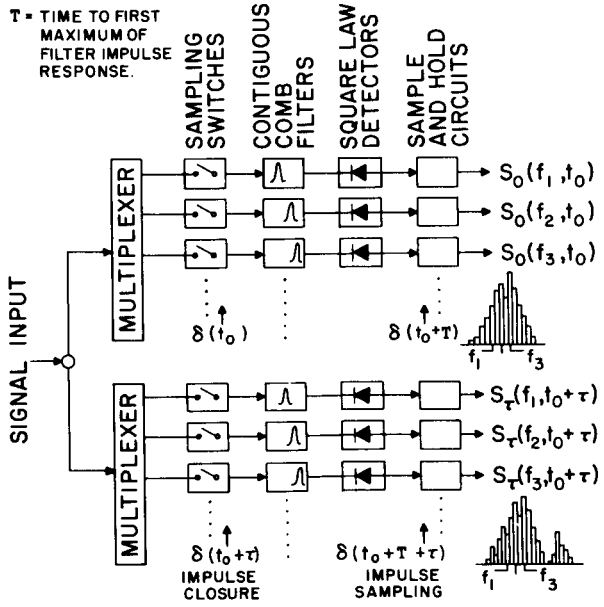

FIGURE 9–5.—Illustrating the measurement of noise spectra for an averaging time τ. The comb filters are assumed to be centered over the range of expected noise frequency components.

†See Reference 10, p. 192 and pp. 492–493, for a discussion of the relative merits of covariance (correlation) and power spectra estimates.

plane of time-frequency elements has been described by a number of investigators (References 4 and 5) in the context of defining *instantaneous spectrum*. In relation to the short-term frequency stability measurement problem, we would expect to obtain sample measurements at the outputs of the filters over a number of switch closure sequences for intervals τ, allowing time between sequences of course for the filters outputs to decay. Long-term drift certainly would cause trouble here, and a smoothing track loop definitely would be required. In the presence of additive noise, a characteristic of any practical system, there is an additional uncertainty limiting the minimum filter bandwidth as given by

$$\Delta t\, \Delta f \geq k/(2E/N_0)^{1/2}, \qquad (18)$$

where Δt and Δf are the minimum rms values simultaneously achievable, E the signal energy, N_0 the additive white noise energy per cps, and k a constant approximately equal to unity.

FLUCTUATION POWER ESTIMATE

Returning to Equation 16, we wish to see how this "average power" statistic can be expected to vary with τ for various spectral distributions for $Q(t)$, and will therefore assume a smoothing operation on $Q(t)$ as in Equation 17. A smoothed $Z'(\tau)$ will be considered:

$$Z''(\tau) = (2/\tau)\int_{-\tau/2}^{\tau/2} [Q''(t)]^2\, dt; \qquad (19)$$

and this $Z''(\tau)$ corresponds to Slepian's $y(t)$ of Equation 1 in Reference 1. $Z''(\tau)$ might be considered the "standardized" (smoothed) mean-square frequency fluctuation power (*SMS* for short) as would be expressed in (cps)^2.

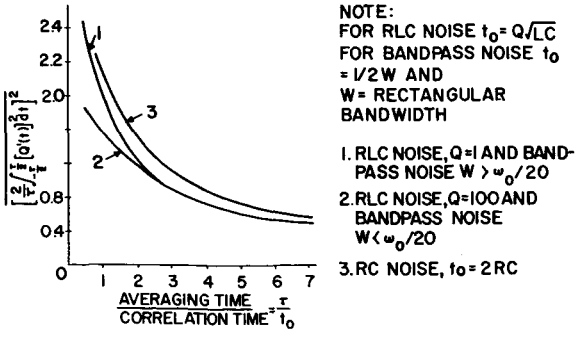

FIGURE 9–6.—Mean square (variance) of the fluctuation statistic $Z''(\tau)$ as a function of the ratio of integration (averaging) time to correlation for the $Q(t)$ process, normalized for a mean time of $z''(\tau) = 1$.

The expressions for the probability density functions for $Z''(\tau)$ are, unfortunately, not in a form suitable for directly computing the maximum likelihood estimates for the moments of $Z''(\tau)$. The variance of $Z''(\tau)$ is obtained, however, and is shown in Figure 9–6 as a function of the ratio of τ to the correlation time of the process $Q(t)$, t_0, defined for the various spectra as follows:

RLC noise:

$$t_0 = \mathbf{Q}(LC)^{1/2}, \quad \mathbf{Q} = \omega_0 L/R,$$

Rectangular bandpass white noise:

$$t_0 = 1/2W, \quad W = \text{Bandwidth},$$

RC noise:

$$t_0 = 2RC.$$

The *RC* and *RLC* noise are assumed to be generated by shaping white noise with the two types of circuits in the usual way.

In the application of Figure 9–6 to the specification of short-term frequency stability, we should recall from Equation 15 that $Z''(t)$ will be applicable to our purposes only when $\tau/t_0 > 1$ (i.e., when the observed $Q(t)$ values spaced τ seconds apart are essentially uncorrelated).

In the absence of an estimation function for the variance of $Z''(t)$, we can only make specific suggestions for approximate estimators which can be expected to be reasonably useful in special cases:

RC noise, $\tau/t_0 > 50$: In this case, $Z''(\tau)$ is approximately normally distributed, and Equation 10 is applicable as the variance estimator.

RLC noise, $\mathbf{Q} < 100$, *but* $\mathbf{Q}\tau/t_0 > 100$: $Z''(\tau)$ also is approximately normally distributed in this case, and Equation 10 can be used to estimate the variance.

RLC noise, $\mathbf{Q} \geq 100$: For such a case, for which—in the limit $\mathbf{Q} \to \infty$ gives $Q(t) = \xi \cos\omega_0 t + \beta \sin\omega_0 t$, the so-called "narrow-band Gaussian process"—the probability densities are modified χ^2 distributions, it is very difficult to make any assumption as to an estimator for the variance.

APPLICATION

Experimentally obtained sample $Q(t)$ functions are shown in Figure 9–7 for two different presenta-

0.1 SECOND EPOCH
3000 cps BW
VERTICAL SCALE:
20 cps PER DIV.
HORIZONTAL SCALE:
10 ms PER DIV

0.01 SECOND EPOCH
3000 cps BW
VERTICAL SCALE:
20 cps PER DIV.
HORIZONTAL SCALE:
1 ms PER DIV.

FIGURE 9–7.

tion time bases. The measurement technique involved the heterodyning of a moderately stable STALO output at 3000 Mc/sec. into a baseband digital discriminator circuit.† The spectrum of the discriminator output was then filtered with an RC combination with $1/RC = 3000$ cps. This provided a known and controllable output correlation time of approximately 0.6 msec. The data presentation permits sampling from 1 to 100 msec, with a frequency resolution of approximately 2 cps. The absence of any measurable amplitude noise, even with signal removed from the discriminator, indicated that these time and frequency resolutions are within the bounds of theoretical limitations, and hence are realistic.

Computed (manually) values of the fluctuation estimates $\hat{M}$ and $S\hat{M}S$ for two values of τ are shown here for comparison:

$\tau = 1$ msec
RC noise, $t_0 = 0.66$ sec
2500 samples, $\tau/10$ int.
$S\hat{M}S$ (Eq. 10) = 16.9 cps
var. (Fig. 9–6) = 15.9 cps
$\hat{M}$ (Eq. 12) = 8.4 cps
rms deviation = 4.1 ± 4.0 cps

$\tau = 10$ msec
RC noise, $t_0 = 0.66$ sec
2700 samples, $\tau/20$ int.
$S\hat{M}S$ (Eq. 10) = 33.6 cps
var. (Fig. 9–6) = 6.7 cps
$\hat{M}$ (Eq. 12) = 10.1 cps
rms deviation = 5.8 ± 2.6 cps

In the absence of an expression for $\hat{M}$, Equation 12 was used to compute M values for a series of τ intervals; and the M value with maximum probability element was chosen for $\hat{M}$. Equation 10 was used to obtain $S\hat{M}S$.

CONCLUSION

A short-term frequency stability measurement model has been suggested as follows:

1. First—Smooth $Q(t)$ over the desired τ interval, as suggested in the section, "Moving Average."

2. Second—take samples of $Q'' = (Q - Q')$ at the intervals appropriate to the chosen statistic and with the system bandwidth and process correlation time limitations in mind.

† As in Figure 9–2.

3. Third—Using the observed sample values and the hypothesized process statistics, compute an estimate of:

(a) For stability averaging times less than, or equal to, process correlation time—the maximum observed frequency deviation over the interval.

(b) For stability averaging times greater than process correlation time—the "standardized mean-square frequency fluctuation."

With probability distribution functions for the chosen maximum likelihood estimates, one can—in principle—immediately determine the variance of the estimator as a confidence interval for the measurement.

Initial experience using $\hat{M}$ and $S\hat{M}S$ indicates that measurement results are more reproducible than with various rule-of-thumb approaches. Manual computation of smoothing and estimation procedures—particularly for $\hat{M}$—is, however, laborious.

REFERENCES

1. Slepian, D., "Fluctuations of Random Noise Power," *Bell System Tech. J. 37*, No. 1, January 1958.
2. Griffin, William D., "A Precision Phase Measurement Technique for Pulsed Signals," *Microwave J.*, Vol. IV, April 1963.
3. Mood, A. M., "Introduction to the Theory of Statistics," McGraw-Hill, 1950.
4. Ville, J., "Theory & Applications of the Notion of Complex Signal," Translation—Rand Report T-92, August 1958. [Reference to original paper (courtesy of Dr. J. Mullen) *Cables et Transmissions 2*, 61 (1948).
5. Gabor, D., "Theory of Communication," *JIEE (London) 93*, 429; also "Theory," RLE Technical Report No. 238, April 1952.
6. Schultheiss, Peter M., et al., "Short-Time Frequency Measurement of Narrow-band Random Signals in the Presence of Wide-Band Noise, *J. Appl. Phys. 25*, No. 8, August 1954.
7. Fano, R. M., "Short-Time Auto Correlation Functions and Power Spectra," *J. Acoust. Soc. Amer. 22*, 546 (1950).
8. Page, C. H., "Instantaneous Power Spectra," *J. Appl. Phys. 23*, 103 (1952).
9. Grenander and Rosenblatt, "Statistical Analysis of Stationary Time Series," Chapters 4 and 5, John W. Wiley, 1957.
10. Blackman, R. B., and Tukey, J. W., "The Measurement of Power Spectra From the Point of View of Communication Engineering," *Bell System Tech. J. 37*, 185 (1958); *ibid. 37*, 485 (1958).

10. A CROSS-CORRELATION TECHNIQUE FOR MEASURING THE SHORT-TERM PROPERTIES OF STABLE OSCILLATORS*

R. F. C. VESSOT, L. F. MUELLER, AND J. VANIER

Varian Associates
Beverly, Massachusetts

A cross-correlation technique for measuring the properties of stable oscillators in the time range 0.01 to 1.0 sec is described. Time-dependent functions representing signals from two separate oscillators are led to a function multiplier, where the instantaneous product of the functions is made. The oscillators are either set to a given phase relation or allowed a small relative drift so that a slow beat frequency is observed. Short-term fluctuations superimposed on the slow beat signal from the multiplier output represent the instantaneous phase difference between the oscillators when the inputs are in quadrature. When the inputs are in or out of phase, the fluctuations represent signal amplitude variations. Sampling times can be specified by filters having certain responses.

The mean-square frequency deviation taken over a given response time is obtained by differentiating, filtering, and squaring the output signal of the function multiplier—data being taken when the input signals are in quadrature. Data from measurements on hydrogen masers are presented, and a comparison of these results with data taken using the zero crossing method over the range 0.1 to 10 sec is given. The effect of thermal noise is seen to be the major factor limiting the short-term frequency stability of the signals.

INTRODUCTION

In describing the frequency stability of oscillators, use has been made by several authors (References 1 and 2) of a model where the rate of phase change of a signal phasor is calculated by considering the effect of adding random noise signals in quadrature with the carrier. These expressions have the general form as given by Edson (Reference 1):

$$\Delta f/f = Q^{-1}(kT/2P\tau)^{1/2},$$

where Δf is the deviation of a set of frequency measurements each made over an interval of time τ. Q is the quality factor of the resonant circuit determining the frequency and, in the case of masers (References 3, 4), is related to the linewidth of the transition involved in generating the energy. The above expression describes the frequency stability of a signal that is considered to exist in the absence of added noise. The influence of noise that has been included in the expression is restricted to the response of the signal vector because of the noise energy that lies within the bandwidth determined by the oscillator Q. The effect of the inevitable noise energy per unit frequency bandwidth $kT\ \Delta\nu$ on the signal, prior to its use or analysis by a particular system, is not included; and, until the recent advent of extremely stable quantum mechanical oscillators such as the hydrogen maser, the effect of the added noise has not been a strong detriment to stability for observation time intervals on the order of 1 msec or greater.

The relation of measuring system bandwidth to observation time is extremely important, as it is this bandwidth that determines the amount of noise energy that is added to the signal energy from the oscillator. Some relation involving a bandwidth proportional to the reciprocal of the ob-

*Work supported by NASA under Contract No. NAS8-260.

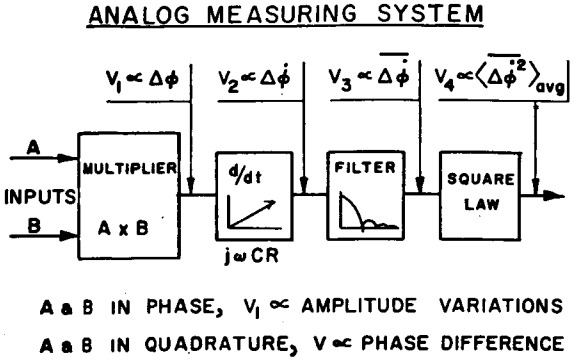

FIGURE 10–1.—Analog measuring system.

servation time should be chosen, depending on the shape of the response of the system. In the system described below, the optimum relation of measuring system bandwidth is maintained for all values of observation time.

It must be remembered, however, that the noise power bandwidth of an oscillator will be finite. This limitation occurs, in the case of a maser, because of the bandwidth of the RF cavity, typically some tens of kilocycles. The total signal-plus-noise power spectrum of the maser can be described as thermal noise over the frequency response of the cavity plus a signal spectrum at its center. If the receiver bandwidth is opened farther than that of the cavity, the cavity will be the overall limiting factor and no further degradation of the frequency stability will result from additive noise. It is possible, as pointed out by Edson (Reference 1), to improve the stability of an oscillator by using an external filter before going to the receiver or measuring system; however, in defining the boundary between the oscillator and the measuring system, one should be careful to state whether or not this filter is included.

Most measurements of frequency stability

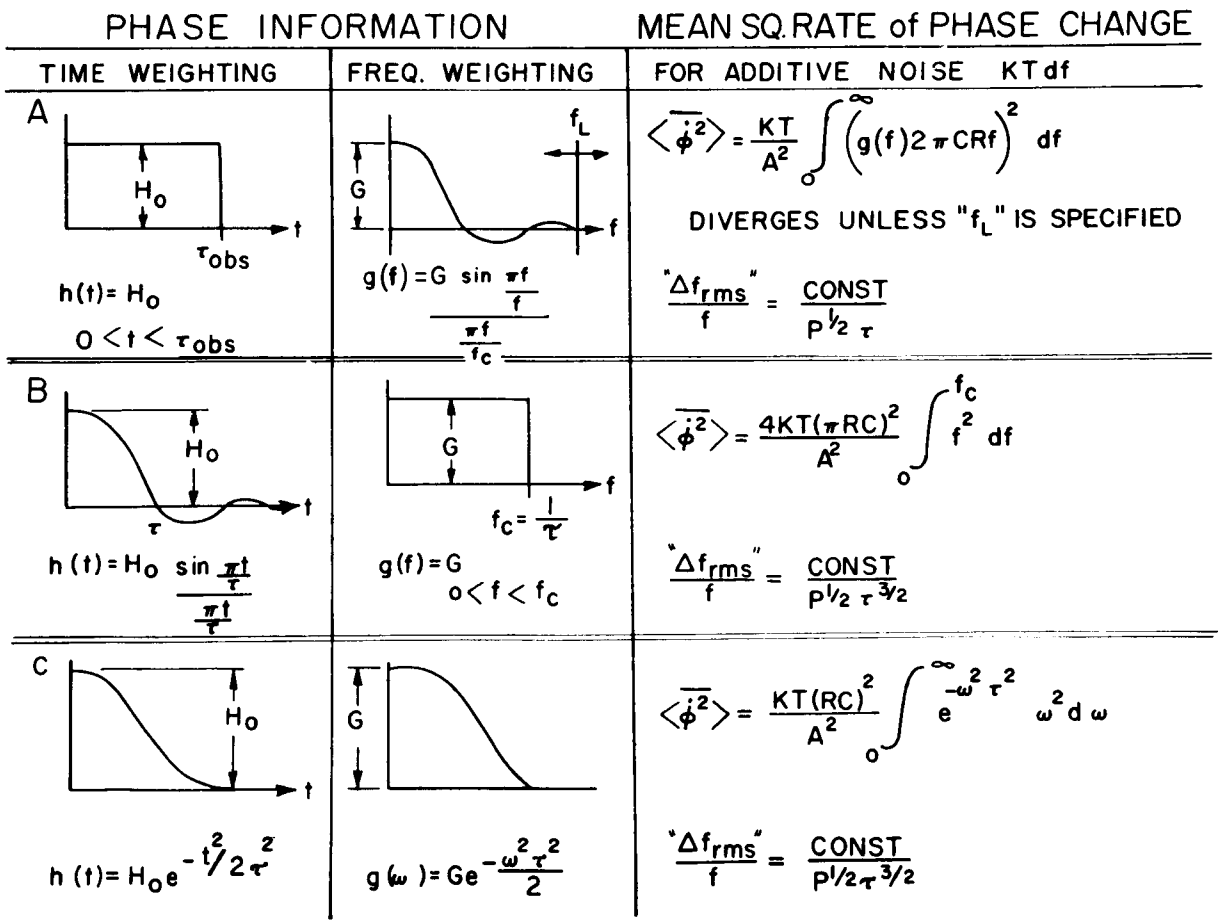

FIGURE 10–2.—Three time-averaging methods.

(References 5, 6, 7, and 8) have been made by timing the zero crossings of signals that result from beating two oscillators together. By making a large number of measurements, each for the same observation time, the standard deviation of the frequency is computed. This is repeated for each observation time. The observation time is generally determined by a fixed number of zero crossings, such as ten 1-sec periods. In most cases some filtering is employed in the signal before it is fed to the period measuring instrument, if only to reduce the effect of spurious counts due to noise pulses that are short compared with the period of the signal. However, in describing the results of such frequency stability measurements, one must give not only the observing time but the overall bandwidth as well. The following will describe a method of making stability measurements by continuously comparing the relative phases of two oscillators. A system that has been used to do this is shown in Figure 10–1 and involves making an analog multiplication of the functions representing the two signals. The low-frequency output signal from the multiplier will represent relative phase fluctuations when the signals are in quadrature and amplitude fluctuations when the signals are in or out of phase. The stability of the signals must be such that the signals can be kept very nearly in quadrature for time intervals very long compared with the observation time desired. In the case of hydrogen masers it is possible to have them stay within a few degrees of each other for about 10 minutes, time enough to make the equivalent of 600 one-tenth second measurements.

The quadrature signal from the multiplier, representing instantaneous phase difference, is led to a filter where a time averaging is performed in a running manner; that is to say, the average phase value over a time interval τ is obtained as a function of real time t. A continuous representation of $\bar{\phi}_\tau(t)$ is obtained and subsequently differentiated, giving $\dot{\bar{\phi}}_\tau$, and an average over a long term is taken of the square of $\dot{\bar{\phi}}_\tau$ to give $\langle \dot{\bar{\phi}}^2 \rangle_{Av}$ by leading the output of the differentiator to an integrating power meter. The reading from this device gives the mean-square rate of phase deviation over a time interval τ; and this, of course, is the mean-square angular frequency deviation of observation time τ.

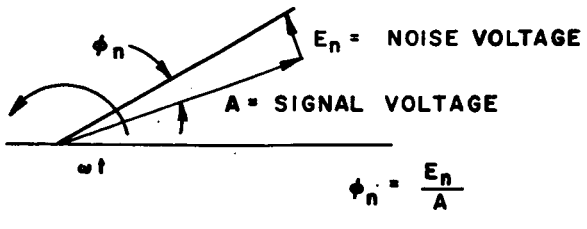

FIGURE 10–3.—Additive noise.

In the system described above, the crucial function is that performed by the filter. The average that is normally made in the time domain is represented by a square window of length τ. To represent this in the frequency domain will require a filter having the response $\sin(\pi f/f_c)/(\pi f/f_c)$, where $f_c = 1/\tau_{obs}$. The filter need not be infinite in frequency extent and can be cut off at a frequency greater than that of the noise power bandwidth of the oscillator.

It is possible to define and relate other time-averaging functions for the phase.

Three such functions and their related frequency-weighting counterparts are shown in Figure 10–2. In the case of the rectangular weighting function shown in Figure 10–2A, it is seen that the filter response multiplied by the response of the differentiator, then squared and integrated over frequency, will lead to a divergent result if a uniform noise power spectrum $kT\ df$ is assumed. In all applications or measurements, there is a bandwidth limit either in the oscillator itself or in the receiver. The magnitude of this bandwidth has a large effect on the frequency stability measured by different systems, since they may not have identical filter characteristics.

The effect of additive noise (Figure 10–3) on rms frequency when the filter has a finite value is given by

$$\Delta f/f = \text{Constant}/P^{1/2}\tau,$$

where P is the power of the oscillator.

In the case of the sharp cutoff low-pass filter, the time-weighting function is

$$H_0\,[\sin(\pi t/\tau)/(\pi t/\tau)\,].$$

In the frequency domain the situation is easy to understand and implement. This method has been used to investigate the noise content near the carrier of the hydrogen maser, and data are given in a later part of this paper.

As shown in Figure 10–2B, the value of $\langle \dot{\bar{\phi}}^2 \rangle_{Av}$ has a definite magnitude, since there are no

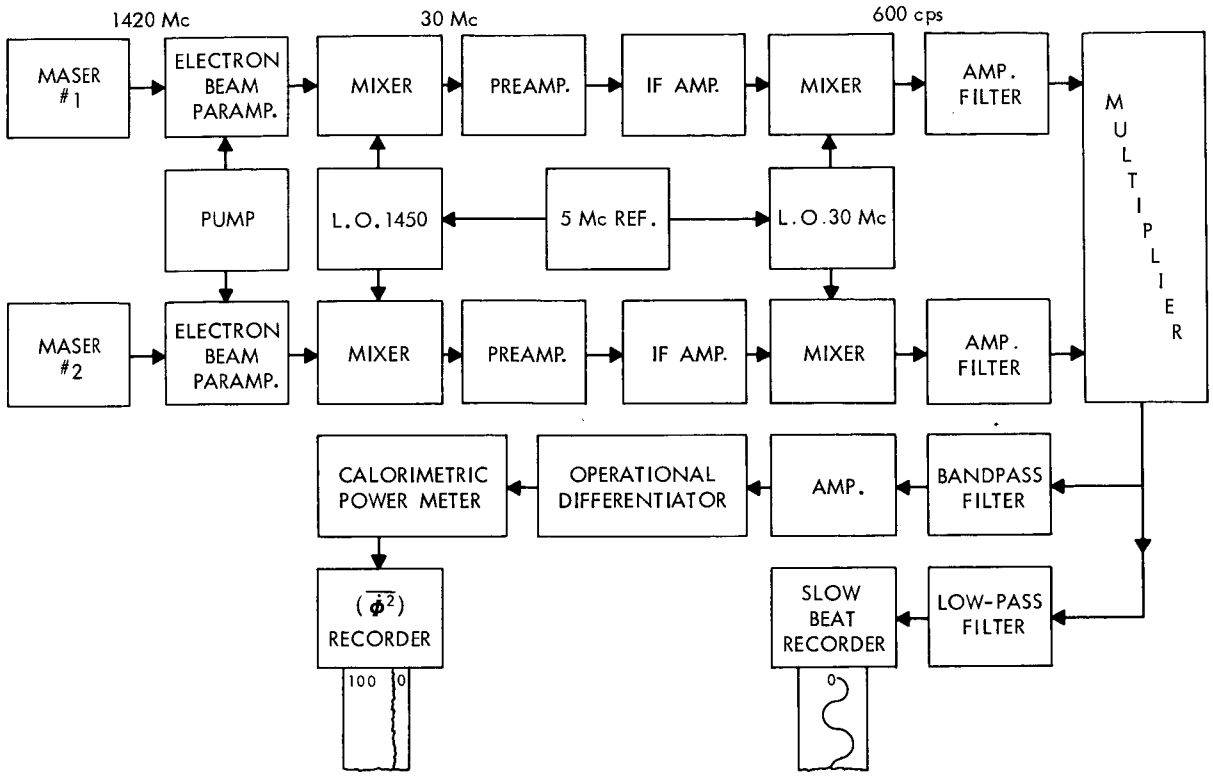

FIGURE 10–4.—Short-term noise measurement system.

ambiguities in the filter parameter. If one relates this bandwidth to the time response by writing $\tau = 1/f_c$, then, for additive noise $kT\,df$,

$$\Delta f/f = \text{Const.}/P^{1/2}\tau^{3/2}.$$

The last case, shown in Figure 10–2C, is for a Gaussian time response $H_0 \exp(-t^2/2\tau^2)$. The frequency response is also Gaussian and has the form $G \exp(-\omega^2\tau^2/2)$. This filter cuts off rapidly enough to allow the mean-square rate phase change $\langle \dot{\phi}^2 \rangle$ to converge, and the relation of the rms frequency stability with τ is

$$\Delta f/f = \text{Const.}/P^{1/2}\tau^{3/2}.$$

The only case that performs mathematically the averaging in time as normally defined is that shown in Figure 10–2A. The other systems do not rigorously provide a $\Delta f_{rms}/f$ over an averaging time τ but nevertheless are useful in describing the properties of an oscillator.

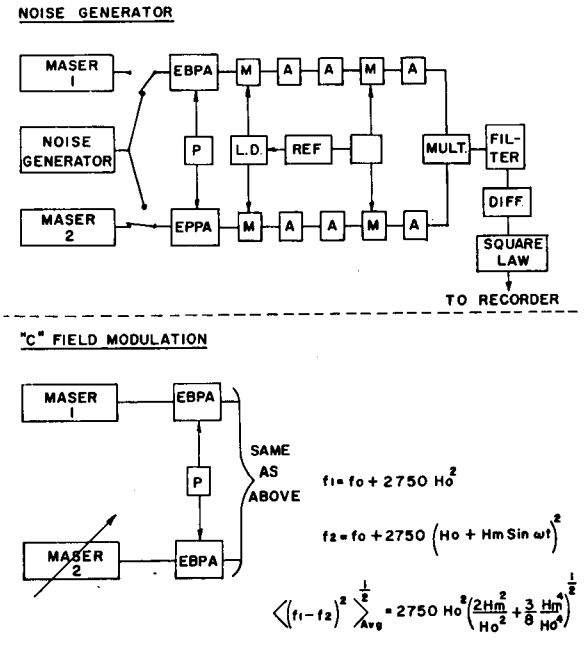

FIGURE 10–5.—Calibration methods.

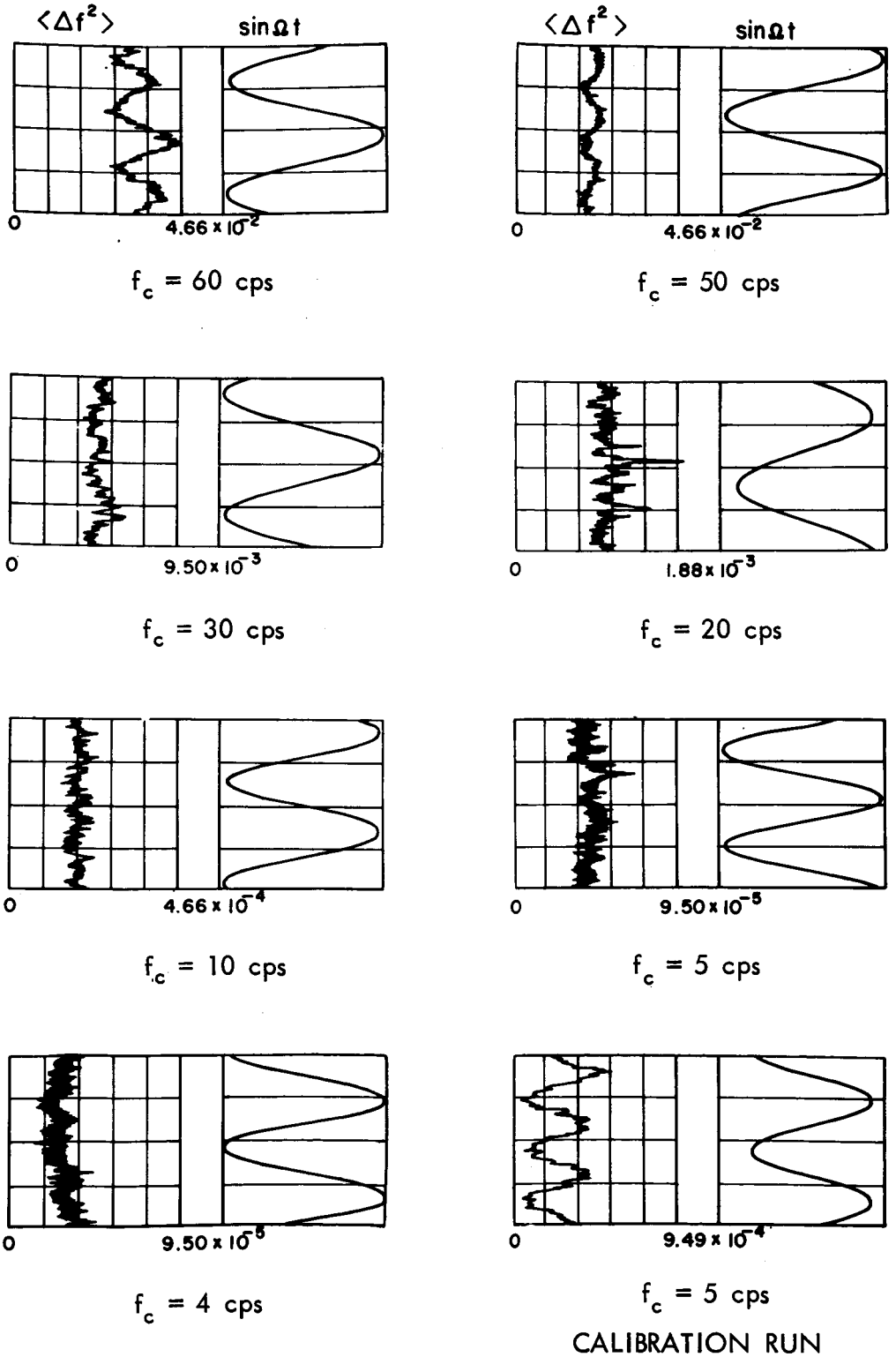

FIGURE 10–6.—Four-minute samples of data from cross correlator.

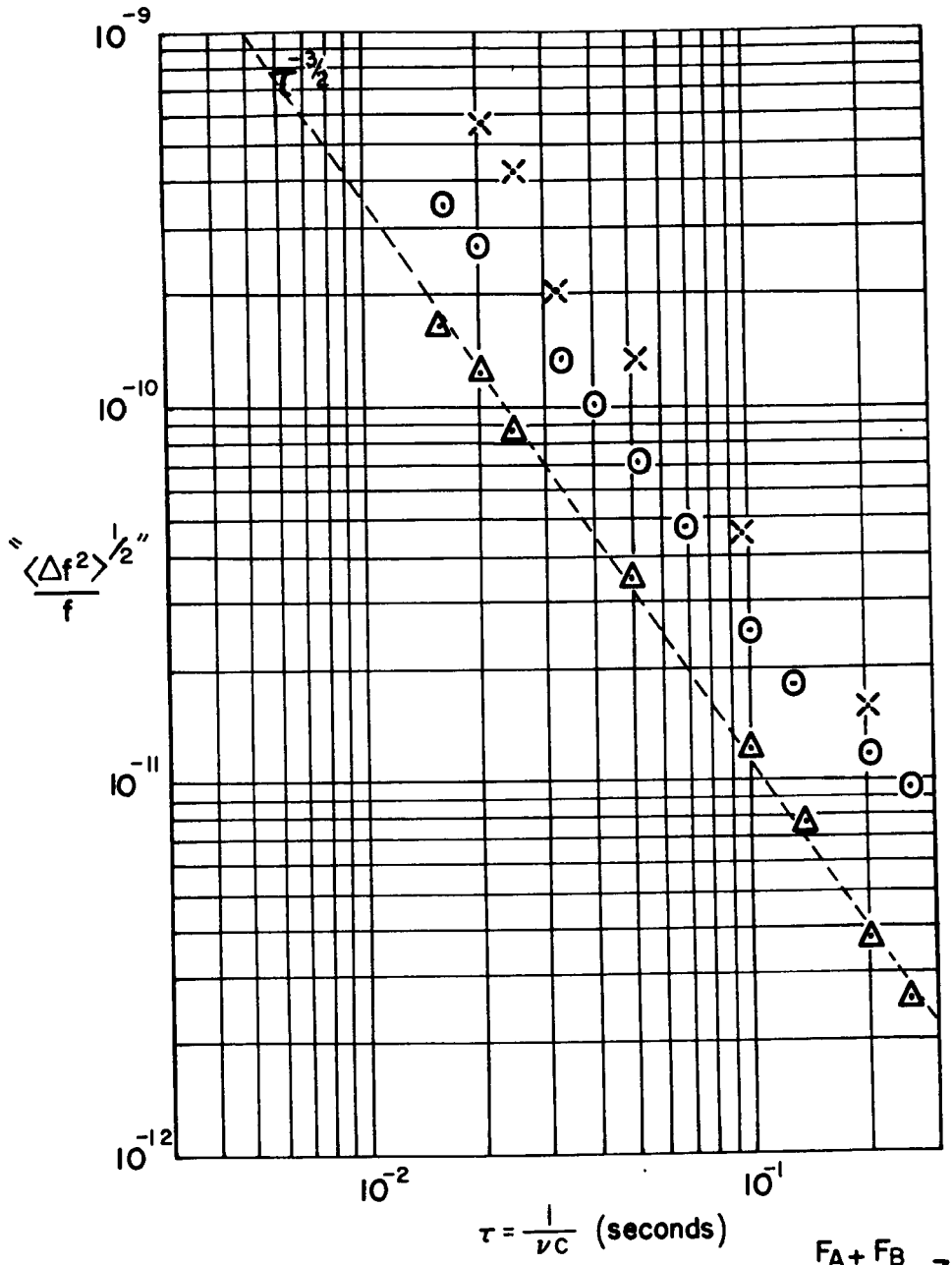

FIGURE 10–7.—Fractional frequency stability of one atomic hydrogen maser.

EXPERIMENTAL

Experiments have been performed on hydrogen masers using the system shown in Figure 10–4 and the sharp cutoff filter given as Case B of Figure 10–2. Two methods of calibration were used. The first method shown in Figure 10–5 involves the use of a noise generator to obtain the noise factors F_1 and F_2 or channel 1 and 2, respectively. The expression relating averaging time to rms "frequency deviation" is given by

$$\Delta f/f = f^{-1}P^{-1/2}[kTF/3\tau^3]^{1/2}$$

for a single oscillator. The power level P is determined by a replacement measurement using a signal generator.

The second method of calibration involves the use of the second-order frequency dependence with magnetic field that is characteristic of the hydrogen maser. The perturbation is in frequency only, and this may be verified from observing the data shown in Figure 10–6. On each 4-minute sample the left-hand plot is of $\langle \Delta\nu^2 \rangle$, the right-hand plot is $\sin\Omega t$, the beat frequency between the masers. In the sample marked "calibration run" it will be seen that, f/f has its maximum values when the signals are in quadrature, indicating that phase variations are being observed. The increase due to the applied perturbation agrees with the calculated perturbation to within 10 percent.

Other samples show data taken for different filter cutoff frequencies and are related to time by

$$\tau = 1/f_c.$$

As the cutoff frequency approaches 60 cps, it is possible to observe amplitude modulation as shown by maxima that coincide with the 0 and π radians condition of the beat signal.

The system provides a means of measuring not only frequency modulation but also amplitude modulation.

A plot of several runs of data taken at different power levels is given in Figure 10–7. The average noise figures are given, and the numbers apply to a single maser—not the difference between two masers.

CONCLUSION

It is seen in Figure 10–4 that the $\tau^{-3/2}$ law is a good fit to the data, indicating that, for the frequency intervals defined as

$$f_c = \tau^{-1},$$

the dominant effect is thermal noise $kT\ df$ and the effect of the noise factor of the receiver.

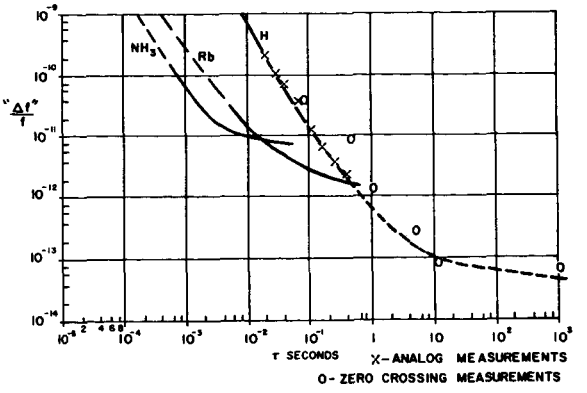

FIGURE 10–8.—Comparison of short-term performance.

From a knowledge of the relaxation rates and power outputs of hydrogen, rubidium, and ammonia masers it is possible to predict, on the above basis, what performance to expect under conditions where systematic variations, such as long-term drifts due to temperature changes, are not included.

In Figure 10–8, the plots are shown for the masers under the following conditions:

Maser	Power (watts)	Frequency (cps)
Hydrogen	10^{-12}	1.42×10^{9}
Rubidium	10^{-10}	6.8×10^{9}
Ammonia	10^{-10}	2.4×10^{10}

Systematic variations are shown by the dotted continuations of the curves. The crosses show the points on the previous figure. The circles are measurements made by counting slow beats and taking the rms value of a histogram.

For hydrogen the effect of systematic variations begins at about 10 sec, and the fractional rms frequency stability for 1 hour averaging, using a zero crossing counting method, is about 8×10^{-14}.

ACKNOWLEDGMENTS

The authors are indebted to Prof. Campbell Searle and to Dr. Richard Lacey for many informative discussions.

REFERENCES

1. EDSON, W. A., *Proc. I.R.E. 48*, 1454 (1960).
2. GOLAY, M. J. E., *Proc. I.R.E. 48*, 1473 (1960).
3. SHIMODA, K., WANG, T. C., and TOWNES, C. H., *Phys. Rev. 102*, 1308 (1956).
4. KLEPPNER, D., GOLDENBERG, H. M., and RAMSEY, N. F., *Phys. Rev. 126*, 603 (1962).
5. PACKARD, M. E., and REMPEL, R. C., "The Rubidium Optically Pumped Frequency Standard," *NEREM Record*, Nov. 1961.
6. VESSOT, R. F. C., and PETERS, H. E., "Frequency Beat Experiments With Hydrogen Masers," *Proceedings 17th Frequency Control Symposium.*
7. VANIER, J., and VESSOT, R. F. C., *Appl. Phys. Letters 4*, 122 (1964).
8. MCCOUBREY, A. O., "Frequency Control by Atomic Resonance," *Microwave Journal*, 1961.

11. EFFECTS OF LONG-TERM STABILITY ON THE DEFINITION AND MEASUREMENT OF SHORT-TERM STABILITY

J. A. BARNES AND D. W. ALLAN

National Bureau of Standards
Boulder, Colorado

Several authors have reported the measurement of a "flicker noise" spectrum for the frequency fluctuations, below a few cycles per second, of good quartz crystal oscillators. Experimental work carried out at the National Bureau of Standards at Boulder is in good agreement with these results.

The influence of this longer term type of noise turns out to be of considerable importance in the definition and measurement of shorter term noise, since averages of this short-term noise normally cover a total averaging time well into the flicker noise region. A mathematical formalism which satisfactorily avoids convergence difficulties has been developed around a set of physically meaningful quantities. Some theoretically reasonable definitions of short- and long-term stability are given.

It has been established by many people that quartz crystal oscillators are frequency-modulated by a "flicker" or $1/\omega$ type of noise which extends to at least as low a frequency as 1 cycle per year and probably even lower. Because the frequency emitted by any physically realizable device is bounded, this flicker noise behavior must cut off at some low, nonzero frequency ϵ.

It is possible to construct some measure of frequency stability $\langle \chi \rangle$ as the time average of a function $\chi(t)$ of the frequency. This function may or may not depend critically on the cutoff frequency ϵ. Thus, it might be that, if one measures the average value of $\chi(t)$ for some finite time T, this average value $\langle \chi \rangle_T$ will begin to approach $\langle \chi \rangle$ only after T is several times larger than $1/\epsilon$. Such a stability measure is thus said to be "cutoff-dependent" and is an inconvenient measure of frequency stability, since averaging times in excess of several years may be required to obtain a reasonable approximation to $\langle \chi \rangle$.

It is apparent that a necessary condition (not a sufficient condition) on any cutoff independent stability measure $\langle \chi \rangle$ is that $\langle \chi \rangle$ exists in the limit $\epsilon \to 0$. One can show that such quantities as the variance of frequency fluctuations around a uniform drift of frequency are, in fact, cutoff-dependent and hence not a very useful measure of frequency stability.

Some measures of frequency stability which are *not* cutoff-dependent and have direct use in various applications are: (1) variance of frequency fluctuation for finite sampling and averaging times, and (2) the variance of the nth finite difference of the phase for $n \geq 2$.

GENERAL PROBLEM

As stated, it has been established that quartz crystal oscillators are frequency-modulated by a "flicker" or $1/\omega$ type of noise spectrum. It even has been shown that this flicker-noise type of spectrum extends to 1 cycle per year and probably even lower. While this spectral region is not in the realm of "short-term" frequency fluctuations, it does have a very profound influence on their definition and measurement.

This can be seen by considering a crystal oscillator whose frequency fluctuations Ω from a nominal value have a (power) spectral density given by

$$G_\Omega(\omega) = g(\omega) + (h/|\omega|), \qquad (1)$$

where $g(\omega)$ predominates for the higher values of ω and thus gives rise to the "short-term" frequency fluctuations. The second term on the right is the flicker noise term. The total mean square of the instantaneous frequency fluctuation $\langle(\Omega)^2\rangle$ is then given by

$$\langle(\Omega)^2\rangle = 2\int_{\epsilon}^{\infty} G_{\Omega}(\omega)\, d\omega, \qquad \epsilon \geq 0. \tag{2}$$

Since any physical device must emit a finite frequency, Ω *must* be bounded; and thus the integral in Equation 2 must exist. This requires that $\epsilon \neq 0$ in order to insure the existence of

$$\int_{\epsilon}^{\infty} (h/|\,\omega\,|)\, d\omega.$$

From the preceding comments, it is apparent that this "cutoff" frequency ϵ is not known but is certainly less than 1 cycle per year. Thus, any meaningful measure of frequency stability should, in effect, be cutoff-independent; otherwise, averaging times exceeding several years must be employed.

It is possible to consider some function $\chi(t)$ obtained from the frequency (or phase) of the oscillator:

$$\chi(t) = X[f(t)]. \tag{3}$$

The expectation value of $\chi(t)$ is then given by

$$\langle\chi\rangle = \lim_{T\to\infty} T^{-1}\int_{-T/2}^{T/2} \chi(t)\, dt. \tag{4}$$

In principle, it is possible to obtain the Fourier transform of Equation 3 and substitute this in the integral of Equation 4. In this situation, the only quantities $\chi(t)$ which have physical significance (in the sense of being easily measurable) are quantities which do not depend critically on ϵ as $\epsilon \to 0$. In other words, $\lim_{\epsilon\to 0^+}\langle\chi\rangle$ must exist for meaningful quantities. Table 11–1 shows several functions of the frequency which do *not* exist as $\epsilon \to 0^+$. Physically, this can be pictured as follows: One can measure the quantity

$$\langle\chi\rangle_T = T^{-1}\int_{-T/2}^{T/2} \chi(t)\, dt \tag{5}$$

for some given time T, then extend the averaging time to NT and obtain $\langle\chi\rangle_{NT}$. If the sequence $\{\langle\chi\rangle_{NT}\}$ is considered, one might find that

$$\lim_{N\to\infty}\{\langle\chi\rangle_{NT}\} \to \infty.$$

For any finite N and T, the quantity $\langle\chi\rangle_{NT}$ certainly may exist. In the limit, however, the quantity may or may not exist.

TABLE 11–1.—*Cutoff-Dependent Quantities*

Name	Expression
Auto-covariance function of the phase fluctuations	$\lim_{T\to\infty} T^{-1}\int_{-T/2}^{T/2} \phi(t)\phi(t+\tau)\, dt$
Auto-covariance function of the frequency fluctuations	$\lim_{T\to\infty} T^{-1}\int_{-T/2}^{T/2} \bar{\Omega}(t,\tau)\bar{\Omega}(t+\tau',\tau)\, dt,$ where $\bar{\Omega}(t,\tau) = [\phi(t+\frac{1}{2}\tau) - \phi(t-\frac{1}{2}\tau)]/\tau$
Standard deviation of the frequency fluctuations	$\lim_{T\to\infty}\left\{T^{-1}\int_{-T/2}^{T/2}[\bar{\Omega}(t,\tau)]^2\, dt - \left[T^{-1}\int_{-T/2}^{T/2}\bar{\Omega}(t,\tau)\, dt\right]^{-2}\right\}$

MEANINGFUL QUANTITIES

The method of (power) spectral densities is a powerful and often meaningful way of encompassing a broad range of measurements. It certainly has application to the case of flicker noise (Reference 1). Occasionally, however, the quantities of physical interest are not simply related to the spectrum or the spectrum contains more information than is needed. Thus, other measures of frequency stability have been devised. Two additional methods are considered here.

RMS FREQUENCY FLUCTUATIONS

As was stated in Table 11–1, the quantity

$$\sigma_f^2(\tau) = \lim_{T\to\infty}\left\{T^{-1}\int_{-T/2}^{T/2}\left[\frac{\phi(t+\tau)-\phi(t)}{\tau}\right]^2 dt - \left[T^{-1}\int_{-T/2}^{T/2}\left(\frac{\phi(t+\tau)-\phi(t)}{\tau}\right)dt\right]^2\right\} \quad (6)$$

is cutoff-dependent. However, if one does not pass to the limit $T\to\infty$ but specifies T and τ, the integral most certainly exists even in the limit $\epsilon\to 0$. Thus, one measure of frequency stability is the function

$$\sigma_f^2(\tau,\ T) = T^{-1}\int_{-T/2}^{T/2}\left[\frac{\phi(t+\tau)-\phi(t)}{\tau}\right]^2 dt - \left[T^{-1}\int_{-T/2}^{T/2}\left(\frac{\phi(t+\tau)-\phi(t)}{\tau}\right)dt\right]^2, \quad (7)$$

which unfortunately depends on *two* parameters τ and T.

THE METHOD OF FINITE DIFFERENCES

It is of value here to digress from short-term stability and consider how quartz crystal oscillators are used in clock systems—a problem in long-term stability. Typically, an oscillator is used as sort of a "fly wheel" in a clock system between regular calibrations with a frequency standard. Thus, one measures an average frequency $\bar{\Omega}$ during some interval $t-\frac{1}{2}\tau$ to $t+\frac{1}{2}\tau$, say. One predicts, then, that (on the average) the total phase accumulated by the oscillator $\Delta\Phi$ in the larger interval $t-\frac{1}{2}T$ to $t+\frac{1}{2}T$ is given by

$$\Delta\Phi \approx T\bar{\Omega} = T\left[\frac{\phi(t-\tfrac{1}{2}\tau)-\phi(t+\tfrac{1}{2}\tau)}{\tau}\right] \quad (8)$$

While this may be true "on the average," the frequency fluctuations of the oscillator cause some error $\delta\Phi$, given by

$$\delta\Phi = \Delta\Phi - T\bar{\Omega},$$

$$\delta\Phi = \phi(t+\tfrac{1}{2}T)-\phi(t-\tfrac{1}{2}T) - (T/\tau)[\phi(t+\tfrac{1}{2}\tau)-\phi(t-\tfrac{1}{2}\tau)]. \quad (9)$$

If one now sets $T=3\tau$ and defines the variable ϕ_n defined on the discrete range of the integer n by the relation

$$\phi_n \equiv \phi(t_0+n\tau)$$

and if one writes $t=t_0+\frac{1}{2}T$ in Equation 9, $\delta\Phi$ can be written in the simpler form

$$\delta\Phi = \Delta^3\phi_n, \quad (10)$$

where $\Delta^3\phi_n$ is the third finite difference of the variable ϕ_n (see Table 11–2). Thus the precision of an oscillator used in this system is related to the quantity

$$\langle(\delta\Phi)^2\rangle = \langle(\Delta^3\phi_n)^2\rangle, \quad (11)$$

which certainly must exist if the clock is any good at all.

Indeed, if one considers Equation 10 in the case of flicker noise (Reference 2), not only is $\Delta^3\phi_n$ a stationary function, but the correlation with $\Delta^3\phi_{n+k}$ for $k\geq 3$ is so small that the convergence of the quantity

$$N^{-1}\sum_{n=1}^{N}(\Delta^3\phi_n)^2$$

for large N is essentially that of a random un-

TABLE 11–2.—*Finite Phase Differences*

Variable	Definition	
ϕ_n	ϕ_n	$\phi(t_0+n\tau)$
$\Delta\phi_n$	$\phi_{n+1}-\phi_n$	$\phi_{n+1}-\phi_n$
$\Delta^2\phi_n$	$\Delta\phi_{n+1}-\Delta\phi_n$	$\phi_{n+2}-2\phi_{n+1}+\phi_n$
$\Delta^3\phi_n$	$\Delta^2\phi_{n+1}-\Delta^2\phi_n$	$\phi_{n+3}-3\phi_{n+2}+3\phi_{n+1}-\phi_n$

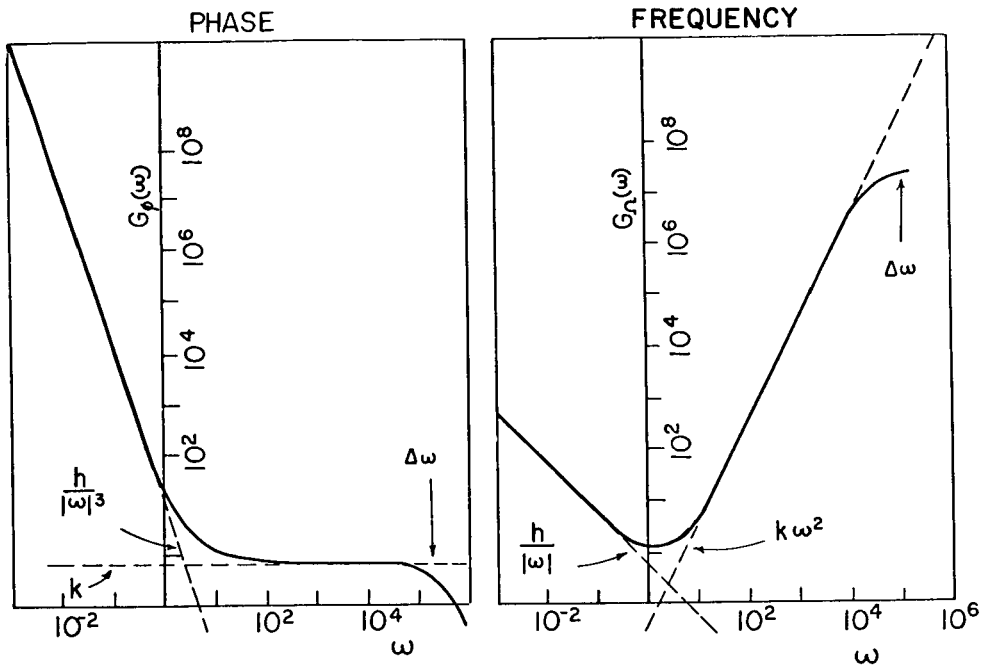

FIGURE 11–1.

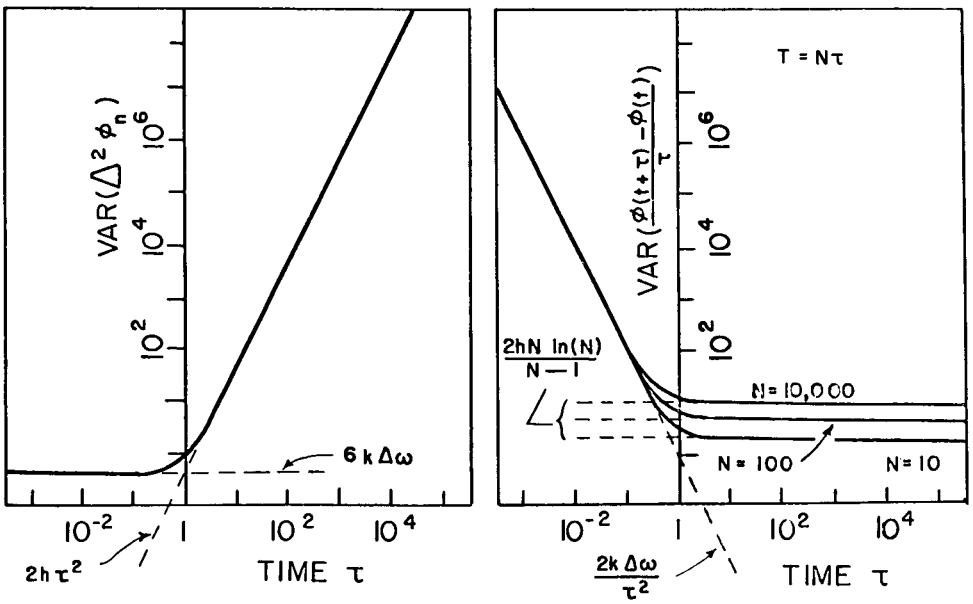

FIGURE 11–2.

correlated variable. Similarly one finds in general that $\Delta^k\phi_n$ is a stationary, cutoff-independent function for $k \geq 2$.

CONCLUSIONS

It is of value now to tie these types of frequency stability together by applying each method to the same theoretical model of an oscillator; in particular, consider an oscillator whose frequency is modulated by a flicker noise. Also, let the system generate an essentially white noise over its bandpass. Since this noise will appear to be half AM and half FM, the spectral densities of frequency and phase will appear as indicated in Figure 11–1. On the basis of this model, the graphs of Figure 11–2 were obtained.

It is interesting to note that the effects of flicker noise on the variance of frequency fluctuations depend on the total averaging time (see Equation 7). Thus, if one were to let $N = T/\tau = 2$ (the smallest possible number for a variance), the oscillator would "appear" better than for any other N. However, one should take the ensemble average of many variances for $N = 2$ to obtain an acceptably precise figure for the variance.

The asymptotes of the curve showing the variance of the second difference differ from the asymptotes of the frequency curve by a function of N and a factor of τ^2. For this specialized case the three numbers k, h, and $\Delta\omega$ serve as a complete measure of frequency stability instead of giving values of a continuous function, such as spectral distribution or variance of the nth finite difference. For the variance of the frequency fluctuations, one has a stability measure which is a function of *two* continuous variables. It also is worth noting that this model, in fact, fits very well a broad class of commercially available oscillators.

One is led to the conclusion that there are some commonly quoted measures of frequency stability which are very impractical. The autocovariance function of phase and frequency and the total rms frequency fluctuations are not useful concepts in the definition of frequency stability, since it is very difficult to obtain them experimentally. While the rms frequency fluctuations for specified sample and averaging times is a meaningful quantity, it is very inconvenient to have a stability measure be a function of two variables. Thus, it is suggested that the more meaningful concepts are (power) spectral densities of phase and frequency fluctuations and the variances of the second and higher finite differences of the phase.

With the difficulty of defining an rms frequency, one sees also the difficulty of measuring the true (power) spectral density of the output voltage of an oscillator. Indeed, as one makes his analyzer narrower in bandwidth and takes longer to sweep the line, the spectrum looks worse and worse.

REFERENCES

1. LIGHTHILL, M., "Introduction to Fourier Analysis and Generalised Functions," Cambridge, 1962.
2. BARNES, J. A., "Atomic Timekeeping and the Statistics of Precession Signal Generators," to be published.

12. THE EFFECTS OF NOISE ON CRYSTAL OSCILLATORS

E. HAFNER

U. S. Army Electronics Command
Fort Monmouth, New Jersey

A first-order perturbation analysis has been used to derive an explicit expression for the output signal of an oscillator with noise sources at several locations in the circuit. While differing in detail, the essential features of the output signal—with only one noise source acting—are found to be the same for each noise source in the circuit. An additional white-noise component, however, is contributed by the source across the output. The common features of the signal reveal two aspects of oscillator behavior to be present simultaneously, which heretofore have variously been assumed to exist separately, to the exclusion of one another. The first one is characterized by the random-walk phase disturbance and low-frequency amplitude modulation, while the other is the action of the oscillator as an extremely narrow-band noise filter. The manner in which these aspects are reflected in the power density spectrum of the signal and in its short-term frequency stability are discussed.

Although the problem of noise in regenerative feedback oscillators has received considerable attention in the past (References 1–6), there is ample evidence that the existing theories provide only partial descriptions of a many-sided phenomenon. In fact, some of the most prominent aspects of oscillator behavior, persistently observed in the course of experimental investigations, apparently cannot be explained by these theories. As a consequence, there exists a serious lack of useful guidance for the development of improved devices and hence a definite need for additional work.

The present paper represents an attempt to clarify further the manner in which the Johnson and shot noise affect the signal in an oscillator and to arrive at a sufficiently detailed understanding of the controlling parameters to indicate the direction in which improved performance can be found.

1. STATEMENT OF THE PROBLEM

A circuit configuration which closely resembles a quartz crystal oscillator, and yet is still manageable analytically, is shown in Figure 12–1. The $R_3-C_3-L_3$ branch approximates the behavior of the quartz crystal unit. The active device in the oscillator is assumed to have infinitely high input and output impedances and to generate a current i_1 which is a nonlinear function of the output voltage of the feedback network:

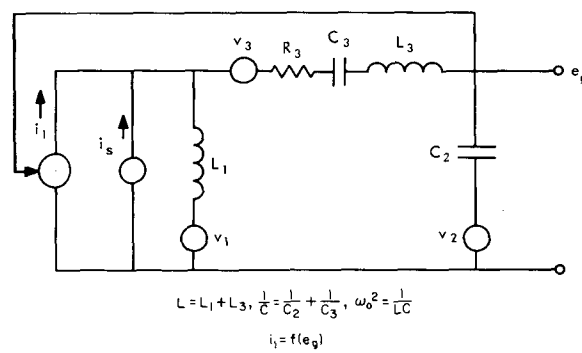

FIGURE 12–1.—Oscillator Model. The feedback network is fed from an ideal current generator whose strength i_1 is a non-linear function of the output voltage e_g. The generators i_s, v_1, v_2 and v_3 are, for the purposes of this paper, assumed to be white noise sources. The R_3, L_3, C_3 branch approximates, by proper choice of the parameter values, the action of a quartz crystal unit.

$$i_1 = f(e_g) \tag{1.1}$$

The current generator i_s and the voltage genera-

tors v_1, v_2, and v_3 inject extraneous signals into the oscillator whose effects are to be evaluated.

The differential equation describing the form and behavior of the output voltage e_g is best derived from the equation

$$e_g=\frac{z_1z_2}{z_1+z_2+z_3}(i_1+i_s)+\frac{z_2}{z_1+z_2+z_3}(v_1+v_3)+\frac{z_1+z_3}{z_1+z_2+z_3}v_2, \quad (1.2)$$

which follows readily from Figure 12–1, by regarding s in, for example, $z_1=sL_1$ as an operator (Reference 7): $s\rightarrow d/dt$. One finds with Equation (1.1), after some rearrangement,

$$\left[\frac{d^2}{dt^2}+\frac{L_1}{LC_2}\left(\frac{R_3C_2}{L_1}-\frac{df(e_g)}{de_g}\right)\frac{d}{dt}+\omega_0^2\right]e_g=F(t), \quad (1.3)$$

whereby

$$L=L_1+L_3,$$

$$C^{-1}=C_2^{-1}+C_3^{-1},$$

$$\omega_0^2=(LC)^{-1} \quad (1.4)$$

and

$$F(t)=(L_1/LC_2)(di_s/dt)+\omega_0^2(C/C_2)(v_1+v_3)+[(d^2/dt^2)+(R_3/L)(d/dt)+(C/C_3)\omega_0^2]v_2. \quad (1.5)$$

It is noted that Equation (1.3) is only of second order; with $L_3\rightarrow 0$ and $C_3\rightarrow\infty$, it reverts to the equation for a conventional single-tuned circuit.

Of major concern in this paper are the properties of the solutions of (1.3) when the extraneous signals are random noise. Stable, nearly harmonic solutions of (1.3) will be assumed to exist without further discussion; and only the stationary state properties of such solutions will be dealt with in the following (i.e., the initial buildup of the oscillations is assumed to be in the infinite past).

If the noise sources in Figure 12–1 are quiescent, Equation (1.3) becomes completely deterministic; and it is well known that, with $F(t)=0$, there are steady-state solutions which are oscillatory in nature, provided certain conditions are met (References 8 and 9). The action of the noise sources is not essential for these solutions to exist; rather, with increasing intensity, the noise sources cause progressively more severe random disturbances of the deterministic solutions.

The solutions of (1.3) with $F(t)=0$ are perfectly periodic in the steady state and can be represented in the form

$$e_{g0}=\sum_n A_{n0}\cos(n\omega_1t+\varphi_n). \quad (1.6)$$

For an harmonic oscillator capable of steady state oscillations, the A_{n0}'s will not all be zero and ω_1 will be in the neighborhood of ω_0 defined in (1.4). With all transients in the infinite past, the A_{n0}'s and φ_n's are constants whose values, as well as the value of ω_1, can—at least in principle—be determined to any desired accuracy. [When Equation (1.6) is substituted into (1.3), with $F(t)=0$ and the principle of the harmonic balance (Reference 10) is applied, an infinite set of nonlinear algebraic equations results which can be solved by an iteration procedure.]

The noise sources in Figure 12–1 introduce transients into the system, and the steady state is never maintained exactly; the various harmonics of the solution of (1.3) never have sharply defined amplitudes and phases. For the present purposes it is most appropriate to write e_g in the form

$$e_g=\sum_n[A_{n0}+x_n(t)]\cos[n\omega_1t+\varphi_n+\phi_n(t)], \quad (1.7)$$

where the $x_n(t)$'s and $\phi_n(t)$'s are stochastic variables representing the amplitude and phase disturbances caused by the noise. When the $x_n(t)$'s and $\phi_n(t)$'s are so small that only terms linear in these quantities are of significance, e_g can be approximated by

$$e_g=e_{g0}+u(t), \quad (1.8)$$

with e_{g0} defined by (1.6) and $u(t)$ given by

$$u(t)=\sum_n[x_n(t)\cos(n\omega_1t+\varphi_n)-A_{n0}\phi_n(t)\sin(n\omega_1t+\varphi_n)]. \quad (1.9)$$

It is apparent that, to within this approximation, all disturbances caused by the noise—and only the disturbances—are represented by $u(t)$ in Equation (1.8). The fact that the approximation is justified, in particular that

$$|\phi_n(t)|\ll 1, \quad (1.10)$$

remains to be verified once $u(t)$ is computed for any particular situation.

Because e_{g0} is the solution of the unperturbed equation and the approximation of (1.5) by (1.6) implies already that terms of higher order in $u(t)$ are negligible, substitution of (1.8) into (1.3) results in

$$\left\{\frac{d^2}{dt^2}+\frac{L_1}{LC_2}\left[\frac{R_3C_2}{L_1}-\frac{df(e_{g0})}{de_{g0}}\right]\frac{d}{dt}+\left[\omega_0^2-\frac{L_1}{LC_2}\frac{d}{dt}\frac{df(e_{g0})}{de_{g0}}\right]\right\}u(t)=F(t). \quad (1.11)$$

This is a linear differential equation for $u(t)$; its time variable coefficients depend only on e_{g0}, the steady-state solution of the homogeneous equation (1.3), and hence are known.

The most realistic representation of the noise current i_s and the noise voltages v_1, v_2, and v_3 in $F(t)$ are series of delta functions of variable strength and variable occurrence, and these are also representations for which the solution of (1.11) is readily found and conveniently interpreted. In the following it will be assumed, therefore, that

$$i_s=\sum_k a_{sk}\,\delta(t-t_k)$$

$$v_r=\sum_k a_{rk}\,\delta(t-t_k) \qquad (r=1, 2, 3). \quad (1.12)$$

Once e_{g0} is determined, the stationary state solution of Equation (1.3) can be found with (1.8), according to the linear superposition principle, when (1.11) has been solved for a single impulse from each one of the noise sources in the circuit in Figure 12–1.

Only an approximate solution of Equation (1.3) will be sought and dealt with in this paper.

2. THE DISTURBANCES OF THE FUNDAMENTAL COMPONENT

2.1 The Approximations

When the nonlinear terms in the current voltage characteristic (1.1) of the active device are small and/or the feedback network in Figure 12–1 is highly selective, the second and higher harmonics in (1.6) will be much smaller than the fundamental and can be considered negligible to a first approximation. These conditions will be assumed justified in the following, and (1.6) will be approximated by

$$e_{g0}=A_1\cos(\omega_1 t+\varphi). \quad (2.1)$$

Only a first approximation to the disturbances of the fundamental frequency component of e_g can now be evaluated reasonably. This is found from (1.11) by letting $u(t)$ in (1.8) become

$$u(t)=x_1(t)\cos(\omega_1 t+\varphi)+y_1(t)\sin(\omega_1 t+\varphi), \quad (2.2)$$

with

$$y_1(t)=-A_1\phi_1(t). \quad (2.3)$$

The next higher approximation to the disturbances of the fundamental frequency component apparently can still be determined from the linear perturbation equation (1.11) if the noise sources are weak. It requires that successively higher harmonics in e_{g0} as well as in $u(t)$ be included in the analysis, whereby the first improvement in $x_1(t)$ and $\phi_1(t)$ cannot be expected until at least the third harmonic is considered.* When any one or all of the extraneous sources i_s, v_1, v_2, and v_3 are strong, higher order terms in $u(t)$ will no longer be negligible—even if $u(t)$ is approximated by (2.2) and e_{g0} by (2.1)—and a nonlinear perturbation analysis becomes necessary. It will become apparent later on, however, that this latter case can be of significance in practical oscillators only when the perturbing forces are signals other than thermal or shot noise.

Any attempt to actually compute the higher order approximations to $u(t)$, or to evaluate the limitations on the validity of the first-order approximations to be derived, is beyond the scope of this paper.

2.2 The Unperturbed Signal

Without imposing undue further restrictions (Reference 8) on the following analysis, the current voltage characteristic (1.1) of the active

* When dealing with crystal oscillators, it must additionally be observed that crystal units generally have an overtone response close to the third electrical harmonic of the oscillator frequency. Especially under high drive conditions, the two frequencies can coincide. The presence of this crystal response in the feedback network then becomes very significant and must be considered in the analysis.

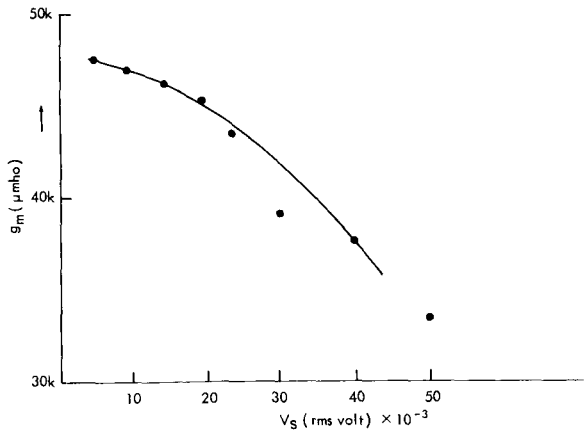

FIGURE 12–2.—Typical behaviour of the effective transconductance g_m as a function of signal level. Dots are experimental points obtained on a 2N2808 transistor, operated at $i_e = 2$ *ma*.

device will be assumed to have the form

$$i_1 = f(e_g) = g_{m0}e_g - \beta e_g^3. \tag{2.4}$$

In order for (2.1) to be a reasonable approximation to (1.6), $\beta e_g^2 \ll g_{m0}$ is desirable, expecially when the transfer impedance of the feedback network at the harmonic frequencies is not extremely low.

When (2.4) and (2.1) are inserted into (1.3) with $F(t) = 0$, the values of A_1 and ω_1 can be determined to

$$A_1^2 = (4/3\beta)[g_{m0} - (C_2R_3/L_1)],$$
$$\omega_1 = \omega_0. \tag{2.5}$$

It is useful to note that the approximation (2.1) to the steady-state signal of the unperturbed oscillator is the solution of the linear differential equation

$$\ddot{e}_{g0} + (L_1/LC_2)[(C_2R_3/L_1) - g_{m0} + \tfrac{3}{4}\beta A_1^2]\dot{e}_{g0} + \omega_1^2 e_{g0} = 0, \tag{2.6}$$

which results when the equivalent linearization procedure is applied to (1.3) [with $F(t) = 0$]. The damping term in (2.6) vanishes only when (2.5) is satisfied. The quantity

$$g_m = g_{m0} - \tfrac{3}{4}\beta A_1^2 \tag{2.7}$$

will be recognized as the effective transconductance (Reference 12) of the active device for signals of amplitude A_1. With g_{m0} and β both positive, (2.7) indicates that g_m decreases monotonously with increasing A_1, as shown in Figure 12–2. This behavior actually was observed under nearly all reasonable conditions in tests on a large number of active devices. The values of g_{m0} and β to be used in (2.4) and in the following relations thus can be determined from the measured g_m vs. signal amplitude curves.* Because (2.5) or (2.6) require (Reference 13),

$$C_2R_3/L_1 = g_m, \tag{2.8}$$

the amplitude A_1 of the steady-state oscillations can be adjusted by proper choice of the circuit parameters.

With (2.1) and (2.5), the steady-state signal in the undisturbed oscillator, as it will be used in the present analysis, is defined; and the perturbations of its amplitude and phase due to the noise must be determined next.

2.3 The Impulse Response

The general equation (1.11) for the perturbation $u(t)$ assumes with (2.1), (2.4), and (2.5)—

* A more detailed examination (Reference 11) of the contributing factors shows that a $\beta^* < \beta$ actually should be used in the following sections pertaining to u(t), whereby β^* is the coefficient of the third-order term when the instantaneous function $f(e_g)$ in (1.1) is developed into a Taylor series. Since the coefficients of the Taylor series depend on the bias conditions of the active device and since the bias conditions change, almost invariably, with amplitude, the g_m vs. amplitude curves, measured under static conditions, include implicitly the effects of the even-order terms in $f(e_g)$, particularly the second-order term. The difference between β and β^* is not very significant except in oscillators with artificial level control, such as AGC or lamp bridge oscillators. In AGC oscillators the change in the bias conditions is artificially magnified and utilized to adjust g_{m0} and β such that the damping term in (2.6) vanishes (Reference 13) for a very small value of A_1. In a lamp bridge oscillator the value of R_3 in (2.6), or its equivalent, depending on the actual circuit, varies with signal amplitude and adjusts itself to the value at which the damping term is zero, while g_{m0} and β remain essentially unchanged. All amplitude-dependent changes in bias conditions—or in R_3—require a finite time to become effective, governed by an $R-C$ time constant, while the first effects of a noise impulse occur instantaneously. The function (2.4) is understood, therefore, to represent the instantaneous relation between i_1 and e_g for the purposes of the present analysis. Any delayed action will only affect the envelope function of e_g and, if necessary, can be accounted for by imposing suitable constraints on the behavior of this function after the instantaneous behavior has been established.

the form

$$\ddot{u}+\omega_1\gamma[1+2\cos 2(\omega_1 t+\varphi)]\dot{u}$$
$$+\omega_1^2[1-4\gamma\sin 2(\omega_1 t+\varphi)]u=F(t), \quad (2.9)$$

whereby the parameter γ is conveniently defined by either of the two equivalent expressions

$$\gamma=(\omega_1 C_2)^{-1}(L_1/L)\tfrac{3}{4}\beta A_1^2,$$
$$\gamma=(L_1/L)[(g_{m0}-g_m)/\omega_1 C_2]. \quad (2.10)$$

It will become apparent later on that $2/\omega_1\gamma$ is the time constant which controls the decay of disturbances in the oscillator.

Equation (2.9) is of the Mathieu type and, through proper transformation (Reference 14), could be brought into the standard form. This, however, appears to be of no assistance in its solution. Rather, with the aid of the identity

$$F(t)=F(t)\cdot 1=F_c\cos(\omega_1 t+\varphi)+F_s\sin(\omega_1 t+\varphi),$$
$$F_c=F(t)\cos(\omega_1 t+\varphi),$$
$$F_s=F(t)\sin(\omega_1 t+\varphi) \quad (2.11)$$

and with $u(t)$ given by (2.2), Equation (2.9) is rewritten in the form

$$(\ddot{x}_1+2\omega_1\dot{y}_1+2\omega_1\gamma\dot{x}_1-F_c)\cos(\omega_1 t+\varphi)$$
$$+(\ddot{y}_1-2\omega_1\dot{x}_1-2\omega_1^2\gamma x_1-F_s)\sin(\omega_1 t+\varphi)$$
$$+(\dot{x}_1+3\omega_1 y_1)\omega_1\gamma\cos 3(\omega_1 t+\varphi)$$
$$+(\dot{y}_1-3\omega_1 x_1)\omega_1\gamma\sin 3(\omega_1 t+\varphi)=0, \quad (2.12)$$

For (2.12)—and hence (2.9)—to be satisfied identically for all t, it is certainly sufficient that the following conditions be met:

$$\ddot{x}_1+2\omega_1\dot{y}_1+2\omega_1\gamma\dot{x}_1=F_c,$$
$$\ddot{y}_2-2\omega_1\dot{x}_1-2\omega_1^2\gamma x_1=F_s, \quad (2.13)$$
$$\dot{x}_1+3\omega_1 y_1=0, \qquad \dot{y}_1-3\omega_1 x_1=0. \quad (2.14)$$

Since the trigonometric functions in (2.12) are linearly independent and $x_1(t)$—and in a sense $y_1(t)$ too—represent small disturbances of large constants, it appears plausible that (2.13) and (2.14) are both necessary and sufficient for (2.12) as a perturbation equation to be satisfied. While we have not been able to prove this rigorously as yet, we proceed under the assumption that the solutions of (2.13) contain all significant aspects of the solution of (2.9) [i.e., we assume that other possible solutions of (2.12) are of no consequence for the present work].* The solutions of (2.14) provide the possibility to account for permanent phase shifts in the third harmonic, but to within the present approximation they do not affect the disturbances of the fundamental and need not be dealt with further here.

It is important to note that Equations (1.11), and hence (2.9) and (2.13), follow from (1.3) by assuming only that $u(t)$ in (1.8) is so small that higher order terms are negligible. The method of slowly varying amplitude and phase (Reference 15) has not been used nor was the narrow-band approximation (Reference 16) introduced. $u(t)$, and hence $x_1(t)$ and $y_1(t)$, need only be small; but their rate of change with time is not restricted. To neglect their second derivatives (References 1 and 5) is seen to be arbitrary and emphatically is not justified.

Equations 2.13 are linear, and the superposition principle can be applied to find the response of the system to the combined action of all the noise sources if the response to a single impulse from each of the noise sources is known. The method used here to find the impulse response will be indicated briefly for v_3. With

$$i_s=0, \qquad v_1=v_2=0, \qquad v_3=a_{3k}\,\delta(t-t_k), \quad (2.15)$$

F_c and F_s become, because of (1.5) and (2.11),

$$F_c=(C/C_2)\omega_1^2 a_{3k}\,\delta(t-t_k)\cos(\omega_1 t+\varphi),$$
$$F_s=(C/C_2)\omega_1^2 a_{2k}\,\delta(t-t_k)\sin(\omega_1 t+\varphi). \quad (2.16)$$

The Laplace transform of (2.13) with (2.16) is

$$(p^2+2\omega_1\gamma p)X_{13}+2\omega_1 p Y_{13}$$
$$=(C/C_2)\omega_1^2 a_{3k}\cos(\omega_1 t_k+\varphi)\exp(-pt_k),$$
$$-2\omega_1(p+\omega_1\gamma)X_{13}-p^2 Y_{13}$$
$$=(C/C_2)\omega_1^2 a_{3k}\sin(\omega_1 t_k+\varphi)\exp(-pt_k). \quad (2.17)$$

The initial conditions for x_1 and y_1 and their first derivative are zero when, at $t=t_k$, the oscillator is assumed to be in the state which would result if the last impulse—prior to the one considered—would have been in the infinite past.

* See Appendix A.

The inverse transforms of the solutions X_{13} and Y_{13} of (2.17) are:

$$\begin{aligned}
x_{13k} &= -(\omega_1 C/2C_2)\, a_{3k} \sin(\omega_1 t_k+\varphi)\, \exp[-\omega_1\gamma(t-t_k)] \\
&\quad +(\omega_1 C/2C_2)\, a_{3k} \cos(\omega_1 t_k+\varphi)\, \exp[-(\omega_1\gamma/2)(t-t_k)] \sin 2\omega_1(t-t_k) \\
&\quad +(\omega_1 C/2C_2)\, a_{3k} \sin(\omega_1 t_k+\varphi)\, \exp[-(\omega_1\gamma/2)(t-t_k)] \cos 2\omega_1(t-t_k), \\
y_{13k} &= (\omega_1 C/2C_2)\, a_{3k} \cos(\omega_1 t_k+\varphi) \\
&\quad -(\omega_1 C/2C_2)\, a_{3k} \cos(\omega_1 t_k+\varphi)\, \exp[-(\omega_1\gamma/2)(t-t_k)] \cos 2\omega_1(t-t_k) \\
&\quad +(\omega_1 C/2C_2)\, a_{3k} \sin(\omega_1 t_k+\varphi)\, \exp[-(\omega_1\gamma/2)(t-t_k)] \sin 2\omega_1(t-t_k).
\end{aligned} \tag{2.18}$$

The terms periodic with $2\omega_1$ in x_{13k} and y_{13k} are correlated; their presence in (2.18) is indicative of some of the difficulties frequently encountered (Reference 17) when dealing with amplitude and phase functions. In the present case the problem is readily resolved when $u(t)$ is formed according to (2.2). One finds with (2.18), as the solution of (2.9),

$$\begin{aligned}
u_3(t) &= -(\omega_1 C/2C_2)\, a_{3k} \sin(\omega_1 t_k+\varphi)\, \exp[-\omega_1\gamma(t-t_k)] \cos(\omega_1 t+\varphi) \\
&\quad +(\omega_1 C/2C_2)\, a_{3k} \cos(\omega_1 t_k+\varphi)\, \sin(\omega_1 t+\varphi) \\
&\quad +(\omega_1 C/2C_2)\, a_{3k} \exp[-(\omega_1\gamma/2)(t-t_k)] \sin\omega_1(t-t_k).
\end{aligned} \tag{2.19}$$

In (2.18), and hence in (2.19), terms with γ or γ^2 as factor have been neglected and $\gamma^2 \ll 4$ was assumed. This is justified because γ is already restricted to very small values, once all other assumptions made to arrive at (2.9) are met. Since βe_{g0}^2 in (2.4) should be much smaller than g_{m0}, it follows approximately from (2.10a), with (2.7) and (2.8), that

$$\gamma = (L_1/L)(\omega_1 C_2)^{-1} \tfrac{3}{4}\beta A_1^2 \ll (L_1/L)(\omega_1 C_2)^{-1} g_{m0} \approx (L_1/L)(\omega_1 C_2)^{-1} g_m = R_3/\omega_1 L \tag{2.20}$$

(i.e., $\gamma \ll R_3/\omega_1 L$). When (2.19) and (2.1) are substituted into (1.8), e_g can be written as

$$e_g = [A_1+\alpha_k(t)] \cos[\omega_1 t+\eta_k(t)+\varphi]+n_k(t), \tag{2.21}$$

whereby, for a single impulse generated at time t_k by v_3 in Figure 12-1,

$$\begin{aligned}
\alpha_k(t) &= \alpha_{3k}(t) = -(\omega_1 C/2C_2)\, a_{3k} \sin(\omega_1 t_k+\varphi)\, \exp[-\omega_1\gamma(t-t_k)], \\
\eta_k(t) &= \eta_{3k}(t) = -A_1^{-1}(\omega_1 C/2C_2)\, a_{3k} \cos(\omega_1 t_k+\varphi), \\
n_k(t) &= n_{3k}(t) = (\omega_1 C/2C_2)\, a_{3k} \exp[-(\omega_1\gamma/2)(t-t_k)] \sin\omega_1(t-t_k).
\end{aligned} \tag{2.22}$$

This representation shows that the oscillator signal suffers at the time of the impulse an instantaneous change in amplitude by the amount $-(\omega_1 C/2C_2)\, a_{3k} \sin(\omega_1 t_k+\varphi)$—which subsequently decays to zero at a rate determined by γ—and an instantaneous and permanent change in phase by the amount η_{3k} in (2.22). This type of behavior has been derived, or concluded to exist, by numerous writers in the past. Blaquiere (Reference 3) has discussed at length the fact that the magnitude and sign of the amplitude and phase changes depend on the phase of e_{g0} at the time t_k.

The third term $n_{3k}(t)$ in (2.21) appears simply as an additive component. It is the impulse response function of the passive network in Figure 12-1, with the loss term R_3 partially eliminated by the action of the active device. The quality factor of the resulting network is $1/\gamma$ which, according to (2.20), is substantially higher than the effective quality factor of the passive elements in the circuit. The existence of the term $n_{3k}(t)$ in the solution of (1.3) reveals that the oscillator, in addition to generating the signal e_{g0}, simultaneously acts as a narrow-band noise filter of relative band width $\Delta\omega/\omega_1 = \gamma$. Although

the third term in (2.19) is, at $t=t_k$, equal to the sum of the two other terms and hence an important part of the solution, it is eliminated from the equations when the method of slowly varying amplitude and phase is applied. It apparently has not been observed before for this reason.

In a manner similar to that used in the derivation of the expressions (2.22) for the noise sources as shown in (2.15), the response of the system to a single impulse from each of the other noise sources in Figure 12–1 can be evaluated in turn. From (1.5) it is apparent that an impulse from v_1 leads again to (2.22) if a_{3k} is replaced by a_{1k}. When

$$i_s=a_{sk}\,\delta(t-t_k), \qquad v_1=v_2=v_3=0,$$

the solution of (1.3) has again the form (2.21), whereby now

$$\alpha_k(t)=\alpha_{sk}(t)=(L_1a_{sk}/2LC_2)\times\cos(\omega_1t_k+\varphi)\,\exp[-\omega_1\gamma(t-t_k)],$$

$$\eta_k(t)=\eta_{sk}(t)=-A_1^{-1}(L_1a_{sk}/2LC_2)\times\sin(\omega_1t_k+\varphi),$$

$$n_k(t)=n_{sk}(t)=(L_1a_{sk}/2LC_2)\times\exp[-(\omega_1\gamma/2)(t-t_k)]\cos\omega_1(t-t_k); \quad (2.23)$$

while, for

$$v_2=a_{2k}\,\delta(t-t_k), \qquad i_s=0, \qquad v_1=v_3=0,$$

one finds

$$\alpha_k(t)=\alpha_{2k}(t)=(\omega_1L_1/2L)[1+(R_3/\omega_1L_1)^2]^{1/2}a_{2k}\times\sin(\omega_1t_k+\varphi+\psi)\,\exp[-\omega_1\gamma(t-t_k)],$$

$$\eta_k(t)=\eta_{2k}(t)=A_1^{-1}(\omega_1L_1/2L)\times[1+(R_3/\omega_1L_1)^2]^{1/2}a_{2k}\cos(\omega_1t_k+\varphi+\psi),$$

$$n_k(t)=n_{2k}(t)=a_{2k}\,\delta(t-t_k)-(\omega_1L_1/2L)[1+(R_3/\omega_1L_1)]^{1/2}a_{2k}\times\exp[-(\omega_1\gamma/2)(t-t_k)]\sin(\omega_1t-\omega_1t_k-\psi), \quad (2.24)$$

with

$$\tan\psi=R_3/\omega_1L_1.$$

Comparison of like expressions in (2.22), (2.23), and (2.24) shows that, except for numerical differences and differences in phase, the response of the system to an impulse from any one of the noise sources is the same in each case, with only one significant exception: The original impulse from v_2 appears directly in e_g, in addition to creating a system response like that caused by the other noise sources. The importance of this fact, reflected in the expression for n_{2k} in (2.24), will be discussed in greater detail at a later point.

The Laplace transforms of derivatives of delta functions, required to obtain the results shown in (2.23) and (2.24), are readily found according to established techniques (Reference 18). As in (2.22), terms with γ or γ^2 as a factor have been neglected in (2.23) and (2.24).

2.4 Amplitude and Phase Disturbances

When n_k in (2.21) is decomposed into components parallel and orthogonal to e_{g0}, one can write e_g in the form

$$e_g=[A_1+x_k(t)]\cos[\omega_1t+\varphi+\phi_k(t)]. \quad (2.25)$$

For a single impulse from v_3, one finds from (2.22) that

$$\phi_k(t)=\phi_{3k}(t)=-A_1^{-1}\{1+\exp[-(\omega_1\gamma/2)(t-t_k)]\}\times(\omega_1C/2C_2)a_{3k}\cos(\omega_1t_k+\varphi) \quad (2.26)$$

and

$$x_k(t)=x_{3k}(t)=-\{\exp[-\omega_1\gamma(t-t_k)]+\exp[-(\omega_1\gamma/2)(t-t_k)]\}\times(\omega_1C/2C_2)a_{3k}\sin(\omega_1t_k+\varphi). \quad (2.27)$$

These relations show that a single impulse from v_3 in Figure 12–1 causes an instantaneous change in the signal phase, which slowly decays with a time constant $2/\omega_1\gamma$ to half its original value. The amplitude also suffers an instantaneous change which, however, is completely corrected with time by the action of the active element. The magnitude of the respective initial changes in amplitude and phase depend on the phase of the underlying sinusoid at the time of the impulse. The effective time constants involved in (2.26) and in (2.27) are sensibly the same in the oscillator model treated here, which is representative of self-limiting oscillators. In AGC and related-type oscillators, however, the amplitude disturbances are artifically corrected in a very

much shorter time, without thereby affecting the phase of the signal in first order (Reference 19). Even in this case, then, the time constant in (2.26) remains determined by the nonlinearity in the active device according to (2.10) and (2.4), while the exponential functions in (2.27) should be replaced by $\exp[-(t-t_k)/T]$ if T is the time constant of the AGC loop or its equivalent.

The exponentially decaying term in (2.26), or a term similar to it, must be expected to exist whenever electrical pulses or impulses are applied to the oscillator, such as when voltage variable capacitors are used for modulation purposes. While the present analysis does not extend to these cases, it must be expected further that the phenomenon responsible for the existence of the exponentially decaying term in (2.26) will act to limit the modulation rate attainable in crystal oscillators by means of voltage variable capacitors.

To reduce the length of time over which the effects of any particular disturbance are noticeable in the signal phase, it is necessary for γ to be as large as possible; because of (2.10) this means that both β, the nonlinearity in the active device, and A_1, the signal amplitude, should be large. This point will be further discussed in Section 3.3.

The expressions corresponding to (2.26) and (2.27) for a single impulse from i_i in Figure 12–1 can be obtained from (2.23) by the same procedure as above; those for an impulse from v_1 are given by (2.26) and (2.27) with a_{1k} substituted for a_{3k}.

The components of $u(t)$ in response to a single noise impulse from v_1, v_3, or i_s in Figure 12–1 are infinitesimal; and there is no question about the equivalence of (2.21) and (2.25). The response of the oscillator to an impulse from v_2, however, contains the original impulse as seen from $n_{2k}(t)$ in (2.24). Since the impulse—by definition—is an infinitely large signal, the procedure used before can be applied only to the second part of $n_{2k}(t)$. Until the signal e_q has been acted on by the filter in the output amplifier, the impulse in $n_{2k}(t)$ must be carried as an additive component to (2.25).

To facilitate the following developments, $\phi_k(t)$ in (2.25) will be represented as

$$\phi_k(t) = \eta_k + \vartheta_k(t), \tag{2.28}$$

whereby η_k represents the permanent shift in the signal phase discussed in Section 2.3 and $\vartheta_k(t)$ the exponentially decaying part of the phase disturbance (i.e., the out-of-phase component of the impulse response of the oscillator acting as a narrow-band filter). The output signal from the oscillator, disturbed by a single impulse from any one of the noise sources, becomes

$$e_q = [A_1 + x_k(t)]\cos[\omega_1 t + \varphi + \eta_k + \theta_k(t)] + a_{2k}\,\delta(t-t_k). \tag{2.29}$$

2.5 The Response to White Noise

The response of the oscillator to white noise is obtained by linear superposition of the effects of all the individual impulses in (1.12). The undisturbed signal e_{q0} used in deriving the response to the impulse at time t_k was assumed previously to include all permanent effects of the impulses prior to t_k. Hence, the phase angle φ in (2.1) and consequently in (2.29) is of the form

$$\varphi = \sum_{l}^{k-1} \eta_{kl}$$

and need not be carried farther. The oscillator signal, as disturbed by the action of the white-noise sources in Figure 21–1, becomes

$$e_q = [A_1 + x(t)]\cos[\omega_1 t + \eta(t) + \vartheta(t)] + v_2(t), \tag{2.30}$$

with

$$\begin{aligned} x(t) &= x_1(t) + x_2(t) + x_3(t) + x_s(t), \\ \eta(t) &= \eta_1(t) + \eta_2(t) + \eta_3(t) + \eta_s(t), \\ \vartheta(t) &= \vartheta_1(t) + \vartheta_2(t) + \vartheta_3(t) + \vartheta_s(t), \end{aligned} \tag{2.31}$$

when—for $x_{jk}(t)$, $\eta_{jk}(t)$, and $\vartheta_{jk}(t)$ in

$$x_j(t) = \sum_k x_{jk}(t), \qquad \eta_j(t) = \sum_k \eta_{jk}(t), \qquad \vartheta_j(t) = \sum_k \vartheta_{jk}(t) \tag{2.32}$$

—the appropriate expressions following from (2.22), (2.23), and (2.24) according to the procedure described in Section 2.4 are used. The summations in (2.32) extend over all values of k for which $t_k \leq t$; and $j = 1, 2, 3, s$.

The process indicated by (2.31) and (2.32) has considerable merit conceptually. The individual impulses in (1.12) are caused by the

elemental phenomena involved in the transport of electrical charges and, though exceedingly numerous, are extremely weak. The addition of the effects of any one of these impulses to x, η, and ϑ in (2.31) changes these quantities by only infinitesimal amounts. There never can be any doubt that the linear perturbation equation (2.9) applies and that the out-of-phase components of $u_k(t)$ can be taken into the argument of the sinousoid.

Nevertheless, the statistical properties of e_g are evaluated more readily when the sums in (1.12) are replaced by continuous functions. Without discussion of the essentially philosophical questions involved thereby (Reference 20), it will be assumed from here on that the output of the noise sources in Figure 12–1 is

$$i_s = B_s(t),$$
$$v_r = B_r(t) \qquad (r=1, 2, 3), \tag{2.33}$$

whereby each $B(t)$ is Gaussian, has zero mean, and is delta-correlated:

$$\langle B_j \rangle = 0,$$
$$\langle B_j(t_1) B_j(t_2) \rangle = B_j^2\, \delta(t_2 - t_1),$$
$$\langle B_i(t_1) B_j(t_2) \rangle = 0, \qquad (i \neq j). \tag{2.34}$$

The a_k's in (2.22) to (2.24) now are to be replaced by

$$a_{jk} = B_j(t)\, dt, \tag{2.35}$$

and the sums in (2.23) become integrals.

The final solution to the problem of determining the explicit form of the signal in the oscillator shown in Figure 12–1, where v_1, v_2, v_3, and i_s are white-noise sources, can now be stated as follows: The signal at the output of the feedback network is given by (2.30), with (2.31) and

$$x_2(t) = (\omega_1 L_1/2L)[1+(R_3/\omega_1 L_1)^2]^{1/2} \int_0^t B_2(\xi)\, \sin[\omega_1\xi + \eta(\xi) + \psi] \times \{\exp[-\omega_1\gamma(t-\xi)] + \exp[-(\omega_1\gamma/2)(t-\xi)]\}\, d\xi,$$

$$\eta_2(t) = A_1^{-1}(\omega_1 L_1/2L)[1+(R_3/\omega_1 L_1)^2]^{1/2} \int_0^t B_2(\xi)\, \cos[\omega_1\xi + \eta(\xi) + \psi]\, d\xi,$$

$$\vartheta_2(t) = A_1^{-1}(\omega_1 L_1/2L)[1+(R_3/\omega_1 L_1)^2]^{1/2} \int_0^t B_2(\xi)\, \cos[\omega_1\xi + \eta(\xi) + \psi] \exp[-(\omega_1\gamma/2)(t-\xi)]\, d\xi; \tag{2.36}$$

$$x_3(t) = -(\omega_1 C/2C_2) \int_0^t B_3(\xi)\, \sin[\omega_1\xi + \eta(\xi)] \{\exp[-\omega_1\gamma(t-\xi)] + \exp[-(\omega_1\gamma/2)(t-\xi)]\}\, d\xi,$$

$$\eta_2(t) = -A_1^{-1}(\omega_1 C/2C_2) \int_0^t B_3(\xi)\, \cos[\omega_1\xi + \eta(\xi)]\, d\xi,$$

$$\vartheta_3(t) = -A_1^{-1}(\omega_1 C/2C_2) \int_0^t B_3(\xi)\, \cos[\omega_1\xi + \eta(\xi)] \exp[-(\omega_1\gamma/2)(t-\xi)]\, d\xi; \tag{2.37}$$

$$x_s(t) = (2C_2)^{-1}(L_1/L) \int_0^t B_s(\xi)\, \cos[\omega_1\xi + \eta(\xi)] \{\exp[-\omega_1\gamma(t-\xi)] + \exp[-(\omega_1\gamma/2)(t-\xi)]\}\, d\xi,$$

$$\eta_s(t) = -A_1^{-1}(2C_2)^{-1}(L_1/L) \int_0^t B_s(\xi)\, \sin[\omega_1\xi + \eta(\xi)]\, d\xi,$$

$$\vartheta_s(t) = -A_1^{-1}(2C_2)^{-1}(L_1/L) \int_0^t B_s(\xi)\, \sin[\omega_1\xi + \eta(\xi)] \exp[-(\omega_1\gamma/2)(t-\xi)]\, d\xi. \tag{2.38}$$

The expressions for x_1, η_1, and ϑ_1 are identical to those for x_3, η_3, and ϑ_3, respectively, and are obtained if only $B_3(\xi)$ is replaced by $B_1(\xi)$. It will be observed that the integrals for $n(t)$ are of the type familiar from the theory of the Brownian motion (Reference 20), indicating that the phase of the carrier executes a random walk.

Of the various assumptions which had to be made in deriving the above expressions as an approximation to the solution of (1.3), the one regarding the absence of harmonic components—particularly of the third harmonic in the undisturbed signal—is considered to be the most serious. In general, it must be expected to limit the validity of the result to oscillators operating at low signal levels. Nevertheless, the expressions do give a detailed description of the effects of noise on the oscillator signal, which becomes increasingly more accurate as the harmonic content is reduced. Since no restrictions had to be placed on the magnitudes of L_3 and C_3 in Figure 12–1, the above approximation to e_g applies equally to crystal oscillators and L−C oscillators.

3. THE POWER SPECTRAL DENSITY OF THE SIGNAL

3.1 Proof of Ergodicity

With the oscillator signal available in explicit form, its statistical properties can be evaluated.

The properties of $\eta(t)$ in (2.30), with (2.36) to (2.38), must be determined first. According to (2.34), the B_j's have zero mean and are not correlated to one another. Hence, the mean and variance of $\eta(t)$ are

$$\langle \eta(t) \rangle = 0, \tag{3.1}$$

$$\sigma^2 = \langle [\eta(t)]^2 \rangle = \sum_j \langle [\eta_j(t)]^2 \rangle, \quad (j = 1, 2, 3, s). \tag{3.2}$$

For example, with the aid of Fubini's integration theorem and considering that $B_3(t)$ and $\cos[\omega_1 t + \eta(t)]$ are independent, one finds the variance of $\eta_3(t)$ as

$$\begin{aligned}
\sigma_3^2 &= \langle [\eta_3(t)]^2 \rangle \\
&= (1/A_1^2)(\omega_1 C/2C_2)^2 \left\langle \int_0^t B_3(u) \cos[\omega_1 u + \eta(u)]\, du \int_0^t B_3(v) \cos[\omega_1 v + \eta(v)]\, dv \right\rangle \\
&= (1/A_1^2)(\omega_1 C/2C_2)^2 \int_0^t \int_0^t \langle B_3(u) B_3(v) \rangle \langle \cos[\omega_1 u + \eta(u)] \cos[\omega_1 v + \eta(v)] \rangle\, du\, dv \\
&= (1/A_1^2)(\omega_1 C/2C_2)^2 (B_3^2) \int_0^t \{1 + \langle \cos 2[\omega_1 u + \eta(u)] \rangle\}\, du \\
&= (B_3^2/2A_1^2)(\omega_1 C/2C_2)^2 t + (B_3^2/2A_1^2)(\omega_1 C/2C_2)^2 \int_0^t \langle \cos 2[\omega_1 u + \eta(u)] \rangle\, du.
\end{aligned} \tag{3.3}$$

Even if $\langle \cos 2(\omega_1 u + \eta(u)) \rangle$ is not zero for all u in $0 \leq u \leq t$, the integral always remains finite while the first term goes beyond all bounds when $t \to \infty$. Similar expressions are obtained for σ_1^2, σ_2^2, and σ_s^2. It is apparent that, if an ensemble of oscillators of identical construction is observed at a very long time after they were turned on (i.e., at $t = t_0$ with $t_0 \to \infty$), the phase angles $\eta(t_0)$ are found to have no preferred value; they are evenly distributed between zero and 2π.

At very large values of t, the oscillator signal $e_g(t)$ in (2.30) is seen to represent a stationary ergodic random process (Reference 22); and ensemble averages can be used throughout to determine its statistical properties.

3.2 The Autocorrelation Function

The power spectral density $G_{ee}(f)$ will be computed from the autocorrelation function $\Gamma_{ee}(\tau)$ of e_g according to the well-known relations (Reference 23)

$$G_{ee}(f) = 4\int_0^\infty \Gamma_{ee}(\tau)\cos\omega\tau\, d\tau, \tag{3.4}$$

$$\Gamma_{ee}(\tau) = \langle e_g(t)e_g(t-\tau)\rangle. \tag{3.5}$$

It is convenient to consider e_g in (2.30) as the sum of four components:

$$\begin{aligned} e_g &= E_C + E_A + E_\vartheta + E_N \\ &= A_1\cos[\omega_1 t+\eta(t)]+x(t)\cos[\omega_1 t+\eta(t)] \\ &\quad -A_1\vartheta(t)\sin[\omega_1 t+\eta(t)]+B_2(t), \end{aligned} \tag{3.6}$$

whereby E_C represents the carrier and E_A the amplitude disturbances. E_ϑ are the out-of-phase disturbances of the oscillator action as a narrow-band noise filter; and E_N is the white noise from v_2, the source in the oscillator output. The autocorrelation function of e_g is then

$$\Gamma_{ee}(\tau) = \Gamma_{CC}(\tau)+\Gamma_{AA}(\tau)+\Gamma_{\vartheta\vartheta}(\tau)+\Gamma_{NN}(\tau). \tag{3.7}$$

All cross correlations are zero.

The determination of the various terms in (3.7) is, if reasonably straightforward, rather laborious and, except for Γ_{CC}, which will be treated separately, requires repeated application of the general procedure used in (3.3). In some cases the required operations are more readily performed when the transformation

$$\int_0^t g(\xi)h(t-\xi)\, d\xi = \int_0^\infty g(t-\xi)h(\xi)\, d\xi \tag{3.8}$$

is used in the expressions for $x(t)$ and $\vartheta(t)$ in (2.31), with (2.36) through (2.38). Only the results of these calculations will be given here:*

$$\begin{aligned} \Gamma_{AA} &= (\omega_1\kappa^2/\gamma)\{\tfrac{7}{24}\exp(-\omega_1\gamma\tau) \\ &\quad +\tfrac{5}{12}\exp[-(\omega_1\gamma/2)\tau]\}\cos\omega_1\tau, \end{aligned} \tag{3.9}$$

$$\Gamma_{\vartheta\vartheta} = (\omega_1\kappa^2/4\gamma)\exp[-(\omega_1\gamma/2)\tau]\cos\omega_1\tau,$$

$$\Gamma_{NN} = B_2^2\,\delta(\tau),$$

$$\begin{aligned} \kappa^2 &= \frac{1}{4}\left(\frac{L_1}{L}\right)^2\left[\left(\frac{\omega_L}{\omega_1}\right)^2(B_1^2+B_3^2)\right. \\ &\quad \left.+\left(1+\frac{R_3^2}{\omega_1^2L_1^2}\right)B_2^2+\left(\frac{1}{\omega_1C_2}\right)^2B_s^2\right], \end{aligned} \tag{3.10}$$

$$\omega_L^2 = (1/L_1C_2). \tag{3.11}$$

The autocorrelation function of E_C is (Reference 4) with, $t_2-t_1=\tau$,

$$\begin{aligned} \Gamma_{CC}(\tau) &= (A_1^2/2)\ \langle\cos[\eta(t_2)-\eta(t_1)]\rangle\cos\omega_1\tau \\ &\quad -(A_1^2/2)\ \langle\sin[\eta(t_2)-\eta(t_1)]\rangle\sin\omega_1\tau. \end{aligned} \tag{3.12}$$

The statistical average of a continuous random variable such as $\cos[\eta(t_2)-\eta(t_1)]$ is given by (Reference 24)

$$\langle\cos[\eta(t_2)-\eta(t_1)]\rangle = \langle\cos\phi\rangle = \int_{-\infty}^{+\infty} p(\phi)\cos\phi\ \alpha\phi, \tag{3.13}$$

whereby $p(\phi)$ is the probability density function of ϕ. It was assumed previously that the $B_j(t)$'s are Gaussian; hence $\eta(t_2)-\eta(t_1)$ is Gaussian and, if σ^2 is the variance of ϕ,

$$p(\phi) = [(2\pi)^{1/2}\sigma]^{-1}\exp(-\phi^2/2\sigma^2). \tag{3.14}$$

Hence,

$$\langle\cos[\eta(t_2)-\eta(t_1)]\rangle = \exp(-\sigma^2/2). \tag{3.15}$$

---

* In the calculations leading to (3.9) it is assumed that $[\eta(t_2)-\eta(t_1)]\approx 0$ because $\eta(t)$ for each oscillator in the ensemble changes only a very slight amount during the time intervals (t_2-t_1) of significance here. Since all noise components in $x(t)$ and $\vartheta(t)$ have lost their correlation when (t_2-t_1) becomes larger than $1/\omega_1\gamma$, this assumption is justified. It is further assumed that γ is negligibly small compared with 1. Terms of the form $(1/\omega_1)\cos\omega_1(t_2\pm t_1)$ and $(1/\omega_1)\sin\omega_1(t_2\pm t_1)$ are not considered next to $(1/\omega_1\gamma)\cos\omega_1(t_2-t_1)$. Therefore averages of the form $\langle\cos[\omega_1t_1+\eta(t_1)]\rangle$ and $\langle\sin[\omega_1t_1+\eta(t_1)]\rangle$ are zero when t_1 is very large because, as discussed in the text, $\eta(t_1)$ is then evenly distributed between zero and 2π.

The integral (3.13) for $\sin\phi$, and hence the second term in (3.12), is zero; and it remains to determine the variance σ^2 of $\eta(t_2)-\eta(t_1)$. From (2.37) one finds that, for example,

$$\eta_3(t_2)-\eta_3(t_1)=\int_{t_1}^{t_2} B_3(\xi)\,\cos[\omega_1\xi+\eta(\xi)]\,d\xi$$

$$=\int_0^{\tau} B_3(\xi)\,\cos[\omega_1\xi+\eta(\xi)]\,d\xi$$

$$=\eta_3(\tau), \tag{3.16}$$

whereby $\eta_3(\tau)$ differs from $\eta_3(t)$ [dealt with in (3.3)] by the fact that now the integration interval involves only very large values of t (except when $\tau\longrightarrow\infty$ which is of no consequence). It follows that the term $\langle\cos 2[\omega_1 u+\eta(u)]\rangle$ in (3.3) is now zero; and with similar considerations for the other η_j's in (2.31) one obtains the variance σ^2 in the form:

$$\sigma^2=(\omega_1^2\kappa^2/2A_1^2)\tau, \tag{3.17}$$

with κ^2 given by (3.10).

The autocorrelation function of E_C becomes with (3.12), (3.15), and (3.17)

$$\Gamma_{CC}(\tau)=(A_1^2/2)\,\exp[-(\omega_1^2\kappa^2/4A_1^2)\tau]\cos\omega_1\tau. \tag{3.18}$$

The relations (3.9) and (3.18) with $\tau=0$ can be used to determine the total average power (Reference 25) contained in each component of e_0 as given by (3.6). The average power in the carrier is $A_1^2/2$. A comparison of $\Gamma_{AA}(\tau)$ and $\Gamma_{\vartheta\vartheta}(\tau)$ shows that the noise power contained in the in-phase (amplitude) components of the disturbances, given by E_A in (3.6), is nearly three times as much as that contained in E_ϑ. However, less than one-half of the first term of Γ_{AA} remains if the action of the oscillator as a narrow-band noise filter is disregarded.

It is interesting to compute the autocorrelation function of the signal component $n(t)$ due to the action of the oscillator as a narrow-band noise filter alone. From the representation of the signal shown in (2.21), it follows that

$$n(t)=n_1(t)+n_2(t)+n_3(t)+n_s(t), \tag{2.31a}$$

with

$$n_j(t)=\sum_k n_{jk}(t), \qquad (j=1, 2, 3, s), \tag{2.32a}$$

whereby the $n_{jk}(t)$'s are given in (2.22) to (2.24), disregarding for now the term $a_{2k}\,\delta(t-t_k)$ in n_{2k}. After the transition to the integral as in Section 2.5, one can obtain the autocorrelation function $\Gamma_{nn}(\tau)$ of $n(t)$ as

$$\Gamma_{nn}(\tau)=(\omega_1\kappa^2/2\gamma)\,\exp[-(\omega_1\gamma/2)\tau]\cos\omega_1\tau, \tag{3.9a}$$

with κ^2 defined in (3.10).

If one were to impose the requirement that the noise filter action yield an average power of $A_1^2/2$, a value of

$$\gamma=\omega_1\kappa^2/A_1^2 \tag{3.19}$$

would be required. Although $\Gamma_{CC}(\tau)$ and $\Gamma_{nn}(\tau)$ would become formally identical, it follows from the origin of $\Gamma_{CC}(\tau)$ and $\Gamma_{nn}(\tau)$ that the two signal processes are certainly not identical. The form of $\Gamma_{CC}(\tau)$ is due to cumulative random phase disturbances only—the amplitude of the carrier remains constant at all times—while the output of a narrow-band noise filter varies, both in amplitude and phase, with both disturbances exponential in character.

The fact that the autocorrelation functions are identical for the two different signal processes proves that, without additional assumptions, it is not possible to derive the properties of a signal if only its autocorrelation function, or its power spectral density function, are given.

The magnitude of γ demanded by (3.19) is in the order of 5×10^{-21}, with values for κ^2, A_1^2, and ω_1 representative of a typical precision crystal oscillator. Considering (2.10a) and the development of Section 2.2, it readily is realized that a mode of operation where the entire output is due to the noise filter action will not be encountered in crystal oscillators, regardless of their design.

3.3 The Spectrum

Proceeding now to the power spectral density of e_0, one finds $G_{ee}(f)$ from (3.9) and (3.18),

with (3.4) and (3.7), as the sum of the following components:

$$G_{CC}(f)=\frac{4A_1^4/\omega_1^2\kappa^2}{1+(4A_1^2/\omega_1\kappa^2)^2[1-(\omega/\omega_1)]^2},$$

$$G_{AA}(f)=\frac{\frac{7}{12}(\kappa^2/\gamma^2)}{1+(1/\gamma)^2[1-(\omega/\omega_1)]^2}+\frac{\frac{5}{3}(\kappa^2/\gamma^2)}{1+(2/\gamma)^2[1-(\omega/\omega_1)]^2},$$

$$G_{\vartheta\vartheta}(f)=\frac{\kappa^2/\gamma^2}{1+(2/\gamma)^2[1-(\omega/\omega_1)]^2},$$

$$G_{NN}(f)=4B_2^2. \tag{3.20}$$

The relations (3.20) show the contributions of the individual signal components as given by (3.6) to the power spectral density and are useful for more detailed work. To simplify the following discussion, however, the sum of G_{AA} and $G_{\vartheta\vartheta}$ will be replaced by a single peak of bandwidth $(\gamma/1.6)$. $G_{ee}(f)$ becomes approximately

$$G_{ee}(f)=\frac{4A_1^4/\omega_1^2\kappa^2}{1+(4A_1^2/\omega_1\kappa^2)^2[1-(\omega/\omega_1)]^2}+\frac{\frac{13}{4}(\kappa^2/\gamma^2)}{1+(1.6/\gamma)^2[1-(\omega/\omega_1)]^2}+4B_2^2, \tag{3.21}$$

whereby κ^2 is still given by (3.10). If, in addition $LC=L_1C_2$ is assumed and (2.10a) is used, one finds

$$\frac{\kappa^2}{\gamma^2}=\frac{4}{9}\frac{\omega_1^2C_2^2}{\beta^2A_1^4}\left[(B_1^2+B_3^2)+\left(1+\frac{R_3^2}{\omega_1^2L_1^2}\right)B_2^2+\frac{B_s^2}{\omega_1^2C_2^2}\right]. \tag{3.22}$$

The expression (3.21), with (3.10) and (3.22), shows that the power spectral density of the oscillator output consists of three distinct parts: the carrier; a spectral response mainly due to the action of the oscillator as a narrow-band noise filter; and a white-noise component which, in all practical cases, is further acted on by the bandpass characteristics of the amplifier stage.

As a numerical example, let

$$\omega_1L_1=100\ \Omega,\quad \omega_1=2\pi5\times10^6,\quad g_{m0}=\tfrac{1}{20},$$
$$R_3=100\ \Omega,\quad L_1/L=10^{-6},\quad \beta=10,$$
$$1/\omega_1C_2=20\ \Omega,\quad A_1^2/2=4\times10^{-5}V^2,\quad \gamma=1.2\times10^{-8},$$
$$P_3=(A_1^2/2)\,R_3(\omega_1C_2)^2=10^{-5}\text{ watt}. \tag{3.23}$$

The parameters for the active device are typical for a 2N2808 transistor; the values for R_3 and L_1/L could apply to a precision crystal unit. The power spectral density of Johnson noise is $4kTR$ and that of shot noise in a transistor $2kTg_m$; hence because of (2.28), (3.4), and (3.5)

$$B_j^2=kTR_j,\qquad (j=1,\,2,\,3),$$
$$B_s^2=\tfrac{1}{2}kTg_m. \tag{3.24}$$

The resistive components R_1 and R_2 have not been considered so far because, with $R_3=100\ \Omega$, their effect on the results does not extend significantly beyond their action as noise generators. Rather pessimistic assumptions (Reference 26) about the effective values of R_1 and R_2 lead to 10 ohms each. With the above values, and $kT=5\times10^{-21}$ watt-sec, the power spectral density of the oscillator signal—in the form (3.21)—becomes approximately

$$G_{ee}(f)=\frac{1.4\times10^8}{1+[2/(3.5\times10^{-20})]^2[1-(\omega/\omega_1)]^2}+\frac{3.8\times10^{-15}}{1+[2/(1.5\times10^{-8})]^2[1-(\omega/\omega_1)]^2}+2\times10^{-20}. \tag{3.25}$$

A sketch of the three components of the spectrum is shown in Figure 12–3. The half-power bandwidth of the carrier is $(\Delta\omega/\omega_1)=3.5\times10^{-20}$, and that of the noise response is $(\Delta\omega/\omega_1)=1.5\times10^{-8}$. The width of the carrier spectrum, when its magnitude is 3.8×10^{-15}, is 2.2×10^{-9} or about 15 percent of the half-width of the noise response. For frequencies more than about 1 part of 10^9 away from the center of the carrier, the spectrum of e_g soon becomes dominated by the noise response. At a frequency three parts in 10^6 away from the center of the carrier, the tail of the

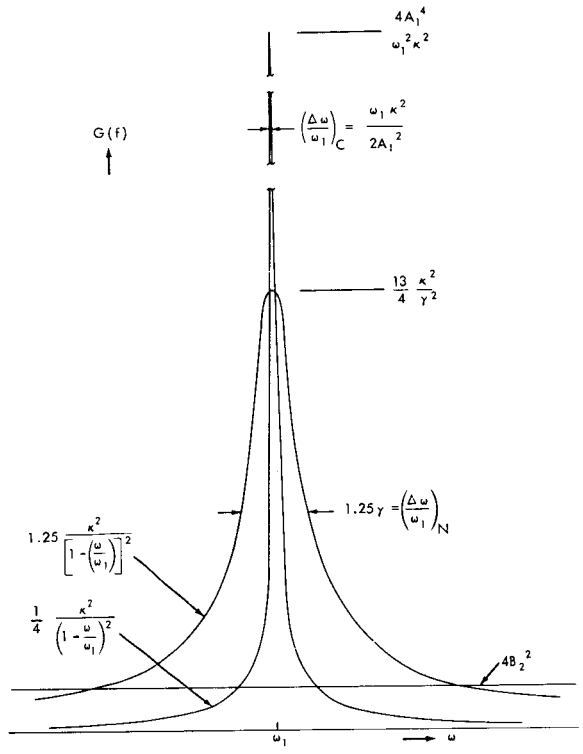

FIGURE 12–3.—The power spectral density of the oscillator output signal e_g is the sum of the three components shown. For a discussion see text.

noise response is equal in magnitude to the white-noise component. For frequencies farther out from the carrier, the white noise—and the manner in which it is modified by the output amplifier—determines the spectrum of the signal.

The dependence of the magnitude and shape of the spectrum of e_g on the various parameters involved can be evaluated from (3.21) together with (2.10), (3.10), and (3.22). The spectrum of the carrier depends prominently on the amplitude A_1, on frequency, on the (L_1/L) ratio, and of course on the strength of the noise sources. Since the peak height of the noise response also depends very strongly on A_1, the most obvious way to reduce the effects of the noise is to operate the oscillator at high power levels. In crystal oscillators the upper limit in A_1 is set by: (1) the amplitude-frequency effect in crystal units which, as a rule of thumb, causes a change of 1 part in 10^6 in resonance frequency per 1 mw change in the crystal drive; and (2) the increase in harmonic content in the signal and the possible serious deterioration of the noise spectrum due to interaction of these harmonics and the crystal resonances at every odd harmonic of the fundamental frequency (Reference 27). The amplitude-frequency effect makes an increasingly tighter control of the drive level necessary at higher amplitudes if the carrier frequency should remain stable.

The noise response given by the second term in (3.21) depends on frequency only via the admittance of C_2. Furthermore, it is noted that all noise response curves, regardless of the value of γ, fall inside the curves described by $[(13/4\times1.6^2)\kappa^2]/[1-(\omega/\omega_1)]^2$ and follow these curves for frequency differences $(\omega-\omega_1)$ much larger than their respective half bandwidths. This behavior is sketched in Figure 12–4. For a given strength of the noise sources, the form of the limiting curves can be changed only by a variation in (L_1/L). The peak values of the noise response depend according to (3.22), in-

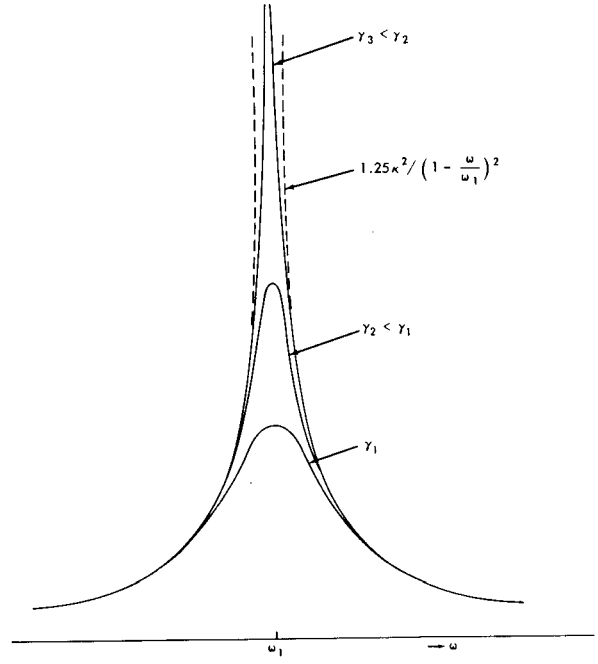

FIGURE 12–4.—The relationship between peak value and half power bandwidth of the power spectral density curves is most easily visualized with the aid of the limiting curves. Illustration applies to the noise response.

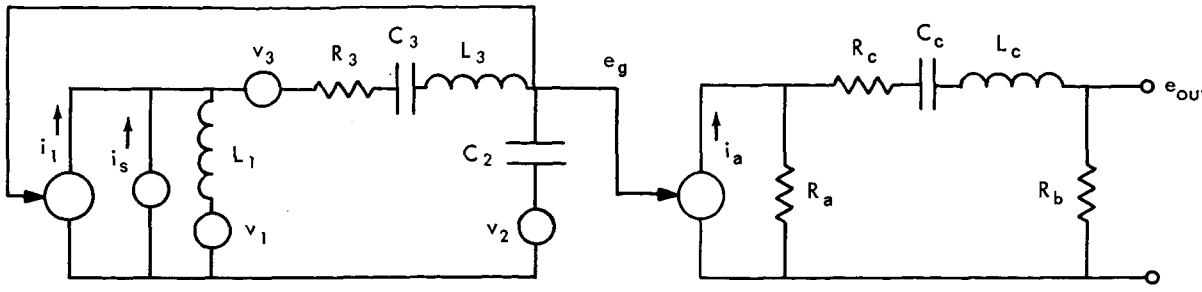

FIGURE 12–5.—Model of oscillator with output amplifier. The filter in the output amplifier serves primarily to shape the white noise component in e_g, which stems from v_2. Its effect on the carrier and on the noise response of the oscillator loop is negligible in the nearly harmonic case, i.e., when γ is small.

versely on $(\beta A_1^2)^2$, which clearly indicates that—especially at low values of A_1—a large β (i.e., a large nonlinearity in the active device) is desirable.

The fact that the limiting curves are independent of γ provides a very simple means for visualizing the properties of the spectral density curves. If, as in Figure 12–4, the limiting curves are drawn, it is necessary only to measure off the peak value of the response at $\omega=\omega_1$; the spectral curve can then be sketched in between the limiting curves. The half-power bandwidth of the spectral curve is only slightly less than the width of the limiting curves at the respective half-power points.

3.4 Effects of the Output Amplifier

To describe the spectrum of the output signal completely, it is necessary to include the effects of the amplifier following the oscillator stage into the analysis. As a simple example consider the circuit in Figure 12–5. The oscillator stage is the same as shown in Figure 12–1. The signal e_g enters a linear active device whose output current i_2 is assumed to be

$$i_2=g_{m2}e_g. \tag{3.26}$$

The output voltage from the filter section is then

$$e_{out}=g_{m2}e_g\frac{R_aR_b}{R_a+R_b+R_c+sL_c+(sC_c)^{-1}}. \tag{3.27}$$

When

$$Q_c=\gamma_c^{-1}=\frac{\omega_1L_c}{R_a+R_b+R_c}\ll\gamma^{-1}, \tag{3.28}$$

with γ defined in (2.10), and

$$L_cC_c=1/\omega_1^2,$$
$$g_{m2}[R_aR_b/(R_a+R_b+R_c)]=1 \tag{3.29}$$

are assumed,* only the white-noise component in e_g is affected appreciably by the filter stage; the other components are passed essentially unchanged. All equations and formulas derived in the preceding sections for e_g apply equally for e_{out} with the following exceptions:

Replace $a_{2k}\,\delta(t-t_k)$ in $\begin{cases}(2.24)\\(2.29)\end{cases}$ by $a_{2k}(\omega_1/Q_c)\exp[-(\omega_1\gamma_c/2)(t-t_k)]\cos\omega_1(t-t_k)$,

Replace $\begin{cases}v_2\\B_2\end{cases}$ in $\begin{cases}(2.30)\\(3.6)\end{cases}$ by $(\omega_1/Q_c)\int_0^t B_2(\xi)\exp[-(\omega_1\gamma_c/2)(t-\xi)]\cos\omega_1(t-\xi)\,d\xi$,

Replace $B_2^2\,\delta(\tau)$ in (3.9) by $(\omega_1/Q_c)(B_2^2/2)[1+Q_c(R_3/\omega_1L)]\exp[-(\omega_1\gamma_c/2)\tau]\cos\omega_1\tau$; (3.30)

* The second requirement in (3.29) obviously was imposed only to avoid a constant for the gain of the amplifier to appear in each one of the expressions.

and, furthermore, replace $4B_2^2$ in (3.20) and in (3.21) by

$$4B_2^2 \rightarrow \frac{2B_2^2[1+Q_c(R_3/\omega_1 L)]}{1+(2/\gamma_c)^2[1-(\omega/\omega_1)]^2}. \quad (3.31)$$

The cross correlations and cross-power spectra of E_N with E_A and E_ϑ are now not zero, but the ones not considered in (3.31) are negligibly small when $Q_c \ll 1/\gamma$; and the above substitutions are fully adequate in this case.

Since the filter removes the delta function from e_y in (2.21), it is obvious that the development of Section 2.4 can now be applied to all of $n_{2k}(t)$ in (2.29) [i.e., the response of the output filter to the white noise from v_2 also can be decomposed into components parallel and normal to e_{y0} and appropriately included into $x(t)$ and $\vartheta(t)$].

The replacement term (3.31) controls the power spectral density of e_{out} at frequencies far away from the carrier, and specifies the magnitude of $Q_c = 1/\gamma_c$ required to suppress the spectrum at these frequencies below a certain level (Reference 28). It is obvious that more effective filter configurations than the one considered here for demonstration purposes could be used to this end.

4. THE SHORT-TERM FREQUENCY STABILITY

The frequency of a periodic of quasi-periodic signal can be obtained by integrating the phase θ over a time τ and dividing the result by τ:

$$\omega_\tau = \tau^{-1}\int_{t-\tau}^{t} d\theta = [\theta(t)-\theta(t-\tau)]/\tau. \quad (4.1)$$

In general, ω_τ is a function of the time t at which the integration is carried out. When $\theta(t)$ can be assumed to have the form

$$\theta(t) = \omega_1 t + \phi(t), \quad (4.2)$$

whereby ω_1 is a constant and $\phi(t)$ a random variable of zero mean, the short-term frequency stability of the signal for integration times of τ seconds can be defined as the square root of

$$\langle 4[(\omega_\tau-\omega_1)^2/\omega_1^2]\rangle = (4/\omega_1^2\tau^2)\{\langle[\phi(t)]^2\rangle + \langle[\phi(t-\tau)]^2\rangle - 2\langle\phi(t)\phi(t-\tau)\rangle\}; \quad (4.3)$$

that is,

$$S(\tau) = 2[\langle(\omega_\tau-\omega_1)^2/\omega_1^2\rangle]^{1/2}. \quad (4.4)$$

While ω_τ and $S(\tau)$ are readily evaluated when $\phi(t)$ is known, the reverse process, that is, the determination of the characteristics of the signal phase from the properties of ω_τ can only be carried out in a very restrictive sense.

With the output signal of the oscillator derived explicitly in the preceding sections, its short-term frequency stability can be computed. In the following, the effects of the output amplifier on the signal e_y as discussed at the close of Section 3 will be included in the analysis. The output signal e_{out} differs from the e_y dealt with earlier only by the terms shown in (3.30); and these terms will be considered used from here on, whenever the relations pertaining to e_y are cited in reference to e_{out}.

For the present purpose, the output signal e_{out} is required in the form

$$e_{out} = [A_1 + x(t)]\cos[\omega_1 t + \phi(t)], \quad (4.5)$$

with

$$\phi(t) = \phi_1(t) + \phi_2(t) + \phi_3(t) + \phi_s(t). \quad (4.6)$$

Except for $\phi_2(t)$, the terms in (4.6) are already known from Sections 2.4 and 2.5. Applying now the procedure used there to (2.24) with (3.30), one finds for $\phi_2(t)$ the expression

$$\phi_2(t) = A_1^{-1}(\omega_1 L_1/2L)[1+(R_3/\omega_1 L_1)^2]^{1/2}\int_0^t \{1+\exp[-(\omega_1\gamma/2)(t-\xi)]\}B_2(\xi)\cos[\omega_1\xi+\eta(\xi)+\psi]\,d\xi$$

$$-A_1^{-1}(\omega_1/Q_c)\int_0^t B_2(\xi)\exp[-(\omega_1\gamma_c/2)(t-\xi)]\sin[\omega_1\xi+\eta(\xi)]\,d\xi. \quad (4.7)$$

The operations on $\phi(t)$ required for (4.3) are of the type

$$\langle \phi(t_1)\phi(t_2) \rangle$$

and, because of (2.34), can be carried out separately on the each of the four components in (4.6).

The process used here to find $S^2(\tau)$ will be indicated below with $\phi_3(t)$ as an example. When $t_1 \leq t_2$ but $t_1 \to \infty$,*

$$\langle \phi_3(t_1)\phi_3(t_2) \rangle = \frac{1}{A_1^2}\left(\frac{\omega_1 C}{2C_2}\right)^2 \int_0^{t_1}\int_0^{t_2} \langle B_3(u)B_3(v)\, \cos[\omega_1 u+\eta(u)]\cos[\omega_1 v+\eta(v)]\rangle \times\{1+\exp[-(\omega_1\gamma/2)(t_1-u)]\}\{1+\exp[-(\omega_1\gamma/2)(t_2-v)]\}\, du\, dv$$

$$= \frac{B_3^2}{2A_1^2}\left(\frac{\omega_1 C}{2C_2}\right)^2 \int_0^{t_1} \{1+\exp[-(\omega_1\gamma/2)(t_1-u)]+\exp[-(\omega_1\gamma/2)(t_2-u)] +\exp[-(\omega_1\gamma/2)(t_1+t_2-2u)]\}\, du$$

$$= \frac{B_3^2}{2A_1^2}\left(\frac{\omega_1 C}{2C_2}\right)^2 \left\{t_1+\frac{2}{\omega_1\gamma}+\frac{3}{\omega_1\gamma}\exp[-(\omega_1\gamma/2)(t_2-t_1)]\right\}. \tag{4.8}$$

Hence, with $t_2-t_1=\tau$,

$$S_3^2(\tau) = (B_3^2/2A_1^2)(C/C_2)^2(1/\tau^2)(\tau+(6/\omega_1\gamma)\{1-\exp[-(\omega_1\gamma/2)/\tau]\}). \tag{4.9}$$

The first term in (4.9) is the familiar result (Reference 1) obtained when only the cumulative effect of the permanent phase shifts caused by the individual noise impulses is considered, while the second term is due to the action of the oscillator as a narrow-band noise filter.

The other components of $\phi(t)$ in (4.6) can be treated in a similar manner, and one finds the complete autocorrelation function of $\phi(t)$ in the form

$$\langle \phi(t)\phi(t-\tau) \rangle = (\omega_1^2\kappa^2/2A_1^2)\{t-\tau+(2/\omega_1\gamma)+(3/\omega_1\gamma)\exp[-(\omega_1\gamma/2)\tau]\} +(\omega_1 B_2^2/2A_1^2Q_c)\{\tfrac{1}{2}Q_c(R_3/\omega_1 L)+[1+Q_c(R_3/\omega_1 L)]\exp[-(\omega_1\gamma_c/2)\tau]\}. \tag{4.10}$$

The short-term frequency stability of the signal follows now from (4.3) and (4.4):

$$S^2(\tau) = (2\kappa^2/A_1^2)(\tau^2)^{-1}(\tau+(6/\omega_1\gamma)\{1-\exp[-(\omega_1\gamma/2)\tau]\}) +(4B_2^2/A_1^2Q_c)(\omega_1\tau^2)^{-1}[1+Q_c(R_3/\omega_1 L)]\{1-\exp[-(\omega_1\gamma_c/2)\tau]\}. \tag{4.11}$$

κ^2 in (4.10) and (4.11) is given by (3.10) and γ by (2.10); $Q_c=1/\gamma_c$ is the quality factor of the output filter in Figure 12–4. The conditions (2.20) and (3.28) are assumed satisfied.

The first term in (4.11) has the same character as (4.9). The second term is due to the white-noise component in e_g and depends strongly on the properties of the output filter. Unless the effective quality factor of this filter is very high, it is this second term which dominates the short-term frequency stability of the oscillator signal.

With the numerical values for the various parameters as chosen in Sections 3 and with $Q_c=10$, (4.11) becomes

$$S^2(\tau) = 44\times10^{-28}/\tau^2\{\tau+(3/0.2)[1-\exp(-.2\tau)]\} +8\times10^{-24}/\tau^2[1-\exp(-1.6\times10^6\tau)]. \tag{4.12}$$

A sketch of the two components of $S(\tau)$ as specified by (4.12), is shown in Figure 12–6. It is noted that the contribution of the first component varies with $1/(\tau)^{1/2}$ for integration times τ of less than 1 second and again for τ larger than about 10 seconds with the slope changing to $1/\tau$ during the transition (around $\tau=5$ sec) of the curve from a higher to a lower level.

* If $t=0$ is chosen to be a time long after the ensemble of oscillators is first turned on, $\eta(u)$ is evenly distributed between zero and 2π for any u in the integration interval; and $\langle \cos 2[\omega_1 u+\eta(u)]\rangle = 0$ holds throughout.

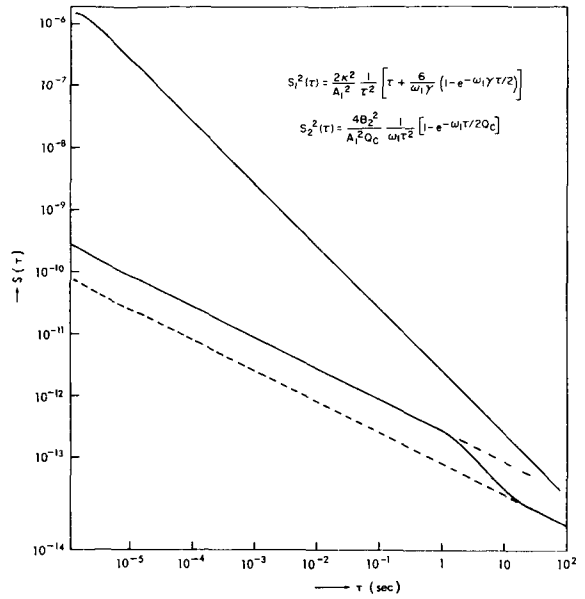

FIGURE 12–6.—The short term frequency stability of a crystal oscillator as a function of integration time τ is the sum of the two solid curves. The lower curve, given by $(S_1^2)^{\frac{1}{2}}$, is due to effects inside the oscillator loop. It includes the effects of the random walk phenomenon in the carrier phase and of the noise response of the oscillator. The upper curve, given by $(S_2^2)^{\frac{1}{2}}$, is due to the additive white noise from the source in the oscillator's output (v_2 in Fig. 5) as acted upon by the filter in the output amplifier. The numerical values of (4.12) apply.

The value of τ at which the transition takes place depends on γ and thus on the nonlinearity of the active device. The magnitude of this component of $S(\tau)$, in an oscillator whose noise generators have a given strength, depends primarily on the (L_1/L) ratio and on the signal amplitude, with some adjustments possible by means of the (ω_L/ω_1) ratio as seen from (3.10).

The contribution to $S(\tau)$ of the second component in (4.12) varies with $1/\tau$ for integration times larger than 1 microsecond; and, at $\tau = 1$ sec, it is greater than that of the first component by more than an order of magnitude. It follows from (4.11) that the significance of this component in relation to the first one can be reduced for a given B_2^2 by increasing the quality factor of the output filter. When Q_c is larger than 10^4, the short-term stability of the signal frequency in this example is essentially given by the first term in (4.12).

An important conclusion can be drawn from the fact that the second term in (4.11) is, as long as $Q_c \ll \omega_1 L/R_3$, independent from the properties of the oscillator feedback network and the active device characteristics. This term stems from the white noise injected directly into e_g by that source, which in effect appears directly at the input of the amplifier. It follows that, as long as the second term in (4.11) is much larger than the first, the short-term frequency stability of the oscillator can be expressed approximately by

$$S(\tau) = \tau^{-1}[2(kTR_2/\tfrac{1}{2}(A_1^2)\omega_1 Q_c)]^{1/2}$$
$$= (2/\omega_1\tau)(V_N^2/V_S^2)^{1/2}, \qquad (4.13)$$

whereby

$$V_N^2\omega_1 B_2^2/2Q_c \qquad (4.14)$$

is the mean-square noise voltage measured at the amplifier output when the crystal unit is disconnected, and V_S^2 the mean-square output voltage when the oscillator is operating normally. The advantage of (4.13) for practical design work is obvious.

To determine the short-term frequency stability of the signal according to (4.3) and (4.4), it was necessary to compute (4.10), the autocorrelation function of the phase disturbances. This autocorrelation function could, of course, be used with (3.4) to determine the power spectral density of the signal phase. The resulting function, however, is simply related to the short-term frequency stability only when both are dominated by the white noise from the oscillator output (i.e., when the Q of the output filter is low). Because of its limited usefulness, the phase spectrum will not be given here.

It is further noted, that the relation between the power density spectrum of the signal, dealt with in Section 3, and the short-term frequency stability also is rather complicated. Only when the Q of the output filter is low is there a direct relation between $S(\tau)$ in (4.13) and the spectral components of the signal far away from the carrier.

5. THE SIGNAL AFTER FREQUENCY MULTIPLICATION

For many applications it is necessary to multiply the frequency of the oscillator signal, and the

properties of the signal at the output of the multiplier have to be known. Provided the multiplier does not contribute significant noise components, the short-term frequency stability of the multiplied signal still is properly represented by the expressions derived in Section 4. The power spectral density of the signal, however, is modified by the multiplication process; and the character of these modifications, under idealized conditions, will now be determined.

Taking again the disturbances caused by a single impulse generated by v_3 in Figure 12–1 as an example, the output voltage from the amplifier in Figure 12–4 was previously determined as

$$e_{out}=[A_1+x(t)]\cos[\omega_1 t+\varphi+\phi_{3k}(t)], \quad (5.1)$$

with $\phi_{3k}(t)$ and $x_{3k}(t)$ given by (2.26) and (2.27), respectively. An ideal n-times multiplier will remove all amplitude disturbances and multiply the phase of the signal by n:

$$e_{Mk}=A_1\cos n[\omega_1 t+\varphi+\phi_{3k}(t)]. \quad (5.2)$$

When (2.28) is used and the magnitude of $\phi_{3k}(t)$ for a single noise impulse is considered, (5.2) is approximately

$$e_{Mk}=A_1\cos n(\omega_1 t+\bar{\varphi})-n(\omega_1 C/2C_2)a_{3k}\cos(\omega_1 t_k+\bar{\varphi})\exp[-(\omega_1\gamma/2)(t-t_k)]\sin n(\omega_1 t+\bar{\varphi}), \quad (5.3)$$

whereby

$$\bar{\varphi}=\varphi+\eta_{3k}.$$

The effects of all other noise impulses add linearly; and, proceeding to the integral representation, the output signal from the multiplier becomes—if only v_3 is acting—

$$e_{M3}=E_{1M3}+E_{2M3}, \quad (5.4)$$

with

$$E_{1M3}=A_1\cos n[\omega_1 t+\eta_3(t)], \quad (5.5)$$

$$E_{2M3}=-n(\omega_1 C/2C_2)\int_0^t B_3(\xi)\cos[\omega_1\xi+\eta(\xi)]\exp[-(\omega_1\gamma/2)(t-\xi)]\,d\xi\,\sin n[\omega_1 t+\eta_3(t)]. \quad (5.6)$$

The other noise components in the oscillator signal can be treated in a similar manner, and the total multiplier output signal is found to be

$$e_M=E_{1M}+E_{2M}, \quad (5.7)$$

with E_{2M} representing the sums of components of the form (5.6) while E_{1M} is, with $\eta(t)$ defined in (2.31),

$$E_{1M}=A_1\cos n[\omega_1 t+\eta(t)]. \quad (5.8)$$

The power spectral density of e_M can now be computed, following the procedure used in Section 3. One finds

$$G_{e_M e_M}=\frac{4A_1^4/n^2\omega_1^2\kappa^2}{1+(4A_1^2/n\omega_1\kappa^2)^2[1-(\omega/n\omega_1)]^2}+\frac{n^2\kappa^2/\gamma^2}{1+(2n/\gamma)^2[1-(\omega/n\omega_1)]_2}+\frac{n^2B_2^2[1+Q_c(R_3/\omega_1 L)]}{1+(2n/\gamma_c)^2[1-(\omega/n\omega_1)]^2}, \quad (5.9)$$

with κ^2 defined in (3.10) and γ in (2.10).

The first term in (5.9) is the carrier of the multiplied signal. The second term is due to that part of the phase disturbances in e_{out} which stems from the action of the oscillator as a narrow-band filter; the third term is due to the white noise from the oscillator output. At frequencies sufficiently removed from the carrier, it is again this latter component that dominates the spectrum; and a large $Q_c=1/\gamma_c$, [i.e., a high Q filter in the output amplifier (or in the multiplier chain!)] is obviously desirable. In practical applications it must be expected that a fourth component will be found in the spectrum of e_M, representing the residual amplitude modulation of the signal.

It is interesting to compare (5.9) with the spectrum of

$$\bar{e}_{out}=A_1\cos[\omega_1't+\eta(t)]-A_1\bar{\vartheta}(t)\sin[\omega_1't+\eta(t)], \quad (5.10)$$

which is the signal from the output amplifier with all amplitude disturbances removed. $\bar{\vartheta}(t)$ thereby represents the out-of-phase components of that term in (3.30) which replaces $B_2(t)$ in (3.6), added to $\vartheta(t)$. The spectrum of (5.10) is

$$G_{\bar{e}_{out}\bar{e}_{out}}=\frac{4A_1^4/\omega_1'^2\kappa^2}{1+(4A_1^2/\omega_1'\kappa^2)^2[1-(\omega/\omega_1')]^2}+\frac{\kappa^2/\gamma^2}{1+(2/\gamma)^2[1-(\omega/\omega_1')]^2}+\frac{B_2^2[1+Q_c(R_3/\omega_1'L)]}{1+(2/\gamma_c)^2[1-(\omega/\omega_1')]^2}, \quad (5.11)$$

It is noted from (3.20) with (3.31) that $G_{\bar{e}_{out}\bar{e}_{out}}$ is equal to

$$G_{CC}+G_{\vartheta\vartheta}+\tfrac{1}{2}G_{NN}.$$

The limiting curves for the three terms in (5.9) are, respectively,

$$\frac{\kappa^2/4}{[1-(\omega/n\omega_1)]^2}, \quad \frac{\kappa^2/4}{[1-(\omega/n\omega_1)]^2}, \quad \frac{(B_2^2/4Q_c^2)[1+Q_c(R_3/\omega_1L)]}{[1-(\omega/n\omega_1)]^2}, \quad (5.12)$$

while those for the three terms in (5.11) are

$$\frac{\kappa^2/4}{[1-(\omega/\omega_1')]^2}, \quad \frac{\kappa^2/4}{[1-(\omega/\omega_1')]^2}, \quad \frac{(B_2^2/4Q_c^2)[1+Q_c(R_3/\omega_1'L)]}{[1-(\omega/\omega_1')]^2}. \quad (5.13)$$

Obviously, the corresponding limiting curves in (5.12) and (5.13) are identical on a relative frequency scale. According to the remarks at the end of Section 3.3, the effects of the multiplication process on the spectrum of the signal can be readily assessed, therefore, when only the peak densities of the components in (5.9) are compared with their counterparts in (5.11). Evidently, the signal-to-noise ratio in the neighborhood of the carrier deteriorates with the fourth power of the multiplication factor, which demonstrates quite drastically that only low multiplication factors can be employed gainfully when the multiplied signal is to be used directly.

When the spectral density of the multiplied signal is to be compared with that of a signal generated at $\omega_1'=n\omega_1$—without considering the amplitude disturbances—the values of κ^2, A_1, B_2 appropriate for the high-frequency oscillator have to be used in (5.11) and (5.13), and those for the oscillator operating at ω_1 in (5.9) and (5.12). The relations then can be used to arrive at a decision as to which source is to be preferred for a particular application, or whether the multiplied signal derived from a crystal oscillator is best used directly or to phase-lock an auxiliary oscillator at the high frequency. In most cases it will be adequate thereby to consider only the first and third terms in (5.9) and (5.11).

With the amplitude disturbances disregarded, the effects of the oscillator action as a narrow-band filter on the spectrum, represented by the second terms in (5.9) and in (5.11), do not appear to be very serious because the limiting curves are the same as for the carrier.

CONCLUSIONS

An effort has been made to analyze an harmonic oscillator, with noise sources in the circuit, with all the mathematical rigor appropriate for a first-order perturbation analysis. The disturbances in the oscillator signal caused by the action of the noise sources can be derived in all cases of practical significance from a linear perturbation equation with time-dependent coefficients. A first approximation to the solution of this equation is obtained under the assumption that the unperturbed oscillator signal is a pure sinusoid of the form $A_1\cos(\omega_1t+\varphi)$. An investigation of the effects of harmonics in this signal, especially the third harmonic, on the solution of the perturbation equation is left for future work.

To proceed beyond the prior state of the art, it was necessary to develop a technique for the solution of the perturbation equation which does not rely on the method of slowly varying amplitude and phase nor on the narrow-band approximation. As a result, an explicit expression for the

signal in an oscillator with noise, which describes the more important aspects of oscillator behavior under the influence of noise and defines their relative significance, was obtained.

The statistical analysis of the signal shows that the components which are eliminated from the solution of the perturbation equation when the slow phase and narrow-band approximations are introduced are of considerable importance for the description of the noise limitations on the practical performance aspects of the oscillator. A white-noise component in the oscillator signal causes the observed inverse first-power dependence of the short-term frequency stability on integration time and controls the magnitude of the spectral components of the signal sufficiently far removed from the carrier. The influence of this component can be significantly reduced by using a high Q filter in the output amplifier of the oscillator.

Components in the output signal due to the action of the oscillator as a narrow-band noise filter control the spectral density of the signal at frequencies close to the carrier. The major significance of this aspect of oscillator behavior, however, lies in the fact that it causes the recovery time of phase disturbances of any origin to be very long, even when the amplitude disturbances are corrected in a much shorter time—for example, by AGC. The influence of these components can be reduced by increasing the nonlinearities in the oscillator circuit whenever the signal amplitude has to be kept to a relatively low level.

The relations given in this paper for the short-term frequency stability and the power spectral density are equally valid as first approximations for crystal oscillators and for L−C oscillators, provided the parameter γ remains smaller than the inverse of the quality factor of the feedback network. They can be used, therefore, to select an acceptable compromise for a given application and to obtain a quantitative estimate for the performance to be expected from a given device.

In terms of general guide lines, it can be concluded that a signal with good spectral characteristics and high short-term frequency stability can be derived from an oscillator that has a very narrow band filter in the output channel, is operated at a high signal level, and has a strong instantaneous nonlinearity in the circuit. When frequency multiplication is involved, the multiplication factor must be low. The recommendations regarding the signal amplitude and the nonlinearity can be made only conditionally, since higher order effects have not been evaluated.

APPENDIX A—THE PASSIVE FEEDBACK NETWORK

When the active device is removed from the circuit in Fig. 1, i.e., when $i_1=f(e_g)=0$ is assumed, the differential equation (1.3) becomes

$$\ddot{u}+\omega_1\gamma_T\dot{u}+\omega_1^2u=F(t) \tag{A.1}$$

$$\gamma_T=R_3/\omega_1L \tag{A.2}$$

It describes the performance of the output voltage from the passive feedback network under the influence of the noise generators. With $i_s=0$, $v_1=v_2=0$, $v_3=a_{3k}\ \delta(t-t_k)$ the solution of (A.1) is

$$u_{3k}=(\omega_1C/C_2)\,a_{3k}\exp[-(\omega_1\gamma_T/2)\,(t-t_k)]\times\sin\omega_1(t-t_k). \tag{A.3}$$

u_{3k} in (A.3) has the same form, but twice the magnitude of $n_{3k}(t)$ in (2.22), the response of the oscillator to an impulse from v_3. The time constant $2/\omega_1\gamma_T$ in (A.3), however, is, because of (2.20), substantially larger than that of n_{3k}. The time constant of the latter is controlled by γ which, with (2.10) and (2.8) can be written as

$$\gamma=\frac{(L_1/C_2)\,g_{m0}-R_3}{\omega_1L} \tag{A.4}$$

Clearly, n_{3k} is the response of the passive feedback network to an impulse $(a_{3k}/2)\ \delta(t-t_k)$ from v_3 if only R_3 in Fig. 1 is replaced by a resistive component of the much smaller value $[(L_1/C_2)\,g_{m0}-R_3]$. The action of the active element raises the quality factor of the passive network to a much higher effective value.

When the procedure used in Section 2.3 to solve the equation (2.9) is applied to (A.1), one

finds with (2.2) and (2.11)

$$\ddot{x}+2\omega_1\dot{y}+\omega_1\gamma_T\dot{x}+\omega_1^2\gamma_T y=F_c$$
$$\ddot{y}-2\omega_1\dot{x}+\omega_1\gamma_T\dot{y}-\omega_1^2\gamma_T x=F_s \qquad \text{(A.5)}$$

as the equations for the passive feedback circuit, which correspond to (2.3) for the perturbations on the fundamental component of the oscillations. The solution of (2.3) for a single impulse from v_3 is given by (2.18); the corresponding solution of (A.5) is

$$\begin{aligned}
x_{3k}(t) &= -(\omega_1 C/2C_2)a_{3k}\sin(\omega_1 t_k+\varphi)\exp[-(\omega_1\gamma_T/2)(t-t_k)]\\
&\quad+(\omega_1 C/2C_2)a_{3k}\cos(\omega_1 t_k+\varphi)\exp[-(\omega_1\gamma_T/2)(t-t_k)]\sin 2\omega_1(t-t_k)\\
&\quad+(\omega_1 C/2C_2)a_{3k}\sin(\omega_1 t_k+\varphi)\exp[-(\omega_1\gamma_T/2)(t-t_k)]\cos 2\omega_1(t-t_k)\\
y_{3k}(t) &= (\omega_1 C/2C_2)a_{3k}\cos(\omega_1 t_k+\varphi)\exp[-(\omega_1\gamma_T/2)(t-t_k)]\\
&\quad+(\omega_1 C/2C_2)a_{3k}\cos(\omega_1 t_k+\varphi)\exp[-(\omega_1\gamma_T/2)(t-t_k)]\cos 2\omega_1(t-t_k)\\
&\quad+(\omega_1 C/2C_2)a_{3k}\sin(\omega_1 t_k+\varphi)\exp[-(\omega_1\gamma_T/2)(t-t_k)]\sin 2\omega_1(t-t_k). \qquad \text{(A.6)}
\end{aligned}$$

Except for the value of the time constant, the second and third terms in $x_{3k}(t)$ and $y_{3k}(t)$ are identical to the corresponding terms in (2.18). When x_{3k} and y_{3k} are inserted into (2.2), these terms add up to one half of (A.3); the first terms in (A.6) provide the other half of the total solution to (A.1). In (2.18), the second and third terms add up to n_{3k}, while the character of the first terms is modified by the oscillation process.

The nature of the solutions (2.18) and (A.6) can now be interpreted as follows: The operations (2.2) and (2.11) transform the original system into an equivalent set of two systems, one a low pass system, the other a bandpass system centered at $2\omega_1$ (without imposing any band limitations). One half of the original forcing function acts on either. In a passive system both halfs produce the same effect and the correct result can be obtained by doubling the response of the low pass part of the equivalent set.

The reaction of the low pass part of the active system, however, is different than that of the band pass part, as evidenced by (2.18) and (2.19); and considering only the low pass part, as is done when the method of the slowly varying amplitude and phase is applied, produces only one aspect of the full solution.

The fact that the methods used in Section 2.3 to solve the perturbation equation is fully adequate to solve the corresponding equation for the passive network is considered a strong support for the validity of our assumption that other possible solutions of (2.12) are of no consequence for the present work.

The autocorrelation function of the output of the passive network, when all noise sources are acting (white noise), is

$$\Gamma(\tau)=2(\omega_1\kappa^2/\gamma_T)\exp[-(\omega_1\gamma_T/2)\tau]\times\cos\omega_1\tau+B_2^2\,\delta(\tau) \qquad \text{(A.7)}$$

the first term of which compares with (3.9a). Because the weighted noise intensity κ^2 is the same in both expressions, it follows that the results of this paper can be most readily generalized to oscillators of arbitrary circuit configurations when the impulse response of the passive network is first evaluated by standard techniques.

REFERENCES

1. Rytov, S. M., "Fluctuations in Oscillating Systems of the Thomson Type I and II," *Soviet Physics 2*, 217–235, March 1956.
2. Spälti, A., "Der Einfluss des thermischen Widerstandsrauschens und des Schrotteffektes auf die Störmodulation von Oscillatoren," *Bulletin des Schweizerischen Electrotechnischen Vereins 39*, 419–427, June 1948.
3. Blaquiere, A., "Effet du Bruit de Fond sur la Frequence des Auto-Oscillateurs a Lampes," *Annal. Radio Elect. 8*, 36–80, January 1953; and "Spectre de Puicance d'un Oscillateur Non-Lineaire Perturbe par la Bruit," *Annal. Radio Elect. 8*, 153–179, August, 1953.
4. Edson, W. A., "Noise in Oscillators," *Proc. IRE 48*, 1454–1466, August 1960.

5. MULLEN, J. A., "Background Noise in Non-Linear Oscillators," *Proc. IRE 48*, 1467–1473, August, 1960.
6. GOLAY, M. J. E., "Monochromaticity and Noise in a Regenerative Electrical Oscillator," *Proc. IRE 48*, 1473–1477, August 1960; and "Equations of the Regenerative Oscillator," *Proc. IEEE 52*, 1311–1330, November 1964.
7. KRYLOFF, N., and BOGOLIOBOFF, N., "Introduction to Non-Linear Mechanics," Princeton: Univ. Press, p. 63 ff, 1949.
8. VAN DER POL, B., "The Non-Linear Theory of Electrical Oscillations," *Proc. IRE 22*, 1051–1086, 1936.
9. LE CORBEILLER, P., "Two-Stroke Oscillators," *IRE Trans.* CT-7, 387–399, December 1960.
10. CUNNINGHAM, W. J., "Introduction to Non-Linear Analysis," New York: McGraw-Hill, 1958.
11. HAFNER, E., "Analysis and Design of Crystal Oscillators," Tech. Rept. E-2474, USAEL, Fort Monmouth, N. J., May 1964, App. I and II.
12. MCLACHLAN, N. W., "Ordinary Non-Linear Differential Equations," Oxford: Clarendon Press, p. 110, 1950.
13. REICH, H. J., "Functional Circuits and Oscillators," Princeton: d Von Nostrand, pp. 327 and 353, 1961.
14. MCLACHLAN, N. W., "Theory and Application of Mathieu Functions," Oxford: Clarendon Press, 1947.
15. KRYLOFF, N., and N. BOGOLIOBOFF, N., *op. cit.*, p. 10.
16. BENNET, W. R., "Methods of Solving Noise Problems," *Proc. IRE 44*, 609–638, (Eq. 223 ff.), May 1956.
17. GABOR, D., "Theory of Communication," *Jour. IEE 93*, 429–457, 1946.
18. DAVENPORT, W. B., Jr., and ROOT, W. L., "Random Signals and Noise," New York: McGraw-Hill, p. 369, 1958.
19. Time constants in the order of several minutes for the recovery of phase disturbances were observed in AGC oscillators during pulse modulation experiments by W. W. Smith of BTL. Private communication.
20. CHANDRASEKHAR, S., "Stochastic Problems in Physics and Astronomy," Selected papers on noise and stochastic processes, N. Wax, Edit. New York: Dover Pub., p. 22, 1954.
21. WANG, M-C., and UHLENBECK, G. E., "Theory of the Brownian Motion," Select. papers on noise and stochastic processes, N. Wax, Edit. New York: Dover Pub., p. 122, 1956.
22. BENDAT, J. S., "Principles and Applications of Random Noise Theory," New York: John Wiley and Sons, p. 79, 1958.
23. RICE, S. O., "Mathematical Analysis of Random Noise," *BSTJ. 23*, 282–332, 1944; and *24*, 46–156, (Eq. 2.1-5), 1945.
24. DAVENPORT, W. B., and ROOT, W. L., *op. cit.*, p. 79.
25. BENNET, W. B., *op. cit.*, Eq. 137.
26. CHENETTE, E. R., "Low Noise Transistor Amplifiers," *Solid State Design 5*, 27–30, February 1964.
27. This effect is the probably cause of the eventual deterioration of the short-term frequency stability of crystal oscillators at very high drive levels reported by M. Block at the 18th Annual Frequency Control Symposium of USAEL, Fort Monmouth, May 1964, Atlantic City, N. J.
28. The importance of auxiliary filtering in improving the spectrum was already pointed out by Edson in Reference 4 above.

Page intentionally left blank

PANEL DISCUSSION

SESSION II: THEORY

Chairman	WILLIAM A. EDSON
Panel Members	MALCOLM W. P. STRANDBERG
	MARCEL J. E. GOLAY
	JAMES A. MULLEN
Authors	R. D. LINCOLN
	L. S. CUTLER
	T. F. CURRY
	R. F. C. VESSOT
	J. A. BARNES
	E. HAFNER

Dr. Strandberg.—Some years ago, when I was active in the field more than I am now, I got ulcers, and now, when I come back and see how many people know so much about it, I get an inferiority complex. There are some things that are nice, however, that I see have changed. One is that there seems to be a common feeling among most people that they are for spectral distribution descriptions. This seems to be a common type of acceptance now, just like being for motherhood, I guess, and most people are against sin, which in this case is a residual FM description of frequency stability. It seems to me that this was entirely different five years ago.

One other thing that I notice is that people are very cavalier in using multipliers now. I sat through frequency symposia in the past, where multipliers were the most suspect element in the whole chain, and yet nobody has said anything about it, except that you can multiply by large numbers and no damage done.

I disagreed with the people who were worried about them before, and now I sort of have to get on the other end of the fence and say, well, you can have trouble if you are not careful.

One other thing that I have seen, as an outsider, developed today; there seems to be a feeling that one can go from a frequency to a time domain characterization of oscillators if you choose the right statistical parameters. I mean you can't certainly at an instant of time or one short interval of time go from the time domain into the frequency domain. This is not really well understood, if I understand questions that have been asked today. However, if one takes a proper statistical average in the time domain, there seems to be an agreement that one can go from that into a statistical average in the frequency domain by well-known techniques.

Dr. Mullen.—One of the things that has struck me, too, has been that the field has made much progress, as shown by the papers we have heard in this session. There has been a consolidation of what we knew a few years ago and the discovery of a number of second generation problems.

The paper by Drs. Baghdady, Lincoln and Nelin is an excellent exposition and will be very useful. On that account especially, I would like to add a few bibliographical notes.

I think that the use of the $(\sin x)^2/x^2$ weighting for the phase difference was published first by Develet [*Trans. IRE Sp. Elec. Tel.* (1961) pp. 80–85, viz., Eq. 34)] and was done with reference to radar in originally classified work by W. W. McLeod, Jr., of the Raytheon Missile Systems Division late in 1955.

Noise in oscillators with AFC loops, i.e., average power control, was discussed already by Dr. Edson [Vacuum Tube Oscillators, John Wiley and Sons, Inc., New York (1953) sec. 15.3] and then by Dr. Golay [Proc. IRE, Aug. 1960 and Nov. 1964]. Noise in oscillators with instantaneous nonlinearities was discussed first by Berstein [*Doklady Akad. Nauk USSR 20*, 11 (1938) (the original paper is in English)] and next by Blaquière [*Ann. Radio él. 8* (1953)].

With respect to Dr. Curry's paper, I think that the use of a window function in spectral analysis is one of the real physical conditions that we have to deal with, and cannot really be avoided. The maximum likelihood estimator is very useful to connect the things that we are measuring to the theory of optimal estimates, but his bank of continuous filters is limited in resolution by essentially a window function. This is as it should be: in each case we have to decide whether we want to emphasize resolution or precision in the individual estimates.

With respect to the papers on the masers, I wonder where the $1/f$ comes from physically. For instance, Drs. Blaquière and Grivet [Proc. IEEE *51*, 1606 et seq. (1963)] have pointed out that if we represent the nonlinearity as a polynomial including quadratic terms, there is the possibility of base band flicker noise beating into the spectral band around the oscillating frequency. (Quadratic terms have generally been neglected since van der Pol pointed out long ago that they are irrelevant as regards limit cycle behavior.) This might be a physical mechanism for bringing the $1/f$ noise up to the frequencies at which we see it. On the other hand, perhaps there is some

sort of modulation in the same way as power supply ripple modulates oscillators. It would be an interesting theoretical advance, if we had some reason to believe that one of these was a more appropriate description than the other.

I think that Dr. Hafner's paper is really very useful and is a step forward in including several different oscillator sources, and in getting more down to design considerations than we have had before, or that I have been aware of before.

I must say that I am not convinced that a noise generator inside the loop gives a direct noise effect in the output. I feel that noise generators inside the loop ought to introduce just modulation and not show up additively. Now, there is no doubt that additive noise in the amplifiers or the filters following the oscillating loop itself is bound to give additive contributions and it is going to be quite a delicate job to disentangle the one effect from the other.

Even in the curves as presented, it would be hard to distinguish the two effects. The difference would show up most clearly in the short-term frequency stability measurements. Of course, in this case, both theories must be applied to the same circuit, and Dr. Hafner's circuit is all the more appropriate for being realistically complicated. With the double tuned circuit of Dr. Hafner's Fig. 1, both theories will predict the second order shaping factor that appears in the short-term stability spectra that he obtained.

Dr. Hafner has kindly informed me that noise in oscillators with AVC control has been treated in 1948 by A. Spalti [*Bull. Ass. Suisse. Elec. 39*, 419 (1948)]. To be more specific than was appropriate in the verbal discussion, the part of Dr. Hafner's paper that leaves me unconvinced is the use of a sufficient condition to separate Eq. (2.12), where I believe that only necessary conditions are admissible. Under the additional constraint of slowly varying amplitude and phase, which I believe to be physically well grounded, the separation becomes necessary.

Dr. Golay.—I should like to begin with the remark that while this was a frequency stability symposium, everyone has acted and talked like it were the opposite, namely a frequency instability symposium. Every measure I have seen given on the screen was a measure of instability. As instability goes up and as stability goes down, that measure increases, so that we have had a very nice series of papers on short-term frequency instability.

I should like to make a remark about Dr. Hafner's paper. He has very rightly, for quartz oscillators, taken a non-linear element with a cubic term like the van der Pol oscillator, and this is indeed correct for an oscillator of the quartz type where you have a vacuum tube feedback.

However, I believe the theory should be extended to oscillators of the Meacham type in which there is a lamp circuit, or to masers and lasers. In these latter there is a given excess of high over low quantum state population which gives you appropriate amplification of the light beam. If the intensity of that beam increases, it takes a little time for that population to decrease. Therefore, in order to develop an adequate study of these oscillators we should introduce a delay in the servo circuit controlling regeneration. The brief studies I have made have indicated that this delay in the servo circuit can introduce profound changes in some aspects of the spectral distribution of the oscillator output.

I would like to congratulate Mr. Barnes for having come with an extremely logical measure of instability of oscillations. After all, a stable oscillator is one in which the phase increases perfectly linearly with time so that the slope of the representative straight line is the frequency. Two points on that straight line define the frequency. Therefore, it is completely logical, if we want to measure departure from stability, to use three equidistant points on the phase vs time curve to determine its short-time curvature. But then you should divide this second phase difference by tau squared, and as the second phase differences are already proportional to one over the square root of the time interval tau, then you do not arrive as Vessot has done with a tau to the minus three-halves term. You arrive at a tau to the minus five-halves term, because you have divided the double difference by tau squared, as you should have.

So this then raises an interesting question: What is the term that Vessot and his associates have obtained which is proportional to tau to the minus three-halves power? I believe it is not a measure of instability from instant to instant, but

rather a measure of the departure of the frequency as measured from instant to instant from its average taken over a time large compared to tau.

I have also an even more serious question about the beautiful work and the meaning of the beautiful work of Vessot showing such nice agreement of theory with experiment. Is it really legitimate to charge the oscillator you are studying with a noise which is added to it by our way of looking at it? Should we not do better justice to it?

Now, we have an oscillator. We add to it a lot of noise and then we make short-term measurements which are effected by that noise. Should we not first, as Edson has suggested, pass its output through a high Q circuit? But a high Q circuit is difficult to get. It is difficult to do justice to a maser or a laser, with a high Q circuit. So in order to obtain a really high Q circuit, we should phase lock, slave an oscillator to the maser. When we do that, of course, we want to take an oscillator which has some nice properties, and is not worse than the maser in every respect. It should be worse than the maser in some respects and better in other respects.

So what we want is something like a quartz oscillator, which has an excellent short-term stability with a high power output, but which, after a while will tend to have its phase drift, and must then be told by a maser how to correct its phase path.

In other words, we have the case of the blind carrying the paralyzed. The paralyzed is the weakly but purely oscillating maser and the blind is the powerful but phase drifting quartz oscillator. The maser is carried by the quartz oscillator which takes a steady, strong pace, but would depart from a straight line after a while unless nudged in the right direction by the maser.

Now, this problem is a real nice and tricky problem, and I believe it to be very worthwhile solving. In fact, I should think a symposium on only the subject of phase locked oscillators would be worthwhile, because of the dualism which exists between the properties of oscillators and the kinds of phase locked loops you want to design to slave oscillators to each other. If the two oscillators never depart by more than their bandwidth, you want a simple loop of the first degree. If the oscillators might drift more and more, you want a loop with a phase motor which is geared to the condensor of the tank circuit of some slaved oscillator and which eventually brings the phase of the slaved oscillator where it should be. The differential equation governing such a loop is of the second degree, and so on to loops of the third or even higher degree.

Consider for instance a similar problem: that of a nearly perfect oscillator carried by a planetoid which goes around the sun. That perfect oscillator emits a one watt signal which must be received from some fifty million miles away. Because the planetoid has a velocity, and an acceleration, and a jerk, etc., we must do the best we can to receive that signal. We have to consider all these factors. We must design a phase locked loop which controls an earth bound oscillator by means of that signal, so that we may receive any information carried by some modulation of that same signal. I believe that the problems of phase locked loops and of oscillators are intimately connected with each other and should be studied as a whole.

Dr. Edson.—One, I am convinced from the numerous data that there is a $1/f$ phenomenon. I think Dr. Mullen has suggested a mechanism that may lead to this. I wasn't fully satisfied, but I think that maybe this is a possibility.

I would suggest this thought, that we find the short-term stabilities and the higher-order terms almost certainly connectable with thermal noise. That in effect is threshing a phase, forward or backward in time, either in the oscillator loop or after it escapes and is out as a sinusoidal signal. All of this implies that the resonator has a fixed unique frequency and we essentially so far escaped talking about what that frequency is. We know practically, that all kinds of resonators have smooth long-term drifts. There is no obvious reason why that is essentially a continuous process, and at least I think that we should not give up looking. This, by the way, is going back in time, I am sure, because ten years ago this is exactly where everyone would have looked for random jumping of the frequency rather than the subtleties of the phase being pounded around. I think we should go back and have a look at that, to see if this is the source of $1/f$.

Dr. Strandberg.—Just one point. Maybe I should direct it to Dr. Golay, really. The point

that Vessot made, I think, was an important one, really; that one can go from the frequency to the time domain, but if one tries to do this in the laboratory, he is going to have difficulties. That is, if you take a rectangular window in the time domain, you are going to have experimental difficulties trying to repeat those measurements in the frequency domain.

Dr. Golay.—I quite agree with that. The point I made was not that point.

Dr. Strandberg.—One is going to get into difficulties, though, if you try to visualize a frequency domain result in terms of a time domain function, which, say, turned out to be a $\sin x/x$ kind of function.

Dr. Edson.—Aren't we going to have to be careful about this part?

Dr. Golay.—You mean taking the second difference and dividing it by tau squared? It would lead us to—

Dr. Strandberg.—What I am just trying to say: suppose he takes a square filter in the frequency domain, then this is a $\sin x/x$ sampling in the time domain. Now he is going to pick out some—

Dr. Golay.—Oh, you can always test these things.

Dr. Edson.—If I might comment, the square filter is little honored by anybody. I mean, a generation ago people discovered transients coming out of the filter before they went it, because there were assumptions about transmission and phase, and I would urge anyone to study filters that are physically realizable—that is, in mathematical models. I think Dr. Vessot here—

Dr. Vessot.—I would like to interpret my own paper, if I may. Really, what we are out to show is that there were no other sources of noise present in the signal from the hydrogen maser. There are plenty of things that can happen. We have atoms rattling about in a bottle, and they make about 10^4 collisions before they come out and after spending about a second in the bottle. Therefore, you would expect that you could generate other frequencies or you might find some other type of perturbation.

Now, it is true that we did not extend ourselves far enough in the frequency domain to investigate these very closely. But really the object was to show that the representation that we have obtained—that is, the model—is that of a very sharp spectrum, which we have said nothing about, in a field of added noise which we could almost call white noise, except that this white noise does terminate. Otherwise, we would be really in deep trouble.

The origin of the noise might be the cavity itself, which generally has a Q of about ten thousand. However, we don't do it this way. We have an isolator, and I don't know what the Q of the isolator is, but it does have a bandwidth of several megacycles. So the origin of the noise is difficult to establish.

The whole thing is in thermodynamic equilibrium. We don't know whether it came from the cavity or whether it came from the line or losses elsewhere, but we do know that it is limited in bandwidth in some way, very likely by the receiver.

In making the measurement, we chose to limit the bandwidth of the receiver because it was something that we understood, rather than to try to control something that we had less of a handle on.

Dr. Edson.—If I might add one word: I think essentially Dr. Vessot has said that we are currently studying a perfectly pure sine wave with additive white noise and finding out what statistics we get from that, which is a perfectly proper model, and it is not by any means what Dr. Hafner studied, or rather it would be a skipping, except the terms that he finally represented as a horizontal line. In his pictures it would be a vertical line of zero width, plus a horizontal line of white noise. And this is a model that certainly can be approximated. And I think that is quite interesting, that the instrumentation fits the statistical model you get in studying the phase perturbations of that.

Mr. Cutler.—This business of white additive noise is something that we have looked at quite a bit too. If you recall in my paper I showed that for a fixed system bandwidth with white additive noise, you are looking for times longer than the reciprocal half bandwidth of the filter. The noise should go down as one over tau, or the fluctuation should go down as one over tau.

Now, if at the same time you shrink the system bandwidth in the same proportion that you are lengthening your averaging time, tau, you get exactly the one over three-halves behavior that

Dr. Vessot sees, and the origin is precisely the same; namely additive noise on top of a signal whose intrinsic fluctuations are much smaller than those induced by the additive noise.

The two methods of looking at this is somewhat different in that Dr. Vessot allows the bandwidth of the white noise to shrink, whereas we in our system of measurement hold the bandwidth constant; consequently, you would get a one over tau behavior.

Dr. Golay.—Is not the challenge here that you have a perfectly beautiful oscillator in front of you and you are not able to see what it is doing? Isn't there some method of looking at it so that we can see what it is doing, by using a properly designed phase lock loop? I mean are we forever to have a beautiful oscillator there and not know anything about it?

Mr. Cutler.—If you take your sampling time sufficiently long, or consequently your system bandwidth sufficiently narrow, that the spectral density of the actual oscillator signal itself is of the same size or larger than the white noise spectral density that is added in, then you will most assuredly see the oscillator.

Dr. Golay.—And if you do not, then you are not looking at the oscillator.

Mr. Cutler.—That's right.

Dr. Edson.—I must quote a line that I stole from Dr. Vessot. The analogy is the man playing a beautiful violin in a boiler factory; and apparently, this is what a maser is. I think Dr. Golay is trying to stop the boilermakers and I think it is hard to get rid of them. I think they are inherent in the system.

Dr. Golay.—Yes, but I don't think it is impossible.

Dr. Baghdady.—I would like to make what I consider an interesting remark about these laws, $1/f$ and so forth. If you approach the modeling of oscillators from the blackbox viewpoint as opposed to what we call physical causes, one of the interesting models that has come up is just a band of noise—a band of gaussian noise, whose spectrum you can assign a variety of shapes and you would be amazed at how many different laws emerge. Out of that you get $1/f$, you get higher powers, you get almost anything you want. It depends on the shape of the spectral density function of that band of noise, no sine wave, just a lot of guys talking at the same time with somebody constraining the shape of the spectrum of their combined chatter. Change the spectral shape and look at the instantaneous frequency, you find some beautiful laws that look like $1/f$ and others. And, incidentally, in agreement with one of the questions that Mr. Barnes brought out, namely that this $1/f$ phenomenon has to taper off eventually, they all taper off, these "one over something" spectra. They don't just keep going: they rise and then they taper off.

Dr. Helgesson (Varian Associates).—I seem to detect here that people are a little bit squeamish about making one measurement in the time domain and a different measurement in the frequency domain. Or maybe they think they should be able to repeat a time domain measurement in the frequency domain, which of course is unrealizable for the sort of things that we have been talking about here.

I don't think this is a particular disadvantage. I think that both types of measurements are equally valid. They apply to different sorts of applications.

The period count, of course, applies to something where a period count is going to be used in an actual setup; for instance, a period count of a doppler frequency. This measurement is very applicable. The frequency domain averaging with a square filter is something that is not only applicable to the hydrogen maser but I think also to any type of stable oscillator. This has, I think, very important applications in frequency lock loops and any other situation where you are constraining the bandwidth in the same way that you are constraining it in the measurement technique. I think that we should recognize that both of these types of measurements exist, and they are useful. Perhaps, we shouldn't actually specify our oscillator in terms of both measurements, because certainly the numbers don't come out the same when you perform both types of measurement on the same oscillator.

We intend to talk a little bit more about this tomorrow in terms of some measurements that we made on atomic standards.

Prof. Searle (MIT).—There has been a lot of talk about the frequency domain versus the time domain. I talked with Prof. Strandberg and a couple of other people on the panel, and they

thought it would be helpful if I stole a slide from the talk that I have to give tomorrow afternoon, to try to put this in block diagram form in hopes that it will focus attention a little bit more on the relations between these two domains. I don't want to make a big deal out of it; obviously, but there has been an awful lot of talk, and I thought one slide might be worth a few thousand words, if the projectionist has the slide.

Essentially, this is nothing different than what a lot of people have been saying already, and this is nothing new, obviously, but it does put it down in some organized fashion, I think [see Figure 24–2]. People have been talking about various methods of performing the operation indicated in the top line, taking the derivative, passing through some type of window function, finding the mean square value of this, and finally down in the lower righthand corner, finding the various answers.

Now, there are very simple relationships, obviously, existing between the time domain and the frequency domain. This slide just summarizes those quickly and indicates that it is readily possible to move back and forth from one of these domains to the other, via the autocorrelation or various Fourier transforms. I thought this might possibly clarify some of the discussion and get the picture in one place at one time.

Dr. Strandberg.—Then what is the problem with the varied measurements, where they seem to feel there is a difference between time and frequency domain?

Prof. Searle.—I can't answer without just taking a guess that it is all tied up in this business that Dr. Vessot and I have been talking about, the window function.

What I had shown on the slide is what I consider to be the mathematically correct way of describing what you mean by a frequency average over a given interval of time, and this amounts to a square box, stepped impulse response $H(\tau)$, which is a $\sin x/x$ frequency response.

Now, if you do anything else other than that, the kinds of functions that you are dealing with, especially when you are talking about white phase noise, have a great deal of power energy in the higher frequencies when you multiply by ω squared. Thus any signal within the responses of the filter which you consider as insignificant the first time through turns out to be vitally important to what happens in the long run.

Dr. Vessot's paper describes this very succinctly, where he shows the tremendous difference between taking a simple square filter in the frequency domain as compared to a $\sin x/x$ filter. It makes a tremendous difference in the data.

Dr. Mullen.—I must say that I feel much better now that you said that it was "vitally important" to consider the functions that we are dealing with. I think it is not really the conceptual question of whether or not we can get mathematical descriptions of both of these things that are equivalent that matters: the question is whether an actual experiment done one way can be interpreted in terms of an actual experiment done the other way. This depends on a balance of experimental difficulties which are different in the two systems.

Dr. Golay.—Of course, if you have a square window in the time domain you have a frequency distribution in the frequency domain, which if multiplied by f, blows up in your face. But it doesn't mean at all that you have to have $\sin t/t$ in the time domain in order to have a manageable expression in the frequency domain. You can apodize your time as the French opticians say. You can take a finite time but make sure that you weight your samples in the proper manner by for instance a cosine function. Then you succeed in so diminishing the high frequency response that the moment of inertia or second moment of that frequency response, will be finite again.

Prof. Searle.—Dr. Golay, the only thing that I don't understand is this notion that something is blowing up somewhere. The only thing that has been said is that if you have something completely flat, white phase noise, then you end up with an infinity when you take the integral. As far as I am concerned, this is the right answer. If you have a completely flat unlimited white phase noise, then you have infinite frequency noise, and therefore your stability should be infinitely bad. So I don't see that there is any worry about realizability. We have done our stuff on the computer. You know this means that you don't have to go to the trouble of constructing a $\sin x/x$ filter, and the answer is perfectly realizable. If the answer is infinite, then you ought to get infinity, and I don't blame this

on the filter. Everybody is blaming this problem on the filter, and it is a problem of the system that you have chosen, which happens to have infinite instability.

Dr. Golay.—I don't believe the worry is real. It requires a bit of thinking.

Dr. Vessot.—I think what Dr. Golay was suggesting was that we describe ahead of time some manner of making a filter that everybody would agree to and, of course, this is very difficult. It is like falling in love with the same woman. I, for one, don't know what shape the filter should have. I have pretty good ideas on the other.

Mr. Lincoln.—If I might add one thing, the type of problem that you have in this filter can be avoided. When you are dealing in spectral regions where additive noise seems to have a significant contribution, that results in a parabolic frequency spectrum, then one is dealing with a flat phase spectrum. One can, for instance, make less than a two percent error in the use of a third-order filter, measuring that phenomenon and getting quite accurate information about the spectrum. Correspondingly, the flatter of the two spectra, right close to the origin is the frequency instability spectrum and this would be the one that would be most logical for analysis at that point.

One can get around, to an extent and, I think, to a very reasonable extent, the additive noise problem, simply by turning to the different phenomena, and as all of us said so many times before, the frequency and phase spectra are very clearly related.

Mr. Sherman (General Electric).—I know this is entitled "Theory," and yet today there were two very hard practical experimental things brought in that possibly went by a little too fast. One of them was the use of three carriers while we tried to talk about and measure one carrier. There was an awful lot of talk that presumes that we know what a frequency is or what an interval of time is. Very rapidly, Mr. Lincoln talked about using three carriers in order to take the data in pairs and compute the data applicable to one. This data is referenced to the average frequency of the three, but at least it gives you something to talk about in terms of measured quantities, which can actually be ascribed to one carrier.

There is one other thing that seems to have gone by me in one of the other papers, the discussion of flicker noise didn't seem to have sufficient distinction drawn between long-period flicker noise and what I have always thought of as being an aging phenomenon. I think there is a true long-term frequency instability for periods of time approaching infinity. Where periods of time approaching the year and periods of time approaching infinity, can be separated, I am not sure.

But there needs to be some way of discussing periods which are short, periods which are long, periods which are years, that is long periods, periods which are lifetimes, that is long, and discuss them separately. I hope that we can talk about short-term frequency stability or instability.

Dr. Golay.—A man, who having heard that crows live two hundred years, decided to make the experiment, and to that purpose acquired a young crow . . ..

Now, I believe that we can speak very well of statistics for one second or for maybe one day, long samples, but when we are dealing with long periods, we are no longer dealing with statistics, we are dealing with history.

A certain oscillator will behave very well over a long period of time, and another one will not behave so well. You compare the two, you decide after a while which has given you the most consistent data. Perhaps you had better have three to have the two which agree with each other outvote the third, but you don't really perform statistics. Statistics belong to the short-term average, and when you deal with history, you just observe and do the best you can and foresee your next step.

Mr. Sherman.—This gets involved again in the flicker noise. It was introduced as a perturbation to the conversation this afternoon. It has become a real stumbling point for me.

Mr. Baugh (Hewlett-Packard).—I think my question has already been answered to a certain extent. Dr. Baghdady in his Olympian viewpoint stated that the spectral density flicker noise just had to go to zero, or decrease for smaller and smaller frequencies. I was wondering if he had any evidence to substantiate this.

Dr. Baghdady.—I'm sorry, I didn't say it had

to decrease to zero. I just said it flattens out. Well, let me tell you what I said.

I said it is interesting to note that you can get one over something, one over omega ($1/\omega$) to a power type noise, by taking a band of gaussian noise and shaping its spectrum in various ways, and computing for each shape what the spectral density function of the instantaneous frequency comes out to be. This is a problem that has been worked out to death and a lot of curves on it have been published. If you look at the curves, they show you a lot of laws that have been worked out, say, for a gaussian shape or a rectangular shape and a single tuned shape and so forth.

The spectral density of the instantaneous frequency fluctuations doesn't go down to zero ultimately as ω goes to zero. It just flattens out or humps down. And there you can rationalize that the noise has a lot of zero crossings in instantaneous amplitude and many phase steps, giving rise to instantaneous frequency pulses that have a flat spectrum. So you would expect to have a flat spectrum to zero, you see, rather than one that goes up indefinitely.

It seems to start from a nonzero value, go through a hump, and then goes down like $1/f$ or one over some other power of frequency, and so forth, depending on the original RF spectral shape. I didn't say it goes down to zero at $\omega=0$.

Dr. Mullen.—Well, no one really knows that the $1/f$ spectrum does not keep on going up. Every time anyone makes a measurement of some physical thing, it ought to give rise to a $1/f$ phenomenon because of some kind of surface noise or contact noise, and as the experimenters keep on lengthening their averaging time, the $1/f$ noise simply keeps going up.

I think that Dr. Golay's point is the correct one, that the difficulty shades off from statistics to history. Perhaps the way that Messrs. Barnes and Allen have obtained measures in which one does not have to know the $1/f$ cutoff frequency adequately avoids the problem. But I do not think that anyone has a model of flicker noise which gives a cutoff in a truly natural manner at the low frequency end.

Dr. Baghdady.—Excuse me. If you consider the shape of the original bands of noise, if you consider the oscillation to be just a band of noise running around and being squeezed through an extremely high Q resonator, some of these extremely stable resonators, you can hardly see a bandwidth to them. You can immediately get the idea that you still have a ways to go, and when you have gone, according to this model, and I don't say that this describes the real world, but it is interesting, it may well do that.

You might say if you have to go to near zero, then your estimate of the bandwidth of the resonator, if such a thing can be defined, would approach a point after which the thing will taper off and stop rising, because this is what this analysis I told you about shows. This stuff is all confined within roughly a range which is equal to the original bandwidth of the noise that you are analyzing.

Dr. Mullen.—You certainly could find models that have a cutoff someplace, but—the problem is to get a physical mechanism that gives flicker noise and is plausible, as a physical mechanism. We can always make up a gaussian noise with any spectrum that we want. That is a good theorem, but to find a physical mechanism that gives a $1/f$ spectrum naturally, with a natural cutoff, is a very, very difficult unsolved problem.

Mr. Lincoln.—I would like to make one suggestion that might be an alternative to this, and that is the following: Suppose one can make spectral measurements down to a low enough frequency where one can determine that a $1/f$ phenomenon is occurring and assign a parameter value to it. Then, although the analysis (including the examples of tone ranging, period counting and so forth) shows a $\sin x/x$ filter effect which asks one to integrate right to the origin, one perhaps might make a case (as some of the Russians have tried) for setting a nonzero low-frequency point in the spectrum near $\omega=0$ beyond which one does not care what happens to the $1/f$ behavior. The choice of the nonzero low-frequency limit may be based upon a consideration of operating time of the oscillator, or recalibration or so forth. One can thus continue considering the $1/f$ behavior as continuing all the way to the origin, but just integrate just so far back and have an answer that is quite good, even if one is not able to measure all the way back that distance toward $\omega=0$. This I offer as an alternative to the problem of what happens eventually as ω goes to zero.

Dr. Edson.—I think that we may very well.

First of all, certainly, this $1/f$ phenomenon is not short-term frequency stability, that is one thing. I can cheerfully rule it out as being non-germane to the Symposium.

I think this is a poor idea, but I think it very possibly is a mathematical trap. I think that it may well be that the mathematics is more obscure than the physics or at least maybe that the mathematics obscures the physics.

Mr. Barnes.—First of all, I think if you were to consider klystrons, I think your definition of "short-term stability" might then stop at one millisecond because your flicker noise for such a device is quite a bit higher in frequency, I believe. Although I haven't made any studies on that. You can avoid the problem mathematically, as I have attempted to show, by treating cutoff-independent quantities.

Mr. Bickford (Raytheon Company).—Several of the authors showed discussions in which they would multiply a change of one nature or another, in which the detecting device was attributed to be a true phase detector.

Now, my question is have the output of these phase detectors been monitored as a function of time, and how do they behave? Are there any discontinuities, are things nice and smooth or do you get a nice $1/f$ behavior?

Dr. Vessot.—In the case that I described, we are not using multipliers in the sense that we multiply frequencies. The multiplier that is used is a function multiplier that represents the product in real time of two signals $F_1(t)$ and $F_2(t)$, and gives a product of F_1 times F_2. All the other systems, merely translated the spectrum down. They were subtractors, perhaps, of frequency, but not multipliers. Therefore I think you are quite right in saying that the spectrum has been retained tolerably well, which you certainly would not do if you put the thing into a times ten multiplier, for instance.

Dr. Spence (University of London).—I would like to hear comments on the use of oscillators as active filters, with particular reference to two applications. This question may be out of order and may be more appropriate for tomorrow, and please say so.

First, some Russian worker suggested a few years ago that a reduction of oscillator noise could be obtained by the interaction of a number of oscillators. Second, it is possible to operate a synchronized oscillator as an amplifier, but whether this is better than using the same active device as an amplifier, I do not know. I would like to ask if anyone has any comments on these two particular uses of an oscillator as an active filter.

Dr. Mullen.—It seems to me that it all depends. I don't think there is any other real answer. You have to study each application separately and the actual active devices that you have to work with.

Dr. Golay.—A phase lock loop is an extremely high Q filter, which is employing an active element in the form of a VCO.

Dr. Baghdady.—Dr. Golay took the words out of my mouth about the phase locked loop. I was going to mention, also, the AFC loop. They both simulate active filters, but I don't think you can make them do the job on the scale I think you have in mind. You can bring the noise bandwidth down to small fractions of cycles per second, and so forth. If you are talking much narrower than this, then it gets trickier all the time.

III. DEVICES

Call to Session	JOHN T. MENGEL GSFC
Chairman	NORMAN F. RAMSEY Harvard University
Discussion Panel	WARREN L. O. SMITH Bell Telephone Laboratories DONALD L. HAMMOND Hewlett-Packard Company ARTHUR O. MCCOUBREY Varian Associates FREDERICK H. REDER Institute of Exploratory Research U.S. Army Electronics Laboratory

13. SHORT-TERM STABILITY OF PASSIVE ATOMIC FREQUENCY STANDARDS

R. F. LACEY,* A. L. HELGESSON,** AND J. H. HOLLOWAY*

Varian Associates

Beverly, Mass., and Palo Alto, Calif.

The stability of passive atomic frequency standards is limited by shot noise introduced by the atomic reference. The contribution of shot noise to the frequency instability can be described in terms of a figure of merit for the atomic reference, and this figure of merit is used to compare references now existing and proposed. The figure of merit is calculated for atomic beam and vapor cell systems, and the asymptotic expressions for the rms frequency fluctuation for long and short averaging times are expressed in terms of it. Measurements of the rms frequency fluctuation of a cesium beam standard show the expected $T^{-\frac{1}{2}}$ dependence on averaging time and agree in magnitude with the calculated values. It is feasible to build atomic beam standards where the contribution of shot noise to the frequency fluctuation for averaging times less than 1 second is less than that due to the crystal oscillator. Rubidium vapor frequency standards currently meet this specification.

Passive atomic frequency standards use an atomic resonance frequency as a reference to control a quartz crystal oscillator. There are three types currently used to any extent: standards using cesium and thallium atomic beams, and those using rubidium vapor cells. The principle of operation is fundamentally the same in all cases. As shown below, shot noise introduced by the atomic reference puts a limit on the frequency stability of the controlled system. It is useful to describe the atomic reference, apart from the quartz oscillator and the associated electronics, by a figure of merit in order to compare the intrinsic performance of various designs with respect to the instability caused by the shot noise. The behavior of a standard can then be predicted from the figure of merit, the parameters of the electronic control circuit, and the short-term stability characteristics of the crystal oscillator.

*Beverly, Mass.
**Palo Alto, Calif.

PRINCIPLE OF OPERATION OF ATOMIC REFERENCES

The complete descriptions of the cesium atomic beam tube and rubidium gas cell as used to control frequency have been given elsewhere (References 1 and 2). We include brief descriptions sufficient to make clear the subsequent material. All atomic references make use of the ground-state hyperfine structure separation of the atom—cesium, thallium, or rubidium—used in the reference. In particular, the transition

$$(F=f,\ m_F=0)\rightarrow(F=f\pm1,\ m_F=0)$$

is used because of the relative insensitivity of the energy separation of these states to the applied magnetic field.

In a typical atomic beam tube, illustrated in Figure 13-1, atoms from a source pass between the poles of a state selector magnet, which deflects a fraction of the atoms in some of the ground level states (including the $(F=f,\ m_F=0)$ state] into a microwave structure. In this region a small,

constant magnetic field is applied parallel to the oscillating magnetic field induced in the microwave cavity at the path of the atomic beam, so that $\Delta m_F = 0$ transitions can be induced. If the frequency of the oscillating magnetic field has the proper value, atoms in the $(F=f, m=0)$ state will undergo transitions to the $(F=f\pm 1, m=0)$ state.* On passing through the second state selector magnet, atoms which are in the latter state will be deflected toward a detector, while the rest of the atoms in the beam will be deflected away. The detector consists of a hot metallic surface of high work function at which the atoms are ionized. (For thallium, oxidized tungsten is most commonly used, while tungsten, tantalum, or niobium are used for cesium.) The ions evaporating from the surface are accelerated

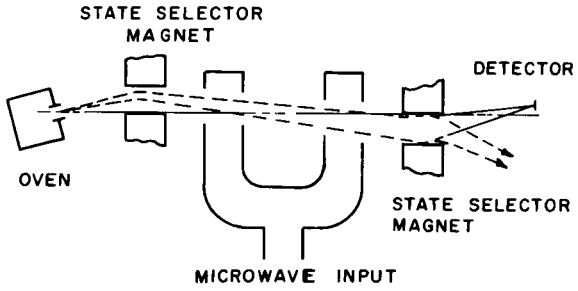

FIGURE 13–1.—An atomic beam tube.

into the first dynode of an electron multiplier, from which secondary electrons are multiplied in succeeding stages. For the Ramsey type of structure used in these devices, the signal at the detector as the frequency of the oscillating magnetic field is varied is shown in Figure 13–2. The width of the central component of the line is typically of the order of 100 Hz, while the width of the pedestal is of the order of 10,000 Hz.

In a standard, the output of a quartz oscillator is multiplied to the proper microwave frequency and modulated about the frequency of the control component: 9.19+ GHz for cesium, and 21.3+ GHz for thallium. If the central frequency does not coincide with that of the line, an error

*For cesium and thallium, F can have two values: 4 and 3, and 1 and 0, respectively. The system can be designed so that the first state selector magnet selects either of the pair of values; and the transition will then be made to the other, which will be deflected by the second state selector magnet to the detector.

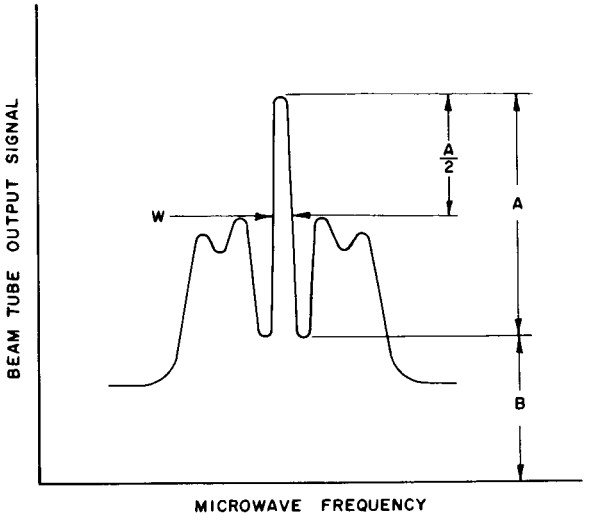

FIGURE 13–2.—Resonance line shape in an atomic beam tube with a Ramsey-type microwave structure.

signal at the modulation frequency appears at the detector, and this error signal is used in a feedback circuit to control the frequency of the quartz oscillator.

A diagram of the optical system of a Rb standard is shown in Figure 13–3. Light from a Rb^{87} lamp propagates through a Rb^{87} gas cell in a microwave cavity and is detected by a photo detector. The microwave transition between the $(F=2, m_f=0)$ and the $(F=1, m_f=0)$ hyperfine levels in the ground state of Rb occurs at 6.84+ GHz, and the microwave cavity is tuned to this frequency. The atomic system has three energy levels, with separations at the microwave frequency and two optical lines at approximately 7900 A. The light from the Rb^{87} lamp contains both optical components. To obtain a population inversion for the microwave transition, a Rb^{85} isotope filter which has an absorption line that overlaps the optical line of longer wavelength from the lamp is used. This optical line is essentially eliminated from the system, so that the

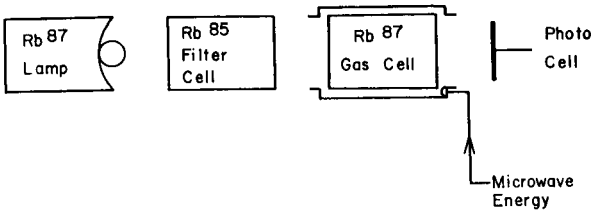

FIGURE 13–3.—A rubidium vapor cell.

photo cell measures the transmitted intensity of the remaining line as modified by the absorption of the gas cell. The microwave frequency is modulated, and the output from the photo cell is synchronously detected to produce a signal whose amplitude is directly proportional to the difference between the average microwave frequency and the reference frequency of the Rb. This signal is integrated and used to correct the frequency of the crystal oscillator from which the microwave signal is derived. The line width is typically 500 Hz and the photon flux about 2×10^{14} per second. The control circuit, shown schematically in Figure 13–4, is fundamentally

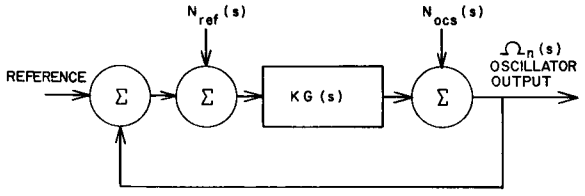

FIGURE 13–4.—Servo model of the frequency control system.

the same for rubidium vapor and atomic beam standards. The spurious error signal, shown as N_{ref} and caused by shot noise of the atomic beam or the light beam, is the cause of the instability with which we are primarily concerned. The noise from the oscillator, shown as N_{osc}, also is important to the performance of the frequency standard, of course, and—as will be discussed below—becomes dominant for sufficiently short averaging times.

FIGURE OF MERIT

The quantity long recognized as a measure of the accuracy of measurement of a resonance frequency is the signal-to-noise ratio divided by the resonance line width. We have found it useful in designing frequency standards to adopt this concept and define a figure of merit for an atomic reference as the reciprocal of the short-term rms frequency fluctuation caused by its noise, assuming optimum amplitude of modulation and a 1-Hz rectangular bandwidth for the control circuit.

The central component of the resonance line in an atomic beam tube with a Ramsey-type structure can be approximated by the function (Reference 3)

$$S=\tfrac{1}{2}A(1+\cos\Omega T)+B,$$

where Ω is the difference between the applied frequency and the atomic resonance frequency in radians per second, T is the time of flight between the separated interaction regions, A is the peak-to-valley amplitude, and B is the background. Let A and B be the current at the output of the electron multiplier. The line width W equals $1/2T$ in Hz.

With a modulated and detuned applied signal,

$$\Omega T=\delta+\Delta\phi\sin\omega t,$$

where

$\delta/2\pi T$ = amount of detuning,

$\Delta\phi/2\pi T$ = modulation amplitude,

$\omega/2\pi$ = modulation frequency.

Then

$$\tfrac{1}{2}A\cos(\delta+\Delta\phi\sin\omega t)=\tfrac{1}{2}A\cos\delta\cos(\Delta\phi\sin\omega t)-\tfrac{1}{2}A\sin\delta\sin(\Delta\phi\sin\omega t).$$

Expanding the right-hand side in a Bessel series and dropping harmonic terms in ωt which a narrow-band synchronous detector would reject, we get

$$S'=B+\tfrac{1}{2}A[1+J_0(\Delta\phi)\cos\delta]-A\sin\delta J_1(\Delta\phi)\sin\omega t.$$

The optimum modulation maximizes the last term. The first maximum of $J_1(\Delta\delta)$ is 0.5819 for $\Delta\phi=1.84$ radians.

For synchronous detection when δ is small,

$$I(\text{noise rms})=\Phi(M/\eta)^{1/2}\times(e\{B+A[1+J_0(\Delta\phi)-J_2(\Delta\phi)]/2\}\,\Delta f)^{1/2}=M\Phi(eI_{dc}'\,\Delta f)^{1/2},$$

where

Δf = noise equivalent bandwidth (assumed to be 1 Hz),

M = overall multiplication of electron current in the electron multiplier,

Φ = noise multiplication due to ion conversion and electron multiplication,

I_{dc}' = equivalent noise-producing dc ion current with sinusoidal modulation.*

η is the ion-to-electron conversion efficiency at the first dynode of the electron multiplier, which is approximately 1. It can be shown that (Reference 4)

$$\Phi=[1+\eta+(1-1/M)/(M^{1/n}-1)]^{1/2}(\eta)^{1/2},$$

where n is the number of stages of electron multiplication. Equating the noise and error signals, we find

$$\delta=\frac{M\Phi(2eI_{dc}'\,\Delta f)^{1/2}}{AJ_1(\Delta\delta)},$$

$$\Omega_{rms}=2\pi\,\Delta\nu_{rms}=\delta/T=2\,\delta W.$$

Therefore,

$$(\Delta\nu_{rms})^{-1}=\frac{\pi AJ_1(\Delta\phi)}{WM\Phi(2eI_{dc}'\,\Delta f)^{1/2}}=F,$$

when

$$\Delta f=1\text{ Hz},$$

where F is the figure of merit.

For a flop-in system with negligible background

$$A\doteq e\eta MN_0,$$

or

$$I_{dc}'\doteq e(N_0/2),$$

where N_0 is the peak ion current into the first dynode. Therefore,

$$(\Delta\nu_{rms})^{-1}=(1.83\eta/W\Phi)\,(N_0/\Delta f)^{1/2};$$

$$F=(1.83\eta/W\Phi)\,(N_0)^{1/2}\qquad\text{for }\Delta f=1\text{ Hz}.$$

If one measured the total noise current for a 1-Hz bandwidth at the output of the electron multiplier, with the microwave frequency set at a half-amplitude point of the resonance line, one would measure

$$I_{noise}=M\Phi(2eI_{dc}'\,\Delta f)^{1/2}.$$

Defining I_{sig} as A,

$$(\Delta\nu_{rms})^{-1}=(1.83/W)\times(I_{sig}/I_{noise}).$$

In the above derivation, we have made several assumptions. One is that our modulation rate is slow enough so that time-of-flight effects of the atoms through the apparatus may be neglected; another is that our measurement of $\Delta\nu_{rms}$ is for measurement intervals small compared with 0.5 second, corresponding to the assumed 1-Hz noise equivalent bandwidth.

In a rubidium vapor reference, the current in the photo detector is proportional to the number of photons received per second and may be expressed as

$$I=\eta N_0e[1-A(1+x^2)^{-1}],$$

where

η = quantum efficiency of the detector,
N_0 = number of photons per second incident,
e = charge of an electron,
A = peak fractional absorption of the gas cell,
x = frequency difference function.

The frequency difference function may be expressed as

$$x(t)=(\delta\nu+\Delta\nu\,\cos\omega t)/\tfrac{1}{2}W,$$

where $\delta\nu$ is the amount the average microwave frequency is detuned from resonance, $\Delta\nu$ the modulation amplitude, ω the modulation frequency, and W the full width at half amplitude of the absorption line. Solving for the current components in the photo detector, the error signal current at the fundamental of the modulation frequency is

$$I_e(t)=I_e\,\cos\omega t=(8A\,\delta\nu\;\Delta\nu\eta N_0e/W^2)\;\cos\omega t,$$

and the direct current component is

$$I_{dc}=\eta N_0e\left[1-\frac{A}{1+2(\Delta\nu/W)^2}\right]\doteq\eta N_0e,$$

since $A\ll1$. Equating the rms error signal to the rms noise amplitude as before, we find

$$(\Delta\nu_{rms})^{-1}=(4A\;\Delta\nu/W^2)\,(2\eta N_0/\Delta f)^{1/2},$$

or

$$\Delta\nu_{rms}/\nu_0=(W^2/4A\;\Delta\nu\nu_0)\,(\Delta f/2\eta N_0)^{1/2},$$

again assuming synchronous detection and an equivalent rectangular bandpass Δf for the control circuitry. As in the case calculated for atomic beam devices, these quantities represent the limiting value of the stability caused by reference

*We wish to thank L. S. Cutler for pointing out to us that the noise current with modulation and synchronous detection does not in general correspond exactly to that calculated from the dc component of the modulated ion current.

noise alone for very short averaging times or for very large bandwidths.

Typical parameters for a rubidium vapor standard are:

$$A = 0.001,$$
$$\Delta\nu/W = 0.2,$$
$$\eta = 0.9,$$

For $\Delta f = 1$ Hz,

$$F = 1.07 \times 10^{-3}(N_0/W)^{1/2}.$$

It is not appropriate to compare the constant 1.07×10^{-3} with that of 1.83 obtained for an atomic beam device because the values of N_0 are vastly different. In fact, rubidium vapor standards are far superior to current atomic beam standards with respect to the instability introduced by shot noise.

STABILITY AND TIME AVERAGING

In the foregoing derivations of the figure of merit, it was implicitly assumed that the time interval over which the frequency deviation is measured is small compared with $1/\Delta f$. Below, we derive—following Bagnall (Reference 5) and Cutler (References 6 and 7)—the general behavior of the rms frequency fluctuation for any averaging interval:

$$\langle \Delta\nu \rangle_T^2 = \lim_{\tau\to\infty}(\tau T^2)^{-1}\int_{-\tau/2}^{\tau/2} dt \times \int_t^{t+T} \Delta\nu(t')\, dt' \int_t^{t+T} \Delta\nu(t'')\, dt'',$$

when $\langle \Delta\nu \rangle_T^2$ is the mean-square fluctuation in frequency averaged over an interval T, $\Delta\nu(t)$ is $\nu(t) - \nu_0$ (the "instantaneous" frequency minus the average frequency) and

$$\nu(t) = (1/2\pi)\,(d\theta(t)/dt),$$

where $\theta(t)$ is the elapsed phase.

The expression above can be manipulated to give

$$\langle \Delta\nu \rangle_T^2 = T^{-1}\int_{-T}^{0} dt[1 + (t/T)]R(t) + T^{-1}\int_0^T dt[1 - (t/T)]R(t).$$

$R(t)$ is the autocorrelation function of the frequency deviation

$$R(t) = \lim_{\tau\to\infty}\tau^{-1}\int_{-\tau/2}^{\tau/2} dt'\ \Delta\nu(t)\ \Delta\nu(t'+t) = \frac{1}{2\pi}\int_{-\infty}^{\infty} \exp(j\omega t)\, S(\omega)\, d\omega,$$

$S(\omega) = |\ \Omega(j\omega)\ |^2$, and is the spectral power density of the frequency deviation. Substituting the Fourier transform of $S(\omega)$ for $R(t)$, we find that

$$\langle \Delta\nu \rangle_T^2 = \pi^{-1}\int_{-\infty}^{\infty} d\omega[S(\omega)\,(1 - \cos\omega T)]/(\omega T)^2 = \frac{1}{2\pi}\int_{-\infty}^{\infty} d\omega[S(\omega)\ \sin^2\omega T/2]/(\omega T/2)^2.$$

If the frequency-regulating control circuit can be described by the diagram shown in Figure 13–4, then

$$\Omega(j\omega) = [1 + KG(j\omega)]^{-1}N_{osc}(j\omega) + \frac{KG(j\omega)}{1 + KG(j\omega)}N_{ref}(j\omega),$$

where

$KG(j\omega)$ = open-loop response of the control circuit,
N_{osc} = equivalent noise signal of the oscillator,
N_{ref} = equivalent noise signal of the atomic reference.

Assuming for the moment that oscillator noise is negligible and recognizing that the reference noise has a flat spectrum, we can express the mean-square frequency fluctuation as:

$$\langle \Delta\nu \rangle_T^2 = (N_{ref}^2/2\pi) \times \int_{-\infty}^{\infty} d\omega \left| \frac{KG(j\omega)}{1 + KG(j\omega)} \right|^2 \frac{\sin^2\omega T/2}{(\omega T/2)^2}.$$

For the usual sort of control circuit the expression between the parallel lines approaches 1 as ω approaches zero, and goes to zero as ω becomes large. We therefore can readily find the asymptotic limits when T is very large and when T is very small.

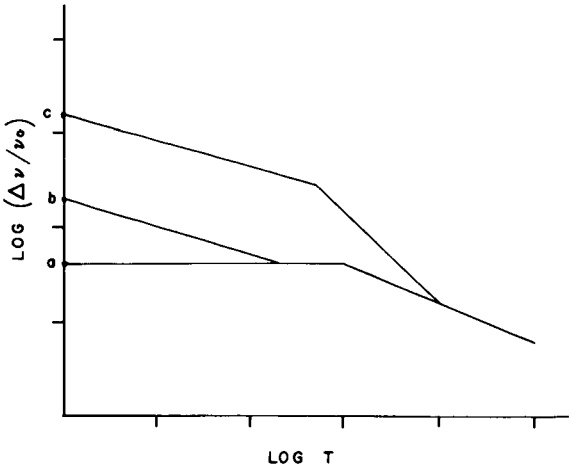

FIGURE 13–5.—Asymptotic behavior of the frequency stability as a function of averaging time for an oscillator controlled by a reference.

For very small T,

$$\langle \Delta\nu \rangle_T^2 = \frac{1}{2\pi}\int_{-\infty}^{\infty} d\omega S(\omega) = 2N_{ref}^2\, \Delta f,$$

where Δf is the equivalent rectangular bandwidth. When T is very large,

$$\langle \Delta\nu \rangle_T^2 = N_{ref}^2/T.$$

The two asymptotes intersect when the averaging time $T_{int} = 1/2\Delta f$. Making use of the definition of the figure of merit, we see that

$$N_{ref} = 1/(2F)^{1/2},$$

so that

$$\langle \Delta\nu \rangle^2 = \Delta f/F^2 \qquad (T \text{ short})$$

and

$$\langle \Delta\nu \rangle_T^2 = 1/2F^2T \qquad (T \text{ long})$$

The latter expression leads to the familiar result that

$$\Delta\nu_{rms}/\nu_0 = 1/\nu_0 F(2T)^{1/2} \propto 1/T^{1/2}.$$

In practice the frequency fluctuation will not decrease indefinitely with increasing averaging time, being limited sooner or later by long-term drifts and fluctuations caused by aging and changes in such ambient conditions as temperature and magnetic field.

If we now consider just the oscillator's random frequency fluctuation and make use of its known flat power spectrum, we can do the same calculations done for the shot noise. In particular, if $KG(j\omega) = K/j\omega$, the asymptotic limits are readily seen to be

$$\langle \Delta\nu \rangle_T^2 = N_{osc}^2/T \qquad (T \text{ short}),$$

$$\langle \Delta\nu \rangle_T^2 = N_{osc}^2/KT^2 \qquad (T \text{ long}).$$

The two asymptotes intersect for $T = 1/K$, which is one-half the value of T_{int}, the averaging time where the shot-noise asymptotes intersect. Figure 13–5 is a plot of the asymptotes of $\Delta\nu_{rms}$ as a function of averaging time, reproducing the results of Bagnell (Reference 4). Curve a is the contribution of noise from the reference alone. Curve b represents the asymptotic behavior when the oscillator frequency fluctuations for averaging times of the order of the control circuit time constant are less than those introduced by the reference, while curve c represents the opposite case. If random frequency fluctuations introduced by the atomic reference are larger than those of the quartz crystal oscillator, the best short-term stability is obtained by decoupling the oscillator from the atomic reference by making Δf sufficiently small so that, for the short averaging times of interest here (<1 sec), the performance is limited by the oscillator. If the oscillator-induced frequency fluctuations are the larger, then the best overall results are obtained by making the response time of the frequency control circuit as short as is practical.

Although above we have discussed the rms frequency fluctuations in terms of an average over an interval of time, one can also consider frequency fluctuations "averaged" in the frequency domain by limiting the frequency range of the frequency fluctuation $\Delta\nu(t)$ by a low-pass filter. For a rectangular passband low-pass filter we have

$$\langle \Delta\nu \rangle_f^2 = 2\int_0^f S(\omega)\, df,$$

where f is the bandwidth and $\langle \Delta\nu \rangle_f^2$ is the mean-square fluctuation averaged over the bandwidth f. This definition is useful for communications systems, since the rms quantity is equal to the noise that would be present in a frequency demodulator at the output of a postdetection filter of bandwidth f. Considering just the effect of

reference noise, if we substitute $1/2f$ for T, we have the same asymptotic limits for frequency interval averaging as for time interval averaging. The actual functions, as opposed to the asymptotic limits, will not be identical but will be quite close in value. The effect of oscillator and other noise introduced in the system will in general be different with frequency interval averaging than with time interval averaging.

PERFORMANCE OF VARIOUS ATOMIC REFERENCES

In Table 13–1 are given the figures of merit and values of $\Delta\nu_{rms}/\nu_0$ for a 1/2-Hz equivalent noise bandwidth (or a 1 second averaging time) for various atomic references. The numbers for thallium tubes, for instance, do not represent the ultimate performance that might be obtained from tubes of this type. While some are clearly superior to others, obviously there are considerations other than short-term stability for a frequency standard—long-term stability, for example, or size.

Figure 13–6 shows the predicted $1/T^{1/2}$ dependence of $\Delta\nu_{rms}/\nu_0$ for a standard using a BLR-2 cesium beam reference. The time constant of the control circuit of this standard is considerably less than 1 second, so that the leveling off expected for short averaging times does not appear. The measured frequency fluctuation agrees quite well with that expected from shot noise. The frequency fluctuation was measured by comparison with a rubidium vapor frequency standard. Two synthesized frequencies, one from each standard, were mixed. The period of an appropriate number of beat cycles to correspond to the desired averaging time was measured many times, and the frequency fluctuations were then calculated from the measured fluctuations in the length of the period. Since the short-term stability of the rubidium standard is considerably better than that of the cesium standard, the measured fluctuations essentially are due to the latter.

TABLE 13–1

Standard	Type	F	ν/ν_0 (1-sec averaging time)
V–4700	Rb vapor	15	6.8×10^{-12}
BLR–2	25″ Cs beam	1.8	4.4×10^{-11}
BLR–3	16″ Cs beam	0.6	1.3×10^{-10}
BLR–4	27″ Cs beam	*(40)	(2×10^{-12})
—	17.6″ Tl beam	(2.1)	(1.6×10^{-11})
—	17″ double resonance Tl beam	(5.5)	(6×10^{-12})
—	30″ Tl beam	(13)	(2.6×10^{-12})

*Numbers in parentheses are estimated values for devices not yet built or of hypothetical design.

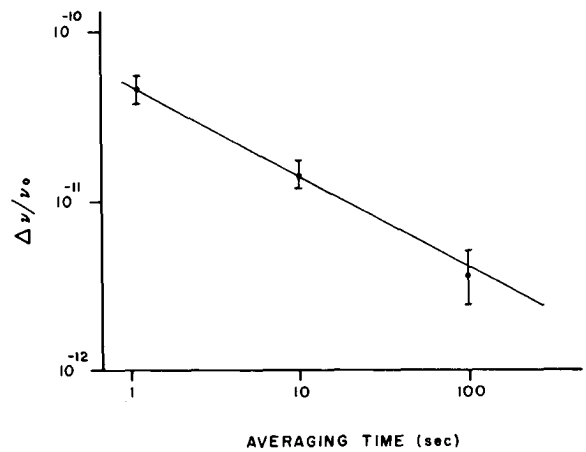

FIGURE 13–6.—Experimental dependence of frequency stability on averging time for a frequency standard using a BLR–2 cesium beam tube.

CONCLUSION

From averaging times less than 1 second, the stability of a quartz crystal oscillator is impaired by coupling it to an atomic reference with too low a figure of merit. To make a standard where the frequency fluctuations introduced by the reference would be less than those of the crystal oscillator—1×10^{-11} for a 1-second averaging time—a figure of merit greater than 12 for a rubidium vapor standard, 8 for a cesium beam tube, or 4 for a thallium beam tube would be required. For a sufficiently large figure of merit, it obviously is possible to obtain a superior short-term performance from a frequency-controlled oscillator than from an independent one over a certain range of averaging times. Current rubidium vapor standards already meet this criterion, and it appears to be completely feasible in small,

portable atomic beam tubes. One such cesium tube, the BLR-4, is currently being constructed, and other high-performance tubes may be expected in the future. We believe also that there are still improvements to be obtained in rubidium vapor standards in the area of short-term stability, both in the atomic reference and in other noise-contributing parts of the system.

REFERENCES

1. Mockler, R. C., Beehler, R. E., and Snider, C. S., "Atomic Beam Frequency Standards," *IRE Transactions on Instrumentation I*—9, 120 (1960).
2. Packard, M. E., and Swartz, B. E., "Rubidium Vapor Frequency Standard," *IRE Transactions on Instrumentation I–11*, 215 (1962).
3. Ramsey, N. F., "Molecular Beams," London: Oxford University Press, 1956.
4. Shockley, W., and Pierce, J. R., "A Theory of Noise for Electron Multipliers," *Proc. IRE 26*, 321 (1938).
5. Bagnall, J. J., Jr., "The Effect of Noise on an Oscillator Controlled by a Primary Reference," *NEREM 1959* Record, pp. 84–86.
6. Cutler, L. S., Private Communication.
7. Bagley, A. S., and Cutler, L. S., "A Modern Solid-State Portable Frequency Standard," in: *Proc. 18th Annual Symposium*, Atlantic City: U.S. Army Electronics Labs., May 4–6, 1964, pp. 344–365.

14. AN OPTICALLY PUMPED Rb^{87} MASER OSCILLATOR*

P. DAVIDOVITS

Columbia University
Columbia Radiation Laboratory
New York, New York

A self-sustained Rb^{87} maser oscillator has been developed. The maser oscillates on the Rb^{87} hyperfine transition frequency (approximately 6,835 Mc/sec). Because of its simplicity and potential frequency stability, the device promises to be a very useful frequency standard.

A few months ago we developed at the Columbia Radiation Laboratory a rubidium maser oscillator which we think will be a very useful frequency standard (Reference 1). The physical size of the device is about a cubic foot; the operating temperature is about 60°C. Because of its relatively high output power, this device may have the best short-term stability of any other frequency standard so far developed.

Because of the frequency shift caused by buffer gas, the rubidium maser will not be a primary standard. As a secondary standard, however, it may be a device of unsurpassed stability and simplicity.

Figure 14–1 shows a simplified energy level diagram for Rb^{87}. The ground state is the $5S_{1/2}$ state. The quantum numbers $F=2$ and $F=1$ designate the two ground-state hyperfine levels. The energy difference between the two levels corresponds to 6835 Mc/sec. The substates designated by the m_F numbers are the Zeeman sublevels. It is between the $F=2$ and $F=1$ ground-state levels that we want to obtain maser oscillation. The $P_{3/2}$ and $P_{1/2}$ states are separated from the ground state by energies corresponding to 7800 A and 7947 A, respectively. To obtain maser action, an excess population must be produced in the $F=2$ state with respect to the $F=1$ state. Overpopulation can be produced by optically exciting atoms out of the $F=1$ state into one or both $5P$ states. From the $5P$ states the atoms decay into both the ground-state $F=2$ and $F=1$ levels. Since atoms are excited out of the $F=1$ state only, while the decay proceeds into both states, an excess population is built up in the $F=2$ state. This process is an example of optical

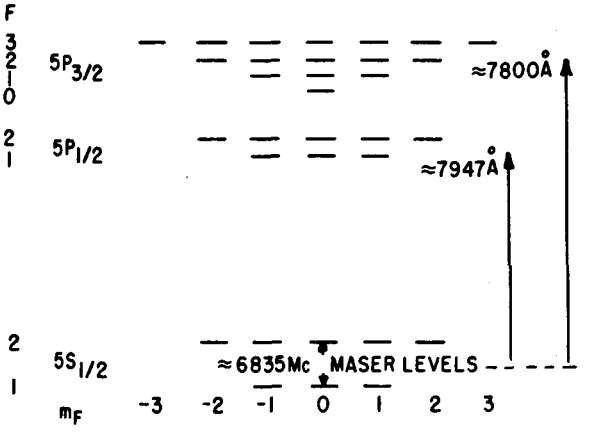

FIGURE 14–1.—Simplified energy level diagram for Rb^{87}.

pumping. The pumping light needed here must, of course, be free of radiation connecting the $F=2$ state with the $5P$ states. Resonance radiation from a Rb^{87} discharge lamp will contain the desired $5S_{1/2}$ $F=1\rightarrow 5P$ pumping light as well as the unwanted $5S_{1/2}$ $F=2\rightarrow 5P$ component. The ground-state $F=2$ and $F=1$ levels are too close together to be separated by conventional optical

*This work was supported wholly by the Joint Services Electronics Programs (U.S. Army, U.S. Navy, and U.S. Air Force) under Contract DA-36-039 SC-90789.

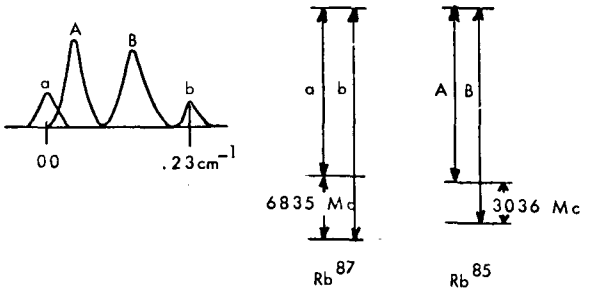

FIGURE 14–2.—Hyperfine structure of rubidium resonance line (see Reference 2).

filters. A method of filtering the undesired component has been described by Bender (Reference 2). The method utilizes the energy-level differences between Rb^{87} and Rb^{85}, which is the other stable isotope of rubidium.

Figure 14–2 shows a very simplified energy diagram for Rb^{87} and Rb^{85}. The desired light component is designated by *b*. The upper hyperfine levels of the two isotopes (levels *a* and *A*) overlap, whereas the lower hyperfine levels are distinct. Thus, if Rb^{87} resonance radiation is passed through a Rb^{85} filter cell, component *a* is absorbed by component *A* while component *b*, which is the desired pumping light, passes through the filter essentially unaltered.

Figure 14–3 shows the effectiveness of this filtering technique. With the Rb^{85} filter-cell temperature at 69°C, most of the undesired component is filtered out.

The Rb^{87} is deposited at the tip of a glass cell designed to fit a TE_{011} microwave cavity. The rubidium vapor in the cell is in equilibrium with the deposit in the tip. The cell also contains an inert buffer gas whose purpose will be described later. The cell is placed inside the microwave cavity, and the system is illuminated by pumping light to produce overpopulation. If the amplification of the atomic system by stimulated emission is large enough to compensate for the system losses, self-sustained maser oscillation will be obtained.

There are a number of factors influencing the maser gain. Some of them are: buffer gas, system temperature, pumping light intensity, and cavity design. Not all of these will be examined in this paper but, to illustrate the method, the effect of the *buffer gas* will be described.

It was stated that the Rb^{87} is contained with an inert buffer gas. The purpose of the buffer gas is: (1) to reduce the Doppler width, (2) to increase the Rb^{87} diffusion time to the walls, and (3) to increase the optical pumping efficiency by quenching reradiation from excited levels.

It has been shown both classically (Reference 3) and quantum mechanically (Reference 4) that, by reducing the mean free path of a radiating atom, the Doppler width can be reduced. For example, for the hyperfine transition of Rb^{87} the Doppler width at room temperature is 9.6 kc/sec. By containing the rubidium with 10 torr of nitrogen buffer gas, the Doppler width is reduced to 20 cps.

Collisions of the atoms with the container walls are almost completely disorienting. In the absence of a buffer gas the mean time for wall collisions would be about 10^{-4} sec, resulting in a bandwidth of about 3 kc. Nitrogen buffer gas at 10-Torr pressure reduces this bandwidth to about 2 cps.

Reradiation from the excited $5P$ states will depopulate the $F=2$ states and so significantly reduce the pumping efficiency. Reradiation can be prevented by collisions of the second kind with buffer-gas atoms. In these collisions the rubidium

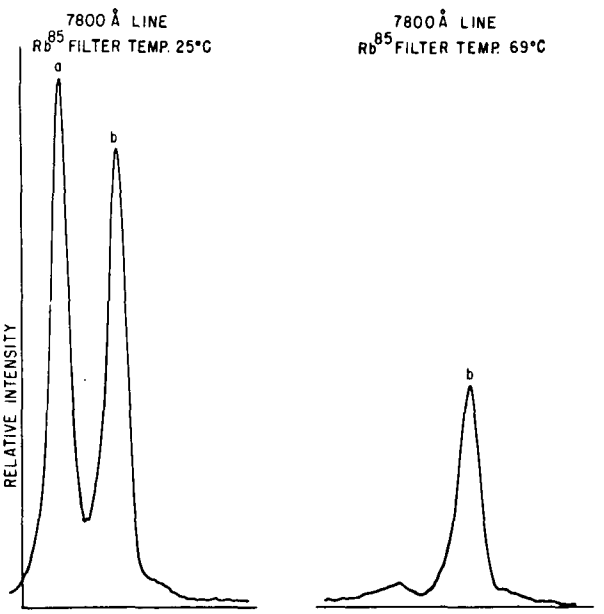

FIGURE 14–3.—Spectra of Varian X49–609 Rb^{87} spectral lamp at two Rb^{87} filter temperatures.

is deexcited by transmitting its energy to the buffer-gas atom. This process is called *quenching.*

The maser gain depends on the inert buffer-gas pressure. At an insufficiently low pressure, there are not enough buffer-gas molecules to perform the stated tasks. If an excess of buffer gas is used, the disruptive effect of collisions between oriented Rb^{87} atoms and buffer-gas molecules becomes significant and the maser gain decreases. Hence, there is an optimum buffer gas pressure for maximum gain. The effectiveness of nitrogen, neon, helium, argon, and hydrogen buffer gases was tested. Nitrogen at 11-Torr pressure yielded maximum gain. These results are shown in Figure 14–4. Various mixtures of buffer gases were tried, and the results are shown in Figure 14–5. The gain was measured for various pressures of nitrogen with argon, neon, and helium. The effect of argon with nitrogen also is shown. It can be seen that the addition of nitrogen in each case initially increases the gain. Since the pressure of the original gas is sufficient to render wall collisions and Doppler width insignificant, it can be concluded that adding nitrogen improves the quenching. From similar considerations it also can be shown that, for maximum maser gain, there are optimum

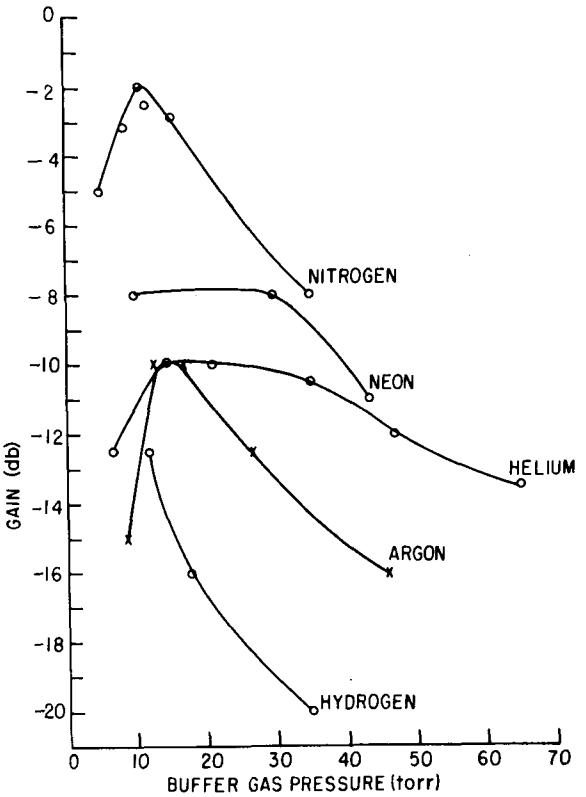

FIGURE 14–4.—Gain vs. buffer gas pressure.

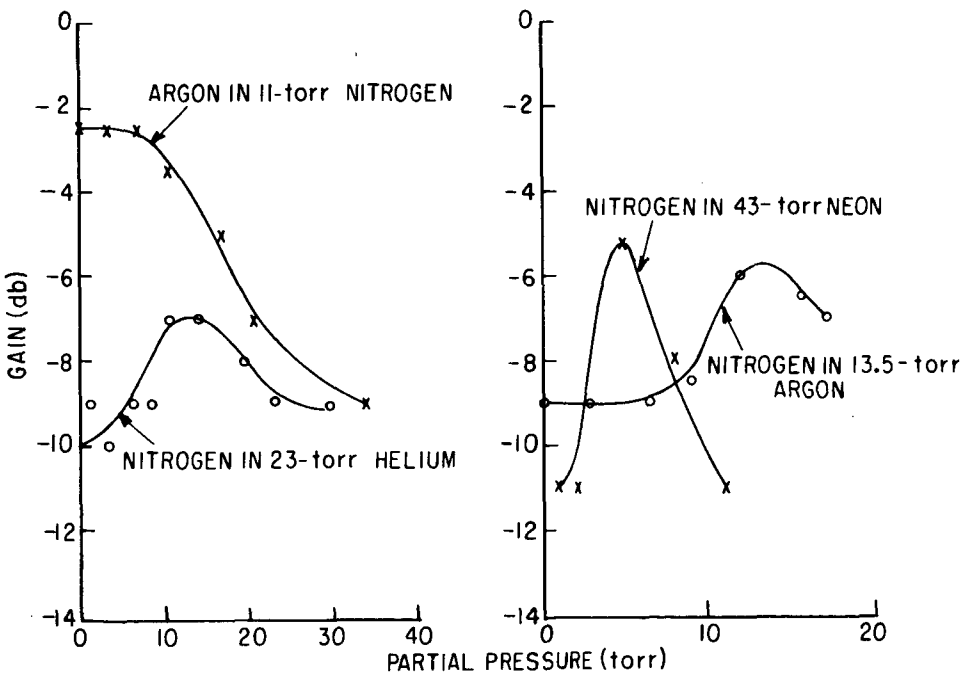

FIGURE 14–5.—Gain vs. partial buffer gas pressure.

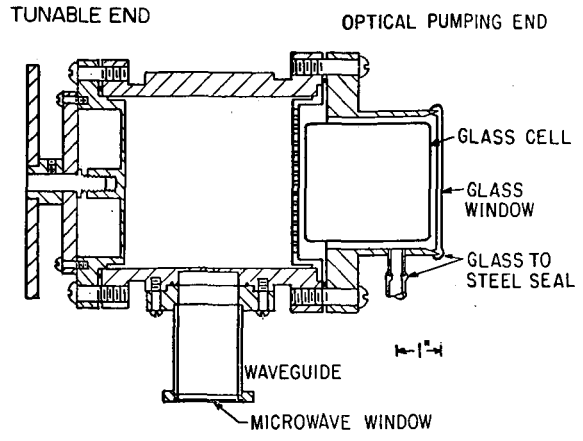

FIGURE 14–6.—Vacuum-tight cavity.

values for the operating temperature and the pumping light intensity.

For frequency stability it is desirable to obtain maser oscillation at the

$$(5^2S_{1/2}\ F=2,\ m=0)\rightarrow(5^2S_{1/2}\ F=1,\ m=0)$$

transition, since this transition is first-order magnetic-field independent.

Even with all parameters optimized, the gain of the first model rubidium maser was not sufficiently high to obtain oscillation on the field-independent transition. The maser gain may be increased by reducing the magnetic field until the hyperfine Zeeman transitions overlap. In this way, stimulated emission from the hyperfine Zeeman levels adds. This technique requires that the net field be reduced to 100 μG or less. Self-sustained maser oscillation was produced in a magnetically shielded system. The shield consisted of three concentric Moly-Permalloy cylinders with suitable end caps.

A few weeks ago we obtained self-sustained oscillation between the

$$(5^2S_{1/2}\ F=2,\ m=0)\rightarrow(5^2S_{1/2}\ F=1,\ m=0)$$

first-order field-independent transition. Oscillation occurred in a magnetically *unshielded* system.

Oscillation on the single

$$(F=2,\ m=0)\rightarrow(F=1,\ m=0)$$

transition was achieved by increasing the maser gain through the use of a higher Q cavity than with the earlier oscillator. The new microwave cavity is vacuum-tight.

The vacuum cavity is made of copper-plated stainless steel type 304. Tests indicate that neither copper nor stainless steel react significantly with rubidium vapor at temperatures up to 250°C. The cavity is designed to operate in the TE_{021} mode and has an unloaded Q of approximately 50,000. Thus, the cavity has a Q about two times as high as the TE_{011} cavity used in the previous maser oscillator. The higher Q is achieved by using the higher mode configuration and by the elimination of the glass cell used to contain the Rb^{87}. The glass cell lowered the cavity Q.

The salient features of the cavity are shown in Figure 14–6. The cavity can be tuned over a range of ± 3 Mc/sec by means of a flexible membrane at one end. Pumping light is admitted through the other end, where the cavity is terminated by a perforated end plate and a stainless-steel-to-glass feather-edge seal. The microwave port, which is designed for approximately 20 percent coupling to the transmission line, is sealed by means of a mica-to-steel seal. Although this seal is magnetic, it is far enough removed from the cavity so that the maser performance is unaffected. The evacuated glass cylinder placed between the perforated end plate and the glass window prevents absorption of pumping light by rubidium vapor, which would be there in the absence of the cell. The rubidium is distilled into the cavity through the side arm shown in the figure. All vacuum seals are made with annealed aluminum O-rings.

Self-sustained maser oscillation is observed at a cavity temperature of about 50°C. The oscillator power output is approximately 10^{-11} W and is limited by the intensity of the pumping light. In the present system, pumping is done from one end only. Furthermore, there is a considerable distance between the pumping light and the active portion of the cavity. More intense pumping light and design improvements should raise the output power to 10^{-10} W, or higher. Simple estimates indicate that it may be possible to increase the power output to 10^{-8} W. In the earlier magnetically shielded maser, the optical pumping

efficiency was higher and the power output was 10^{-10} w. The high power output of this maser will insure better short-term stability than is obtainable from any other existing frequency standard.

Calculations by Dr. R. Vessot, presented in an earlier paper at this conference (*These Proceedings*, paper 10), show that the rubidium maser may have a short-term stability two orders of magnitude better than the present hydrogen maser.

There are three important factors which limit the long-term stability of the rubidium maser oscillator: (1)t he temperature-dependence of the frequency shift resulting from the presence of the buffer gas, (2) the temperature-dependence of the cavity frequency and consequent line pulling, and (3) the light shift. Calculations show that a long-term stability of 1 part in 10^{12} is possible.

REFERENCES

1. DAVIDOVITS, P., "An Optically Pumped Rb^{87} Maser Oscillator," *Appl. Phys. Letters 5*, 15 (1964).
2. BENDER, P. L., "Atomic Frequency Standards and Clocks," *Quantum Electronics*, C. H. Townes, Ed. (Columbia University Press: New York), pp. 111–112, 1960.
3. WITTKE, J. P., and DICKE, R. H., "Redetermination of the Hyperfine Splitting in the Ground State of Atomic Hydrogen," *Phys. Rev. 103*, 620 (1956).
4. DICKE, R. H., "The Effect of Collisions upon the Doppler Width of Spectral Lines," *Phys. Rev. 89*, 472 (1953).

15. MEASUREMENTS OF SHORT-TERM FREQUENCY STABILITY USING MICROWAVE PULSE-INDUCED EMISSION

M. ARDITI

ITT Federal Laboratories
Nutley, New Jersey

Measurements of short-term frequency stability of microwave signals can be simplified if a source of good short-term stability can be used for comparison. Microwave pulse-induced emission in the alkali vapors can provide such a signal for periods of 10 to 20 msec. The short-term frequency stability of such a signal in a rubidium gas cell has been measured at 6834 Mc by beating two nearly identical gas cells against each other. A photographic method was used to measure the period of the beat frequency over periods of time of a few milliseconds. The results of the measurements show that the short-term frequency stability was as good, or better, than the resolution of the method—in this case: 1 part in 10^9 for periods of measurement of 1 millisecond. The microwave pulse-induced emission signal from the rubidium cell also was used to measure the short-term frequency stability of microwave signals produced from crystal oscillators and varactor harmonic generators. The results of the tests indicate that such signals can be relatively free of phase instability, even for such large multiplication factors.

In some modern airborne radar, the requirements for a stable microwave frequency source are such that the stability is needed only for a very short time corresponding to the two-way propagation time of the radar signal. The need arises, then, for a method of measuring short-term frequency stability of a microwave source for periods of the order of milliseconds, for example.

The methods of measurements are simplified if a source of microwave signal of very good short-term stability can be used for comparison with the radar source.

Stable sources of microwave energy can be obtained with stable crystal oscillators and well-designed multipliers and varactor harmonic generators, with spin oscillators, with masers, or with klystrons phase-locked to crystal oscillators or to masers.

The remarkable spectrum purity of the microwave oscillation from ammonia or hydrogen masers has been reported in the past (References 1 and 2). In this paper we will study the frequency stability of microwave pulse-induced emission in alkali vapor. Like the masers, the pulse-induced microwave emission does not require any feedback to lock a crystal oscillator to an atomic resonant frequency; and, consequently, the short-term frequency stability is not limited by the time constant in the feedback loop circuit.

The microwave pulse-induced emission is relatively easier to obtain than maser action because it does not require population inversion or atomic beam separation, or to satisfy the threshold condition for self-sustained oscillation; and it is applicable in a wide range of microwave frequencies from 1420 Mc for hydrogen, to 1771 Mc for sodium, 3035 Mc for rubidium 85, 6834 Mc for rubidium 87, and 9192.6 Mc for cesium, for example. The pulse-induced emission signal also is less sensitive to frequency-pulling by the tuning of the cavity than the maser signal and consequently is less susceptible to short-term frequency instabilities due to mechanical vibrations. However, the microwave pulse-induced emission signal is damped by relaxation processes within a relatively short time; and special techniques must be adapted to use this signal for the measurements of the short-term stability of crystal oscillators and multiplier chains—or other sources of microwave

oscillations. Before describing the methods used for these measurements, a brief description of the characteristics of microwave pulse-induced emission in alkali vapors will be given. Although rubidium 87 will be considered more particularly, the discussion applies also to other alkali metals such as hydrogen, sodium, or cesium.

MICROWAVE PULSE-INDUCED EMISSION

A comprehensive article on microwave pulse-induced emission has been published by Dicke and Romer (Reference 3).

In the case of the microwave pulse-induced emission in an alkali vapor, optical pumping (Reference 4) is applied to a rubidium cell, for example, to produce a greater difference in the populations of the $F=2$ and $F=1$ hyperfine levels in the ground state. The $\Delta F=1$, 0–0 transition is used because of its relative insensitivity to magnetic field. The cell is contained in a microwave cavity, and a short pulse of microwave energy at the resonance frequency of a microwave hyperfine transition is applied to the cavity. At the end of the exciting pulse, the pulse-induced emission from the atoms radiating in the cavity is detected in a microwave superheterodyne receiver. It is not even necessary that the microwave frequency of the exciting pulse should be exactly at the resonance frequency since, if the pulse length T_p is sufficiently short and the spectrum sufficiently broad, there will be enough energy at the resonance frequency to induce the transition.

Signal Power

For a low pulse repetition rate, it can be shown (Reference 3) that there is an optimum in the length of the exciting pulse T_p for maximum induced emission power. This has been checked experimentally, as shown in Figure 15–1 where the amplitude of the microwave pulse emission signal just after the end of the exciting pulse has been plotted as a function of T_p. In most experiments, the smallest value of T_p is chosen; and normally this corresponds to values of 1 to 5 msec for the cells used.

It has been noticed also that for a given length of T_p the amplitude of the pulse-induced emission signal is a maximum for several frequencies of the exciting microwave, centered around the resonant frequency and separated by $1/T_p$, with a maximum maximorum of the amplitude at the resonance frequency.

The pulse-induced emission power radiated from the microwave cavity is given approximately (Reference 3) by Equation 1.

$$W \approx \pi(n_1-n_2)^2 V Q_0 \omega |\mu_{121}|^2 (\hbar\omega/2kT_0)^2, \qquad (1)$$

where $|n_2-n_1|$ represents the number of atoms per cm^3 of the excess population of two energy levels between which the transition takes place, V the volume of the cavity, and Q_0 the unloaded Q of the microwave cavity.

This assumes, when the gas is excited by a microwave pulse, that the memory of the phase of previous pulses has been destroyed by some relaxation mechanism. For sufficiently long inter-

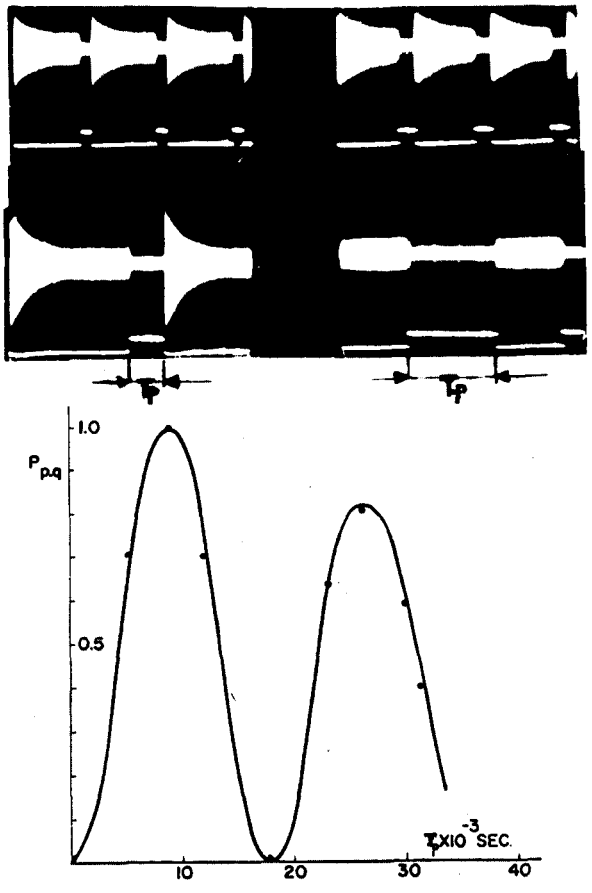

FIGURE 15–1.—Amplitude of emitted signal at end of exciting pulse as a function of pulse size.

vals between pulses, thermal relaxation would be enough; but even for shorter pulse intervals a strong relaxation could be obtained if a pulse of resonant light is used before each microwave exciting pulse—because then the rubidium atoms are raised to excited states, with almost complete disorientation of the spin system and with a resulting loss of the phase memory of the preceding pulse.

If Equation 1 is applied to the case of a rubidium cell optically pumped, in the best conditions, a power between 10^{-11} and 10^{-12} watt could be expected from the pulse-induced emission. This also has been checked experimentally; and, since this is not a large power, sensitive receivers and filter techniques are necessary to make full use of this power.

Relaxation Processes

The calculations of the power expressed in Equation 1 assume that the component of the macroscopic dipole moment in the direction of the exciting field is constant. Actually this power is damped by several relaxation processes, such as: the relaxation produced by spin exchange in collisions between rubidium atoms, the relaxation due to collisions between the rubidium atoms and the buffer gas atoms, the relaxation due to collisions between rubidium atoms and the wall of the cell, the relaxation due to the light used in optical pumping if continuous illumination of the cell is used, and the relaxation due to magnetic field inhomogeneities. A discussion of these various relaxation processes is beyond the scope of this paper but can be found in a number of papers recently published (Reference 5).

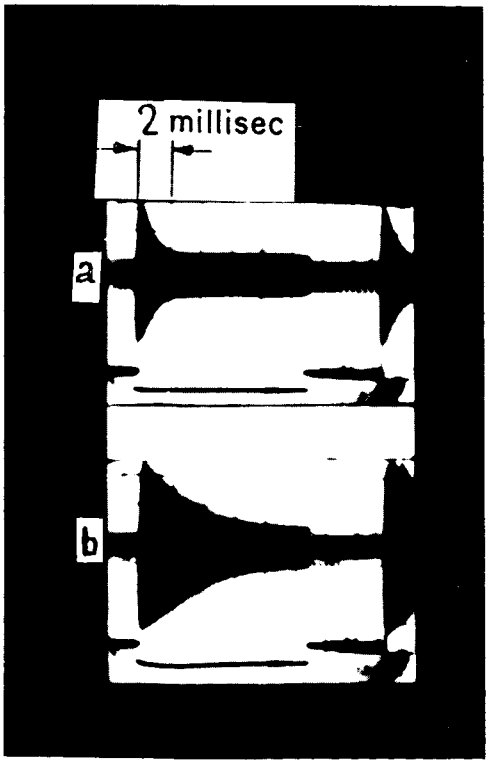

FIGURE 15–2.—Relaxation of emitted signal produced by light from optical pumping; (a) continuous illumination, (b) pulse of light terminated before end of exciting pulse.

As an example, in the case of the $\Delta F = 1$, 0–0 transition in rubidium, the relaxation produced by the light is shown in Figure 15–2, which is a photograph of the exponential decay of the pulse-induced emission signal: In (a), the cell is under continuous illumination; and, in (b), the cell receives a pulse of light which is terminated before the end of the microwave exciting pulse so that the atoms relax in the dark. It can be seen that in this case a much larger relaxation time is obtained. Also by pulse-exciting the lamp used for the resonant light, a somewhat better optical pumping efficiency is obtained, resulting in a larger signal for the microwave pulse-induced emission than with continuous illumination.

As an order of magnitude, and again for the case of the $\Delta F = 1$, 0–0 transition, relaxation times of the order of 10 to 20 milliseconds can be obtained in a rubidium vapor cell filled with neon as a buffer gas at a pressure of about 10 Torr, in a temperature range from 45° to 30°C. Somewhat longer relaxation times could be obtained with coated cells without buffer gas (Reference 6), but data are lacking for the signal-to-noise ratio of the detection of the pulse-induced emission in such cells.

Frequency Stability

Long-term frequency stability

For a given cell, at a fixed temperature and fixed ambient magnetic field, the frequency of the pulse-induced emission signal of the 0–0 transition is very stable. The long-term frequency

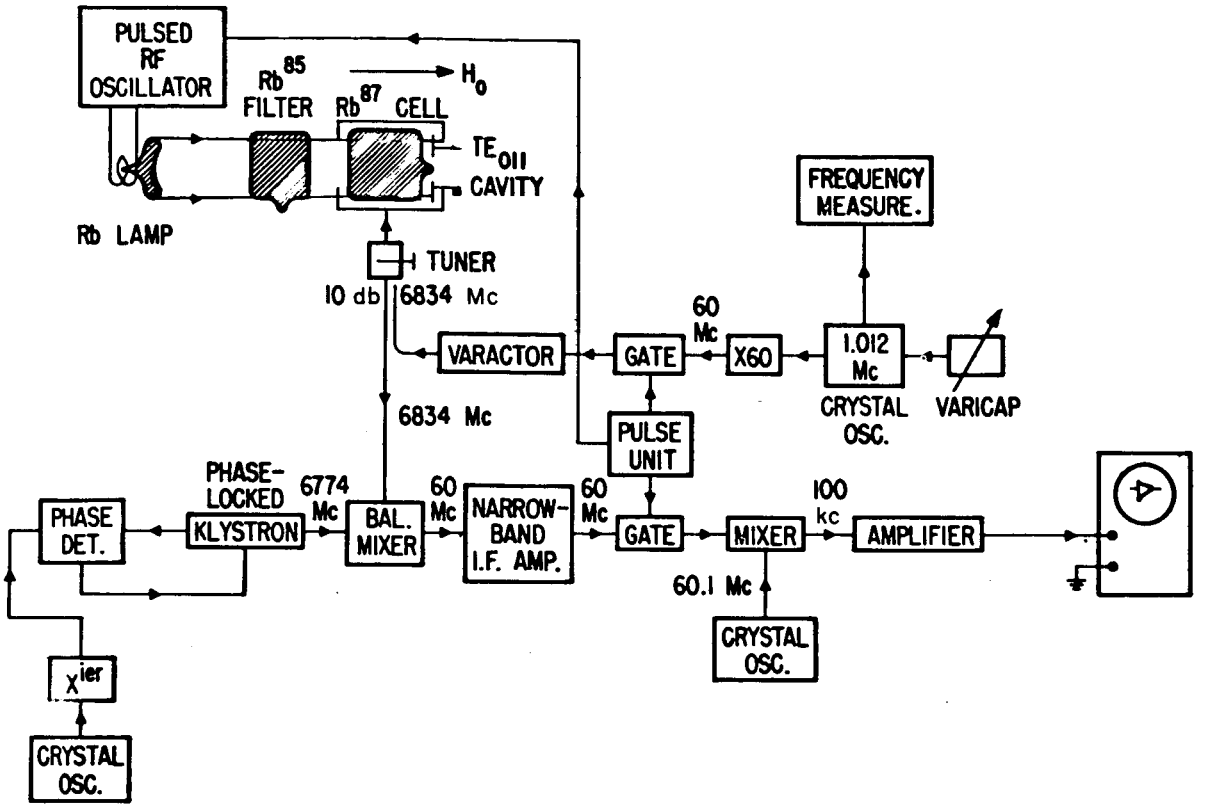

FIGURE 15–3.—Measurement of long-term stability of microwave pulse-induced emission signal. Experimental setup.

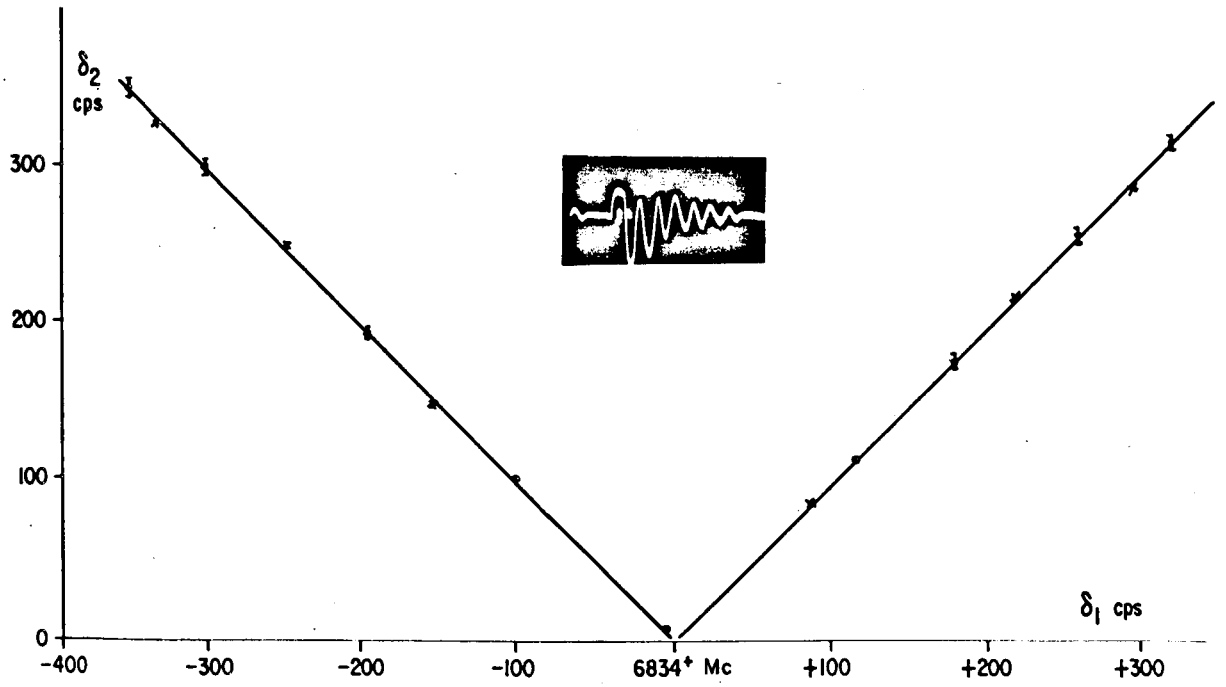

FIGURE 15–4.—Frequency of beat signal as a function of frequency difference between frequencies of microwave excitation and microwave-induced emission.

stability of the emitted signal has been checked experimentally in the following way:Referring to Figure 15–3, a rubidium vapor cell containing a buffer gas is enclosed in a microwave cavity operating in the TE_{011} mode. The cavity is excited by a pulse of microwave energy at a frequency near the resonance frequency of the 0–0 transition. This microwave energy is produced from a relatively stable crystal oscillator and multiplier chain up to 60 Mc and varactor harmonic generation up to 6834 Mc. In the multiplier chain a gated amplifier, controlled by a pulse unit, permits the microwave energy to be delivered in pulses of known timing and duration. The same pulse unit controls the RF oscillator of the lamp used for optical pumping, so that the light is cut off during the detection of the pulse-induced emission signal. This detection is made with a microwave superheterodyne receiver, with double mixing to reduce the bandwidth of the receiver and increase the signal-to-noise ratio of the detection. In order not to overload the receiver, a gate in the IF amplifier cuts off the receiver for the duration of the microwave pulse excitation.

The emitted signal is mixed in the receiver with a small signal derived from the exciting microwave radiation, and the beat note is displayed with a broadband detector on an oscilloscope. It was observed that the beat frequency varies linearly with the frequency of the microwave excitation, to an accuracy of a few parts in 10^{10} for measuring times of 30 msec, showing that the frequency of the emitted signal was constant to this accuracy, independent of the frequency of the microwave excitation and of the length and strength of the exciting pulse (Figure 15–4).

By using a pulse of light terminating before the end of the microwave exciting pulse, it has been found also that the frequency of the emitted signal is independent of the intensity of the pumping light, thus removing the "light-shift" effect (Reference 7) associated with optical pumping under continuous illumination. Under these conditions the frequency of the emitted signal depends only on the buffer gas pressure, the temperature of the cells, and the magnitude of the ambient magnetic field (Reference 7). These effects can be greatly reduced by proper mixtures of buffer gases and adequate magnetic shielding of the cell (Reference 8).

Finally, another interesting feature of the pulse-induced emission is its relative insensitivity to the tuning of the microwave cavity. No frequency pulling has been found here comparable with the effect observed in auto-oscillator masers (Reference 9). For example, a detuning by more than 500 kc on each side of the cavity tuning at 6834 Mc did not produce any noticeable frequency shift—none, at least, greater than a few parts in 10^{10}, which was the limit of accuracy of our measurements. A somewhat similar effect has been observed (Reference 10) in the molecular beam generator with two resonators through which a beam of excited molecules passes in series. It was observed in this case that maser oscillations took place in the first cavity and that oscillations were also excited in the second resonator, but that the frequency of these oscillations did not depend on the tuning of the second cavity.

As a suggestion, this effect could be used for tuning a hydrogen maser in the following way: The signal from a self-sustaining oscillation from a hydrogen maser could be mixed in a detector with the induced emission signal from a pulse-excited hydrogen cell—at the same gas pressure—and the tuning of the hydrogen maser cavity adjusted until a zero beat is obtained.

Short-term frequency stability

Although the previous measurements of the frequency of the pulse-induced emission were made over short periods of time—smaller than 30 msec, for example, they could not be considered conclusive with regard to the short-term frequency stability of the emitted signal because it would have been difficult to ascertain the part due to instabilities in the crystal oscillator and multiplier chain used for comparison. For this reason, the short-term stability was measured by comparing the pulse-induced emission signals produced by two nearly identical gas cells pulse-excited by the same oscillator.

The experimental setup is shown in Figure 15–5. A beat signal is obtained at the output of the receiver and can be detected with a broadband detector or passed into a narrow-band receiver and then detected (Figure 15–6). In this latest case, some care should be taken in the measurements because a transient produced by the pulse in the narrow-band amplifier could be superimposed on the emitted signal and thus could

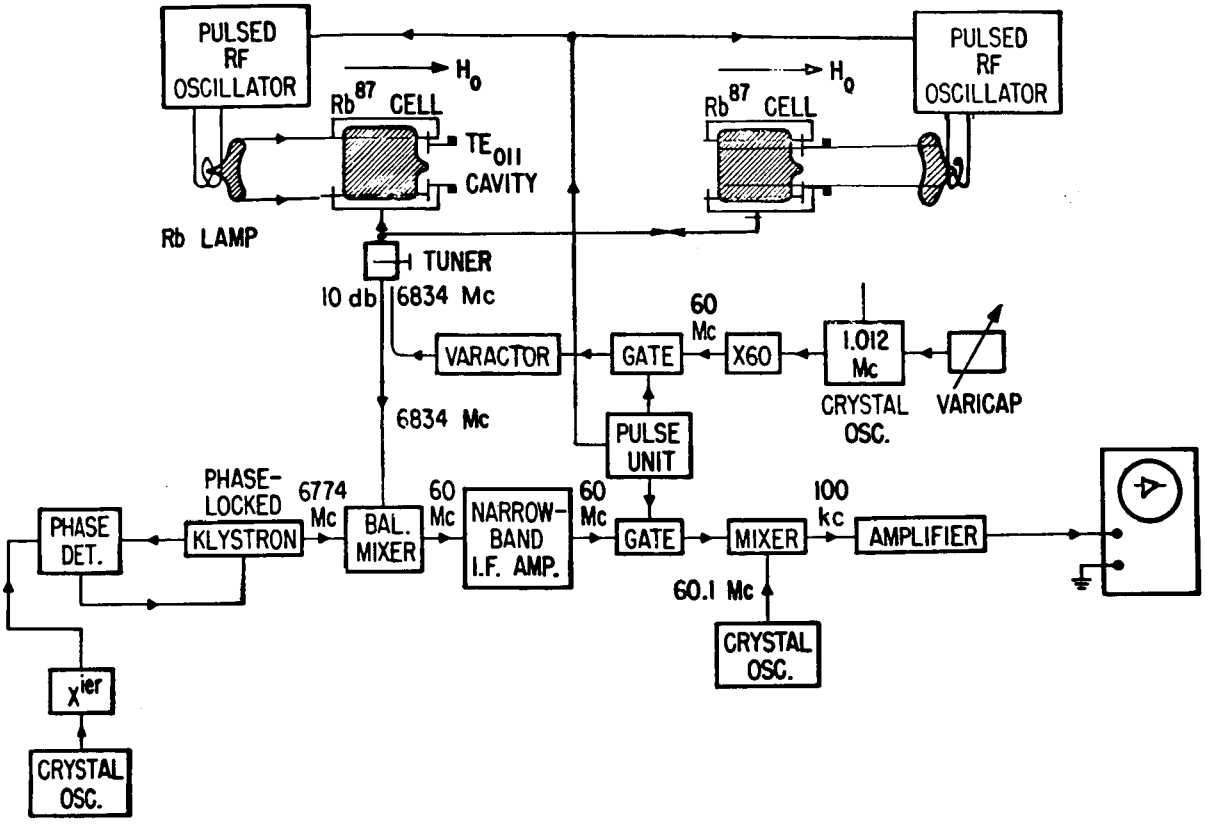

FIGURE 15–5.—Measurement of short-term frequency stability of microwave pulse-induced emission. Experimental setup.

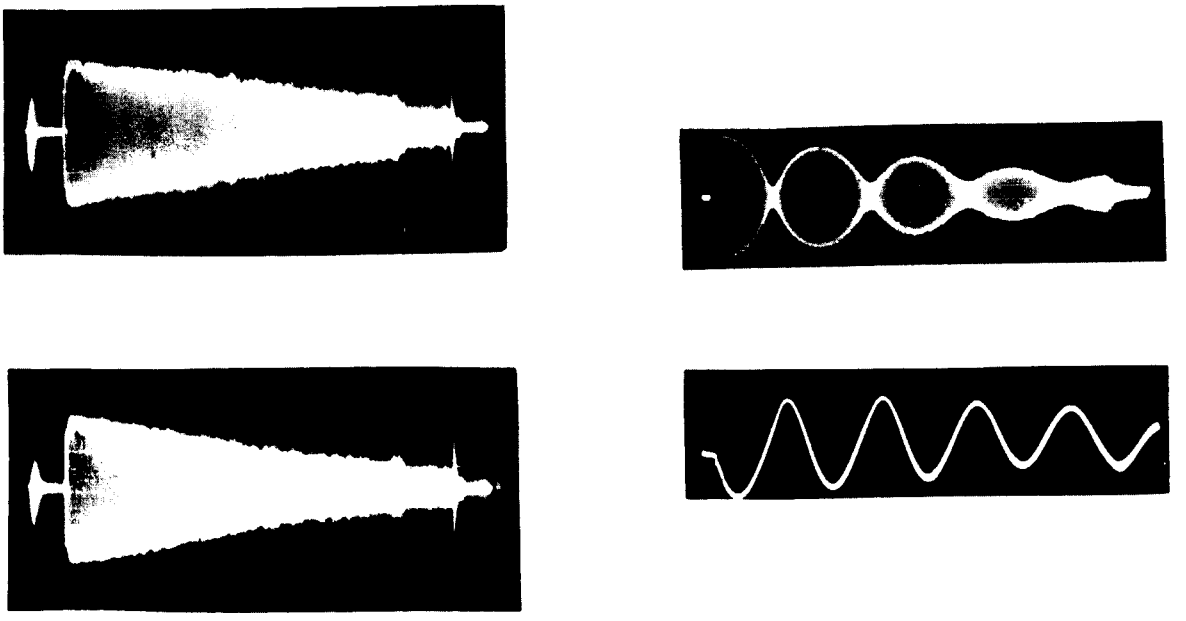

FIGURE 15–6.—Beat signals from pulse-induced emission signals from two cells. At left, exponential decay of emitted signal from each cell; at right, beat signal in a broadband detector or through a narrow-band amplifier and detector.

reduce the accuracy of the measurements; this transient should then be sufficiently short compared with the total time available for the measurement. This effect puts a lower limit on the bandwidth of the receiver.

The frequency of the beat signal can be measured in a number of ways. For example, an electronic counter with a period-measuring device can be used to count the number of zero crossings in a given time interval, or a frequency discriminator or phase-detector can be used. For practical reasons an oscilloscope with a calibrated time base was used here, and photographs were taken of a single scan corresponding to 33.3 milliseconds total sweep time. The time interval between maxima or zero crossings of the beat signal was then determined, and the short-term frequency stability was determined by statistical analysis of the results.

Theoretically, the short-term frequency stability of masers (References 1, 9–11) or spin oscillators (Reference 12) is limited only by the intrinsic linewidth of the Fourier spectrum of the oscillation; and the rms fractional frequency deviation for a measurement made in a time interval t_0 is given by Equation 2:

$$\langle d\omega^2\rangle^{1/2}/\omega_0 = 0.113/Q_l\ (kT/P_0t_0)^{1/2} \qquad (2)$$

where k is the Boltzmann constant, T the absolute temperature, P_0 the microwave power in the cavity, and Q_l the line Q.

This would probably be true also in the case of the pulse-induced emission if the emission was not damped; and, assuming for example that $t_0 = 10^{-3}$ sec, $P_0 = 10^{-12}$ watt, $Q_l = 0.25 \times 10^9$, an upper limit for the short-term frequency stability of pulsed emission would be of the order of 1 part in 10^{12} for a period of measurement of 1 millisecond.

However, usually, the short-term frequency instabilities one measures are not due so much to the intrinsic instabilities as given by Equation 2 but are due mostly to errors introduced in the measurements by the noise in the receiver used to detect the emitted signal. For example, in measuring the time interval t_0 between two maxima or two zero crossings, it can be shown (Reference 12) that the error $\langle dt^2\rangle^{1/2}$ is such that

$$\langle dt^2\rangle^{1/2} = t_0/\rho. \qquad (3)$$

The error on the beat frequency is then

$$\langle df^2\rangle^{1/2} = 1/\rho t_0, \qquad (4)$$

where ρ is the signal-to-noise ratio of the detected signal for the time interval considered.

It follows that

$$\langle df^2\rangle^{1/2}/f = 1/f\rho t_0, \qquad (5)$$

where f is the microwave frequency of the emitted signal, since the frequency translation through the local oscillator of the receiver does not change the frequency difference between the two signals giving the beat note.

Equation 5 represents the relative error in frequency for a period of measurement of t_0 seconds. Expressing ρ in terms of F, the noise factor of the receiver, we obtain Equation 6:

$$\langle df^2\rangle^{1/2}/f = FkT\Delta f/P_0 f t_0, \qquad (6)$$

where Δf represents the bandwidth of the receiver.

Usually, the values of frequency errors given by Equation 6 are much larger than the values obtained with Equation 2. For example, assuming $F = 8$ db, $\Delta f = 2 \times 10^4$ cps, $P_0 = 10^{-12}$ watt, $f = 6.83 \times 10^9$ cps, the short-term frequency stability could not be measured with an accuracy greater than 1 part in 10^{10} for a period of measurement of 1 msec.

Because of the damping effects, ρ is not constant during the entire period of measurement, and consequently the experimental values differ somewhat from the values obtained from Equation 6; but the order of magnitude is in agreement, and a resolution of about 1 part in 10^9 for a period of measurement of 1 msec has been obtained. Some improvement could be achieved by using the more advanced methods of measurements which have been developed for a similar problem in the case of magnetometers using the proton-free precession method (Reference 13).

Experimentally, by analyzing the beat frequency signal from the two gas cells, during a period of about 15 to 20 msec, it was possible to detect a spurious frequency modulation at a rate of 240 cps with a maximum frequency excursion of 12 cps. This would correspond to a frequency excursion of about 1 part in 10^9 for each cell. It is believed that this modulation was produced by some stray ac field acting on the cells, since no magnetic shield was used on the cell operating in the earth's field. Such stray modulation could be removed easily with adequate magnetic shielding.

In resumé, the measurements show that the

pulse-induced emission signal has a short-term frequency stability comparable with, or better than, the resolution of the method of measurement (i.e., of the order of 1 part in 10^9 for period of measurement of 1 msec).

SHORT-TERM FREQUENCY STABILITY OF A MICROWAVE SIGNAL PRODUCED BY A CRYSTAL OSCILLATOR AND VARACTOR HARMONIC GENERATOR

A stable crystal oscillator (Sulzer type 5P) at 4.99 Mc, followed by a multiplier chain up to 60 Mc and varactor harmonic generator up to 6834 Mc, was used to produce a microwave signal near the frequency of the rubidium resonance. This signal was mixed with the microwave pulse-induced emission signal in a receiver, and the beat frequency was analyzed to determine the short-term frequency stability.

The measurements were carried out in two ways:

In a *first method*, the crystal oscillator served as a common source for both the microwave excitation producing the pulse-induced emission signal and the microwave signal to be compared in the receiver.

In a *second method*, an independent oscillator was used to produce the pulse-induced emission signal in the cell, and a continuous microwave signal derived from the Sulzer oscillator was compared in the receiver.

In the first method there is a synchronization between the phase of the pulse-induced emission signal and the phase of the microwave exciting signal, which makes it easier to detect any frequency modulation of the oscillator and multiplier chain being tested.

In the second method no such synchronization exists, and only a detailed statistical analysis of the measurements of the time interval between maxima or zero crossings can give the short-term stability information.

The following experimental results were obtained:

The Sulzer oscillator model 5P was preliminary-tested using a method similar to the one described in Reference 14 but using a period counter instead of a frequency discriminator. The standard for comparison was a Varian rubidium frequency standard model V-4700A. The standard deviation of the frequency was found to be 5 parts in 10^{11} for periods of 1 sec and 1 part in 10^{11} for periods of measurements of 20 sec. Since these values include the instabilities of the rubidium standard, the stability of the Sulzer oscillator for periods of 1 sec was probably better than 3 parts in 10^{11}.

Using the first method of measurements, the short-term stability of the oscillator was found to be of the order of the resolution of the method (i.e., about 1 part in 10^9 for periods of measurement of 1 millisecond). A small frequency modulation at 60 cps of less than 5 parts in 10^{10} was barely detectable.

When frequency modulation is present in the signal to be measured, the distance between maxima or zero crossings is not constant for the various cycles of the beat signal. This can be determined on the photographs of the CRT display, but a convenient method of making the measurements is to adjust the sweep of the CRT in such a way that the end of the emitted signal is superimposed—on the CRT screen—with the beginning of the signal. This is shown in Figure 15–7, where in (a) the beat signal is displayed in the conventional manner—showing one full scan of the signal, and where in (b) the sweep of the CRT is adjusted in such a way that the maxima and minima at the beginning and at the end of the emitted signal are superimposed. This superposition of the signals depends on the relative frequencies of the microwave excitation and the microwave-emitted signal; and, by changing the frequency of the crystal oscillator, one can move continuously the pattern corresponding to the beginning of the emitted signal with respect to the pattern corresponding to the end of the emitted signal. This is shown in Figure 15–7(c) and (d), and the frequency change necessary to move one maxima to a minima corresponds to the pulse rate of synchronization—30 cps in this particular case. It is possible to adjust the superposition to better than 5 cps at 6834 Mc. In one set of measurements, using a manual setting of the oscillator through visual observation of the scope pattern, the standard deviation of the resettings was better than 5 parts in 10^{10}. (Incidentally, this is a very convenient way to adjust the frequency of an oscillator to various given values, separated

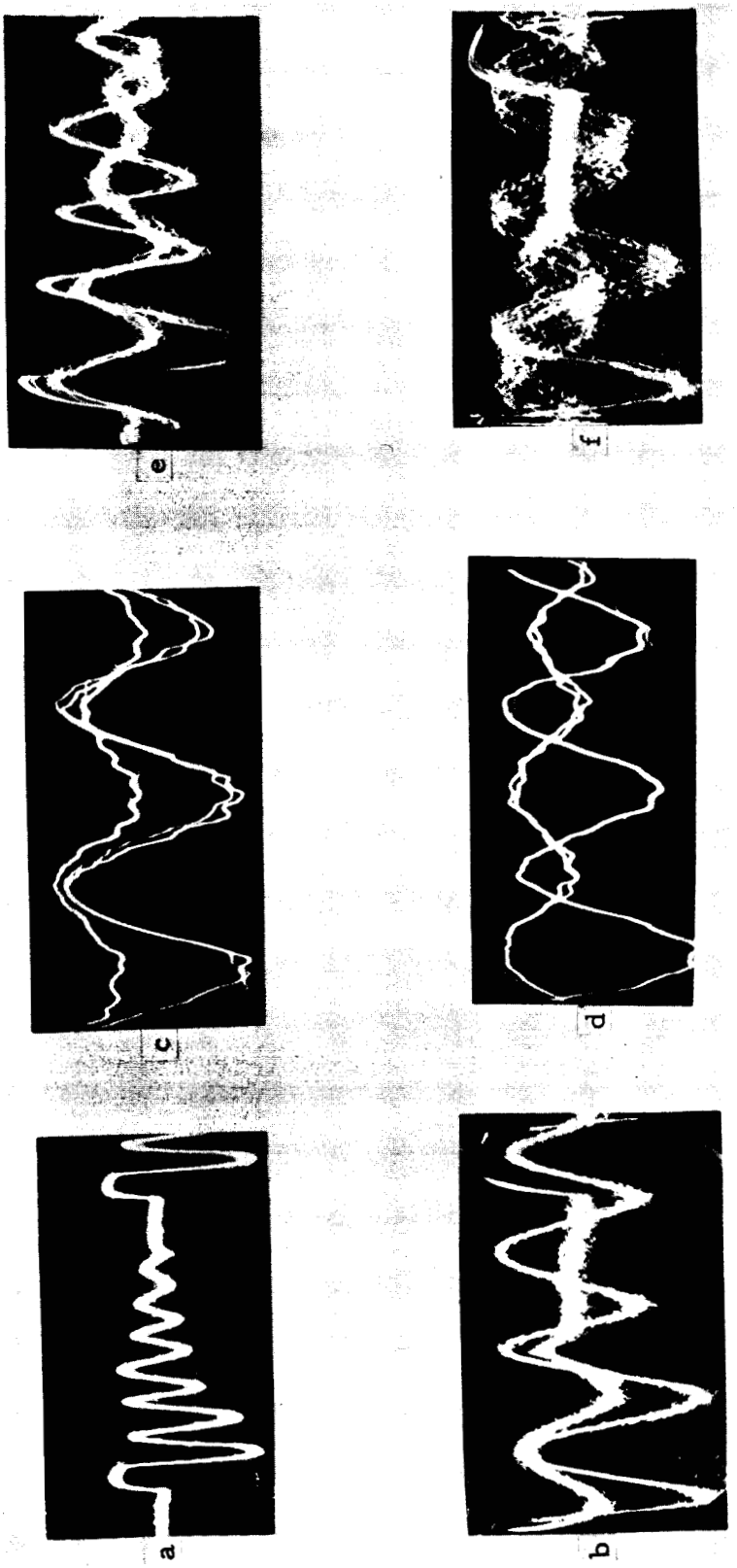

FIGURE 15-7.—Beat signals for various CRT displays showing frequency modulation of oscillator.

by 30 cps at 6834 Mc, with a high degree of precision.)

With this technique it is possible by examination of the coincidence between maxima to detect a frequency modulation of a few parts in 10^{10} for periods of measurements of 10 msec. Figure 15–7(e) shows, for example, the pattern obtained when a 60-cps frequency modulation was applied to the crystal oscillator through a varicap. When the modulation frequency does not correspond to an integer of the sweep scan frequency, the synchronization is lost and a fuzzy picture—more difficult to interpret—is obtained [see Figure 15–7(f)].

With the second method of measurements, the statistical analysis of the histograms of the time intervals between maxima or zero crossings gave essentially the same results as the first method.

In resume, these measurements show that a stable crystal oscillator and multiplier chain up to 60 Mc, followed by a varactor harmonic generator up to 6834 Mc, can be used to obtain a microwave signal of very good short-term stability (i.e., better than 1 part in 10^9 for 1 msec). These results are in agreement with similar observations previously reported and obtained by different techniques of measurements (References 2–15).

CONCLUSIONS

The measurements of the short-term frequency stability of the microwave pulse-induced emission in alkali vapors show that this signal has a stability of 1 part in 10^9, or better, for period of measurement of 1 msec. This microwave signal could be used advantageously in Doppler radar and for the measurement of the short-time stability of other microwave sources.

REFERENCES

1. Kleppner, D., Goldenberg, H. M., and Ramsey, N. F., "Theory of the Hydrogen Maser," *Phys. Rev. 126*, 603 (1962). Vessot, R. F. C., "Frequency Stability Measurements between Several Atomic Hydrogen Masers," Quantum Electronics, *Proc. 3rd Intern. Congress*, Ed. P. Grivet and N. Bloembergen, Dunod Editeur Paris, and Columbia University Press: New York, Vol. 1, page 409, 1964.
2. Barnes, J. A., Allan, D. W., and Wainwright, A. E., "The Ammonia Beam Maser as a Standard of Frequency," *I.R.E. Trans. Instrumentation I*, 26 (1962).
3. Dicke, R. H., and Romer, R. H., "Pulse Techniques in Microwave Spectroscopy," *Rev. Sci. Inst. 26*, 915 (1955).
4. Kastler, A., "Optical Methods of Atomic Orientation and of Magnetic Resonance," *J. Opt. Soc. Am. 47*, 460 (1957).
5. Franzen, W., "Spin-Relaxation of Optically Aligned Rubidium Vapor," *Phys. Rev. 115*, 850 (1959).
   Bouchiat, M. A., "Relaxation Magnetique d'atomes de rubidium sur des parois paraffinees," *J. Phys. Radium 24*, 379, 611 (1963).
   Balling, L. C., Hanson, R. T., and Pipkin, F. M., "Frequency Shifts in Spin Exchange Optical Pumping Experiments," *Phys. Rev. 133*, A607 (1964).
   Jarret, S. M., "Spin-Exchange Cross-Section for Rb^{85}–Rb^{87} Collisions," *Phys. Rev. 133*, A111 (1964).
   Moos, H. W., and Sands, R. H., "Study of Spin-Exchange Collisions in Vapors of Rb^{85}, Rb^{87}, and Cs^{122} by Paramagnetic Resonance," *Phys. Rev. 135*, A591 (1964).
   Franz, F. A., and Luscher, E., "Spin Relaxation of Optically Pumped Cesium," *Phys. Rev. 135*, A582 (1964).
   Arditi, M., and Carver, T. R., "Hyperfine Relaxation of Optically Pumped Rb^{87} Atoms in Buffer Gases," to be published in *Phys. Rev.* (Nov. 2, 1964).
6. Robinson, H. G., Ensberg, E. S., and Dehmelt, H. G., *Bull. Am. Phys. Soc. 3*, 9 (1958).
   Alley, C. O., Jr., "Investigations of the Effect of Gas Collisions and Optical Pumping on the Breadth of Spectral Lines," Final Report, U.S. Army Signal Corps Engineering Laboratory, September 30, 1960, page III–9.
   Bouchiat, M. A., and Brossel, J., "Etude de le relaxation hyperfine de la vapeur de rubidium," *Compt. Rend. Acad. Sci. Paris 254*, 3650, 3828 (1962) and *257*, 2825 (1962).
7. Arditi, M., and Carver, T. R., "Pressure, Light and Temperature Shifts in Optical Detection of 0–0 Hyperfine Resonance of Alkali Metals," *Phys. Rev. 124*, 800 (1961).
   Barrat, J. P., and Cohen-Tannoudji, C., "Etude du pompage optique dans le formalisme de la matrice densite," *Compt. Rend. Acad. Sci. Paris 252*, 93 (1961) and *252*, 255 (1961).
   Cohen-Tannoudji, C., "Observation d'un deplacement de raie de resonance magnetique causee par l'excitation optique," *Compt. Rend. Acad. Sci. Paris 252*, 394 (1961); also: "Advances in Quantum Electronics," page 114, J. R. Singer, Ed., Columbia Univ. Press: New York and London, 1961.
   Heitler, W., "The Quantum Theory of Radiation," 3rd ed., Sec. 20, Oxford University Press: London, 1954.
   Shearer, L. D., "Energy Shifts of the Magnetic Sub-Levels of $^3S_1$ Helium Caused by Optical Pumping," *Phys. Rev. 127*, 512 (1962).
8. Arditi, M., and Carver, T. R., "Frequency Control

by Gas Cell Standards," *Proc. 15th Annual Symposium on Freq. Control*, Atlantic City, N.J., May 31–June 2, 1961, U.S. Army Signal Research and Development Lab., Ft. Monmouth, N.J., p. 181 (1961).

9. SHIMODA, K., WANG, P. C., and TOWNES, C. H., "Further Aspects of the Theory of the Maser," *Phys. Rev. 102*, 1308 (1956).
10. BASOV, N. G., ORAEVSKY, A. N., STRAKHOVSKY, G. M., and TATARENKOV, V. M., "An Emission of the Molecules being in the Mixed Energy State," *Quantum Electronics Proc. 3rd Intern. Congress*, Ed. P. Grivet and N. Bloembergen, Dunod Editeur Paris, and Columbia University Press: New York, Vol. 1, p. 377 (1964).
11. EDSON, W. H., "Noise in Oscillators," *Proc. I.R.E. 48*, 1454 (1960).
12. GRIVET, P., and BLAQUIERE, A., "Masers and Classical Oscillators," *Proc. Symposium on Optical Masers*, Polytechnic Institute of Brooklyn, April 16–19, 69 (1963).

GRIVET, P., and BLAQUIERE, A., "Nonlinear Effects of Noise in Electronic Clocks," *Proc. I.R.E. 51*, 1606 (1963).

13. GRIVET, P., BLAQUIERE, A., and BONNET, G., "Magnetometres a Maser et a Oscillateurs de Spin," *Quantum Electronics, 3rd Intern. Congress*, Ed. P. Grivet and N. Bloembergen, Dunod Editeur Paris, and Columbia University Press: New York, Vol. 1, p. 248 (1964).

SERVOZ-GAVIN, P., and GAUTHIER, D., *J. Phys. Radium* (to be published) and *Bull. Ampere 9*, 629 (1960).

FAINI, G., FUORBES, A., and SVELTO, O., "A Nuclear Magnetometer," *Energia Nucl. 7*, 705 (1960) and *8*, 295 (1961).

BONNET, G., Ph.D. Thesis (unpublished), Grenoble 1961.

SALVI, A., Ph.D. Thesis (unpublished), Grenoble 1961.

14. HASTINGS, H. F., and KING, P. B., Jr., "A Technique for Precise Measurements of Short and Long-Term Stability of Oscillators," *IRE Trans. Instrumentation I*, 248 (1962).
15. BUCK, J. R., HEALEY, D. J., III, and MEISELES, M., "Measurement of Phase-stability of Quartz Crystal Oscillators for Airborne Radar Applications," *IEEE Convention Records, Part B, Instrumentation*, p. 34, 1964.

16. NOISE SPECTRUM PROPERTIES OF LOW-NOISE MICROWAVE TUBE AND SOLID-STATE SIGNAL SOURCES

H. MAGER,* S. L. JOHNSON,† AND D. A. CALDER†

Raytheon Company
Massachusetts

Microwave signal sources, used as local oscillators and transmitter chain exciters in many of today's high-performance coherent tracking and guidance radars, require very low residual frequency or phase modulation. The modulation rates of the residual modulation of interest for these radars extend from 10 cps on out to 150 kc/sec. In this paper, experimental data are presented on the residual FM of low-noise L- to X-band tubes, "solid-state klystrons," and solid-state chains. The tube types include klystrons, magnetrons, and triodes. Data are presented on solid-state chains of the type consisting of a VHF crystal-controlled transistor oscillator, followed by a VHF transistor power amplifier and a varactor frequency multiplier chain. The spectral shape of the solid-state chain is shown to differ appreciably from those of the microwave tube sources and that of the solid-state klystron. The relation between the various parameters of the chain—such as the crystal Q and the amplifier noise figure, and the magnitude and spectral shape of the residual FM of low-noise solid-state chains—are discussed.

Papers in Session I of this Symposium (Reference 1) have indicated that adequate definition of frequency stability requires a description of the *spectrum* of the signal source. Experience of the Raytheon Company with both microwave tube and crystal-controlled solid-state chains has given emphasis to this requirement, since the spectral shapes of these two types of sources are very different—a fact which is lost when stability is measured in the time domain with averaging intervals of tenths of a second or longer.

This paper will present data showing the state of the art of low-noise microwave signal sources. We will concern ourselves with residual FM at modulation rates of 10 cps to 150 kc/sec, that is, with that portion of the spectrum extending from 10 cps to 150 kc/sec from the carrier. The first section of the paper will deal with low-noise klystrons, magnetrons, and triodes; the second section will include data on solid-state chains and "solid-state klystrons" and will delineate comparisons where appropriate. For some devices, mention will be made of the extent to which correlation exists between theoretical noise models and experimental data.

The topic of experimental techniques and equipment will not be discussed, since the subject is amply covered in the first paper of Session II of this Symposium (Reference 2). However, a VHF discriminator will be discussed, since it is not covered elsewhere. Most measurements were made using either a dc Pound discriminator, a carrier nulling microwave bridge discriminator with IF, or the Allscott Noise Measuring Equipment.

TUBES

The two-cavity klystron is the source with the lowest FM noise for RF frequencies at S-band or higher, and for noise modulation frequencies above 1 or 2 kc/sec. Figure 16-1 shows data on the Raytheon QKK1106 and the Sperry SOX-239 klystrons; both of these tubes produce greater than 1-watt output. The spurious FM decreases from about $\frac{1}{2}$ cps per kc/sec at 1 to 2 kc/sec from the carrier, to about 0.2 cps per kc/sec at 100

*Bedford, Mass.
†Wayland, Mass.

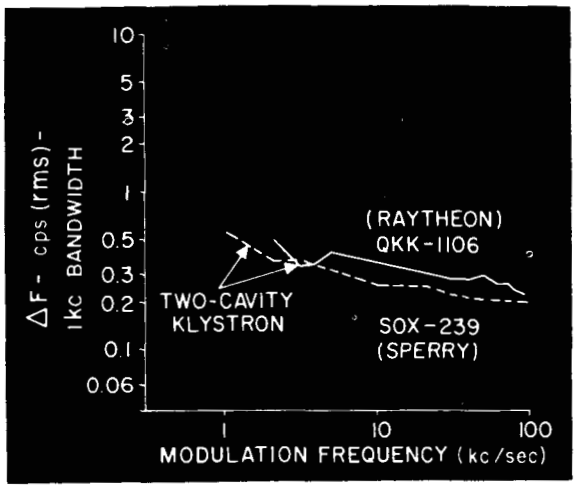

FIGURE 16–1.—FM noise low-power two-cavity klystron.

kc/sec from the carrier. Manufacturer's data on the Varian VA-514, a tube similar to those above, indicates roughly the same FM noise.

Life test noise data on a Raytheon QK896, a 50 to 100-watt two-cavity klystron is shown in Figure 16–2. The FM noise is about the same as that of the lower power tubes, as is indicated by the photographs of noise with a Panoramic ultrasonic analyzer IF bandwidth of 1 kc/sec. The Varian 572 is another two-cavity klystron having similar power output and noise performance.

A summary of FM noise of typical low-noise tubes is given in Figure 16–3. They are all characterized by a rapidly changing deviation below 5 kc/sec and a relatively flat deviation above 20 kc/sec. The noise of the TRAK, model 9186–1017, triode oscillator (using a 7910 triode); the Varian

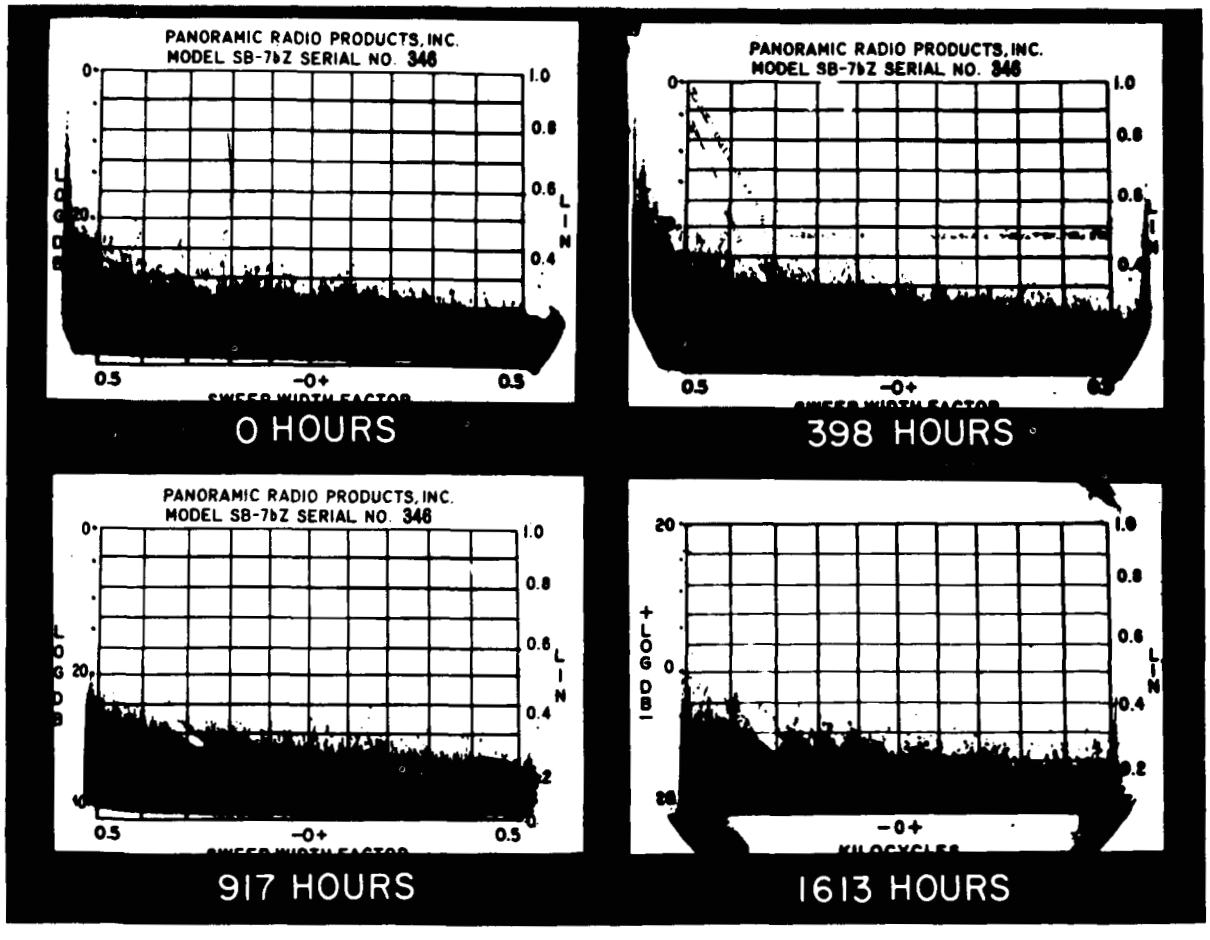

FIGURE 16–2.—QK896 No. 1499 FM noise 10–70 kcs (0.9 cps full scale).

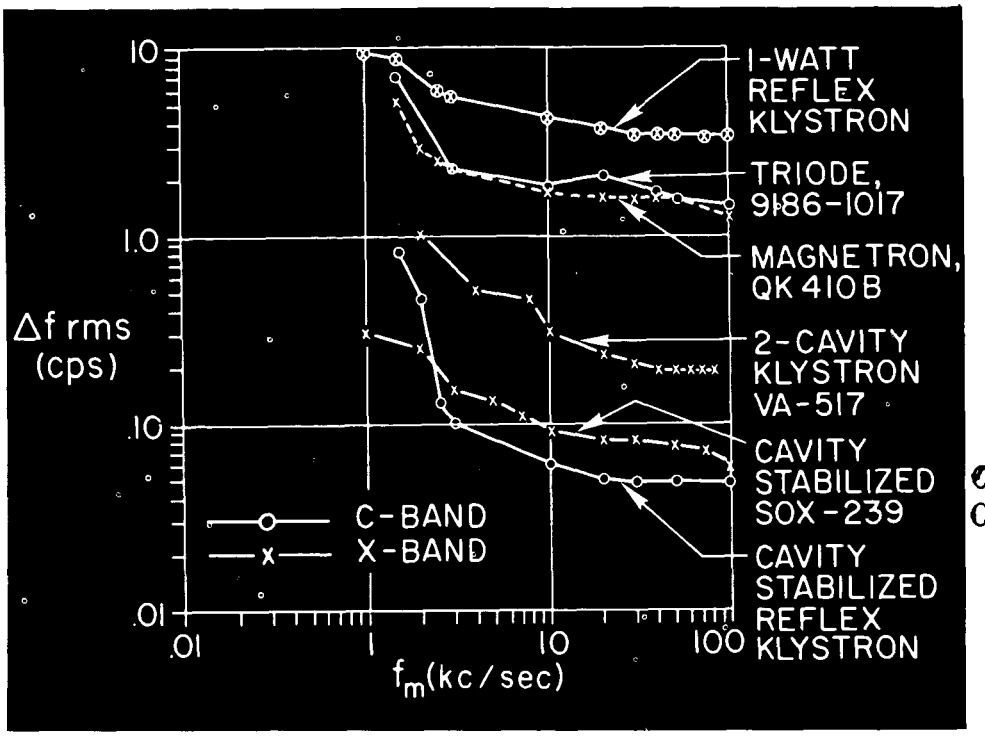

FIGURE 16–3.—Comparative FM noise spectra of tubes.

1-watt reflex klystron; and the Raytheon QK410B magnetron are about the same: 5 to 10 cps per kc/sec at 1 kcps from the carrier, decreasing to 1 to 4 cps per kc/sec at 100 kc/sec from the carrier. The spurious FM of the VA–517 as shown has been discussed. The figure also shows what has been achieved with passive cavity stabilization. The data on the stabilized SOX–239 were obtained from sales literature (Reference 3); the stabilized reflex is the 1-watt tube shown at the top.

FM noise measurements have been extended down to 100 cps and up to the megacycle region on some of the tubes discussed; the noise continues to rise at low frequencies and remains relatively flat at high frequencies. Also, for a given tube type, noise has been found to be relatively independent of microwave frequency.

The 50-watt two-cavity klystrons have been tested under 1-g vibration, and the noise increases to a few hundred cycles coherent with the vibration frequency in the 500 to 2000 cps region.

For applications requiring lower noise than that shown in Figure 16–3, Raytheon has employed an active degeneration technique, with a microwave discriminator and the transmitter in a closed-loop system. The photographs of Figure 16–4 show the FM noise of three such transmitters. Full scale is 0.1 cps (i.e., noise is of the order of 0.01 cps per kc/sec.

SOLID-STATE SIGNAL SOURCES

During the past two to three years there has been an increasing use of solid-state microwave sources as local oscillators and transmitter chain exciters in radar systems. The design of solid-state sources is a relatively new and evolving art, made possible by the relatively recent development of high-power, very high frequency transistors and efficient varactor diodes.

Solid-state sources fall into two broad categories. In one category can be placed those sources which have been called the *solid-state chain type.* These sources, in most cases, use a VHF crystal-controlled transistor oscillator, followed by a VHF transitor power amplifier and a varactor frequency multiplier chain of high overall order of multiplica-

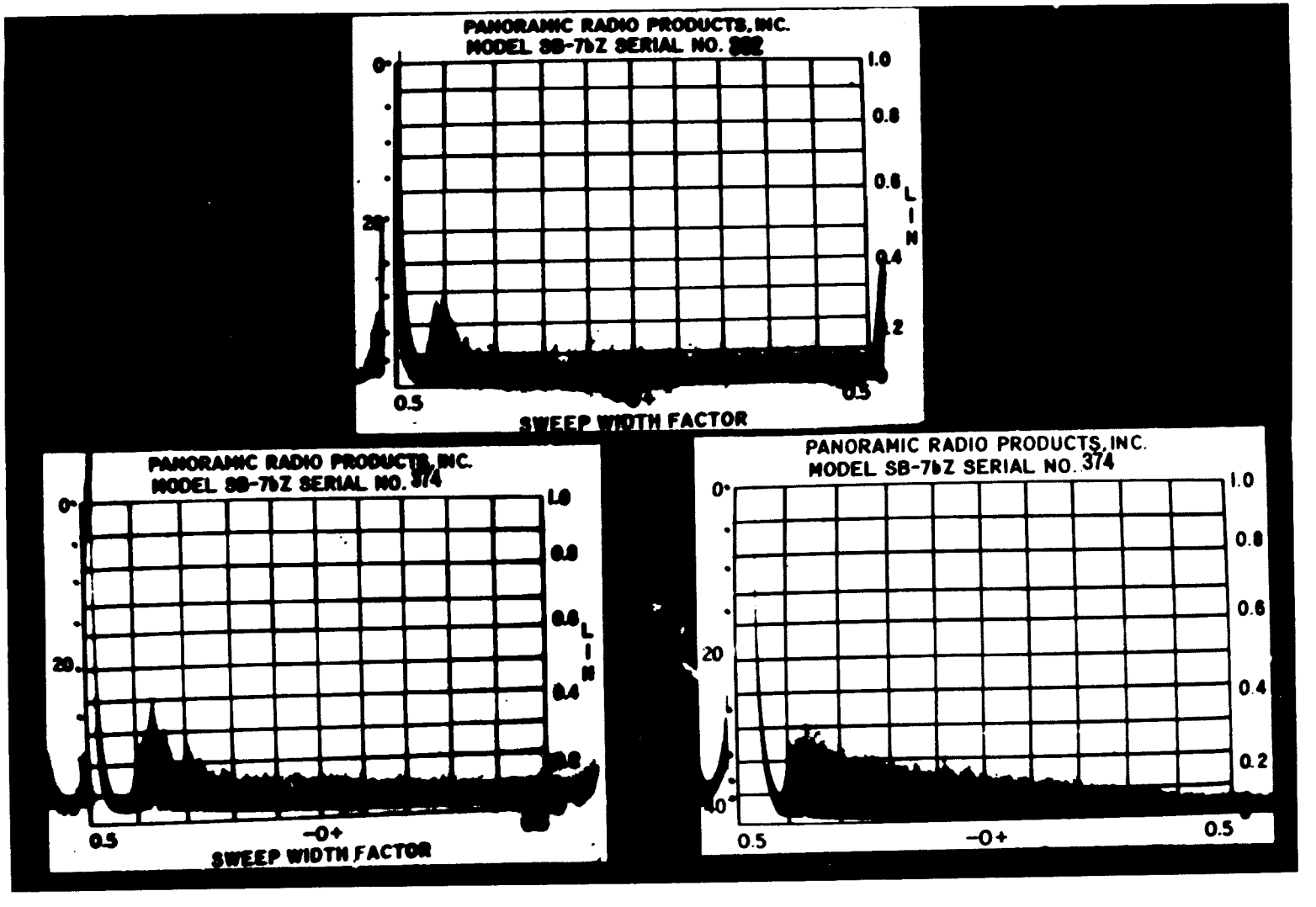

FIGURE 16–4.—FM noise (2–70 kc) of three transmitters (0.1 cps full scale).

tion. Today it is entirely possible to construct solid-state sources of this type capable of delivering up to 250 mw with 2 to 3 percent of bandwidth at X-band; 750 mw with 5 to 7 percent bandwidth at C-band; and 3 watts and higher, with up to 10 percent bandwidths at L-band. An increase in power output efficiency and bandwidth can be expected (in some cases, it has already been achieved) with further development of these devices.

In the other category can be placed those solid-state sources which have been called *solid-state klystrons*. The solid-state klystron is a relatively new device, presently marketed by three manufacturers: Western Microwave Laboratories, Fairchild Semiconductor, and Frequency Sources, Inc. Western Microwave has coined the trade name "Solistron" for their units.

Published circuit information on these devices is very limited, since all three manufacturers have kept this information proprietary. It is generally considered, however, that these devices use a transistor(s) oscillating at substantial power levels in the 1 to 2 Gc/sec region, which is followed by a one or two-stage varactor or step recovery diode frequency multiplier. These devices can be made very compact and lightweight, and can be powered from low-voltage (24–28 volts dc) supplies. Typical power outputs for the solid-state klystrons presently being marketed range from a few watts at L-band to 10 milliwatts at X-band. Some of the units can be voltage-tuned by as

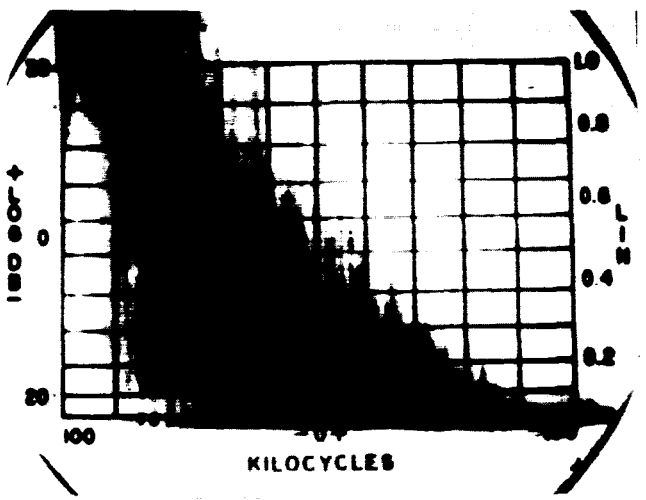

BIAS VOLTAGE	15 v
POWER OUT	20 mw
RF FREQUENCY	1266 Mc/s
FULL SCALE	10 cps
VAR. BAND PASS	1.7 - 200 kc/sec
INTEGRATED NOISE	80 cps rms
SWEEP WIDTH	200 kc/sec
CENTER FREQUENCY	100 kc/sec

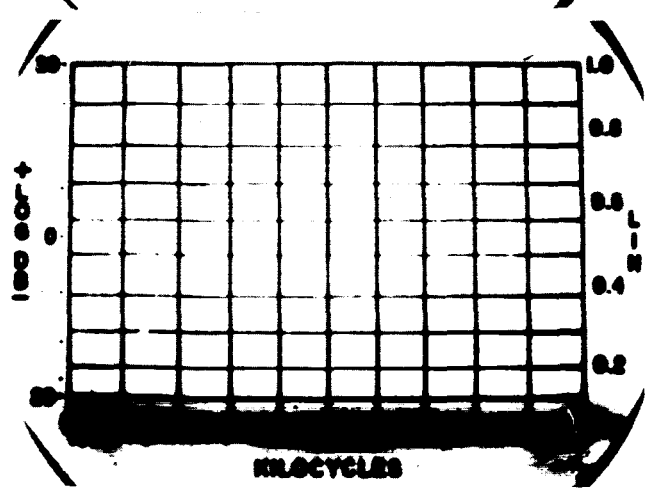

BIAS VOLTAGE	15 v
POWER OUT	27 mw
RF FREQUENCY	1266 Mc/s
FULL SCALE	5 cps
VAR. BAND PASS	1.7 - 200 kc/sec
INTEGRATED NOISE	3 cps rms
SWEEP WIDTH	200 kc/sec
CENTER FREQUENCY	100 kc/sec

FIGURE 16–5.—Solid-state klystron spectra.

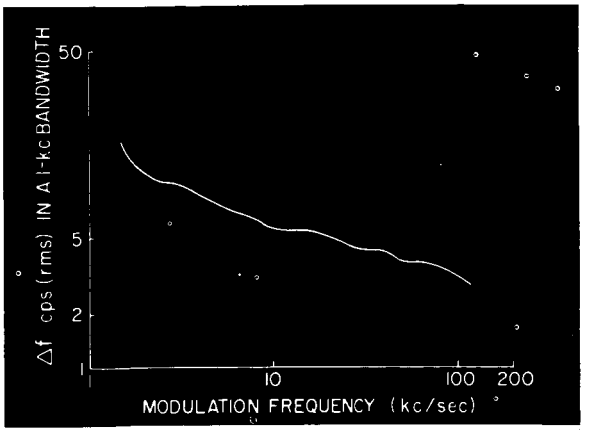

FIGURE 16–6.—FM noise of C-band solid-state klystron (Fairchild MS11).

much as one-half octave. Significant increases in power output, efficiency, and bandwidth of solid-state klystrons are expected with further development of these devices.

SOLID-STATE KLYSTRONS

The data for solid-state klystrons are very limited, primarily because these devices are relatively new. Figure 16–5 (upper photograph) is a display, obtained with an ultrasonic analyzer, of the noise spectra of a Western Microwave L-band "Solistron." The sweep width of the display is 200 kc/sec, centered at 100 kc/sec. On this range the analyzer had a resolution of approximately 2 kc/sec. Full-scale deflection corresponds to a frequency deviation of 10 cps.

The L-band "Solistron" had a power output on the order of 20 mw and exhibited a spectra having decreasing deviation (Δf) with increasing modulation frequency (frequency from carrier). The integrated noise of the 200 kc/sec swept band was 80 cps rms (noise below 1.7 kc/sec was filtered out).

An unusual feature of the L-band "Solistron" was that, at a particular position of the fine tuning control, an appreciable reduction in the FM noise could be achieved. The analyzer display for this particular condition is shown in the lower photograph of Figure 16–5. The integrated noise under this condition was 3 cps rms.

Figure 16–6 presents FM noise data in the modulation frequency range of 1 to 200 kc/sec of a C-band solid-state klystron. The data, kindly furnished by the manufacturer, are for the Fairchild MS 111 solid-state klystron. The MS 111 is a mechanically tuned unit covering the frequency range 5.9–6.4 Gc/sec. It provides 20 milliwatts of output power over this range. The device consists of a transistor oscillator/doubler and a X4 diode multiplier. The MS 111 displays an FM noise spectrum shape typical of solid-state klystrons. The frequency deviation, as measured in a 1 kc/sec bandwidth, is approximately 10 cps (rms) at 2 kc/sec from the carrier and decreases to approximately 3 cps (rms) at a modulation frequency of 100 kc/sec.

SOLID-STATE CHAINS

The FM noise of solid-state sources of the chain type has been investigated both theoretically and experimentally. Figure 16–7 presents the measured FM noise data of an X-band low-noise chain developed at Raytheon. This source has undergone considerable development over the past two years and possibly represents the lowest FM noise achieved to data in X-band solid-state sources.

The frequency deviation at X-band, as measured in a 1 kc/sec bandwidth, is 1.0 cps (rms) at 1 kc/sec modulation frequency, dips slightly, and then rises to approximately 2.3 cps at 100 kc. This chain illustrates a distinctive feature of the

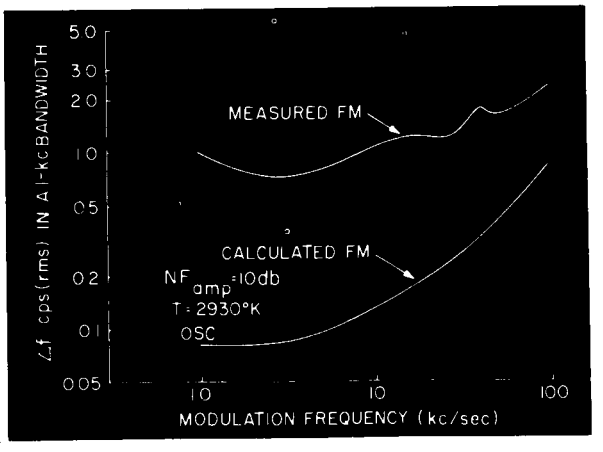

FIGURE 16–7.—FM noise of X-band solid-state chain.

chain-type sources: that of a rising deviation with increasing modulation frequency, as contrasted with a falling Δf with increasing FM, characteristic of microwave tubes and solid-state klystrons.

The X-band source is comprised of a VHF oscillator and buffer, a four-stage VHF transistor amplifier, and a varactor frequency multiplier consisting of two doublers, two quadruplers, and a final doubler. A block diagram of the X-band source is shown in Figure 16–8.

The 80-Mc/sec crystal oscillator is a modified Clapp circuit using a type 2N2808 transitor. The oscillator and buffer amplifier are housed in a component oven to achieve good long-term frequency stability. The power amplifier, which delivers 5 watts, consists of two 2N2224 amplifier stages driving two cascaded class "C" power amplifier stages using 2N2887 transistors.

The amplifier and multipliers were purposely designed to have better than 2.5 percent fixed tuned bandwidth, so that any frequency in this band could be selected simply by changing crystals in the oscillator. No attempt was made to achieve better FM noise performance by band-limiting in the amplifiers and multipliers.

A simplified FM noise model for the solid-state chain, presented in Appendix A, explains the spectral shape of the FM noise. The FM noise contribution from the oscillator (at chain output) as given by Equation A4 of Appendix A is

$$\Delta f = NB_x(KT/P_{cx})^{1/2}$$

(rms cps per cycle of bandwidth),

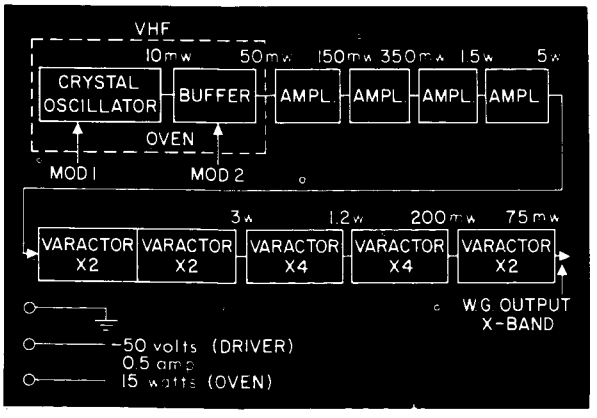

FIGURE 16–8.—X-band solid-state source.

where

N = multiplier chain multiplication factor,
B_x = loaded crystal bandwidth in cps,
T = equivalent noise temperature in degrees Kelvin of parallel conductance of crystal tank circuit,
P_{cx} = crystal signal power in watts.

The FM noise contributed by the amplifier (at chain output) is given by Equation A6 in Appendix A:

$$\Delta f = Nf_m(KT_a/P_{ca})^{1/2}$$

(rms cps per cycle of bandwidth),

where

f_m = modulation frequency (frequency from carrier) in cps,
$T_a = FT_0$ where F is amplifier noise figure; T_0 is 293°K,
P_{ca} = carrier power at input to amplifier.

A comparison of Equation A6 with Equation A4 reveals that the contribution of Δf from the oscillator is independent of f_m,, whereas the contribution from the amplifier is proportional to f_m. For large values of f_m, the amplifier contribution will be predominant, and Δf will increase linearly with f_m until limited by amplifier or multiplier bandwidth.

The total chain FM noise can be calculated by suitably combining the oscillator and amplifier noise contributions. A plot of the calculated chain FM noise is shown along with the measured data for the X-band source in Figure 16–7. The following measured or assumed parameters were used in calculating the total FM noise:

$$F = 10 \text{ db},$$
$$T_{osc} = 2930°\text{K},$$
$$P_{cx} = 10^{-3} \text{ watt},$$
$$P_{ca} = 10^{-2} \text{ watt},$$
$$B_x = 4000 \text{ cps}.$$

The shapes of the calculated curve and the measured curve are in reasonable agreement, considering the number of simplifying assumptions that were made in the noise model. Closer absolute agreement between measured and calculated data would result by assuming a higher oscillator effec-

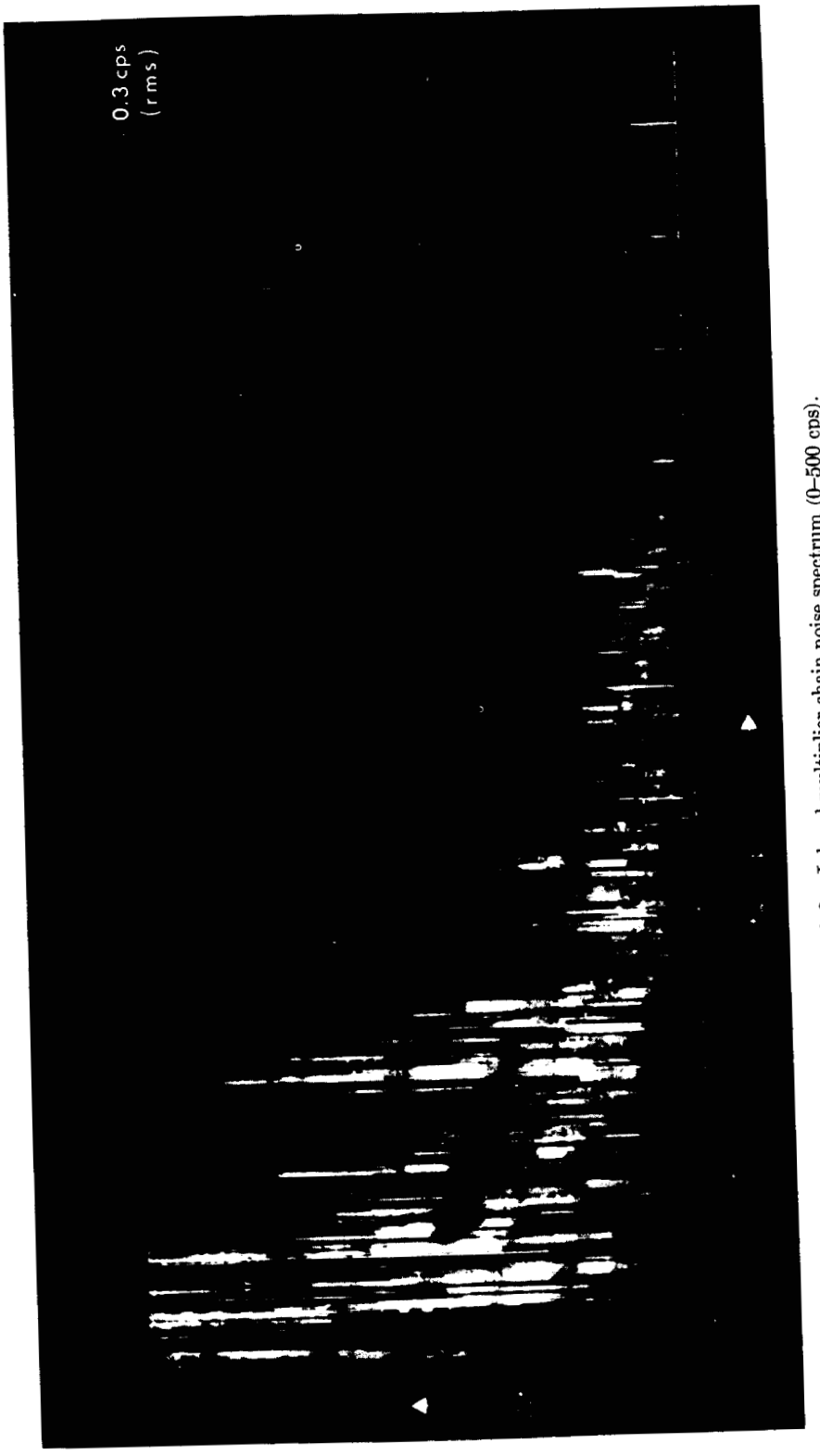

FIGURE 16-9.—L-band multiplier chain noise spectrum (0–500 cps).

tive noise temperature or larger loaded crystal bandwidth.

FM noise data very close to the carrier (below 500 cps) on solid-state chains are very difficult to obtain. Figure 16-9 presents what limited data are available on an L-band chain for modulation frequencies below 500 cps. The L-band unit uses a Valpey Crystal Corp. oscillator and a Microwave Associates' multiplier and amplifier which were built to Raytheon specifications. The source delivers 2 watts at L-band.

The spectral plot shown in Figure 16–9, taken with an analyzer having a bandwidth of about 1.2 cps, covers the modulation frequency range from approximately 1 cps to 500 cps. The large coherent signals are pickup at 60 and 400 cps, which are suspected to be mostly from the test equipment (the source operated from 60 cps; the test equipment from 60 cps, 400 cps, and batteries). The spectral plot is presented primarily to show the rapid increase in Δf as the carrier is approached.

CONCLUSIONS

This paper has presented FM noise data on a wide variety of low-noise microwave signal sources. At C- and X-band, under nonvibratory operation, two-cavity klystrons are capable of providing a carrier with FM noise of less than 0.5 cps (rms) per kc/sec bandwidth at 1 kc/sec modulating frequency, decreasing to 0.2 cps (rms) per kc/sec at 100 kc/sec. The measured FM noise of typical low-noise triodes, magnetrons, reflex klystrons, and solid-state klystrons at C-band and above is presently about one order of magnitude higher.

Data have been presented on the FM noise performance of an X-band crystal-controlled solid-state chain specifically designed for low noise. This source is capable of providing a carrier with FM noise less than 1 cps (rms) per kc/sec at 1 kc/sec modulating frequency, rising to 2.3 cps (rms) per kc/sec at 100 kc/sec.

The low-noise tube sources exhibit an FM noise spectrum which has a deviation (Δf) which initially decreases with increasing modulation frequency and then subsequently becomes constant. The FM noise of low-noise tube sources from S- to K_u-band has been observed to be relatively independent of carrier frequency.

The solid-state chains for which data have been presented exhibit a deviation which initially decreases with increasing modulation frequency, passes through a minimum, and then increases at a rate approximately 6 db per octave at frequencies well removed from the carrier. The FM noise deviation for solid-state chains is dependent directly on N, the multiplier multiplication ratio, and will decrease with decreasing carrier frequency.

ACKNOWLEDGMENTS

The authors wish to acknowledge the support under various contracts of the Bureau of Ships and the Bureau of Weapons of the U. S. Navy, and of the Army Missile Command for measurements on microwave tubes, the Advanced Research Projects Agency for development of the L-band solid-state chain, and the Bureau of Weapons for the development of the X-band solid-state chain. The authors also wish to acknowledge the early work of Mr. Roy. E. Byington in predicting noise performance of solid-state sources. Acknowledgment is also given to Dr. Robert B. Borts and Messrs. Willard W. McLeod, Jr., John R. Caswell, and Philip R. Shutt for their guidance and technical direction.

REFERENCES

1. *These Proceedings: Symposium on the Definition and Measurement of Short-Term Frequency Stability, Session I, Users' Viewpoint and Requirements*, November 23, 1964.
2. CAMPBELL, R. A., *Ibid, Session IV, Measurement Techniques*, "Stability Measurements in the Frequency Domain," Paper 19, November 24, 1964.
3. CAIN & COMPANY, "Cain Circuit," Volume 3, No. 1; March 1964.
4. STEWART, J. L., "Frequency Modulation Noise in Oscillators," *Proc. IRE 44*(3), 372 (1956).
5. EDSON, W. A., "Noise in Oscillators," *Proc. IRE 48*(8), 1454 (1960).
6. MULLEN, J. A., "Background Noise in Nonlinear Oscillators," *Proc. IRE 48*(8), 1467 (1960).
7. BALDWIN, L. D., COLLINS, F. P., JOHNSON, S. L., and PRIEST, W., "Operating Characteristics and Design Criteria of an All-Solid-State 13.3 Gc, 50 mw Microwave Source," *International Solid-State Circuits Conference Digest*, Volume 6, pp. 50–51, February 1963.
8. HINES, M. E., "Microwave Power Sources Using Varactor Harmonic Generation," *The Microwave Journal 6*(4), 74 (1963).

APPENDIX A

Simplified Model for FM Noise in Solid-State Chains

The basic diagram of a solid-state source consists of three significant blocks, as shown in Figure 16–A1. A stable crystal-controlled transistor oscillator generates the basic frequency, which is amplified to a suitable power level by a one or more stage amplifier. The output of the amplifier is applied to a multiplier chain consisting of a series of efficient varactor multiplier stages. The oscillator frequency and the overall multiplication factor of the chain are chosen to provide the desired output frequency.

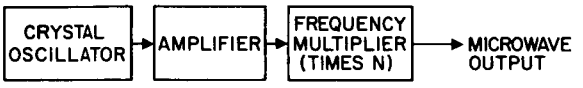

FIGURE 16–A1.—Solid-state source.

Each of the basic blocks is significant in determining the FM noise at the output, and each will be examined separately.

Oscillator FM Noise

The problem of noise in oscillators has been examined by a number of investigators—among them Stewart (Reference 4), Edson (Reference 5), and Mullen (Reference 6). All three authors have analyzed the effects on self-excited oscillators of broad-band noise, such as shot or thermal noise, at or near the oscillator frequency. Stewart has restricted his analysis to FM noise in oscillators, whereas Edson & Mullen have treated both the AM and FM noise case.

Following Edson, in Equation 68 in Reference 5, the square of the FM noise voltage spectrum from the oscillator is given by

$$V_2^2(\omega) = \frac{2kTG}{(\omega_0^2 CkT/2PQ^2)^2 + 4C^2(\omega_0-\omega)^2} \text{ effective volts}^2/\text{cycle}, \quad \text{(A1)}$$

where

k = Boltzmann constant, 1.38×10^{-23},
G = equivalent parallel conductance of crystal tank circuit,
T = equivalent noise temperature in degrees Kelvin of conductance G; the noise contributed by active elements in oscillator have been lumped with thermal noise generated in crystal tank circuit,
C = capacitance of crystal tank circuit,
ω_0 = short-term average frequency of oscillation in radians/sec,
ω = variable angular frequency,
P = total power generated in crystal,
Q = crystal-loaded Q.

In the range of frequencies 1 to 200 kc from carrier, and for the range of parameters which will be considered, the first term in the denominator is negligible with respect to the second term.

The FM noise power spectrum can be readily derived from Equation A1 by multiplying through by G and making an appropriate substitution for C:

$$P_{sx} = \tfrac{1}{2}(KT)(B_x/f_m)^2 \text{ watts/cycle}, \quad \text{(A2)}$$

where

B_x = loaded crystal bandwidth in cps
$f_m = (1/2\pi)(\omega-\omega_0)$ in cps.

The FM noise can be expressed as an equivalent FM deviation using the expression:

$$\Delta f = \sqrt{2} f_m (P_s/P_c)^{1/2} \text{ rms cps}, \quad \text{(A3)}$$

where

f_m = modulation rate or separation from carrier in cps,
P_s = noise power in specified band f_m cycles from carrier,
P_c = carrier signal power.

This expression, which is valid for small modulation index, is derived in most standard texts on FM theory. In this instance, where noise is the modulating signal, the assumption of small modulation index is certainly justifiable.

Substituting Equations A2 in Equation A3, the following relation is obtained:

$$\Delta f = B_x(KT/P_{cx})^{1/2} \text{ rms cps per cycle of bandwidth}, \quad \text{(A4)}$$

where P_{cx} is the crystal signal power in watts.

Referring to Equation A4, it is seen that the

FM noise contribution from the oscillator can be reduced by decreasing the equivalent noise temperature and the crystal bandwidth or by increasing the crystal power. This is in marked contrast to the criterion for long-term stable sources, which require minimum crystal power to reduce aging effects.

Amplifier FM Noise Contribution

The contribution of the amplifier to the FM noise can be calculated readily if it is assumed that the amplifier is linear and its gain characteristics are flat over the FM range of interest. For most solid-state sources, the first assumption of linear operation is not strictly valid, since the final stages of the amplifier are generally operated nonlinear for maximum efficiency. A more rigorous analysis of FM noise would take into account the effects on noise of nonlinear operation in the final stages.

Referred to the input of the amplifier, the total noise power per cycle of bandwidth is

$$P_{in}=KT_a \text{ watts/cycles}, \qquad \text{(A5)}$$

where

$$T_a=FT_0$$

and

$T_0=293°\text{K}$,
$F=$amplifier noise figure.

P_{in} can be considered as half AM and half FM noise. Substituting for P_{in} in Equation A3, an expression can be derived for equivalent FM deviation:

$$\Delta f=f_m(KT_a/P_{ca})^{1/2}$$

rms cps per cycle of bandwidth, (A6)

where P_{ca} is the carrier power at input to amplifier. It is seen that the FM noise contribution for the amplifier can be reduced by improving the amplifier noise figure or by increasing the signal level at the input to the amplifier.

Multiplier FM Noise Contribution

The remaining significant block to be considered in the FM noise model is the varactor frequency multiplier. In passing through the multiplier, the frequency deviation will be multiplied N times, where N is the multiplication ratio:

$$\Delta f_{in}=N\Delta f_{out}.$$

This is equivalent to stating that the FM sidebands (power) will be increased by N^2.

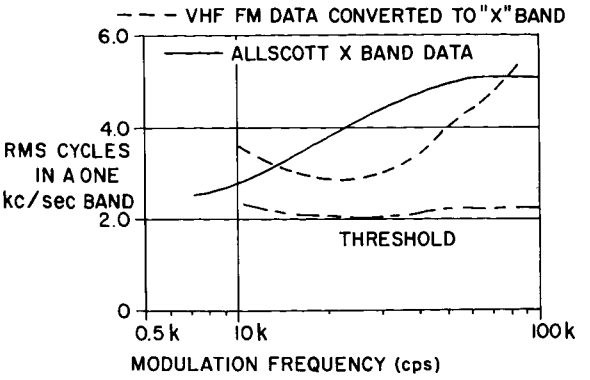

FIGURE 16–A2.—FM comparison, VHF and X-band.

Apart from the FM noise sideband enhancement in the multiplier, which is predictable, there are other mechanisms in the multiplier which could conceivably produce noise. Included in this category are parametric instabilities, avalanche breakdown in the varactors, as well as $1/f$ and shot noise from forward conduction in the varactors.

The problem of avalanche breakdown and parametric instabilities are discussed in References 7 and 8. These particular mechanisms can be significant sources of noise. With proper design of the multiplier chain, however, they can be eliminated—in fact, must be eliminated if low noise is desired.

An investigation was undertaken to determine whether there were any extraneous sources of noise in the varactor multipliers chains which would produce a significant increase in FM noise at the output above that predicted by the N^2 law. The FM noise on the VHF signal at the input to the multiplier chain and the FM noise on the output were measured. A very sensitive VHF discriminator, which is described in Appendix B, was constructed to measure the FM noise on the VHF drive signal. The measured FM noise on the VHF signal, when extrapolated to X-band using the N^2 law, was in close agreement with the actual measured X-band performance. Figure 16–A2 shows the experimental results.

APPENDIX B

VHF DISCRIMINATOR

A diagram of the discriminator is shown in Figure 16–B1. The discriminator requires an input of approximately 50 mw. It consists of two separate channels with sufficient gain to provide a 75-volt peak detected output when tuned to the carrier. Each channel has a bandwidth of 150 kc,

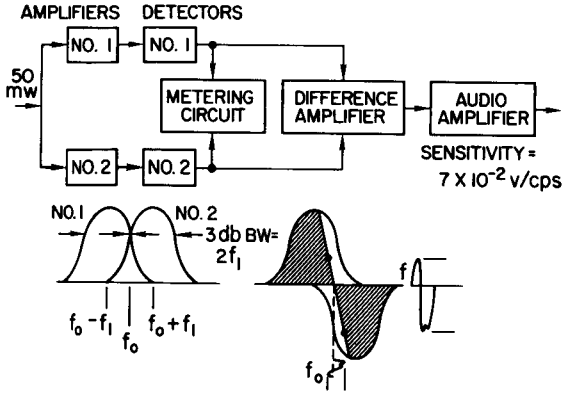

FIGURE 16–B1.—VHF discriminator.

which is obtained by using helical resonators with loaded Q's of between 500 and 600 in each final amplifier plate.

The amplifiers are set up by tuning each channel to carrier frequency by a peaking meter. Then, channel no. 1 is tuned down to put the carrier on its upper 3-db point, and channel no. 2 is tuned above carrier in a similar manner. A difference amplifier inverts one signal and combines them, thus providing a discriminator response similar to the one shown. The additional audio amplifier, which has a gain of 37 db, provides an overall sensitivity of $S = 14$ millicycles/millivolt at 80 Mc, or $S' = 1.8$ cps/mv at "X" band. The use of a Hewlett–Packard type 310 spectrum analyzer with its 1-kc bandwidth gives millivolts in a 1-kc band which are readily converted to rms cycles in a 1-kc band. The microphonically generated signal from the test set limits its usefulness below 10 kc/sec. The threshold noise was determined as 1.1 mv/kc (2 cps per kc/sec at X-band) by driving from a vacuum tube oscillator calculated to give less than 0.1 cps per kc/sec at X-band.

17. SHORT-TERM FREQUENCY STABILITY MEASUREMENTS OF A CRYSTAL-CONTROLLED X-BAND SOURCE*

J. R. BUCK AND D. J. HEALEY III

Westinghouse Electric Corporation
Baltimore, Maryland

A crystal controlled X-band source providing a high degree of spectral purity and 750 milliwatts power output was designed and evaluated by the Westinghouse Electric Corporation. The results of the evaluation revealed that, when the oscillator is built to yield high spectral purity, the harmonic generator and transistor amplifier can limit the attainable purity at X-band.

Results of measurements of spectral purity when the oscillator and harmonic generator are subjected to vibration environment are given.

Certain products manufactured by Westinghouse require the incorporation of low-noise microwave signal sources. Klystron oscillators are capable of providing the required spectral purity in a laboratory environment; but vibration effects, power supply ripple, and acoustical noise degrade the performance to unacceptable levels in vehicular systems. For a number of years, Westinghouse therefore has employed an AFC circuit invented by C. H. Grauling, Jr., as a means of stabilizing the spectrum of reflex klystrons against degradation under the environmental conditions that are encountered. Although the AFC is entirely satisfactory for many applications, there are some systems demanding more stringent long-term stability than is provided by the AFC. These applications also, however, require the very short-term stability provided by the AFC.

For these applications, it is natural to consider the use of a quartz crystal unit as the frequency-determining element. This paper describes a source utilizing quartz crystal control that was designed and evaluated by Westinghouse.

*This paper is based on work performed in connection with the Bureau of Naval Weapons Contract NOw 63-0280/di.

PERFORMANCE CHARACTERISTICS REQUIRED

Crystal oscillator frequency band	HF
Output frequency band	X
Power level	750 milliwatts
Long-term stability	5×10^{-5}
Short-term stability	See Figure 17–1

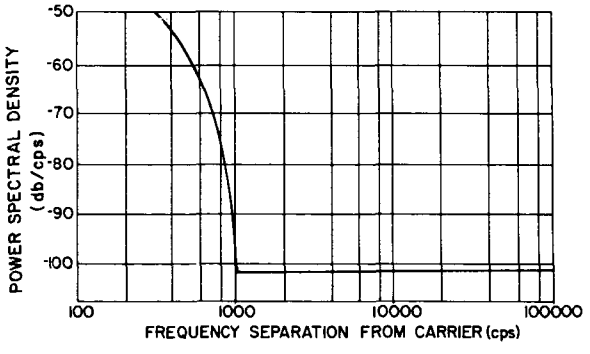

FIGURE 17–1.—Short-term stability requirement.

MECHANIZATION

Quartz Crystal Unit

Typical requirements are that the phase modulation appearing on the X-band signal at a dis-

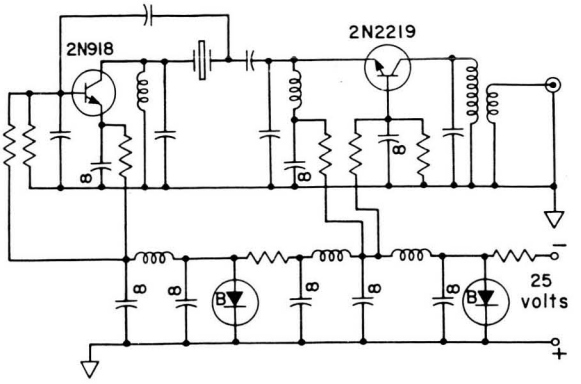

FIGURE 17–2.—Oscillator circuit.

crete modulating frequency be less than 10^{-4} radian. Our experience with quartz crystal units has revealed that this requirement is difficult to satisfy under a vibration and acoustic environment. Excluding the amplification of the applied vibration as a result of excitation of the quartz-crystal-unit mounting structure, we have measured phase modulation indices between 0.5 and 3.0 degrees per g at X-band for various AT-cut resonators operating in the HF and VHF range. Thus, to meet a 10^{-4} radian requirement, the permissible g-level applied to the quartz plate is on the order of 0.01 to 0.0016 g. A serious problem arises when isolation is designed to satisfy such requirements for vehicular environment and when the space available is small. The isolation system always has considerable amplification at a low frequency; and, when typical vibration input spectra are applied to the system, nonlinearities are exhibited by the isolation system. The result is that the harmonics of the vibration input excite the mechanical resonance of the quartz-crystal-unit mounting structure. The effective g-levels at the crystal unit that are allowed at mount resonant frequency are on the order of 0.001 g, and sometimes much less.

The crystal unit developed by Sykes, Spencer, and Smith (see Reference 1) was found to be the best for our applications. The measured mount resonance in this crystal unit varied between 3.0 and 3.5 kc on a number of units tested. On all the other crystal units we have tested, the mount resonance was lower in frequency. In our application, the frequency of the mount resonance is not important unless the harmonics occurring in the mechanical system as a result of nonlinearities are significantly less at the higher resonant frequencies. A number of isolation schemes were tried, and the final design is similar to that which was made by BTL, except that it was necessary to make the enclosure larger and to use a precompressed sponge rubber instead of Curon for isolation.

Oscillator Circuit

The oscillator includes a sustaining circuit and a buffer amplifier. Measurements were made on several configurations of oscillators, which included temperature compensation circuitry and Automatic Level Control (ALC). It was concluded that temperature compensation could not be employed with simple thermistor-varactor circuitry because of the degradation of the spectral purity at the frequencies of interest. The final circuit employed was a modified Pierce circuit followed by a transistor buffer amplifier in a grounded base configuration. The oscillator circuitry is shown in Figure 17–2. Figure 17–3 shows the oscillator package.

Harmonic Generator

The harmonic generation circuitry utilized varactor diodes and VHF transistor amplifiers. Many harmonic generators employing varactor

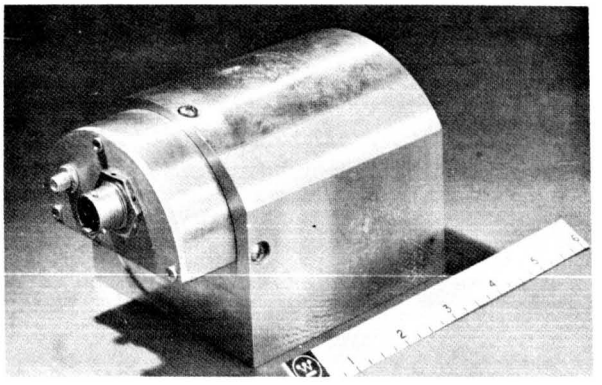

FIGURE 17–3.—Oscillator package.

diodes utilize not simply the variation of depletion-layer capacitance but also the charge storage effects. In such operation, harmonic generation is primarily a function of the reverse current pulse resulting from the return of stored *minority* carriers—the charge carriers which cross the junction when the diode is forward biased but which are not permitted to remain sufficiently long to allow recombination with majority carriers.

Such operation leads to power handling capability and efficiencies which are greater than can be achieved by using depletion-layer capacitance variation alone for obtaining the energy conversion. Two commercially available harmonic generators which produced 100 milliwatts of power at X-band and utilize the step-recovery phenomena resulting from charge storage in some stages were measured, and it was found that at X-band the noise at 2000 cps from the carrier was −50 db in a 500-cps bandwidth. It appeared, therefore, that such operation of varactor diodes was unsatisfactory for our application. Unfortunately we were not able to determine whether the degradation was entirely caused by the varactor operation or whether it was caused by the transistor amplifiers required to drive the varactor chain. However, we had observed at various times in the past that forward pumping of VHF varactor stages resulted in an increase of the noise spectrum of the SHF signal, although such operation appeared to be tolerable in high SHF stages. Therefore, the design of the X-band source was based on only using the depletion-layer capacitance variation.

When such a design is made, very good agreement is obtained with the theory given by Penfield and Rafuse.

The basic design of the harmonic generator involved the design of an output frequency selective filter whose input impedance at the output frequency was a resistance having the magnitude required for maximum power handling capability. Also, the input impedance at the input frequency and intermediate frequencies, such as the second harmonic of the input frequency, was a pure reactance-frequency slope.

Similarly, the input circuit was designed to produce a resistance at the input frequency which was the value necessary to pump the varactor

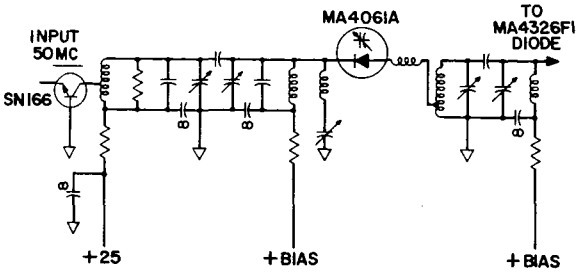

FIGURE 17–4.—Harmonic generator stage.

junction with the available input power, so that the requisite harmonic elastance variation was obtained. At frequencies other than the input frequency, the circuit appeared as an effective capacitive reactance. In designing the networks, it was necessary that they be made so that the net reactance seen by a current flowing through the varactor junction was zero at the input and output frequencies. Doubly tuned circuits satisfied our requirements, although more complex output filters would have been desirable. A typical harmonic generator circuit is shown in Figure 17–4.

Since the restriction was placed on the varactor operation that no forward pumping would be permitted and, further, that the reverse junction potential would not be permitted to exceed about 0.8 of the avalanche potential, it is not possible to produce the required 750 milliwatts of power at X-band by direct harmonic generation. Approximate expressions which relate the power handling capability of the varactor to its characteristics when the series resistance of the diode is small are as follows:

Simplified Equations for
The Doubler and Tripler Stages

Doubler:

Power output

$$P_{out} \approx 0.012[(V_{max}-V_{min})^2/(S_{max}-S_{min})]2\pi f_0$$

$$R_L \approx 0.145\ S_{max}/4\pi f_0$$

$$R_{in} \approx 0.07\ S_{max}/2\pi f_0$$

$$\text{Efficiency} \approx 1-27.6\ (\omega_0/\omega_c)$$

$$\omega_c = (S_{max}-S_{min})/2\pi R_s$$

$$\text{bias} \approx 0.41\ (V_{max}-V_{min})-V_{min},$$

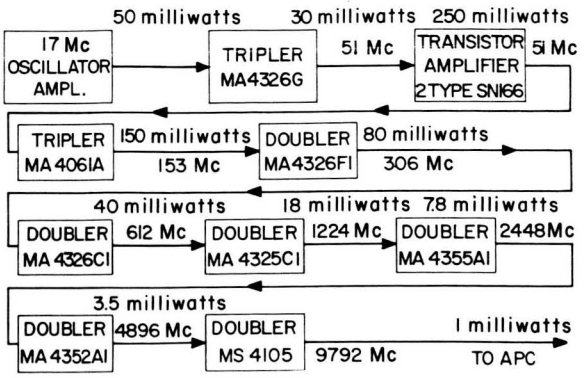

FIGURE 17–5.—Complete harmonic generating configuration.

where

f_0 = excitation frequency
V_{max} = max. instantaneous reverse voltage across junction
V_{min} = min. instantaneous reverse voltage across junction
$S_{max} = 1/C_{min}$; C_{min} = junction capacitance at V_{max}
$S_{min} = 1/C_{max}$; C_{max} = junction capacitance at V_{min}

R_s = series resistance of diode. (The effective reactance must be resonated out.)
C_{eff} at exciting freq. $\approx (1/0.68)\ C_{min}$
C_{eff} at second harmonic $\approx (1/0.67)\ C_{min}$

Tripler:

$$P_{out} \approx [0.024(V_{max} - V_{min})^2/(S_{max} - S_{min})]2\pi f_0$$
$$R_L \approx 0.17\ (S_{max}/6\pi f_0)$$
$$R_{in} \approx 0.13\ (S_{max}/2\pi f_0)$$
$$\text{Efficiency} \approx 1\text{–}35\ (\omega_0/\omega_c)$$
$$\omega_c = [(S_{max} - S_{min})/2\pi R_s]\{1/2[1-\gamma]\}$$

where γ is exponent in:

$$C_j = K/(V-\phi)^\gamma$$
C_j = junction capacitance
V = reverse voltage
ϕ = contact potential

Power limitation occurs in the VHF range. At the time this carrier source was designed, the only satisfactory high-frequency power transistor appeared to be the SN166. This transistor has a 20-watt dissipation rating at 25°C.

All our designs, however, are based on operating junction temperatures of not more than 120°C and maximum ambient temperatures of 95°C, to guarantee a particular reliability specification. With such constraints, the permissible dissipation is only 3 watts. It was highly undesirable that multiple transistors be employed. High-power VHF transistor amplifiers have been designed and built at Westinghouse, using special combining network techniques; but cost, space, and weight precluded such circuits from being used. It was desirable also to employ the transistors as Class A amplifiers to permit the use of RF feedback techniques if required and thus minimize phase modulation effects resulting from collector supply noise. For these reasons the amplifier was built to operate at 50 Mc and was designed for an available power output of only 250 milliwatts. With such restrictions on the design, the available output at X-band is only 1.0 milliwatt. However, the design permits the use of a single varactor diode in each stage. For wide bandwidth, it would be desirable to use two or four varactors in each stage, but such designs were not pursued.

Figure 17–5 shows the harmonic generator arrangement that was employed. It is interesting to note that at 50 Mc the full power handling capability of the MA4106 is being employed when it is operated without utilizing any benefits from forward driving of the diode, and at X-band the available junctions are all too large to permit efficient pumping. The inefficient pumping and cartridge parameters lead to a much narrower bandwidth than was desired in the SHF doublers. Figure 17–6 is a photograph of the harmonic generator.

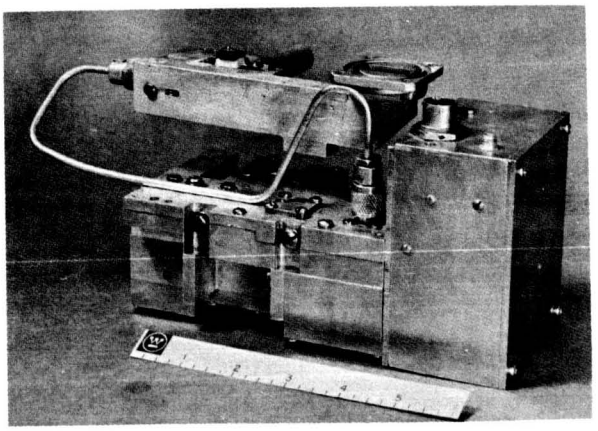

FIGURE 17–6.—Harmonic generator.

750-Milliwatt Generator

The 1.0-milliwatt signal is employed to phase-lock an X-band reflex klystron. Figure 17–7 shows the basic automatic phase control (APC) loop that is employed. The purpose of the APC loop is to slave the klystron oscillator to the frequency of the signal obtained from the harmonic generator plus the frequency of the offset oscillator. The offset oscillator also is sometimes employed to impart certain periodic information to the carrier signal, which is the klystron output. The APC loop must provide a gain versus frequency characteristic that will reduce frequency deviations of the klystron arising from power supply noise and vibration to the level of the reference frequency. The ability of the APC loop to perform this function in our applications depends on the ultimate phase noise of the product demodulator (phase detector). Noise in the product demodulator output is not merely determined by the noise figure of the X-band to demodulator circuits but depends on the nonlinearities that exist in these circuits. With the carrier signal, which is the beat between the klystron frequency and the frequency from the harmonic generator present, the effective noise figure is much worse when measured in a 500-cps bandwidth at a 2000-cps modulating frequency than when measured in the usual manner with the carrier not present.

Our measurements on various amplifier and product detector configurations have shown that the output carrier-to-noise level (C/N) does not increase linearly with the input C/N as the carrier is increased beyond a certain level. This level is much below the level at which noticeable

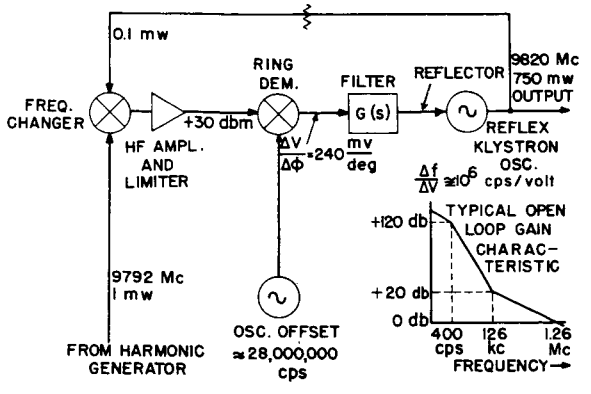

FIGURE 17–7.—Basic APC loop.

(1 db) compression occurs, and C/N trypically ranges between 110 and 135 db in a 500-cps bandwidth centered 2000 cps from the signal carrier frequency. Typical noise figures for the X-band to audio circuits are about 13 db, so that the maximum carrier-to-noise level is realized with 0-dbm signal power. With circuitry exhibiting maximum C/N of 110 db, the signal level need not exceed −24 dbm. In many applications, this condition is acceptable; and a −20 dbm signal level is employed. For example, for carrier sources required to be −80 db at 2000 cps in a 500-cps bandwidth, the error detector noise would be at least 30 db below the allowable noise on the source.

The APC loop must provide gain sufficient that frequency excursions of the klystron resulting from vibration, acoustics, power supply ripple, and dynamic load variations (pulling) be reduced to a level which satisfies the spectral purity requirements of the carrier frequency. A loop having an open-loop gain on the order of 120 db at 400 cps is capable of satisfying our requirements in some cases. When a feedback loop has such gain, it is necessary to reduce the gain to unity before intolerable time delays occur. A 40 db per decade cutoff at 400 cps is required. This typically may change to a 20 db per decade rolloff at a gain of about 20 db, yielding an APC bandwidth on the order of 1200 kc. With careful design of the amplifier and demodulator circuitry, additional filtering will not occur below a frequency of several megacycles, and the resulting gain versus frequency characteristic provided by the APC loop is adequate to reduce to an acceptable level the klystron frequency deviations resulting from all environmental disturbances. With transistor circuitry, one must be extremely careful in the design to minimize phase modulation of the carrier signal resulting from variation of circuit susceptance with noise on the collector supplies.

Figure 17–8 shows a typical IF amplifier and product detector circuit that is employed. The ac-to-dc conversion with the circuit shown is about 240 millivolts per degree of phase shift. The use of feedback as shown permits a reduction of phase noise resulting from power supply noise of approximately two orders of magnitude greater than is achieved with simple transistor circuitry.

Thus, with careful design of the APC loop the klystron can be disciplined to the reference

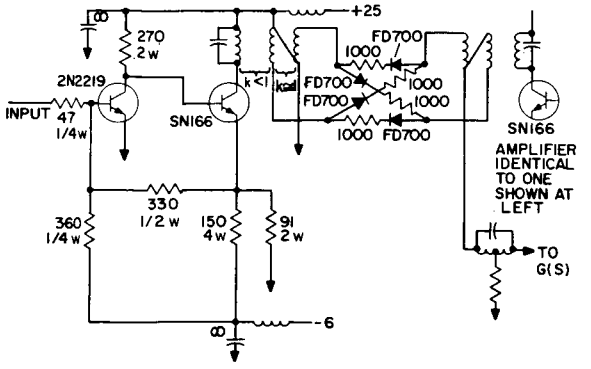

FIGURE 17-8.—IF amplifier and product detector.

frequency derived from the harmonic of the quartz crystal oscillator.

MEASURED PERFORMANCE CHARACTERISTICS

Stability of Complete Source

The complete source includes the APC loop and reflex klystron oscillator. The APC loop was evaluated separately from the oscillator-harmonic generator by utilizing a low-noise microwave oscillator in a laboratory environment as the reference frequency. The APC loop characteristics satisfied the design objectives and therefore did not need to be included in evaluating the crystal oscillator–harmonic generator.

The oscillator–harmonic-generator output frequency spectrum was measured by two methods. One method involved the use of the James Scott noise measuring equipment. The other method involved the use of a frequency discriminator whose input was the beat note obtained by heterodyning two completely independent oscillator–harmonic-generator units. The output of the frequency discriminator was measured with a narrow bandwidth wave analyzer. The noise bandwidth of the analyzer was 7 cps; and a 20-second time constant smoothing circuit was employed, so that the average value of the noisy envelope of the signal appearing at the output of the 7-cps bandwidth bandpass filter could be observed. The results of the measurements made on two identical sources is shown in Figure 17–9.

A previous paper (see Reference 2) described the instrumentation and results obtained in testing the oscillator. The measured results at the time the paper was written indicated that the harmonic generator did not degrade the X-band signal purity, as compared with the oscillator purity, except for the expected increase by the frequency multiplication ratio. Efforts, however, continued on improving the oscillator-amplifier circuits, and the results shown in Figure 17–8 included these improvements. The results now indicated that there was a slight degradation of the spectral purity caused by the harmonic generating circuits. Although we believed that at last we had a sufficiently stable oscillator and that harmonic generator instabilities were the limiting factor, the difference between measured and predicted results was too small to permit a definite conclusion to be reached. An evaluation therefore was made of the stability of the components in the harmonic generator.

Stability Under Vibration

The stability also was measured under vibration. Figure 17–10 shows the results when the harmonic generator was subjected to 1-g vibration input over a vibration frequency range from 100 to 2000 cps. Low-frequency vibration was also applied, and the spectrum was measured over the range of 100 to 6000 cps. Vibration input of 0.15-inch double amplitude from 10 to 30 cps was applied, and no discernible change in the power spectrum was observed. However, when the vibration input was increased to 10 g, the noise level increased by 3 to 6 db uniformly over the 100- to 6000-cps range. Although extremely rigid

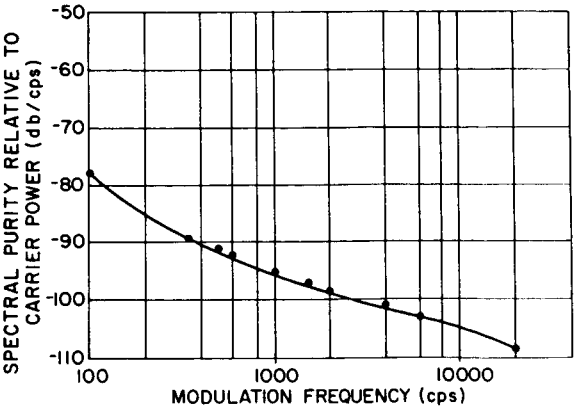

FIGURE 17–9.—Spectra of beat between two sources.

contruction and strip line circuits were employed (Figure 17–6), structural deficiencies were experienced at 10 g.

Oscillator Performance

To determine whether the harmonic generator degrades the stability, it is necessary to have knowledge of the oscillator spectrum. The results shown in Figure 17–9 are for an X-band signal source which is obtained by frequency-multiplying the output of a 17-Mc crystal oscillator by 576. The spectrum of the oscillator must then be 55 db better than that of Figure 17–8 if the results do not represent the oscillator performance. Therefore, an instrumentation technique is required

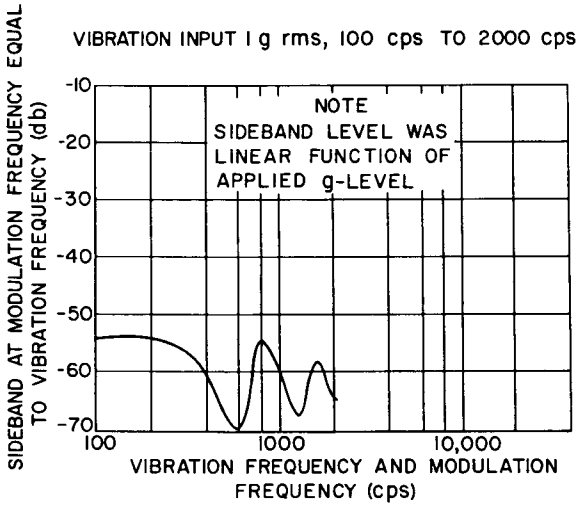

FIGURE 17–10.—Stability under vibration.

that is capable of measuring carrier-to-noise ratios on the order of 160 to 170 db/cps at frequencies separated from 2000 to 100,000 cps from the carrier. A technique that we found to be suitable for such measurement has been described previously (see Reference 2). Figure 17–11 shows the arrangement that is employed.

The secret of making such measurements is to recondition the carrier and exalt the noise sidebands. The latter is obtained by a carrier nulling technique as shown in Figure 17–11. This avoids the noise-carrier intermodulation problem that was discussed in connection with the APC error detection.

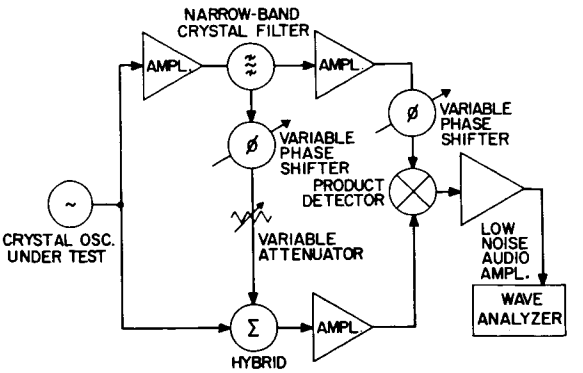

FIGURE 17–11.—Oscillator measuring instrumentation.

Calibration of instrumentation, such as shown in Figure 17–11, is made by several methods to insure that the desired information can be measured. A technique which is simple and straightforward involves the addition of a small signal to the carrier. Such a signal may be obtained from a frequency synthesizer and can be precisely set to be 100 db smaller than the carrier. The resultant is an equivalent single sideband signal. Such a signal consists of a set of symmetric and antisymmetric sidebands. These are equal in magnitude, and the antisymmetric set corresponds to phase modulation of the carrier with a modulation index that produces a −106 db sideband level. The product detector is a quadrating device; and, by properly adjusting the phase shifter shown in Figure 17–11, approximately 40-db discrimination against the AM component is realized. Measurement of the product detector output with the wave analyzer, together with knowledge of the

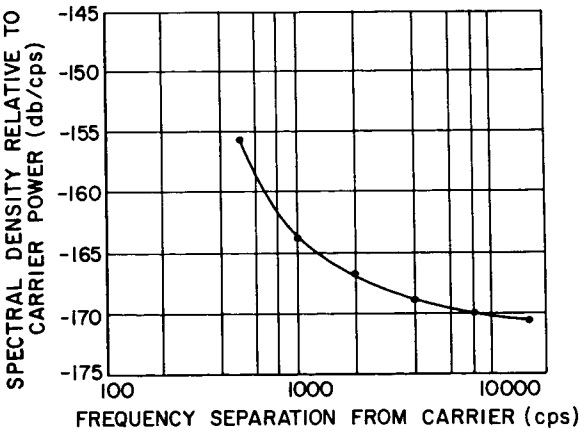

FIGURE 17–12.—Oscillator spectrum.

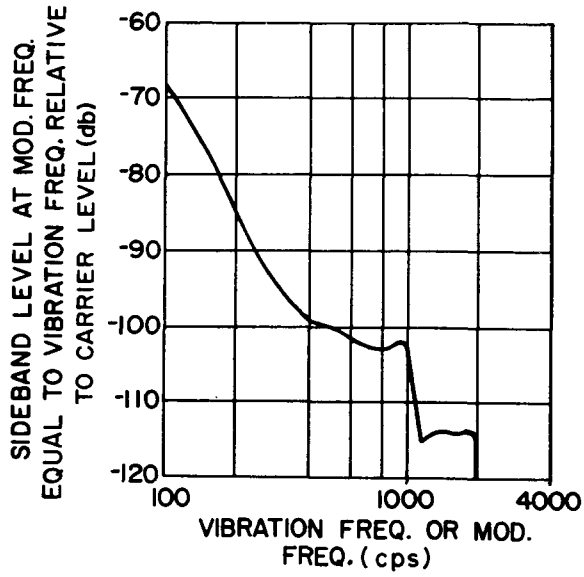

FIGURE 17–13.—Oscillator spectrum with vibration of 1 g rms, 100 to 2000 cps. [Note: (1) Sideband levels were linear function of applied g-level (2) Mount resonance at 3.4 kc was not excited as a result of nonlinearities in isolation for 109–2000 cps 1-g vibration output.]

signal levels at the summation point, then provides calibration of the measuring apparatus. This measuring technique has been perfected so that, at a frequency of 17 Mc, the ultimate sensitivity is better than a 170-db C/N in a 1-cps bandwidth at frequencies more than 2000 cps from the carrier.

The results of measurement of the oscillators employed in obtaining the results shown in Figure 17–9 are given in Figure 17–12.

The oscillators also were measured under vibration environment. The results for a 1-g vibration input are shown in Figure 17–13. At 2000 cps, the sideband level is −120 db/cps. Thus, isolation on the order of 800-to-1 is required in typical system applications, in addition to that which exists in the oscillator package.

Performance of Individual Stages of the Harmonic Generator

Since the X-band output spectrum and measurement of the oscillator spectrum revealed that degradation was occurring when our best oscillators were used, the individual stages of the harmonic generator were measured. Two identical circuits driven by the oscillator were measured by multiplying their outputs in a product detector. Detectors were constructed for each frequency of interest up to 300 Mc. This permitted individual stages and combinations of stages to be measured. The results include noise from each of two channels except in the case of the amplifiers. Since there is no frequency change involved, the source can be directly applied to the product detector when measuring an amplifier. Referred to X-band, the instrumentation noise at 50 Mc was −114 db/cps.

The results of these measurements revealed that the first two triplers and the 50-Mc amplifier both exhibited noise which accounted for the observed X-band spectrum. The first tripler and amplifier exhibited noise of −103 db/cps at 2000 cps from the carrier referred to X-band. The second tripler exhibited noise of approximately 101 db/cps at 2000 cps from the carrier referred to X-band.

The harmonic generator providing 300 Mc to X-band was measured as an entire unit, using a microwave phase detector. The noise contribution of this portion of the harmonic generator was −118 db/cps at 2000 cps from the carrier at X-band.

CONCLUSIONS

The results of the evaluation of the signal purity of an X-band source derived by generating an X-band harmonic from a 17-Mc crystal oscillator, using varactor diode harmonic generation circuits, indicate that the oscillator can be so good that harmonic generator degradation of the spectral purity becomes important.

When the signal purity at X-band must be better than was obtained with the mechanization described in this paper, it would seem advisable to utilize the harmonic of a VHF crystal oscillator rather than the harmonic of an HF crystal oscillator. If it is assumed that the same carrier-to-noise ratio realizable at HF can be achieved in the sustaining circuit and amplifier at VHF, the VHF oscillator should provide the same X-band spectrum as the HF oscillator when ideal harmonic generators are employed with both oscillators.

The TO-5 cold-welded crystal unit developed

by BTL should be well suited for this application. Preliminary results of vibration tests of such units at Westinghouse indicate that they are about two orders of magnitude better under the vibration environment than was the 17-Mc crystal unit.

There was no measurable increase in the spectral noise at the frequencies corresponding to the inharmonic resonances of the 17-Mc crystal units. In the use of the VHF crystal unit, the inharmonic responses might be a problem.

The transistor amplifiers can be greatly improved because of the availability of the RCA 2N3375 transistor. Using this transistor, extremely phase stable circuits—obtained using feedback techniques—can be realized at 50 Mc.

Step recovery diodes possibly can be employed for the high UHF and SHF stages of the harmonic generator. The fact that the harmonic current is proportional to the input signal level over a wide range of input implies that the bandwidth problems associated with cascading nonlinear varactor stages would be relieved.

It appears that, with little effort, an X-band carrier generator providing a carrier-to-noise level of 115 db/cps at 2000 cps from carrier should be realizable.

REFERENCES

1. Spencer, W. J., and Smith, W. L., "Precision Quartz Crystal Oscillator for Severe Environmental Conditions," in: *Proc. of the 16th Annual Symposium on Frequency Control*, pp. 405–421, April 1962.
2. Buck, J. R., Healey, D. J., III, and Meiseles, M., "Measurements of Phase Stability of Quartz Crystal Oscillators For Airborne Radar Applications," in: *1964 IEEE International Convention Record*, Part 8, pp. 34–42, 1964.

18. A LOW-NOISE PHASE-LOCKED-OSCILLATOR MULTIPLIER

H. P. STRATEMEYER

General Radio Company
West Concord, Massachusetts

A 100-Mc crystal oscillator can be phase-locked to any submultiple frequency between 1 and 10 Mc/sec. The use of a keyed phase detector makes it possible to obtain a wide range of multiplication ratios without adjustments of the circuit. Exceptional flexibility for experimental purposes and large multiplication ratios in a single stage are obtained with only moderate complexity. The bandwidth of the multiplier can be made over 5 kc/sec wide at 100 Mc/sec, so that the characteristics of the driving source are reproduced for averaging times down to less than 100 μsec. The noise level of the multiplier is less than −145 db per cps bandwidth at the 100-Mc output.

Figure 18–1 is a block diagram of the multiplier. A short pulse, generated at the input frequency, keys the phase detector. The output from the phase detector is proportional to the amplitude of the 100-Mc signal when the input pulse is generated. This output is used to correct the frequency of the crystal oscillator. This arrangement permits any integral ratio between output and input frequency (e.g., if the ratio is 20, every 20th cycle is sampled; if the ratio is 100, every 100th cycle is sampled). As long as the pulse

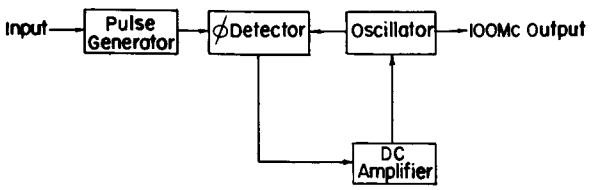

FIGURE 18–1.—Phase-locked oscillator multiplier (PLOM).

generator (Figure 18–2) can produce pulses at the input frequency and the loading on the detector is negligible, there is no theoretical limit on frequency ratio. Very high ratios have been successfully used in experimental units (Reference 1).

Figure 18–3 is a simplified diagram of the phase detector. Several factors limit the frequency ratio: (1) The pulse must be shorter than $\frac{1}{2}$ cycle of the waveform to be sampled, (2) the source impedance of the high-frequency signal and the "on" resistance of the switch S must be low enough to charge the holding capacitor C_H during one sample, and (3) the load impedance across C_H must be high enough to prevent decay of voltage across C_H between samples. The larger C_H is, the longer is the holding (discharge) time constant; but the source impedance must be lower

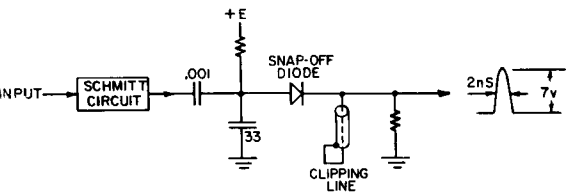

FIGURE 18–2.—Keyed phase detector.

and lower to charge C_H to the amplitude of the signal during the "on" period of S. If the output frequency is 100 Mc/sec, a ratio of 100:1 is easily obtained by conventional techniques.

For the unit described, a two-diode bridge with Gallium Arsenide diodes, a holding capacitor of about 20 pf and an input impedance of the dc amplifier of 1 MΩ gave satisfactory results.

The input circuits that generate the sampling pulse determine the noise contribution of the unit inside the lock-loop passband. It is convenient to

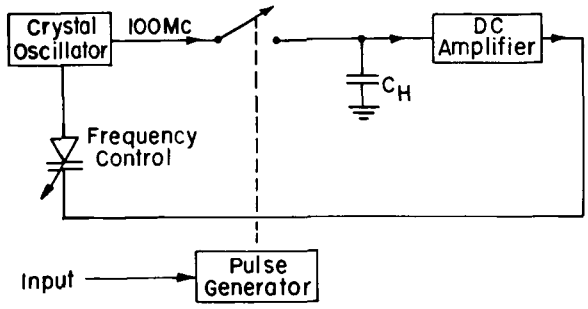

FIGURE 18–3.—Pulse generator.

use an equivalent resistance to describe this noise. This resistance is independent of the multiplication ratio. Several circuit arrangements have been investigated. In all of them, a snap-off (step-recovery) diode generates the pulse (References 2 and 3) for the keyed phase detector. They differ only in the way the input signal, generally a sine wave, drives the snap-off diode. A simple three-stage, overdriven amplifier was used originally but did not provide sufficient squaring at low input frequencies. The next circuit was a Schmitt trigger circuit and amplifier; all data presented in this paper were obtained with this circuit, which accepts a wide range of input frequencies and amplitudes. A tunnel diode circuit can be made more sensitive and can be used at frequencies into the hundreds of megacycles, but allows little range of input amplitude. While the tunnel diode may have somewhat less noise, the experimental use of the multiplier described made it impractical to limit the input amplitude to the 2:1 range of the tunnel-diode circuit. If a multiplier of this type is to be used for output frequencies over a few hundred megacycles, the tunnel diode may be required.

Design parameters of phase-locked oscillators have been treated extensively in the literature and are well understood (References 1 and 4). To understand the requirements of this unit, one need keep in mind only that the phase-locked oscillator will follow the modulating frequency of the controlling signal inside the passband of the lock loop. Outside the passband the noise of the oscillator alone is seen. The phase-lock loop acts as a low-pass filter for noise on the controlling signal and as a high-pass filter for the noise of the locked oscillator. The capture range can be made as wide as the lock range but can be restricted by an additional low-pass filter in the lock loop. If a multiplier is to be used to evaluate the performance of the low-frequency source, the capture range must be made as wide as possible (i.e., the frequency response of the lock loop should not be limited by anything but the lock range of the oscillator which, in turn, should be as wide as possible). Figure 18–4 shows the static characteristic of the 100-Mc crystal oscillator. The usable range is about ±100 ppm.

Figure 18–5 shows the overall response of a multiplier lock loop and the test setup for the measurement. A 5-Mc signal is multiplied to 100 Mc/sec in one channel. The same 5-Mc signal is fed to the other multiplier channel through a phase modulator. The two 100-Mc signals are connected to a phase detector, and the output is recorded as a function of the modulating frequency. The response is flat to about 9 kc/sec (−3 db) and rolls off at 20 db/decade beyond

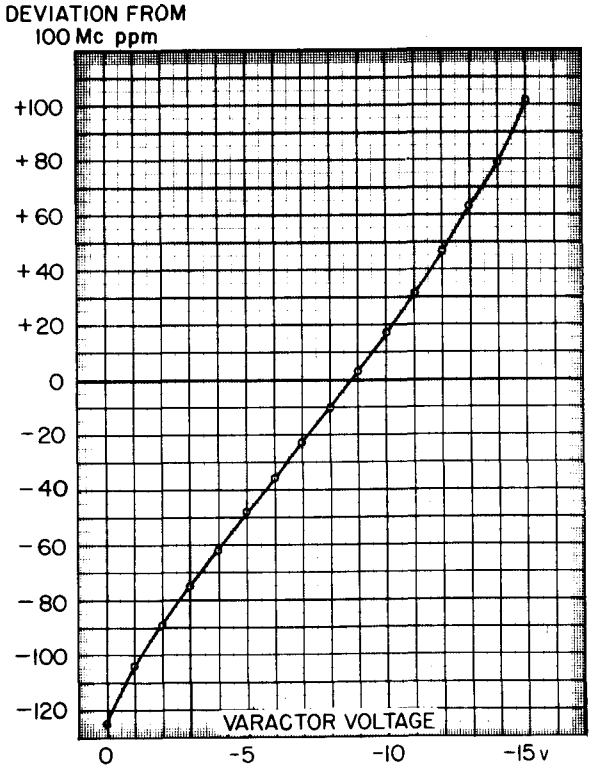

FIGURE 18–4.—Static characteristic voltage-controlled 100-Mc crystal oscillator.

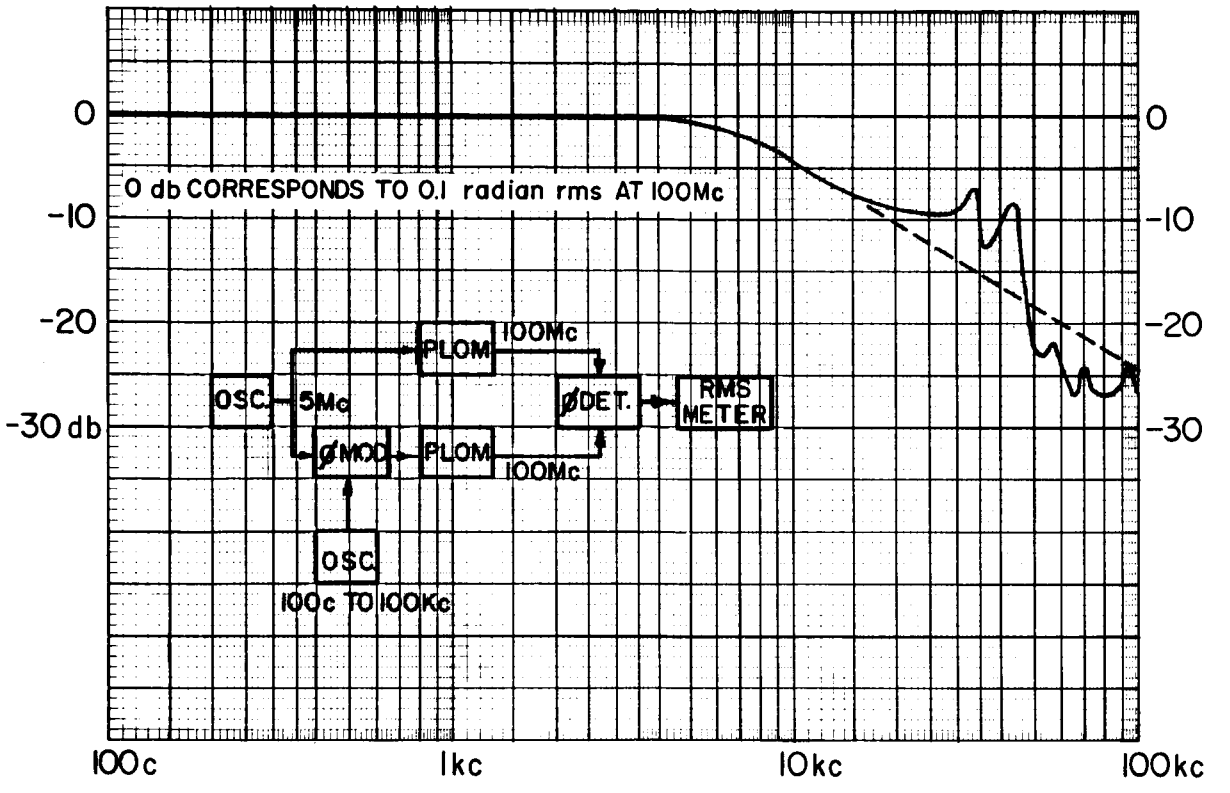

FIGURE 18–5.—Overall response of phase-lock loop of PLOM.

10 kc/sec. The peaks at 34 and 44 kc/sec are caused by spurious modes of the 100-Mc crystal in the locked oscillator. Figure 18–6 shows the spurious responses of the crystal alone. The main mode, at 100 Mc/sec, has a series resistance of 90 ohms; the nearest spurious mode at +34 kc/sec is 800 ohms; and the next, at +44 kc/sec, about 450 ohms.

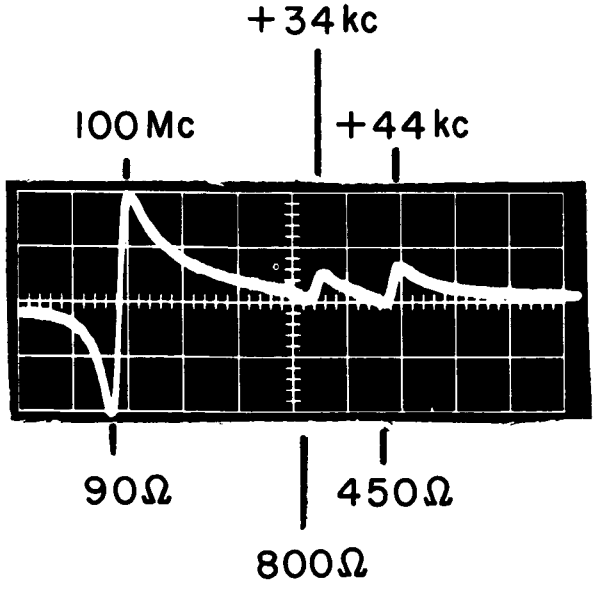

FIGURE 18–6.—Spurious modes of 100-Mc crystal.

EVALUATION OF PERFORMANCE

To determine the noise of the multiplier, coherent drive was applied to two identical multipliers; and the outputs were compared. Noise common to both inputs does not appear as output if the two multiplier channels have similar characteristics, whereas noise introduced by the multipliers shows up in the output. A wave analyzer can be used to plot the noise spectrum. At the 100-Mc

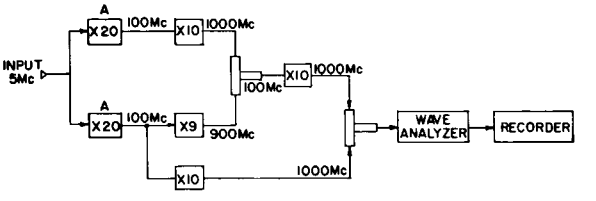

FIGURE 18–7.—Measuring system for noise tests.

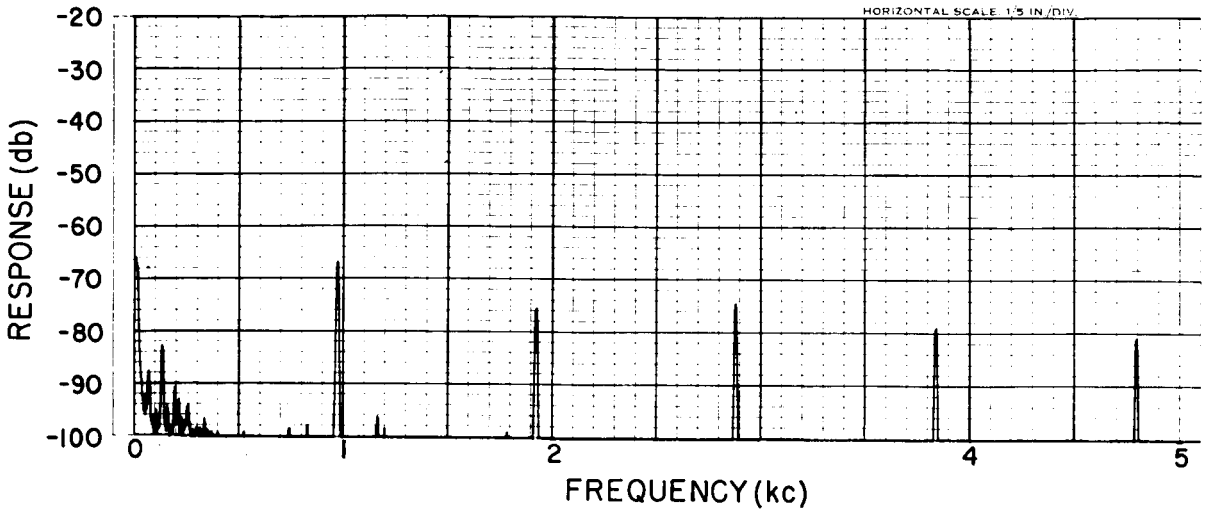

FIGURE 18–8.—X-band spectrum of klystron multiplier only. 100-Mc coherent drive; analyzer bandwidth, 10 c.

output of the phase-locked oscillator multipliers, the noise is too low to be measured, and additional multiplication is required. Figure 18–7 is a block diagram of the setup used for this purpose. This system multiplies phase deviations by 100 so that the spectrum is that which would be obtained at X-band. The multipliers in Figure 18–7 are phase-locked klystron multipliers with 100-kc bandwidth in their lock loops. Unfortunately, these units introduced rather strong sidebands at their power frequency. To separate these sidebands from anything that might be introduced by the phase-locked oscillator multipliers under test, the primary power was obtained from a power oscillator of about 1 kc/sec rather than from 60 cps. The spectrum of Figure 18–8 shows the output from the klystron multipliers with coherent 100-Mc drive to both chains (0 db corresponds to 1 v rms). Note the absence of noise down to the −100 db level except at the low-frequency end. The low-frequency components are caused by a combination of $1/f$ noise in the mixer, direct pickup of 60 and 120 cps through ground loops, and carrier unbalance in the wave analyzer. Relatively strong components are present at the 1-kc power frequency and its harmonics.

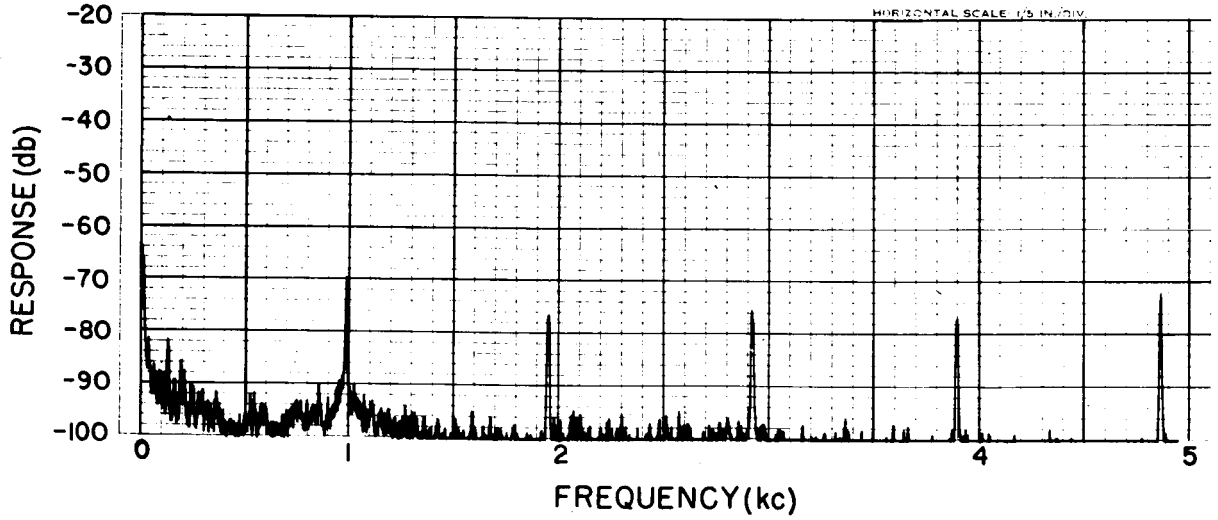

FIGURE 18–9.—X-band spectrum of complete system with 5-Mc coherent drive to PLOMs. Analyzer bandwidth, 10 c.

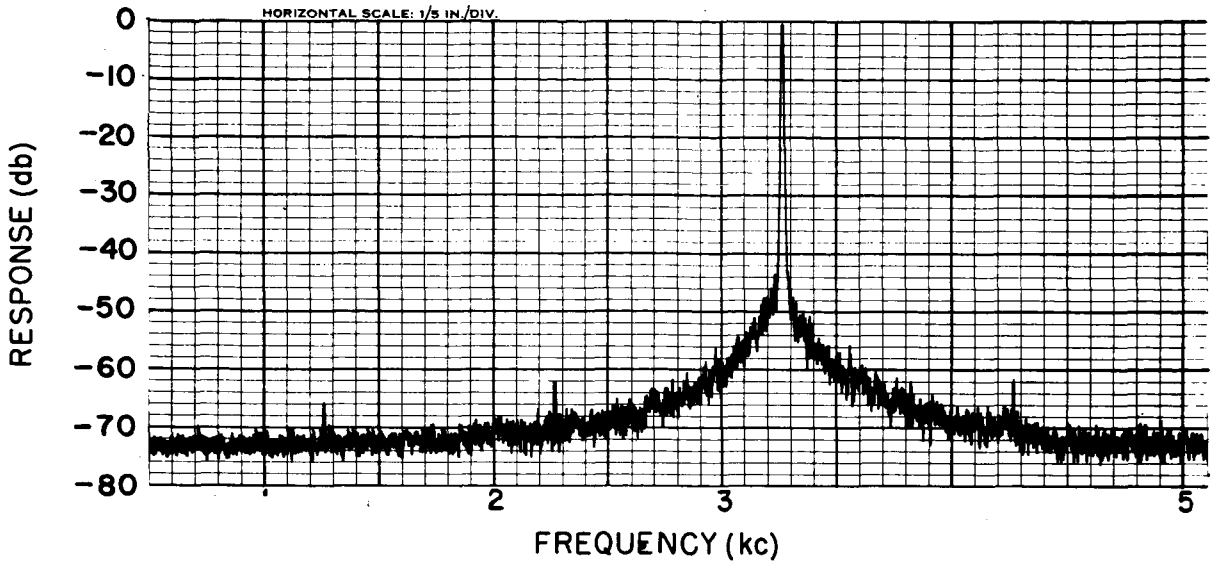

FIGURE 18–10.—X-band spectrum of two 5-Mc oscillators. Analyzer bandwidth, 10 c.

Figure 18–9 shows a spectrum obtained with coherent 5-Mc drive to the two phase-locked oscillator multipliers. The noise level is increased slightly and is between −96 db at a few hundred cps and −100 db above 3 or 4 kc/sec. This is the output from two equally noisy devices and corresponds to −99 to −103 db for one unit. As the spectrum was obtained with 10-cycle bandwidth, another 10 db must be subtracted to get the noise level for a 1-cycle bandwidth, so that the noise at X-band is between −109 and −113 db per cycle bandwidth. This can be reduced to −149 to −153 db referred to the 100-Mc output from the phase-locked oscillator multipliers, or to −175 to −179 db per cycle bandwidth for the 5-Mc input. Expressed in terms of equivalent noise resistance at the multiplier input terminal, the noise is less than that generated by a 200-ohm resistor at 300°K.

A typical application for these multipliers is the measurement of the noise spectrum of two 5-Mc precision sources with crystal drive levels of about 0.7 microwatt. Figure 18–10 shows a typical X-band spectrum.

REFERENCES

1. REY, T. J., "APC With Pulse Reference," MIT Lincoln Laboratory Report 47G–0019, November 9, 1960.
2. BOFF, A. E., MOLL, J., and SHEN, R., "A New High Speed Effect in Solid State Diodes," in: *Digest of Technical Papers, 1960 International Solid State Circuit Conference*, Philadelphia: IRE and Univ. of Pennsylvania, February 11, 1960.
3. DIETRICH, A. F., and GOODALL, W. M., "Solid State Generator for 2×10^{-10} Second Pulses, *Proc. IRE 48*(4): 791 (1960).
4. MCALEER, H. T., "A New Look at the Phase-Locked Oscillator," *Proc. IRE 47*(6): 1137 (1959).

PANEL DISCUSSION

SESSION III: DEVICES

Chairman	N. F. RAMSEY
Panel Members	W. L. SMITH
	D. L. HAMMOND
	A. O. MCCOUBREY
	F. H. REDER
Authors	A. L. HELGESSON
	P. DAVIDOVITS
	M. ARDITI
	H. MAGER
	S. L. JOHNSON
	D. J. HEALEY, III
	H. P. STRATEMEYER

Prof. Ramsey.—For one thing, I am very pleased and honored by the fact that several of the authors used the hydrogen maser for comparing how their device was as a short-term frequency standard.

But I really want to point out in the case of Davidovits and Arditi that their comparison was with a hydrogen maser that was designed for long-term frequency stability, deliberately designed not to have short-term frequency stability. In particular the hydrogen maser, as normally used when long-term stability is the principal desire, has a line that is made as narrow as possible. This means that the atoms are stored in the bottle for times of the order of a second or more for the purpose of getting a very sharp line. On the other hand, that does one no good if he is looking for very short-term stability. Furthermore, it does harm for short-term stability in that one must then diminish the power output of the device. This power limitation was true of the hydrogen maser with which the comparisons were made; we normally run with about 10^{12} atoms per second coming into the maser. This means that we were operating at 10^{-12} watts output, which from the point of view of short-term stability is somewhat unfavorable because of the low power output.

On the other hand, with the maser that we have at present, we could multiply the beam intensity by at least a factor of a hundred, and it is, I think, quite easy. It would be quite feasible with just a little bit of improved design to get still another factor of ten. This would essentially increase the average power of the maser, operated in a continuous fashion by about 10^3, in that case making it run at about 10^{-9} watts. This is very helpful on the short-term stability where the noise in the receiver is the dominant limitation as correctly pointed out by Arditi, Davidovits and others.

It is also true that with a hydrogen maser, one could do pulsed operation, that is where one deliberately operates the device somewhat intermittently. Under that circumstance, we could certainly get an additional factor of at least ten or perhaps even a hundred more beam intensity. The main limitation that would come at some stage is simply pumping speed to handle the hydrogen flow in the maser. On the other hand, this can for short intervals of time be overcome by giving short periods of bursts.

So I think for very good short term stability one could very well have a factor of at least 10^4 in beam intensity, which would therefore correspond to 10^{-8} watts or about the same as that discussed by Davidovits.

Now, this remark is not in any way meant to belittle the usefulness of the other devices, particularly the rubidium maser that was described, which has many great virtues of simplicity and is indeed a very attractive device for short-term stability measurements.

On the other hand, this remark does correct the statement that the rubidium maser could be two orders of magnitude better than the hydrogen maser for short term stability. This statement is only true of hydrogen masers designed for different functions. If both were designed for the same function actually they would be about comparable. There is a place at which one would change over from preferring the hydrogen maser to probably doing it with, say, a rubidium maser at somewhere in the order of—oh, probably on the order of 10^{-2} seconds. For longer times than that, the hydrogen maser, if you want high precision, is significantly better. For shorter times than that, the two devices are beginning to get fairly comparable, in which case one might as well take the simplest of the devices. For sufficiently short term stability it is really basically the power output that is relevent and if the hydrogen and rubidium masers are each operating about 10^{-8} watts, they would be somewhat comparable.

Mr. Smith.—It was most interesting this morning to hear reference made to devices with which I am familiar; namely, crystals and crystal oscillators, as compared to other devices with which I am less familiar.

The other point of considerable interest to me, at least, was the fact that for about the first time this morning we heard an actual suggestion

for a method to specify short-term stability. Whether or not the rms frequency definition in a given bandwidth is the best and simplest way is something still to be decided.

To me it appears that one needs probably different pieces of information for different applications. A complete specification, at least from a manufacturer's point of view is probably highly impractical because of the expense and the difficulty of making all of the measurements on a particular device. In most cases in which this very high degree of short-term stability is required, however, at least referring to crystal oscillators, there will be involved fairly lengthy multiplier chains, as was pointed out this morning by one of the speakers.

After multiplication of frequency, it matters little whether you start with AM or FM sidebands, you end up with a phase modulation. So probably, for practical purposes if we could specify the total spectrum at an equivalent microwave frequency, we could satisfy the practical needs of nearly all of the users of stable microwave sources.

This is presented for what it is worth. We have a long way to go, I believe, to reach a common ground for definition.

Just in passing, I was most interested in noting that the figures quoted for crystal oscillator chains are in pretty close agreement with a few measurements that we have made at Bell Laboratories so far. This gives me a little more confidence that perhaps we are not too far off in our attempts. We are a ways away from actual microwave chains. We have been using the systems of frequency differences very similar to that described by Mr. Stratemeyer and have come out with comparable numbers to those quoted by Westinghouse and Raytheon this morning.

Dr. Reder.—The paper by Stratemeyer, I thought, was interesting because it gives a very nice method for flexible testing. It has an interesting feature since one portion of a crystal signal is compared with another portion of the same signal, whose phase is controlled by the input to the trigger.

I wonder, on the next to the last paper, what the definition of "medium-short-term" stability is? But it is not an important question.

As to the paper on noise spectrum porperties of low-noise microwave tube and solid-state signal sources, I thought it was very useful because it presented a lot of data which was missing in some of the other papers. It looks as if there is hope that we shall get a solid-state microwave source which can be used as a flywheel for atomic frequency standards in the microwave range.

Now I would like to make a few comments on the paper on measurements of short-term frequency stability using microwave pulse-induced emission. It was stated that both this device and the masers have the advantage that they are not time-constant limited because there is no loop which locks anything. While this is true in general, actually the atom-cavity system also forms a loop with a time constant determined by the cavity Q, I don't think that this feature is of much importance in practice. You can hardly use these sources of high short-term stability without some amplification. And usually, I believe, one would employ a phaselocked klystron circuit which introduces a time-constant limitation.

It is also claimed that the pulse-emission device does not require steady inversion. This is true, but it still does require, or makes it desirable for output power, to have the difference between the two populations increased by optical pumping. So again, I do not think that this advantage is too important in practice, at least not as long as you stick to Rb for which achievement of steady inversion is not too difficult anyway.

I understand from the title of the paper that the pulse-emission device is primarily applicable to measurements of the spectrum of, for instance, crystal oscillators, and not so much as a source per se of high short-term stability signals of sufficient power level in the microwave range.

I also wonder what the effect of spectrum asymetry would be in case the frequency of the driving signal does not exactly agree with the atomic frequency. Since your (Dr. Arditi's) measurement precision was limited to about 2 parts in 10^{10}, you may not have seen such an effect.

I think the same might hold, at least in part, for the claimed absence of any light-shift. I just wonder whether there is absolutely no light-shift in a device like this in which you turn off the light before you look at the microwave signal

or whether a small light-shift is still possible depending on the time interval between "light-off" and "microwave receiver-on".

I do not believe in the suggestion that the pulse-emission device should be used for tuning the hydrogen maser. Because if one uses it for maser tuning one degrades the H-maser accuracy by the lower accuracy and stability of the pulse-emission device.

The paper on an optically-pumped rubidium maser oscillator brought a very nice surprise, that is, Columbia University got this maser finally oscillating between the $m=0$ levels. What arouses my suspicion, however, are claims that several discussed improvements can be achieved "easily". I wonder—other well-experienced people work so hard for years just to accomplish moderate improvements—I hope they know what they are doing.

I do not believe that the Rb maser is a suitable—well, let us say competitive, standard for long-term frequency stability. It is plagued by the bad feature of any maser, namely cavity pulling. You do not have this serious problem with passive standards.

Also I believe that there are still many technical problems to be solved. Many of those at first easily-taken technical problems turn out to be really nasty problems in the end. For instance, take the all-metal cavity with the glass-to-metal seals exposed to Rb vapor. Rb reduces metal oxide which is a vital element of the seal. Of course, one may overcome this trouble by painting the seal with a suitable film.

This sealing problem aggrevates leak testing (something serious for all gas cell standards) which is important for long-term stability and quite complicated because of the 10 Torr, or so, buffer gas pressure. If a leak develops in the metal-glass seals, you have no ready means of detecting it except by measuring frequency changes.

The paper mentions that the Rb maser uses a magnetic microwave window. I think it would be desirable to replace it with a nonmagnetic window which is now available on the market.

Again, I am very skeptical about an "easily" achievable 10^{-8} watt power output. I never have seen an improvement by a factor of 1,000 which came about "easily". I do believe in the potential of the Rb maser as an excellent short-term stability source and I would like to recommend strongly that the Government support work on the solution of various technical problems. Such work can best be done by industry, and it would do no harm to do it in parallel to further research at Columbia University which is concerned with more basic problems, e.g., finding buffer gas mixtures with better temperature stability and reducing light shift.

Now about the first paper, according to its title it should have treated all passive atomic standards equally. But I think it was heavily influenced by the beam-tube people. There was very little information in this paper on gas cell standards which, offhand, look to me to be by far better standards for "short-term" stability. Also, I think it would have been quite useful if the obvious spread in the f value of the various beam tubes would have been explained.

Finally, if I may, I would like to show, just for the fun of it, a beat note recording between two Rb standards. It was recorded at 100 Mc and with a time constant of the Parzen frequency comparator of 0.01 sec. This specific beat note was established by tuning one standard as close as possible within a reasonable time to the other. It shows, therefore, phase noise for considerable time intervals around the cross-over points. In this specific case the beat cycle was about 6 hours long. I do not claim that gas cell standards always behave like this, but it is an interesting case. It means that the offset here was 5 parts in 10^{13}. Since such numbers are thrown around here freely, I see no reason why I should not throw one, too.

Dr. Vessot.—It is set there, though; it didn't get there by itself.

Dr. Reder.—This is right. I did not claim it. I said so specifically.

Unfortunately, the projector here does not work with this record. Well, I will leave the record here on the podium during lunch time, and those interested can look at it.

Dr. McCoubrey.—I wanted to comment first on the fact that I think we are witnessing at this conference some new viewpoints which are particularly important to the topic of the conference, short-term stability. These new viewpoints

are represented by the paper on the rubidium maser and the remarks of Professor Ramsey concerning the hydrogen maser, with particular respect to its short-term stability.

The point is this, there will always be a need for oscillators which can be slaved by phase locking methods to very stable master oscillators, such as the hydrogen maser, or which can be used as flywheel oscillators, frequency locked to a very stable atomic reference such as the cesium atomic beam tube, possibly later on a thallium tube and the rubidium buffer gas cell.

Now, the point is that these references provide the long-term stability that you want, and whatever degree of short-term stability that you require will have to come from either the slave or flywheel oscillator that is used. So far crystal oscillators have been used exclusively in this kind of work.

But I think that now the picture is changing, and with the developments that we see coming, these active maser oscillators having excellent spectral purity, will provide some opportunities that we haven't had in the past.

The aging characteristics of quartz crystals and their high sensitivity to mechanical acceleration, vibration, microphonic effects, etc., place some real demands upon the design of feedback systems; the feedback systems associated with phase lock circuits, or the feedback systems associated with frequency control circuits.

From a practical viewpoint these effects are absent or at least they are reduced by many orders of magnitude in the case of the active atomic oscillators, hydrogen masers and rubidium oscillators. I think if these devices are developed, for their optimum spectral purity, they will be particularly useful for slave oscillators or flywheel oscillators in feedback systems. This optimum design will involve the high power output without sacrificing the Q associated with the atomic transitions.

I think it was evident in the talks that the rubidium oscillator will certainly be important because of its size and simplicity. Which of these oscillators will actually have the highest degree of spectral purity, I think, remains to be seen. The details are not obvious to me now, at this point in any case.

The second thing I would like to comment on, I find it a little hard, is this question of the pulsed emission. I have the feeling that, if we gathered ten experts in the room, it would be about an hour before we are all talking about the same thing. This may or may not have something to do with short-term stability; I don't know. The point, though, is that it is difficult to compare what is happening in the pulse case with what we have been talking about at other times during the conference. I think that it is necessary to look very, very closely at the fundamentals of what is taking place in each case. What I would like to try to do is to focus attention on three points. It is particularly hard because I find I have to jump between this concept of spectral purity in one case and short-term stability in the time domain in another case, and I can't do that very well.

But, first, in the case of the cavity tuning effect, such as in the transient case of pulsed emission, one is dealing with radiation which is emitted over a short period of time, the time of the pulse. You are dealing with atoms that radiate typically over a period of, say, ten milliseconds, a hundredth of a second. There is a spectral distribution associated with this. We might call it a spectral distribution associated with the atomic transition, typically, it might be a hundred cycles per second or about a part in 10^8.

In the steady-state case the radiation that we are dealing with is concentrated in a much narrower spectrum simply because it is a steady-state case.

Cavity tuning and cavity pulling effects arise because there is a weighing inside of the maser between the atomic transition function and the cavity tuning function itself. Now, it turns out that the magnitude of this effect is given by the width of the spectrum associated with the atomic transitions, which is important in the transient case which was discussed. This width multiplied by a fraction, a quantity which is a cavity detuning, expressed as a fraction of the cavity width between the half-power points, and in any practical case this is a very small quantity. So any cavity pulling effects are small compared to the spectral width of the radiation associated with the transient case.

As far as the maser tuning suggestion is concerned, on which Dr. Reder has already com-

mented, I think it is important to recognize that here you are trying to tune the maser by zero beats with radiation spread over a spectrum which is a part in 10^8 wide. In cases of interest, we are talking about tuning these things in parts to 10^{12}. This can be done quite well, and we are approaching a part in 10^{13} in this connection.

Third, I would like to focus attention on the comparison of the short-term stability measurement with those discussed in other papers at this conference. The situations can be very, very different and I don't think it is valid to make a simple comparison. For example, in the transient oscillator, in addition to the length of the samples which one is comparing, there is also the rate of decay associated with the radiation which enters. In the case of the short-term stability of the active maser oscillator, it is oscillating continuously, this decay rate is not present, the thing is oscillating steadily, but instead you have the much smaller effect of thermal noise which gives rise to the spectral width. In both cases, of course, the additive noise enters.

Mr. Hammond.—I would like to talk a little bit about some of the characteristics of short-term frequency stability, characteristics of quartz crystal units.

I refuse to have an inferiority complex after hearing the discussions of atomic frequency standards. I think that we all have a great deal of appreciation for the short-term frequency stability that is possible with the rubidium maser, and it is a very tantalizing thought of coupling this with a cesium beam standard to get an excellent long-term/short-term device, using both of them in combination. I think this solves a problem of high frequency, high spectral purity, to a few orders of magnitude. It still leaves us with the question of short-term frequency stability at lower frequencies, which incorporate divider problems in getting from the higher frequencies down. I think this is a much smaller problem, because the people who are really concerned with high frequencies are at the high frequency region already.

In the case of quartz crystals, I think this is still an important matter, because a great deal of our present applications for short-term frequency stability are geared around quartz crystal units. There are basically a number of origins of short-term frequency instability that we understand pretty well; the thermal effects in the oscillator, i.e., the shot noise, but I think more important still, this $1/f$ noise. I think $1/f$ is probably not a very good term. Probably it would be better to call it device noise. It is a characteristic of a unit of the resonator, of the mechanical elements that are involved.

I would like to say that there seems to be a problem in the minds of all of us about what happens as the frequency goes to zero, and I think this is a very legitimate question. Certainly the $1/f$ noise is related to long-term aging. And as an element of experimental fact, I would like to point out that if you observe short-term frequency stability over a period of time that there is a correlation between the aging rate and the short-term frequency stability.

What this says is that the power spectrum, the amplitude and its characteristics are time dependent. This function that we carry out to get from the time domain to the frequency domain is itself a variable in quartz crystals, and because this variable does relate to long-term stability, this certainly gives me reason to believe that you can push this function a good deal closer to zero, the $1/f$ a good deal closer to the zero point than we have talked about earlier.

I think that one of the stumbling blocks here has been the concept involved with this $1/f$ noise approaching zero; that this implies an infinite aging in infinite time. This isn't too surprising. If you look at some of the mechanisms in the device that can cause this $1/f$ noise, one of these is the evaporation of contaminants. Let's suppose that after a while you run out of contaminants. This simply means that the spectrum is changing in amplitude, the function changes. Or, putting it another way, if you integrate to infinite time and expect to predict what the frequency will be, you will have to consider the fact that the thing that you are integrating, the function of stability out to long-term time elements, is itself changing. Even in the case of a quartz crystal unit, we think of this piece of quartz as being an inert device; it is not going to go anywhere; it is not going to disappear. Yet I point out to you that it does have a finite vapor pressure, and although this is extremely small, infinite time is a long period of time, and con-

ceptually there is nothing wrong with evaporating all of the quartz away.

Now if you will permit me to put my tongue in my cheek and say that there have been some articles recently predicting that the gravitational constant is decreasing with time due to either the expansion of the universe or the decrease in angular rotation of the galaxy, then you would expect due to this observed or predicted aging rate that we should have some $1/f$ noise in a pendulum clock.

And if we turn this around and we eventually observe some $1/f$ noise in atomic frequency standards, maybe we can have some justification for thinking that our fundamental concepts are changing.

Dr. Davidovits.—Professor Ramsey, I certainly didn't imply that the rubidium maser is going to replace the hydrogen maser. Obviously, the hydrogen maser has long-term stability and in addition, it is much more a primary standard than the rubidium maser. Of course, in a short talk of this sort, one can only sing praises to his own device.

I think, however, Dr. Reder made some comments which were somewhat pessimistic. I didn't mean to imply, and I certainly don't imply, that the device whose pictures I flashed on the screen going to be the ultimate rubidium maser which is going to give the stability or the power output which I quoted. What you are saying is certainly true, the walls may indeed form oxides, but it is certainly not out of the question with good techniques and enough money spent that one can make a cell which will not deteriorate. As far as the power output is concerned, I mean, you say you don't believe 10^{-8} watts is possible. Well, all I can say is that I do.

Dr. Arditi.—I would like to make some comments about the light shift in the case of the pulse-induced emission.

We have changed the light intensity over quite a large range of more than five to one, and could not detect any frequency shift. It was measured to 1×10^{-10} at least. And this has been checked by using the technique of beating the output frequency of two cells, but also with a technique using pulse induced emission where we could use several pulses before an excitation pulse was applied, and in that case we could make a rather narrow line in the order of ten or fifteen cycles at 6834 Mc, and could not see any shift of the center of this line with variation of light intensity. I believe this is due to the fact that those light shifts are really due to virtual transitions, and there is a certain lifetime to those transitions which is of the order of 10^{-7} seconds, which will not persist once the light is turned out.

Mr. Mager.—Professor Searle yesterday commented on the possibility of translating between the frequency domain and the time domain. As a radar engineer, I should like to apply for help here in making the data that we presented today more useful and meaningful to a much wider audience. In other words, let us consider a typical case of a two-cavity klystron in which we have a microwave demodulator feeding a bandpass filter centered at 10 kc, let's say a fourth-order Butterworth filter, with a 1 kc bandwidth, and say that this filter feeds a true rms voltmeter with a detector averaging time of a few seconds. My appeal is to translate this now to something meaningful to frequency control engineers.

Mr. Barnes (National Bureau of Standards).—Dr. McCoubrey, I believe that you suggested that the spectral width of pulsed masers limits measurements to this spectral width or about one part in 10^8. I believe that it is the total number of photons emitted which limits the precision of measurement and not the duration of the pulse. Hence, you can measure the average frequency much more precisely than the spectral width.

Dr. McCoubrey.—I said that I felt that the spectrum associated with the decaying radiation had frequency components spread over a region that wide. I think the details of how you measure this, obviously you can measure it to a fraction of that width, depending on the techniques, the distortion, the shape of the spectral function, and questions of this sort. I would agree that you can measure to a small fraction of that.

Dr. Mullen (Raytheon Research Division).—I am not sure that I understood the figure of merit. It appears to me that in the inverted equation you find out that you have a delta nu, by which is meant the frequency uncertainty, and which is related to the line width divided by the square root of a power signal-to-noise ratio, so this is the kind of pulse splitting that you can get if you have a good signal-to-noise ratio. Is

that what the figure of merit refers to, the number of parts that you can split the line width into?

Dr. Helgesson (Varian Associates).—This figure of merit is intended for comparison of standards at the same frequency. For instance, in the comparison of cesium standards, it is essentially the—I guess you have described it a little bit differently in saying this is how fine you can split the line. Perhaps, if you take this and calculate the frequency stability from the figure of merit, then you can describe essentially how fine you can split the line for any definition of averaging time or averaging bandwidth, and we made this comparison for one second averaging time. I don't know if this answers your question or not.

Maybe you are confused because the figures of merit were not related directly to the frequency stability that we calculated for one second averaging time. The reason here was that we were comparing several things that operate at different atomic reference frequencies.

Dr. Mullen.—Well, it appeared to me that it involved a line width, too. That the one over delta nu was the signal-to-noise ratio over some W. So was the W the natural line width, or was that the line width of that central peak?

Dr. Helgesson.—That is the line width of the central peak, and in the gas cell it was the line width of the absorption in the gas cell. Since in the beam device we operate strictly on the central peak, this is the parameter that is important in deriving that stability or the figure of merit.

Dr. Alley (University of Maryland).—I would like to address a question to Dr. Davidovits regarding the light shift, the self energy effects in the presence of a real radiation field. Have you had a chance to measure this with the oscillating rubidium cell?

Dr. Davidovits.—Not quantitatively. But there are light shifts just as one would expect, and we are now presently trying to measure them quantitatively and devise methods of minimizing them.

Dr. Alley.—You have no idea of the order of magnitude of those present in an oscillating device, compared to those in a passive device?

Dr. Davidovits.—No, I don't. All I can say is that they are present, we have observed them, yes.

Prof. Searle(MIT).—I would like to address a statement to Dr. Helgesson on the first paper. I am sorry that my paper didn't come after the previous one, because it is very pertinent. This is on this darn averaging time business that we kicked around yesterday and which came up again this morning. Let me just try to say it as briefly as possible this way, because of the peculiar nature of this particular measurement problem where we are involved in taking the derivative of the phase, or in the frequency domain, that is multiplying by omega squared, the high frequency noise in any one of these systems is greatly emphasized, and therefore the nature of the high frequency properties of the filter that you use become very, very critical. That is, that the filter, the high-frequency properties, the parts that you are being casual about, have a profound influence on the frequency stability number that you quote.

Dr. Helgesson mentioned sort of casually that when you use the averaging in the "frequency domain" that this sometimes gives you a little bit better criteria and this can be used to advantage. Let me just say for a simple-minded example that I picked, the difference between these two methods was several orders of magnitude, and in a word, let the buyer beware.

Prof. Ramsey.—It seems to me to be an advantage to take something like a gaussian average since this isn't so sharp on the edge and then the exact shape makes less difference.

Dr. Helgesson.—I would like to say that of course when you make a measurement of frequency domain averaging, and you do not use a filter that is purely rectangular, there is some noise that comes through above the cutoff frequency. However, the measurements we have made used a filter that drops off at 24 db per octave.

If it looked like this was not sufficient, one could provide whatever rejection is necessary in order to make a valid measurement; attenuate the high-frequency components to the extent that is needed to get a valid measurement. We felt for the measurements that we made that this was sufficient.

Dr. Vessot (Varian).—I am mystified a little by the pulse method. I agree that the coherence within the pulse is very, very good. But I think it would be very difficult to try and make a

statistic on one sample pulse. I think the difficulty of creating a method for doing this thing is probably one order of magnitude greater than the difficulty of agreeing on a way of specifying frequency at this conference.

I agree that the light shift is absent, however, Dr. J. Vanier's calculation has shown that this happens. The other thing is that one does get phase shift in passive standards. I direct this to Dr. Reder. These are the shifts in phase at the ends of the Ramsey cavity, so therefore there is a cavity problem with the passive standards. It is a different kind of cavity problem, but it certainly is not negligible.

The other comment is that I think we are between two fires here on the rubidium maser and the hydrogen maser, and I would just like to point out that one is like a wrist watch and the other is like a tower clock, and I would not like to wear a hydrogen maser in my pocket whereas I would consider carrying a rubidium maser some distance. There certainly will be places where each will be of paramount importance.

As to the question of the power level, I believe both can be raised and I think that a common limit is going to occur that is apt to be something like the spin exchange process. You end up having molecules, or atoms so close together that they cannot endure each other's presence and there is a cutoff of oscillation. In the case of hydrogen, you have to get rid of the unwanted atoms, and that requires large pumps. I believe there may be some other things, such as intensified optical pumping required in the rubidium maser and that presents further problems.

Dr. Reder.—I would like to answer first the remark by Dr. Vessot about the cavity pulling. I did not say that the passive standard is completely free of cavity pulling. What I say is that a maser has a considerably larger cavity pulling effect than a passive device, and the factor is the ratio of the two involved Q values.

Dr. McCoubrey.—On the comment which Mr. Barnes made, I think he hit a nail on the head there, and that is in the pulse case there will be advantages. There is a potential advantage in that you can arrange that more quanta be emitted during the time of interest than you could arrange in the corresponding continuous oscillator case. That is, take advantage of the fact that you can concentrate all of the quanta in the time that is of interest, rather than having them dribble out continuously.

Mr. Ashley (Sperry Tube Division).—I want to defend the honor of the two-cavity klystron a little bit. The data that we have seen this morning is a good type oscillator, but I want you to know that there are many other specifications that went into that, and the noise was compromised to a small amount in meeting other specifications. There is room for improvement in the two-cavity oscillator. In England, the people at Ferranti reported at the Paris Tube Conference that they have an oscillator which by optimizing the beam and the coupling of the beam to the gap in the cavity they have reduced the frequency modulation by a factor of some seven to ten over the data that you saw presented this morning.

As the data that several papers have shown indicates, the principal defects in the klystron oscillator are mechanical. It is the frequency modulation which results when you insist upon vibrating it. I would say that in engineering the oscillators that have been built to this day, the primary consideration has been on the electronics and on the achievement of the low residual FM during non-vibrating conditions, and we pretty much take what we get on the vibration characteristics.

Recently we have been doing a reflection tube where we have been worried about the other end of it more than the mechanical end of it, and we brought the reflection tube to a competitive position with this two-cavity oscillator in terms of frequency modulation when you vibrate. Now, this shouldn't be. The electronics very much favor the two-cavity oscillator because it is a high voltage device and does not have grids. I think if somebody were really to apply themselves to the mechanical design that the residual FM of the two-cavity oscillator could be reduced by a factor of at least a hundred, or a factor of at least ten and probably a hundred over the mechanical vibration figures that have been given previously.

Now, the last comment is that I have been trying to keep up with solid-state competition

and I measured one C Band chain and got a curve which was very much in agreement with that theoretical curve which was presented by Johnson in his talk.

Mr. Johnson (Raytheon Co.).—Well, I suppose some reply is needed. I thank the gentleman for presenting some data in support of the solid state chain performance.

I also would like to comment on his statement that we could expect improvement in the order of ten to a hundred in the vibration sensitivity or a decrease in the vibration sensitivity of klystrons. I say well, let's go at it, we sure could use it.

Mr. Grauling (Westinghouse, Baltimore).—I would like to ask the gentleman from Sperry if the data on the vibration of the two-cavity tube includes also vibrating the power supply, which could be a problem?

Mr. Ashley.—No, the tube plus a Sperry isolator on the vibration table, everything else—

Mr. Grauling.—I just want to point out that we have to take the power supplies along with us.

Mr. Chi.—I would like to make one observation. In the morning session there were two speakers, and perhaps there will be other people, wondering if we know what is short-term frequency stability. I think it is fair to say that we know what short-term frequency stability is.

The core of the problem is that there are too many definitions. We know what we are looking for. What we are seeking is one standard definition and measurement technique.

IV. MEASUREMENT TECHNIQUES

Call to Session ROBERT J. COATES
GSFC

Chairman CAMPBELL L. SEARLE

Discussion Panel CHESLEY H. LOONEY, JR.
GSFC
BENJAMIN PARZEN
Parzen Research, Inc.
GEORGE E. HUDSON
Boulder Laboratories, NBS
GERNOT M. R. WINKLER
Institute of Exploratory Research
U.S. Army Electronics Laboratory

19. STABILITY MEASUREMENT TECHNIQUES IN THE FREQUENCY DOMAIN

R. A. CAMPBELL

Raytheon Company
Bedford, Massachusetts

The general art of demodulating RF signals has been practiced for many years, but this art becomes more difficult when the information to be extracted is oscillator noise—especially when an accurate quantitative measurement is desired. This paper surveys the general subject of time versus frequency domain measurements and investigates the frequency domain more thoroughly.

The paper is largely devoted to CW frequency demodulators used in noise measurements. Comparisons are made with respect to sensitivity, equipment noise, power levels required, and rejection of other modulation modes.

Varied aspects of postdetection equipment are also considered, especially video filter noise bandwidths and current attempts to standardize bandwidth to facilitate establishment of a noise specification. A brief discussion of the various types of readout devices (oscilloscopes, voltmeters, etc.) is included.

Calibration—both direct and indirect—is discussed, along with the applicability of the various methods available.

TIME VERSUS FREQUENCY DOMAIN

Frequency stability is determined by measuring the instability of a signal source. The two general methods of this measurement are the so-called *time* and *frequency domain* approaches. *Time domain* measurements produce—as an end result—an accurate plot of frequency versus time, the measured points being the average frequency over some time interval. For example, a typical measurement may determine the frequency by counting cycles for 1 sec, successive points being taking from every second to every hour, depending on the results desired. Stability (or instability) is then determined by statistical methods from the measured values.

Frequency domain measurements, on the other hand, deal with the frequency spectrum of the signal and define stability in terms of the energy outside the center frequency of the signal. This definition of stability also includes amplitude instabilities, since they also put energy into sidebands. In some applications, frequency and amplitude variations are indistinguishable, as far as the end result is concerned.

The task of the frequency domain measurement is, therefore, one of demodulating the signal so that the spectrum may be processed in a quantitative manner. Two general techniques present themselves. One typically involves a narrow-band receiver that can view any portion of the spectrum directly. This is undesirable, since it cannot distinguish between AM and FM sidebands. The other involves demodulating the signal in a calibrated detector and viewing the spectrum with the center frequency translated to zero frequency. Ideally, this detector should be linear with frequency and amplitude, and insensitive to any modulations other than FM. Because of the modulation levels encountered, signals are small; so postdetection gain is required. The amplified signals are then analyzed in an appropriate manner with voltmeters, spectrum analyzers, etc.

FREQUENCY MODULATION DETECTORS

The general form of a frequency modulation detector (Figure 19–1) is a comparison of a sample of the signal that has been passed through some dispersive network with an unmodified sam-

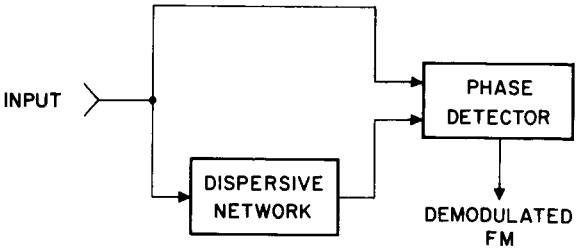

FIGURE 19–1.—Generalized diagram of FM detector.

ple. The comparing circuit ranges from a simple video crystal detector to an amplitude-insensitive phase comparator. The net result is a conversion of a portion of the frequency modulation sidebands into amplitude sidebands, which can then be detected. The various types of detectors are merely combinations of different dispersive networks with various phase comparators and different amplitude detectors.

The simplest detector—with the exception of the slope detector—is the interferometer, where the dispersive element is a long line (Figure 19–2). This is usually used for wide-band applications, with its accompanying low sensitivity. More sensitive versions require an excessively long line and are characterized by multiple responses.

Detectors classed as discriminators are characterized by the use of resonant networks as the dispersive element. One type uses a reactance cavity (Figure 19–2) on a hybrid to obtain the dispersed signal. In its usual application, the fourth arm of the hybrid has a short to supply the undispersed signal. The net circuit is, basically, the interferometer with a cavity instead of a long line. A second type uses a transmission cavity

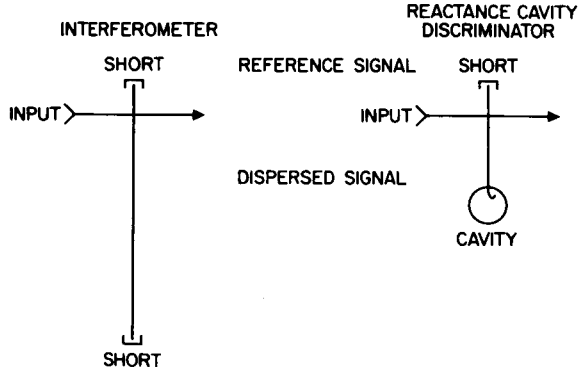

FIGURE 19–2.—Dispersive networks.

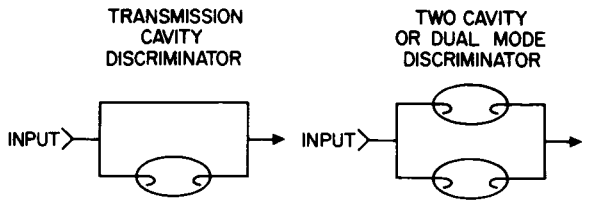

FIGURE 19–3.—Dispersive networks.

(Figure 19–3) with separate paths for the dispersed and undispersed signals. Power division and recombination are usually accomplished with hybrids. A third type uses the two-cavity, or dual-mode cavity, approach (Figure 19-3) wherein the two signals are both dispersed—but in opposite senses—by tuning the two cavities to opposite sides of the carrier.

A common non-microwave discriminator used at microwave frequencies is the LO–IF method (Figure 19–4). In this case, the input signal is mixed with a local oscillator signal to produce an IF signal. Frequency demodulation is then achieved with an IF discriminator.

In any of the above circuits, detection may be accomplished by merely putting a crystal detector at the indicated output. Better signal-to-noise ratios, as well as greater AM rejection, can be achieved by using a phase comparator between the two signals. Implementation of the phase detector is shown later, when actual discriminators are discussed. The crystal detector has the advantages of simplicity and reliability; however, it has the disadvantage of operating in the worst possible portion of the crystal noise spectrum. A much smaller detector noise level is obtained by using the crystal at an IF frequency as a mixer. The IF noise level of a crystal is much lower than its video noise level, and the use of IF amplifiers reduce the noise contribution of the final video detector to an insignificant level.

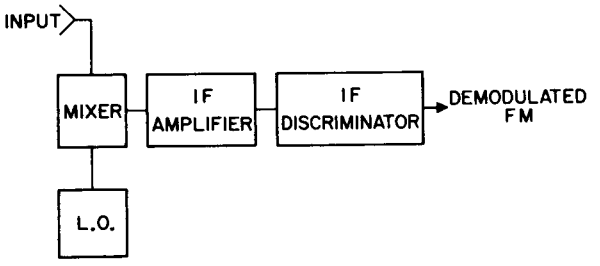

FIGURE 19–4.—Local oscillator—IF discriminator.

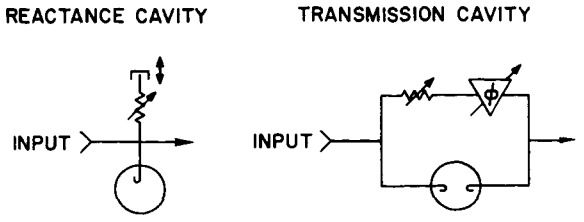

FIGURE 19–5.—Carrier nulling.

Two permutations of the above components which further increase the performance of the discriminator are available. One is to incorporate IF sections into the two signal paths, rather than merely using them as a low-noise detector. One advantage to this method is that the detected signal at the lower modulating frequencies is very small compared with the sideband levels that produced it, because the phase shift between the sidebands of the two signals is small. By incorporating the IF sections before the phase comparison, the entire sideband is converted to IF with a resulting larger signal-to-noise ratio. Obviously, the final detector or phase comparator is at the intermediate frequency.

The other permutation is the use of a carrier nulling technique (Figure 19–5). In this scheme two signals are produced as if a discriminator were being made, except that phase and amplitude are adjusted in the two signals so as to cancel the carrier. This has the effect of raising the sideband-to-carrier power ratio by almost the same factor to which the carrier was nulled. Then, by increasing the input power to raise the carrier up to the same level as used in the non-nulling discriminator.

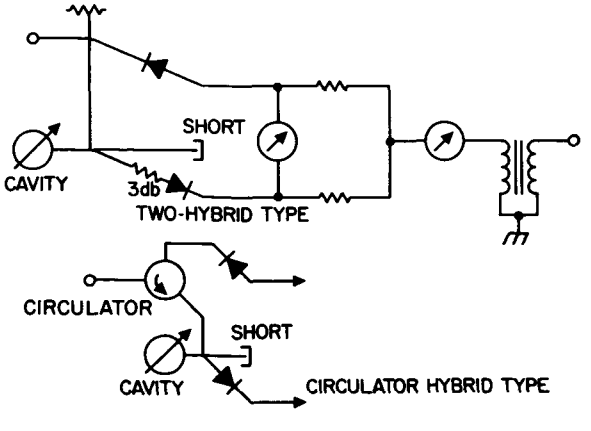

FIGURE 19–6.—Dc pound discriminator.

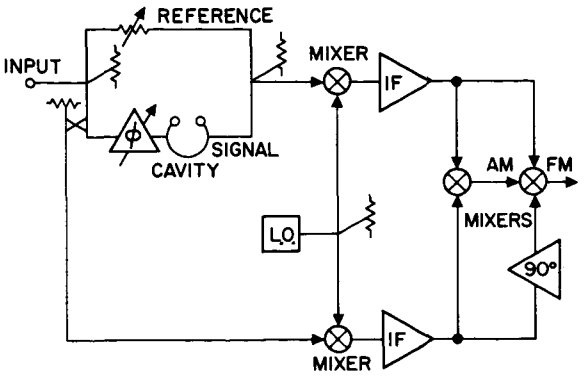

FIGURE 19–7.—Carrier null, IF discriminator.

an apparent increase of the modulating index is achieved. The combining of the two signals in this manner reduces the net phase shift of the sideband by roughly one-half, but this is a slight effect compared with the factor of 100 or more that is gained by carrier nulling.

Typical discriminator circuits are shown in the next figures. The Pound discriminator (Figure 19–6), used at Raytheon for many years because of its ease of operation, has a noise level of about $\frac{1}{3}$ cps per kilocycle bandwidth at 1-kc modulating frequency, to about one-tenth of that at 100-kc modulating frequency. It uses the reactance cavity with video crystal detectors. The figure shows the technique used to obtain a balanced phase detector output from what earlier appeared to be a single output circuit.

The transmission cavity approach, along with the IF and carrier nulling permutations, are used in the Raytheon high-performance discriminator (Figure 19–7), having a noise level of about 0.01 cps per kilocycle. This illustrates the fact that the carrier nulling circuit is not a discriminator,

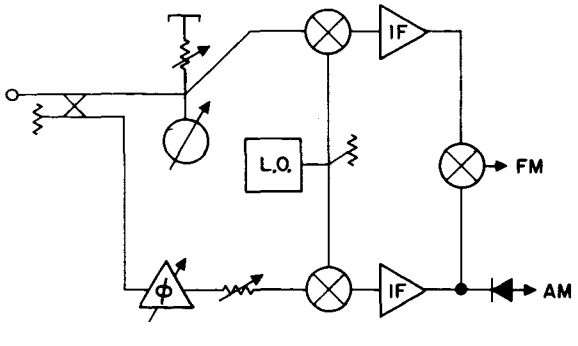

FIGURE 19–8.—Allscott, Varian discriminator.

but merely serves as the dispersive element. The same approach, with a reactance cavity, is shown in the Allscott equipment (Figure 19–8), having a noise level of about 0.06 cps per kilocycle. The dual mode discriminator is commonly found as the STALO frequency degenerating feedback sensor.

VIDEO SIGNAL PROCESSING

Signal processing after detection is a matter that is usually determined by the requirements of the system application. Nevertheless, the processing equipment invariably consists of video amplifiers, bandwidth limiting filters, and some type of voltage sensor. Sometimes, the total noise within the video bandwidth only is required; therefore broadband fixed filters are used. At other times, a series of measurements will be taken across the video bandwidth in a narrower filter. This has the advantage of showing the spectral shape of the noise rather than just a total noise content. Presently, several laboratories are attempting to standardize this narrower band to 1 kilocycle, although other bandwidths are used, especially at video frequencies below 1 kilocycle, where narrow bandwidths are obviously required.

One available device, the spectrum analyzer, bandwidth-limits and detects in a single instrument. Otherwise, a great variety of instruments, such as true rms voltmeters, oscilloscopes, wave analyzers, etc., are used.

PULSE APPLICATION

All above applies directly only to CW measurements. Measurements on a pulse system are more difficult to perform because of equipment limitations. The direct approach for pulsed signals is to filter out all the pulse sidebands except the carrier. The measurements are then made as if it were a CW system. This filtering rarely can be accomplished at microwave frequencies, however; so a detector is required that has a wide dynamic range. In this manner, the noise sidebands can be observed without producing an overload situation at the detector input, where all the pulse sidebands will be found. If the same detector input power is used, then the carrier is reduced, compared with the CW case, with the accompanying reduction in sensitivity. If the same carrier level is used, the crystals frequently are unable to handle the total power of the carrier and all the pulse sidebands.

AMPLITUDE MODULATION

A brief discussion on amplitude modulation is appropriate at this point. The video detector for AM is a simple crystal detector; but, in the more refined discriminators, AM is measured as well as FM—however, with a 90-degree phase shift introduced into one signal path. This has no bearing on the subject of this symposium but is very convenient when constructing test equipment to measure both AM and FM.

PRECAUTIONS

An important point gained from our experience in producing various noise measuring equipment is that the details of construction are as important as the type of discriminator used. All discriminators with the phase comparator detection can be made AM-insensitive; but the degree of insensitivity is controlled by such bothersome details as microwave mismatches, closeness of the match between the two crystals, etc. Similarly, the net discriminator sensitivity is not only a function of the cavity Q and power level but also of such secondary parameters as the coupling between the cavity and the transmission line. Needless to say, noise levels in all portions of any equipment must be controlled if maximum sensitivity is to be realized.

CALIBRATION

Calibration is generally a problem in any microwave discriminator, except the LO–IF discriminator, where a point-by-point voltage versus frequency plot may be made. The commonest calibration techniques are: (1) the *substitution method*, where a specific video signal is substituted for the discriminator output; (2) the *comparison method*, where a microwave discriminator is compared with a directly calibrated LO–IF discriminator; and (3) the *Bessel null method*, where a linearly modulating source is modulated at the index which produces the first carrier null. This index is 2.405 and may be determined through the use of a microwave spectrum analyzer. The first method is not safe because the microwave components are not included in the calibration. The other two methods may be employed to an

accuracy within $\frac{1}{2}$ db, if care is taken. Raytheon uses a *fourth technique*, which employs a ferrite rotator to produce sidebands in a line separate from the line containing the carrier. The relative amplitudes of the carrier and sidebands therefore are independently adjustable, so any index may be made using a power measurement as the primary accuracy-determining factor. The accuracy of this device is about 0.2 db.

DETAILED ANALYSES

The bibliography lists sources that deal with these devices in detail.

BIBLIOGRAPHY

CAMPBELL, R. A., "Analysis of the Pound Discriminator," Raytheon Bedford Memo RTD–2176, June 1, 1964.

GINDSBERG, J., "A Precision Calibrator for Microwave Demodulators," *IRE Trans. on Instrumentation*, I–7: 332–339, December 1958.

MAGER, H., "Analysis of a Suppressed-Carrier Microwave Demodulator," Raytheon Bedford Memo RTD–439, November 20, 1961.

MCLEOD, W. W., Jr., "A Survey of Microwave Discriminators," (declassified August 1964) Raytheon Bedford Report M/R–16–866, May 10, 1956.

WHITWELL, A. L., and WILLIAMS, N., "A New Microwave Technique for Determining Noise Spectra at Frequencies Close to the Carrier," *The Microwave Journal* 2(11): 27–32, November 1959.

Page intentionally left blank

20. SHORT-TERM STABILITY MEASUREMENT TECHNIQUES AND RESULTS

R. H. HOLMAN AND L. J. PACIOREK

Syracuse University Research Corporation
Syracuse, New York

In applications where there is a need for short-term frequency stability or spectral purity in microwave sources, we have found it practical to measure this property by means of spectral plots and by fine discrimination techniques. Frequency variations which occur over periods of less than 1 millisecond to about 1 second have been of major concern.

Four techniques (including the traditional short-term stability measurement) used to measure short-term perturbations or noise in a source are described, and the relations existing are discussed. The technique using a spectral plot or wave analysis is the one primarily used; and typical measurement results on the outputs of devices such as a crystal frequency standard. multiplier chains a traveling wave tube (TWT) and the helium–neon (He–Ne) gas laser are shown.

The Syracuse University Research Corporation (SURC) became involved with the specification of STAble Local Oscillators (*stalos*) for Doppler radar applications about 5 years ago. This work led to the development of stable microwave sources which were tunable and had the short-term stability of a crystal oscillator. Oscillators and multipliers were needed for this source development; therefore, the task of designing these units with short-term stability as the prime objectives was undertaken. The problem of how to specify and measure stability, faced early in this work, resulted in the establishment of a facility for oscillator noise measurement. This measurement facility is continuously being improved. At present, quartz crystal frequency standard oscillators are used as the reference; however, the addition of ammonia masers to the measurement facility in the near future will give us a greater capability in oscillator stability measurement. Our quest for stable low-noise oscillators led to the investigation of the spectral characteristics of CW lasers to determine the feasibility of using the output as a short-term frequency standard for microwave frequencies.

Four of the techniques used at SURC to measure short-term perturbations or noise in oscillators will be described, and the relations existing will be discussed. One of them is the traditional short-term stability measurement. However, since our application called for spectral purity, most of the tests were obtained by measuring the spectrum. Typical results will be displayed, and the work with the He–Ne laser will be discussed.

TECHNIQUES FOR MEASUREMENT OF SHORT-TERM INSTABILITIES

The reason for measuring the stability of a source is to provide data that will lead to the selection of the best source for a particular application or to provide a check of a system or signal source. The data should be in a form that is easy for the user to interpret. For example, the system designer may require a source having good spectral purity, and the amount of energy in the sidebands near the carrier could be important. The data in this case should be in the form of a spectral plot. On the other hand, if the source were used in a system where the rms frequency deviation is important—such as in a counter, the data would be useful in a form relating stability to integration time. It is possible

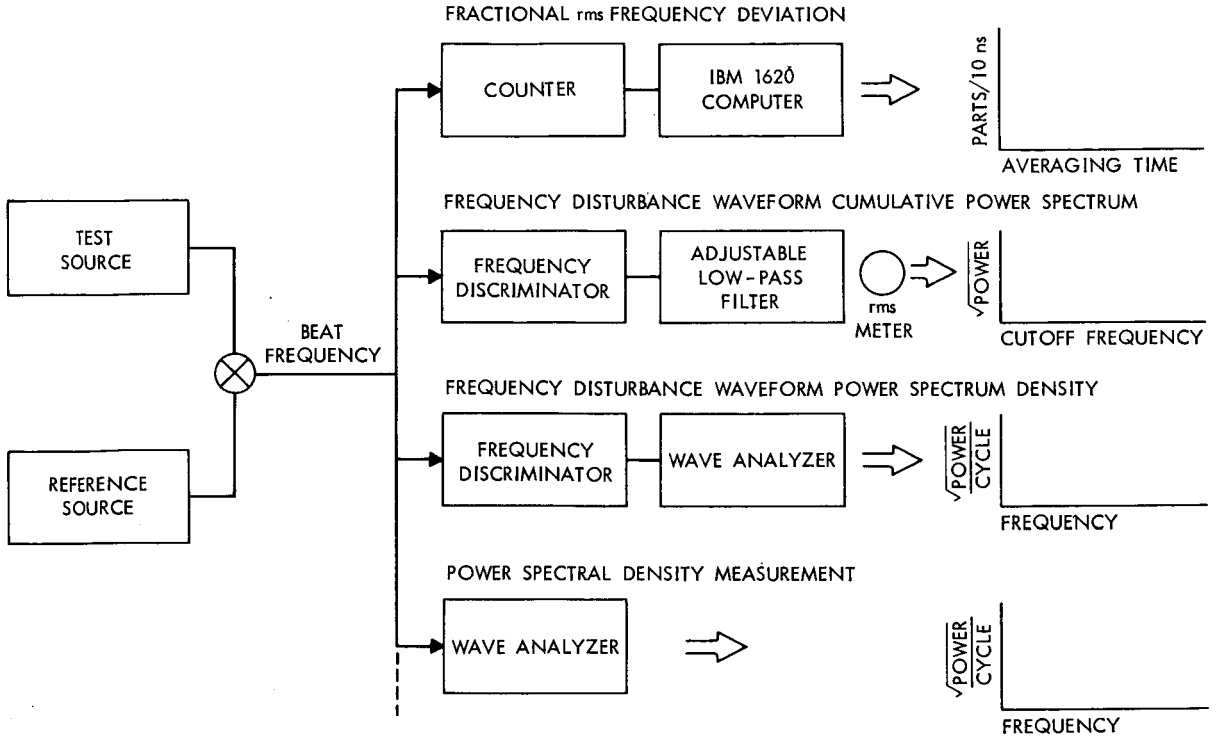

FIGURE 20–1.—Techniques for short-term frequency perturbation measurement.

that a system designer may wish to predict the output of a frequency or phase discriminator in order to specify the residual noise in a system. In this case, the output from a discriminator would be of interest. From these examples, it is clear that different applications of a source require different data; as a result, the data should be presented in a form useful to the user.

At least six techniques to measure short-term instabilities of a source have been used at SURC. Four of these techniques will be discussed, and are shown in block diagram form in Figure 20–1. In many cases, the test oscillator is multiplied and beat against the multiplied output of a reference oscillator. The test oscillator is offset slightly in frequency to obtain a beat frequency out of the mixer. The first technique shown, termed here as the *Fractional rms Frequency Deviation*, is the traditional short-term stability test used by many. In this test, fractional rms frequency deviation is obtained as a function of averaging time. The second technique, termed the *Frequency Disturbance Waveform Cumulative Power Spectrum*, for many years has been used to measure the short-term instabilities in MTI radar stalos. A military test set called the UPM-72 was developed with this technique. In this method, a sensitive calibrated discriminator is used to measure the energy in the waveform of the frequency disturbance. The third technique, called the *Frequency Disturbance Waveform Power Spectral Density*, is a variation of the second technique. The *Power Spectral Density Measurement* is the fourth technique employed. It is the measurement recently called the "spectral purity" by many. In our application, the spectrum of a source is most important; therefore, the spectral density technique is generally used at SURC; it was described by Barnes and Mockler in 1960 (Reference 1).

There are other techniques that could be added to the list. For instance, at SURC a phase discriminator has been, at times, substituted for the frequency discriminators in techniques 2 and 3. These have not been included for the sake of brevity.

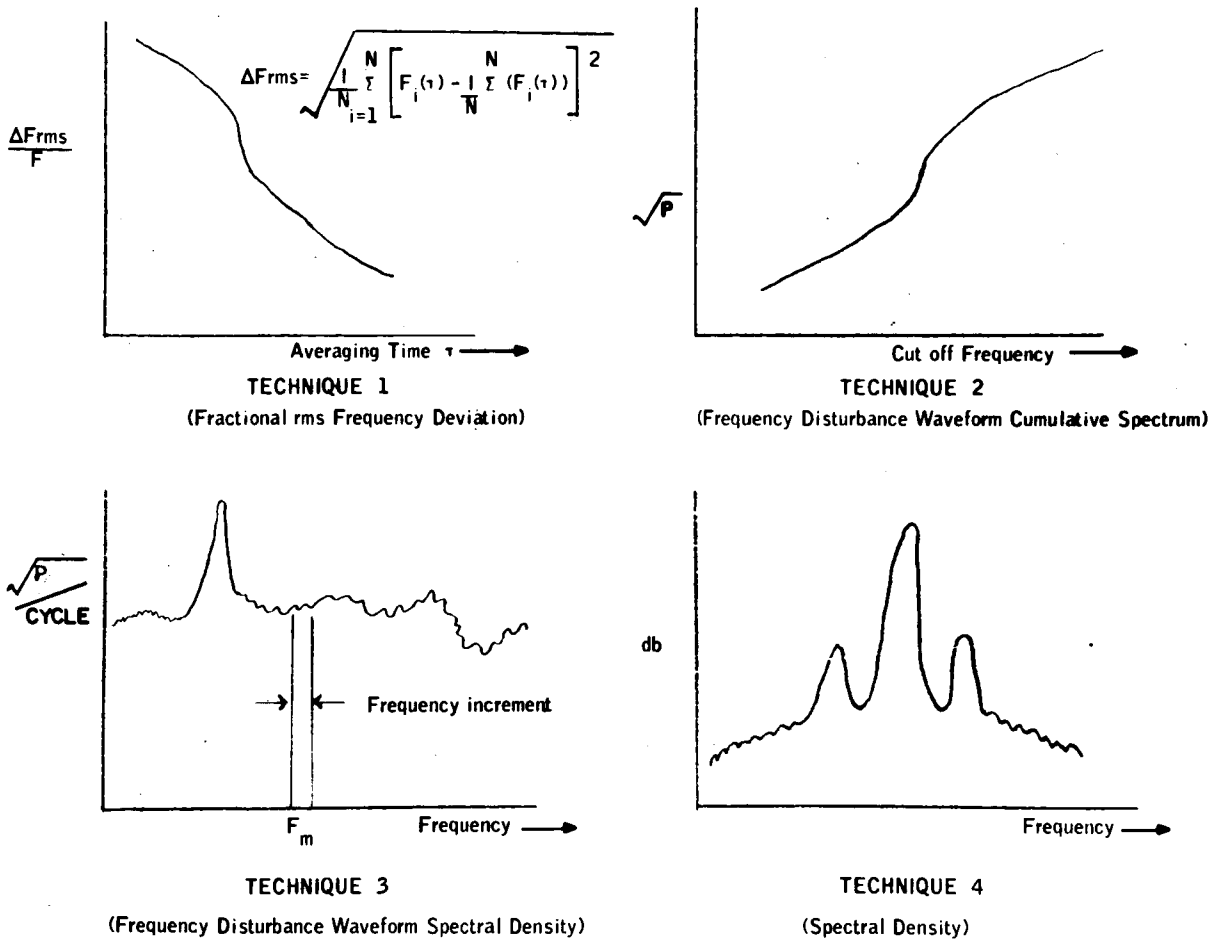

FIGURE 20–2.—Typical outputs from various techniques.

Sample results of the four techniques are shown in Figure 20–2.

Technique 1: Fractional rms Frequency Deviation

In this technique, many measurements of a frequency are taken for a fixed averaging time, and the rms frequency deviation of the sample of N measurements is calculated. The result is one point on the curve shown; other points are obtained by changing the averaging time. The result is a plot relating rms frequency deviation to averaging time; this is commonly called the *short-term stability measurement.* Usually, only a few points are measured on the curve to specify the source stability; as a result, the plot does not describe the source in detail. This is unfortunate, because a more detailed plot would be more useful in diagnosing a source.

Technique 2: Frequency Disturbance Waveform Cumulative Power Spectrum

In this technique, a sensitive calibrated discriminator is followed by a variable cutoff frequency low-pass filter and then a true rms meter. The meter can be calibrated to indicate rms frequency deviation. The results can be plotted relating rms frequency deviation to cutoff frequency. For a given cutoff frequency, the energy in the disturbance waveform below the cutoff frequency is measured. Thus, by varying the cutoff, a plot of rms frequency deviation versus cutoff is obtained. Since the discriminator is calibrated, the output is a measure of the sideband energy of a source.

To relate this to the first technique, the ordinate (Δf rms) can be divided by f, the carrier frequency, to obtain fractional rms frequency devia-

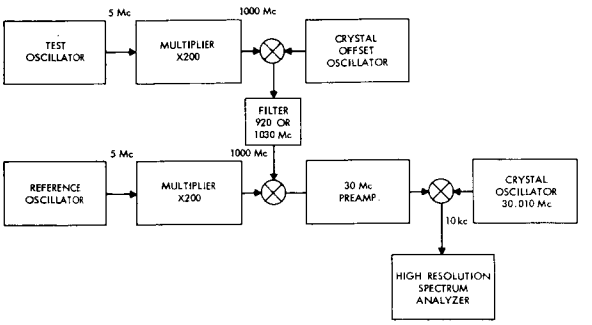

FIGURE 20–3.—Setup for frequency standard tests.

tion. The ordinate is now identical to that of Technique 1. The abscissa can be expressed as the time constant of the low-pass filter. In this form, the two plots are related.

The advantage of this method over Method 1 is the ease of obtaining points at high cutoff frequencies that correspond to short averaging times, which are difficult to obtain in Technique 1.

Technique 3: Frequency Disturbance Waveform Power Spectral Density

In Technique 3, the frequency disturbance waveform out of the discriminator is wave-analyzed, giving the spectral power density of the disturbance waveform. If the energies of each of the frequency increments in the disturbance waveform are independent, this plot is related to the result of Technique 2. In fact, the plot of Technique 3 is the derivative of the plot of Technique 2.

The advantage of this method (and Method 4 as well) is the ease of obtaining detailed results. These detailed results have proven useful in the development of evaluation of oscillators.

Technique 4: Power Spectral Density

In Technique 4, a high-resolution spectrum analyzer is used to obtain the power spectral density of the source with its sideband energy. This measurement recently has become popular, since the results are highly descriptive of a source and are easily obtained. As mentioned previously, this is the method generally used at SURC.

Relation Between Technique 2 and Technique 3

We will next show how the power spectrum is related to the power density spectrum of the frequency disturbance waveform, the result of Test 3. Assume that there are no amplitude variations and that the power spectrum is symmetrical.

For the purpose of drawing the desired relation, assume that the result of Technique 3, the spectral density of the disturbance waveform, is known. If an increment of frequency of the disturbance is considered a sinusoidal modulation component at a frequency f_m of a peak deviation of Δf, obtained from the discriminator constant, we can apply FM theory. Furthermore, if we assume $\Delta f/f_m$ (the modulation index) is much less than 1 (a reasonable assumption for a quality oscillator), we can apply narrow-band FM theory. FM theory gives us Equation 1, which relates carrier sideband energy in a ratio of the carrier energy to this modulation component. Applying narrow-band theory results in Equation 2. The final simple result is given in Equation 3. Note that a discrete frequency disturbance component from Technique 3 at a frequency f_m accounts for a pair of sideband components to the carrier. This result (3) allows a simple superposition to be applied such that the Frequency Disturbance Waveform Power Spectral Density can be mapped to obtain the carrier sideband power spectral density.

$$\frac{P_{SB}}{P_c} = \frac{J_1^2(m_f) + J_2^2(m_f) + J_3^2(m_f) + \cdots}{J_0^2(m_f)}, \quad (1)$$

where

$$m_f = \Delta f/f_m.$$

If $m_f \ll 1$, the Bessel functions can be approximated by

$$J_0(m_f) = 1,$$
$$J_1(m_f) = \tfrac{1}{2}m_f,$$
$$J_2(m_f), \quad J_3(m_f), \cdots = 0, \quad (2)$$

resulting in

$$P_{SB}/P_c = J_1^2(m_f) = \tfrac{1}{4}m_f^2;$$

or, in terms of voltage, which is the form in which most analyzers present the data:

$$V_{SB}/V = \tfrac{1}{2}m_f = \Delta f/2f_m. \quad (3)$$

INSTRUMENTATION FOR SPECTRAL PLOTS

In all the tests, the source output frequency is translated down to a frequency where a narrow

crystal filter can be employed. Since the crystal filter frequency cannot be changed, the beat to be analyzed must be varied to move the spectrum through the filter. A commercial wave analyzer is used which incorporates a swept Local Oscillator (LO) in the audio range, and a crystal filter. The filter bandwidth is 10 cps, and the range of frequencies that can be swept is 0 to 20 kc.

OSCILLATOR TESTS

The test setup for comparing frequency standards in the 5-Mc range is shown in Figure 20–3. The output from each standard under test is multiplied to 1000 Mc. One of the signals is then offset by a 30-Mc crystal oscillator, and the resulting signal at 1030 Mc or 970 Mc is filtered and fed to a mixer, where it is mixed with the 1000 Mc from the other source. The resulting 30-Mc signal is amplified in a low-noise preamplifier and mixed with a 30.010-Mc crystal oscillator to obtain a 10-kc beat that is wave-analyzed. Figure 20–4 shows the spectral plot of the beat between two 5-Mc quartz crystal frequency standard oscillators. Two atomic frequency standards were substituted for the quartz oscillators, resulting in the plot of Figure 20–5. This plot illustrates the utility of the spectral technique in diagnosing system ills. In this case, the high sidebands were caused by a faulty servo system in the frequency lock loop of the flywheel oscillator.

In the development of oscillators, the spectral technique has been used as a diagnostic tool. For example, Figure 20–6 shows the schematic of a simple crystal oscillator, and the resulting spectrum after multiplication to 3000 Mc and beat against a harmonic of a crystal reference oscillator. The oscillator was modified by putting an emitter follower into the circuit to drive the crystal from a lower impedance source. Figure 20–7 shows the resulting plot. Comparing the 60-cycle sidebands in both plots indicates a reduction of 15 db in the emitter coupled circuit. In laying out an

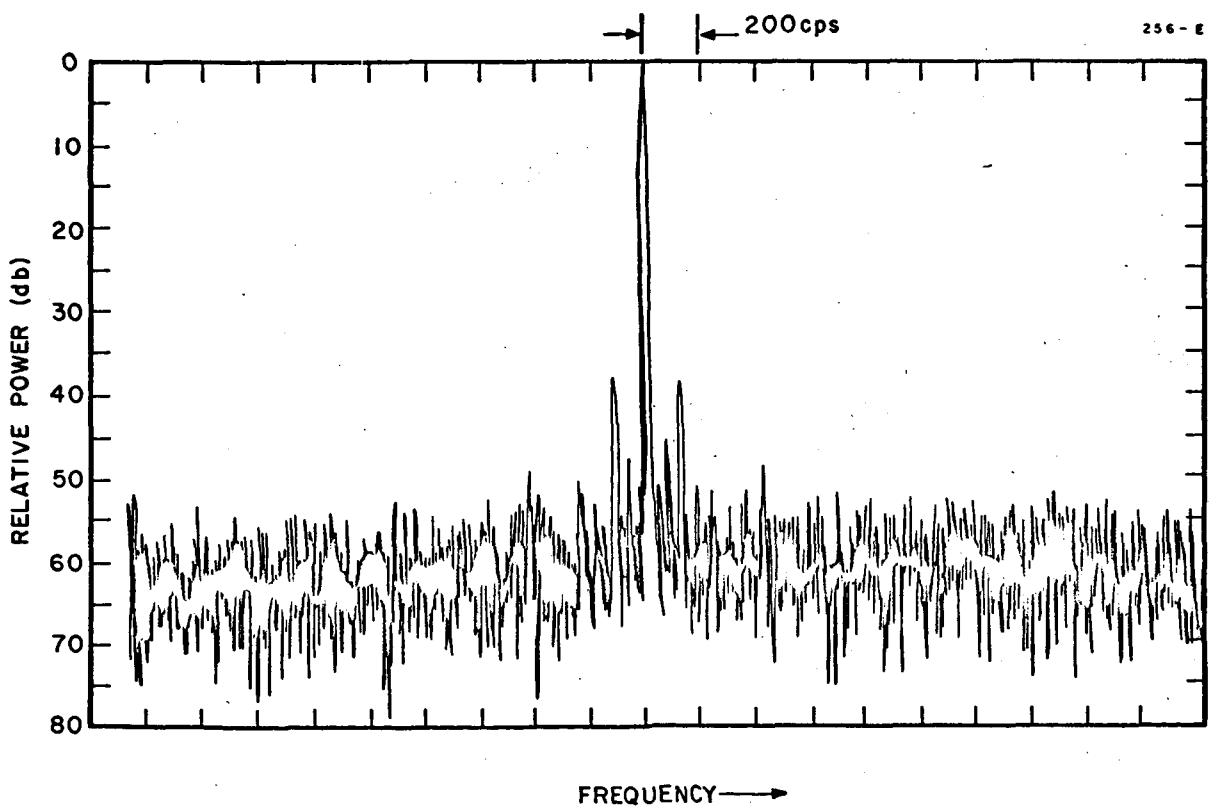

FIGURE 20–4.—Comparison of two quartz crystal 5-Mc frequency standards at 1 Gc.

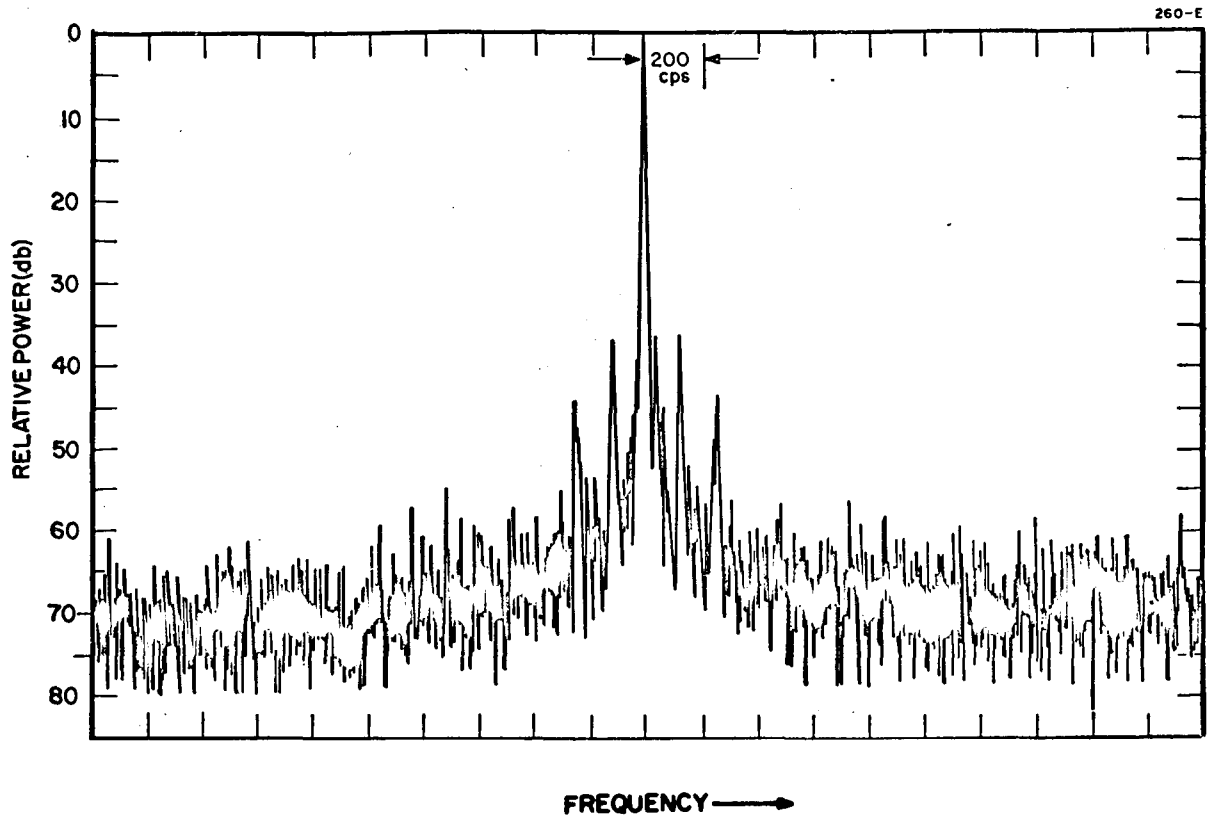

FIGURE 20–5.—Comparison of two rubidium vapor frequency standards at 1 Gc.

oscillator, it is important to keep the interconnecting wires as short as possible to reduce the hum pickup. To exemplify this, a clip lead was attached to a wire in the oscillator circuit; the resulting spectrum is shown in Figure 20–8. A comparison of Figure 20–8 and Figure 20–7 clearly indicates the importance of proper circuit layout.

MULTIPLIER

One technique for obtaining a stable source at microwave frequencies is to multiply the output of a low-frequency (<100 Mc) crystal oscillator. It is possible that the multiplier could degrade the signal from the oscillator. When evaluating multipliers, the basic idea is to drive two identical units with the same source. Thus, the contribution of the driving source tends to be reduced in the resulting plot. Figure 20–9 shows a typical setup for multiplier testing.

A phase-locked multiplier (×20) was evaluated, and the bandwidth of the phase-lock loop was varied. Figure 20–10 shows the spectral plot when two multipliers were driven commonly from the same 5-Mc frequency standard. The bandwidth of the phase-lock loop was changed from 500 cycles to 50 cycles, and then to 5 cycles. The results shown in Figure 20–11 and Figure 20–12 indicate that an improvement in signal-to-noise level can be obtained by a phase-locked multiplier. The multipliers contained vacuum tubes. A similar experiment with transistor multipliers also was performed. Figure 20–13 shows the plot of a wide-band transistor multiplier, and Figure 20–14 shows the resulting spectrum of a narrow bandwidth (50 cps) phase-lock-loop transistor multiplier.

TWT AMPLIFIER TESTING

A block diagram of the test setup for amplifier evaluation is shown in Figure 20–15. In this case, a TWT amplifier was tested. A stable source was fed to a 3-db coupler. The signal from one port is

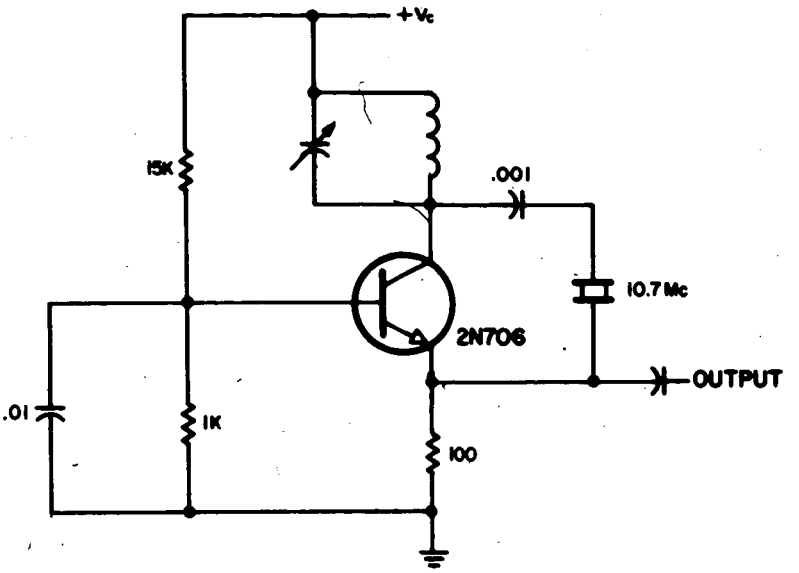

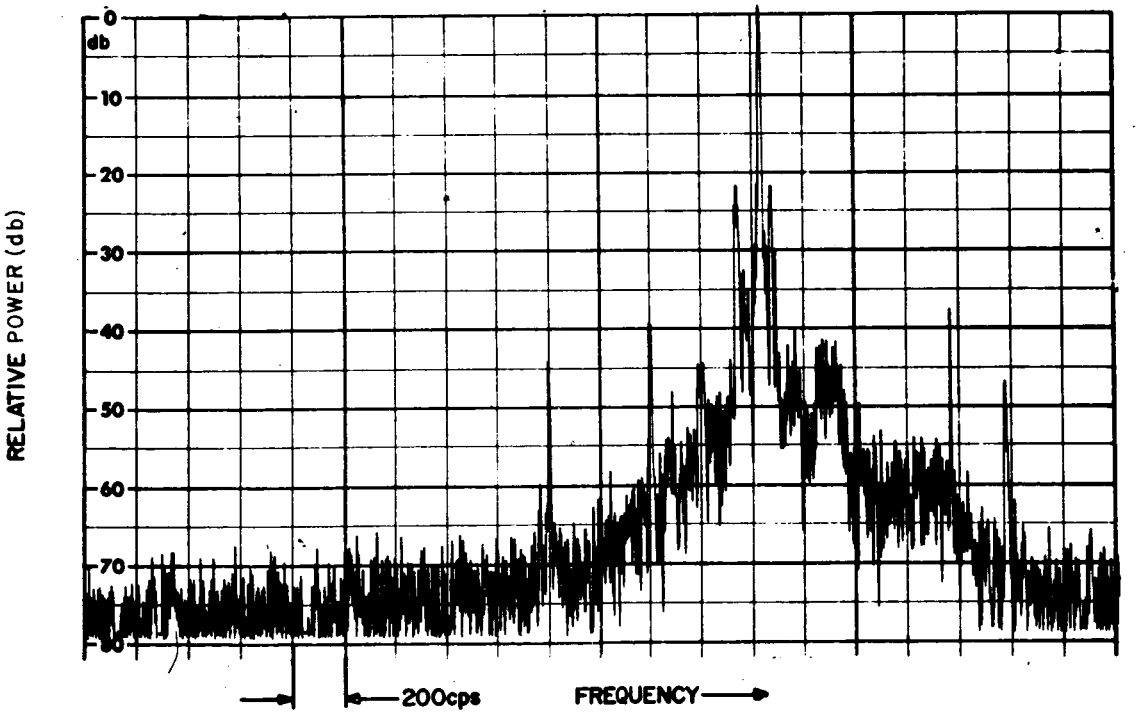

FIGURE 20–6.—Spectrum of 10.7-Mc crystal oscillator multiplied to 3000 Mc.

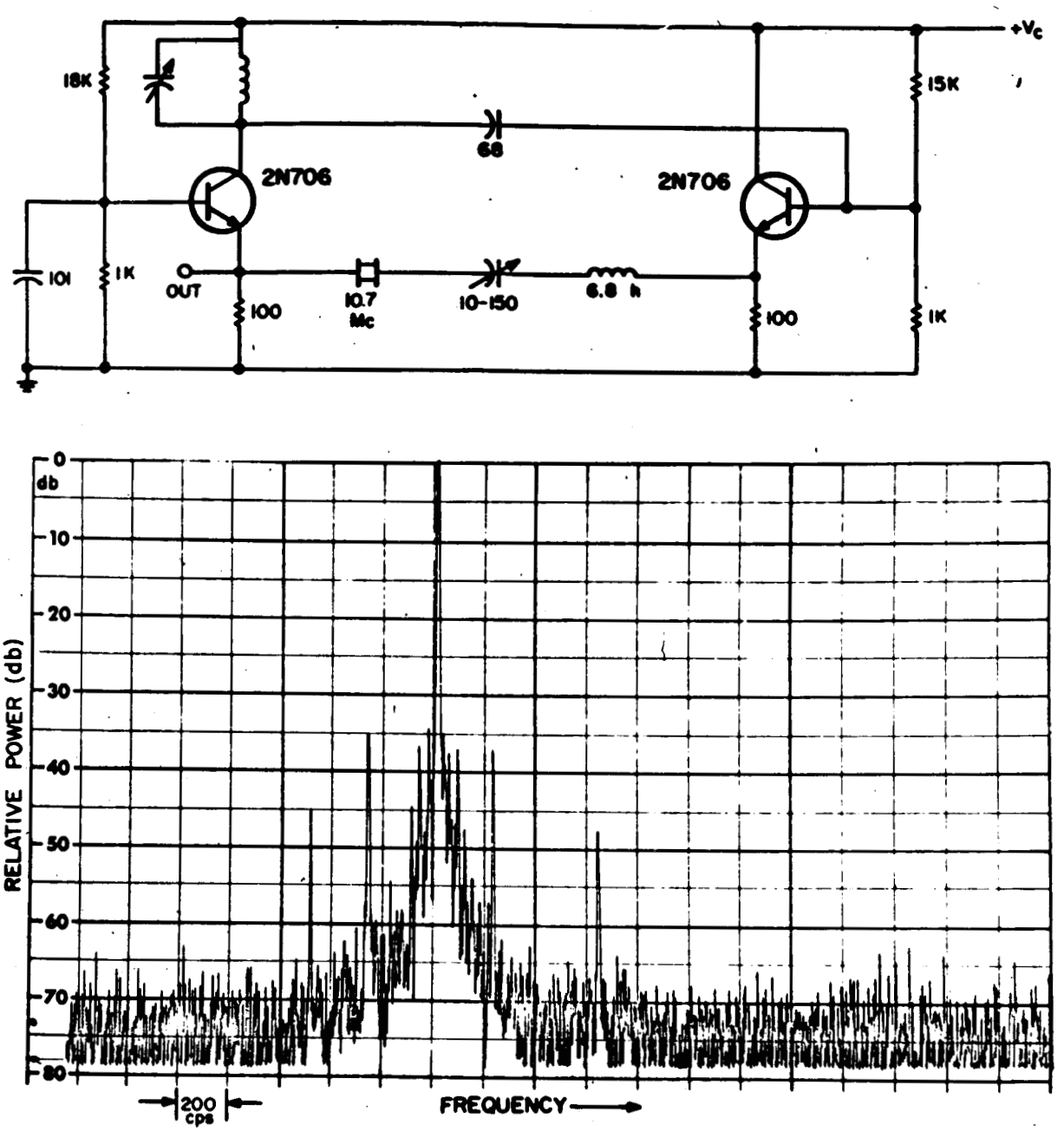

FIGURE 20–7.—Spectral plot of emitter-coupled oscillator at 3000 Mc.

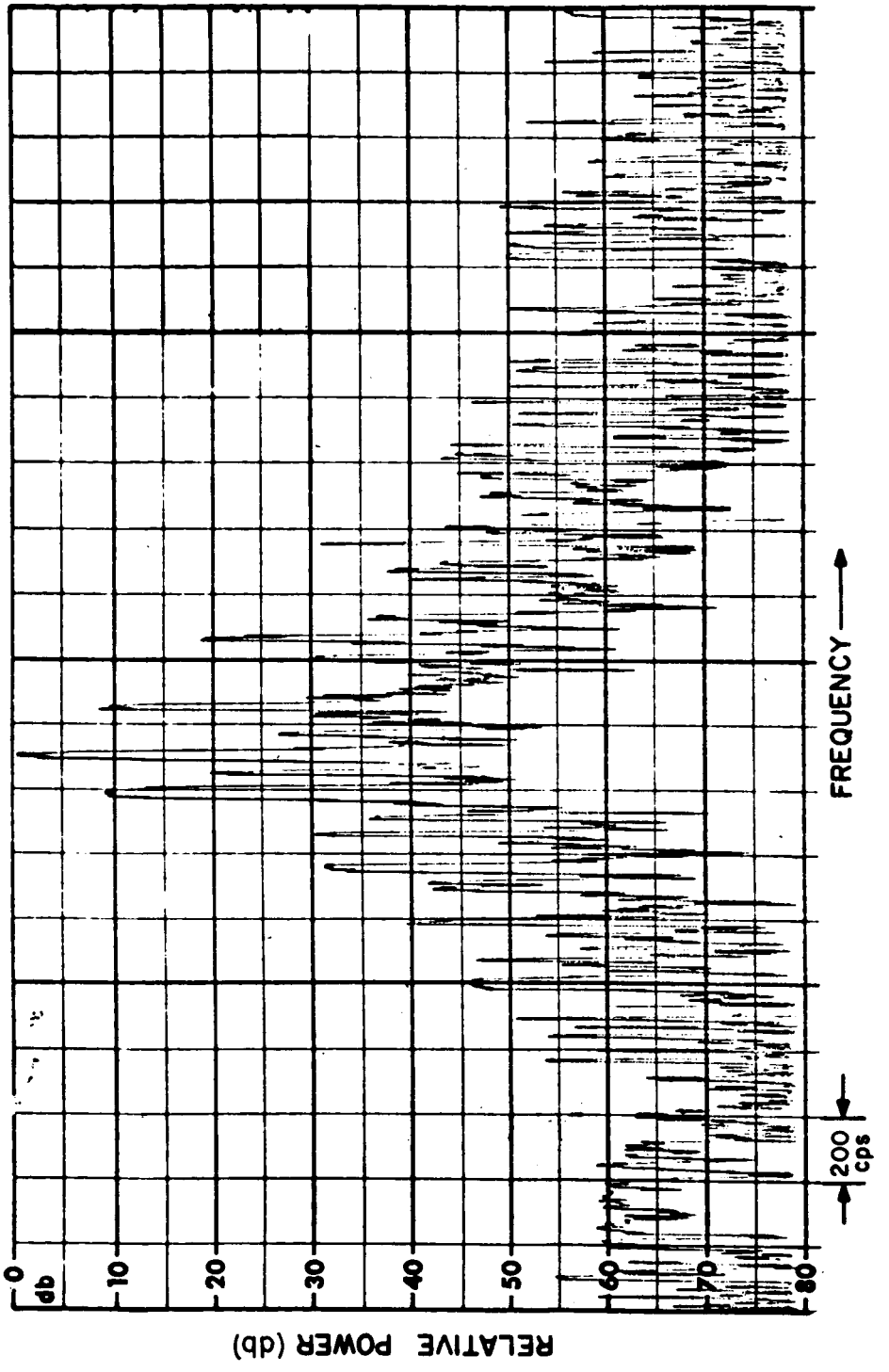

FIGURE 20–8.—Clip lead placed on interconnecting wire in emitter-coupled oscillator.

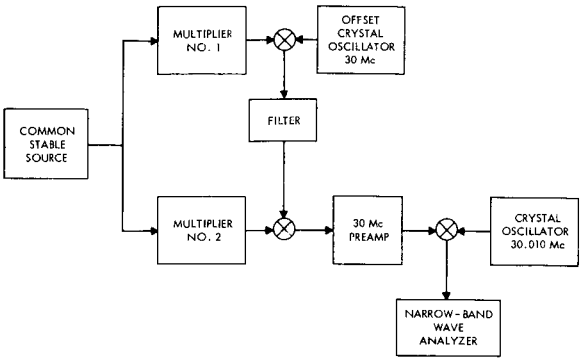

FIGURE 20–9.—Multiplier test setup.

offset by 30 Mc, and the other signal is fed directly to the TWT amplifier and a variable attenuator. The TWT-attenuator channel can be bypassed with a cable. A control plot taken without the TWT is shown in Figure 20–16b. The TWT was switched in and the attenuator adjusted for the same signal level into the mixer; Figure 20–16a shows the resulting plot. A comparison clearly indicates the amount of hum and noise introduced by this particular TWT amplifier. In this case, most of the noise is attributed to a poor power supply.

RESULTS OF EVALUATING A CW LASER

A CW laser can be adjusted so that the output contains many frequency components, as shown in Figure 20–17. The frequency difference between components is given by

$$\Delta f = (c/2L) + \text{pulling term},$$

where

c = speed of light,

L = laser cavity length.

By feeding the laser output into a photo multiplier tube, mixing occurs; and the output of the photo multiplier will be equal to Δf. For practical lasers, the length of the cavity is such that the frequency out of the photo multiplier is in the microwave region. In the laser at SURC, the beat frequency is about 240 Mc. This beat was translated to 10 kc, and a spectral plot of the output

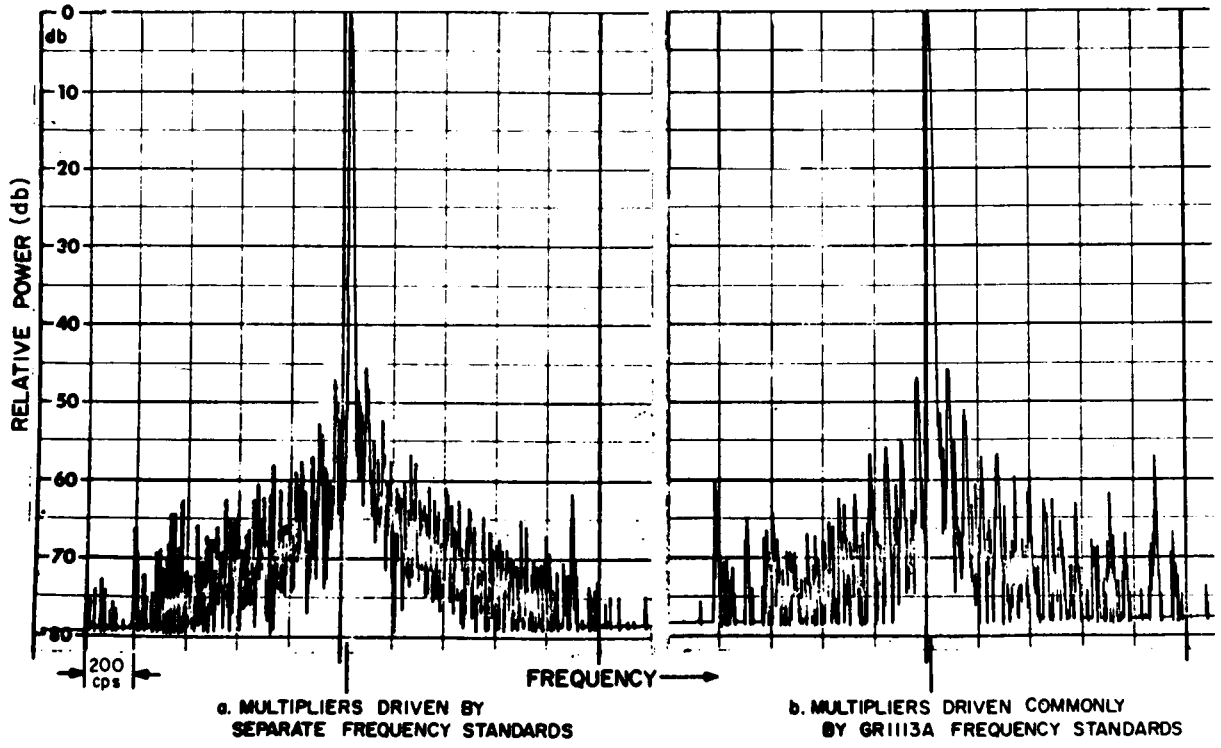

FIGURE 20–10.—Comparison at 1 Gc of two frequency multipliers with 500-cps bandwidths.

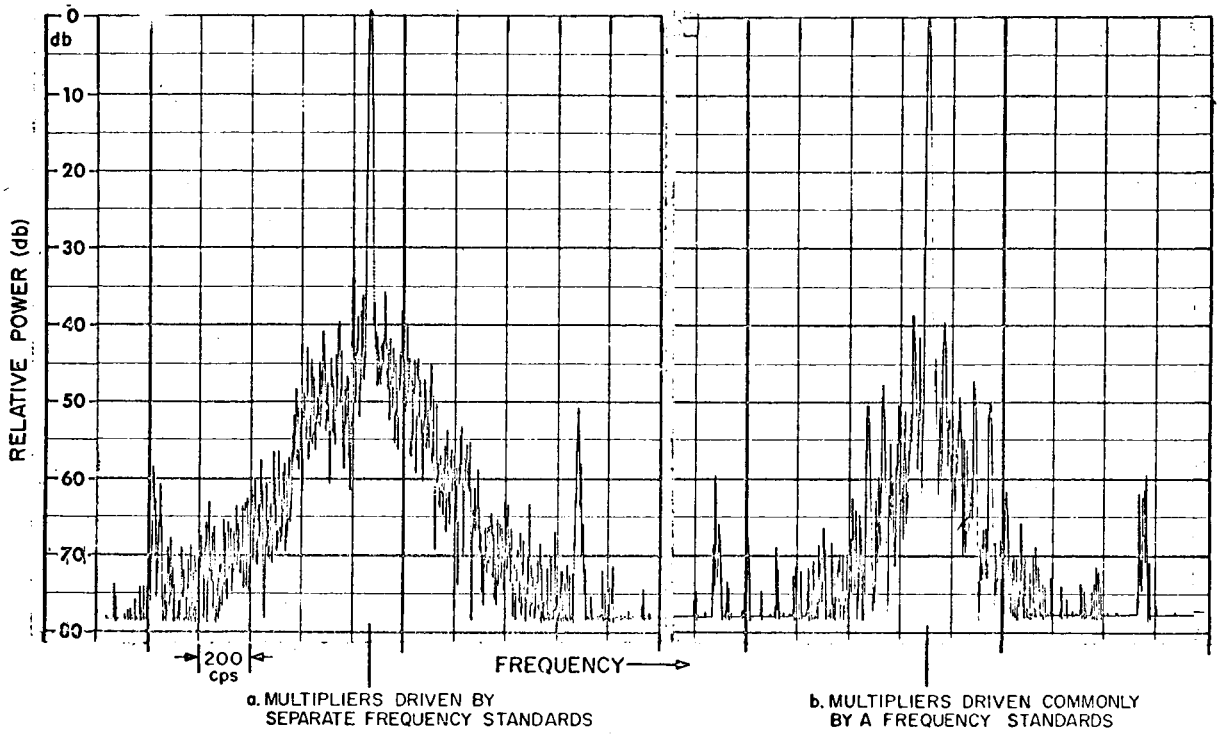

FIGURE 20–11.—Comparison at 3 Gc of two frequency multipliers with 50-cps bandwidths.

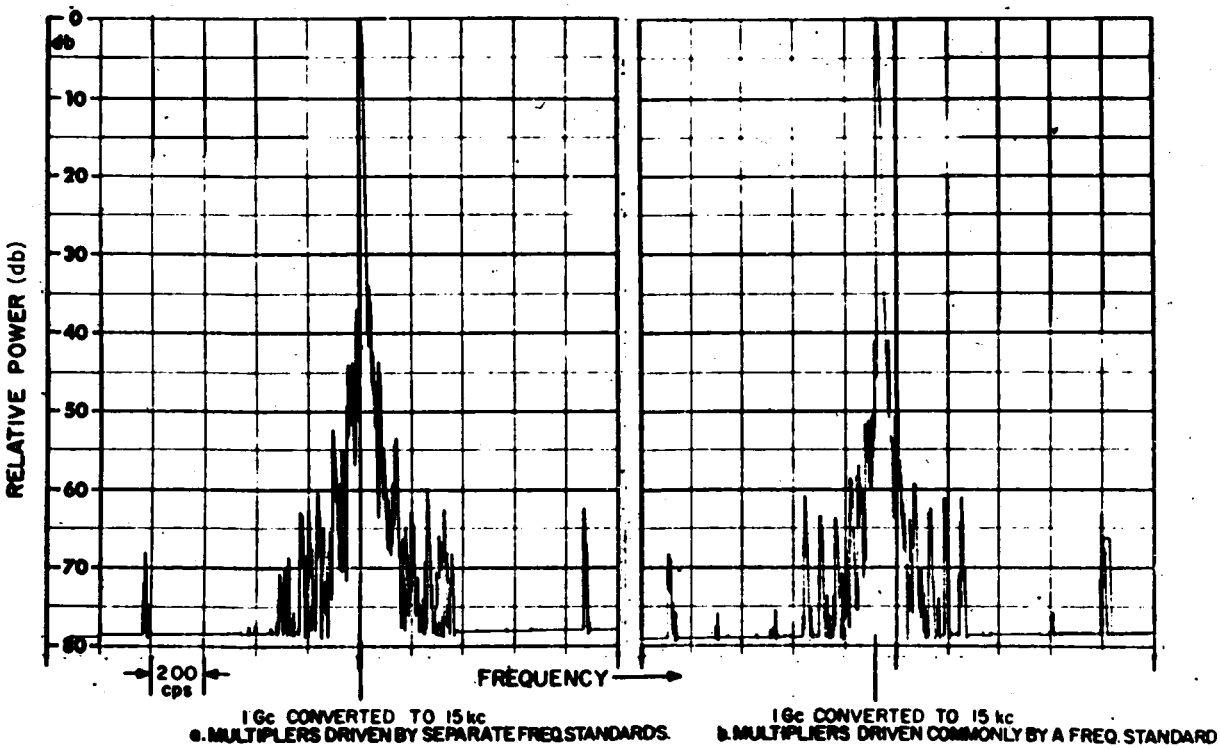

FIGURE 20–12.—Comparison at 1 Gc of two standard frequency multipliers with 5-cps bandwidths.

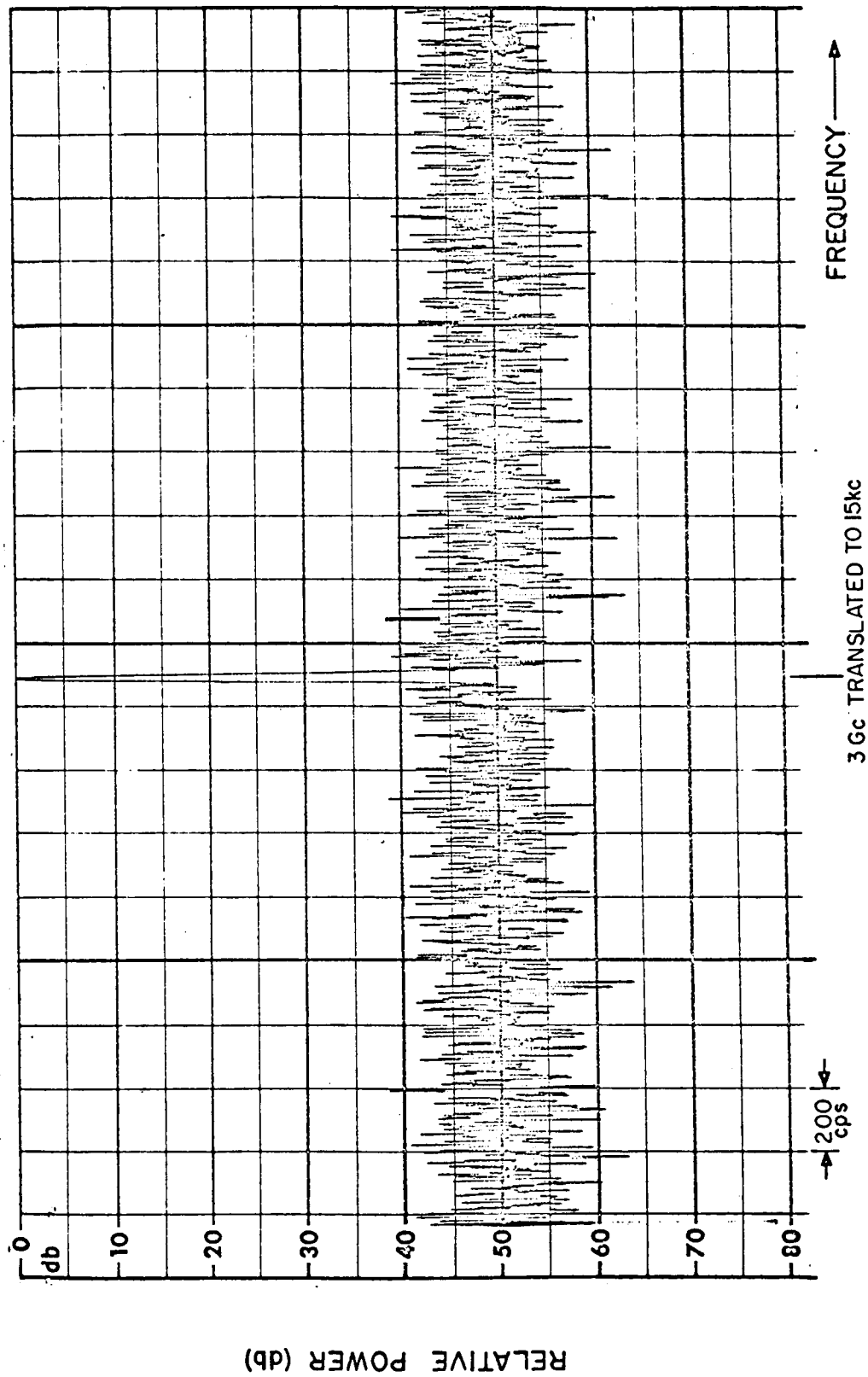

FIGURE 20–13.—Spectral plot of wide-band transistor multipliers beat at 3 Gc.

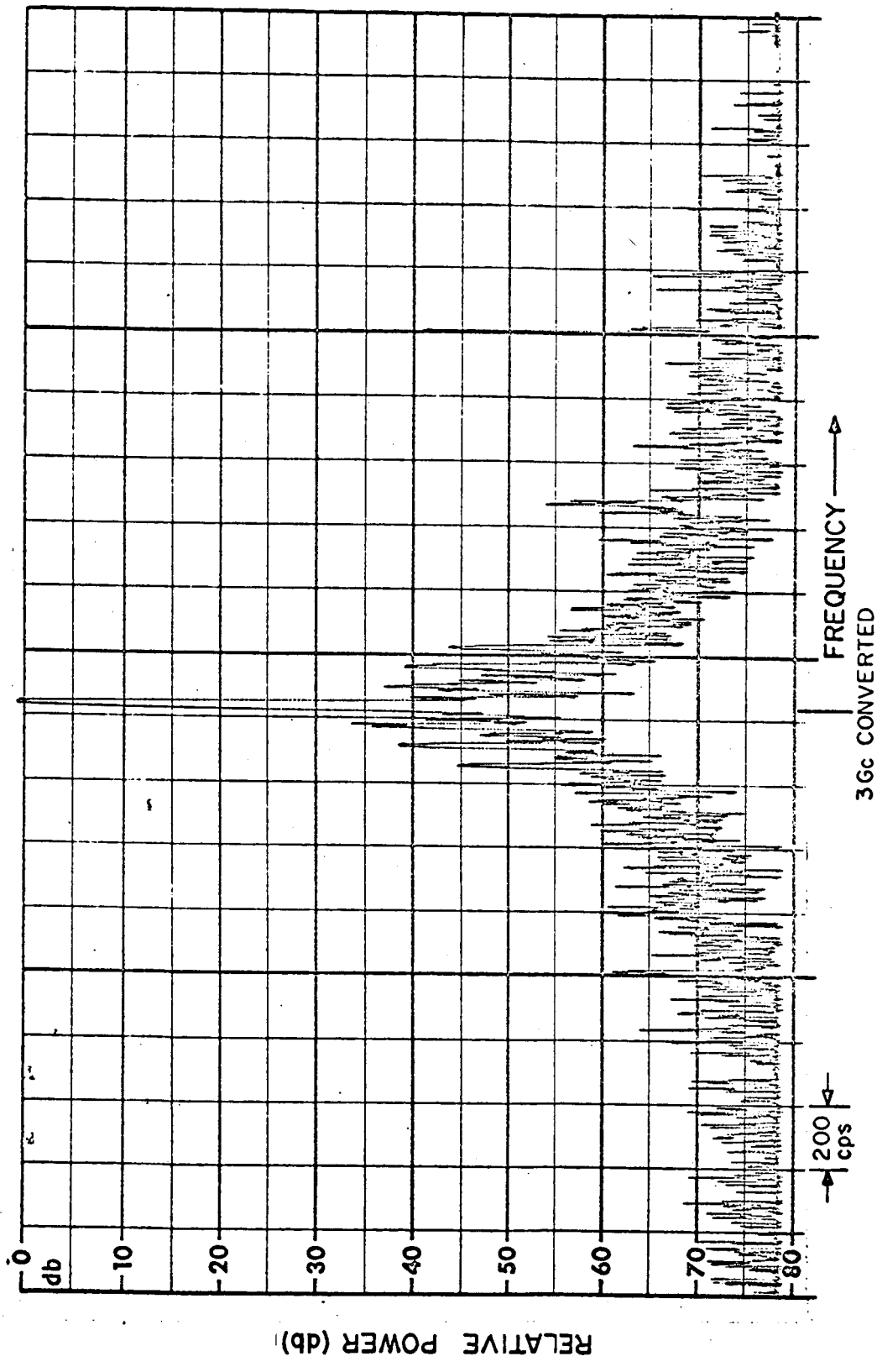

FIGURE 20–14.—Spectral plot of narrow-band transistor multipliers beat at 30 Gc.

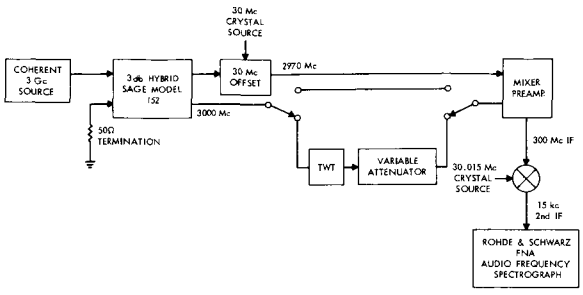

FIGURE 20–15.—Test setup for amplifier evaluation.

was taken; Figure 20–18 shows the resulting spectral plot. This spectral plot is poor compared with the plots obtained from crystal sources.

To stabilize the laser self-beat, a phase-lock loop was assembled as shown in Figure 20–19. The light frequencies of the laser were mixed in a photo multiplier and the resulting signal mixed with a crystal oscillator harmonic to get a 30-Mc beat that was amplified and fed to a phase discriminator. The reference for the phase detector was a 30-Mc crystal oscillator. The resultant correction signal out of the discriminator was used to change the length of the laser cavity by means of the rear mirror mounted on a PZT crystal. Once phase-locked to the crystal reference, the plot in Figure 20–20 was obtained—a considerable improvement over the plot obtained in the unlocked mode.

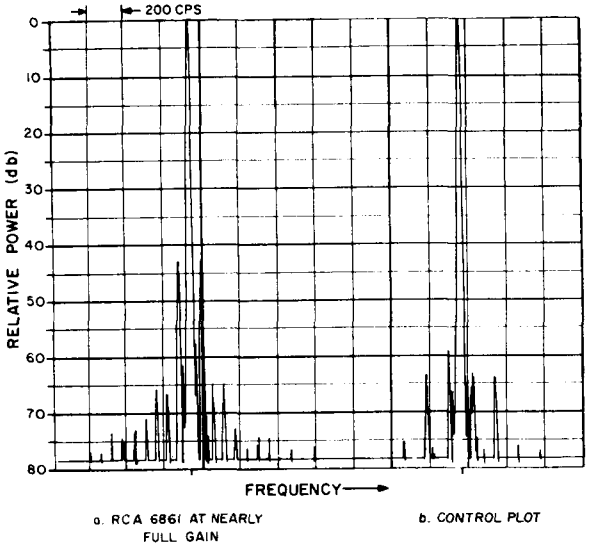

FIGURE 20–16.—Incidental modulation in a low-noise solenoid TWT.

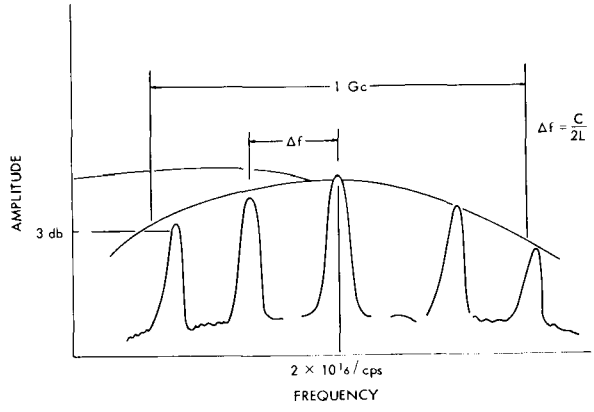

FIGURE 20–17.—Laser spectrum.

CONCLUSION

The methods used to measure short-term stability at SURC have been described, and some comparison between methods has been shown. Typical results using the *spectral technique* have been presented. This technique was used mostly because of the large dynamic range possible with an audio spectrograph and because of the ultimate use of the data, which called for spectral purity.

REFERENCE

1. BARNES, J. A., and MOCKLER, R. C., "The Power Spectrum and Its Importance in Precise Frequency Measurements," *IRE, Transactions on Instrumentation*, September 1960.

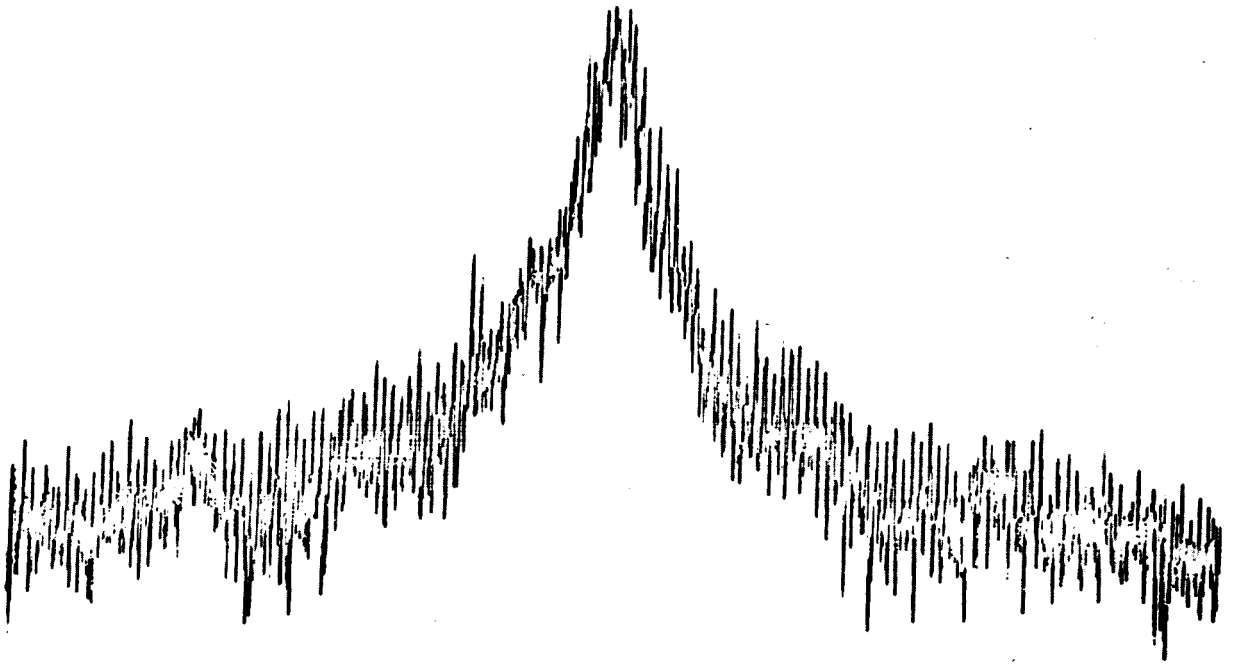

FIGURE 20–18.—Unlocked laser vs. crystal oscillator.

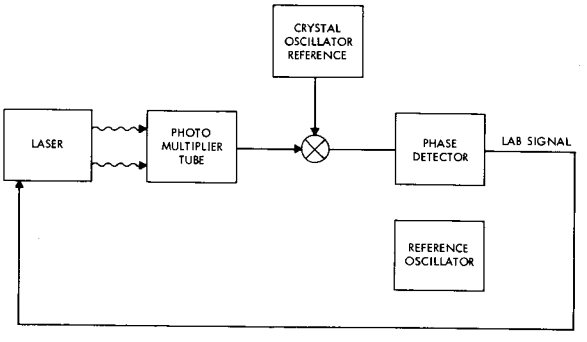

FIGURE 20–19.—Phase-lock loop for laser.

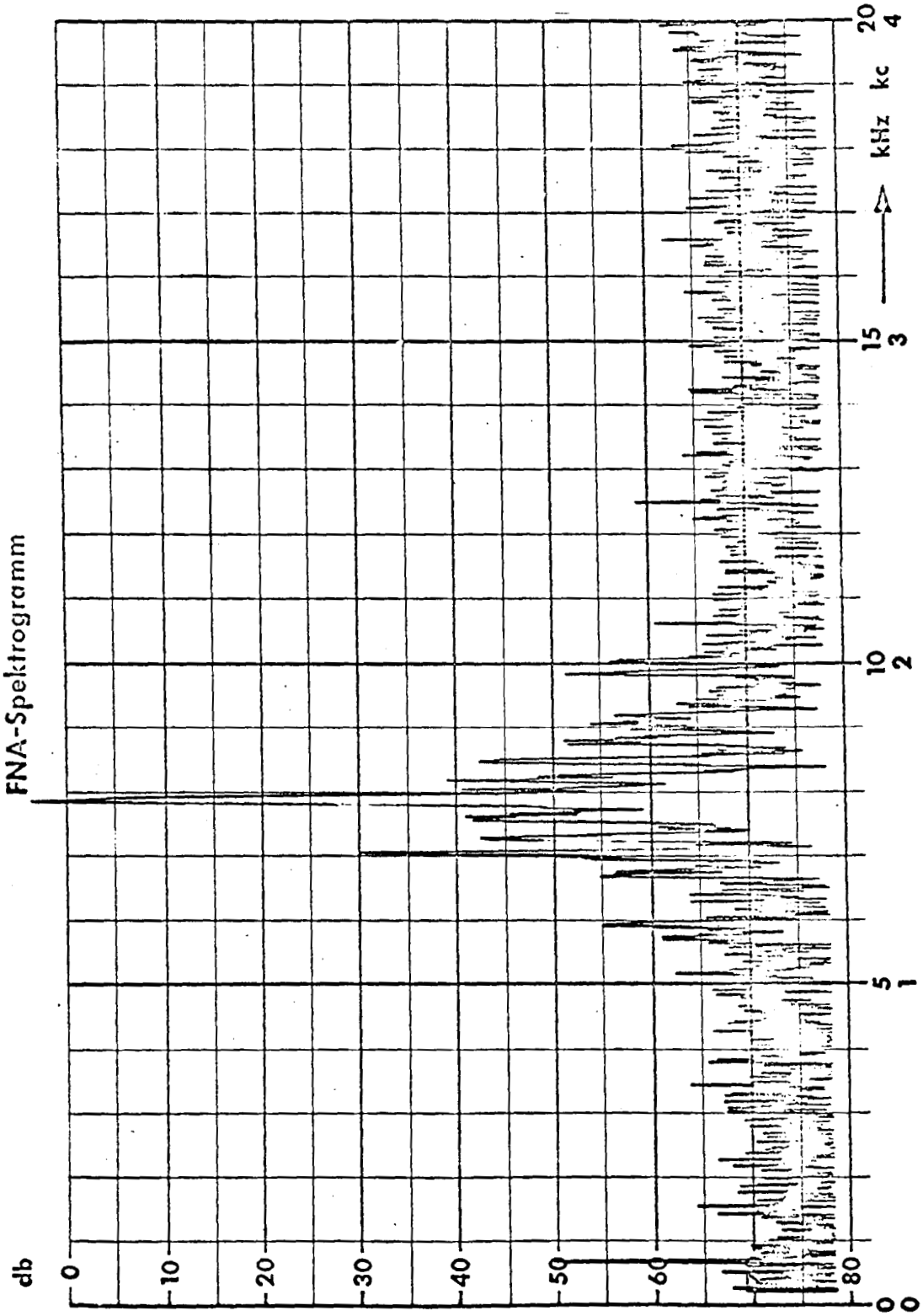

FIGURE 20–20.—Phase-locked laser self-beat.

21. SELF-CALIBRATING AND SELF-CHECKING INSTRUMENTATION FOR MEASUREMENT OF THE SHORT-TERM FREQUENCY STABILITY OF MICROWAVE SOURCES*

C. H. GRAULING JR., AND D. J. HEALEY III

Westinghouse Electric Corporation
Baltimore, Maryland

The short-term frequency stability of a phase-stable source, or stalo, is best expressed in terms of sideband levels. This paper discusses the apparatus that is employed to measure a spectral density of −115 db/cps at 1000 cps from the carrier frequency at X-band. A passive reference is employed, although use of an active reference source is considered. Two types of passive measuring apparatus are discussed in detail: the RRE discriminator, and a Westinghouse-developed test set. The latter provides a number of significant features that are not obtained with the RRE discriminator; for example, the capability of direct calibration, direct determination of the limiting sensitivity, and the measurement of intentional modulation appearing on the source.

Specification of short-term frequency stability, averaging times less than 1 millisecond, is usually more meaningful to users when the stability is expressed in terms of modulation sidebands or spectrum distribution rather than in terms of the linewidth or the fractional frequency stability. The latter, however, is still frequently given as a measure of stability, although it has significance only when the averaging time is greater than several seconds.

Measurement of short-term frequency stability therefore requires apparatus which can analyze the spectrum of the signal near the carrier. This paper will discuss several methods that might be considered and will describe in some detail the approach used by Westinghouse in the design of a test set for this purpose, suitable for field use by relatively unskilled personnel.

The signals to be measured have such stability that they may be represented as a very narrow carrier line surrounded by low-level noise sidebands, the total power content of the sidebands being very small compared with that of the carrier itself. A suitable test set is, then, one which measures the sideband energy in a prescribed bandwidth over a frequency range corresponding to the modulation frequencies of interest.

The desired sensitivity of such a test set to satisfy current as well as anticipated future needs at Westinghouse is −115 db/cps of bandwidth for frequencies 1000 cps and greater from the carrier. At frequencies below 1000 cps, reduced sensitivity can be tolerated.

In many cases the amount of power available from the source for the measurement of source stability is rather small, and the test set should desirably provide the sensitivity of −115 db/cps with input signals on the order of a few milliwatts.

An important requirement for any test set of this sort is that calibrating and checking features be provided. These functions should be operable when the expected signals are present in the equipment. Finally, operation of the test set should be simple, so that a relatively unskilled operator can obtain reliable measurements of the stability of the source under test.

*This paper is based on work that was performed in connection with Bureau of Naval Weapons Contract NOw 63-0280/di.

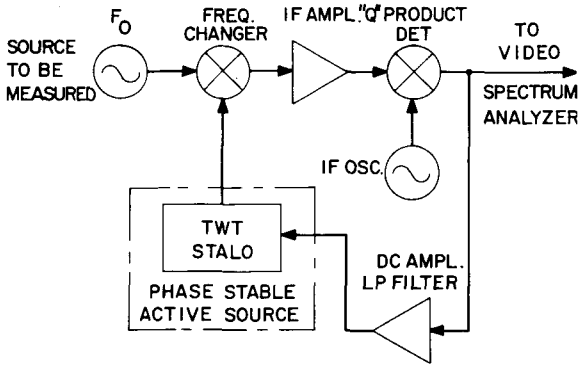

FIGURE 21–1.—Microwave stalo as active reference source.

MEASUREMENT TECHNIQUES

All of the possible stability measuring devices have one feature in common: The signal to be measured is compared with some form of local reference, and any differences between signal and reference are read out as a measure of the short-term stability. The local reference may be an *active source*, such as a stalo of known characteristics, or a *passive device*, such as a cavity resonator.

Test sets using a passive reference form the subject of the next two sections and will not be discussed further at this time.

The *active* reference is readily utilized in a phase-lock loop controlled by the signal to be measured. Figures 21–1 and 21–2 show simplified block diagrams for such test apparatus. Figure 21–1 shows a microwave stalo as an active reference source. The stalo employs a Traveling Wave Tube (TWT) and a resonant cavity as an oscillating loop. Figure 21–2 shows a crystal oscillator and harmonic generator as the active reference source. The use of an active reference has the advantage of providing a direct phase comparison between the reference standard and the unknown frequency; it does not introduce effective attenuation of the sidebands to be measured, as occurs in the use of a passive reference.

The problem, however, is that the measured output can be no better than the active reference; and the state of the art has not progressed to the point where "standard stalos" having performance characteristics significantly better than those required from the source under measurement can be made available.

The evaluation of a highly phase stable source, therefore, usually involves intercomparison of three identical units. Consequently, measurement of sources that may be operated at any frequency in a band such as X-band would be extremely costly. In addition, field testing without a procedure to check the standard could not be tolerated.

Theoretical calculations indicate that the TWT stalo may give adequate performance; but no experimental data to substantiate the theory, at the sideband levels of interest, are known to exist. A companion paper (Reference 1) indicates that a crystal oscillator and harmonic generator should give about the stability required, but it cannot be considered a "standard stalo" at the present time.

A significant disadvantage is encountered when the signal to be measured contains intentional phase or frequency modulation of large index. The maximum modulation index that can be satisfactorily measured is limited to approximately 1 radian when additional frequency tracking loops are not provided.

THE RRE DISCRIMINATOR

Principle of Operation

The most satisfactory technique for measuring the angle modulation noise on SHF sources involves the use of a microwave frequency discriminator, with a video spectrum analyzer for measurement of the discriminator output wave-

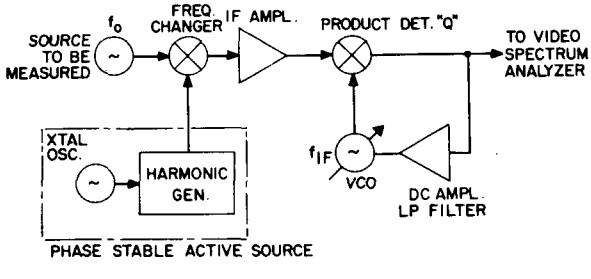

FIGURE 21–2.—Crystal oscillator and harmonic generator as active reference source.

form. Of the various discriminators that might be employed, those which minimize the carrier frequency signal appearing at the input of the SHF to audio conversion circuits provide the greatest sensitivity. A discriminator that is widely used is the RRE discriminator (Royal Radar Establishment, Malvern Works, U. K.). Figure 21–3 shows the basic configuration of such a discriminator. The signal to be measured is applied to a waveguide bridge circuit containing a matched cavity resonator. Assume that the 3-db coupler, cavity resonator, and the load on port 3 are all perfectly matched. When the cavity resonator is tuned precisely to the carrier frequency of the source, the signal appearing at port 4 of the 3-db coupler is the result of small changes in the reflection coefficient as the instantaneous frequency changes from the resonant frequency of the resonator. Having been disdipated in the resonator, the carrier itself will not appear at port 4.

The impedance of the cavity can be expressed as

$$Z=Z_a[1+j(2\Delta f/BW_u)], \tag{1}$$

where

Z = impedance at a particular detuning Δf,
BW_u = unloaded bandwidth of cavity resonator,
Z_a = impedance at the resonant frequency of the cavity.

The reflection coefficient is given by

$$\Gamma=(Z-Z_0)/(Z+Z_0), \tag{2}$$

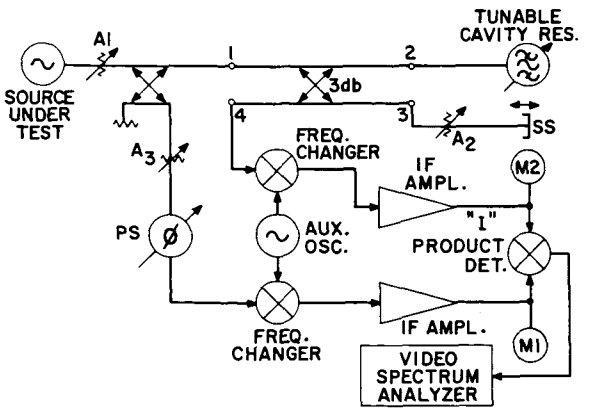

FIGURE 21–3.—RRE discriminator.

where

Z = impedance of cavity,
Z_0 = surge impedance of coupler.

With a perfectly matched cavity, $Z_a=Z_0$; hence,

$$\Gamma=\frac{j_0(\Delta f/BW_u)}{2Z_0[1+j(\Delta f/BW_u)]}. \tag{3}$$

A major objective is the measurement of spectra which are more than 60 db below the carrier power. The highest modulation frequency of interest is on the order of 200,000 cps. Now, the sideband level for very small sidebands can be written as

$$\text{Sideband (db)}=20\log_{10}(\Delta f/2f_m), \tag{4}$$

where

Δf = peak deviation of the carrier frequency,
f_m = modulating frequency causing this peak deviation;

Δf is, then, largest for a given sideband level at the highest modulating frequency. Thus, −60 db at 200,000 cps corresponds to a peak deviation of 400 cps.

The cavity resonator has a Q_L that will typically range between 10,000 and 20,000 at X-band. This yields a loaded bandwidth

$$BW=f_0/Q_L=500 \text{ kc to } 1 \text{ Mc}, \tag{5}$$

and an unloaded bandwidth half this value. For most measurements, therefore, the second term of the denominator in Equation 3 is small; and the peak reflection coefficient is essentially

$$\Gamma=2\Delta f/BW. \tag{6}$$

In practice, Z_a is not precisely equal to Z_0. The small mismatch that is encountered is accommodated by the short-circuited attenuator connected to port 3 of the 3-db coupler shown in Figure 21–3.

The magnitude and phase of the mismatch at port 3 is controlled by the variable attenuator and by the position of the sliding short circuit, respectively. Adjustment of these two parameters is made to produce a small reflection that is antiphased at port 4 with that resulting from the coupler and cavity mismatch when $\Delta f=0$.

The signal from port 4 is a double-sideband suppressed carrier signal representing the phase noise of the source under measurement, provided the amplitude noise on the source is much less than the phase noise. The amplitude of the signal is directly proportional to the frequency deviation of the carrier when the deviation is small. It also is directly proportional to both the loaded Q of the cavity resonator and the signal level at port 1 of the coupler.

The modulating signal waveform is obtained by applying both the bridge output and carrier signals to an "I" product detector. A spectrum analysis of the demodulated waveform then yields the frequency deviation spectrum *when the AM spectrum is less than the PM spectrum.*

Ultimate Sensitivity

As shown in Figure 21–3, the double-sideband suppressed carrier signal is applied to a frequency changer which converts the frequency to an HF or VHF intermediate frequency. The signal directly from the source also is applied to a similar frequency changer for the purpose of obtaining the carrier (as well as its sidebands) for reinsertion. An auxiliary oscillator (SHF oscillator) is used in common to both frequency changers.

The signals from the frequency changers are separately amplified and applied to a product detector, which is operated as an "I" or synchronous detector to recover the modulation waveform corresponding to the incidental noise modulation of the source under test.

Envelope detectors are provided to monitor the signal appearing at the inputs to the product detector. A diode detector monitors the reinserted carrier level, which is read on M1. Another diode detector monitors the suppressed carrier signal channel; but, since the modulation sidebands are small, the meter M2 will show a deflection only when significant carrier appears at port 4 of the 3-db coupler. M2 is therefore basically used as a null indication for proper tuning of the tunable cavity resonator and adjustment of attenuator A2 and short SS. The sensitivity of the discriminator output of the product detector—when phase shifter PS is adjusted for "I" detection—may be determined by monitoring the voltage of the reinserted carrier by means of M1 and by knowing the cavity Q_L as well as the gains or losses of the IF amplifiers, frequency changers, product detector, microwave transmission path, and attenuator A3.

The characteristic of the measuring apparatus can be expressed as

$$V_{out} = KV_1 \, \Delta f(Q_L/f_0), \tag{7}$$

where

V_1 = voltage at the reference detector as read on M1,
K = constant accounting for the transmission losses and gains noted above,
Q_L = loaded quality factor of the tunable microwave resonator,
f_0 = carrier frequency,
Δf = peak deviation of the carrier frequency at f_m.

Assume that the group delays of the two channels from frequency changers to product detector, *including* network associated with the product detector, are exactly identical; then the noise of the auxiliary oscillator is suppressed, and the minimum value of Δf that can be measured is determined when V_{out} equals thermal noise. When

$$V_{out} = V_{noise},$$

$$\Delta f_{min} = \frac{B_r B_a^{1/2}}{(S/N)_{max}}, \tag{8}$$

where

B_r = 3-db bandwidth of the tunable cavity resonator,
B_a = noise bandwidth of the analyzer,
$(S/N)_{max}$ = maximum signal-to-noise ratio that is obtainable at the product detector output per cps (voltage).

B_r is fixed at a value between 500 kc and 1 Mc to provide measurements over the desired modulating frequency spectrum. The maximum S/N depends on the noise-carrier intermodulation occurring in the signal channel. As noted in a previous paper (Reference 2), a typical S/N of a signal channel as shown in Figure 21–3 is about 137 db/cps.

In practice it is found that, without special feedback techniques, manual adjustment of the

tunable cavity resonator permits about 40 db carrier rejection to be realized when measuring sources having moderately good long-term stability (i.e., averaging over times greater than 1 second). For such conditions the minimum frequency deviation in a 1-cps bandwidth is then

$$\Delta f_{min} = \frac{(10^6)\ (1)}{\frac{1}{20}\ \text{antilog}_{10}\ (137+40)} = 1.4\times10^{-3}\ \text{cps}. \tag{9}$$

The ultimate sensitivity is 0.014 cps in a 100-cps analyzer bandwidth, and 0.044 cps in a 1000-cps bandwidth.

When greater sensitivity is needed, the carrier signal at port 4 of the 3-db coupler must be further attenuated. Using feedback techniques to control the resonator tuning, 60 db of carrier rejection might be realized. This would increase the sensitivity by a factor of 10 times, provided the input signal under measurement is increased by 20 db. It was stated in the introduction to this paper that the requirements at Westinghouse are for measurement to -115 db/cps at 1000 cps f_m. This corresponds to 0.00358 cps peak deviation and, as seen by the above discussion, can be realized with manual tuning of the resonator provided adequate power is available from the source.

Calibration

Calibration of the RRE discriminator is best accomplished by providing a modulating signal to modulate the source under test. This technique can, of course, be employed only if the device under test can be modulated and has a linear modulation characteristic. The modulation signal is increased until a microwave spectrum analyzer shows that the carrier vanishes. For this condition,

$$\Delta f = 2.405 f_m, \tag{10}$$

where

2.405 = argument of the zero-order Bessel function of the first kind for which the function first becomes zero,
Δf = peak deviation,
f_m = modulating frequency.

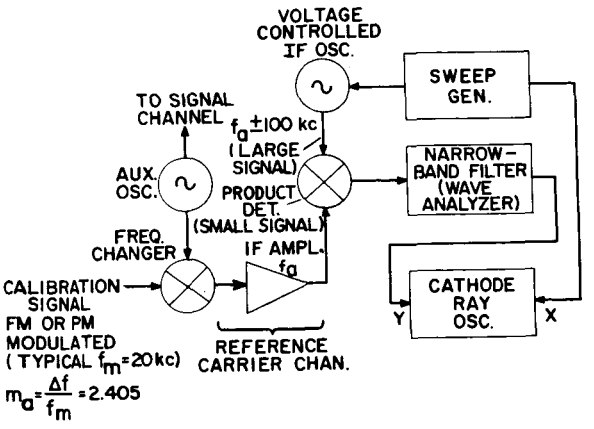

FIGURE 21–4.—Use of components in discriminator for microwave spectrum analyzer to permit modulation index of calibrating signal to be set to 2.405.

When the source under test and the auxiliary oscillator provide fairly good long-term frequency stability, it is possible to use the reference channel as the spectrum analyzer by applying an IF swept frequency oscillator as the carrier switching signal to the product detector and the reference IF as the signal spectrum. Figure 21–4 shows the arrangement that is used. Typical instabilities necessitate that the spectrum display be about 200 to 500 kc and modulation frequencies greater than 20 kc to avoid operator confusion in adjusting the modulation index to 2.405. A precision audio attenuator is employed to reduce the modulating signal so that the deviation is within the dynamic range of the analyzer used to measure the product detector output. This is readily adjusted to any particular Δf once the modulation level to produce 2.405 f_m has been established.

Alternatively, a standard source may be used when the source under test cannot be modulated, or measured values of gains Q_L and attenuator A3 used to establish a calibration number. A direct calibration using the source under test is, however, preferable.

Measurement (Calibration) to Establish Ultimate Sensitivity

It is not possible to make a direct determination of ultimate sensitivity. If a noise tube is introduced to make the measurement, an optimistic figure is obtained since the residual carrier from

port 4 of the coupler is not present. The effective noise figure at the particular analyzer frequency band therefore is not determined. If an IF crystal oscillator is used to introduce the residual carrier voltage, the limitation caused by noise on the SHF auxiliary oscillator is not measured.

There are two commercially available test sets that employ the arrangement shown in Figure 21–3. In both of these test sets, the IF amplifier–product detector circuits are of poor design, so that considerable differential group delay is exhibited. As a result, serious limitation of ultimate sensitivity occurs because of angle modulation noise appearing on the auxiliary oscillator unless an AFC or APC loop is employed to force the IF frequency to remain constant. With such AFC circuitry, suppression of auxiliary oscillator noise of greater than 60 db over the modulation frequency band of interest has been measured. With AFC, a gas tube and IF oscillator can be employed to estimate the ultimate sensitivity.

Amplitude Modulation Measurement

AM noise can be determined by measurement of both the carrier level and the fluctuations from the reference detector, provided the AM noise exceeds the ultimate sensitivity imposed by the effective noise figure in the analyzer frequency band at which measurement is made. Measurements show that almost all the microwave sources measured at X-band indicate −126 db in a 100-cps bandwidth at a 1000-cps modulating frequency, and −134 db in a 100-cps bandwidth at 150,000-cps modulating frequency. This, then, apparently is the instrumentation noise; and one must conclude that we have not in fact been able to measure the AM noise of the sources under test.

Limitations

A limitation encountered with use of passive references is that they respond not only to angle modulation but also to amplitude modulation. The basic purpose of the reference is to operate on the input signal to produce a modified signal that can be cross-correlated against the input (in the product detector) to recover a particular modulation on the reference. In the case of the RRE discriminator, the output from the bridge may be considered as a pair of double-sideband suppressed carrier (DSSC) signals representing the PM and AM sidebands on the input, along with a replica of the input which has been attenuated and phase-shifted. The latter signal is the result of imperfect bridge balance. Since the effective carrier cancellation is between 20 and 40 db without additional feedback techniques, sidebands only 20 to 40 db below the input can exist on the bridge output. The PM sidebands on this uncancelled signal cause no trouble, but the AM sidebands may present a problem. If phasing is proper, additional suppression will be obtained in the "I" detector; however, the additional suppression is a function of the manner in which the microwave bridge unbalance occurs, and it may not be obtained. The discriminator provides a sensitivity $\Delta V/\Delta f$ which is a constant for small Δf, independent of modulating frequency. Thus, for a constant sideband level the output is proportional to the modulation frequency, since for constant sideband level $\Delta f/f_m$ is constant. This amounts to a reduction in the FM or PM sidebands appearing on the source by the conversion characteristic of the bridge, which produces an effective attenuation of $2f_m/BW$ to the low-frequency input sidebands while creating a signal suitable for demodulation.

At a low modulating frequency f_m measurement of the angle noise on the source, therefore, becomes difficult when bridge unbalance exists and the AM on the source is significant. As an example, consider the case when the modulating frequency is 1000 cps and the cavity bandwidth is 1 Mc. The sidebands from the bridge representing the FM on the source at 1000-cps f_m are attenuated by

$$20 \log_{10} [(1{,}000{,}000)/(2)(1000)] = 54 \text{ db}$$

relative to those on the source. If the AM sidebands on the source were equal to the FM sidebands, the bridge balance would need to be greater than 60 db to insure measurement of the FM—assuming the worst case of no additional suppression in the "I" detector. Thus, for the

typical 40-db balance, it would be necessary that the AM be more than 20 db below the FM at 1000 cps from the carrier of the source under test to insure measurement of the FM sidebands.

As noted, the manner in which the unbalance occurs is important. By further adjustment of the three variables—cavity tuning, attenuator A2, and the sliding short SS—it is possible to realize additional discrimination as a result of the quadrating property of the "I" detector; however, practical use of such critical adjustment requires that a proper sensing technique be provided.

Another serious problem is the dimensional instability of the discriminator in the presence of vibration and acoustic environment. Acoustic shielding is essential in the Westinghouse Aerospace Division Laboratories to permit measurement in excess of -110 db/cps at 1000-cps f_m.

Measurement of a modulated carrier such as encountered in high PRF pulse Doppler radar sets usually is not possible, since the first upper and lower sidebands resulting from pulse amplitude modulation of the carrier appear at port 4 as a residual signal.

WESTINGHOUSE TEST SET

Principle of Operation

This test set utilizes a passive resonant cavity as the frequency reference element. In developing this set, the following features were considered:

1. Provision of adequate sensitivity for Westinghouse requirements.
2. Simplicity of operation, so that trained but relatively unskilled personnel can obtain reliable measurements with minimum judgment on their part.
3. Incorporation of self-checking and self-calibrating features to maintain performance in field usage.

All signal processing prior to conversion to audio frequency is done at microwave frequencies, so that no auxiliary microwave oscillators and associated power supplies are required in the test set. The output from the microwave circuits is an audio signal, the detected modulation waveform, which is examined in a video spectrum analyzer. A simplified diagram of the Westinghouse test set is shown in Figure 21–5.

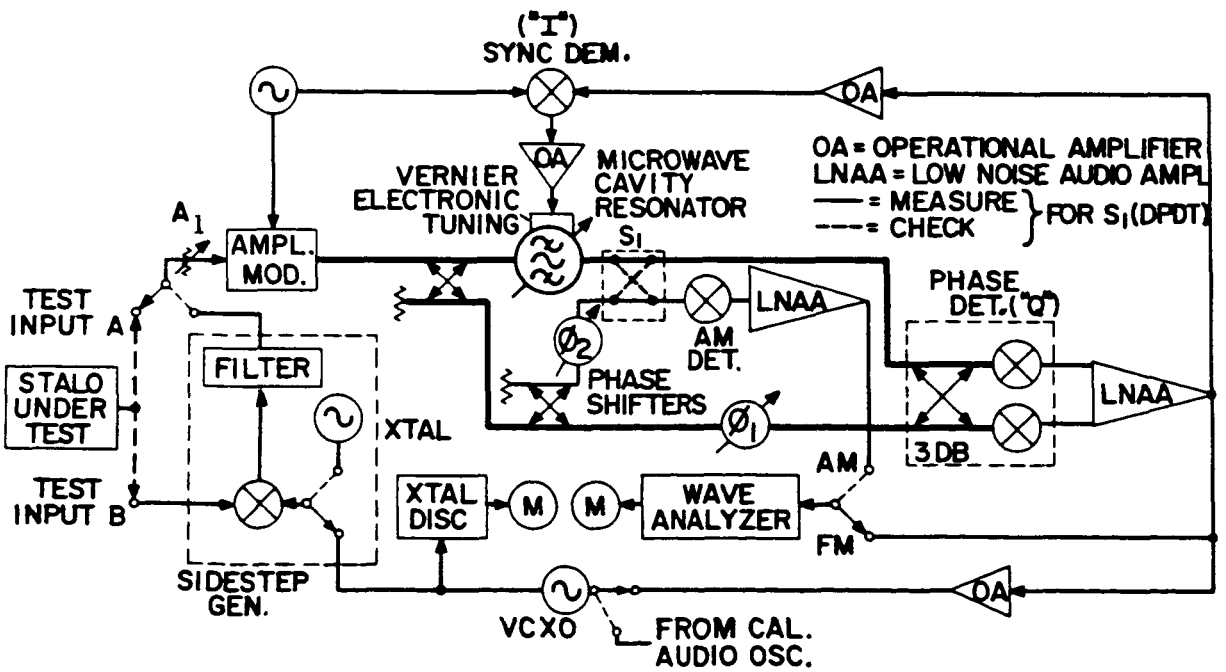

FIGURE 21–5.—Westinghouse test set.

The heart of the test set is a microwave cavity resonator and a "Q" product detector. The latter consists of a 3-db hybrid and special low-noise mixer crystals. The output of the "Q" detector is applied to a low-noise audio amplifier. A signal from the source to be measured is applied to "Test Input A." This signal is routed in two paths by the directional coupler. Part of the signal power passes through the cavity resonator to one input port of the "Q" detector. The remaining part of the input signal power is applied directly to the second input port of the "Q" detector through a variable phase shifter. The phase shifter is adjusted so that the output of the "Q" detector is zero when the cavity is tuned to the frequency of the source under test. When Δf of the source is not zero, the additional phase perturbation appearing on the signal which passes through the resonator produces an output from the "Q" detector which is amplified by the audio amplifier. The signal at the output of the audio amplifier, representing the angle modulation waveform, may then be examined by using the spectrum analyzer.

In this discriminator arrangement, the angle modulation noise is converted to a phase modulation that can be demodulated by the "Q" detector. Specifically, a DSSC signal which carries the desired modulation information is generated. These sidebands are attenuated by a factor of $2f_m/BW$ plus the insertion loss in the cavity as compared with the input PM sidebands. For low modulating frequencies, both the AM and PM sidebands—as well as the carrier—pass through the cavity unchanged (except for some attenuation) and are applied to one port of the "Q" detector along with the DSSC signal containing the information. Discrimination against AM is then provided by the quadrating property of the detector. A separate channel consisting of a crystal detector and a separate low-noise audio amplifier provides capability for AM measurement. This arrangement not only eliminates low-level signal switching but also provides additional calibration capability.

Adjustment and Calibration

Measurement of angle modulation (FM or PM) with the test set depends on a frequency-to-phase conversion in the transmission cavity resonator. For proper operation, it is necessary that the cavity resonator be accurately tuned to the carrier frequency of the source being measured and that the phase shifter be adjusted so that good AM rejection can be realized from the "Q" detector.

Drift of the carrier frequency of the source relative to the resonant frequency of the cavity resonator will introduce a static phase error that will cause AM noise to appear at the "Q" detector output.

An automatic balancing scheme therefore has been provided. The AM loop shown in Figure 21–5 provides proper tuning of the resonator. An AM modulator is driven by a low-frequency signal—the modulation frequency being an order of magnitude lower than the frequency band of interest for which the source spectrum is to be examined—to provide a carrier for the balancing loop. The signal at this frequency that appears at the "Q" detector output is a measure of the unbalance of the "Q" detector as a result of a difference between the carrier frequency and the resonant frequency of the cavity (or misadjustment of the variable phase shifter).

The amplified error from the "Q" detector is cross-correlated with the AM modulating signal in an "I" detector, the output of which is employed to control the tuning of the cavity resonator. The key to providing this feature is the vernier electronic tuning provided in the microwave resonator.

The adjustment of the discriminator to permit measurement of the angle modulation of a source is as follows:

1. The amplitude modulation is turned *off*, the electronic tuning of the resonator is set to the center of its range, and the cavity is manually tuned to the carrier frequency of the source to be measured.

2. The amplitude modulation is turned *on*, but the AM feedback loop is left *open*. The phase shifter is next adjusted to produce minimum output from the audio amplifier at the amplitude modulating frequency.

3. The AM loop is *closed*, and the discriminator

remains properly tuned as long-term frequency drifts occur.

It is obvious that initial adjustment does not need to be as precise as in the RRE discriminator because of the incorporation of the low-frequency AM loop. The AM loop permits full benefit of the quadrating property of the "Q" detector in discriminating against AM on the source.

The test set includes a sidestep generator and a voltage-controlled crystal oscillator (VCXO) whose FM output can be employed for calibration of the test set. This FM is monitored by a discriminator utilizing quartz crystal resonators, thereby providing accurate measurement of small frequency deviations appearing on the oscillator (i.e., 1- to 10-cps peak deviation).

To calibrate the test set, the source is connected to Test Input B shown in Figure 21–5, and attenuator A_1 is adjusted to set the power level to a prescribed value that yields the correct level at the "Q" detector. This power level is monitored from the output of a coupler ahead of the resonator (not shown in Figure 21–5).

The VCXO is connected to the calibrating audio oscillator and is modulated at the frequency f_m for which calibration is to be made. The resultant deviation is monitored by connection of the wave analyzer to the crystal discriminator output. The sidestep generator adds this frequency deviation to the source under test, and the resultant signal is applied to the test microwave discriminator. The wave analyzer is then connected to the output of the low-noise audio amplifier, and a calibration point is obtained. The VCXO is removed from the balanced modulator in the sidestep generator, and a fixed-frequency crystal oscillator having high spectral purity is substituted in its place. The reading obtained from the wave analyzer is the sum of the frequency deviation of the source under test and the crystal oscillator. Since the latter is about 2 orders of magnitude less than the deviation on the source, it does not influence the measurement.

In cases where the source can be conveniently changed in frequency, it can be applied to Test Input A, thereby eliminating any contribution of the sidestep generator. In some systems the sidestep generator is an essential part of the source under test; and in those cases the source is always connected to Test Input A, and the output of the VCXO is connected to the sidestep circuits associated with the source. The crystal discriminator also is used to monitor deliberate modulation that may appear on the source under test. When the sidestep generator is connected to the VCXO and the control signal for the VCXO is obtained from the low-noise audio amplifier, the deliberate modulation appearing at the input to the cavity is effectively removed. The discriminator output is a direct measure of the deliberate modulation under these conditions.

In some cases, it may be desired to measure the noise on the source under test with the sidebands resulting from deliberate modulation being considered as noise. For this case, the sidestep generator merely is connected again to the fixed-frequency offset oscillator.

A feature of this mechanization for the test set is that it provides means for complete maintenance in the field with a minimum of additional equipment. No microwave sources other than an operating source to be measured are required for field maintenance.

Ultimate Sensitivity

As noted previously, the ultimate sensitivity of a microwave discriminator for these noise tests is limited by the maximum attainable signal-to-noise ratio at the audio output to the wave analyzer and the degree of sideband exaltation that can be provided.

Sideband exaltation was not provided in the Westinghouse test set because the power available from many of the sources to be measured was rather limited. The Westinghouse test utilizes a microwave "Q" detector (i.e., the phase-modulated output from the resonator, which is a measure of the angle modulation on the source under test, is converted directly to an audio signal). The arrangement has proven satisfactory because of the availability of microwave diodes exhibiting reduced $1/f$ noise.

Initial measurements using Philco diodes type L4154 show that the effective noise figure in the modulating frequency range of concern is about 10 db less than can be achieved with the 1N23-type crystals. The Low-Noise Audio Amplifier

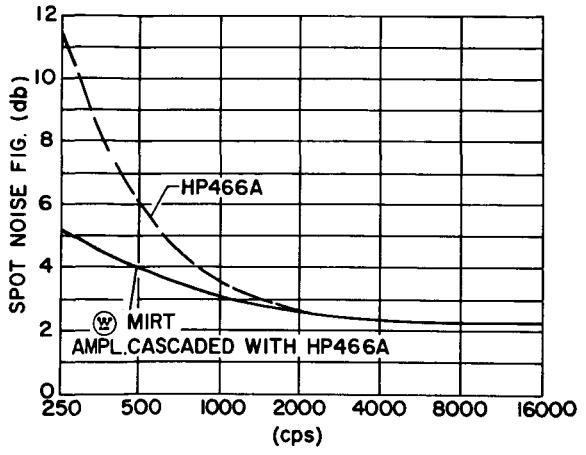

FIGURE 21–6.—Noise figure of low-noise audio amplifier.

(LNAA) likewise must have a low noise figure in the modulating frequency band of interest. Figure 21–6 shows the noise figure of a Westinghouse molecularized amplifier designed for low noise at low audio frequencies, compared with an HP466A low-noise amplifier. Both of these audio amplifiers are entirely adequate for use in the test set as the LNAA. Measurements showed that the resulting sensitivity with the L4154 diodes and the low-noise audio amplifiers of Figure 21–6 is -163 db/cps of bandwidth at 1000 cps from the carrier ($f_m = 1000$ cps).

As noted previously in connection with IF amplification prior to conversion to audio (e.g., the arrangement of Figure 21–3), a typical signal-to-noise ratio was about 137 db/cps at 1000 cps. The performance of the Westinghouse test set thus is comparable with that achieved with the commercially available versions of the RRE discriminator when 20-db carrier cancellation is achieved.

The conversion of angle modulation noise appearing on the source to a phase modulation that can be measured by the "Q" detector depends on the modulating frequency and the cavity resonator bandwidth. With cavity bandwidth of 500 kc, the conversion at a modulating frequency of 1000 cps is -48 db. The ultimate sensitivity at 1000 cps from the carrier is then $-163+48 = -115$ db/cps.

A feature of the test set is that the ultimate sensitivity limit can be measured directly. Switch S1, shown on Figure 21–5, is a double-pole, double-throw reversing switch. When it is placed in CHECK position, both signals to the "Q" detector are obtained through paths which have no difference in group delay. Therefore, by merely adjusting phase shifter ϕ_2 for minimum noise output from the audio amplifier, the noise voltage is the limiting noise level of the test set and, in conjunction with the calibration previously described, yields the ultimate sensitivity.

Limitations

The sensitivity of the test set is adequate for our purpose. However, measurement of smaller frequency deviations necessitates either a significant increase in maximum S/N or a carrier nulling technique. The test set can be modified to provide carrier nulling and exaltation of the sidebands by the addition of another coupler, attenuator, and phase shifter to bridge the cavity. The penalty, however, is the necessity of having more power available from the source under test. Alternatively, the "Q" detector could be operated as an "I" detector, and the RRE discriminator employed. However, the ultimate sensitivity may be greater using the bridged transmission cavity; and, in addition, the adjustment procedure is considerably simplified. There is also the possibility that the minimum Δf that can be measured can be reduced by a factor of 2 to 3 with use of diodes other than the L4154.

CONCLUSIONS

Westinghouse has chosen to utilize a *passive reference* for measurement of short-term stability of microwave sources rather than an active standard frequency source. The reason for this is associated with the need for providing simple calibration and maintenance of performance in the measuring set. Westinghouse also has chosen to use a transmission cavity rather than a reflection cavity in the discriminator, together with "Q" detection, because this provides means for simple checking of ultimate sensitivity. Such a technique is feasible because an acceptable effective noise figure can actually be realized by direct conversion from microwave frequencies to audio frequencies. The output test S/N ratios at low

audio frequencies are, in fact, comparable to the best that have been realized with intermediate conversion to an HG signal prior to demodulation to audio.

REFERENCES

1. Buck, J. R., and Healey, D. J. III, "Short-Term Frequency Stability Measurements of Crystal-Controlled X-Band Source," *Proceedings of Symposium on the Definition and Measurement of Short-Term Frequency Stability, Goddard Space Flight Center; NASA and IEEE*, Paper No. 17, November 24, 1964.
2. Buck, J. R., Healey, D. J. III, and Meiseles, M., "Measurements of Phase Stability of Quartz Crystal Oscillators for Airborne Radar Applications," *1964 IEEE International Convention Record*, Part 8, pp. 34–42, 1964.

Page intentionally left blank

22. SHORT-TERM STABILITY MEASUREMENTS IN THE SURVEYOR SPACECRAFT SYSTEMS*

B. E. ROSE

Aerospace Group
Hughes Aircraft Company
Culver City, California

The telecommunications link for the Surveyor Spacecraft utilizes a receiving and transmitting link at a frequency of approximately 2200 Mc. Both the spacecraft and the ground station use phase-lock loop receivers. To prevent loss of phase lock due to vibration caused by the vernier engine and retro engine burning and the landing shock, the transmitter and receiver must meet short-term stability requirements, expressible as a maximum phase jitter of 45 degrees, peak-to-peak, measured in a phase-locked loop of 425-cps noise bandwidth, under conditions of 3 g's zero-to-peak vibration from 10 cps to 10 kc.

Measurements of phase jitter in the oscillator modules are presented in the report, and the method of measurement is discussed. Excessive phase jitter was found to occur at approximately 400 cps in the transmitter and 1100 cps in the receiver. These frequencies were found to be the crystal-mount mechanical resonant frequencies for the HC–18/U (transmitter) and HC–6/U (receiver) crystals.

Two methods for reduction of phase jitter are described: The first utilizes a foam vibration isolation mount, and the second used a component with a greatly improved internal mounting structure for the quartz plate.

To complete the mission of a soft landing on the lunar surface, the Surveyor spacecraft must survive and operate through the flight phases of take-off, injection into orbit, midcourse maneuver, landing, and touchdown.

In particular, during midcourse maneuver and during descent, it is required to maintain communications with the DSIF stations for engineering data, telemetry transponder mode tracking, and television picture transmission. Because the spacecraft retro rocket and vernier engines are operated during these maneuvers, the telemetry systems will be subject to vibration. The problem of maintaining phase lock during vibration is discussed in this paper in three parts: (1) the Surveyor block diagram and the phase jitter specifications imposed on the transmitter signal and receiver local oscillator signal, (2) the test setup used to make jitter tests—under vibration conditions—and the phase-locked loop test set used in making the tests, (3) the measured phase jitter observed with conventional crystals in a hard mounting and in vibration isolators, and finally with ribbon-mounted crystals.

SYSTEMS BLOCK AND SPECIFICATIONS

Figure 22–1 shows a simplified block diagram of the spacecraft transmitter and receiver. The signal source for the transmitter is selectable from either the transmitter VCXO or the receiver VCXO. When connected to the receiver VCXO, the transmitter signal is phase-locked to the received signal. The transmitter utilizes a multiplication ratio of 120 and the receiver, 108.

Phase Jitter Specifications

45 degrees peak-to-peak phase jitter, 3σ value—measured in a 425-cps loop bandwidth—at 3 g's zero-to-peak sine vibration, 10 to 10,000 cps

*This paper presents results of one phase of research carried out under Contract 950056 for Jet Propulsion Laboratory, California Institute of Technology, under Contract NAS 7–100 sponsored by the National Aeronautics and Space Administration.

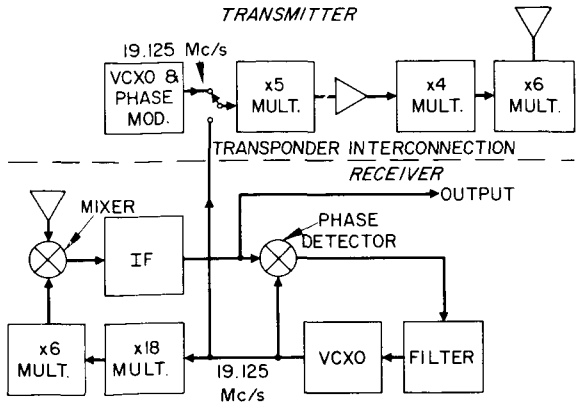

FIGURE 22–1.—Spacecraft transmitter and receiver (simplified diagram).

These jitter specifications are referred to the S-band output frequency. Initial phase measurements on transmitter and receiver did not satisfy specifications. The source of the phase jitter was traced to the crystals used in the receiver and transmitter voltage-controlled oscillators. The transmitter crystal was an HC-18 case style wire-mounted crystal of conventional design; the modules. Since the phase jitter originated in the modules containing the crystals, further testing was performed on these modules—at 19.125 Mc/sec—rather than on the complete transmitter and receiver. A receiver and transmitter module were specially built without foam around the crystal, so that it could be removed or remounted. The vibration table was capable of delivering the full 3 g's at frequencies up to 2000 cps. Tests above 2000 cps were made using whatever g-level was obtainable.

TEST SETUP

The phase jitter at the output of the module under test was measured with a phase-locked loop test set. The schematic of this loop is shown in Figure 22–2. The loop noise bandwidth was 425 cps. The loop was calibrated by the use of an oscillator/phase modulator which was itself calibrated by using the vanishing carrier method. The output of the phase-locked loop was observed on an oscilloscope.

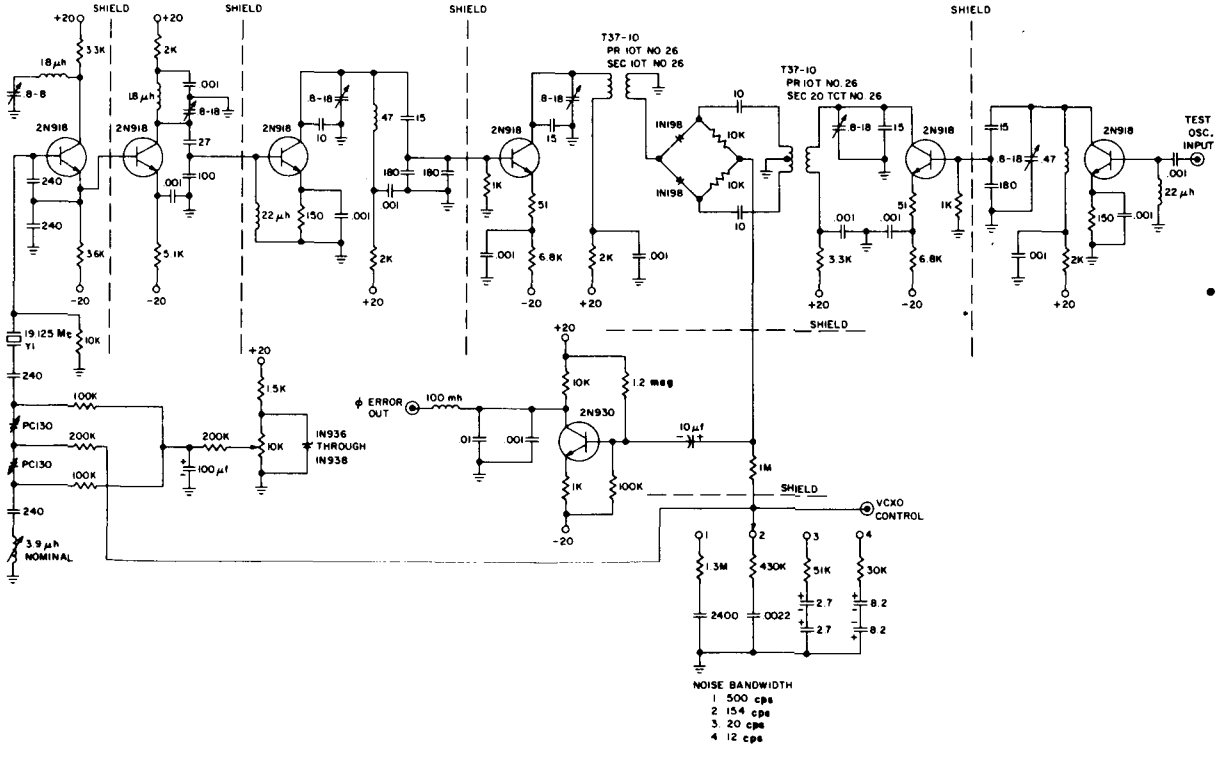

FIGURE 22–2.—Phase jitter detector.

TEST RESULTS

Conventional Crystals in a Hard Mounting

Phase jitter with the standard crystals hard-mounted in the modules was measured to be as much as 1000 degrees (referred to S-band) at approximately 400-cps vibration frequency on the HC-18 crystals and at 1100 cps on the HC-6 crystals. These mechanical resonances had approximately 1-percent bandwidth. These frequencies were found to correspond to the cantilever resonance of the internal spring-mass of the crystal and its mounting wires. Numerous crystals of the HC-18 type were tested. It was found that, although the resonant point almost always occurred at 400 cps, plus or minus 40 cps, the magnitude of the phase jitter varied by as much as 20 to 1 from crystal to crystal.

X rays of several crystals failed to reveal visual differences between high- and low-jitter crystals. It is not known why there was a large variation between crystals of the same lot.

Vibrator Isolator

Figure 22–3 is a sketch of the vibration isolator built to reduce the vibration level at the crystal. An isolation factor of approximately 10 was achieved in this unit. The purpose of the third lead is to ground the case of the crystal to reduce phase jitter caused by capacity variation between the isolator and the crystal case at the natural mechanical resonance of the foam-crystal combination. Even with this third lead, it was found that the amount of isolation which could be achieved at 400 cps was limited by the occurrence of phase jitter at the lower mechanical resonance of the mount. That is, lowering the isolator resonant

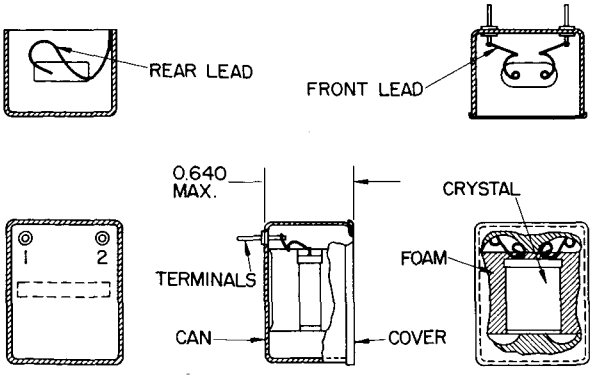

FIGURE 22–3.—Vibration isolator.

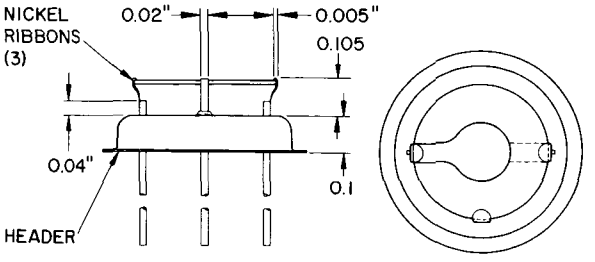

FIGURE 22–4.—Ribbon-mounted crystal.

frequency (by mass-loading the crystal case, for example) tends to increase the phase jitter at the isolator resonance since the excursion is increased; and therefore lead-to-lead and lead-to-case capacitance varies more. The final mount was resonant at about 150 cps.

Ribbon-Mounted Crystals

Several types of commercially available rugged mount crystals were hard-mounted and tested for phase jitter. Although the resonant frequency of these mounts was higher than non-rugged types, they were found to exhibit large phase jitter when vibrated at resonance. Although not much data are available on the subject, the aging rate and temperature behavior of these rugged mounts are reported to be inferior to that of the standard mount.

A type of crystal which seems very promising for this application is the ribbon-supported, transistor header mounted crystal, which was developed by Bell Telephone Laboratories. This crystal is now becoming available from a number of crystal manufacturers. These crystals are mounted on two or three nickel ribbons of 1–3 mil thickness. A sketch of a typical unit is shown in Figure 22–4. Because of the mounting method, the length of the supporting ribbons can be made very short—resulting in a very stiff structure. Tests of two- and three-ribbon crystals show a maximum phase jitter of less than 10 degrees—an improvement of 2 orders of magnitude compared with the standard mount. Preliminary tests indicate aging rates equal to, or better than, those found with conventionally mounted crystals.

Results of preliminary tests and evaluation of prototype models of these ribbon-mounted crystals indicate that there is a good prospect that they will achieve the specified limits of phase jitter. When tests are completed, these components will be submitted for approval for use in flight spacecraft.

23. SHORT-TERM STABILITY MEASUREMENTS

V. VAN DUZER

Hewlett-Packard Company
Palo Alto, California

The short-term stability of a signal can be specified by a limit plot of phase noise and spurious signals versus frequency-of-offset plot. Such a specification will allow evaluation and comparison of signals for a particular application with appropriate system band-limiting, etc. This paper deals with the physical measurement techniques used to obtain such data for high-quality signal sources. A low-noise double-balanced mixer, a low-noise amplifier, a low-frequency wave analyzer, and similar signal sources are the elements of such a system. The measurement capability here should be about 160 db relative per root cycle, or something better than $\Delta f/f$ of 4×10^{-13} for 1-second averaging with 30-kc bandwidth at 1 Mc. This technique is readily extended to the measurement of the short-term stability of resonant devices and signal-processing circuitry. Some aspects of practical measurement experience in connection with a high-quality frequency synthesizer are presented.

The measurement of and the specifications on short-term frequency stability for high-quality signal sources have been serious problems. Lacking well-defined standards for specifications, the equipment manufacturers have presented the users with a confusing array of data that sometimes defy comparison of signal sources *and* evaluation of these sources for a particular application. The short-term stability of a signal source can be specified by a limit plot of phase noise and spurious signals versus frequency-of-offset from the desired signal. Such a specification would allow the user to evaluate the signal source for his particular application. Conversion to other terms with appropriate system band limitations could be readily accomplished, and comparisons of signal sources for the particular application would be greatly facilitated. Note that the same type of plot is useful in connection with performance, phase modulation cleanup, or degradation of a signal-processing circuit such as frequency dividers, multipliers, etc.

The amplitude modulation is assumed to be much smaller than the phase modulation for a high-quality signal; but, if this is not the case, a similar limit plot of this would be of interest because of direct effects and easy (undesired) conversion to phase modulation in the application of the signal. Also, as a practical matter, the effects of environment on the short-term stability should be indicated. This paper will deal with the measurement system used to obtain the signal quality information indicated above.

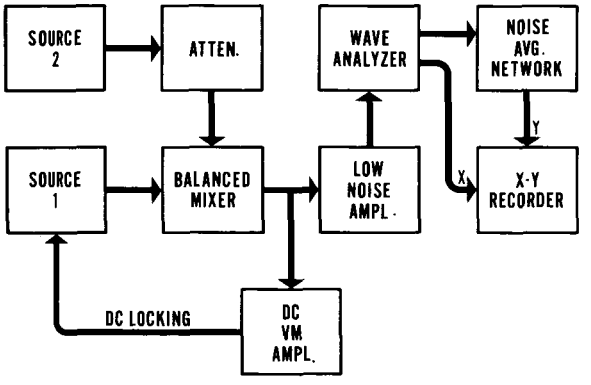

FIGURE 23-1.—Measurement system.

SUGGESTED SYSTEM

Figure 23-1 shows the block diagram of the proposed system. The sources either are two of the type to be evaluated or one is a reference standard of greater stability than the source to be evaluated. The attenuator is used in the cali-

bration of the system and in adjusting the level of the linear input to the mixer.

The mixer used in our work is a very broadband (100 kc to 500 Mc) double-balanced type using diodes with very low $1/f$ noise. The conversion loss is 6 db, and all the ports are a nominal 50 ohms. Balancing against both inputs is required so as not to demodulate the amplitude noise of either input. Balancing on the order of 40 db is obtained over the HF frequency range. The low-noise amplifier can be either a parametric or a transistor amplifier. The mixer output impedance of 50 ohms allows a broadband output; and it makes the use of a transistor amplifier quite appropriate, whereas a field-effect amplifier would seriously limit the system performance. The parametric (down to 1 cycle) or transistor (down to 100 cycles) amplifier can have a short-circuit input noise voltage per root cycle of 2×10^{-9} volt, whereas the best field-effect amplifier will be more than 10 times that bad. The noise-averaging network used has been one with a 1-sec time constant, but this is not critical.

To calibrate the system, Source 2 (Figure 23–1) is offset in frequency slightly (or a substitute offset source is used); and the attenuator is used to reduce the signal level as appropriate for plotting on the x–y recorder with reduced analyzer sensitivity, so that the signal is above the noise level. The attenuator setting, wave analyzer gain, and recorder gain are noted for the calibration. To record the phase modulation, Source 2 is restored to Source 1 frequency; and the attenuator is reset to allow the maximum linear input to the mixer. The dc output of the mixer is set to zero by shifting the frequency adjustment of one of the sources. The dc-locking holds the two sources in quadrature while the noise plot is being made. The noise plot is calibrated with corrections for average to rms, double-sided to single-sided noise, two sources (if one is not a standard), the change in system gain from the calibration setup, and a bandwidth correction to noise voltage per root cycle if a 1-cycle bandwidth analyzer was not used. As the offset frequency increases, it becomes advantageous to use a wider bandwidth analyzer to allow a faster frequency sweep. In special cases, it is appropriate to use a band-defining filter and rms reading voltmeter in place of the wave analyzer and recorder.

SYSTEM PERFORMANCE

The system described above, with a transistor amplifier, has a sensitivity (equal to noise) of 4×10^{-9} volt per root cycle referred to the mixer input for offset frequency above 100 cycles. (The noise voltage goes up as $1/f$ below 100 cycles.) This compares with 9×10^{-10} volt per root cycle for 50-ohm thermal noise. The mixer used is quite linear up to 4×10^{-1} volt input,* so that we have a noise per root cycle to signal voltage ratio of 10^{-8}, or 160 db. (There should be no difficulty in measuring spurious signals.)

To characterize the performance in terms of $\Delta f/f$ for a particular averaging time τ, we need to know the RF system noise bandwidth of interest. To shape—or weight—the phase noise voltage curve corresponding to τ, we apply the factor $\sin\pi\tau f$ to the noise voltage per root cycle E_N (versus offset frequency f_0) components below $1/2\tau$. The weighted rms noise voltage can then be calculated. The ratio of this value to the rms carrier level gives $\Delta\phi_\tau$, the rms phase deviation; and division by $2\pi\tau$ will yield Δf_τ, the rms frequency deviation.

As a hard-usage example, consider an RF bandwidth of 200 cycles corresponding to a 100-cycle $1/f$ corner in the measurement system and assume that a 1-second averaging time is desired.

$$E^2_N = E^2_{NA} + E^2_{NB} + E^2_{NC},$$

$$E^2_{NA} = E^2_{N1}\int_0^{1/2\tau} (\sin^2\pi\tau f)\, f^{-2}\, df$$

$$\approx 3.8\tau E^2_{N1}$$

$$= 60\times10^{-14}$$

for $1/2\tau$ below the $1/f$ corner f_c, where E_{N1} is the noise voltage per root cycle at 1 cycle.

$$E^2_{NB} = E^2_{N1}\int_{1/2\tau}^{f_c} f^{-2}\, df$$

$$= E^2_{N1}[(2\tau)^{-1} - f_c^{-1}]$$

$$= 7.8\times10^{-14},$$

$$E^2_{NC} = 0,$$

*Another factor of 2 in measurement capability can be obtained by overdriving this input and using a special calibration.

with f_c considered as the upper offset frequency limit.

$$E^2_{N\tau} \approx 68\times10^{-14}, \qquad E_{N\tau} = 8.25\times10^{-7},$$

$$\Delta\phi_\tau = 8.25\times10^{-7} \div 4\times10^{-1} = 2.12\times10^{-6} \text{ radian},$$

$$\Delta f_\tau = \Delta\phi_\tau / 2\pi\tau = (2.12\times10^{-6})/(2\pi\times1)$$

$$= 3.37\times10^{-7} \text{ cycle}.$$

With a 5-Mc carrier frequency, this would correspond to a fractional frequency deviation of 6.75×10^{-14}.

For an example of the capability when used in a broader band system, consider a 30-kc RF bandwidth and 1-second averaging. We then have to include a term for the flat noise voltage E_{NF}:

$$E^2_{NC} = E^2_{NF}(15{,}000\text{–}100) = 24\times10^{-14},$$

$$E^2_{N\tau} = 92\times10^{-14}, \qquad E_{N\tau} = 9.6\times10^{-7},$$

$$\Delta\phi_\tau = 9.6\times10^{-7} \div 4\times10^{-1} = 2.4\times10^{-6},$$

$$\Delta f_\tau = (2.4\times10^{-6})/2\pi = 3.82 \text{ cycles} \times10^{-7}.$$

With a 1-Mc carrier frequency, this would correspond to 3.8×10^{-13} for a fractional frequency deviation number at 1 Mc with 1-second averaging. It is seen that this system is able to measure the short-term stability of the best available HF sources. The system is more attractive for shorter averaging times.

SYSTEM APPLICATIONS

Figure 23–2 shows the type of plot described above, obtained with the Hewlett-Packard Frequency Synthesizer Model 5100A as the signal source. Model 5102A performance is about 10 db better on the 1-Mc range and about 20 db better on the 100 kc range.

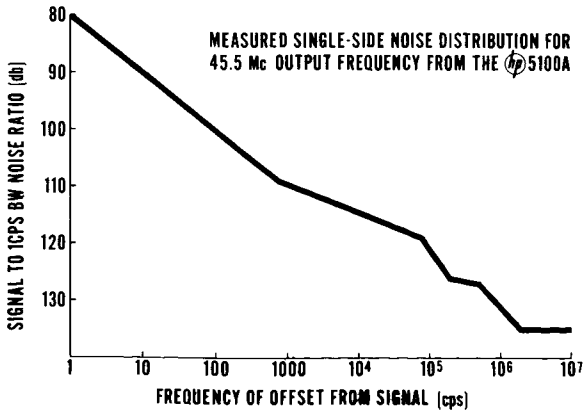

FIGURE 23–2.—HP Model 5100-A phase noise.

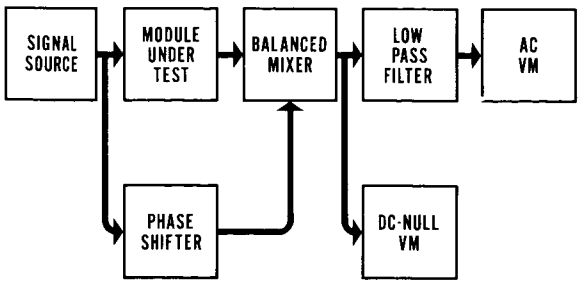

FIGURE 23–3.—Module test.

To assure the short-term stability of this frequency synthesizer, each of the modules is production-tested for phase noise by using a system similar to the one described above, with a band-limiting filter and voltmeter substituted for the wave analyzer; and the sources are replaced by the input and the output of the module under test, as shown in Figure 23–3. The module also is subjected to very light shocks in this test position as a very effective method of locating potential problems such as loose screws, faulty components, and bad solder joints indicated by abnormal readings on the ac voltmeter or sudden steps in the dc voltmeter reading. A similar system is used as a production check on the completed synthesizer, with latching lights to indicate a failure to meet production limits on the rms and peak* phase noise during a final test run—including an ambient temperature excursion.

This method should be of particular interest to those interested in checking the short-term frequency stability of a resonant element such as quartz crystal with a minimum of extraneous circuitry. For example, consider a 1-Mc crystal with 10 ohms series resistance and a Q of 10^6, and a test arrangement as shown in Figure 23-4. Assume that the crystal is placed in a 50-ohm system so that the Q is reduced to 10^5. Now, for

*It is interesting to note that the peak-phase noise voltage in the absence of shock or vibration does not exceed 3 times the rms value—the noise is not completely Gaussian.

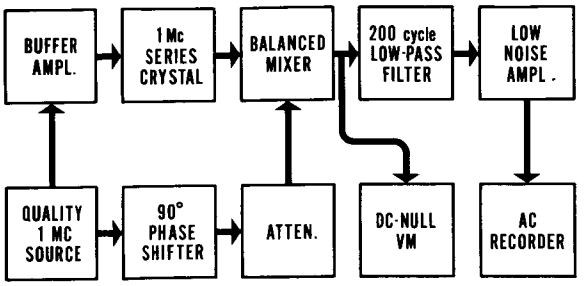

FIGURE 23–4.—Testing crystal stability.

a Δf in the crystal resonant frequency, we have a resultant

$$\Delta\phi = 2Q\ \Delta f/f.$$

It will be found that the bulk of the crystal instability components will lie well within 200 cycles of the resonant frequency, so that the 200-cycle low-pass filter will allow sufficient bandwidth for the crystal evaluation. From the performance indicated earlier, we can measure 2×10^{-6} radian in this setup. In crystal terms,

$$\Delta f/f = \Delta\phi/2Q = 10^{-11}$$

is the measurement capability here. Somewhat more resolution is available by lowering the resistance in the crystal circuit, reducing the noise measuring bandwidth, and overdriving the mixer. A test like this is used at Hewlett–Packard to evaluate the short-term stability of a crystal for a critical filter application. In this case, the crystal is subjected to an ambient temperature excursion while the test is being run.

CONCLUSION

A versatile and practical system for measuring and specifying short-term frequency stability is suggested. The measurement capability is sufficient to evaluate the best available signal sources. The actual performance of such a system was outlined, and some application information was presented.

24. COMPUTER-AIDED CALCULATION OF FREQUENCY STABILITY*

C. L. SEARLE, R. D. POSNER, R. S. BADESSA, AND V. J. BATES

Research Laboratory of Electronics, MIT
Cambridge, Massachusetts

In April 1962 we reported at the 16th Annual Frequency Symposium concerning a method of calculating frequency stability via autocorrelation. The autocorrelation of the phase difference between two oscillators can be readily calculated on a computer, and the resulting function can be converted very easily to any of the usual methods of specifying frequency stability.

This paper reviews briefly the relations between the autocorrelation of the phase information and varous methods of specifying frequency stability. Then we discuss an experiment currently underway which uses this method to find the frequency stability of two oscillators.

D. A. Brown, in his Master's thesis (Reference 1), derived in signal-processing terms a number of expressions relating to the specification of oscillator stability. Some of this work was presented in April 1962 at the 16th Annual Symposium on Frequency Control. The one relation from that paper which is pertinent to this discussion is the expression relating the variance of the frequency to the autocorrelation of the phase.

$$\sigma^2_{f_{av}\cdot T_0} = (1/2\pi)^2(2/T_0^2)[\phi_{11}(0) - \phi_{11}(T_0)]. \quad (1)$$

This expression is derived below.

In Figure 24–1, two oscillators are compared by recording the phase difference between them as a function of time. This phase can, in general, be split into two terms. The first is a ramp equal to $\bar{\omega}t$, where $\bar{\omega}$ is the average frequency difference between the two oscillators. The second is the random phase fluctuations between the two oscillators; that is,

$$\phi(t) = \bar{\omega}t + \theta(t). \quad (2)$$

The frequency difference averaged over a time T_0 can now be found by the equation

$$f_{av.T_0} = [\phi(t+T_0) - \phi(t)]/2\pi T_0 \quad (3)$$

$$= (1/2\pi)\left[\bar{\omega} + \frac{\theta(t+T_0) - \theta(t)}{T_0}\right]. \quad (4)$$

This frequency is, of course, itself a function of time. What we want is the variance of this function:

$$\sigma^2_{f_{av}\cdot T_0} = \lim_{T\to\infty} (1/2T)\int_{-T}^{T} [f_{av.T_0} - (\bar{\omega}/2\pi)]^2\, dt \quad (5)$$

$$= (1/2\pi)^2 \lim_{T\to\infty} \frac{1}{2T}\int_{-T}^{T}\left[\frac{[\theta(t-T_0)]^2 + [\theta(t)]^2 - 2\theta(t)\theta(t-T_0)}{T_0^2}\right] dt. \quad (6)$$

*This work was supported in part by the U.S. Army, Navy, and Air Force under Contract DA36-039-AMC-03200(E).

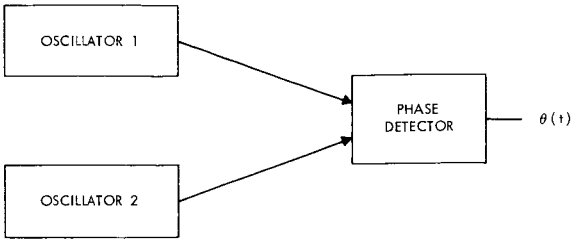

FIGURE 24–1.—Setup for comparison of two oscillators.

If $\theta(t)$ is a stationary time function, the terms in Equation 6 can be identified in terms of the autocorrelation function as follows:

$$\sigma^2_{f_{av}\cdot T_0} = [1/(2\pi)^2](2/T_0^2)[\phi_{11}(0) - \phi_{11}(T_0)], \quad (7)$$

where $\phi_{11}(0)$ is the autocorrelation of the *random part of the phase* for zero delay [i.e., the mean square of $\theta(t)$] and $\phi_{11}(T_0)$ is the autocorrelation of the *random* part of the phase for delay T_0. Thus, the variance of the *frequency* as a function of averaging time T_0 can be found very easily from the autocorrelation of the random part of the *phase*. This simple equation provides the direct link between the two equivalent methods of data reduction, namely

1. Variance or mean-square deviation of frequency,
2. Power spectrum of frequency.

Most simple laboratory determinations use one of the systems shown in the upper part of Figure 24-2 to reduce data [see Packard and Rempel (Reference 2) and Vessot (Reference 3), for example]. For finding one or two points on the curve of variance versus averaging time T_0, these methods are adequate. But if we want a more complete variance-versus-T_0 curve—or the complete power spectrum—these measurements and calculations become laborious. Under these circumstances, computer-aided analysis can be very useful.

The computer can, of course, perform any of the functions shown in Figure 24-2. It could, for example, take the derivative of $\theta(t)$, convolve with $h(t)$, and find the mean-square value of the resulting signal for all values of $h(t)$ corresponding to various averaging times T_0—thereby finding the variance of frequency-averaged-over-T_0 versus T_0. Examination of the above derivation will show, however, that with *the same number of multiplications and summations* the computer can form $\phi_{11}(\tau)$, the complete autocorrelation function of the phase. As shown in the diagram, it is now a simple matter to find the variance of frequency by using Equation 1. With equal ease, we can calculate the power spectrum of phase, or the power spectrum of the frequency without averaging or for any averaging time T_0. All these

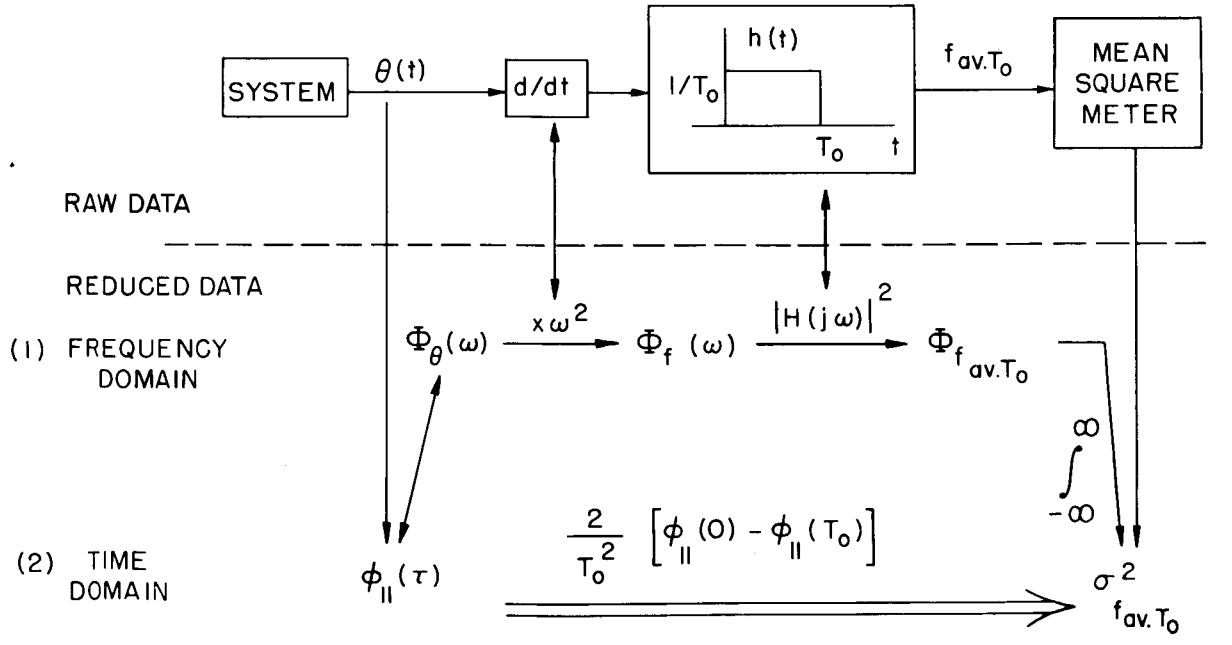

FIGURE 24–2.—Ways to obtain the variance of the frequency (all quantities in radians).

calculations based on $\phi_{11}(\tau)$ are on *reduced data* and thus can often be performed easily by inspection. Simplicity of calculation also is assured by working in the frequency domain as much as possible. All the insight into the relative shapes of autocorrelation functions and power spectra can be brought into play in performing these calculations and interpreting the results.

On the basis of Figure 24–2, the relation between the variance and the power spectrum of either phase or frequency is now simple and direct in terms of *reduced data*. Thus the variance can be readily calculated from the power spectrum (and vice versa, provided we know $\phi_{11}(0)$, the mean-square value of the phase).

Several alternate methods for calculating the variance are shown in Figure 24-2. There is no particular "best" method, because the choice of analysis method depends so strongly on the form of the data. For example, if the function has a flat frequency spectrum versus ω—that is, $\Phi_f(\omega) = K$—then the variance can be calculated easiest in the frequency domain, by multiplying

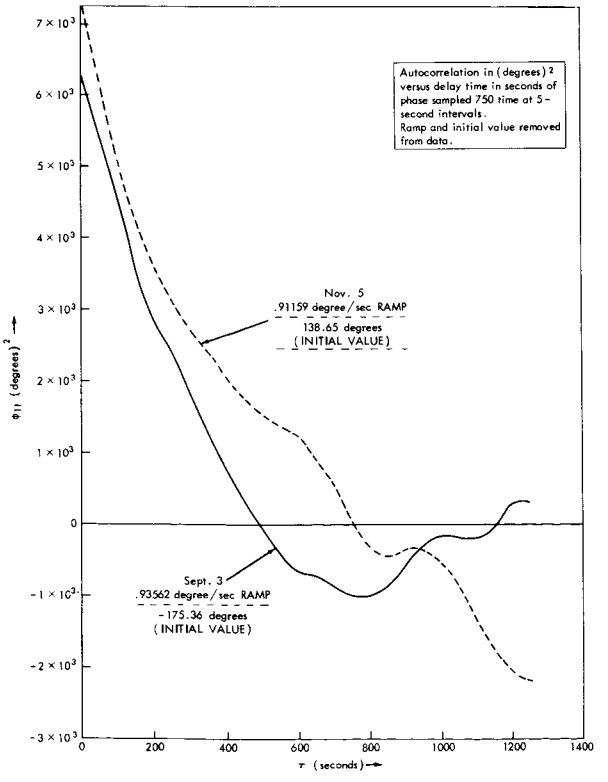

FIGURE 24–3.—Autocorrelation for two different runs.

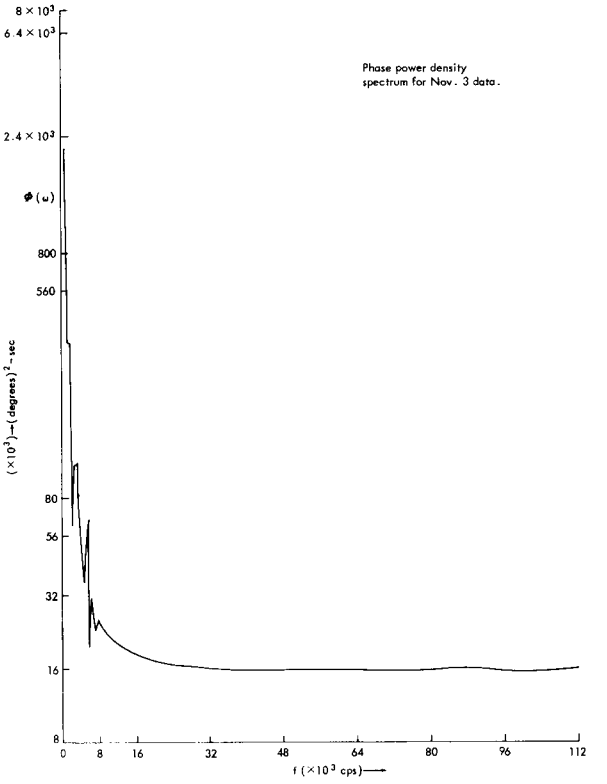

FIGURE 24–4.—Phase power density spectrum.

by

$$|H(j\omega)|^2 = (\sin^2\omega T_0/2)(\omega T_0/2)^2 \qquad (8)$$

and finding the area under the resulting power spectrum. Note, however, that the alternate routes provide an important check on computations.

As a specific example of this method, we have calculated on our PDP–1 computer $\phi_{11}(\tau)$, $\Phi_\theta(\omega)$, and $\sigma^2_{f_{av}\cdot T_0}$ for two oscillators. To avoid the phase ambiguities usually present in a phase detector, we used in our detection system two synchronous detectors which form $\sin\theta$ and $\cos\theta$. These signals were then fed to the PDP–1. The computer was programmed to find $\theta(t)$ from $\sin\theta$ and $\cos\theta$. Then it calculated $\phi_{11}(\tau)$ and its Fourier transform $\Phi_\theta(\omega)$, and the variance. The results of these calculations are shown in Figures 24–3, 24–4, and 24–5. Because the total length of the sample was only 1 hour, the autocorrelation beyond 5 or 10 minutes is suspect, as is the low-frequency portion (below 10 cycles per hour) of the power spectrum.

To check further on the method of analysis, a

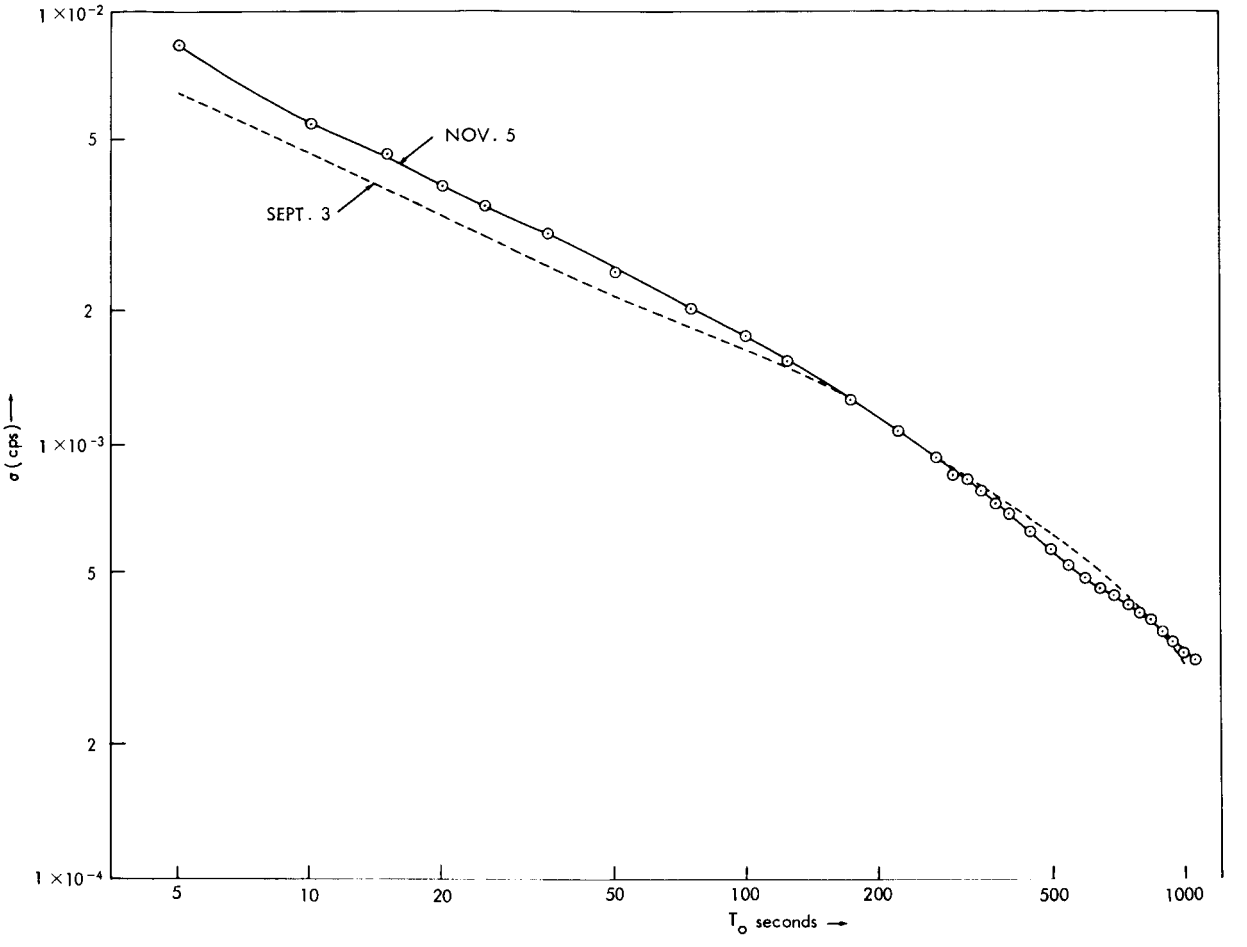

FIGURE 24–5.—Standard deviation vs. delay time for two different runs.

second run was taken on the two clocks about 2 weeks after the first run. The results are added to Figures 24–3 and 24–5. The agreement between the two experiments is good.

We conclude four things from these experiments:

1. If computer analysis is used, the *autocorrelation function* of the phase and *power spectrum* of phase or frequency are a logical pair to calculate.

2. Because the variance and the power spectrum are related in a fairly direct way through Equation 1 and the Fourier Transform of $\phi_{11}(\tau)$, the choice of which of these methods of data abstraction to use is not fundamental. Rather, it is one of convenience for the problem at hand. However, because of the relation between the time domain and the frequency domain through the Fourier Transform, it would seem that more detail in short-term stability information will be evident in the power spectrum; whereas long-term stability information may be better displayed in the time domain via the variance.

3. There are some important bounds on the shape of the autocorrelation function. For example, the function must be maximum for $\tau=0$, and for random phenomena it will go to zero for large τ. Also, for periodic phenomena, the autocorrelation is periodic. These bounds on the autocorrelation function, when reflected through Equation 1, place bounds on the variance of frequency which can be of great assistance as a rough check on experimental results.

4. Figure 24–2 provides several alternate routes for calculating the variance. The "best" route depends on the particular problem, but the alter-

nate routes provide a useful check on computations.

ACKNOWLEDGMENTS

The authors gratefully acknowledge the help of Professors J. W. Graham, R. P. Rafuse, and J. G. King at the Massachusetts Institute of Technology, and R. Vessot at Varian Associates—all of whom contributed much to the shaping of this paper in the course of many discussions.

REFERENCES

1. Brown, D. A., "Statistical Measurement of Frequency Stability," Master's Thesis, Massachusetts Institute of Technology, August 1962.
2. Packard, M. E., and Rempel, R. C., The Rubidium Optically-Pumped Frequency Standard, *NEREM Record*, November 1961.
3. Vessot, R., Mueller, L., Vanier, J., "A Cross Correlation Technique for Measuring the Short Term Properties of Stable Oscillations," Varian Associates, *Q.E.D. Activity*, Beverly, Mass., November 1964.

PANEL DISCUSSION

SESSION IV: MEASUREMENT TECHNIQUES

Chairman	C. L. SEARLE
Panel Members	C. H. LOONEY, JR.
	B. PARZEN
	G. E. HUDSON
	G. M. R. WINKLER
Authors	R. A. CAMPBELL
	L. J. PACIOREK
	C. H. GRAULING, JR.
	D. J. HEALEY, III
	B. E. ROSE
	V. VAN DUZER
	V. J. BATES
	R. S. BADESSA
	R. D. POSNER
	C. L. SEARLE

Mr. Looney.—In the first paper, which I thought quite interesting, in fact I thought all of the papers were quite interesting, I would like to hear some additional remarks by the first speaker, if this is possible, in terms of some of the sources of noise in his various discriminators.

I am not familiar with some of the commercial discriminators he used. In his written paper he points out certain noise levels from the various discriminators, and I would like to hear some comments as to the various sources of this noise.

I thought, too, in his paper, the calibration technique of using the rotating phase shifter to develop the side bands independently was quite interesting and deserves perhaps a bit more attention.

The paper from Syracuse, by Mr. Paciorek, I thought was an excellent survey. I wished for better slides, some of the information perhaps could go a bit more into the fine detail that was available from some of the measurements.

I thought it was an excellent survey of techniques. I thought that again a few words on instrumental noise sources might be helpful.

Your slide, Figure 3, with its multi-oscillators; I thought it might be helpful to have a little more information on the noise that would be generated within the instrument itself.

The paper from Westinghouse gives quite a detailed treatment of one approach. It is, of course, in the frequency domain only. The paper as you will find when you get to the written proceedings, is exhaustive and I felt that it conveyed a great deal of information which was only possible to hint at in the spoken word today.

I appreciated the comments made by Mr. Rose in which he said his paper cut across all of the disciplines of all of the sessions of the symposium.

It did not deal to a large extent with measurement techniques but did deal with device parameters more than might have been expected in this particular session.

The Hewlett–Packard paper by Mr. Van Duzer was, I thought, exceedingly good. I should say the definition that he proposes is quite interesting and I think there is a great deal of food for thought in the ideas.

Mr. Parzen.—Well, I should first like to make some general statements and then make some comments about at least one specific paper.

The general statement that I would like to make first concerns the question of AM and PM. Everybody seems to disregard AM. However, it is important because, in general, any device to which a signal is fed has a tendency to convert AM into PM. So after a while you really don't know. Now, as a matter of practice, I have found this: when you feed two separate signal sources to most measuring systems the PM component is more important than the AM components unless one of the sources has a defective design. Very often it is true that many sources are defective. As a result, the AM is so big that it overrides the PM component. However, we should not treat poor design as a good example. In those cases, we have measured the resolution of a measuring system and the tendency there is to feed the same source into both input jacks. It turns out that the AM very often seems to be the predominating effect that you see. Sometimes you will wrongly confuse the resolution of the system as being too poor when actually the source you are feeding into it has poor AM characteristics. On the other hand, this can be used advantageously to determine whether the source does have AM because, if you feed a source into an instrument and get a poor reading out of the instrument, then you know that there is AM present. So that is about as important.

Now, I found it interesting that the most obvious and least controversial definition of frequency has not even been stated. The definition is really implied in the real meaning of the word frequency, namely, as a number of cycles per unit of time. The average time of this quantity for specified sampling time is obtained with such devices as frequency counters. This method, obviously, is capable of furnishing high fractional frequency resolution only when the frequency being measured has a certain number of cycles for the required sampling time. However, the

availability of such devices as frequency mixers and large factor frequency multipliers has made this method useful even for relatively low frequencies. For example, a one-megacycle frequency standard has been consistently measured to within one part in 10^{12} for a one-second sampling time. This, of course, implies that the effective multiplication factor is at least 1 million.

So, obviously, it is possible to build frequency multipliers, to obtain a large number of cycles, and so in some way to solve the dilemma of how to state frequencies. I am not saying that you do this all the time but, at least, it should be a method that should be considered when you want to evaluate the total picture.

Now, there are some things that one should cover in a symposium. One thing that I want to mention is the use of error-multiplied systems of effectively obtaining large multiplication factors which possess important features for both making measurements and obtaining greater understanding of the measurement process and the quantities being measured. The system has been described at previous symposia and in the literature. There was one application in an earlier paper at this session, I believe by General Radio.

I would like to ask some questions about the Hewlett-Packard paper, which incidentally is very, very important because, in one way, it negates the $1/f$ noise that we have been talking about so much.

He has basically a balanced mixer or what has been called a product detector, which yields obviously very low noise close to zero frequency. This is a rather important development. I would like to know some more about the mixer itself, the diodes used in the mixer, and also the accompanying amplifier which makes possible the very good performance of this system.

There were other questions that I would like to ask: how is the locking and the zero-phase-shifting scheme actually employed in a real system where two independent sources are available and how do you make this locking scheme noncontributory to the total noise of the system? This seems to be a rather difficult problem.

Dr. Winkler.—Well, actually, I think these presentations and papers have been most interesting and I believe that the conference really has made a great step towards some common understanding in regards to standards so that we can write proper specifications, so that we can design uniform test procedures, and verify these specifications.

Until Searle's paper, I was under the belief that, at the first step, it would be wise to live with the present situation for a while and to prefer simplicity to what is more or less recognized generally to be a more sophisticated approach and to leave this to later.

But now I have been convinced that the sophisticated approach can really be the most simple one. Your [Searle] paper has been very excellent.

I still think, however, that for many laboratory applications, it is useful to look at the situation with a more simple approach. It is my understanding, collected through these talks, that we have a practice of expressing stability or instability in basically three different ways; two of them in the so-called time domain, rms frequency deviation and rms phase deviation, and the spectral characteristics that we can assign to a frequency source.

I believe for the time being that it is good reasoning to use both of these. Assume for example, somebody gives me information that we have a source with a carrier and two sidebands separated by one-hundredth of a cycle with an average power of 3 db below carrier frequency. This set of conditions is not as obvious to me as if I were given the information that we have an oscillator which exceeds its frequency specification due to oven cycling or something like that and the frequency deviation is .01 cycles, or expressed in phase deviation, accumulated during one of these cycles as one radian, I believe. In other words there is room for expressing these figures in both ways as long as one states clearly what one is doing. Here I agree perfectly with Professor Searle.

Another remark which I would like to make is, for most applications, we can make simple numerical assumptions. This may be helpful to come to an easy understanding to make quick guesses, engineers' estimates on the performance of oscillators, and ramifications of such figures. For example, we are interested many times with systematic frequency modulation when we put a device on the shake table. For many purposes

this can be considered as sinusoidal modulation and we can get quick estimates and a good picture. If we are interested in low noise applications, we may then be interested in real phase deviation.

I believe that the phase information is generally preferable over frequency figures. Probably this would have come into more general practice if people weren't used to thinking in powers of ten, or in parts to 10^9 and so on. Everybody gets his kicks out of having as high a number as possible and the phase information looks less impressive. I believe that phase information is probably simpler to use; I really think so.

Also, basically, as was pointed out in the last paper, they are completely equivalent of course with one exception. The conversion or actually the transformation from one domain into another, of course, requires integration of an infinite interval. Since we always have information lacking here, it couldn't be done completely accurately in practice. I believe this is another reason why we should be able to live with two sets of standards or specifications or definitions, if you please.

It is a matter of course that whatever is neglected becomes the most important part in the frequency domain. For example, if we convert from the frequency domain into the time domain—then we have to neglect the very high frequencies—we couldn't extend our considerations to infinite frequencies. But this profoundly effects our figures if we go down into very, very short measuring intervals.

I believe that there is a place for two languages here and I think that an attempt to unify our language at too early a stage may be harmful until we have enough experience. I have no more specific comments except my great enthusiasm about the general meeting. I would like to take this opportunity to extend my compliments to the organizers and to this organization. I think it has been a most useful meeting, at least as far as I am concerned.

I have only two questions in regards to papers 20 and 21.

Paper 20; am I correct in stating that oscillations in an oscillator originating in different modes are not coherent to each other? I believe that maybe this picture of what we have seen in the beat note of two masers and the frequency spectrum may not be too meaningful.

Paper number 21, in regard to the choice of a passive and an active reference, again I want to put this into a question: am I correct in assuming that this may be dictated mainly by the requirements to measure very short-term frequency stability? In other words, if one desires to measure very close around the carrier one probably requires the use of an active standard.

Dr. Hudson.—By definition, since I am a member of this panel, I must be an expert on measurement techniques. I kept telling myself this, but unfortunately it isn't so. I am, however, really interested in the theory of measurement, and so I will take my prerogative as a member of this panel, and address myself to some general remarks in this vein.

I have been struck by certain aspects of these problems, that is the definition and the measurement of short-term stability. Some of the aspects are simply ones of terminology.

I have also been struck by the similarity between these problems and the problem of large scale and small scale turbulence. There seems to be a certain analogy between the whole series of problems that people ran into in the discussion of turbulence, and the ones that we have been discussing here. It might be instructive to look into this further.

The very terminology, short-term stability, suggests that part of the specification of short-term versus long-term stability could be made clearer by the introduction of what might be termed a characteristic time. For times less than this, or of the same order of magnitude, one would speak of short-term stability.

The time could be chosen according to one of many criteria. It might be the observation time or the averaging time. It might be an autocorrelation time as shown in the slide of Professor Searle's or it might be a correlation time of a signal with a stable reference oscillator, i.e., a standard oscillator that would be stable by definition. It might be just a period of a signal. Thus we have a whole series of times that could possibly be chosen as the characteristic time, helping define short-term stability.

This has been noticed in some of the papers here that we have such a wide gamut of times. In any event, once one does specify a time which he might call a sample time, then certain sta-

tistics, characteristic of a signal over this sample time, could specify the stability or instability.

To be a useful characteristic, it should be one which is invariant over the sample populations. The statistics might be the spectral purity or some rms deviation, the power in the sidebands, and so forth.

Long-term stability, I think, strictly ought to be measured by or specified with reference to statistics of signals which are characteristic of the signal in the limit of infinite times—or anyway, very long compared to the short-term characteristic time.

We have seen here that there are very many short-term stability measures. Perhaps we should be speaking not so much of short-term stability but rather of time dependent stability characteristics. When one computes an average, he must take it over a certain time. The way in which the average quantity varies with this time, that is, its statistical random properties may actually be the best characteristic of the signal in speaking of its short-term stability.

Now this is all that I wanted to conjecture about generally. In the main, I concur with the other members of the panel in their evaluations of the various papers but I have one or two specific comments of my own. Compliments are due Mr. Van Duzer for an excellent slide presentation.

In the last paper, particularly, I was impressed by the recognition that the statistics should be plotted versus the time. This is an example of what I meant in my foregoing general comments.

I want, however, to question the specific model that you set up, Professor Searle. In this model the difference in phase between two oscillators is a linear function of time plus a random function.

In many cases you would at least have a quadratic term that would make some difference. As for the random function it might not be a stationary function, and one should investigate the significance of this very carefully.

Mr. Campbell.—The specific question is what is the source of noise in the test equipment; it almost invariably turns out to be the crystals. It is obviously so in the video case, in the $1/f$ discriminator, especially with carrier nulling, and again it turns out to be the crystal in the $1/f$ mixer.

The calibrator that I mentioned, is written up in the IRE transactions for instrumentation, I believe, by Joseph Ginsberg, the reference is in the paper.

Mr. Van Duzer.—I would like to apologize for making my paper so short, maybe I left some things out that I should have said.

One thing, with regard to the conversion of the phase to frequency deviations, it is going to be very difficult to make this conversion if we start without phase noise data that goes down to one cycle. It is going to be very difficult, if not impossible, to convert that to one second averaging. So this conversion is only going to hold if we are between these, provided that we have enough data, of course. It is very convenient to get data, phase noise data, down to one cycle, so we should be able to make a relatively accurate conversion then, for averaging times that are short compared to a second between these.

I would like to answer Mr. Parzen's questions. He seems to be an advocate of the error multiplier technique; the error multipliers that I have seen have been limited by a narrow bandwidth in their noise measurements. And at least the ones I have seen are largely useful for measuring very slow changes in frequency, looking at very low frequency components of phase noise, if you will.

The $1/f$ noise that I spoke of is quite interesting in the transistor amplifier that we build, which is using a PNP silicon transistor on the input. The $1/f$ noise starts in at about 100 cycles, between 50 and 100 cycles.

I used the $1/f$ term quite loosely. It turns out in the power expression for this amplifier that if you take V^2S equal to some constant times frequency to some exponent, that exponent for this amplifier, in the "$1/f$ region" is about 1.85. It is very high.

The diodes used in the mixer on the other hand are very close to an exponent of 1, they run about 1.2. These are hot carrier diodes, they don't exhibit any noticeable storage effects, provided the frequencies they are concerned with are not above 500 megacycles.

The DC locking that I referred to, showed in the diagram there, one must make the bandwidths in that lock loop low enough so that it doesn't effect the measurements. If you are going down to one cycle on your phase noise plot, then

you shouldn't pass anything appreciable in that loop that comes anywhere near one cycle. In our measurements what we always do is check to see that the locking is not affecting measurement.

Mr. Paciorek.—A couple of questions have been directed towards the second paper. One in particular dealt with the source of instrumentation noise.

In this presentation, owing to the lack of time, I did not discuss the fact that we take the control plot before each measurement to measure the noise level of the system.

In the one spectral plot that I showed of the laser self beat, it is true that the self beat is noncoherent. However, one slide I did not show indicates the results after phase locking the self beat. In other words this was the output from one laser, the self beat, the laser was beat in a photomultiplier and the resulting beat was then stabilized. However, I didn't show the laser slide, and I asked the projectionist if he would get if for me. It was down in reproduction, so if he has that—good.

The first slide I would like to show is the one of the unstabilized laser self beat.

Okay. This is the other one. This is after the self beat was phase locked to a harmonic of the crystal oscillator. You will note here that the sidebands close to the carrier are greater than 40 db down. Now the scale here is 4000 cycles along the abscissa and 80 db along the ordinate.

Now if I can have the other slide—This is the same scale; however, the grid lines were not included on this. You can see the improvement in the spectrum of the self beat by phase locking it to a harmonic of a crystal oscillator by comparing this spectrum with the one that we looked at first.

Mr. Grauling.—I would like to try to answer Dr. Winkler's question on the question of the active reference. I am afraid that I am going to have to ask him to repeat the question because of the acoustics on the stage.

Dr. Winkler.—You gave some criteria why one would select a passive or an active reference. I believe it could be restated and could be said that you could get away with a passive reference, which of course is much simpler, as long as you are interested in a far out part of the spectrum, which corresponds to very short-time fluctuations, but couldn't do it with a passive device if you were interested in, let's say, three-eighths of one-hundredth of a second or 0.1 second.

Mr. Grauling.—Yes, this is definitely so. In the range of modulating frequencies or separation from the carrier that we have interest in, which is somewhere in, say, the hundred to thousand cycle range at the bottom and a fraction of a megacycle at the top; in this region we can employ the passive reference as you pointed out.

At very, very low frequencies or fractions of a cycle, this would not be the case. The term that I referred to, which is an effective attenuation of the sidebands, involves the sideband frequency divided by the bandwidth of the cavity. Under these conditions the attenuation of the output sidebands that you can get from either equivalent time delay or the cavity, is so great that you would just not be able to see the sidebands for the noise.

Mr. Looney.—I would like to ask Mr. Paciorek to educate me a little further. I am afraid that I missed the significance here of your laser experiment. Are we seeing anything here more than simply the filtering action of the phase lock loop?

Mr. Paciorek.—Luckily, we have the man that performed that experiment with us today, so maybe I can call him up here and then he could go into the intimate details of the experiment if you would like.

Mr. Goldick.—The object of this experiment; one of the mirrors was mounted on a piezoelectric crystal and this mirror then tracked with the noise variations within the cavity. Any vibrations that would cause the mirrors to move were tracked out. I mean it is as simple as that.

Mr. Looney.—I say, again, what do we gain by this over and above the filtering action of the phase lock loop? What significance is there to this measurement?

Mr. Paciorek.—I guess the ultimate use of this, of the laser, is the thing that we are hoping that this will lead to. The length of the laser is stabilized by locking to a harmonic of a crystal. You can then hold the length of the laser cavity to so many parts per and it is hoped that this stability will be translated to the light frequencies so that you can then hold the average frequency of the spectrum up at light frequencies to the stability of your crystal reference. The significance of this

is the fact that you can phase lock the self beat and thereby control the length of the laser cavity.

Mr. Looney.—I see your point. I am still puzzled as to whether it does provide you this stability, or whether it is simply a technique for modulating a laser.

Dr. Reder.—I think all that it does is transfer the quartz stability to the laser as he pointed out, but the paper, as it was presented, gave the impression that this would be something better than the spectrum of quartz but I think that was not your intention.

Mr. Paciorek.—That is absolutely correct.

Dr. Winkler.—I would like to comment here. What it really does is transfer the quartz stability not to the laser frequency, but to the difference of two modes.

Mr. Paciorek.—That's right. However, since the laser frequency is a function of the cavity length, the light frequency has to be an integral number of wave lengths.

Dr. Winkler.—It will stabilize the cavity but it will not eliminate any other interferences, of course, which will act approximately equal on both modes.

Mr. Paciorek.—Yes.

Dr. Winkler.—Any frequency shifts or phase disturbances, for example, due to the gas or due to the excitation will not be cancelled or reduced. You will lock the cavity to make the beat coherent.

Mr. Paciorek.—Okay.

Dr. Winkler.—But nothing more. Am I right?

Dr. Reder.—If there is any instability between the two modes, this will now be transferred to the laser frequency.

Voice.—There are higher orders of effects that would effect this different frequency, the modes, and I think one could hope to achieve a much better degree of stability by doing this.

To ask a question, have you tried to instrument two different CW lasers in this way and then compare beat notes between those to give you some indication of the stability of the actual optical frequencies involved rather than this mode difference frequency?

Mr. Paciorek.—No, we only have one laser. We built another one, though, so we should be able to try this out shortly.

Dr. Curry(Curry, McLaughlin and Len, Inc.).—This is sort of a shotgun question and I think generally a quash question and comment covering several papers.

I think Dr. Hudson's general comments actually have covered the subject. First, I am happy to see the function which Professor Searle is using. This is exactly my Equation 15 in my paper yesterday. The important point here is that this is a statistic which on the short-term, as Dr. Hudson has already mentioned, is itself a random variable.

Now what we want to do to get some reproducable results is obtain a confidence interval on this. In other words, what we would like to do is, based on hypothesized statistics, predict what the probability distribution function for this whole expression is, hopefully. As I showed yesterday, if you assume the interval sampling average time is much greater than the correlation time for the process that you have hypothesized then the second term, which is your correlation function, is zero and you can deal with simply the integral of the average power. Thereby you get the results which Slepian, I think, obtained for the probability density function.

Going on now to, for example, Mr. Van Duzer's paper; he throws me a little bit into shock talking about 140 db below the carrier. He is talking about a one cycle per second bandwidth.

What bothers me is that the spectrum which he shows of the wave analysis plot is smooth, and my question to him is "Is this a smooth function of a large number of runs or just what is this?" In other words, you didn't show any actual data, you show a smooth output.

The next comment is to Mr. Paciorek, and it is in the same vein. The spectra that you take—having looked at several hundred thousand of these over the last three years—what do you see?—you run about several hundreds of these and then you take all the best looking ones, and this is simply saying that this is a random variable and what you do is smooth the data.

Mr. Van Duzer.—The number is 160 db. We are very close to thermal noise here and we are operating with a one cycle bandwidth analyzer, when I say 160 db down.

Dr. Curry.—Was this the HP analyzer?

Mr. Van Duzer.—No, it is not commercially available.

Dr. Curry.—It is not commercially available?

Mr. Van Duzer.—Right.

Dr. Curry.—Okay. That's below what you can do with your analyzer, your commercially available unit.

Mr. Van Duzer.—Yes. Your other question was with regard to the smoothing of the data. This is what you would get taking an average through the phase noise plot. It is the same thing that would happen if you increased your averaging time at the output of the analyzer, and slowed down your sweep.

Dr. Curry.—Yes, you are taking a cut though, you see, in time and in frequency. Right?

Mr. Van Duzer.—Yes.

Dr. Curry.—Right. If you could look at all time-frequency elements of that plane simultaneously, what you would see would be sort of a smear of data which would be hopping up and down with time. What we want is an rms value. Let's say that you ran a hundred of these spectral analyses and then smoothed them. A mathematician would say he is running a regression analysis under some criterion but the point is that we can lay them on top of each other and draw an eyeballed line through the data. Is this what your data represented?

Mr. Van Duzer.—Yes, sir.

Mr. Lincoln(ADCOM).—This question is directed to Professor Searle. If I understand you correctly you presented a function which represented the frequency rms deviation in terms of the autocorrelation of the phase, I believe. Well, this is the same thing as an integral across the entire spectrum of phase deviation. Now in the case of a random walk phenomenon as many men have pointed out, such as Rice, there was a singularity at the origin. In other words, to work with the autocorrelation in phase you must have a Fourier integral function. I might suggest that the autocorrelation of frequency deviation, might be preferable in this case because I don't think that anyone could really stick in an oscillator to determine the autocorrelation of phase at zero.

A second point is that in your demonstration, assuming a flat phase spectrum, band limited, from which you calculated the autocorrelation function of phase and from this the fractional frequency deviation, I think it could be readily shown that the value you get is quite indeed a function of the bandwidth over which you chose that phase. Therefore a very critical and necessary function in any of these fractional frequency curves which are similar to a period counting technique would be this bandwidth because they can be moved arbitrarily depending on the badnwidth of the measurement. Would you care to comment on that, sir?

Prof. Searle.—The first question has come up several times. Dr. Hudson posed it previously and I was referring to it when I mentioned the work of Jim Barnes and the talk we had about the problem of a random walk of phase.

The interesting fact is that even though the autocorrelation obviously is not stationary when you are dealing with a random walk problem; when you take the first difference, you already get a criterion which has some meaning, (even though it is a function of the length of the sample). What Jim Barnes is suggesting is that if you take the second difference, then hopefully we will get to a criterion that no longer is a function of the length of the sample.

In other words—and this is the best that I can do to answer your problem, I am not ignoring it at all, it is very serious.

Refresh me on the second question, will you?

Mr. Lincoln.—The importance of bandwidth.

Prof. Searle.—Oh, yes. The bandwidth question. That is the reason that I originally sketched up that function. What you say is completely correct. I originally sketched up that function in a discussion with Dr. Vessot about the fact that the bandwidth of the noise must appear the way I formulated it, and hence must appear as one of the characteristics of rms frequency deviation versus averaging time. In Vessot's model of a square filter in the frequency domain, this factor involving the bandwidth of the noise is not present, and this is the whole key to the argument. I appreciate your focusing attention on that.

Mr. Looney.—Let's let Mr. Barnes have a word. We have been mentioning his name a number of times.

Mr. Barnes(National Bureau of Standards).—In regard to this problem that I think may be worrying somebody about the Fourier integrability of flicker noise, I can give you a very beautiful reference which is C. M. Lighthill, "*Fourier Analysis and Generalized Functions.*" It treats the problem of such annoying functions

as flicker noise in a very concise and nice way. That is the only comment that I wish to make.

Dr. Vessot(Varian).—Mr. Parzen brought a question up, and I hope what he meant was not the number of cycles in a given time, but the quantity of phase. The number of cycles implies that there is something finished, that there is something magic about the number 2 pi. But it is the amount of phase that is elapsed. I think this is what he meant.

The other thing is the question that he raised about the amplitude as well as the phase modulation; it is very important, and I would like to—

Mr. Parzen.—Are you talking about the definition of frequency or what?

Dr. Vessot.—Yes.

Mr. Parzen.—Well, frequency, what does one mean by frequency? Obviously it is the number of times an event takes place per unit of time.

Dr. Vessot.—I question this. I think it is more the amount of phase that is elapsed in a sinusoidal oscillator, and here is where the blood begins to run.

Mr. Parzen.—One cycle is 2 pi.

Dr. Vessot.—One cycle is 2 pi.

Mr. Parzen.—That's right.

Dr. Vessot.—But you must allow time to go by so that 2 pi radians have elapsed.

Mr. Parzen.—This is right.

Dr. Vessot.—And unfortunately, time now is the dependent variable rather than the independent variable. The time window is no longer a rectangular one. If I ask you what the stability of that same oscillator is for a time, that does not coincide with 2 pi radians, then I think—

Mr. Parzen.—Then you have something to resolve. In other words, if you are willing to actually forget about the effect of one cycle then there isn't any problem and if you have enough cycles, it really doesn't make any difference.

Dr. Vessot.—Anyway, there is room for hair-splitting.

The other point that I wanted to make: I concur with you completely that amplitude information is also very important and the method of multiplying two functions together will yield this. I think this could be a very useful way of determining this property.

Mr. Parzen.—Providing there isn't any circuitry in between.

Dr. Vessot.—Provided that you know what you are doing.

Mr. Parzen.—And usually there is, unfortunately.

Dr. Vessot.—Yes. And I also agree that Dr. Winkler's double standard is a very valuable one, depending on who is going to apply the problem. In one case indeed the sharp cutoff filter probably has its use and in the other case the sharp time window.

Dr. Winkler.—Yes, that is exactly what I am concerned with because I couldn't see why one should try to convert. If you have a requirement, for example freedom from modulation, then we very well should say so and give the limits.

Dr. Vessot.—But the thing that we should continue to point out is that the sharp rectangular frequency window as Campbell Searle and others, pointed out, does not give the same definition of stability as a time window which is rectangular.

Mr. Morgan(Bureau of Standards).—Since the subject of our symposium here is the measurement and the definition of short-term frequency stability, this implies that we must have something to measure against. This also implies to me some kind of a standard. Everybody has chosen their own standard and this makes it difficult to compare our results. It seems to me that one of the first things that we can do here or through some kind of a committee would be to decide on some kind of a standard. Right now the standard seems to be whatever is available in the laboratory. If we could somehow decide on a standard against which these measurements are made, then some of these things will fall into place, I think.

Prof. Searle.—Go ahead, right there.

Mr. Sherman.—I would like to respond to a cry for help from Mr. Rose who said that he had no basis for observing the correlation or a distinction between crystals which were noisy and crystals which were not under vibration.

You used an x-ray but you didn't use it in the right manner. That is, you didn't determine the orientation of mounting the crystals in the springs.

There is a fairly good theory relating the susceptibility of the resonant frequency of a crystal to radial forces which is being used in conjunction with bi-metals to adjust the frequency of a crystal to produce a compensated crystal with no oven. This was explored rather thoroughly by Louie

Dick (James Knight Co.) in the middle 50's, in the development of some shock mounted AT cut crystals.

There are two axes on which a crystal can be mounted, such that the resonant frequency of the crystal is insensitive to radial force. If it is mounted on these axes, there is a minimum of noise, FM noise, under vibration. If it is mounted off these axes, there are two maxima, one of them is larger than the other.

Now, you can't go down to your friendly neighborhood crystal shop and buy the crystal that he wants to sell you, and count on having this crystal be optimum for your properties, the desired properties. You have to specify your desired properties recognizing that they are going to cost you something. They are going to cost you a great deal of difficulty in communication. They are going to cost you a great deal of difficulty in delivery time. They are also going to cost you something in money. They are going to cost you a little bit in Q, that is you are going to lose about 15 percent of Q, in order to achieve this quietness.

I think that Dr. Winkler saying that he didn't particularly care if we talked about several things—several different ways of talking about stability—got close to the problem that we have here in communication. However, on the other side, I think it is important that we should know our literature and know our conversion factors. That is, maybe we need to be bilingual or polyglotal in some sense. I can very easily see a crystal manufacturer not being aware of the work of Dick trying to solve this problem all over again, and I can very easily see a manufacturer of equipment receiving two problems which are essentially identical, solving them separately, and coming up with two equally satisfactory solutions to the same problem because they are presented in different terminologies.

Dr. Guttwein(U. S. Army Electronics Laboratory).—I want to elaborate a little bit on the remarks of Mr. Sherman. What he is essentially saying is any AT cut crystal has insensitive axes to compression. This insensitive axis is located 60 degrees off the X axis of the crystal. This is fine, however, for practical applications. There are some added difficulties because if you vibrate that crystal you do not get only strictly compressional forces, you get other kinds of forces, especially bending forces. These bending forces elimininate to a certain extent the advantage which you would gain by mounting that crystal 60 degrees off the X axis. Also, it is true, this is a good way of mounting it, but it doesn't eliminate all of the problems. You still will have a vibration sensitive crystal.

I would like to say something else to Mr. Rose. He requested some comments on these crystals. You said that you have tried a stiff-mounted crystal, however you are afraid that they have a higher aging rate. I don't think this is true.We have made a lot of experiments with stiffly mounted crystals at 32 megacycles. The mount had a resonant frequency of about 2000 cycles and we found a very good phase stability in these. The aging rate of these crystals will be the same as any normal military metal enclosed crystal.

You can have a crystal which is two orders of magnitude better in aging. I don't know how much aging is of importance to you. This would be a glass enclosed crystal. This crystal is not mounted in spring mounts. It would have a resonant frequency. The first resonant frequency of the mount would be about a thousand cycles. It also would be possible, as Mr. Sherman pointed out, if you are willing to pay the price, to develop special crystals for your applications.

I also feel that the crystals which you mentioned, going back to that transistor design pioneered by Bell Telephone Laboratory, probably will meet your requirements in terms of aging and vibration sensitivity, although we didn't have an opportunity to test these crystals but the design looks very good. I think you are probably very well off, trying this crystal as the next step.

Dr. Winkler.—I would like to answer this remark of before. I did not mean to say that it makes no difference how you specify. I beleive that the standardization should be sought. However, I believe that we may be forced to maintain the two separate languages because I couldn't see how an rms frequency fluctuation would satisfy, for example tube manufacturers and vice versa. I think there is some need for two different languages, but I do agree with you for a need of standardization.

Mr. Chi.—Thank you, Professor Searle, for the

interesting discussion. Drs. Strandberg and Golay will now attempt to summarize the symposium.

Dr. Strandberg.—I cannot talk fast enough to summarize the symposium in three minutes. As a matter of fact, let me be a little funny. I have a feeling that there is a difference between physicists and electrical engineers which will remain different. Vive le difference, in this fashion:

The physicist, no matter what he is working on, thinks he is beating on the frontiers of science. It might have been done sixty years ago by Lord Raleigh but he still believes he initiated it. He never looks around to see what anybody else is doing.

An engineer, it seems to me, always sits down very carefully and looks into a field as broadly as he possibly can to see what is going on, what is applicable, and what he can steal to make it look like something he developed and so forth. This is very important in this one field, because I think here is a field that has been going on for a long time and there is a lot of work that has not even been brought up at this meeting.

I think actually what this meeting has done in my mind is that it actually has indicated the state of the art today as shown by the interest, the participants, and the apparatus that exists in this field. It certainly underlines the areas that still have to be looked into—such as the theory, the apparatus development, and the utilization of information in other research areas, in which short-term frequency stability is a byproduct of concern.

I think that there has also been enough discussion that one can go ahead with an initial declaration of a possible standard for measuring properties. Let's face it, there has been a good deal of sophistication that has developed in the last few years in the engineering brotherhood. Although I was the brunt of it, it is typified by the degree of sophistication that has developed in the last few years as indicated by the good humor that people had when Professor Searle put up this chart, a graph that I had suggested some years ago in trying to define what I was talking about when I talked about long-term and short-term stability. At that time it was really very important because people only talked about residual FM; it was utter chaos, one could not communicate with anybody. Now it seems trivial and laughable that somebody here could, or even should have to talk about spectra and carrier shifts and so on but that is all to the good because we are willing now to accept that kind of a presentation.

I think there is one byproduct field, for example, where a good deal of information is available and that is in my field of electro-magnetic resonance work. We have been measuring klystron noise, both AM and FM, for twelve or fifteen years because that is the thing that we are battling and although the apparatus is not designed for it; this is byproduct information which is available. The apparatus looks very much like, except more complicated, the FM meters or frequency modulation meters that Westinghouse and RRE (Royal Radar Establishment) have designed especially for the purpose.

I think this $1/f$ noise conversation is very good. I hope the dialogue keeps up. It is a good example of things that have to be talked about among all of us until finally everyone neglects it as being trivial and no longer important.

More data should be made available so that people can give descriptions, whether they are hand waving or not, of the sources of this stuff and how to handle it. Then we can get away from looking at it as an insurmountable barrier but rather one that you can slip around the side of, maybe. I must say, I feel that one is playing chess presently in the measuremnet field with available apparatus. I think that certainly there are indications here that instrumentation is developing in the field which will generate significant data. That is a very good thing and certainly more should be done.

There seems to be enough agreement in my mind for a standard formulation wording committee to be formed to generate a framework of standards for further study and revision and final adoption in this short-term frequency stability field.

Dr. Golay.—Mr. Chairman, ladies and gentlemen, the symposium has been one of the most stimulating and enjoyable symposia I have attended ever. I am sure the reason for this is to a great extent the newness and the pertinence of the subject discussed and of course, it is the host and the guests who make the party.

I won't in these few minutes make any more specific reference to any one paper but I would like to express some thoughts as to the direction our next work could take both conceptually and instrumentally.

Conceptually, I believe a good basic measure of the frequency instability of an oscillator should be the curvature of the phase of that oscillator plotted as a function of time and I would like to suggest some theoretical exploration of alternatives in that direction.

Instrumentally, I believe it is unfair to ask too much of a maser in terms of short-term frequency stability. It is not made for that purpose any more than the Lippizaner horse has been bred to pull a milkwagon. We should study the short-term stability of the oscillators at the second or third hierarchy level of the team which shall constitute a good clock. A low pressure hydrogen maser at the start, master of perhaps a high pressure hydrogen maser and this one in turn master over a quartz crystal. But then, the thing of pertinent interest is the short-term stability of the quartz crystal, the intermediate term stability of the high pressure maser, and the long-term stability of the low pressure maser. Why not study all three, per se? After having the characteristics of each, we shall have the fundamental parameters of the phase locked loops which should be utilized to tie each to the other in a harmonious manner.

In concluding, I would like to think that I can speak for each of us when I say that we are leaving this meeting with more ideas than we had when we came two days ago. I shall look forward to a fresh crop of letters to the editor of the IEEE on the things we have discussed, and perhaps a year or two from now another meeting such as this one will help us survey the ground covered.

Mr. Chi.—From the results of the two-day symposium, which we have had here, I am sure that we would agree with you that there has been much interest stimulated through the discussions and the papers which we have had.

I hope that after the symposium there will be enough interest to stimulate additional exchange of information, either through us, or through the individuals who have interest in the subject matter.

One thing which I want to mention before I give recognition to the other members is this: The symposium proceedings will be ready as soon as we have all of the papers. Those authors who have not deposited their papers with us, please inform Mr. Tom McGunigal, the secretary of the symposium.

At this time I would like to express my appreciation to the chairman of the four sessions Mr. Sykes, Dr. Edson, Professor Ramsey, and Professor Searle for their leadership in conducting the sessions, and most importantly in keeping the schedule of each session. And of course, I would like also to thank all of the panel members for their constructive criticism and illuminating discussions, and the authors for their informative and original papers which will prove to be very useful in the development of a standard.

There will be some work carried on after the symposium with the intent of developing a standard definition and measurement technique. However, the group at the moment wishes not to be announced and we will try to work as quietly as possible.

At this time I would like to recognize the cosponsors of the symposium. I did not do this purposely near the end, but this was the only time that I could find, so I would like to introduce the vice-chairman of the symposium, Mr. Armstrong, who represents IEEE Technical Committee 14 on Standards, Piezoelectric and Ferroelectric Crystals.

I would also take this opportunity to thank the members of the program committee whose names are listed on the program. I would also like to express my appreciation to the various Government agencies who have supported us in planning this symposium and also the officers of the symposium whom I would like to name:

Mr. Tom McGunigal, who is secretary of our symposium; Mr. Charles Boyle, who did most of the detail work for us including all of the correspondence.

The subject is of international interest and we feel quite proud that we have representatives from abroad to attend this symposium.

APPENDIX A — ADDITIONAL PAPERS

The two papers presented in this appendix are of general interest but were not presented at the Symposium.

25. A TUNABLE PHASE DETECTOR FOR SHORT-TERM FREQUENCY STABILITY MEASUREMENTS

A. E. ANDERSON AND H. P. BROWER

Collins Radio Company
Cedar Rapids, Iowa

A test instrument for measuring the phase stability of quartz crystals under vibration was developed in 1961 on a Signal Corps contract. Since then it has proved to be a very useful device for the measurement of phase and short-term frequency stability of frequency-generating and frequency-converting circuits such as crystal oscillators, mixers, multipliers, dividers, and synthesizers.

Consisting of a tunable phase detector and a reference crystal oscillator phase-locked to the average frequency of the test signal, the instrument covers the frequency range of 1 to 110 megacycles. The equipment resolution at 1 Mc is 0.001 degree in a bandwidth of 20 cps to 4 kc. This is equivalent to a sideband level of −101 db or a short-term frequency stability of 3 parts in 10^{10} in a 10 millisecond measuring period. At 100 Mc, the resolution is 0.04 degree or a sideband level of −69 db. By use of a narrow-band audio spectrum analyzer, an additional 20 to 30 db of resolution can be obtained. A chart recorder in conjunction with the spectrum analyzer has made it possible to plot spectrum profiles of signals with sideband resolution of −140 db.

Design considerations of the instrument are discussed, and measurement techniques and typical results are shown for several types of signal sources.

Most commercially available instruments for measuring short-term frequency stability use one of two methods: a short-term period count, or frequency multiplication into the UHF or SHF regions. Some use a combination of the two. A third method—not as generally used—of measuring the relative phase variations between the test signal and a stable reference signal has been found to be quite useful at Collins Radio Company; this method resulted as an offshoot of a development for the Signal Corps several years ago.

The equipment originally was developed for the purpose of measuring the phase stability of quartz crystals under vibration. During its development and subsequent testing, it became apparent that it would be useful in much wider applications—particularly the study of phase stability of complete circuits.

DESIGN CONSIDERATIONS

The specification for the original equipment required a capability of measuring phase stability of crystals from 1 to 110 Mc with a minimum resolution of approximately 0.003 degree at 1 Mc and 0.35 degree at 110 Mc. The crystals being tested would be subjected to 10 g's of vibration in the frequency range of 20 to 2000 cps. Also required were oscillators for the crystals being tested, and means of mounting the crystals to the vibration table and connecting them to the test oscillator.

A number of factors influenced the design approach, the principal ones being to avoid the generation of spurious signals and to minimize the noise contributed by the test circuitry. This was accomplished by making all measurements at the crystal frequency—thus eliminating the need for

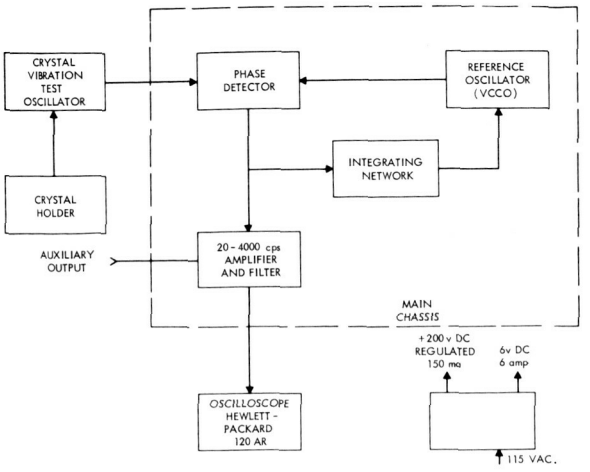

FIGURE 25–1.—The measurement system.

any mixers, multipliers, or injection frequencies. It also was considered desirable to provide most of the gain ahead of the phase detector, to minimize the noise contribution of the phase detector or post detection amplifiers.

The resulting circuit—as shown in the block diagram of Figure 25–1—was basically quite simple and consisted of a phase detector, tunable from 1 to 110 Mc in seven bands, and a reference crystal oscillator using a crystal at the same frequency as the crystal under test. To maintain the reference oscillator at the same frequency as the test crystal, it was designed as a voltage-controlled oscillator, with the control voltage obtained from the phase detector. An integrating circuit in the feedback loop prevents the reference oscillator from following the random or vibration-induced phase variations of the test signal.

Needless to say, minimizing the problems of noise generation and spurious signals by making all measurements directly at the test frequency introduced a few other design problems, particularly in the tunable phase detector. Extreme care in shielding and filtering also were required. These problems and other design details are reported in Reference 1.

PRINCIPLES OF OPERATION

As mentioned previously, the instrument is primarily a tunable phase detector and a voltage-controlled reference oscillator. Designed initially for testing the phase stability of crystals operated in a second oscillator circuit, it can be used for measuring the stability of any relatively stable signal of sufficient amplitude in the frequency range of 1 to 110 Mc. The test signal must be of sufficient stability that the reference oscillator will remain locked to it. Input level required is approximately $\frac{1}{2}$ volt into 100 ohms. The input signals are amplified to levels ranging from approximately 100 volts peak-to-peak at 1 Mc to 20 volts at 110 Mc, providing a phase detector output of 200 volts peak-to-peak at 1 Mc and 40 volts at 110 Mc in the unlocked condition.

In actual operation, the instrument is first calibrated by opening the loop and observing the phase detector output on the oscilloscope (see Figure 25–2). The reference oscillator frequency is adjusted to give a low-frequency beat note, as shown in Figure 25–3. As one complete cycle of the beat frequency represents 360 degrees of phase change, the slope of the waveform at the zero crossover—in degrees per volt (or millidegrees per millivolt)—can be determined. Switch-

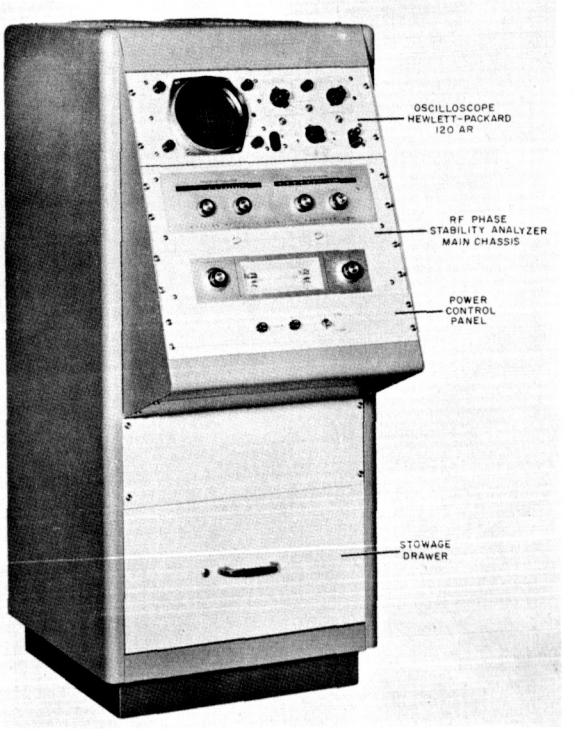

FIGURE 25–2.—The test instrument.

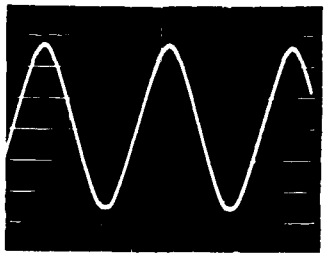

CALIBRATION
SENSITIVITY: 30v/DIVISION
SWEEP: 10 ms/DIVISION
SLOPE: 0.75 m°/mv

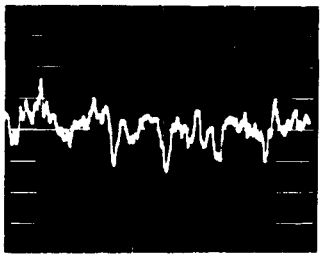

RESIDUAL NOISE
SENSITIVITY: 1mv/DIVISION
SWEEP: 10 ms/DIVISION
RESOLUTION: ≈ 0.75 m° PEAK

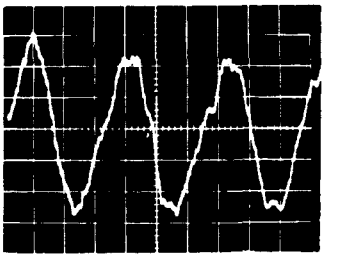

VIBRATION 5g at 30cps
SENSITIVITY: 2mv/DIVISION
SWEEP: 10 ms/DIVISION
PHASE DEVIATION: 3.7 m° PEAK

FIGURE 25–3.—System performance at 1.0 Mc; measurement system 101, USASRDL crystal no. 7.

ing to the *lock* and then to the *operate* position locks the reference oscillator to the average frequency of the signal, but permits the random phase variations between them to be displayed (as shown) by increasing the scope sensitivity. The effect of vibration on the test crystal can be seen in the third picture in Figure 25–3. Switching from the *lock* to the *operate* position also amplifies the output signal by a factor of 10 to provide a higher signal level to the scope.

As the crystals under test were to be vibrated at rates from 20 to 2000 cps, the response of the instrument was required to be flat over this bandwidth, and was intentionally held flat out to about 4 kc to include any 2nd harmonic effects. Above 4 kc it was intentionally rolled off by means of a low-pass filter in the audio amplifier, and below 20 cycles it is rolled off by the time constant of the integrating network between the phase detector and reference oscillator. The low-frequency response could be extended by increasing the time constant, and the high-frequency response could be extended by changing the filter.

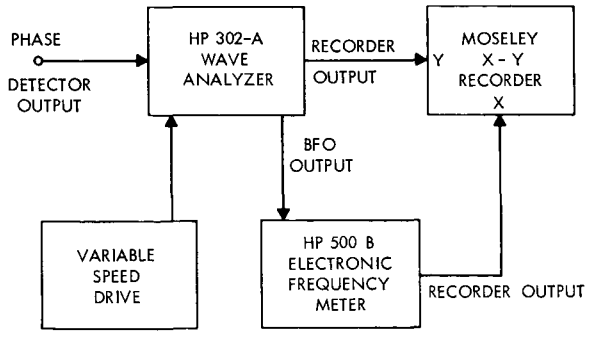

FIGURE 25–4.—Audio spectrum analyzer.

PERFORMANCE CHARACTERISTICS

In measuring the stability of a typical signal—for instance, the output of a frequency synthesizer—the phase detector output will consist of random phase fluctuations in the 20 cycle to 4 kc range plus any discrete components due to spurious frequencies, power supply ripple, etc. As shown in Figure 25–3, the composite level of the test crystal oscillator—prior to vibrating the crystal—was on the order of 0.5 millidegree, with peaks of 1 to 1.5 millidegrees. This is fairly typical for a crystal oscillator and has been found to be a function of drive level, crystal Q, frequency, and other factors. The resolution of the instrument ranges from something less than 1 millidegree at 1 Mc to about 40 millidegrees at 110 Mc. At a 20-cycle modulation rate, this is equivalent to frequency stability of approximately 1 to 3 parts in 10^{10}.

In many cases, the composite noise level is all that is of interest. Frequently, however, the spectral distribution of the noise is of interest; and an audio frequency spectrum analyzer, such as the Hewlett-Packard 302A, has been found to be a useful adjunct to the instrument. It not only permits analyzing the signal for spectral density and discrete components but also provides an additional 20 to 30 db of resolution. Used with a

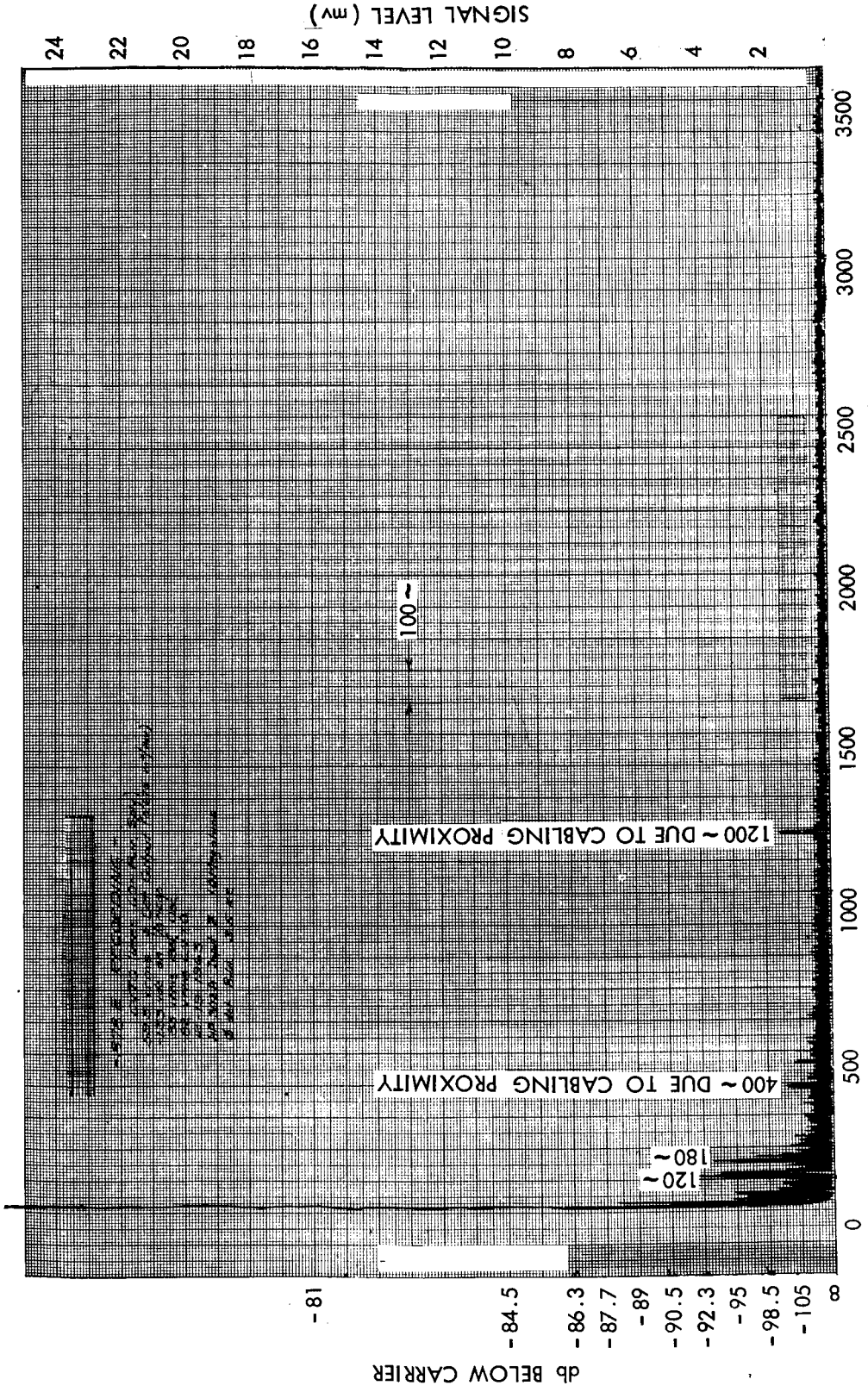

FIGURE 25–5.—Spectral recording of a 3.0-Mc signal from crystal test oscillator using regular power supplies.

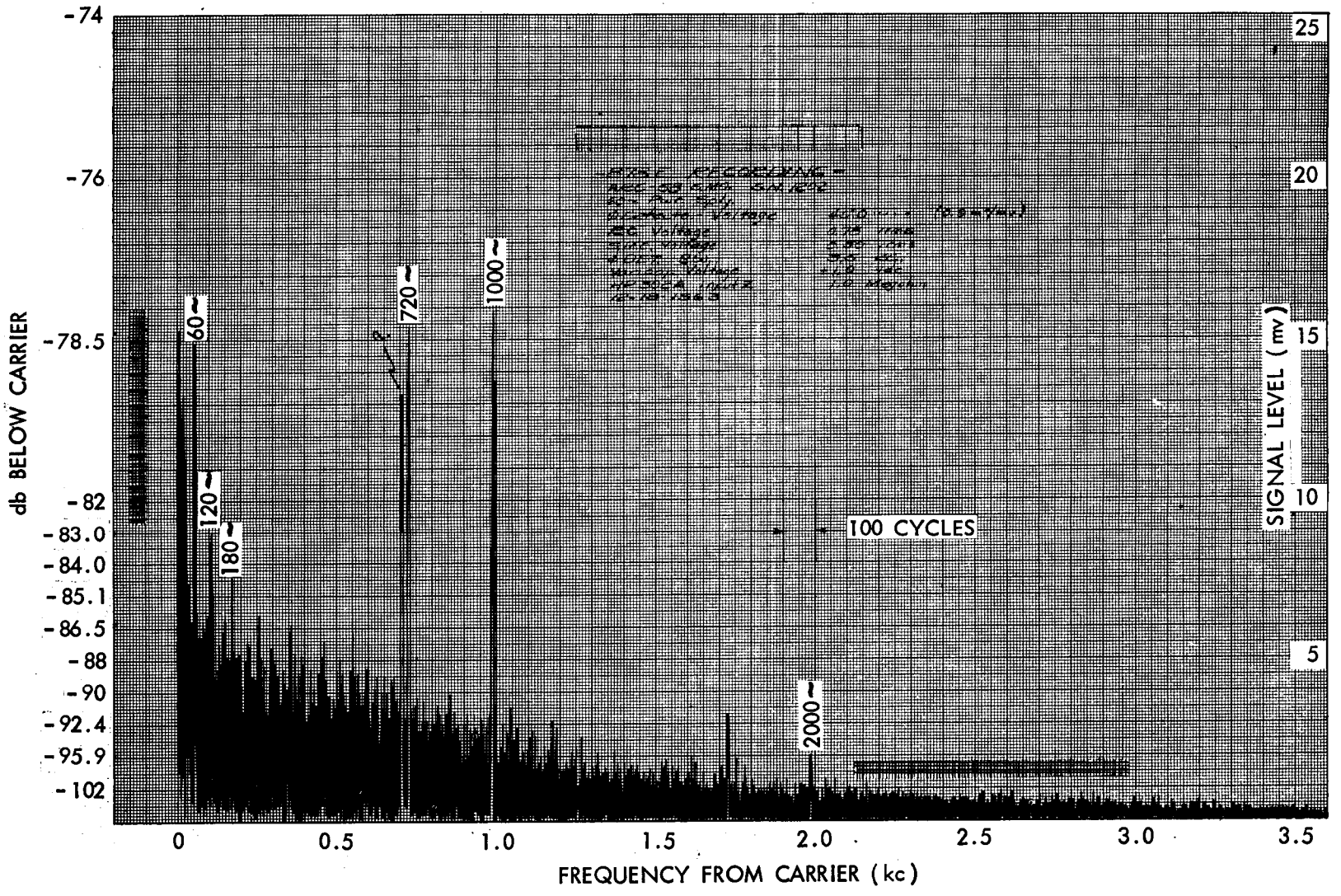

FIGURE 25–6.—Spectral recording of output from stabilized master oscillator in an ARC-58 HF single-sideband transceiver using 60-cps power source.

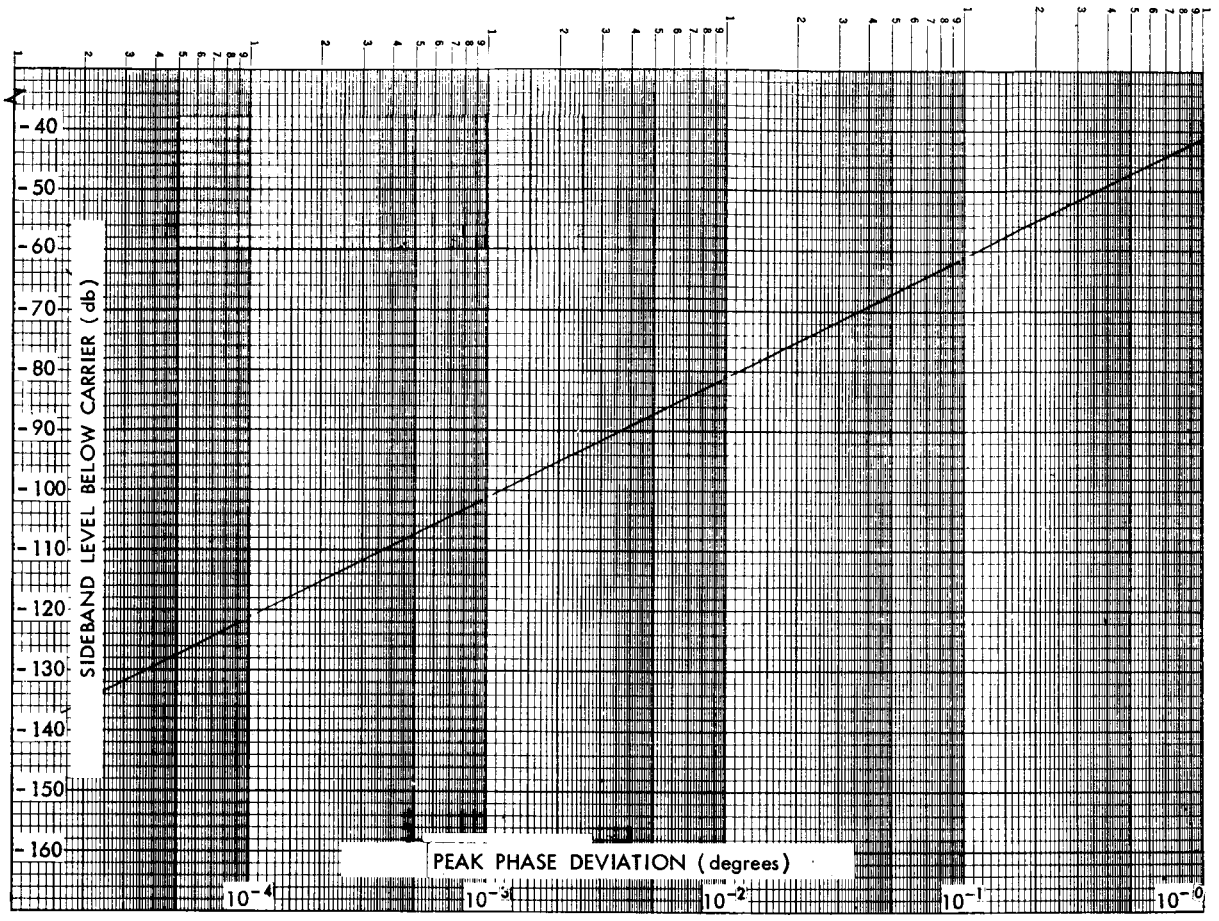

FIGURE 25–7.—Sideband level vs. peak phase deviation (assumed small deviation).

chart recorder—as in the block diagram of Figure 25–4—a plot of the spectrum profile can be drawn as shown in Figures 25–5 and 25–6. Although these recordings are actually the spectra of the phase deviations of the test signals, they were plotted as sideband level below the carrier in db since this had more significance to the system engineer than either phase deviation or short-term frequency deviation. A conversion chart from phase deviation to sideband level in db, calculated from the phase modulation equation (assuming sine wave modulation), is shown in Figure 25–7.

TYPICAL RESULTS

To demonstrate the results obtained with the instrument, data from measurements on different types of oscillators are included: a 3-Mc crystal in the test oscillator, a 3-Mc signal from an ARC-58 SSB transceiver SMO (Stabilized Master Oscillator), a 2.5-Mc signal from a Collins 70K-5 permeability tuned L-C oscillator, a 3-Mc signal from a temperature-compensated crystal oscillator used in single-sideband equipment, and a 31.7-Mc crystal in the test oscillator.

Figure 25–5 shows a spectral recording of a 3.0-Mc signal from the crystal vibration test oscillator, using the regular power supplies for the equipment. The 120- and 180-cps signals were due to the various equipment power supplies and wiring within the screen room where the measurements were made. The 400- and 1200-cps signals were due to the close proximity of 400-cps power cables to the measurement apparatus. The equipment to which these cables were connected

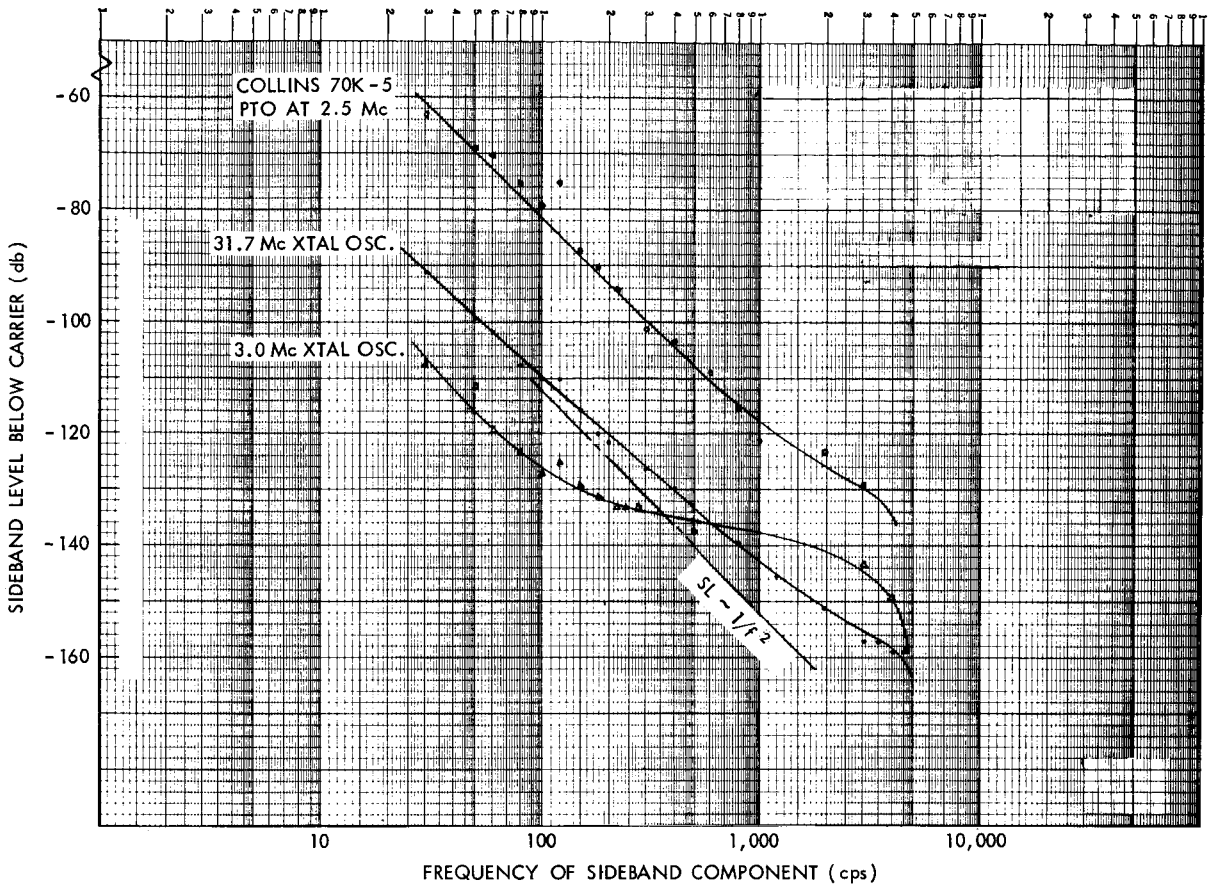

FIGURE 25–8.—Phase stability tests, using phase stability analyzer in totally enclosed magnetic shielded room. (All equipment operated from batteries; bandwidth, 7 cps; HP 302A.)

was not operating at the time, indicating that the electric field was adversely affecting the measurements.

Figure 25–6 is the spectral recording of the output from the stabilized master oscillator (SMO) in an ARC-58 HF single-sideband transceiver when operated from a 60-cps power source. The various signals shown which are not related to 60 cps are generated in the frequency stabilizer. Notice that the average noise level is 10 to 15 db higher than in Figure 25–5.

Figure 25–8 is a plot of data taken with the spectrum analyzer of Figure 25–4, but without the X-Y recorder. Curves are shown for the Collins 70K-5 PTO, a 3-Mc TCXO, and a 31.7-Mc crystal in the test oscillator. The 70K-5 is a transistorized L-C oscillator. The TCXO utilizes a 3-Mc semiprecision fundamental crystal with a minimum Q of 500,000, operated at a drive level of less than 10 microwatts. The 31.7-Mc crystal drive level was about 1 milliwatt. The crystal was a standard third overtone CR-76.

The increasing slope of these curves in the vicinity of 5 kc is due to the characteristics of the audio filter. The odd shape of the 3.0-Mc curve is presently not explainable. Also, no explanation is given for the fact that the slope of these curves approaches $1/f^2$, and not $1/f$ as might be expected if the noise level at the lower frequencies was due to flicker noise.

The ultimate resolution of the instrument depends to some extent on the stray electric fields which may be present. This is portrayed graphically in Figure 25–8, which is a plot of data obtained in a totally enclosed screen room, the walls of which were contructed of magnetic

shielding material. All equipment was operated from batteries in the shielded room.

The offset data points at 120 cps could be placed on the curves by removing the one incandescent bulb in the ceiling of the screen room and then reading the meter with a flashlight!

CONCLUSIONS

In many system applications, the spectrum profile or the phase stability of the signal is more meaningful than short-term frequency deviations. In such applications, measurements utilizing a phase detector at the signal frequency are preferable to presently used techniques.

REFERENCE

1. Final Report for Phase Stability Measuring Equipment. Contract DA–36–039–sc–78310. Defense Documentation Center (ASTIA) Technical Bulletin AD–269–205.

26. SHOT-EFFECT INFLUENCE ON THE FREQUENCY OF AN OSCILLATOR LOCKED TO AN ATOMIC BEAM RESONATOR

P. KARTASCHOFF

Laboratoire Suisse de Recherches Horlogeres
Neuchâtel, Switzerland

For an oscillator—locked to the resonance of an atomic beam tube—the main source of short-term frequency fluctuations is, in most cases, the shot noise due to the atomic beam. Assuming this to be white noise described by Schottky's formula, the spectral density of the controlled variable (i.e., of the instantaneous value of the controlled-oscillator frequency) is calculated for the case of a simple integrating servo loop having only one time constant. It is shown how the standard deviation of measured samples can be calculated by using a formula given by MacDonald. For sampling times which are long compared with the servo time constant, an approximation leads to a simple formula which agrees better with the experimental results than the approximations which do not consider the response of the servo system.

In a frequency standard operating with an atomic beam resonator using the hyperfine transitions of cesium or thallium, the resonance is indicated by a maximum value of the detector beam if the excitation frequency is adjusted to the frequency of the transition. The excitation frequency (9192 Mc/sec for cesium) is produced by means of a crystal oscillator driving a frequency multiplier chain.

Automatic frequency control of the crystal oscillator is obtained by means of a low-frequency phase or frequency modulation on the excitation signal.

This modulation produces a periodic variation of the detected beam intensity. The fundamental component of this intensity variation vanishes if the average frequency of the excitation signal is equal to the frequency of the atomic resonance. The fundamental component appears on either side of the resonance, its amplitude being a function of the amount and its phase depending on the sense of the offset. By means of a synchronous demodulator (chopper) a dc error voltage is obtained, the time integral of which is acting on the frequency of the crystal oscillator.

Figure 26–1 shows a simplified block diagram of the frequency control servo. In this case, we first shall neglect all delaying time constants due to the atomic beam resonator and to the other elements forming the servo loop.

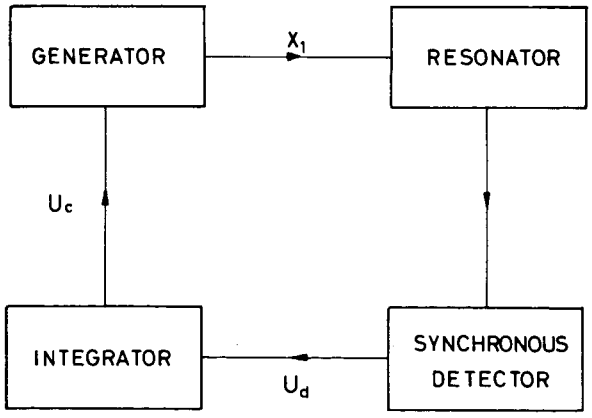

FIGURE 26–1.—The frequency control servo.

For sake of generality, we shall normalize the frequency with reference to the linewidth of the atomic resonator. We get

$$x_1 = 2[(\nu_1 - \nu_b)/\Delta\nu], \tag{1a}$$

$$x_e = 2[(\nu_e - \nu_b)/\Delta\nu], \tag{1b}$$

ν_b being the Bohr frequency of the atomic resonance, ν_1 the frequency of the locked oscillator, ν_e the frequency of the free-running oscillator, and $\Delta\nu$ the linewidth of the atomic resonance.

x_1 and x_e are related by the formula

$$x_1 = x_e - K_f \cdot U_c \tag{2}$$

describing the action of the control voltage U_c on the frequency of the oscillator. The output voltage U_d of the synchronous demodulator being proportional to the offset, we have

$$U_d = Dx_1. \tag{3}$$

The control voltage being the time integral of the voltage U_d, we have

$$dU_c/dt = Ki \cdot U_d. \tag{4}$$

By eliminating U_d and U_c, we get the differential equation

$$dx_1/dt = (dx_e/dt) - K_0 x_1, \tag{5}$$

with

$$K_0 = K_f K i D.$$

The solution of the differential equation is

$$x_1(t) = x_{e0} \exp(-K_0 t) + K_0^{-1} (dx_e/dt)[1 - \exp(-K_0 t)]. \tag{6}$$

We obviously may call K_0 the gain of the servo loop. The solution shows that, in the long term, the systematic offset tends to zero if the crystal oscillator has no drift; otherwise, the systematic offset would be given by the second term of Equation 6.

The frequency fluctuations of the controlled oscillator are due to two main causes:

1. Spontaneous fluctuations of the oscillator frequency which are too rapid to be completely canceled by the action of the control loop.
2. Noise introduced in the control loop due to the shot effect of the atomic beam.

In this paper, we shall consider only the influence of the shot-effect noise and assume that the oscillator is perfectly stable. This point of view is justified in all the cases in which the shot effect is the main cause of the observed frequency fluctuations. Experience has shown that this can be admitted for the atomic beam tubes actually used and for good crystal oscillators.

SIMPLE ESTIMATION NEGLECTING SERVO CHARACTERISTICS

A very simple but rough estimation of the error in measuring the frequency of the atomic resonance can be obtained in the following way:

We call I_1 the total detected ion current and I_R the amplitude of the Ramsey-pattern characteristic of the atomic beam resonator. The central part of this resonance pattern is described by

$$I(x) = I_R \cos(\pi/4)x,$$

which is a good approximation for $|x| < 2$. For $x = \pm 1$ (i.e., on the skirts of the resonance pattern) a current variation ΔI corresponds to a frequency variation of

$$\Delta x = (dI/dx)^{-1} \Delta I = (4/\pi)(\Delta I/I_R). \tag{7}$$

The current fluctuates according to Schottky's formula (References 1 and 2), giving a mean-square value of

$$\langle \Delta^2 I \rangle = 2eI_1 B, \tag{8}$$

where B is the bandwidth of the detection system.

From these relations, we get

$$\langle \Delta^2 x \rangle = (16/\pi^2)(2eI_1 B/I_R^2). \tag{9}$$

If each measurement lasts for a time $\tau \approx 1/B$, we can calculate a relative standard deviation σ' for the measured frequency, which is given by the relation

$$\sigma' \approx 1.8 (\Delta\nu/\nu_b I_R)(eI_1/\tau)^{1/2}, \tag{10}$$

allowing a rapid evaluation of the precision limit set by the shot noise. We shall see that in actual systems this formula gives a result which is too optimistic.

SHOT NOISE ACTING ON THE FREQUENCY CONTROL LOOP

We admit that the noise perturbations are random and that their probability distribution does not change with time.

The mean-square value $\langle x_1^2(t) \rangle$ of the normalized frequency x_1 can be calculated if its spectral density $G_1(\omega)$ is known. $\langle x_1^2(t) \rangle$ is given by the

well-known relation (References 1 and 2)

$$\langle x_1^2 \rangle = \frac{1}{2\pi}\int_0^\infty G_1(\omega)\, d\omega. \qquad (11)$$

The frequency control servo system can be represented as a filter with an input variable representing the noise, and with x_1 as the output variable. If we call $G_b(\omega)$ the spectral density of the noise, the spectral density of the output is given by the relation

$$G_1(\omega) = G_b(\omega) \mid Y_b(i\omega) \mid^2. \qquad (12)$$

For the shot noise, the spectral density is equal to

$$G_b(\omega) = eI_1/\pi, \qquad (13)$$

according to Schottky's formula.

The system transfer function $Y_b(i\omega)$ is established according to the block diagram shown in Figure 26–2. All variables are the Laplace transforms of the original time functions. At the output of the atomic beam tube, we obtain an ion current which is the sum of two terms representing the signal and the noise:

$$I_j = aX_1 I_R F_1(p) + I_N. \qquad (14)$$

The coefficient a is the normalized modulation index of the low-frequency modulation on the excitation signal, described by the relation

$$x_1(t) = x_1 + a \sin\omega_m t,$$

where ω_m is the angular frequency of the LF modulation. $F_1(p)$ is the transfer function of the atomic beam tube:

$$F_1(p) = (1+pT_r)^{-1}, \qquad (15)$$

T_r being the interaction time of the atomic beam (Reference 3). I_N, the second term of Equation 14, is the fluctuating part of the ion current due to shot noise.

The frequency control servo is described by the relation

$$X_1 = -F_2(p)\, U_1 = -F_2(p)\, I_j R_1; \qquad (16)$$

R_1 is the input resistance of the preamplifier. The negative sign is necessary to obtain the proper correcting sense of the servo (cf. Equation 2). By eliminating I_j from Equations 15 and 16, we obtain

$$X_1 = -I_N \frac{R_1 F_2(p)}{1 + aR_1 I_R F_1(p)\, F_2(p)},$$

and thus

$$Y_1(p) = -\frac{R_1 F_2(p)}{1 + aR_1 I_R F_1(p)\, F_2(p)}. \qquad (17)$$

The form of $F_2(p)$ depends on the detailed characteristics of the amplifiers, the synchronous detector, and the integrator. Generally, it can be represented as a ratio of polynomes:

$$F_2(p) = K_s[P(p)/Q(p)], \qquad (18)$$

the degree of $P(p)$ and $Q(p)$ depending on the complexity of the circuits. K_s is a constant which determines the overall gain. The simplest form we can use to represent $F_2(p)$ is

$$F_2(p) = [K_s/p(1+pT)], \qquad (19)$$

where the factor $1/p$ describes the operation of the integrator and T is the time constant of the amplifier. If a selective low-frequency amplifier having a bandwidth of B cps is used, T is about equal to $1/\pi B$.

If the time constant T is large compared with the interaction time T_r, we may neglect T_r with respect to T and put $F_1(p)$ equal to 1. We then have

$$Y_b = -(K_0/aI_R)(p^2T + p + K_0)^{-1}, \qquad (20)$$

with $K_0 = K_s a R_1 I_R$. K_0 is the gain of the servo loop and is similar to the K_0 used in Equation 5.

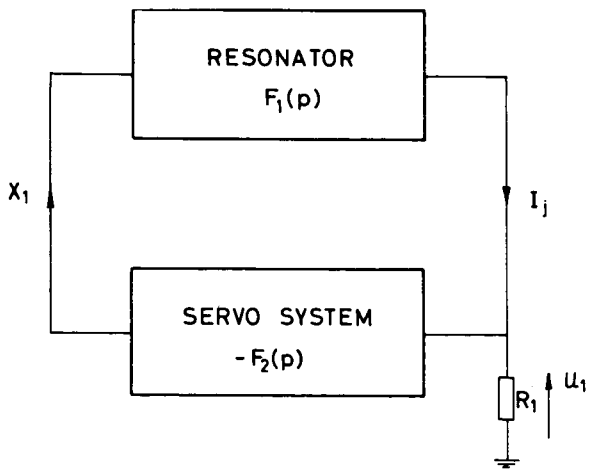

FIGURE 26–2.—Establishment of system transfer function $Y_b(i\omega)$.

Putting $p=i\omega$, we obtain—according to Equation 12—the spectral density of the normalized variable x_1:

$$G_1(\omega)=(eI_1/\pi)\,(K_0^2/a^2I_R^2)\,[(K_0-\omega^2T)^2+\omega^2]^{-1}. \tag{21}$$

By means of Equation 11 we then get the mean-square $\langle x_1^2\rangle$:

$$\langle x_1^2\rangle=\frac{eI_1K_0^2}{2\pi^2a^2I_R^2}\int_0^\infty\frac{d\omega}{(K_0-\omega^2T)^2+\omega^2}. \tag{22}$$

The solution of the integral in this equation is equal to

$$\int_0^\infty\frac{d\omega}{(K_0-\omega^2T)^2+\omega^2}=\frac{\pi}{2K_0}. \tag{23}$$

It is important to note that the value of the integral is not depending on the servo time constant T. Intuitively, we would like to believe that, for a given loop gain K_0, the servo would filter out more noise if T were increased. This is true for the higher frequency components of the noise, but at the same time the servo response becomes oscillatory and less damped. This is why the mean-square fluctuation does not diminish if the time constant is increased.

The mean-square value $\langle x_1^2\rangle$ is equal to

$$\langle x_1^2\rangle=eI_1K_0/4\pi a^2I_R^2. \tag{24}$$

From this we can calculate the standard deviation σ_0, which is a measure of the probability distribution width for the frequency of the controlled oscillator:

$$\sigma_0=(\Delta\nu/\nu_b)\,\langle x_1^2\rangle^{1/2}$$
$$=(\Delta\nu/2\nu_baI_R)\,(eI_1K_0/\pi)^{1/2}. \tag{25}$$

FINITE SAMPLING TIMES

The quasi-instantaneous value of the controlled-oscillator frequency having the standard deviation σ_0 cannot be measured directly. The results of measurements carried out by means of counters always are average values taken over a finite counting or sampling time τ.

Each result is a sample given by the relation

$$x_\tau(t_i)=\tau^{-1}\int_{t_i}^{t_i+\tau}x(t)\,dt. \tag{26}$$

The standard deviation of these measured values

$$\sigma(\tau)=\langle x_\tau^2\rangle^{1/2} \tag{27}$$

depends on the sampling time τ. It is well known that this standard deviation is equal to

$$\sigma(\tau)=(A/2\tau)^{1/2} \tag{28}$$

if the spectral density $G(\omega)$ of $x(t)$ is a constant and equal to A (Reference 2). In our case, the spectral density as described by Equation 21 is not constant; and therefore it is not possible to apply Equation 28.

A more general relation due to D. K. C. MacDonald (Reference 3) allows us to calculate $\langle x_\tau^2\rangle$ from the spectral density:

$$\langle x_\tau^2\rangle=\pi^{-1}\int_0^\infty G_1(\omega)\frac{1-\cos\omega\tau}{\omega^2\tau^2}\,d\omega. \tag{29}$$

It is easy to verify that

$$\langle x_\tau^2\rangle=(A/2\tau)\qquad\text{if } G_1(\omega)=A,$$

as in Equation 28. Furthermore, we have

$$\lim_{\tau\downarrow0}\langle x_\tau^2\rangle=\langle x_1^2\rangle.$$

The integral in Equation 29 cannot be solved in an explicit form and has to be calculated by means of a computer.

To obtain an approximate evaluation of $\langle x_\tau^2\rangle$, we transform the spectral density function $G_1(\omega)$ into a rectangle according to Figure 26–3. From Equation 21 we have

$$G_1(\omega)=G_0\{K_0^2/[(K_0-\omega^2T)^2+\omega^2]\}, \tag{30}$$

with

$$G_0=eI_1/\pi a^2I_R^2.$$

The surface of the equivalent rectangle is equal to the integral

$$\int_0^\infty G_1(\omega)\,d\omega.$$

The width of the rectangle is equal to the cutoff frequency ω_c defined by the relation

$$G_1(\omega_c)=G_0;$$

and thus

$$\omega_c = T^{-1}(2K_0T-1)^{1/2}, \tag{31}$$

which is valid for $K_0T > \frac{1}{2}$.
We then get, with

$$G_m = G_0\pi K_0/2\omega_c, \tag{32}$$

an equivalent spectral density which is constant below ω_c and zero above ω_c. For sampling times τ which are long compared with the period of the cutoff frequency—that is,

$$\tau \gg 2\pi/\omega_c,$$

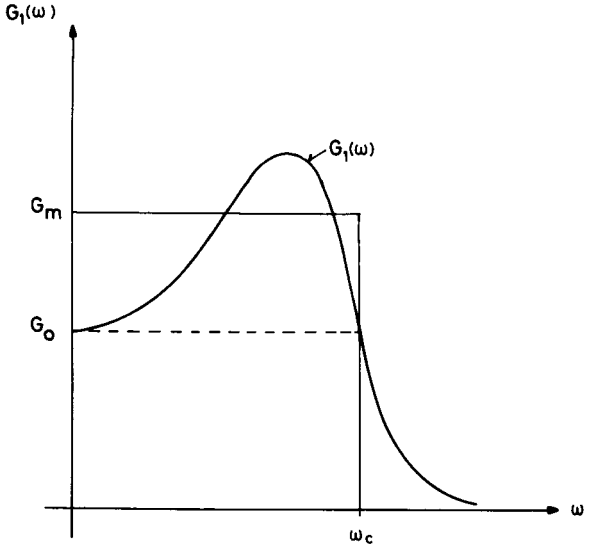

FIGURE 26–3.—Transformation of spectral density function $G_1(\omega)$ into rectangle.

we may neglect the contributions of the high-frequency components. This leads to the estimation

$$\langle x_\tau^2 \rangle = G_m/2\tau = eI_1K_0/4a^2I_R^2\omega_c\tau, \tag{33}$$

from which we obtain the standard deviation

$$\sigma(\tau) = \Delta\nu/2\nu_b a I_R(eI_1K_0/\omega_c\tau)^{1/2}. \tag{34}$$

NUMERICAL EXAMPLES

We have calculated the standard deviations for two cesium beam frequency standards having very different characteristics. Standard 1 uses a Varian BLR 2 tube with an interaction length of 10 inches and Standard 2, the 4-meter-long beam tube of the L.S.R.H. (Reference 4). The data for the two examples are given in Table 26–1.

TABLE 26–1

Deviation	Standard 1	Standard 2
$\Delta\nu$ (cps)	290	35
ν_b (cps)	9.2×10^9	9.2×10^9
a	0.1	0.1
K_0 (sec^{-1})	40	40
I_1 (A)	3.94×10^{-12}	5×10^{-12}
I_R (A)	1.37×10^{-12}	1×10^{-12}
T (sec)	0.027	0.08
ω_c (sec^{-1})	40	18.5

For the three standard deviations $\sigma(\tau)$ according to Equation 34, $\sigma'(\tau)$ according to Equation 10, and σ_0 according to Equation 25, we obtained the results shown in Table 26–2.

From measurements against a Varian 4700A rubidium-gas-cell standard having itself a short-term stability of $1\times10^{-11}\ \tau^{-1/2}$, we obtained the following results:

Standard 1:

$$\sigma_{exp} = 1.1\times10^{-10}\ \tau^{-1/2},$$

Standard 2

$$\sigma_{exp} = 3.5\times10^{-11}\ \tau^{-1/2}.$$

The short-term fluctuations of the crystal oscillators used in the experiments were in the range of 1 to 2 parts in 10^{-11} for a 1-second sampling time, when the oscillators were free-running. The calculated values for $\sigma(\tau)$ agree fairly well with the experimental results, at least for sampling times over 1 second. We, however, have some

TABLE 26–2

Deviation	Standard 1	Standard 2
$\sigma(\tau)$	$9\times10^{-11}\ \tau^{-1/2}$	$2.5\times10^{-11}\ \tau^{-1/2}$
$\sigma'(\tau)$	$3.3\times10^{-11}\ \tau^{-1/2}$	$6.1\times10^{-12}\ \tau^{-1/2}$
σ_0	3.2×10^{-10}	6.4×10^{-11}

doubts as to whether the approximation leading to Equation 34 still would be good for shorter sampling times. Equation 10 leads to results which are too small, but it can be used to compare different types of beam tubes.

To check further the approximation of Equation 34, we have calculated numerically on a desk computer the integral of Equation 29 with the data of Standard 1 and $\tau = 1$ sec; we obtained a result of 7×10^{-11}. This is 20 percent smaller than the value shown in Table 26–2. Further checks might be useful; but, for the time being, we believe that Equation 34 gives a conservative approximation.

REFERENCES

1. James, H. M., Nichols N. B., and Phillips R. S., "Theory of Servomechanisms," M.I.T. Rad. Lab. Series, Vol. 25, McGraw-Hill: New York, 1947.
2. Van der Ziel, A., "Noise," Prentice Hall: Englewood Cliffs, N.J., 1954.
3. McDonald, D. K. C., *Phil. Mag. 40*, 561 (1949).
4. Kartaschoff, P., "Etude d'un etalon de fréquence à jet atomique de césium," thesis, Swiss Federal Institute of Technology, Zurich, 1964.

Page intentionally left blank

APPENDIX B — LIST OF ATTENDEES

D. W. Allen
National Bureau of Standards
Boulder Labs, Colorado

Carroll O. Alley
University of Maryland
College Park, Md.

A. E. Anderson
Collins Radio Co.
Cedar Rapids, Iowa

Harro G. Andresen
Army Electronics Labs.
Fort Monmouth, N.J.

S. Anema
IBM
Bethesda, Md.

M. Arditi
ITT Federal Labs.
Nutley, N.J.

James T. Arnold
Varian Associates
Palo Alto, Calif.

J. Robert Ashley
Sperry Electronic Tube Div.
Gainesville, Fla.

J. H. Armstrong
Bell Telephone Labs.
Allentown, Pa.

Robert M. Aughey
ITT Federal Labs.
Nutley, N.J.

Edward J. Bacon
Booz, Allen Applied Research, Inc.
Bethesda, Md.

Elie J. Baghdady
ADCOM, Inc.
Cambridge, Mass.

A. S. Bagley
Hewlett-Packard Co.
Palo Alto, Calif.

Raymond L. Baker
FAA, Research Div.
National Aviation Fac. Exp. Ctr.
Atlantic City, N.J.

M. Baltas
Defense Communication Agency
Washington, D.C.

C. Baltzer
Tracor
Austin, Texas

Richard H. Bangert
Bendix Pioneer-Central Div.
Davenport, Iowa

Donald S. Banks
Raytheon Co.
Bedford, Mass.

James A. Barnes
National Bureau of Standards,
Boulder Labs.
Colorado

Alex Barvicks
Goddard Space Flight Center

V. J. Bates
Mass. Institute of Technology
Cambridge

Richard Baugh
Hewlett-Packard Co.
Palo Alto, Calif.

Robert C. Beal
Johns Hopkins Applied Physics Lab.
Silver Spring, Md.

Douglass L. Benson
Army Strategic Communications Command
Washington, D.C.

William Bickford
Raytheon Co.
Bedford, Mass.

Don Bissler
IBM
Bethesda, Md.

George K. Bistline, Jr.
McCoy Electronics Co.
Mount Holly Springs, Pa.

Martin B. Bloch
Frequency Electronics, Inc.
Astoria, New York

Chris Boykin
Harry Diamond Labs.
Washington, D.C.

Richard L. Britton
Harry Diamond Labs.
Washington, D.C.

H. P. Brower
Collins Radio Co.
Cedar Rapids, Iowa

Kenneth M. Brown
General Dynamics
Pomona, Calif.

G. Brunins
Westinghouse Electric Corp.
Baltimore, Md.

William M. Bush
Cornell Aeronautical Lab.
Buffalo, N.Y.

David A. Calder
Raytheon Co.
Wayland, Mass.

J. J. Caldwell, Jr.
TRW Space Tech. Labs., Inc.
Redondo Beach, Calif.

Richard A. Campbell
Raytheon Co.
Bedford, Mass.

Andrew R. Chi
Goddard Space Flight Center

A. A. Citro
Goddard Space Flight Center

D. B. Clemson
General Electric Co.
Philadelphia, Pa.

Robert J. Coates
Goddard Space Flight Center

Joseph G. Coolican
General Electric Co., Ltd.
Utica, N.Y.

Kingsley W. Craft
LFE—Electronics, Inc.
Waltham, Mass.

Myron Criswell
Navy Bureau of Ships
Washington, D.C.

Thomas F. Cutty
Curry, McLaughlin & Len, Inc.
Syracuse, N.Y.

Jack A. Curtis
General Electric Co.
Lynchburg, Va.

Leonard S. Cutler
Hewlett-Packard Co.
Palo Alto, Calif.

Walter Dauksher
Airborne Instruments Lab.
Deer Park, N.Y.

Paul Davidovits
Columbia Univ. Radiation Lab.
New York

Duane G. Davis
National Security Agency
Fort Meade, Md.

Charles H. Dawson
Stanford Research Institute
Menlo Park, Calif.

John W. B. Day
Defence Research Telecommunications Est.
Ottawa, Canada

Francis C. Deckelman
Harry Diamond Labs.
Washington, D.C.

Joseph Deskevich
Goddard Space Flight Center

Vincent J. DiLosa
Goddard Space Flight Center

William J. Dougherty
Frankford Arsenal
Philadelphia, Pa.

D. T. Duckworth
Naval Ordnance Test Station
China Lake, Calif.

W. A. Edson
Electromagnetic Technology Corp.
Palo Alto, Calif.

Peter D. Engels
Goddard Space Flight Center

F. D. Erps
Montronics, Inc.
Bozeman, Mont.

Albert W. Felsher, Jr.
Goddard Space Flight Center

Lowell Fey
National Bureau of Standards
Boulder Labs., Colorado

Joseph Flink
Federal Scientific Corp.
New York

Morton L. Friedman
Goddard Space Flight Center

M. S. Friedland
Geo Space Corp.
Melbourne, Fla.

C. Friend
Wright Patterson AFB
Dayton, Ohio

Robert E. Gardner
Naval Research Lab.
Washington, D.C.

Allan F. Gaynor
General Electric Co.
Oklahoma City

Samuel F. George
Naval Research Lab.
Washington, D.C.

M. Giller
Westinghouse Aerospace Div.
Baltimore, Md.

Norman R. Gillespie
Raytheon Co.
Wayland, Mass.

E. H. Gleason
Marshall Space Flight Center
Huntsville, Ala.

Harry J. Goett
Goddard Space Flight Center

Louis P. Goetz
Westinghouse Aerospace Div.
Baltimore, Md.

Marcel J. E. Golay
Perkin-Elmer Corp.
Norwalk, Conn.

Howard D. Goldick
Syracuse Univ. Research Corp.
Syracuse, N.Y.

Raymond L. Granata
Goddard Space Flight Center

C. Grant
Ovenaire, Inc.
Charlottsville, Va.

C. Herbert Grauling, Jr.
Westinghouse Aerospace Div.
Baltimore, Md.

Edward B. Greene
Bendix Systems Div.
Ann Arbor, Mich.

L. J. Grimes
Kennedy Space Center
Cocoa Beach, Fla.

Fred Gross
General Dynamics
Pomona, Calif.

H. E. Gruen
DELTA-f
Carlisle, Pa.

Dr. Gunter K. Guttwein
Army Electronics Labs.
Fort Monmouth, N.J.

Edmund J. Habib
Goddard Space Flight Center

Joseph D. Hadad
Raytheon Co.
Bedford, Mass.

Erich Hafner
Army Electronics Labs.
Fort Monmouth, N.J.

Orville C. Hall
Westinghouse Electric Corp.
Baltimore, Md.

R. Hall
Navy Bureau of Ships
Washington, D.C.

Donald L. Hammond
Naval Research Lab.
Washington, D.C.

Donald L. Hammond
Hewlett-Packard Co.
Palo Alto, Calif.

Atwood H. Hargrove
Defense Electronics, Inc.
Rockville, Md.

C. William Harrison
General Radio Co.
Rockville, Md.

Harris F. Hastings
Naval Research Lab.
Washington, D.C.

Leonard O. Hayden
Naval Research Lab.
Washington, D.C.

Daniel J. Healey III
Westinghouse Electric Corp.
Baltimore, Md.

E. Heber
Bell Telephone Labs.
Whippany, N.J.

Alan Helgesson
Varian Associates
Palo Alto, Calif.

Wilfred B. Hillstrom
Goddard Space Flight Center

D. T. Himes
ITT Federal Labs.
Nutley, N.J.

Howard D. Hinnah
The Bendix Corp.
Davenport, Iowa

Erwin Hirschmann
Goddard Space Flight Center

Urs Hochuli
University of Maryland
College Park

J. G. Holman
Westinghouse Electric Corp.
Baltimore, Md.

Roland H. Holman
Syracuse Univ. Research Corp.
Syracuse, N.Y.

L. W. Honea
National Bureau of Standards
Station WWV
Greenbelt, Md.

Alton B. Hornback
Navy Electronics Lab.
San Diego, Calif.

George E. Hudson
National Bureau of Standards
Boulder Labs., Colorado

K. M. Hueter
Bell Telphone Labs.
Whippany, N.J.

Gerald M. Hyde
MIT Lincoln Lab.
Lexington, Mass.

Robert Hynes
Naval Research Lab.
Washington, D.C.

John H. Jacobi
Goddard Space Flight Center

Stephen A. Jacobs
Goddard Space Flight Center

David B. Jacoby
McCoy Electronics Co.
Mount Holly Springs, Pa.

E. H. Johnson
Goddard Space Flight Center

G. F. Johnson
Hughes Aircraft Co.
Culver City, Calif.

Leland F. Johnson
Pickard & Burns Electronics
Waltham, Mass.

Stanley L. Johnson
Raytheon Co.
Wayland, Mass.

Sam A. Johnston
Amphenol Controls
Janesville, Wis.

George Kamas
National Bureau of Standards, Boulder Labs.

Irving I. Kaplan
Westinghouse Electric Corp.
Baltimore, Md.

Peter Kartaschoff
Laboratoire Suisse de Recherches Horlogères
Neuchâtel, Switzerland

Robert F. Kelly
Army Strategic Communications Command
Washington, D.C.

Robert L. Kent
Damon Engineering, Inc.
Needham Hts., Mass.

Howard I. Kingman
Goddard Space Flight Center

E. Kirkpatrick
Inertial Guidance and Calibration
Newark Air Force Station, Ohio

Richard Klinke
Fairchild Semiconductor
Mountain View, Calif.

Frank K. Koide
North American Aviation, Inc.
Anaheim, Calif.

Elvin Krasin
Motorola, Inc.
Scottsdale, Ariz.

George C. Kronmiller
Goddard Space Flight Center

Bodo Kruger
Goddard Space Flight Center

Richard F. Lacey
Varian Associates
Beverly, Mass.

John Lahzun
Westinghouse Electric Corp.
Baltimore, Md.

James L. Lanphear
General Radio Co.
Rockville, Md.

Roy Larson
National Bureau of Standards, Boulder Labs.
Colorado

Joseph Lattin
Naval Weapons Quality Assurance Office
Washington, D.C.

D. B. Leeson
Hughes Aircraft Co.
Culver City, Calif.
(now at Applied Technology, Inc.)

Frank Leo
Naval Observatory
Washington, D.C.

Gerald L. Lett
General Radio Co.
Rockville, Md.

Hugh Lilienkamp
Naval Avionics Facility
Indianapolis, Indiana

R. N. Lincoln
ADCOM, Inc.
Cambridge, Mass.

W. F. Lineberger
National Security Agency
Fort Meade, Md.

David W. Lipke
Goddard Space Flight Center

Dr. M. S. Lipsett
Perkin-Elmer Corp.
Norwalk, Conn.

David M. Lisbin
Westinghouse Electric Corp.
Baltimore, Md.

John L. Little
National Bureau of Standards

H. Lo
Physics Dept.
University of Maryland
College Park

Chesley H. Looney
Goddard Space Flight Center

Heilbron B. Love, Jr.
Harry Diamond Labs., U.S.A.M.C.
Washington, D.C.

Frank J. Lupo
Dept. of Electrical Eng.
New York Univ.
New York

E. Norman Lurch
Goddard Space Flight Center

Thomas J. Lynch
Goddard Space Flight Center

Howard Mager
Raytheon Co.
Bedford, Mass.

Robert Munn
Motorola, Inc.
Chicago, Ill.

James Morakis
Goddard Space Flight Center

Reed W. Markley
Raytheon Co.
Wayland, Mass.

William Markowitz
U.S. Naval Observatory
Washington, D.C.

Robert J. Martel
Westinghouse Aerospace Corp.
Baltimore, Md.

Paul C. Marth
Johns Hopkins Applied Physics Lab.
Silver Spring, Md.

John B. Martin
Goddard Space Flight Center

A. O. McCoubrey
Varian Associates
Beverly, Mass.

Frank J. McCarthy
Spectra-Electronics, Inc.
Los Altos, California

Joseph E. McColgan
Meteorology & Calibration Directorate
Frankford Arsenal
Philadelphia, Pa.

James C. McDade
Harry Diamond Labs.
Washington, D.C.

R. B. McDowell
Navy Bureau of Ships
Washington, D.C.

Thomas E. McGunigal
Goddard Space Flight Center

Thomas P. McReynolds
Varian Associates
Palo Alto, Calif.

Manfred Meiseles
Westinghouse Electric Corp.
Baltimore, Md.

John T. Mengel
Goddard Space Flight Center

Dove Menkes
Radio Corp. of America
Camden, N.J.

George Milburn
Army Strategic Communications Command, Engineering Directorate
Washington, D.C.

Donald E. Miller
Hughes Aircraft Co.
Los Angeles, Calif.

John E. Miller
Goddard Space Flight Center

Ralph L. Miller
Goddard Space Flight Center

Robert E. Morden
Naval Research Lab.
Washington, D.C.

Alvin H. Morgan
National Bureau of Standards
Boulder Labs.
Colorado

H. J. Morrison
Westinghouse Electric Corp.
Baltimore, Md.

William A. Morton
Goddard Space Flight Center

Robert A. Mostrom
Smith Electronics, Inc.
Cleveland, Ohio

F. H. Mullen
National Co.
Malden, Mass.

James A. Mullen
Raytheon Co.
Waltham, Mass.

John D. Musselman
Smith Electronics, Inc.
Brecksville, Ohio

P. E. Nace
Westinghouse Aerospace
Baltimore, Md.

B. D. Nelin
ADCOM Inc.
Cambridge, Mass.

Alec L. Nelson
General Dynamics
Rochester, N.Y.

Charles J. Neumann
Range Development Dept.
Pacific Missile Range
Pt. Mugu, Calif.

Grady Nichols
Goddard Space Flight Center

Llewellyn W. Nicholson
Goddard Space Flight Center

D. Norar
Eastern Instrumentation
Baltimore, Md.

George O'Connor
Arvin Industry, Inc.
Columbus, Ind.

Arthur Orenberg
National Co.
Malden, Mass.

Leonard J. Paciorek
Syracuse Univ. Research Corp.
Syracuse, N.Y.

Ross A. Parkhurst
Harry Diamond Labs.
Washington, D.C.

Willis S. Parsons
U.S. Army
White Sands Missile Range, N.M.

Benjamin Parzen
Parzen Research, Inc.
Long Island, N.Y.

M. Pittman
Physics Dept.
University of Maryland
College Park

Henry H. Plotkin
Goddard Space Flight Center

R. Pohle
University of Maryland
College Park

Richard D. Posner
Mass. Institute of Technology
Cambridge

Millard Prisant
Frequency Electronics, Inc.
Astoria, N.Y.

David M. Raduziner
Raytheon Co.
Wayland, Mass.

Norman F. Ramsey
Harvard Univ.
Cambridge, Mass.

William Ray
Johns Hopkins Applied Physics Lab.
Silver Spring, Md.

Frederick H. Reder
Army Electronics Labs.
Fort Monmouth, N.J.

Bruno W. Reich
Goddard Space Flight Center

John V. Rende
Goddard Space Flight Center

R. C. Rennick
Bell Telephone Labs.
Allentown, Pa.

John M. Richardson
National Bureau of Standards, Bc lder Labs.
Colorado

Dr. Robert W. Rochelle
Goddard Space Flight Center

Robert J. Rorden
Varian Associates
Palo Alto, Calif.

Brian E. Rose
Hughes Aircraft Co
Culver City, Calif.

Donald E. Rosenbaum
Naval Avionics Facility
Indianapolis, Ind.

Lauren J. Rueger
Johns Hopkins Applied Physics Lab.
Silver Spring, Md.

Werner M. Rupp
Army Electronics Labs.
Fort Monmouth, N.J.

Sachio Saito
Goddard Space Flight Center

Richard Sanborn
Pickard & Burns Electronic
Waltham, Mass.

Glen San Lwin
Johns Hopkins Applied Physics Lab.
Silver Spring, Md.

Dominick Santarpia
Goddard Space Flight Center

Baldwin Sawyer
Sawyer Research Products, Inc.
Eastlake, Ohio

William A. Saxton
Frequency Magazine
Brookline, Mass.

T. C. Sayre
General Electric Co.
Roslyn, Pa.

Paul R. Schultz
Radio Receptor Corp.
Brooklyn, N.Y.

Leonard Schwartz
General Precision, Inc.
Pleasantville, N.Y.

John Schwarz
Army Electronics Labs.
Fort Monmouth, N.J.

R. H. Sear
Westinghouse Electric Corp.
Baltimore, Md.

Campbell L. Searle
Mass. Institute of Technology
Cambridge, Mass.

Richard E. Seifert
General Electric Co.
Lynchburg, Va.

Frederick Sera
Goddard Space Flight Center

Dan S. Serice
NASA Headquarters

J. M. Shapiro
Hallicrafters
Wilton, Conn.

Merrick E. Shawe
Goddard Space Flight Center

Ken Shen
Astro Communication Lab.
Gaithersburg, Md.

Delbert Shepard
Naval Weapons Quality Assurance Office
Washington, D.C.

John H. Sherman, Jr.
General Electric Co.
Lynchburg, Va.

Robert B. Shields
Syracuse Univ. Research Corp.
Syracuse, N.Y.

John H. Shoaf
National Bureau of Standards, Boulder Labs.
Colorado

C. S. Shyman
Westinghouse Electric Corp.
Baltimore, Md.

S. Siahatgar
Dept. of Electrical Engineering
Univ. of Maryland
College Park

Louis Sickles
Radio Corp. of America
Camden, N.J.

Alfred J. Siegmeth
Resdel Engineering Corp.
Pasadena, Calif.

Victor R. Simas
Goddard Space Flight Center

James H. Simpson
General Precision, Inc.
Pleasantville, N.Y.

W. A. Skillman
Westinghouse Electric Corp.
Baltimore, Md.

Frank Slater
Goddard Space Flight Center

Burton Smith
Raytheon Co.
Burlington, Mass.

Charles N. Smith
Goddard Space Flight Center

Kenneth D. Smith
Westinghouse Electric Corp.
Baltimore, Md.

L. A. Smith
General Precision, Inc.
Pleasantville, N.Y.

Ned B. Smith
Cornell Aeronautical Lab., Inc.
Buffalo, N.Y.

Perry Smith
Waltham, Mass.

Warren L. Smith
Bell Telephone Labs.
Allentown, Pa.

P. A. Sorrell
Westinghouse Electric Corp.
Baltimore, Md.

R. Spence
Imperial College
London, England

A. W. Speyers
Vitro Labs.
West Orange, N.J.

Orville J. Stanton
NASA Headquarters

Edward F. Stasik
Westinghouse Electric Corp.
Baltimore, Md.

Clark Stephens
General Technology Corp.
Torrance, Calif.

William Stern
Columbia Univ. Radiation Labs.
New York

D. Stilwell
Naval Research Lab.
Washington, D.C.

C. S. Stone
Tracor
Austin, Texas

John T. Strain
Frequency Electronics, Inc.
Ashton, Md.

M. W. P. Strandberg
Mass. Institute of Technology
Cambridge

Herbert P. Stratemeyer
General Radio Co.
West Concord, Mass.

Richard G. Strauch
Martin Co.
Orlando, Fla.

H. A. Strothers
U.S. Army, Office of the Chief of Communications-Electronics
Washington, D.C.

Harold K. Sutcliffe
Defence Research Staff
British Embassy
Washington, D.C.

Peter G. Sulzer
Sulzer Labs., Inc.
Rockville, Md.

Richard L. Sydnor
Jet Propulsion Lab.
Pasadena, Calif.

Roger A. Sykes
Bell Telephone Labs., Inc.
Allentown, Pa.

J. D. Svedlow
System Technology Center
Philco Corp.
Arlington, Va.

Herbert D. Tanzman
Winslow Teletronics Corp.
Asbury Park, N.J.

Ralph E. Taylor
Goddard Space Flight Center

C. V. Tenney
Navy Electronics Labs.
San Diego, Calif.

J. Toms
Tracor
Austin, Texas

J. H. W. Unger
Bell Telephone Labs.
Whippany, N.J.

James C. Van Caster
General Dynamics/Electronics
San Diego, Calif.

Victor Van Duzer
Hewlett-Packard Co.
Palo Alto, Calif.

J. Vanier
Varian Associates
Beverly, Mass.

Dr. R. F. C. Vessot
Varian Associates
Beverly, Mass.

Edmund Vollrath
Harry Diamond Labs.
Washington, D.C.

Lewis Ott Ward
Parzen Research, Inc.
Westbury, New York

Schuyler C. Wardrip
Goddard Space Flight Center

W. B. Warren, Jr.
RMS Engineering, Inc.
Atlanta, Georgia

William R. Webb
Westinghouse Electric Corp.
Baltimore, Md.

E. F. Weinburg
Raytheon Co.
Bedford, Mass.

Gerald Weiss
Dept. of Electrical Engineering
New York Univ.

Albert L. Whitehead
Goddard Space Flight Center

Dr. G. M. R. Winkler
Institute for Exploratory Research
Army Electronics Labs.
Fort Monmouth, N.J.

Edwin L. Wirtz
Radio Corporation of America
Burlington, Mass.

J. D. Woermbke
Westinghouse Electric Corp.
Baltimore, Md.

Walter H. Wood
Goddard Space Flight Center

R. H. Woodward
Pickard & Burns Electronic
Waltham, Mass.

Mr. Lyn Wooten
Radio Corporation of America
Burlington, Mass.

W. Whittier Wright
RMS Engineering, Inc.
Atlanta, Georgia

Benjamin S. Yaplee
Naval Research Lab.
Washington, D.C.

☆ U. S. GOVERNMENT PRINTING OFFICE: 1965 O - 778-267